

# ELECTRICAL TRANSMISSION AND SUBSTATION STRUCTURES

*Technology for the Next Generation*

---

PROCEEDINGS OF THE 2009 ELECTRICAL TRANSMISSION AND  
SUBSTATION STRUCTURES CONFERENCE

---

November 8–12, 2009  
Fort Worth, Texas

SPONSORED BY  
Electrical Transmission Structures Committee  
of The Structural Engineering Institute (SEI)  
of the American Society of Civil Engineers

EDITED BY  
Marlon W. Vogt, P.E.



Program Channel: [@Seismicisland](http://@Seismicisland)

Published by the American Society of Civil Engineers

# ELECTRICAL TRANSMISSION AND SUBSTATION STRUCTURES

*Technology for the Next Generation*

---

PROCEEDINGS OF THE 2009 ELECTRICAL TRANSMISSION AND  
SUBSTATION STRUCTURES CONFERENCE

---

November 8–12, 2009  
Fort Worth, Texas

SPONSORED BY  
Electrical Transmission Structures Committee  
of The Structural Engineering Institute (SEI)  
of the American Society of Civil Engineers

EDITED BY  
Marlon W. Vogt, P.E.



Published by the American Society of Civil Engineers

Telegram Channel: [@Seismicisolation](https://t.me/Seismicisolation)

## **Copyright and Disclaimer**

ISBN: 978-0-7844-1077-6

Any statements expressed in these materials are those of the individual authors and do not necessarily represent the views of ASCE, which takes no responsibility for any statement made herein. No reference made in this publication to any specific method, product, process or service constitutes or implies an endorsement, recommendation, or warranty thereof by ASCE. The materials are for general information only and do not represent a standard of ASCE, nor are they intended as a reference in purchase specifications, contracts, regulations, statutes, or any other legal document.

ASCE makes no representation or warranty of any kind, whether express or implied, concerning the accuracy, completeness, suitability, or utility of any information, apparatus, product, or process discussed in this publication, and assumes no liability therefore. This information should not be used without first securing competent advice with respect to its suitability for any general or specific application. Anyone utilizing this information assumes all liability arising from such use, including but not limited to infringement of any patent or patents.

Copyright © 2010 by the American Society of Civil Engineers.  
All Rights Reserved.

ASCE and American Society of Civil Engineers—Registered in U.S. Patent and Trademark Office.

*Photocopies and reprints.*

You can obtain instant permission to photocopy ASCE publications by using ASCE's online permission service ([www.pubs.asce.org/authors/RightslinkWelcomePage.html](http://www.pubs.asce.org/authors/RightslinkWelcomePage.html)). Requests for 100 copies or more should be submitted to the Reprints Department, Publications Division, ASCE, (address above); email: [permissions@asce.org](mailto:permissions@asce.org). A reprint order form can be found at [www.pubs.asce.org/authors/reprints.html](http://www.pubs.asce.org/authors/reprints.html).

American Society of Civil Engineers  
ASCE International Headquarters  
1801 Alexander Bell Drive  
Reston, VA 20191-4400 USA

Call Toll-Free in the U.S.: 1-800-548-2723 (ASCE)  
Call from anywhere in the world: 1-703-295-6300  
Internet: <http://www.pubs.asce.org>

# Preface

These proceedings contain papers presented at the 2009 Electrical Transmission and Substations Structures Conference sponsored by the Structural Engineering Institute of the American Society of Civil Engineers, held in Fort Worth, Texas, November 8-12, 2009. This is the fourth specialty conference on utility structures, and begins an attempt to hold the conference on a three-year cycle. The conference originated to provide opportunities for utility engineers to gain further understanding of the industry through technical papers, workshops, plant tours, and networking with other utility professionals.

The electric utility industry faces the impending retirement of approximately half its workforce in the next 10 years. The planning committee designed every aspect of this conference to provide value and knowledge transfer to those in the transmission and substation structures sector of our industry. We specifically focused on the needs of the newer, less-experienced engineers and technicians, hence the title, "Technology for the Next Generation." However, there was also plenty of value for seasoned veterans.

The conference included formal sessions on loadings, analysis and design, foundations, substation design, applied technology, and case studies. The session chairs and editor reviewed all papers included in these proceedings. All papers are eligible for discussion in the Journal of Structural Engineering. The papers are also eligible for ASCE awards.

Marlon W. Vogt, PE, Editor

# Acknowledgments

Preparation of the 2009 Electrical Transmission Conference required time, effort, and dedication by members of the conference steering committee and staff at ASCE/SEI. Therefore, much of the success of the conference is a reflection of the level of effort by this group of volunteers.

The committee would also like to acknowledge the critical support of the sponsors, exhibitors, and participants who contributed to the success of the conference through their participation.

## Conference Steering Committee

### Conference Chair

Marlon W. Vogt, P.E., M.ASCE  
Ulteig Engineers, Inc.

Frank W. Agnew, P.E., M.ASCE  
Alabama Power Company

Gary E. Bowles, P.E., M.ASCE  
Electrical Consultants, Inc.

Ronald Carrington, P.E., M.ASCE  
POWER Engineers

Dana Crissey, P.E., M. ASCE  
Oncor Electric Delivery

Anthony M. DiGioia, Ph.D., P.E.,  
Dist.M.ASCE  
DiGioia, Gray & Associates LLC

Leon Kempner, Jr., P.E., M.ASCE  
Bonneville Power Administration

Otto J. Lynch, P.E., M.ASCE  
Power Line Systems, Inc.

Robert E. Nickerson, P.E., M.ASCE  
Consulting Engineer

Wesley J. Oliphant, P.E., F.ASCE  
ReliaPole Solutions

Archie D. Pugh, P.E., M.ASCE  
American Electric Power

Ronald E. Randle, P.E., M.ASCE  
EDM International

C. Jerry Wong, Ph.D., P.E., M.ASCE  
DHW Engineering LLC

## SEI Staff

James Rossberg  
Debbie Smith  
Barbara Hickman

Donna Dickert  
Seán Scully  
Joanna Colbourne

Telegram Channel: [@Seismicisolation](https://t.me/Seismicisolation)

## Sponsors

### *Platinum*

American Electric Power  
Oncor Electric Delivery

### *Premium*

FWT, Inc.  
Power Line Systems, Inc.  
Thomas & Betts Corporation  
Valmont Newmark

### *Deluxe Plus*

Electrical Consultants, Inc.  
Sabre Tubular Structures

### *Deluxe*

Black & Veatch  
LOCWELD  
POWER Engineers  
SAE Towers

### *Basic*

DIS-TRAN  
Fabrimet, Inc.  
Falcon Steel Company  
KEC International Ltd.  
Underground Devices, Inc.

## Exhibitors

3M High Capacity Conductor  
AIR2  
Birmingham Fastener Manufacturing  
COMENSA  
Commonwealth Associates, Inc.  
Copper Care Wood Preservatives, Inc.  
Crux Subsurface, Inc.  
DiGioia, Gray & Associates LLC  
DIS-TRAN  
Electrical Consultants, Inc.  
Fabrimet, Inc.

Falcon Steel Company  
FWT, Inc.  
GAI Consultants, Inc.  
Helical Pier Systems Ltd.  
Hughes Brothers, Inc.  
John Chance Land Surveys  
Kalpataru Power Transmission Ltd.  
KEC International Ltd.  
Laminated Wood Systems, Inc.  
Lapp Insulators LLC  
LOCWELD

Telegram Channel: [@Seismicisolation](https://t.me/Seismicisolation)

Madison Chemical Industries Inc.  
McKinney Drilling Co.  
MESA Associates, Inc.  
Network Mapping Ltd.  
Osmose Utilities Services Inc.  
Pascor Atlantic  
Patterson & Dewar Engineers  
Pondera Engineers LLC  
Power Line Systems, Inc.  
Preformed Line Products  
ReliaPOLE Solutions, Inc.  
ROHN Products  
RS Technologies

Sabre Tubular Structures  
SAE Towers  
Scarborough Engineering, Inc.  
SEVES USA Inc.  
Synertech Moulded Products/Oldcastle  
Precast  
Terra Remote Sensing Inc.  
Thomas & Betts Corporation  
Threaded Fasteners, Inc.  
Trinity Structural Towers, Inc.  
Underground Devices, Inc.  
Valmont Newmark  
W.I.R.E. Services

Telegram Channel: [@Seismicisolation](https://t.me/Seismicisolation)

# Table of Contents

## Loading I

### **Are Wood Poles Getting Weaker?**

Brent Baker and Michael D. Brown

### **The Chaotic Confusion Surrounding “Wood Equivalent” Non-Wood Poles**

Wesley J. Oliphant

### **Estimation of Containment Loads on a 230kV Steel Transmission Line Using Finite Element Model**

Asim Haldar, Maria Veitch, and Trevor Andrews

### **Common Sag and Tension Errors: It’s Time for Template Technology to be Put in the Drawer Forever**

Otto J. Lynch

## Analysis and Design I

### **Laboratory and Field Testing of Steel Davit Arm Fatigue Failures on Concrete Poles**

Bruce Freimark, Meihuan (Nancy) Zhu, and Robert Whapham

### **Lessons Learned from Design and Test of Latticed Steel Transmission Towers**

Quan He Fan

### **Lessons Learned on Mega Projects**

Michael E. Beehler

### **345 kV High Ampacity OH/UG Project**

Dana R. Crissey

## Foundations

### **Integration of Optimum, High Voltage Transmission Line Foundations**

Freeman Thompson, Nick Salisbury, Anwar Khattak, Aaron Hastings, and Michael Foster

### **Geotechnical Investigations for a Transmission Line Are More Than Drilled Borings**

Kristofer Johnson

### **Transmission Pole Foundations: Alternate Design Methods for Direct-Embedded Round, Wood Transmission Poles**

Cassie McNames and Sivapalan Gajan

### **Assessment and Repair of Steel Tower and Steel Pole Foundations**

Nelson G. Bingel III and Kevin D. Niles

Telegram Channel: @Seismicisolation

## **Substation Design**

### **Substation Bus Design: Current Methods Compared with Field Results**

Keith Malmedal and John Wendelburg

### **3D Automated Design of Substations**

D. R. Lemelin, C. Bégel, C. Benavides, C. Lacroix, and Y. Drolet

### **Seismic Design of Substation Structures**

E. Bazán-Zurita, J. Bielak, A. M. DiGioia Jr., and S. Jarenprasert

### **Analytical Techniques to Reduce Magnetic Force from High Fault Current on Rigid Bus**

T. A. Amundsen, J. L. Oster, and K. C. Malten

## **Loading II**

### **Wind Loading: Uncertainties and Honesty Suggest Simplification**

Alain H. Peyrot

### **Review of Span and Gust Factors for Transmission Line Design**

Roberto H. Behncke and T. C. Eric Ho

### **Wind Load Methodologies for Transmission Line Towers and Conductors**

Leon Kempner Jr.

### **The Effects of Ice Shedding on a 500 kV Line**

Alan B. Peabody and Ron Carrington

## **Analysis and Design II**

### **Fact or Fiction—Weathering Steel Can Provide Effective Corrosion Protection to Steel Structures**

C. Jerry Wong

### **Large Catenary Structures for High Voltage Transmission Lines**

P. G. Catchpole and E. A. Ruggeri

### **Aesthetic Mitigation—The Challenge Confronting Future Expansion of Transmission Lines**

Max Chau, Archie Pugh, and Scott Kennedy

### **Alabama Power Increases Line Capacity Using 3M ACCR Conductor (On Existing Towers)**

Howard A. Samms

## **Case Studies—Foundations**

### **Golden Pass LNG 230kV Double Circuit: Foundations**

Ernest C. Williamson Jr. and Ronald L. Rowland

### **Deepwater Transmission Line Foundations Meet Trophy Bass Lake Environment**

**Telegram Channel: @Seismicisolation**

R. Norman, A. M. DiGioia Jr., and E. J. Goodwin

#### **230kV Lattice Tower Replacement: An Example of Design Loading Not Addressed in the NESC**

Norman P. Hodges

#### **Design and Construction Challenges of Overhead Transmission Line Foundations (NU's Middletown Norwalk Project)**

Christopher L. McCall, James M. Hogan, and David Retz

## **Case Studies—Construction Challenges**

#### **Transmission Line Construction in Sub-Arctic Alaska Case Study: "Golden Valley Electric Association's 230kV Northern Intertie"**

Gregory E. Wyman

#### **The 2008 Iowa Floods: Structural Challenges and Solutions**

James W. Graham, Tim Van Weelden, and Marlon Vogt

#### **Transmission Line at St. Andrew Bay**

Rengaswamy Shanmugasundaram

#### **Construction Challenges of Extra High Voltage Transmission Lines: Building in the Most Difficult Terrain in the World**

Deepak Lakhapati

## **Applied Technologies**

#### **Vegetation Management Through LiDAR Derived CADD Models: Compliance with NERC Reliability Standard FAC-003-1**

N. Ferguson, S. Ryder, S. Verth, P. Richardson, and R. Ray

#### **Sequential Mechanical Testing of Conductor Designs**

Bruce Freimark, Bruce Vaughn, Jean-Marie Asselin, Craig Pon, and Zsolt Peter

#### **H<sub>2</sub>S Entrapment and Corrosion on Direct Embedded Galvanized Steel Transmission Poles**

Ajay Mallik and Andy Cooper

#### **Line Rating: It's All about the Temperature!**

Ryan Bliss

## **Posters**

#### **Dynamic Wind Analyses of Transmission Line Structures**

Ferawati Gani, Frederic Legeron, and Mathieu Ashby

#### **Temporary Support of Lattice Steel Transmission Towers**

Scott Monroe, Rodger Calvert, and John D. Kile

**Telegram Channel: @Seismicisolation**

**Power Restoration Solution after Major Cyclone: "Gonu" Hit Oman in June 2007**

Deepak Lakhapati

**Analysis Challenges in the Evaluation of Existing Aluminum Towers**

Rengaswamy Shanmugasundaram, Jason W. Kilgore, and Roger Calvert

**Electrical and Mechanical Considerations in 765kV (Insulator) Hardware Assembly Design**

John Kuffel, Ziqin Li, Bruce Freimark, and Teja Rao

**Strength of Steel Angles Subjected to Short Duration Axial Loads**

Jared J. Perez, Wendelin H. Mueller III, and Leon Kempner Jr.

**Residual Capacity in Compression of Corroded Steel Angle Members**

L. -V. Beaulieu, F. Légeron, S. Langlois, and S. Prud'homme

**Steel Structure Surface Preparation for Below Grade Coatings**

Edward M. Jacobs

**Impact of Alternative Galloping Criteria on Transmission Line Design**

D. Boddy and J. Rice

Telegram Channel: @Seismicisolation

*This page intentionally left blank*

Telegram Channel: @Seismicisolation

## ARE WOOD POLES GETTING WEAKER?

Brent Baker, P.E.<sup>1</sup> and Michael D. Brown, P.E.<sup>2</sup>

<sup>1</sup>Civil Engineer, The Empire District Electric Co., 602 S. Joplin Ave., Joplin MO 64802, PH (417) 540-6028; email: bbaker@empiredistrict.com

<sup>2</sup>Civil Engineer, Allgeier, Martin and Associates, Inc., P.O. Box 2627, Joplin MO 64803, PH (417) 499-1009; email: mbrown@amce.com

### ABSTRACT

This paper follows the evolution of wood pole design over the last 80 years and an example is used to demonstrate how the relative safety factor has increased. A brief review of the changes in the National Electrical Safety Code (NESC) strength requirements from 1927 to 2007 is presented to show how little it has changed. Technological advances in calculators, computers and computer software make it possible to analyze complex problems. Equations that were once simplified to facilitate computation are now expanded to include components previously ignored. However, the NESC has not adapted to incorporate these changes, resulting in more conservative designs.

### INTRODUCTION

Have you noticed that both transmission and distribution wood pole line designs don't seem to be what they were? Span lengths seem shorter and pole classes seem larger than they used to be? Have the codes changed that much or are the poles just weaker than they were? We submit for your consideration that the methods used for design today are much different than they have been over the last 80 years, resulting in more conservative structure design. The purpose of this article is to walk you through the evolution of wood pole design and demonstrate how the relative factor of safety has increased over the years.

While there have been changes in the National Electrical Safety Code (NESC), the strength requirements have changed very little between 1941 and 2007. In 1927 there were three grades of construction, A, B, and C with overload factors (safety factors) of 3, 2 and 1.33 respectively. The Heavy Load case was an 8 psf wind with  $\frac{1}{2}$ " radial ice. In 1941 the grades were changed to Grade B, C and C at Crossings with overload factors increased to 4, 2 and 2.67 respectively. The Heavy Load case was changed to 4 psf wind with  $\frac{1}{2}$ " radial ice and the "k" factor was introduced (NESC Rule 250B). In 1977 the extreme wind case was introduced (NESC Rule 250C). In 1990 an alternate method was introduced as an option that a designer could use. The alternate, Method B, was an attempt to acquaint line designers with a Load and Resistance Factored Design (LRFD) method as the first of several steps towards

completely revising the strength requirements for wood poles in future editions of the NESC. The 1997 edition made the LRFD method the preferred method, but left the overload factors as the alternate method. The 2002 edition revised the extreme wind case requirements. The 2007 edition introduced an extreme ice with concurrent wind load case (NESC Rule 250D). The 2007 edition also eliminates the alternate overload factor method in 2010, leaving the LRFD method as the only method after that time.

Although sweeping changes were proposed for the 2007 NESC, the majority were not approved. It appears that change continues to generate a lot of controversy and opposition within the industry. Work is now underway on the 2012 NESC. Change proposals were due by July 2008 and a preprint of proposed changes was due in September 2009. The Public Comment period will end on May 1, 2010. It is anticipated that many changes will be proposed for the strength and loading requirements of Part 2 of the NESC. It is also anticipated that the controversy and resistance to change will continue.

Of interest from a historical perspective is that the ultimate fiber stress used for poles was increased sometime between 1961 and 1972, but pole circumferences six feet from the butt were reduced, resulting in about the same groundline moment capacity.

### EXAMPLE 1

For illustrative purposes a simple single pole, single circuit 69kV structure with 4/0-6/1 ASCR conductors and a 3/8" HSS shield wire has been used. The pole top assembly, or crossarm configuration, is a TS-1 assembly as shown in Figure 1. The pole and wire data used in all of the calculations are set forth in Tables 1 and 2

This assembly has been a standard Rural Utilities Service (RUS), formerly the Rural Electrification Administration (REA), assembly for over 60 years. This assembly was selected as thousands of miles of this type of construction has been used by both investor owned utilities and rural electric cooperatives. Many of those lines have been rebuilt or upgraded in some way over the years, but many are still in service. Some would consider this a "standing" testimony to the reliability of this type of construction and the original design methods.

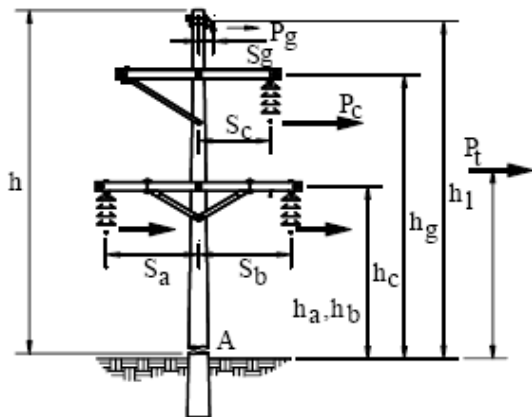


Figure 1. TS-1 Structure

**Table 1.**

POLE DATA		
Species (ultimate bending stress = 8,000 psi)	SYP	SYP
Height - Class	55-1	70-1
Top Circumference (in)	27	27
Groundline Circumference (in)	45.9	49.9
Moment Capacity at A (Ft.-Lb)	204,200	261,900
Moment Due to Wind on Pole (Ft.-Lb.)	3,985	6,835

**Table 2.**

CONDUCTOR LOADS, UNFACTORED		
	NESC HEAVY LOADING	
	VERTICAL	TRANSVERSE
3/8" HSS (LB/FT)	0.8077	0.4533
4/0 – 6/1 ACSR (LB/FT)	0.9520	0.5210

This paper makes extensive references to RUS publications on transmission line design. While these documents may not represent cutting edge technology, they do provide a well-documented history of design practices relating specifically to wood poles for transmission lines. They are publicly available documents and are some of the most widely used manuals or references for transmission line design, perhaps second only to the NESC. The publication names and dates are listed in the References at the end of the paper.

The maximum horizontal or wind span will be determined by several different design methods and the relative safety factor compared. All design calculations will be based on the NESC Heavy Load District for Grade B construction. This load case consists of a  $\frac{1}{2}$ " radial ice thickness on conductors with a 4 psf transverse wind.

**METHOD 1.** The first design method is based on simple statics where the moment capacity of the pole at the ground line is compared to the summation of the horizontal force times the distance from the ground to wire for each wire. The safety factor of 4 required by REA and the NESC could be applied to the strength side or the load side of the equation, but was most commonly used on the strength side to simplify the math. Table 3 shows the summation of moments for a 55-1 pole.

**Table 3. Summation of Moments**

	Force	Distance	Moment
OHGW	0.4533HS	46.9 ft. ( $h_g$ )	21.26HS
Top Phase	0.521HS	44.0 ft. ( $h_c$ )	22.92HS
Bottom Phases	1.042HS	38.0 ft. ( $h_b$ )	39.60HS
Totals			83.78HS

The maximum horizontal span, HS, is found from the following equation:

$$204,200 \text{ ft.-lbs} / 4 = 83.78\text{HS}$$

therefore HS = 609 feet

**METHOD 2.** The second design method is the same as Method 1 except that wind on the pole is considered. This method was built into the chart used in the 1950 REA Transmission Line Manual, but no example or explanation was included. Both the 1961 and 1972 REA Bulletin 62-1 used this method as well. For a 55-1 pole the maximum horizontal span, HS, is found from the following equation:

$$204,200 \text{ ft.-lbs} / 4 = 83.78\text{HS} + 3,985 \text{ ft.-lbs.}$$

therefore HS = 562 feet

**METHOD 3.** The third design method refined Method 2 by including the effects of the unbalanced vertical loads due to the unsymmetrical placement of wires. RUS Bulletin 62-1 (1980) indicated that this could impact span length by 2 to 10 percent, but left it to the engineers' judgment if it was significant enough to include. Again for a 55-1 pole, the maximum horizontal span (HS) is found from the following equation assuming that the vertical or weight span is equal to the horizontal span (which is assumed for all the following methods):

$$204,200 \text{ ft.-lbs} / 4 = 83.78\text{HS} + 3.5\text{HS} + 3,985 \text{ ft.-lbs.}$$

therefore HS = 539 feet

**METHOD 4.** This method is the same as method 3, except that it was done with the aid of a computer program, PLS-POLE (2000). It was done as a basis of comparison, as the rest of the methods addressed by this paper were done using PLS-POLE (2000).

The resulting HS = 533' for the 55'-1 pole.

It should be noted that all previous methods ignored the axial stress component (total vertical load divided by the cross-sectional area of the pole), but the program does account for it. The difference between methods 3 and 4 is attributed, in part, to that axial stress component and to minor differences in the calculation of wind load and pole circumferences. The difference of 1.1% is note worthy, but it certainly is minor when compared to the differences obtained with the other methods.

**METHOD 5.** This method is identical to Method 4 except that the moment capacity is checked at five-foot increments up the pole as well as at the groundline.

The resulting HS = 533' for the 55'-1 pole, indicates that the maximum moment occurred very near the ground line. A second example using a 70' pole, which will be discussed later, had a lower horizontal span indicating that the maximum stress did occur above the groundline.

**METHOD 6.** This method takes into account the P-Delta ( $\Delta$ ) or secondary moment effects. Horizontal loads cause the pole to deflect a distance of delta ( $\Delta$ ). The resultant vertical load  $P$ , times the distance  $\Delta$  results in an additional moment component or secondary moment. This secondary moment causes additional deflection with an additional moment component. This non-linear behavior increases the moment the pole must resist and greatly increases the math the engineer must deal with. Hence the use of the computer program for the rest of the methods.

An equation for pole deflection appeared in the REA Bulletin 62-1 (1961), but the secondary moment was not included in span length calculations until much later.

REA Bulletin 62-1 (1980) indicates that secondary moments are usually not accounted for in wood pole designs stating: “The high overload factor of four for heavy, medium and light district loadings is intended to keep the design simple for low height structures and in line with known strength, foundation response and loading conditions. For tall single pole structures, the designer may want to increase the OCF for NESC district loadings and high wind loadings in order to account for the additional moment due to deflection.”

RUS Bulletin 1724E-200 (1992) provides example calculations with and without consideration of the secondary moments, that are linear and non-linear calculations. The manual further indicates that many designers incorporate secondary moments in their design, but that manual did not provide recommendations either way on it.

A general equation for determining the maximum groundline moment is:

$$M_A \geq (OCF)M_{wp} + (OCF)M_{wc} + (OCF) M_{vo} + (OCF) M_{p\Delta}$$

where:

$M_A$  = the ultimate moment capacity of the pole at groundline

$M_{wp}$  = the groundline moment due to wind on the pole

$M_{wc}$  = the groundline moment due to wind on the wires

$M_{vo}$  = the groundline moment due to unbalanced vertical loads

$M_{p\Delta}$  = the groundline moment due to secondary moments

OCF = the overload capacity factor

Note that the overload capacity factor, as it was called at that time, is applied after the secondary moment is calculated and that the OCF could be applied to either side of the equation. While the axial stress component ( $P/A$ ) is not shown (it is not considered in any of the RUS Manuals), it is incorporated in the computer analysis results provided in this paper.

The resulting HS = 497'

**METHOD 7.** This method has been included to show what would happen if one used Method 6, but placed the entire safety factor on the load side of the equation before calculating the secondary moment. In other words, instead of calculating pole deflection based on a transverse load of  $T$ , one used  $4T$  to get pole deflection.

The resulting HS = 414'

**METHOD 8.** In 1990 the NESC introduced an alternate method, called Method B, which broke the traditional safety factor or Overload Factor into a strength factor component and a load factor component. In accordance with the 2007 NESC, the LRFD method is the only method to be used after July 2010. This LRFD method is fully embraced by the RUS Bulletin 1724E-200 (2005). By the time that manual had been published, RUS was requiring that secondary moments be considered as part of the design on most single pole structures. However, even the 2007 NESC does not require secondary moments be included. NESC Rule 260.A.1 states that "allowance may be made" for deflection "when the effects can be evaluated".

A general equation for determining the maximum groundline moment is:

$$\emptyset M_A \geq (LF)M_{wp} + (LF)M_{wc} + (LF)M_{vo} + (LF)M_{p\Delta}$$

where:

$\emptyset$  = strength factor, 0.65 for wood poles

LF = load factor, varies with the type of load (2.5 for wind loads, 1.5 for applied vertical loads and 1.0 for dead load or self weights)

Again note that the load factor is applied after calculating the secondary moment, which is how RUS intended it to be. NESC Rule 260.A.1 (2007) states that "Such deformation, deflection, or displacement should be calculated using Rule 250 loads prior to application of the load factors in Rule 253." Clearly the intent is to base deflection on an unfactored load, however that is easier said than done. Unless pole strength calculations are done using approximations to simplify manual or spreadsheet calculations, most programs are written to apply the load factor to the loads before calculating deflection. In most other standards and codes, the intent is to apply the load factor first since the load factor accounts for the uncertainty in predicting the load in various return periods. Most other codes have load factors of 1.6 or less instead of the 2.5 required for wind loads when using Grade B construction. Methods 8 through 11 below have the load factor applied before calculating deflection since PLS-POLE (2000) was used for the calculations. The results are therefore more conservative than what the NESC would require or that RUS would recommend.

It should be noted that Methods 1 through 7 used a traditional safety factor of 4, regardless of what side of the equation it was applied, with the exception of dead load. The dead load or self-weight of the pole and structure was not even considered in Method 1 thru 3 and Methods 4 thru 7 used a load factor of 1.0. Methods 8

through 11 are based on the LRFD method and the equivalent safety factor is 3.86 for wind loads (2.5/0.65) and 2.3 (1.5/0.65) for applied vertical loads. Method 8 uses a load factor of 1.0 for dead load for comparison to the previous methods.

The resulting HS = 534' is slightly higher than Method 6 due to the difference in overall safety factors.

**METHOD 9.** This method is just like Method 8 except that the Load Factor for the dead load has been increased from 1.0 to 1.5. The 1.5 load factor is in compliance with the NESC and thus this method probably better represents what most designers that use a non-linear analysis are doing.

The resulting HS = 507'

**METHOD 10.** ANSI 05.1 (2002) incorporated a new requirement in Section 9 that recommends the ultimate fiber bending stress be reduced with pole height. 100% of the published fiber stress can be used at groundline and the fiber stress should be reduced linearly to 75% of the published value at half the pole height above ground. Previously this recommendation had been included in a non-binding appendix of ANSI 05.1 (2002). A major effort was made to adopt this provision in the NESC C2 (2007), however that effort was not approved and the NESC remains based on the ANSI 05.1 (1992). It is anticipated that this issue will be a proposed change for the next NESC. The reduction recommended by ANSI 05.1 (2002) is incorporated in Method 10.

The resulting HS = 430'. Remember in Method 4 and 5 that the maximum stress occurred at the groundline. However this example demonstrates that the reduction in maximum fiber stress would require designers to check the portion of the pole above ground and will probably impact most designs.

**METHOD 11.** As discussed previously, the advent of the computer has allowed or enabled us to do things that we normally would not be able to do. This method builds on the previous method by adding in the weight of the crossarms, braces and insulators and includes the wind load on all of those components. We can even apply the correct drag factors for the flat surfaces of the crossarm and the round surfaces of the insulators.

The resulting HS = 423' is 1.6% less than the Method 10 results and is about the same order of magnitude as that observed in Method 4 over Method 3.

## EXAMPLE 2

The previously described methods are used on the same TS-1 structure with a 70'-1 pole. Logic would indicate that taller poles will deflect more and therefore will be impacted more by methods that include secondary moments. The results are shown in Table 4 and bear out that logic.

## RELATIVE FACTORS OF SAFETY

Each of the different design methods resulted in different horizontal span limitations even though they were designed with the same nominal factor of safety of about four (4). To compare the relative factor of safety for each method of calculation, Method 2 is used as a base with a factor of safety of 4.0. Any of the methods could have been used as the basis of comparison. Method 2 was selected as it is the method that has probably been in use the longest and it is likely that more miles of line were built based on that method than any other method. The ratio of horizontal spans is then used to determine the relative factor of safety. For example, comparing Method 2 to Method 3, the relative factor of safety is  $4*(562/539) = 4.2$ .

As shown in Table 4 the relative factor of safety varies from 3.7 to 5.4 for the 55'-1 pole example and 3.6 to 6.1 for the 70'-1 pole example. Is it any wonder that wood poles seem to be getting weaker?

**Table 4. Summary of Results**

Method	Groundline Check Only	Non-Linear	Strength Factor	Load Factor	55-1		70-1	
					Horizontal Span	Relative Factor Of Safety	Horizontal Span	Relative Factor Of Safety
1	Y	N	0.25	1	609	3.7	590	3.6
2	Y	N	0.25	1	562	4.0	528	4.0
3	Y	N	0.25	1	539	4.2	512	4.1
4	Y	N	0.25	1	533	4.2	501	4.2
5	N	N	0.25	1	533	4.2	493	4.3
6	N	Y	0.25	1	497	4.5	447	4.7
7	N	Y	1.00	4.0	414	5.4	354	6.0
8	N	Y	0.65	V* 2.5W	534	4.2	477	4.4
9	N	Y	0.65	1.5V 2.5W	507	4.4	437	4.8
10	N	Y	0.65**	1.5V 2.5W	430	5.2	352	6.0
11	N	Y	0.65**	1.5V 2.5W	423	5.3	345	6.1

\* Load Factor of 1.0 on dead load and 1.5 on applied vertical loads

\*\* Fiber Stress reduced in accordance with ANSI 05.1(2002)

## CONCLUSIONS

While wood poles may not be getting weaker, it certainly gives that appearance from the results presented herein. Based on these results the following conclusions can be drawn regarding the design of single pole wood structures:

- the NESC heavy loading has changed very little
- the method of calculation has changed drastically
- the method of calculation has a major impact
- secondary moments have a significant impact
- the application of strength and load factors has a major impact on secondary moments
- ANSI 05.1 fiber stress reduction has a major impact
- wood poles are not getting weaker

The methods presented by this paper are not intended to represent all methods that have or could be used to determine the maximum horizontal span. Other methods or different assumptions will result in different relative factors of safety. Other load cases or the use of Grade C construction will also result in different relative factors of safety. For example, structures controlled by extreme wind load cases may display a much narrower range of relative factors of safety since a load factor of 1.6 or less is normally used instead of 2.5, thereby giving more realistic deflections and secondary moments.

## CLOSING THOUGHTS

If thousands of miles of a structure design have been installed and those lines performed well structurally for over 50 years, logic would indicate that the design was satisfactory or perhaps even over designed. Yet all but one of the design methods considered in this paper resulted in a more conservative design. Is it time to re-evaluate our design method? Should we adjust the strength and load factors to be consistent with the design method?

The advent of the computer and the ingenuity of software developers have made it possible to analyze complex problems that could not be done previously. The engineer must decide how best to use that technology to manage our resources while protecting the safety and well being of the public. It needs to be recognized that more conservative designs may not be in the best interest of the public. They may just be more expensive and a waste of resources. The wide variety of design methods in use and the wide margin in relative factors of safety indicate the need for design standards. Perhaps the proposed ASCE Manual of Practice “Design of Wood Utility Pole Structures” will be that standard.

Perhaps Dr. A.R. Dykes summed it up well when he said “Structural Engineering is the Art of moulding materials we do not wholly understand into shapes we cannot precisely analyze, so as to withstand forces we cannot really assess, in such a way that the community at large has no reason to suspect the extent of our ignorance.”

## ACKNOWLEDGEMENTS

A special thanks to Donald Heald of Rural Utilities Services for his assistance in providing older versions of the REA Transmission Line Manual. The authors also extend their gratitude to their employers, The Empire District Electric Company and Allgeier, Martin and Associates, Inc. for the resources they provided in support of this work.

## REFERENCES

ANSI C2(2007), National Electrical Safety Code, Institute of Electrical and Electronics Engineers, Inc., New York, NY

ANSI O5.1(2002), American National Standard for Wood Poles Specifications and Dimensions, Alliance for Telecommunications Industry Solutions, Washington, DC

PLS-POLE(2000), Power Line Systems - Analysis and Design of Pole Structures, Power Line Systems, Inc., Madison, WI

U.S. Dept. of Agriculture, Rural Electrification Administration, *Transmission Line Manual Physical Design Consideration*, Government Printing Office, Washington, D.C

U.S. Dept. of Agriculture, Rural Electrification Administration, Bulletin 62-1(1961), *Transmission Line Manual*, Government Printing Office, Washington, D.C

U.S. Dept. of Agriculture, Rural Electrification Administration, Bulletin 62-1(1972), *Transmission Line Manual*, Government Printing Office, Washington, D.C

U.S. Dept. of Agriculture, Rural Electrification Administration, Bulletin 1724E-200(1980), *Design Manual for High Voltage Transmission Lines*, Government Printing Office, Washington, D.C.

U.S. Dept. of Agriculture, Rural Utilities Services, Bulletin 1724E-200(1992), *Design Manual for High Voltage Transmission Lines*, Government Printing Office, Washington, D.C.

U.S. Dept. of Agriculture, Rural Utilities Services, Bulletin 1724E-200(2005), *Design Manual for High Voltage Transmission Lines*, Government Printing Office, Washington, D.C.

**SEI 2009 Electrical Transmission & Substation Conference  
Technology for the Next Generation**

**The Chaotic Confusion Surrounding  
“Wood Equivalent” Non-Wood Poles**

**Wesley J. Oliphant, PE, F.ASCE**

President, ReliaPOLE Solutions, Inc. 32624 Decker Prairie, Rd., Magnolia, TX  
77355 Phone: (281-259-7000) e-mail: [woliphant@reliapole.com](mailto:woliphant@reliapole.com)

**ABSTRACT**

Unlike the statement in our American Declaration of Independence, which declares “all men are created equal”, electrical transmission and distribution poles are not necessarily so. Yet as an industry, we continue to work very hard to “commoditize” poles of differing structural attributes and material behaviors and we continue to try to relate them as an “equivalent” to ANSI class wood poles. It is easy to understand why we want to do this as we want to keep things simple, foolproof, less work, and “standardized”, etc., etc. etc. But with the industry’s inconsistent application of basic structural principles, the practice can sometimes lead to much confusion – at times chaotic confusion.

Since the development of the ANSI Standard Classification system for wood poles, a reasonable level of consistency and predictable behavior has been established for a highly variable product – natural wood poles. There is no doubt, that wood poles remain an integral and popular choice for supporting electrical power lines in the United States. But, for a variety of reasons utilities are increasingly specifying and installing non-wood poles of tubular steel, prestressed concrete and fiber reinforced polymer (FRP) materials in place of these wood poles for certain line design reasons. Those reasons are NOT the focus of discussion in this paper. Rather, this paper’s discussion is intended to be focused on the potential structural differences that may be experienced when we take a single, quality and dimensional standard for one pole material (natural wood poles), and try to establish “equivalent” structural performance and behavior expectations across a variety of other structural materials. Understanding the performance and structural behavior characteristics of each of the materials is not that difficult. Our consistent specification and communication of desired structural characteristics across all materials is where the confusion seems to be. This paper will attempt to discuss such characteristics as: 1) nominal strength; 2) stiffness; and 3) durability and how they compare across common pole materials. As well, this paper also discusses how the current NESC and various RUS Bulletins deal with the various material strengths, reliability and behaviors.

## The Chaotic Confusion Surrounding “Wood Equivalent” Non-Wood Poles

**Wesley J. Oliphant, PE, F.ASCE**

President, ReliaPOLE Solutions, Inc. 32624 Decker Prairie, Rd., Magnolia, TX  
77355 Phone: (281-259-7000) e-mail: [woliphant@reliapole.com](mailto:woliphant@reliapole.com)

Is it just me or am I the only person that believes these times are already chaotic enough without something else adding to the chaos? I'll grant that this important "pole issue" is not nearly as globally important as watching world economic meltdown occur right before our eyes. But I think I am a reasonably knowledgeable Engineer, and a long time "pole guy" with a great deal of time invested in learning the nuances of the pole industry. The issue of "wood equivalent" non-wood poles is right up there in my list of things I worry about. My family says I need to find a new hobby! Perhaps, but let me try to explain my point of view.

### *What exactly is a “wood equivalent” non-wood pole?*

I hate to break the news, but there is no such thing as a "wood equivalent" non-wood pole". Don't misunderstand, I do fully understand and appreciate why we want to believe one exists. Our industry seems to find a benefit to "commoditizing" or "standardizing" poles of differing structural attributes and material behaviors. We want to try to keep things simple, foolproof, less work, more "standardized", etc., etc. etc. But the practice of specifying "wood pole equivalents" of non-wood poles is leading to much confusion – at times chaotic confusion.

And, do we really want to set up the natural wood pole as the "standard" to which non-wood poles (tubular steel, concrete, and fiber reinforced composites) are measured? As wonderful a job as ANSI 05.1 has done to provide "minimum specifications for quality and dimensions of wood poles that are used for single pole utility structures", I think additional steps can and should be taken to bring this standard to a more consistent structural specification if that is how it will be used. The latest 2008 version of ANSI 05.1 is very much headed in the right direction with the addition of the Reliability Base Design information in appendix C.

As we design structures for electrical transmission, distribution and substation structures, we deal primarily with the material behaviors of strength, stiffness and durability.

### **Comparing nominal strengths:**

When most people refer to "wood equivalent" poles they are really trying to compare nominal strength. We all know that ANSI 05.1 establishes pole "classes" (Classes C10 up to H6) in order to define a consistent load carrying capability across various

species of wood poles. What might be less known and even confusing, is that during the process of selecting a wood pole class, particularly for larger transmission poles, a number of strength adjustments typically need to be made to account for characteristics and processes influencing pole strength and stiffness. One of these adjustments is the height adjustment. On poles taller than 50 ft. the maximum cantilever stress will typically occur some distance above the groundline, not at the groundline as most assume. It is also important to note that the fiber stress values shown in ANSI 05.1 represent “consensus” values (a combination of clear specimen tests, full size pole tests and engineering judgment).

All of this is important to keep in mind as we make very specific strength comparisons between wood poles and steel, concrete and fiber reinforced polymer poles. Keep in mind, the ANSI loads below are intended to be 50 percentile or “mean” strength values.

Horizontal			Horizontal		
Class	load (pounds)	Newtons	Class	load (pounds)	Newtons
H6	11,400	50,710	3	3,000	13,300
H5	10,000	44,480	4	2,400	10,680
H4	8,700	38,700	5	1,900	8,450
H3	7,500	33,360	6	1,500	6,670
H2	6,400	28,470	7	1,200	5,340
H1	5,400	24,020	9	740	3,290
1	4,500	20,020	10	370	1,650
2	3,700	16,500			

Table 1- ANSI 05.1 Horizontal Load Table

In the design methodology of:

$$\square R_n \geq \lambda Q$$

$\square$  is a resistance (strength) factor

$R_n$  nominal resistance (strength)

$\lambda$  is a load factor

$Q$  is the load

We can and should assume that load is consistent, and it applies the same, regardless of the type of pole material selected. I know there are many discussions that can be had with determining appropriate loads, but load should be irrespective of material. It is the resistance side of the equation where we run into multiple problems equating poles of differing materials. Part of the confusion is the manner in which the National Electric Safety Code (NESC) still intermingles and confuses loads and strengths.

Table 2 below shows the strength factors as they apply to structures from table 261-1A of the NESC.

2007 NESC Strength Factors for Structures

	Wood & Reinforced Concrete (not prestressed)	Steel	Concrete (prestressed)	FRP
Rule 250B (Grade B)	0.65	1.0	1.0	1.0
Rule 250B (Grade C)	0.85	1.0	1.0	1.0
Rules 250C & 250D	0.75	1.0	1.0	1.0

**Table 2 - Strength Factors for Structures (excerpted from Table 261-1A of the 2007 NESC)**

Steel, prestressed concrete and fiber reinforced polymer materials used for structures can use the same strength factor, irrespective of the NESC loading rules. Wood poles and reinforced concrete poles (not prestressed) on the other hand, have variable strength factors depending on the NESC load condition. And to what nominal strength do these factors apply – 1%, 5%, 50% (mean), LEL values? Why is it that one pole material is variable, and all other pole materials are fixed? If this is an attempt to inject differing levels of “reliability” into the design of structures, there are better ways of dealing with this. But currently, we have confusion, and chaos.

And of course the confusion and chaos is amplified when we try to compare a standardized steel, prestressed concrete or FRP pole load capacity to a wood pole load class derived from such a “crazy” methodology. If the pole is originally designed as a steel pole to begin with, we will use a 1.0 strength factor no matter what the loading rule. If the pole is originally sized as a wood pole, varying strength factors would have been used depending on the loading condition considered. Does it really make good structural engineering sense that we can utilize 50% more of the steel poles capacity than a wood pole when considering NESC rule 250B, grade B loadings, but only 18% more capacity than a wood pole under NESC rule 250B, grade C loadings? I propose this does not make much sense.

One can argue about the coefficient of variation (COV) being much larger with wood poles than with the other non-wood pole materials. With that COV difference, a larger number of poles, because of the higher variability, will exceed the required loading, assuming that all poles are based on the same nominal strength rating. But that doesn't make much sense either. I believe the goal should be to have the same reliability against failure at a specific load no matter what the material used. We set the loads, and we design poles to withstand those loads. We want to maintain a certain confidence that every pole will hold the required load and we can do that if we standardize the way we define “nominal strength” across all materials.

Most materials define strength as a 5% lower exclusion limit with a 50% confidence level. We should do that with all poles no matter the material and we will gain consistency in how we discuss nominal strength. ANSI 05.1 2008 is now providing the tools to calculate the strength of wood poles at a 5% lower exclusion limit with a 50% confidence. We need to standardize on this for wood poles and as well all other pole materials.

The Rural Utilities Service (RUS) has provided “wood pole equivalency” guidelines and established standard classes of both steel poles and prestressed concrete poles. The table below shows the standard class steel poles. The standard class prestressed concrete poles have the same strength requirements as does the steel pole standard classes. In addition to the tip load requirements, RUS also has several other requirements that are important considerations. These requirements are a defined Point-of-Fixity (POF) that is a distance from the pole bottom that equals 7% of the pole length, and a minimum strength specification at 5 feet from the top of the pole. Both are excellent requirements. But a catalog of non-wood poles designed to meet the RUS requirements of these tables, would meet requirements that are not typically considered with the selection of wood poles. Until we require wood poles to meet the same criteria, there will continue to be confusion of “wood pole equivalency” comparisons when these tables are utilized.

**TABLE 1**  
**Strength Requirements**

Standard Class Designations for Steel Poles	Minimum Ultimate Moment Capacity At Five Feet From Pole Top (Ft.-Kip)	Horizontal Tip Load Applied 2 Ft from Pole Top (Lbs.)
S-12.0	96	12,000
S-11.0	88	11,000
S-10.0	80	10,000
S-09.0	72	9,000
S-08.0	64	8,000
S-07.4	57	7,410
S-06.5	50	6,500
S-05.7	44	5,655
S-04.9	38	4,875
S-04.2	32	4,160
S-03.5	27	3,510
S-02.9	23	2,925
S-02.4	19	2,405
S-02.0	15	1,950

Table 3 - From RUS Bulletin 1724E-214 (available at <http://www.usda.gov/rus/electric/pubs/1724e->

**FIGURE 1**  
**Minimum Ultimate Moment Capacity Diagram along the Pole**

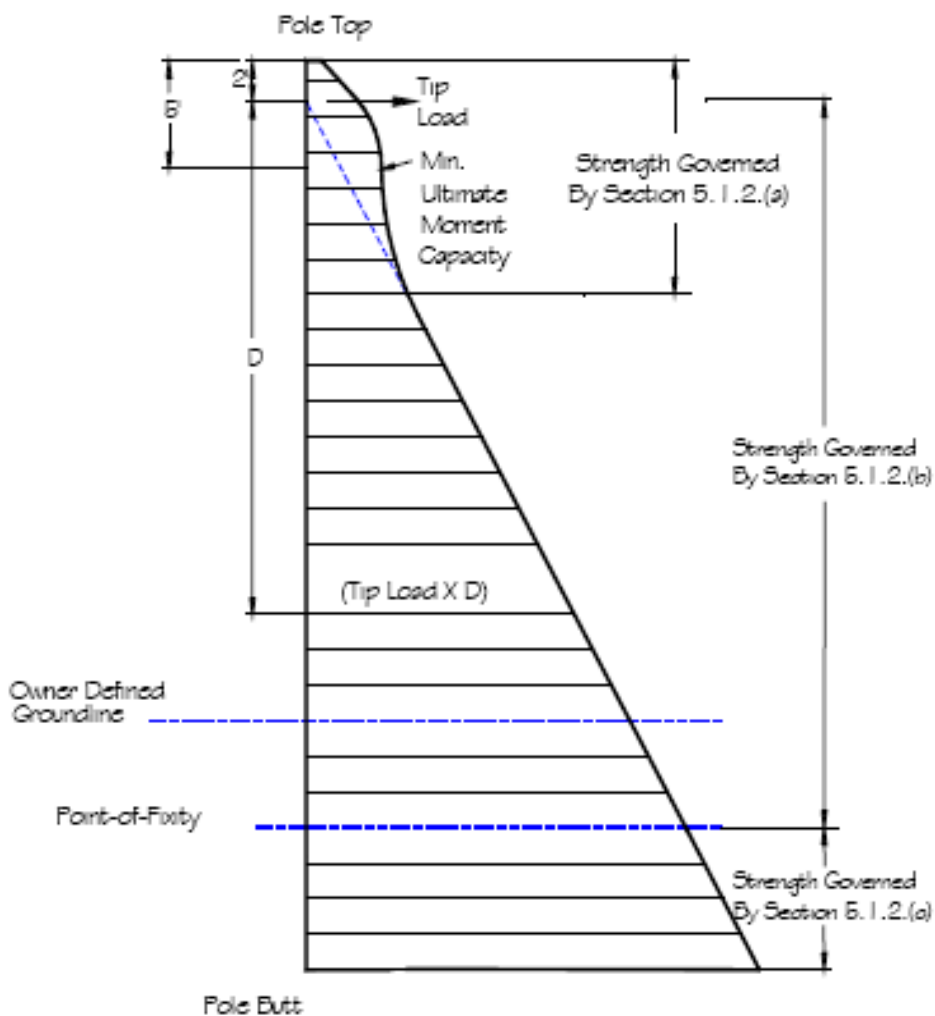


Figure 1 - Taken from RUS Bulletin 1724E-214  
 (available at <http://www.usda.gov/rus/electric/pubs/1724e-214.pdf>)

**Durability:**

Durability and strength are related. When structures deteriorate for whatever reason, they can lose strength. As in real estate, it is location, location, location. A woodpecker hole can be relatively benign structurally unless our friend decides to make a full fledged condo out of the top 20 feet of a pole. The same principle also applies to corrosion on a steel pole. A small bare spot mid way up the pole does not

necessarily reduce strength below that required of the loads. But, losing more than 33% of the wall thickness at groundline will definitely need to be considered significant and analyzed with respect to the expected load.

But how is durability treated with regard to “wood pole equivalency”? NESC Rule 250B allows for the deterioration of wood poles up to 67% of its original installed strength. However, non-wood poles must maintain their original required strength throughout their design life. In Rule 250C & 250D deterioration of wood poles is allowed up to 75% of its original installed strength. Again, non-Wood Poles must maintain the original required strength throughout their design life. If a calculated strength is required to achieve a given design life, then why do we allow reduced strength allowances for wood poles, but not for steel, prestressed concrete, and/or FRP poles? Does that make sense?

### **Stiffness:**

In my experience, the issue of stiffness is the least understood structural characteristic and most likely ignored when making “wood pole equivalent” comparisons. Obviously there are pole top deflection issues.

Wood poles, and steel poles deflect in a typical linear fashion. Apply a load and the tip of the pole will deflect a certain distance. Apply 10 times that load and the tip will deflect roughly 10 times the original distance. Depending on the height of the pole, wood poles will experience pole top deflections typically in the 10%-15% of the pole height at rupture. Steel poles can deflect 10%-20% of the pole height at ultimate load. There are stiffness differences.

Prestressed concrete poles have a variable modulus of elasticity. This is due to the prestressing effects and the composite nature of the combined concrete and steel. Concrete poles are very “stiff” and exhibit very minimum deflection, typically 2%-5% of the poles height for up to 50% of the poles loading range. Beyond approximately 50% of the ultimate loading, a prestressed concrete pole will become very elastic and pole top deflections of 10%-15% of the pole height will not be uncommon.

FRP poles can also be variable in stiffness depending on the nature of the composite. Stiffness is a key design consideration for FRP poles. Especially when considering FRP poles as “wood pole equivalents” special consideration should be given to limiting the deflection to that of the wood pole.

So all poles deflect differently. But let's also discuss the other stiffness related issues that I believe are even more critical. Substituting “wood pole equivalent” steel and concrete structures for existing wood pole guyed structures and multipole structures such as H-Frames, 3-Pole structures, etc should be done with great care. There is a stiffness interaction in these types of structures that may cause guy forces to change

dramatically in guyed pole applications, or x-brace forces to change dramatically with a change in pole stiffness in H-Frame applications. It is highly recommended that poles configured in these kinds of non-cantilevered applications, be specifically designed to determine the forces and reactions generated from the structure component stiffness interactions. It can be very dangerous to simply substitute a load capacity rated pole into these kinds of applications without giving due analysis consideration to the stiffness effects. Wood, steel, prestressed concrete and FRP poles will structurally behave much differently and could have a significant impact on other components, particularly guys and x-braces.

A number of analysis studies were done by various manufacturers over the years to evaluate the replacement of one leg of a wood h-frame with a steel or concrete pole. The analysis from these studies clearly indicated that pole class sizing problems would be encountered if not done carefully and analytically.

### ***Conclusions and Recommendations:***

We have discussed a number of issues related to the concept of “wood equivalent” non-wood poles. From an engineer’s point of view, carte blanch substitution can be dangerous. This is particularly so in structures where the stiffness interactions can dramatically change guy forces and resulting guy anchor loads, x-bracing forces, etc. While we all understand the desire and benefits to “commoditizing” or “standardizing” poles of differing structural attributes and material behaviors, we need to be very smart in how we go about doing so. Understand the structural behavioral differences before such substitutions are made. Also, understand fully the design “equivalency” of nominal strength.

I would recommend as an industry of talented engineers, that we work to eliminate the confusion (and chaos) that currently exists:

1. All pole nominal strengths need to be determined and classified in the same the same way. Within ANSI 05.1 let’s establish and publish tables (and use them) that are based on 5% lower exclusion limits with 50% confidence level. Let’s do the same for all other non-wood poles so that we can be consistently clear when comparing nominal strength of poles made of different materials.
2. Within ANSI 05.1, let’s also clear up the confusion on size effects, class size and method of conditioning and re-calculate the nominal resistance (bending strength) of utility poles with those effects already included.
3. Let’s also encourage the continued move to reliability based LRFD type design standards within the NESC. This is necessary to “fix” the discrepancy with strength factors we currently have with wood vs. other materials in NESC. It simply makes no sense to have variability of wood pole strength

factors dependent on load conditions. Make the load factors variable (50 year recurring events, 25 years recurring events, etc.) if differing levels of reliability are desired.

4. Alternatively, NESC should just consider deferring structural design standards altogether to organizations such as the Structural Engineering Institute of ASCE.
5. Include in ANSI 05.1 the effects of strength degradation over time due to durability issues, or work to exclude from NESC the currently allowed strength reductions that apply only to wood poles.

#### REFERENCES:

1. Institute of Electrical and Electronic Engineers, Inc., "National Electric Safety Code, C2-2007", IEEE, New York, NY
2. American National Standards Institute, "ANSI 05.1-2008, American National Standard for Wood Poles, Specifications and Dimensions" ANSI, New York, NY.
3. Wolfe, Ronald W.; Bodig, Jozsef; Lebow, Patricia. 2001. "Derivation of Nominal Strength for Wood Utility Poles. Gen. Tech. Rep. FPL-GTR-128 rev.). Madison, WI: U.S. Department of Agriculture, Forest Service, Forest Products Laboratory. 11 p.
4. Rollins, H.M. "A Discussion of 'Wood Equivalent' Poles", A technical bulletin prepared for the North-American Wood Pole Coalition, January 2007
5. United States Department of Agriculture, Rural Utilities Service, "Bulletin 1724E-214, Guide Specification for Standard Class Steel Transmission Poles".

## Estimation of Containment Loads on a 230kV Steel Transmission Line Using Finite Element Model

**Asim Haldar<sup>1</sup>, Ph. D, P. Eng., Maria Veitch, B. Eng. and Trevor Andrews, P.Eng.**

<sup>1</sup>Engineering Services Division, Newfoundland and Labrador Hydro, Nalcor Energy, 500 Columbus Drive, St. John's NL, A1B 4K7, Canada, ahaldar@nalcorenergy.com

### ABSTRACT

Overhead transmission lines are designed to withstand meteorological loads such as wind, ice, combined wind and ice and static residual loads due to broken conductor and/or ice shedding. A line could be subjected to dynamic overloading when a triggering event is caused by a component failure. In this situation, a shock wave propagates through the system and a redistribution of the force takes place. If the capacity of the remaining system can not support this force redistribution, the line may experience a cascade failure.

This paper presents a systematic methodology to model both the static and dynamic behaviors of a line due to conductor breakage using the ADINA (Automatic Dynamic Incremental Nonlinear Analysis) program. Based on the analysis, the extent of a cascade damage/failure zone is estimated and a mitigation approach for correcting the situation is provided.

### INTRODUCTION

Newfoundland and Labrador Hydro, a Nalcor Energy company, operates transmission lines at 69 kV, 138 kV, 230 kV, and 735 kV voltage levels. The transmission system consists of wood poles as well as steel and aluminum towers. The transmission line network covers a vast region and is exposed to a very harsh, cold environment. Figure 1 presents the island map showing the study area and the two 230 kV parallel steel transmission lines (Line 1 and Line 2) considered in this study. These lines run from the Bay D'Espoir Terminal station to Sunnyside Terminal Station located on the Avalon Peninsula (shaded area). The lines are approximately 140 km long, and consist of guyed-V tangent towers and self supported latticed (four legged) towers for the heavy angles and dead ends. The lines were constructed in the late 60's. Since their commissioning, the transmission line system within the study area has experienced a number of severe ice storm failures (Figure 2, a glaze ice sample with unit weight 7.8 kg/m). Figure 3 presents the layout of the two parallel lines and their connectivity to the transmission line system on the Avalon Peninsula.

This figure also shows the location of the dead end towers on the two parallel lines (Line 1 and Line 2) considered in this study and the many occurrences of the line failures during the past forty years. It is seen that a large section of the two steel lines does not have an adequate number of dead end towers to provide security against cascade failures. Note that the steel transmission line system on the Avalon Peninsula was upgraded during 1999-2004, considering cascade failure protection (Halder, 2006). The dead end towers on Line 1 and Line 2 were not upgraded.

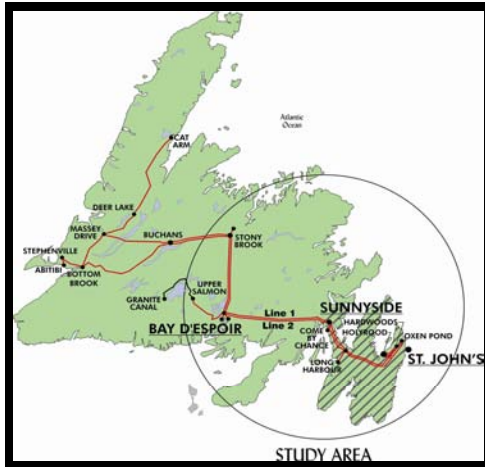


Figure 1 Location of transmission lines



Figure 2 Glaze ice sample (1984 ice storm)

Lines 1 and 2 were designed for (1) 25.4 mm radial glaze ice, (2) 13 mm radial glaze with 117 km/h wind and (3) 160 km/h wind respectively. An overload factor of 1.33 was used. The conductor is 795 MCM 26/7 ACSR and the ruling span in the long section is 430 m. The final tension under everyday condition at  $4^{\circ}\text{C}$  is 27.8 kN. The ratios of span to sag and span to insulator length are 32 and 200 respectively.

## EXISTING TOWER CAPACITY ENVELOPE DIAGRAM

The existing suspension tower was designed for a longitudinal load of 17.8 kN with a 62.0 kN vertical load on each phase or their combinations. Analysis of a typical suspension tower shows that with no ice, the actual longitudinal capacity ( $R_n$ ) under static loading is approximately 30.0 kN per phase or their combinations. This capacity does not include any strength factor ( $\phi=1.0$ ). Figure 4 depicts an interaction diagram of vertical and longitudinal limit loads on the tower. The static capacity can be increased further under short duration dynamic load (Perez et al, 2008) and this issue will be discussed later.

## SCOPE OF THE PAPER

The objective of this paper is to estimate the length of a cascade failure zone due to a broken conductor scenario. The length is estimated based on a finite element

model of a typical 230 kV line section where both transient (peak dynamic) and steady state (quasi static residual) loads are evaluated. The numerical model considers the following cases: (1) first tower next to the break is intact and (2) first tower fails and the force redistribution in the remaining line system is assessed.

Next, a scenario with more than one tower failure is considered. Based on the location of the first surviving tower after a failure, the most probable extent of the failure zone is estimated and the mitigation to strengthen the tower to withstand the required containment load is proposed.

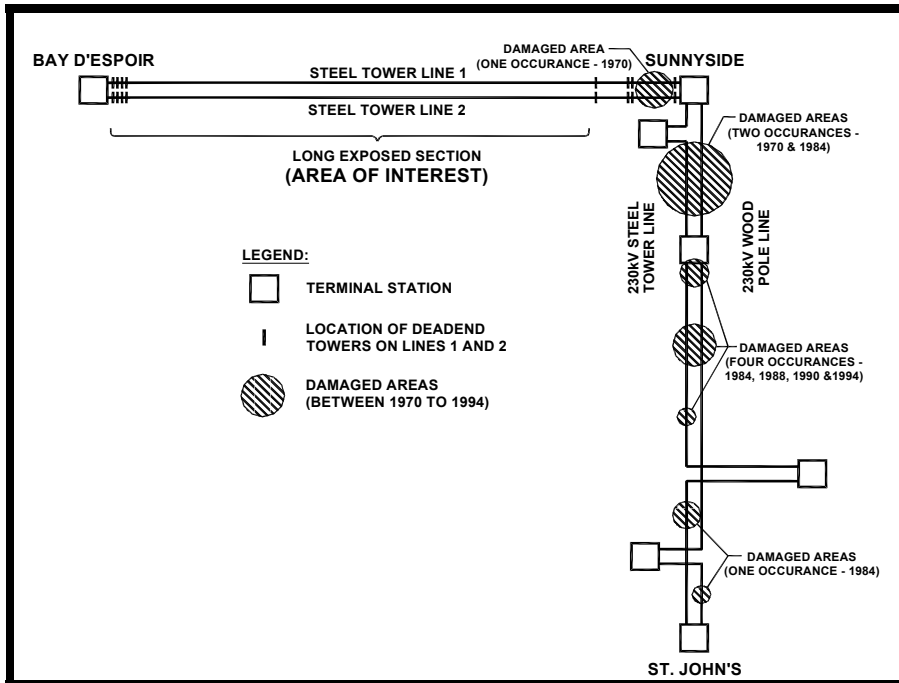


Figure 3 Location of the Dead End Towers on the Existing Two Lines

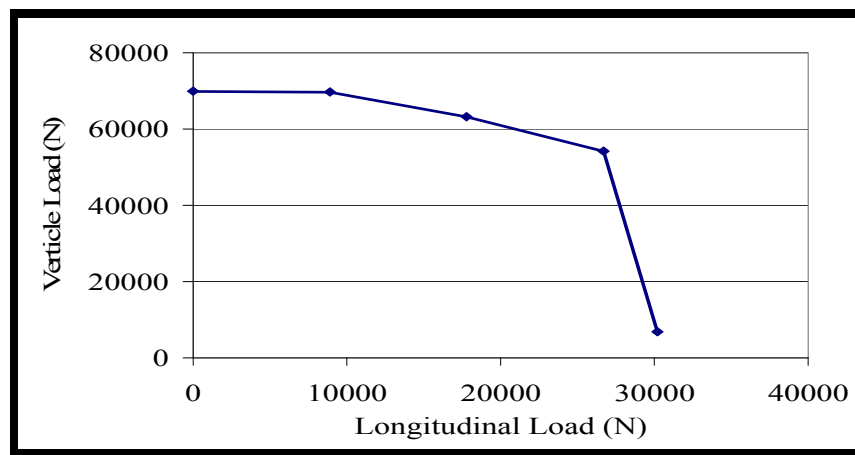


Figure 4 Static Tower Capacity Envelope Diagram under Vertical and Longitudinal Loads

## UNDERSTANDING CASCADE MECHANISM

A cascade phenomenon is defined when the failure zone includes many towers and is well extended beyond the location of the initial triggering event. For example, when a line is overloaded with primary loads (meteorological loads) the failure of the “weakest link” would most likely trigger an event. As the large amount of stored energy is released, substantial dynamic impact loads (transverse and vertical, as well as longitudinal) can be imposed on the remaining components in the system. Depending on the components’ residual (reserved) strengths to withstand these large dynamic impact loads, the failure zone could propagate well beyond the location of the initial failure. It has been reported during the 1998 Quebec storm that a 735 kV line lost as many as 80 self-supported steel latticed towers in three different sections of the line under longitudinal cascade situation (Figure 5).

After the break of a conductor, as the insulator swings, it imposes an unbalanced force on the system (loss of tension on the break side), which was not present before the break. This unbalanced force has two components: (1) a transient (dynamic) part with sharp rise and fall of the tension following a time history response and (2) the residual static part (steady state) where the motion is damped out after a few minutes and the system comes to a rest position. Peyrot et al (1980) has provided an explanation of the sharp rise and fall of the transient phenomenon up to the first two peaks in terms of the system energy before and after the break. Tucker (2007) has shown that one can encounter more than two peaks in a numerical model study.

Current design practices do not consider the load on the surviving tower after a tower or a number of towers have failed either under the dynamic and/or static residual loads. It only considers residual static load on the first tower near the failure assuming that the tower is intact.

## REVIEW OF LITERATURE

BPA (Bonneville Power Administration) uses a containment failure design philosophy where a tower series includes suspension towers designed with varying longitudinal capacities (light verses heavy suspension towers) and are placed strategically to contain the damage/failure under longitudinal load. The design philosophy assumes a limited number of tower failures in a typical line section and is based on the work of Kempner (1997) which showed that under cascade failure, the longitudinal load on the survival tower decreases as the number of adjacent failed tower increases. Figure 6a presents the experimental test setup where the first tower near the failure remains intact and the peak load is measured on each successive tower. Figure 6b presents the scenario where the first, second and the third tower fail in succession indicating that in each case, the peak load has exceeded the tower capacity and thus creates a cascade failure.

Kempner (1997) defined the impact factor as the ratio of the peak load measured on the first surviving tower (T2P, T3P etc.), next to the last failed tower, to

the peak load measured on the first tower adjacent to the broken conductor span, in Figure 6a (T1C). Kempner (1997) showed that this impact factor decreased as the number of failed towers increased. If the first surviving tower withstands the peak impact load after a limited number of tower failures, then the cascade will be prevented and the extent of the failure zone can be estimated assuming symmetry on both sides of the initial failure point. The variation of impact factor with number of failed towers will be shown later.



Figure 5 Loss of a 735 kV Line in Quebec (1998 Ice Storm)

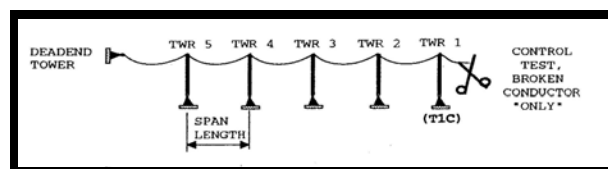


Figure 6a Experimental setup (Kempner, 1997)

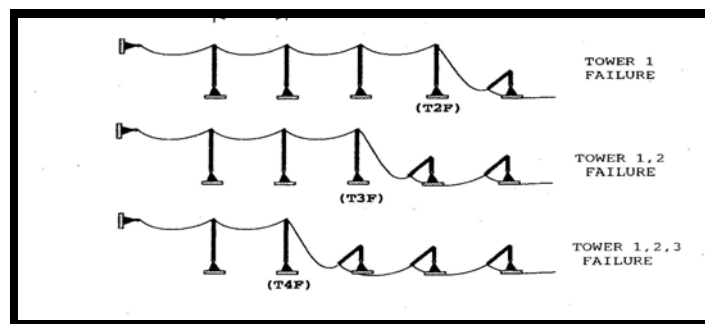


Figure 6b Experimental setup (Kempner, 1997)

McClure and her colleagues (2006) at McGill University have used ADINA extensively to predict the dynamic load on overhead lines due to conductor breakage as well as to study ice-shedding problems. The detailed methodology for modeling overhead lines using ADINA is given in CEATI report (McClure, 2006) and in Tucker (2007). The latter guide was used to develop and validate a numerical model with full scale test data to study the failure of a suspension insulator string and its effect on adjacent towers under dynamic loading condition (Tucker and Halder, 2007).

## METHODOLOGY- FINITE ELEMENT MODEL (FEM) IN ADINA

The general outline for transient response analysis in ADINA requires the development of a finite element (FE) model of the line followed by a static run to ensure that the initial position of the cable geometry under gravity load (self weight) is captured. A routine check on the sag and the tension provides the basis for assuming that the model is correct with respect to initial tension, axial rigidity (EA) and the boundary conditions. Since the ADINA software used for this study had a restriction of 900 nodes, it was important that the model be kept simple to provide insight into the problem for determining whether the development of a more complex model is warranted.

The following provides the highlights of the procedure that was used in the present study to develop an ADINA model.

- The conductor is modeled as truss elements with initial pretension.
- The conductor material can be modeled as elastic (final modulus) or non linear elastic (initial modulus).
- The tower masts and the bridge are modeled as linear elastic beam elements with appropriate stiffness while the guys are modelled as cable elements with axial rigidity and initial tension.
- The load is defined as mass proportional.
- The static model is run first; the result is saved and used as the restart condition for the transient dynamic analysis.
- The transient dynamic analysis is initialized at 1.0 second and the cable “death element” (element removed from the model to simulate a broken conductor) is activated at 1.002 second to simulate the conductor break.

Once the static analysis is completed, the transient response analysis is carried out by invoking the “death element” option in ADINA which allows the simulation of a conductor rupture at any location. If this option is used, the corresponding element group automatically becomes nonlinear. When the conductor element “dies”, the insulators at the break point, as well as insulators in the other spans, are free to swing

fully. A step by step time step integration ( $\Delta t = 0.002$  second) of the equations of motion of the discrete system provides the time history responses of various parameters such as displacement, conductor tension, force in the insulator string and on the tower, etc.

### VALIDATION OF IMPACT FACTORS - A TWO SPAN MODEL

In order to validate the results, a simple two span model (Figures 7 and 8) is used to understand the accuracy of the results with respect to number of elements considered and its impact on various line parameters such as sag, tension and frequency. Figure 9 compares the impact factor values for conductor tension obtained from the analysis with those determined from the full scale EPRI tests (Peyrot et al, 1980). Two impact factors defined by Peyrot et al (1980) are used here for comparison. These are Initial Impact Factor (IIF) and Final Impact Factor (FIF). The IIF is defined as the ratio of the peak dynamic load to the conductor tension prior to the break while the FIF is defined as the ratio of the peak load to the residual load. ADINA model runs with 2% damping compares well with the test results. Figure 10 presents a typical time history plot of conductor tension at the tower adjacent to the broken conductor span. The typical insulator swing was less than  $80^{\circ}$  degree under steady state condition while under transient condition, this was more than  $90^{\circ}$  degree.

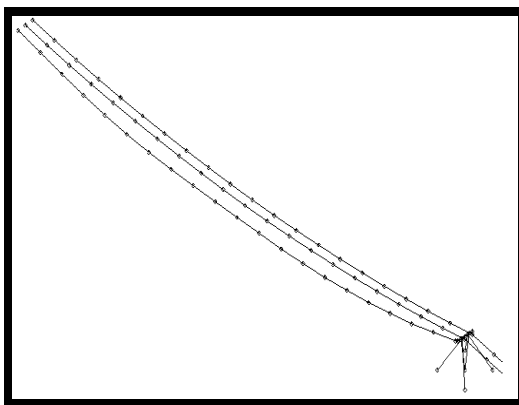


Figure 7 ADINA-Transmission Line Model

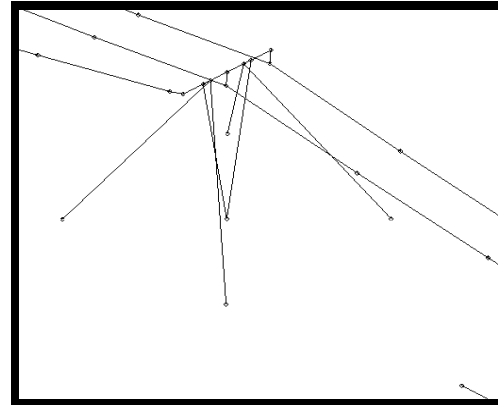


Figure 8 ADINA- Tower Model

### EXTENT OF FAILURE ZONE DUE TO CONDUCTOR BREAKAGE

This section presents the methodology to assess the extent of the failure zone due to conductor breakage. A section of the line is modeled with five equal level spans under every day conductor tension. The failure is considered either in any one single phase or their combinations. This provides five different failure scenarios: (1) outside left phase (2) middle phase (3) outside and middle phases (4) two outside phases and (5) all three phases. Analysis is first carried out assuming that the first tower near the break is intact (conventional model) and later, allowing the first tower to fail. Analysis also considers subsequent tower failures (Figure 6b).

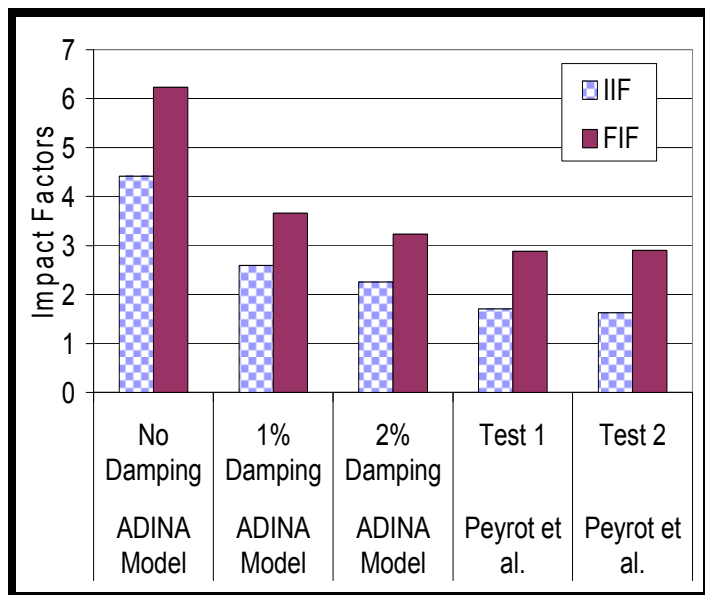


Figure 9 Comparison of Model and Full scale Conductor Tension Impact Factors

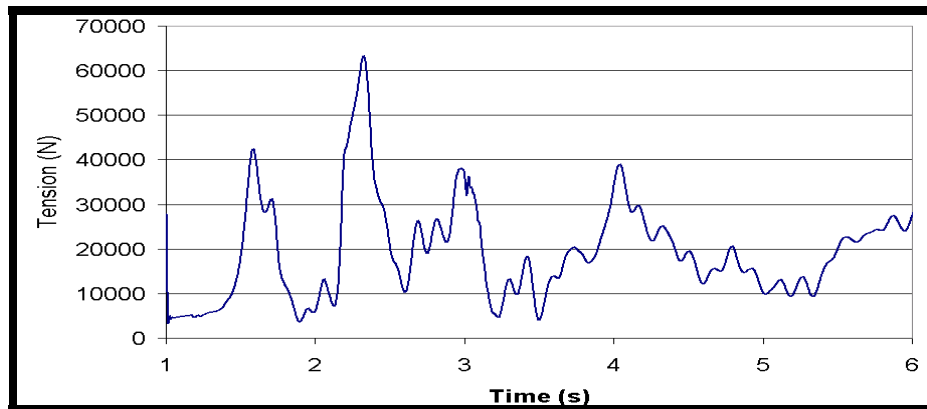


Figure 10 Time History Plot for Conductor Tension

### Line Section Model

As indicated in the previous section, a line section of the steel line (Figure 3) with five equal spans is modelled with cable elements for the conductor and the tower guys, beam elements for the two tower masts and the bridge and a number of truss elements for the insulator strings. Based on a sensitivity study, twenty cable elements were selected for each span.

### Intact System (Broken Conductor, No Tower Failure)

The model developed in the previous section is used to study the effects of the loss of a phase conductor or their combinations on the intact towers (Figure 6a). The ADINA model predicted that the longitudinal force on each tower decreases as the towers are located farther from the failure location. The ratio of the longitudinal force on each tower ( $F_i$ ) divided by the force on the first tower next to the failure location ( $F_1$ ) is shown in Figure 11. The longitudinal force on the towers decreases significantly from tower 1 to tower 2 and continues to decrease at smaller amounts in the remaining towers, conforming to a power trend. This trend was also noted by Kempner (1997) in a small scale model test and is valid in general for broken conductor case. If the tower closest to the failure location survives then it can be assumed that all remaining towers will also survive.

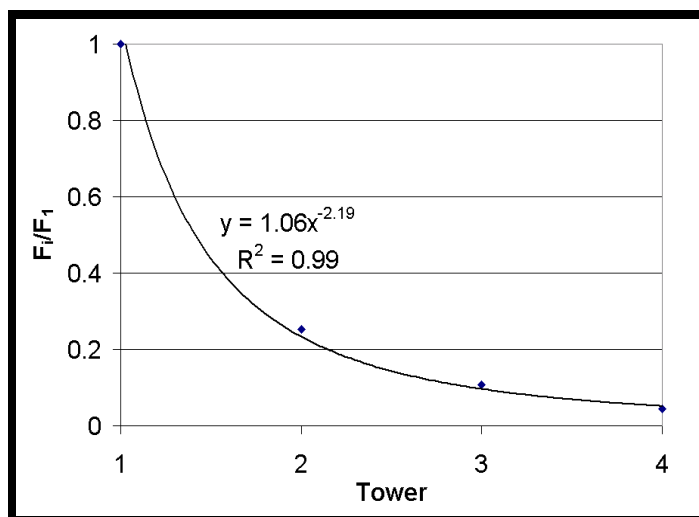


Figure 11 Impact Factors on the Intact Towers (Outside Phase Failure)

### Failed System with One or More Tower Failures

ADINA model runs were made for an initial static tower capacity of 27.6 kN ( $\phi=0.9$ , Figure 4) under everyday loading condition. This capacity does not consider any amplification factor under short duration dynamic load (Perez et al, 2008). Later this static capacity was increased to 35.6 kN and 44.5 kN to reduce the extent of the failure zone (lesser number of tower failures) and to assess the type of mitigation (structural modification) that may be required to withstand the large peak forces. The “tower failure” in ADINA is referred as the failure of the section of the bridge that would be affected by the peak force from a conductor failure. This implies that a single phase failure on one side of the bridge would only affect that side. Therefore, the peak load in excess of the tower capacity imposed on the first tower near the break will cause a tower failure and a significant amount of this longitudinal load will be transferred to the next tower.

To understand the cascade failure mechanism of transmission lines due to conductor failure, the numerical analysis is carried out following Tucker (2007). The model is run for all five load combinations, one at a time.

- 1) Conductor break with no tower failures is modeled first using the methodology described in the earlier section.
- 2) The longitudinal force time history on the first tower is obtained and the peak longitudinal force and the time at which the tower capacity is exceeded are noted.
- 3) The model is updated introducing “death elements” to the effected part of the tower at the noted time.
- 4) Conductor break with one tower failure is modeled and a dynamic analysis is carried out to predict the peak forces on all other surviving towers.

Steps 2 to 4 are repeated for the remaining towers in succession. For each model run, the maximum dynamic longitudinal force on the surviving tower next to the failure location is noted. Figure 12 presents the data for a middle phase failure where the load on the fourth tower is shown to be reduced significantly as we accept the first three tower failures. In this case, the failure zone could be estimated as the length of a line section involving six towers assuming symmetry.

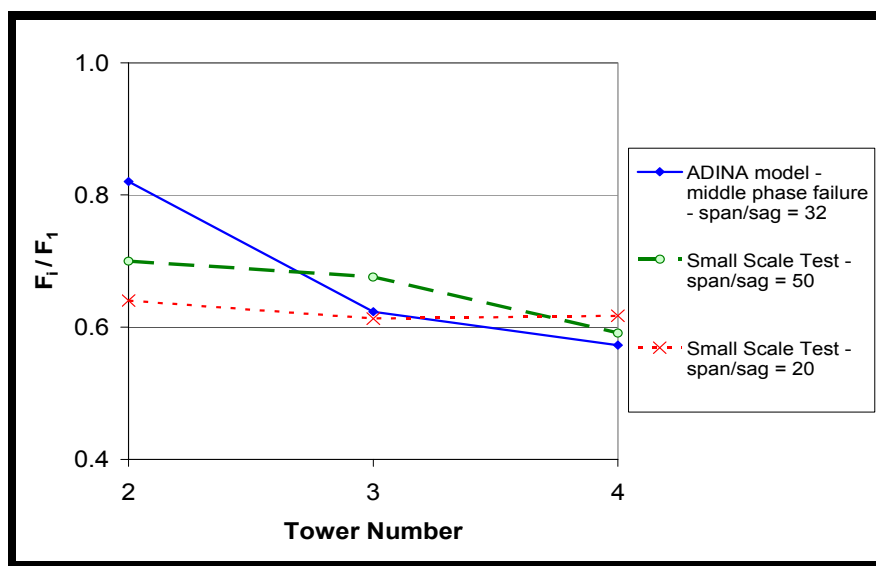


Figure 12 Impact Factors on the Closest Surviving Tower (Middle Phase Failure)

However, the force on the tower is still larger than its static capacity (27.6 kN) and therefore, an extrapolation is done to determine the acceptable number of tower failures to ensure that the imposed force on the surviving tower is less than the static capacity. In this case it is estimated that the failure of five towers on one side will contain the peak load. However the line model could be enlarged to include more spans to see the decrement of this peak force. The comparison plots with the results

presented by Kempner (1997) are also shown in Figures 12 and 13 for similar span to sag and span to insulator ratios. The comparison is reasonable.

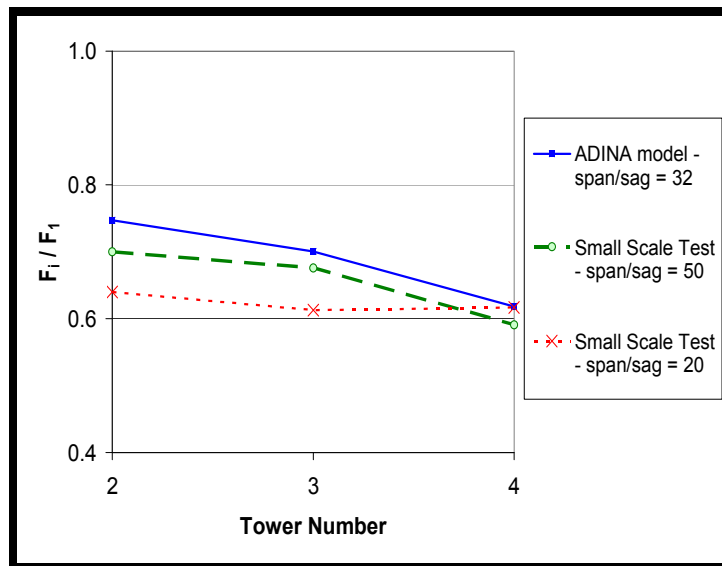


Figure 13 Impact Factors on the Closest Surviving Tower (Three phase failure)

Table 1 presents the acceptable number of tower failures that will be required in containing the peak load under various static capacity assumptions. The numbers are based on the assumption that equal number of towers will fail on both sides of the failure location. Increased static capacity only reduced the expected number of tower failures by 20%. Figure 14 presents the required modification of the selected bridge members under two loading scenarios.

Table 1 Number of Expected Tower Failures under a Cascade Event

Tower Static Capacity (N)	One Phase Failure – Side	One Phase Failure - Middle	Two Phase Failure – Side and Middle	Two Phase Failure – Two Sides	Three Phase Failure
26,700	10	10	10	10	10
35,600	8	10	8	8	8
44,500	2	8	6	6	6

Table 2 Number of Expected Tower Failures Considering Dynamic Capacity

Upgraded Tower Under Dynamic Capacity (N)	One Phase Failure – Side	One Phase Failure - Middle	Two Phase Failure – Side and Middle	Two Phase Failure – Two Sides	Three Phase Failure
53,400	0	2	2	2	2

A separate model run was also made by increasing the 44.5 kN static tower capacity to 53.4 kN by including a dynamic capacity factor of 1.2 (Perez et al, 2008). This was done to consider the effect of short duration peak load. Under this scenario, ADINA model runs show that the line section will lose only one tower on each side of the failure location (Table 2). It shows that the number of tower failures under cascade situation can be reduced by strengthening the tower for increased static capacity and taking into consideration the additional strength due to the effect of short duration force on the tower (Perez et al, 2008). More information on the tower capacity under short term dynamic loading is needed to model the event appropriately.

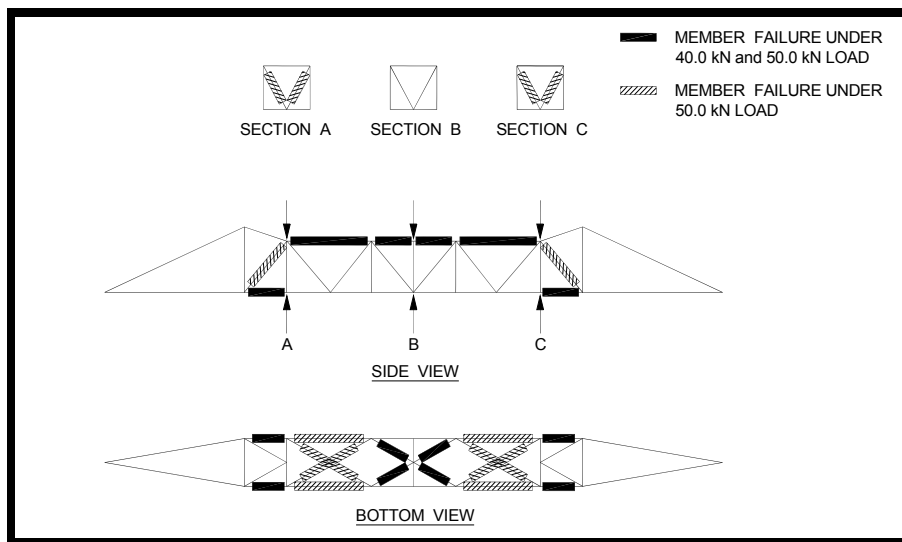


Figure 14 Upgrading of Bridge Members for Increased Capacities

## SUMMARY & CONCLUSIONS

A systematic approach to estimate the most probable cascade length of an existing steel transmission line is presented under broken conductor scenario. A finite element model of a typical line section is developed using ADINA. All possible five load cases are considered in the dynamic analysis. Considering the dynamic capacity of an upgraded tower, the expected tower loss would be as little as two towers while under original static capacity, this could be ten towers. The methodology is quite

robust and is equally applicable with some ice loading on the conductor where the initial tension and the ice weight of the cable would be larger. Reduction of the load on the tower can be achieved further if one chooses to use a load reduction device (Haldar and Tucker, 2008). This part of the work is still being studied.

## REFERENCES

- ADINA (Automatic Dynamic Incremental Nonlinear Analysis) (2003). ADINA R & D, USA
- Haldar, Asim (2006) Upgrading of a 230kV Transmission Line System Using Probabilistic Approach, 9<sup>th</sup> International Conference on Probabilistic Methods Applied to Electric Power System, Stockholm, Sweden, June, 9p
- Haldar, Asim and Tucker, Kyle (2008) Dynamic Finite Element Analysis of a Test Transmission Line Using ANCO Load Reduction Device, CEATI report T053700-3329, Montreal, Canada
- Kempner, Leon, (1997) Longitudinal Impact Loading on Electrical Transmission Line Towers: A Scale Model Study, PhD Thesis, System Science: Civil Engineering, Portland State University, Portland, Oregon, 201 pages.
- McClure, Ghyslaine (2006) ADINA modeling Guide and Benchmark Tests for Component Failure Analysis in Overhead Line Sections, Published Report. CEATI Project T043700-3319A, Montreal, Canada.
- Peyrot, A. H. Klugge, R.O. and Lee, J.W. (1980) Longitudinal Loads from Broken Conductors and Broken Insulators and Their Effects on Transmission Lines. IEEE Transactions Power Apparatus Systems, PAS 99, pp-222-234.
- Perez J, Mueller, W and Kempner, Leon (2008) Strength of Steel Angles Subjected to short Duration Loads, CEATI Report T063700-3336, Montreal, Canada.
- Tucker, Kyle (2007) Validation of Transmission Line Full-Scale and Small-Scale Test Results on Dynamic Loads with Numerical Modeling, M.Eng. Thesis, Memorial University of Newfoundland, St. John's. Newfoundland.
- Tucker, Kyle and Haldar, Asim (2007) Numerical Model Validation and Sensitivity study of a Transmission Line Insulator Failure Using Full Scale Test Data, IEEE Transactions on Power Delivery, October, Volume 22, No. 4, 6p.

## Common Sag and Tension Errors; It's Time for Template Technology to be Put in the Drawer Forever

Otto J. Lynch, P.E.<sup>1</sup>

<sup>1</sup>Vice President, Power Line Systems, Inc., 956 Marynell, Nixa, MO 65714  
PH (417) 724-8292; FAX (417) 724-8492; email: [otto@powline.com](mailto:otto@powline.com)

### ***Abstract***

The calculation of proper sags and tensions of conductors and other wires are the most vital aspect of transmission line design; structure heights and placements are determined by the sags, structure designs are determined by the tensions, and lines are constructed using both of these methods. Mostly gone are the days of plastic sag templates. Or are they? Many use computer software programs thinking that they are using *Technology for the Next Generation*, yet they merely duplicate the archaic plastic template technology and thus their designs have sags and tensions that can have significant error. Additionally, their lines are built using these same assumptions and thus sags can be lower than anticipated or tensions can be higher than anticipated.

This paper will discuss common errors made in the industry and suggest methods for more accurate sag and tension calculations for better structure and line designs as well as construction. It's time that we truly use *Technology for the Next Generation* and not continue to use these Electronic Sag Templates that merely duplicate what we've always done before.

### ***Introduction***

The concept of using an equivalent span for a series of spans has been around for a long time. The method now known as the "Ruling Span Method" was originally developed by E.S. Thayer (Thayer) in 1924.

#### ***What is a Ruling Span?***

Section 9.7.1 in the *Design Manual for High Voltage Transmission Lines* (RUS Bulletin 1724E-200) defines the Ruling Span as follows:

*A ruling span is an assumed uniform design span which approximately portrays the mechanical performance of a section of line between its deadend supports. The ruling span is used in the design and construction of a line to provide a uniform span length which is representative of the various lengths of spans between*

*deadends. This uniform span length allows sags and clearances to be readily calculated for structure spotting and conductor stringing.*

*Use of a ruling span in the design of a line assumes that flexing of the structure and/or insulator string deflection at the intermediate supporting structures will allow for the equalization of tension in the conductor between adjacent spans to the ruling span tension”.*

The Report of the IEEE “Bare Conductor Sag at High Temperature Task Force” entitled “Limitations of the Ruling Span Method for Overhead Line Conductors at High Operating Temperatures” (IEEE Limitations of the Ruling Span Method) states:

*... It (Ruling Span) is a fictitious span with a rate of slack equal to the average rate of slack of the line section.*

### ***How is a Ruling Span Calculated?***

The ruling span is traditionally calculated by the following equation:

$$RS = \sqrt{\frac{\sum S_i^3}{\sum S_i}}$$

Where:

RS = Ruling Span

$S_i$  = horizontal length of individual spans in a Ruling Span section

It is important to note that the ruling span is NOT an average of spans; it is weighted towards the longer spans.

### ***How is a Ruling Span Used***

Once the Ruling Span for a given section of line is calculated, a catenary curve can be developed for its uniform span that will predict the sags of every span within that Ruling Span section. Traditionally, this was made into a plastic template that an engineer could then use for determining the layout of a line design. Line design software has since been developed that can apply these same principles electronically.

### ***What is Ruling Span Error?***

As described above, the Ruling Span concept assumes that the conductor attachments are free to move in order for the tension to equalize. As most conductors are usually clipped to the insulators, this can only be true at the time (and thus for a given conductor temperature) of construction of the line when the longitudinal tensions are equal. Unless all spans in a Ruling Span section are level and equal, this

assumption has varying degrees of error. Spans are usually unequal in length and as the conductor temperature changes; shorter spans will expand and contract less than longer spans. Depending on the structure configurations, this can create various effects:

- In the somewhat hypothetical case of perfectly rigid intermediate structures with perfectly rigid insulator arrangements, a longitudinal load will develop that is equal to the change in tensions between the adjacent spans. In essence, each structure becomes deadend supports and each span becomes its own Ruling Span.
- On the opposing scenario where the structures could be put on rollers to freely slide back and forth to maintain equalized tension in the conductor, the spans would actually vary from the original span and the sags from the varying sag.
- Most structures fall somewhere between these two scenarios; structures and post insulators flex, drop brackets and suspension insulators swing longitudinally, span lengths change, and conductor tensions are unequal. This unequal tension across a structure in turn creates longitudinal loads on the structure, which could potentially cause structural and insulator failures in some situations.

As it is physically impossible to maintain equal tensions and equal span lengths simultaneously, it is clear to see that the Ruling Span assumption becomes “in error” as the conductor temperature changes. The true question becomes not if the Ruling Span is in error, but by how much is that error? The error becomes more pronounced the greater the change in temperature. A line that was constructed (tensions equalized) at 90° F will have a smaller error at a higher operating than if the line was constructed at 30° F. Also, as we tend to operate lines hotter today than ever before, this error is quickly becoming more significant.

The previously referenced IEEE Limitations of the Ruling Span Method addresses this premise in further depth. However, since the publishing of that report, many lines have been flown with LiDAR and this error is easily verified. Further, software programs such as PLS-CADD (PLS-CADD, 1992) that take into account actual longitudinal conductor attachments (structure deflections, insulator deflections, insulator swings, etc.) along with the change in span and conductor lengths, better known as Finite Element (FE) analysis allow for this error to be determined.

One concern that the author wishes to clarify at the conclusion of this section is that structures that have relatively little deflection and insulator movement are shorter structures with short post – or “pin-top” insulators – as often used on distribution lines. It could be argued that the Ruling Span concept is not applicable for such lines and each span should be considered individually and the tension

differentials at each structure properly accounted for in the structure and insulator design.

### ***Inclined Spans***

The calculation of a Ruling Span in inclined spans such as in mountainous construction and some river crossings may not be what it appears to be at first glance. To illustrate this, let's first cover some basic concepts of sag and tension.

The Southwire Overhead Conductor Manual (Southwire) provides that for a level single span of wire, the conductor length can be calculated by the following equation:

$$L = \left( \frac{2H}{w} \right) \sinh \left( \frac{Sw}{2H} \right)$$

Where:

L = total conductor length in a span

H = horizontal component of conductor tension

w = conductor weight per unit length

S = span length

Further, Southwire provides that for a level single span of wire, the sag can be calculated by the following equation:

$$D = \frac{H}{w} \left[ \cosh \left( \frac{wS}{2H} \right) - 1 \right]$$

Where:

D = sag of the conductor in a span

H = horizontal component of conductor tension

w = conductor weight per unit length

S = span length

Using the same example as Southwire, applying these calculations to an example level span of 1000 foot span of 795 kcmil – 26/7 ACSR “Drake” conductor ( $w = 1.094 \text{ lbs/ft}$ ) installed at a tension of 6300 lbs. yields a sag (D) of 21.72 feet and a total length of conductor (L) of 1001.26 feet. It is important to note here that a slack of only 1.26 feet in a 1000 foot long span yields this magnitude of sag of 21.72 feet.

Now, let's take that same example span and incline it 30 degrees by changing the elevation of one attachment by 577.35 feet. This creates a chord distance of 1154.70 feet. Southwire states:

*The midpoint sag, D, in an inclined span is approximately equal to the sag in a horizontal span whose length is equal to the inclined span length.*

In order to create the desired sag in the inclined span to match the level span, the amount of slack must be the same. The obvious answer to this conundrum is to

simply use a more effective ruling span that will accurately predict the expected sag and tension in the incline as expected on a level span. The immediate solution is usually counterintuitive; simply using a Ruling Span of the chord length does not yield the expected sag and tension. The Ruling Span must actually be *shorter* than the actual span so that the expected behavior of the actual span will match. It is important that the slack be calculated properly as the sensitivity of this slack is critical when calculating the sags, particularly when considering temperature and loading effects.

The slack of an inclined span is simply equal to the slack of a level span having the same horizontal projection multiplied by the cosine of the slope of the span chord. Thus, the effective span to use, i.e. the Ruling Span, of an inclined span is simply the horizontal span length multiplied by the cosine of the slope of the span chord. This will result in a theoretical inclined span length the same as the horizontal span length. In our example above, even though the span is 1000', the Ruling Span would be 866.03 feet.

For a series of spans, the traditional Ruling Span can be slightly modified to account for the individual inclined spans and an Improved Ruling Span can be developed as follows:

$$RS = \sqrt{\frac{\sum S_i^4}{\sum C_i}}$$

Where:

RS = Ruling Span

$S_i$  = horizontal length of individual spans in a Ruling Span section

$C_i$  = chord length of individual spans in a Ruling Span section

To prove this concept, we will further explore the example span above using a traditional Ruling Span, an Improved Ruling Span, and exact Finite Element Model (FEM) analyses for a series of inclines, considering temperature and loading effects, and compare those results. The 1000 foot span with four inclines were considered; 0°, 15°, 30°, and 45°. The traditional Ruling Span is of course 1000 foot, and the Improved Ruling Spans are 1000, 966, 866, and 707 feet respectively. The spans are subjected to high (212° F) and low (-20° F) temperatures as well as a loaded (1 inch ice at 30° F) condition. The sags, horizontal tensions, and maximum tensions are summarized in Tables 1 through 3. Numbers in parentheses, when indicated, are percent errors relative to the FEM values.

**Table 1. Sag at Incline**

	Sag at Incline / Error (ft) / %			
	0°	15°	30°	45°
HOT 212 Traditional Ruling Span	31.15 / 0%	32.25 / -1%	35.95 / -6%	43.99 / -14%
HOT 212 Improved Ruling Span	31.15 / 0%	32.78 / 0%	38.56 / 1%	52.74 / 4%
HOT 212 Finite Element Model	31.15 / -	32.72 / -	38.2 / -	50.94 / -
COLD -20 Traditional Ruling Span	16.25 / 0%	16.83 / 1%	18.76 / 4%	22.97 / 7%
COLD -20 Improved Ruling Span	16.25 / 0%	16.57 / 0%	17.61 / -2%	19.79 / -8%
COLD -20 Finite Element Model	16.25 / -	16.65 / -	18.04 / -	21.48 / -
ICE Traditional Ruling Span	29.12 / 0%	30.14 / -2%	33.59 / -7%	41.09 / -17%
ICE Improved Ruling Span	29.12 / 0%	30.45 / -1%	35.11 / -3%	45.84 / -8%
ICE Finite Element Model	29.12 / -	30.67 / -	36.22 / -	49.69 / -

**Table 2. Horizontal Tension at Incline**

	Horizontal Tension at Incline / Error (lbs) / %			
	0°	15°	30°	45°
HOT 212 Traditional Ruling Span	4384 / 0%	4384 / 1%	4384 / 6%	4384 / 16%
HOT 212 Improved Ruling Span	4384 / 0%	4314 / 0%	4088 / -1%	3657 / -3%
HOT 212 Finite Element Model	4384 / -	4321 / -	4126 / -	3787 / -
COLD -20 Traditional Ruling Span	8411 / 0%	8411 / -1%	8411 / -4%	8411 / -6%
COLD -20 Improved Ruling Span	8411 / 0%	8539 / 0%	8959 / 2%	9761 / 9%
COLD -20 Finite Element Model	8411 / -	8502 / -	8748 / -	8993 / -
ICE Traditional Ruling Span	15934 / 0%	15934 / 2%	15934 / 8%	15934 / 21%
ICE Improved Ruling Span	15934 / 0%	15769 / 1%	15248 / 3%	14289 / 8%
ICE Finite Element Model	15934 / -	15658 / -	14783 / -	13184 / -

**Table 3. Maximum Tension at Incline**

	Maximum Tension at Incline / Error (lbs) / %			
	0°	15°	30°	45°
HOT 212 Traditional Ruling Span	4418 / 0%	4719 / 1%	5413 / 6%	6786 / 14%
HOT 212 Improved Ruling Span	4418 / 0%	4647 / 0%	5074 / -1%	5766 / -3%
HOT 212 Finite Element Model	4418 / -	4655 / -	5117 / -	5947 / -
COLD -20 Traditional Ruling Span	8429 / 0%	8872 / -1%	10047 / -4%	12463 / -6%
COLD -20 Improved Ruling Span	8429 / 0%	9004 / 0%	10678 / 2%	14369 / 8%
COLD -20 Finite Element Model	8429 / -	8966 / -	10435 / -	13284 / -
ICE Traditional Ruling Span	16042 / 0%	17102 / 2%	19583 / 7%	24513 / 19%
ICE Improved Ruling Span	16042 / 0%	16932 / 1%	18796 / 3%	22202 / 8%
ICE Finite Element Model	16042 / -	16818 / -	18263 / -	20652 / -

It can be seen that the Improved Ruling Span method gives much better results relative to the more exact FE results than the traditional Ruling Span. While most lines do not have the extreme inclines used to illustrate this theory, there are still differences at the lower inclines and in rare cases of extreme inclines, these differences can become quite significant. It is obvious that Finite Element modeling yields the absolute correct results to design or analyze an overhead line, but should the Ruling Span concept be the method of choice, then the Improved Ruling Span method should be used.

### ***Weight Span Errors***

Another common mistake made in the days of plastic sag templates was in the calculation of the weight span on each structure. Sag templates were traditionally made with the maximum sag condition under temperature and/or ice loading for the proper spotting of structures to maintain proper clearance to the ground. If a shield wire was used, there was most likely a minimum sag condition for that wire used for checking against uplift on a structure and/or hardware binding.

While there are many other inherent problems with using the simplified Wind and Weight span concept for structure analysis, those are beyond the scope of this paper. Without going into depth on the theory of Wind and Weight Span methods and in keeping with the theme of this paper, a brief discussion of this process for understanding its impact will follow. Traditionally, hatch marks were made on the drawings at the low point, or the “belly”, of the maximum sags drawn with the sag template. The distance between these two low points was then measured and multiplied by the unit weight of the wire with ice and/or wind and any load factors to obtain the maximum vertical load on each structure. A variant of this was to reverse calculate the maximum vertical load a structure could support and then divide that by the unit weight of the wire with ice and/or wind and any load factors to obtain the maximum “Weight Span” the structure can support.

The problem with this concept is that the maximum weight span does not occur under the maximum design temperature condition. In reality, other conditions such as cold temperatures, ice, and wind can create a higher vertical load on the structure. See Figure 1. It is nearly impossible to simulate with a plastic template or computerized methods that merely duplicate plastic template technology the effects that wind has on inclined spans as described in detail in “Re-Engineering The Transmission Line Design Process”; this effect alone can increase the weight spans by 50% or more in average terrains.

Figure 1 represents a section of an actual line where the Weight Span under what was assumed to be the maximum sag condition of Maximum Operating condition is 990 feet. The structure was designed for a maximum of 1000 foot Weight Span. Under the “Cold” condition, the weight span increases to 1230 feet and even more critical, it increases to 1357 feet under the Extreme Wind condition. This

ice span is actually slight shorter in this instance, but the vertical load is actually greater due to the weight of the ice in addition to the weight of the conductor.

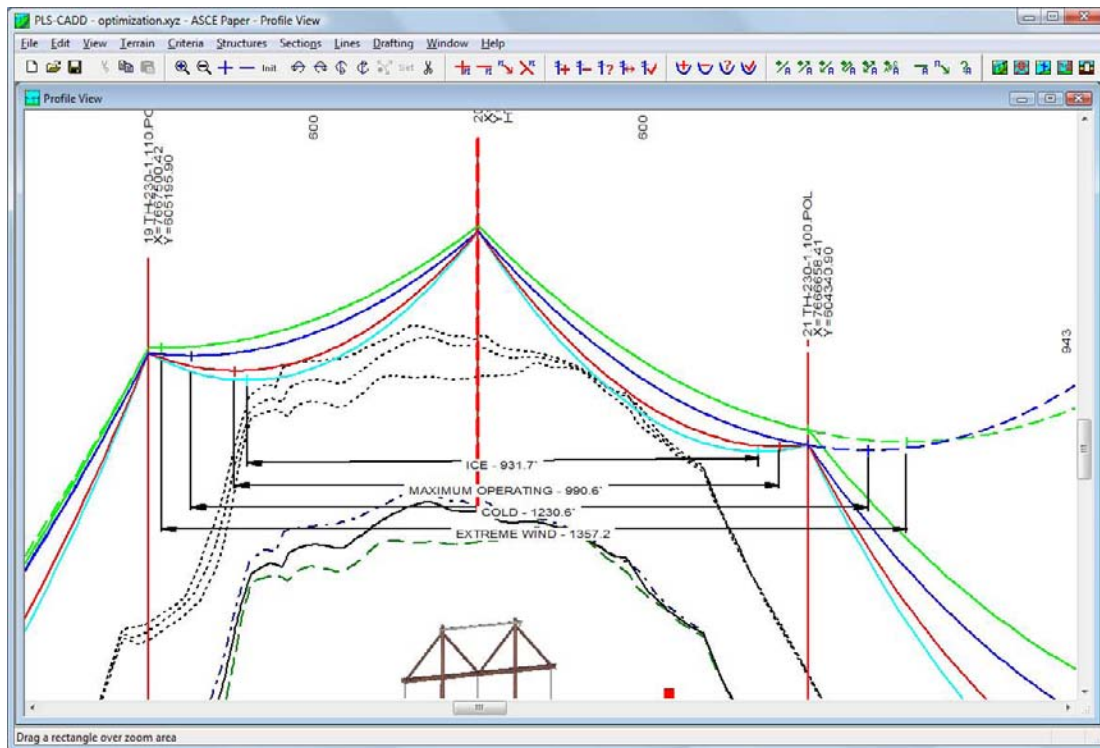


**Figure 1. Traditional Weight Span Error.**

Unfortunately, some overhead line design and drafting programs available today still use this traditional method of measuring weight spans and these errors are never realized. While it is possible to design a more inexpensive line by ignoring these other conditions and only using the “plastic template” methodology of Weight Spans, the design will actually be in error. It is important to know if this is the case and understand the potentially significant errors that can result in vertical structure loading if this archaic method is being utilized.

### ***Designing with the Wrong Ruling Span***

Designing an overhead line with traditional sag templates is a perfect “chicken and egg” enigma: a Ruling Span must be selected to develop a template to spot structures and sag wire, but the Ruling Span can’t actually be calculated until the structures are spotted. The traditional approach would be to assume a Ruling Span, use it for the design, and then calculate the actual Ruling Span when complete. It would be extremely coincidental should the assumed Ruling Span end up being the actual Ruling Span of each of the Ruling Span sections on a line. In theory, this would be an iterative process as the line would need to be redesigned with the actual Ruling Span calculated after the initial spotting, which would end up with a different

spotting and another different ruling span, and this would occur differently for each Ruling Span section of a line.

In the days before templates could easily be made with software and a local print shop, many engineers would simply say “close enough” within some certain range of the actual Ruling Span and the one used for spotting. Some utilities have even gone so far as to require only certain increments (i.e. 300, 600, 900, 1200, etc.) for the Ruling Span and in one case that the author is aware of, a utility designs every line in their system with a single Ruling Span. But just exactly what is “close enough”?

The RUS Bulletin 1724E-200 addresses this in Section 9.7.4 and Table 9-4:

*“9.7.4 Effects of the “Wrong” Ruling Span: It is important that the actual ruling span be reasonably close to the ruling span value that is used to spot the line. If this is not the case, there may be significant differences between the predicted conductor tensions and clearances and the actual values. There have been instances where sags were greater than predicted, resulting in clearance problems, because the wrong ruling span was assumed. Table 9-4 will be of use in determining how conductor sags differ from the predicted value when there are differences between actual and assumed ruling span. Note that tension variation is opposite of that of the sags. Thus, increased sags mean decreased tension and vice versa.”*

Our Drake conductor example above will be used to illustrate these exact effects on various spans and their magnitude. As a basis of comparison for various Ruling Spans and spans, the same horizontal tension of 6300 lbs at 60° F at the Design Ruling Span as used above will remain the constant across the analysis and all spans are assumed to be level.

At the “stringing” condition of 60° F, there is no change in the sag regardless of what Design Ruling Span was assumed (see Table 4). In essence, any errors in the Design Ruling Span versus the Actual Ruling Span will not be apparent during the construction phase.

**Table 4. Design Condition**

		Sag (ft)											Tension (lbs)	
		Actual Ruling Span												
		500	600	700	800	900	1000	1100	1200	1300	1400	1500		
Design Ruling Span	500	5.43	7.81	10.63	13.89	17.58	21.71	26.27	31.27	36.71	42.58	48.89	6300	
	600	5.43	7.82	10.64	13.9	17.6	21.73	26.3	31.3	36.74	42.62	48.93	6300	
	700	5.42	7.81	10.63	13.89	17.58	21.71	26.27	31.26	36.7	42.57	48.88	6300	
	800	5.43	7.82	10.64	13.9	17.6	21.73	26.29	31.3	36.73	42.61	48.92	6300	
	900	5.43	7.82	10.64	13.9	17.59	21.72	26.28	31.28	36.72	42.59	48.91	6300	
	1000	5.43	7.82	10.64	13.9	17.59	21.72	26.28	31.28	36.72	42.59	48.91	6300	
	1100	5.43	7.82	10.64	13.9	17.59	21.72	26.28	31.29	36.72	42.6	48.91	6300	
	1200	5.43	7.81	10.64	13.89	17.59	21.71	26.28	31.28	36.71	42.59	48.9	6300	
	1300	5.43	7.81	10.64	13.9	17.59	21.72	26.28	31.28	36.72	42.59	48.9	6300	
	1400	5.43	7.82	10.64	13.9	17.59	21.72	26.28	31.29	36.72	42.6	48.91	6300	
	1500	5.43	7.81	10.64	13.9	17.59	21.72	26.28	31.28	36.72	42.59	48.9	6300	

The problem occurs when the line is heated up. From our discussion on “slack” in the Inclined Spans section above, the calculation of the final sags under the maximum operating temperature is a function of the slack. If the slack is calculated using the wrong Ruling Span, then the wrong final sag will be estimated. To illustrate this concept, the sag of the conductor at 212° F has been calculated for a 1000' span (i.e. the Actual Ruling Span) using various Design Ruling Spans (see Table 5).

**Table 5. Maximum Operating Condition**

		Sag (ft)											Tension (lbs)	
		Actual Ruling Span												
		500	600	700	800	900	1000	1100	1200	1300	1400	1500		
Design Ruling Span	500	10.78	15.53	21.15	27.63	34.99	43.21	52.32	62.3	73.16	84.9	97.53	3172	
	600	9.73	14.01	19.08	24.93	31.56	38.98	47.18	56.18	65.97	76.55	87.92	3515	
	700	8.94	12.87	17.52	22.9	28.99	35.8	43.33	51.59	60.57	70.28	80.71	3827	
	800	8.35	12.03	16.37	21.39	27.08	33.44	40.47	48.18	56.57	65.64	75.38	4096	
	900	7.9	11.38	15.5	20.25	25.63	31.65	38.31	45.6	53.54	62.11	71.33	4327	
	1000	7.55	10.87	14.8	19.34	24.48	30.23	36.59	43.55	51.13	59.32	68.12	4529	
	1100	7.27	10.47	14.25	18.61	23.56	29.1	35.21	41.92	49.21	57.09	65.56	4705	
	1200	7.04	10.13	13.79	18.02	22.81	28.17	34.09	40.58	47.63	55.26	63.46	4860	
	1300	6.85	9.86	13.42	17.54	22.2	27.41	33.17	39.49	46.35	53.77	61.75	4994	
	1400	6.69	9.63	13.11	17.13	21.68	26.77	32.4	38.57	45.27	52.52	60.31	5113	
	1500	6.55	9.44	12.85	16.78	21.24	26.23	31.75	37.79	44.36	51.46	59.09	5218	

Examining this table for our 1000 foot example level span, if a Design Ruling Span of 1000 foot is used on the 1000 foot Actual Ruling Span, the sag would be 30.23 feet. However, if an 1100 foot Design Ruling Span was used, the sag would be 29.1 feet. Translating this in the design practices, if an 1100 foot Design Ruling Span was used to spot the structures and sag the wire and the Actual Ruling Span ended up being 1000 feet and the line designer said “close enough”, the structures spotted would be 1.13 feet lower than the designer intended. While this probably won’t create clearance issues in every span due to line grading, the only way to verify this is to “redraw” the entire line as spotted with the Actual Ruling Span and make changes where this is necessary.

Figure 2 shows a relationship of Ruling Span difference expressed as a percentage of the design span versus the actual span sag error at 212 degrees, expressed as a percentage.

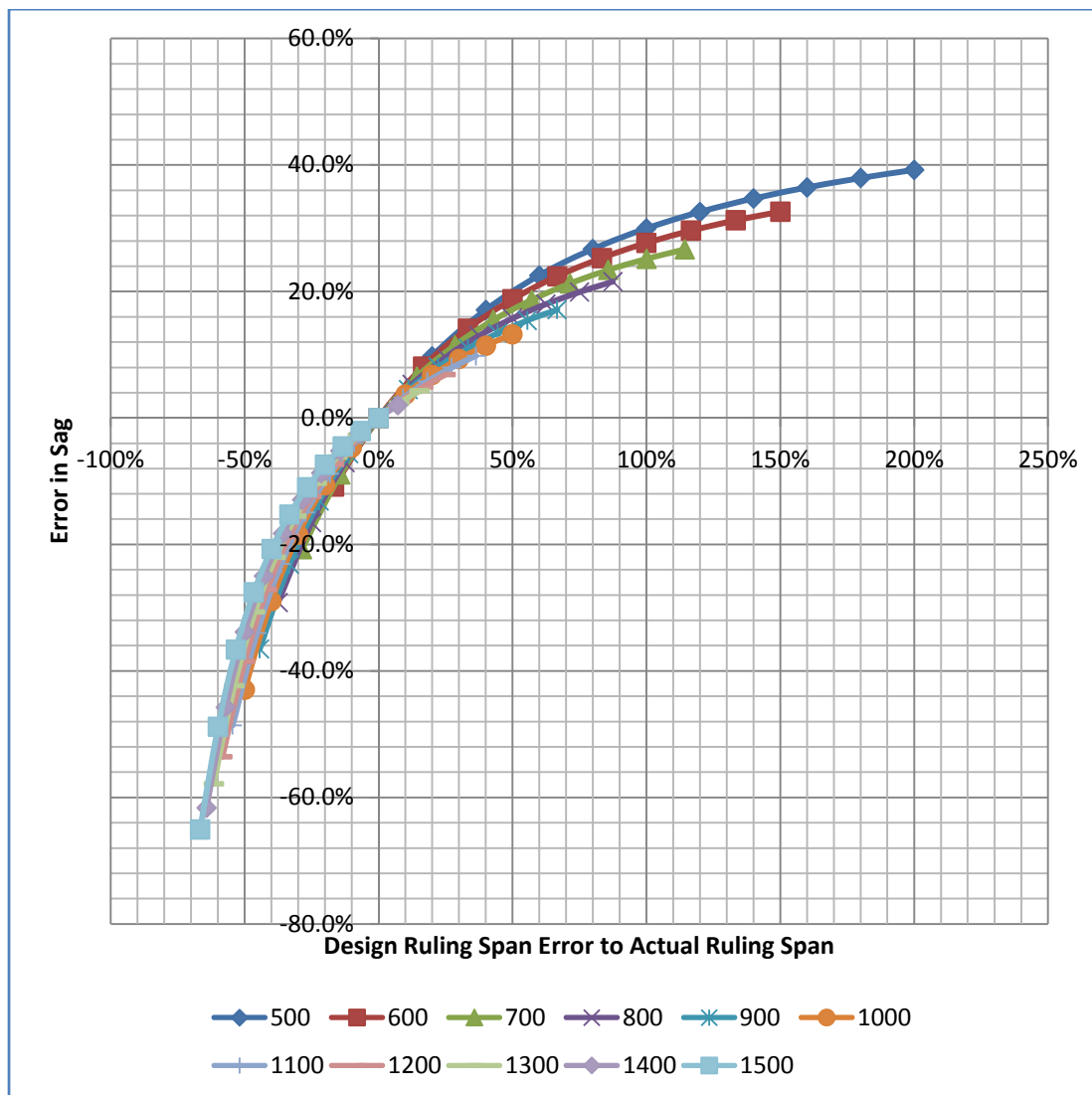
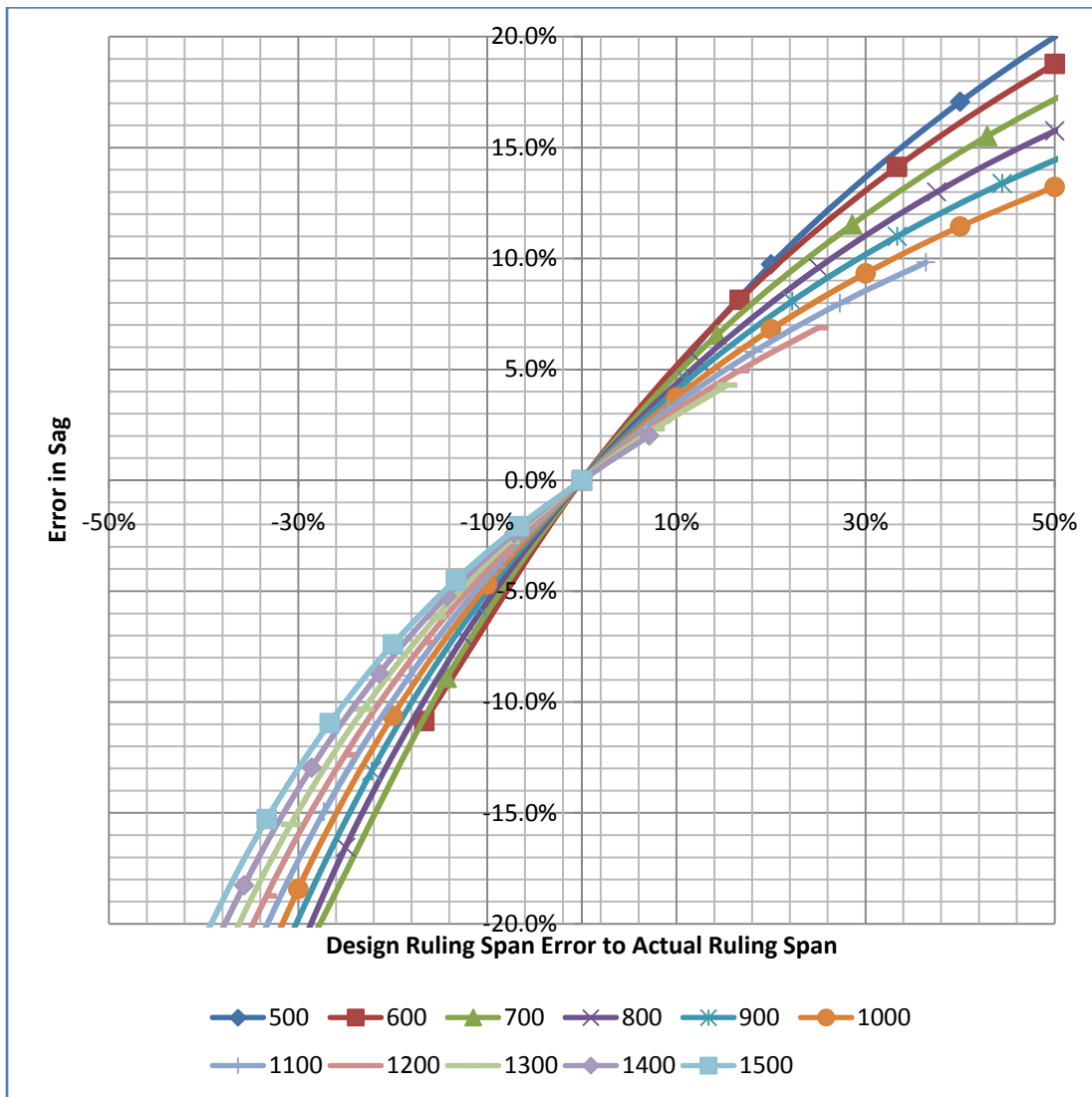


Figure 2. Ruling Span Error Relationship.

For clarification purposes, Figure 3 presents this same data bounded by a more realistic range of  $\pm 50\%$  Assume Ruling Span error.



**Figure 3. Ruling Span Error Relationship.**

The conclusions that can be drawn from our particular example above is that a  $+10\%$  error in the selection of the Design Ruling Span can yield an Actual Ruling Span error of approximately 2-5%, and a  $-10\%$  error in the selection of the Design Ruling Span can yield an Actual Ruling Span error of approximately 3-7%.

To apply this in practice, it is common practice in the industry to apply a 2 foot buffer to ground clearances to account for survey error, construction errors, design errors, etc. For our targeted 1000 foot Actual Ruling Span, this equates to a range of negative 13% to 20% (See Figure 4), which calculates to 870 feet to 1200 feet. As long as the Design Ruling Span is within 870 feet to 1200 feet, this 2 foot buffer will be maintained; however, that uses the entire buffer for the design error

alone. The IEEE Guide to the Installation of Overhead Transmission Line Conductors (IEEE 524) specifies that sagging should be within 6 inches of design sag in any one span. This translates into a much more constrained range to just under 4% allowance for error in our 1000 foot Actual Ruling Span, or 960 feet to 1040 feet Design Ruling Span.

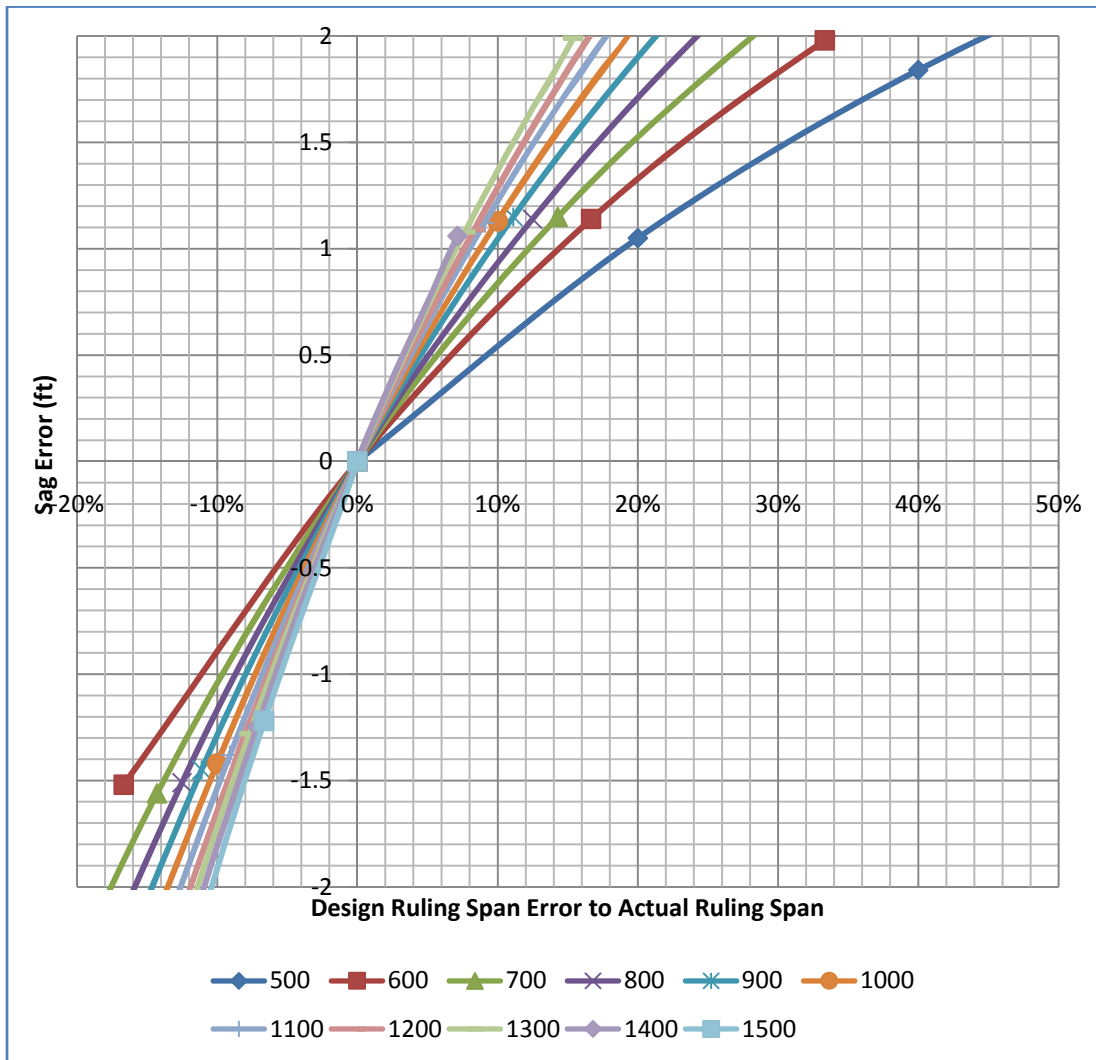


**Figure 3. Dimensional Ruling Span Error Relationship.**

Shorter spans have a greater percentage of error allowed to maintain the same absolute clearance, but the spans are shorter, and conversely, longer spans have a lesser percentage of error allowed to maintain the same absolute clearance. Calculating out the exact error for the range of spans considered in this paper yields around 40 ft,  $\pm 10$  ft for the allowable Design Ruling Span error to maintain the wire within 6 inches of the desired sag at  $212^{\circ}$  F for our example project. It would be the conclusion of this author that the practical Design Ruling Span used on a line with the

above parameters should be within 40 feet of the Actual Ruling Span. However, it would simplest, and most accurate, to just use the Actual Ruling Span on the line. Even better, Finite Element analysis should simply be used as it is the most accurate method available today.

### ***Construction with the Wrong Ruling Span***

Even further compounding this problem is even if the most prudent line design possible has been done, the line is constructed with traditional Stringing Charts where the Ruling Span has been rounded can lead to these same errors.

If the conductor is strung at the same temperature as the reference temperature, the use of the wrong ruling span is insignificant. However, if the temperature varies from this basis temperature, errors will be introduced. If a stringing chart from a shorter ruling span than the actual ruling span is used and the ambient temperature is lower than the reference 60° F, the resulting sag will be less than expected, and if the ambient temperature is higher than 60° F, the resulting sag will be higher. If a stringing chart from a longer ruling span than the actual ruling span is used and the ambient temperature is lower than the reference 60° F, the resulting sag will be higher than expected, and if the ambient temperature is higher than 60° F, the resulting sag will be lower.

In the example above, the basis for the comparison is to assume that the tension at 60° F is 6300 lbs across all Design Ruling Spans. In an Actual Ruling Span section of 1000 feet, if the stringing chart for a 900 foot Ruling Span is used, the sag at 212° F (Initial) will be 31.65 feet versus the 30.23 feet expected by the design. For this reason, it is critical that the stringing charts be used for the Actual Ruling Span.

Further, this is not just a transmission problem; distribution lines can be just as susceptible if not more sensitive to these errors. One cannot “force” a span or a series of spans to behave different than physics dictates.

### ***Conclusion***

By not considering the actual line layout in the calculation of the Ruling Span, the wrong Ruling Span can be selected and the results can be error, particularly in the cases of extreme temperature and loading events. Further, simply using a computer program to calculate the behavior on a level span and then applying those results to an entire line design can lead to an incorrect design and/or analysis. While the Ruling Span certainly served its purpose for approximately designing overhead lines with little temperature changes anticipated and with technology available at that time, modern overhead line designs with the maximum operating temperatures that they are expected to operate at in the 21<sup>st</sup> century should simply use modern *Technology for the Next Generation*. With the tools readily available to the overhead line engineers

in today's world, there is no practical reason why archaic "plastic template technology" should continue to be used at all. We don't send men to space any more with slide rules, so why should we design our ever increasingly important electric infrastructure with the same archaic technology used nearly a century ago.

In addition, there is a need to modernize outdated construction standards. Modern stringing charts should be developed for each project using the actual line design data. Using "standardized" stringing charts based on decades old calculations and rounding off the Actual Ruling Spans to apply them is simply not the accuracy level that is expected in today's world.

It should further be pointed out that just because one may be using a line drafting or design software program to design the entire line thinking that it is extremely accurate, if it the wrong Ruling Span is being manually selected or internally calculated using the traditional Ruling Span method, those same hand method errors are just being done all over again and are merely duplicating the same archaic plastic template technology.

Remember, friends don't let friends use plastic template technology.

### References

- E.S. Thayer, "Computing Tensions in Transmission Lines", "Electrical World", no. 2, pp. 72-73, 1924.
- Report of the IEEE Task Force "Bare Conductor Sag at High Temperature", *Limitations of the ruling span method for overhead line conductors at high operating temperatures*, April 2002, IEEE Transactions on Power Delivery, Volume 14, Issue 2. Motlis, Y. Barrett, J.S. Davidson, G.A. Douglass, D.A. Hall, P.A. Reding, J.L. Seppa, T.O. Thrash, F.R., Jr. White, H.B.
- Otto J. Lynch and Peter Hilger, *Re-Engineering The Transmission Line Design Process*, Autumn 1996, Power Technology International magazine.
- ANSI Committee C2, (2007), *National Electric Safety Code (NESC), 2007 Edition*, Institute of Electronics and Electronics Engineers, Inc. New York, New York.
- PLS-CADD, (1992), *Power Line Systems – Computer Aided Design and Drafting*, Power Line Systems, Inc., Madison, Wisconsin
- Southwire Company, "Overhead Conductor Manual" 2<sup>nd</sup> Edition, 2007, Carrollton, Georgia.
- U.S. Department of Agriculture, Rural Utilities Service, (2004), *Design Manual for High Voltage Transmission Lines, RUS Bulletin 1724E-200*, U.S. Government Printing Office, Washington, D.C.
- IEEE 524-2003, (2003), *Guide to the Installation of Overhead Transmission Line Conductors*, Institute of Electrical and Electronics Engineers, Inc., New York, NY.

## Laboratory and Field Testing of Steel Davit Arm Fatigue Failures on Concrete Poles

Bruce Freimark<sup>1</sup>  
P.E., F.ASCE

Meihuan (Nancy) Zhu<sup>2</sup>  
Ph.D, P.E.,

Robert Whapham<sup>3</sup>  
P.E., SM.IEEE

<sup>1</sup> Principal Engineer, American Electric Power (AEP), 700 Morrison Road, Gahanna, OH 43230, Phone: (614) 552-1944, email: bfreimark@aep.com

<sup>2</sup> Senior Engineer, American Electric Power (AEP), 700 Morrison Road, Gahanna, OH 43230, Phone: (614) 552-1821, email: mzhu@aep.com

<sup>3</sup> Global Market Manager - Transmission, Preformed Line Products (PLP), 660 Beta Drive, Mayfield Village, Ohio 44143, Phone: (440) 473-9202, email: bwhapham@preformed.com

### ABSTRACT

Over the past number of years AEP and other utilities have been experiencing fatigue failures of steel davit arms in our Texas region, especially when used in conjunction with concrete poles. It was assumed that these failures were the result of conductor motion, either as a result of high wind gusts (wind sway) or smooth moderate winds (aeolian vibration).

This paper describes the results of a field vibration study that was conducted on one line which experienced davit arm failures to establish the level of aeolian vibration versus wind velocity and vibration frequency. Also described are the results of extensive laboratory testing that were conducted on a vibration span to determine the relationship between conductor motion, the davit arm motion, and the fatigue stress on the arms. Further laboratory tests were also conducted to determine if dampers used to control aeolian vibration on the conductors would have a mitigating effect on the davit arm failures.

Further long-term field measurements are planned on a line where davit arm failures have occurred to collect data on a full scale span and to verify the preliminary findings of the laboratory testing.

### FIELD VIBRATION STUDY

A two week field vibration study was conducted on a 138KV line in Corpus Christi, Texas in the span adjacent to structures where davit arms have failed (Figure 1).

The line is built with a vertical bundle (12" spacing) of 795 kcmil 26/7 ACSR (Drake) conductor on concrete poles. The ruling span length is approximately 880 feet and the surrounding terrain is very flat farmland (Figure 2).



Figure 1 – Cracked Davit Arm



Figure 2 – Surrounding Terrain

The results of the field vibration study showed that moderately severe vibration activity occurred with the dampers removed at frequencies in the 18 hertz to 24 hertz frequency range, and dropped off at lower and higher frequencies (Figure 3). The 18 hertz to 24 hertz frequency range correlates to a wind velocity range from 6 MPH to 8 MPH for the Drake conductor (based on the Strouhal number), which is consistent with historical data which shows that on most lines vibration activity is the highest for wind velocities in the 6 MPH to 10 MPH range.

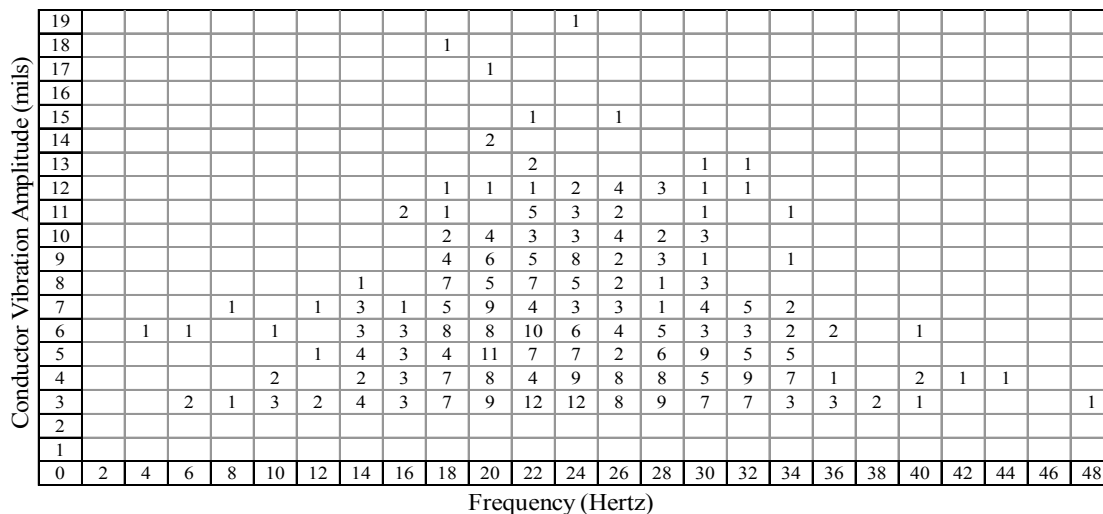


Figure 3 – Field Vibration Records (Amplitude vs. Frequency)

## LABORATORY TESTING – GENERAL SETUP

The initial scope of the laboratory testing consisted of three separate tests: fundamental frequencies (vertical and horizontal) of the davit arms, with and without vertical conductor loading, forced response of the davit arms (vibration shaker attached directly to end of arm), and testing in a 90 foot vibration span. Three different davit arm designs were tested (Figure 4) with both polymer and ceramic insulator assemblies installed.



Figure 4 – Three Davit Arm Designs Tested

For the laboratory testing a special steel pole was fabricated, and equipped with mounting holes in an upper and lower position for the three different test sequences (Figure 5). To deaden the vibration of the pole itself, so its behavior was similar to a concrete pole, it was filled with over a ton of sand.

Initially, strain gauges were attached to the davit arms, adjacent to the weld at the top shoulder (apex) and at the side shoulders on the upper surface (Figure 6 and Figure 7). After beginning the span testing, it was discovered that vertical vibration of the conductor will excite horizontal movements of the insulator string and davit arm (along the conductor axis).

As a result, the strain gauges at the side shoulders were replaced with dual axis strain gauges (Figure 8), and additional strain gauges were added to the sides of the arms (Figure 9) and one positioned 6 inches away from the weld on the mounting plate.



Figure 5 – Test Pole

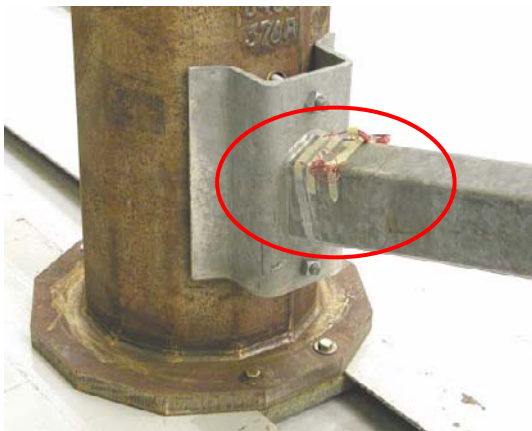


Figure 6 – Strain Gauge Placement

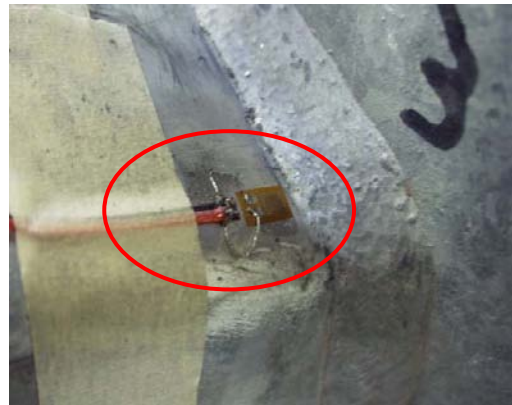


Figure 7 – Strain Gauge on Side Shoulder

Accelerometers were attached to the davit arms as required to monitor both vertical and horizontal dynamic displacements and frequencies of the arms during the tests (Figure 10).



Figure 8 –  
Dual Axis Strain Gauges



Figure 9 –  
Strain Gauge on Side

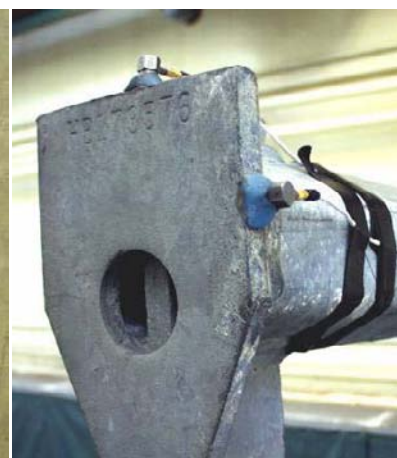


Figure 10 –  
Accelerometers

## FUNDAMENTAL FREQUENCY TEST

The general setup for the fundamental frequency testing of the davit arms is shown in Figure 11. For each weight increment placed at the end of the insulator string, the fundamental frequencies (vertical and horizontal) were recorded. The fundamental frequencies were excited by hitting the end of the arm with a rubber mallet.

Table 1 shows the fundamental frequencies of each arm for vertical loads ranging from 0 lbs to 2,000 lbs. 1,000 lbs represents the approximate load from a 950 ft. span of single Drake conductor, and 2,000 lbs represents a twin (vertical) configuration for the same span length.



Figure 11 – Fundamental Frequency Test Setup

It should be noted that the initial horizontal fundamental frequency tests conducted on Arm No. 1 were with the weights attached directly to the attachment hole at the end of the arm. With the weights in this position the fundamental frequency with a load of 2,000 lbs was 2.7 Hertz, compared to the 8.5 Hertz in Table 1, with the weights at the end of the insulator assembly. It was clear that the horizontal frequency was influenced by the position of the weights, and therefore, all of the data presented in Table 1 is with the weights positioned at the end of the insulator string (the condition that normally exists in the field).

As shown in Table 1, the vertical fundamental frequencies for the three arm designs were very similar, but there was a marked difference in the horizontal fundamental frequencies.

Before the fundamental frequency tests were conducted, the same test setup was used to determine the static stress on the davit arms adjacent to the weld, and the vertical deflection at the end of the arm. Of significant interest was the level of static stress on the arms as determined from the strain gauges. These values, as measured by strain gauges near the welds, were 2 to 3 times higher than a linear calculation of stresses using the arm geometry, material properties, and the position of the load. However, the strain gauge positioned 6 inches from the weld on the mounting plate gave results consistent with the linear calculations.

Possible explanations for this large difference are that there exist concentrated stresses adjacent to the weld due to the shape of the arm and the type (and quality) of the weld. Further proof requires a non-linear, finite element, analysis of the arm shape and welds. However, it is known that higher static stresses on the arm will result in a lower fatigue stress endurance limit within the arm's life cycle as long as the fatigue stress is larger than the fatigue threshold.

Table 1 – Fundamental Frequency vs. Load

Load	Fundamental Frequencies					
	Vertical			Horizontal		
	Arm #1	Arm #2	Arm #3	Arm #1	Arm #2	Arm #3
0#	24.6	25.2	24.5	N/A	7.4	8.6
500#	4.9	4.6	4.8	N/A	6.3	9.0
1,000#	3.6	3.3	3.4	N/A	6.9	7.5
1,500#	2.9	2.5	2.7	N/A	6.0	7.5
2,000#	2.4	2.1	2.4	8.5	5.8	7.5

### FORCED RESPONSE OF ARMS

For this test the arms were mounted to the lower mounting holes on the pole, and the vibration shaker was secured directly to the lab floor (Figure 12). Weight was added to the end of the arm to simulate the conductor vertical loading. Accelerometers were mounted at the end of the arm, at the center, and 1/3 of the distance from the base to monitor arm deflection. The shaker frequency controls were set to sweep from 5 hertz to 60 hertz at a rate of 0.1 hertz per second. A constant force was applied between the shaker and the arm.



Figure 12  
Forced Response Test

It was hoped that from this testing that higher order resonant frequencies of the arms could be found so that this information could be used to determine which frequencies to use in the span testing.

Unfortunately, only the fundamental vertical frequency was apparent when the outputs of the accelerometers were closely reviewed.

### SPAN TESTING

Figure 13 shows the basic setup for the span testing, where the davit arm with insulator is connected to the center of a 90' span of 795 kcmil 26/7 ACSR (Drake) conductor. Figure 14 shows a close-up of the suspension clamp and the weights attached below it to simulate the weight of the conductors.



Figure 13 – Span Test Setup



Figure 14 – Suspension Close Up

The vibration shaker positioned near one end of the span is shown in Figure 15. Figure 16 shows the levered weight basket arrangement at one end of the span used to adjust and maintain the tension on the conductor (15 lbs of tension for each 1 lbs of weight in the basket).



Figure 15 – Vibration Shaker



Figure 16 – Weight Basket

Similar span testing was conducted for each of the three davit arm designs. At a number of discrete conductor tensions (ranging from 10% to 15% of the conductor breaking strength) the span was tuned and held at six or seven resonant frequencies (see Table 2 for example). Therefore, for each arm, as many as 34 different conductor vibration frequencies were investigated.

Table 2 – Lab Span Resonant Frequencies

Tension	Freq 1	Freq 2	Freq 3	Freq 4	Freq 5	Freq 6	Freq 7
4726#	9.94	14.81	19.76	24.86	30.27	36.52	
3976#	9.11	13.57	17.88	22.84	27.72	33.59	40.06
3600#	8.79	12.95	17.36	21.98	26.74	32.42	38.70
3376#	8.49	12.70	16.84	21.42	26.10	31.66	36.98
3150#	8.25	12.39	16.33	20.86	25.43	30.98	36.30

For each resonant conductor frequency the peak-to-peak amplitude of the anti-node of one of the free standing wave loops in the span was held at 0.5”.

By recording the dynamic stress at various points on the arm (with strain gauges), and the vertical and horizontal movement of the arm tip (using accelerometers) it was possible to correlate aeolian vibration activity in the span to movement (vertical or horizontal, or a combination) of the arm tip.

The most compelling test data was at a conductor frequency of 28.35 hertz for one of the arms. As shown in Figure 3, the amplitude of conductor vibration was one of the highest around this frequency during the field vibration study.

The movement of the arm at the 28.35 hertz frequency produced the highest dynamic strain levels. The movement was vertical, and even though the frequency of the span

was 28.35 hertz, the arm was moving at the vertical fundamental frequency of the arm/insulator/weight combination (2.4 hertz), as clearly shown in Figure 17. The measured maximum strain is 100 microstrain, which occurs at the top of the arm.

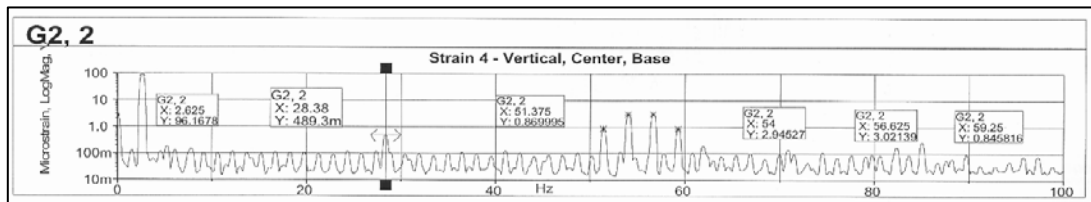


Figure 17 – Strain Spectrum at Center Top of Arm (28.35 hertz)

The arm movement at 28.35 hertz was so significant that it warranted further study. In one case the frequency was held constant while the anti-node amplitude in the span was varied. In the other case the anti-node amplitude was held at 0.5", while the tension in the span (and therefore resonant frequency) was adjusted in small increments. The results of these closer studies are detailed in Table 3.

There are two significant observations that can be made from Table 3. First, in the upper segment of the table where the frequency was held and the amplitude of the vibration was varied, it is clear that there is a threshold value (around 0.33" peak-to-peak) for movement of the arm. This suggests that the arm movement can be mitigated with vibration dampers applied to the span which reduces the vibration amplitude to a value below the threshold.

Table 3 – Additional testing at 28.35 hertz

Frequency (Hz)	Antinode Amplitude (in p-p)	Antinode Velocity (mm/s)	Shaker Power (W)	Comments	Shaker Velocity (m/s)	Shaker Force (N)	Phase Angle (deg)
28.35	0.1	226	1.3	No visible arm motion	0.0632	69.1	128
28.35	0.2	452	6.2	No visible arm motion	0.1593	181.2	115.4
28.35	0.3	679	18.7	No visible arm motion	0.2716	342.1	113.7
28.35	0.32	724	23.6	No visible arm motion	0.2801	374.1	116.8
28.35	0.34	769	27.0	Vertical arm motion	0.2947	393.6	117.8
28.35	0.4	905	41.2	Vertical arm motion	0.3605	461.5	119.7
28.35	0.5	1131	66.1	Vertical arm motion	0.4426	540.8	123.5
28.1	0.5	1121	56.7	No visible arm motion	0.4776	561.5	115
28.15	0.5	1123	48.0	Small vertical arm motion	0.4472	540.5	113.4
28.2	0.5	1125	58.0	Vertical arm motion	0.4557	566.4	116.7
28.5	0.5	1137	67.9	Vertical arm motion	0.4468	525.6	125.3
28.6	0.5	1141	62.8	Small vertical arm motion	0.4291	514.4	124.7
28.65	0.5	1143	59.0	No visible arm motion	0.415	504.2	124.3

During the two-week field vibration study, measurements were also made on phases that had dampers (one per span) installed. Figure 18 shows the standard IEEE<sup>1</sup> formatted results of the testing comparing the undamped vs. damped vibration activity. This clearly shows that the amplitude of vibration was reduced below the threshold for arm movement.

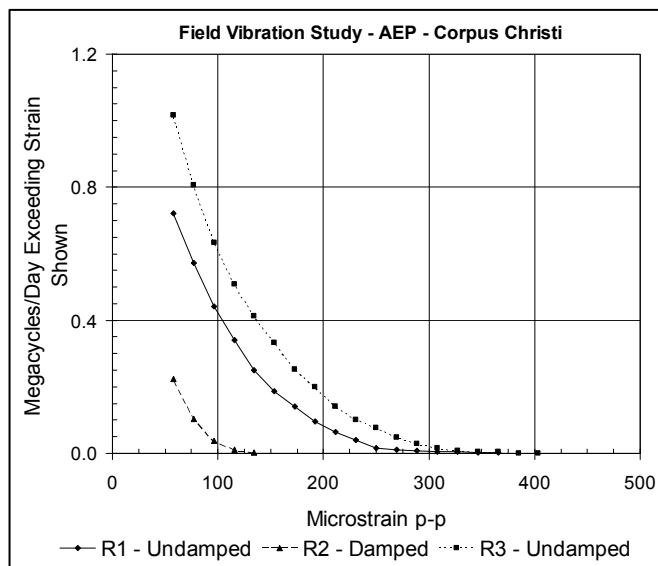


Figure 18 – Dampers vs. Undamped

In the Fall of 2006 the line that experienced davit arm failures, and on which the field vibration study was conducted, was fitted with new vibration dampers. Since the installation of these dampers, this line has not experienced further davit arm failures. This further substantiates the theory of a threshold value.

The second observation comes from the constant amplitude test (bottom segment of Table 3). The test shows that there is a very narrow band (about 0.2 hertz) of frequencies that cause significant arm movement. It further suggests that due to difficulties in making fine adjustments in tension on a short laboratory span, there may have been other span vibration frequencies that could have produced significant arm movement. This also helps to explain that the percentage of arm failures is relatively low.

## PLANNED FIELD MEASUREMENTS

Plans are being made to instrument davit arms on lines in Texas that have experienced davit arm failures. The instrumentation will consist of accelerometers mounted to the tip of the arms to measure both vertical and horizontal (along the conductor) movements. An associated data logger system will collect and store or transmit data over a long period of time. A weather station will also be installed at the monitoring site, with temperature, wind speed and wind direction data being logged.

The planned system will allow for studying the davit arm movements under actual field conditions and full length spans to verify the work that was done in the laboratory. It will also help in determining any other dynamic factors, in addition to

the aeolian vibration of the conductors, which may be affecting the davit arm such as high wind gusts.

By also studying phases with and without dampers with the planned system, the effectiveness of the dampers in mitigating the arm movements can be verified in the field.

A follow up field vibration study is also planned which will allow correlation between the movements measured on the arms with actual vibration data on the span.

## CONCLUSIONS

- The field vibration study showed that there is moderately severe vibration activity on spans without dampers.
- Static stress measurements on the davit arms adjacent to the weld (with strain gauges) were considerably higher (2 to 3 times) than the stress calculated using standard linear analysis.
- Span testing in the laboratory revealed that vertical (aeolian) vibration of the conductor can produce both vertical and horizontal (or combination) movements of the tip of the arms.
- Comparisons of arm movements measured in the lab when using polymer insulators vs. porcelain insulators suggests that the weight of the porcelain insulators can increase the arm movements (both vertical and horizontal).
- Conductor vibration (28.35 hertz) produced by wind velocities in the 6 to 10 MPH range can excite significant vertical arm movement at the arm's fundamental frequency (2.4 hertz).
- Further testing showed that there was a "threshold" value of the free loop anti-node amplitude, below which the arm did not move. This supports the use of dampers to control the level of the vibration in the field to mitigate arm movements and subsequent fatigue failures.

---

## References

<sup>1</sup> "Standardization of Conductor Vibration Measurements", Paper 31 TP-65-156, IEEE Trans. Vol. Pas. 85, 1966

## Lessons Learned from Design and Test of Latticed Steel Transmission Towers

Quan He Fan, P.E., M. ASCE<sup>1</sup>

### ABSTRACT

Design of latticed steel transmission towers is a challenging task which involves lengthy modeling and detailing of significant amount of steel members and connections. Testing of the towers designed validates consistency between modeling and detailing and ensures the towers are designed to withstand design loads without premature failures.

This paper presents lessons learned from design and testing of latticed steel towers in a recent project of developing a family of nine (9) 500kV transmission towers. The paper provides a discussion about the process of selecting bidders for design, detailing and fabrication of latticed steel towers, and a brief discussion of determining materials used in the towers. The paper also discusses comparisons of different tower weights for various tower base widths and foundation reactions to achieve a cost effective design combining both the tower and its foundations. Examples of modeling tower members using beam elements in PLS-TOWER are presented to illustrate the importance of fully understanding the main purpose of using beam elements in TOWER. Variations between tower modeling and detailing are presented with specific attention to member and connection eccentricities. Finally, lessons learned from six (6) tower tests are discussed.

### INTRODUCTION

The majority of 500kV transmission lines in Georgia were constructed in 1970s. All latticed steel towers used in the 500kV transmission lines in Georgia were originally developed by Georgia Power Company (GPC) in the late 1960s and early 1970s. The towers were not designed with working clearances for hot line nor helicopter maintenance.

During the 1980s and 1990s, there was not much demand for building new 500kV transmission lines in Georgia. However, in early 2000s, construction of several hundred miles of new 500kV transmission lines was anticipated. In light of the construction anticipated, studies of 500kV structures deemed necessary in order to provide clearance required for hot line and helicopter maintenance, to comply with the latest national design specifications, and to achieve the most economic design.

### BACKGROUND

In early 2004, Georgia Transmission Corporation (GTC) expected to construct approximately 90 miles of 500kV transmission line in next five to seven years. GTC understood that GPC, another member of the Georgia Integrated Transmission

---

<sup>1</sup> Georgia Transmission Corporation, 2100 East Exchange Place, Tucker, GA 30084; PH (770) 270-7699; FAX: 770-270-7775; Email: [quan.fan@gatrans.com](mailto:quan.fan@gatrans.com)

System (ITS), anticipated a similar need of 500kV transmission line construction. GTC also found that GPC was in process of updating its existing horizontal configuration tower family to comply with the latest National Electric Safety Code (NESC). GTC discussed with GPC on several occasions about jointly developing a new family of 500kV structures to meet the demand of the new construction of 500kV lines in Georgia. GPC and GTC agreed that it would be beneficial for both companies to use same 500kV structure standards in the future construction of 500kV transmission lines in Georgia. At the time, Southern Company transmission line standards team was working on the study of a 500kV Structure Family Evaluation to establish a standard 500kV structure family within Southern Company. GTC joined the study in late 2004 after received an invitation from GPC. The study involved evaluating design and construction criteria and costs for a multitude of 500kV structure families using 35 miles of Mostellar Spring – McGrau Ford 500kV line as a basis for comparison. The study considered the following structural families:

- Existing GPC horizontal configuration towers
- Existing Alabama Power Company (APC) delta configuration self-supporting and guyed towers
- Delta configuration single poles
- Horizontal configuration guyed H-frames

The tangent structures in each family considered are shown in Figure 1.

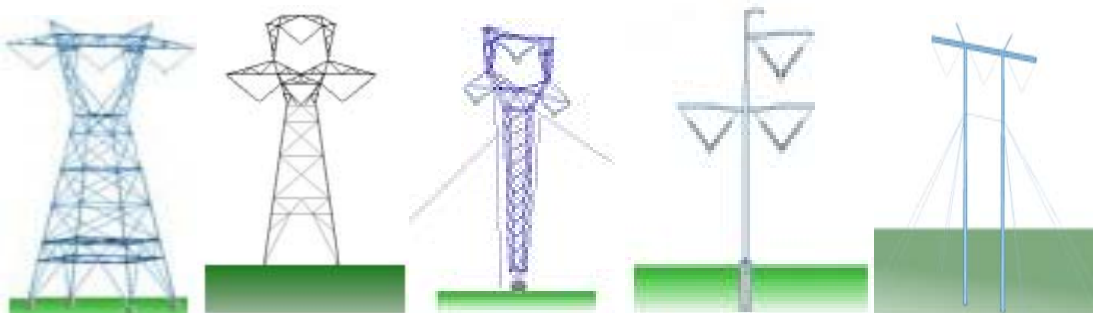


FIGURE 1

After the extensive studies, it was concluded that an upgraded existing APC delta configuration tower family is the desired 500kV standard structures going forward. The new family of structures will have following improvements to the existing structures studied:

- Provide adequate clearance required for hot line maintenance
- Provide adequate phase spacing between shield wires and conductors required for helicopter maintenance
- Provide engineered buzzard shield for protection of insulators from buzzard contamination
- Design an additional angle structure to provide efficient line design with a more completed family of structures
- Accommodate more effectively with 150 feet rights-of-way width under the various loading conditions encountered
- Use more readily available angle sizes and provide interchangeable angles between AISC and metric angles in design and detailing
- Provide better electric behaviors

Based on the assessment of work involved in developing the new family of 500kV structures, a working team consisting of members from Southern Company and GTC was formed. The team was responsible for coordinating design requirements of Southern Company and GTC, setting design parameters, determining bidding process, selecting winning bidder and reviewing design and details submitted by the bidder.

### BIDDING PROCESS

In 2005, the working team started the pre-bidding process. It began with initial contact with consulting firms in the United States which have known experience in design and analysis of 500kV transmission lines. After review of the information collected in the initial contact, considering the scope of the project and capacity of the consulting firms, the following four (4) firms were selected for further consideration:

- |                    |                                |
|--------------------|--------------------------------|
| - Black & Veatch   | - Commonwealth Associates Inc. |
| - Burns & McDonald | - Power Engineers              |

The working team conducted face to face interviews with each of above consulting firms. The interview started with the consultant's presentation on experience of latticed steel tower design, recent 500kV transmission line work, and design software, particularly PLS-TOWER (TOWER). Then detailed discussions on project scope, schedule, quality control process, tower detailing and tests, tower fabrication, tower erection and other related topics were carried out. It was intended initially to have a consulting firm perform all engineering work including design, analysis and detailing of the family of tower. However during the interview and discussions, it was found out that the consultants have either very limited or no capacity at all for detailing of latticed steel tower. After much deliberation, it was decided that the project would be better carried out in two steps. First, the team would solicit proposals from the consulting firms to develop design specifications for the latticed steel towers. Then a tower supplier would be selected to provide services in design, analysis, detailing and testing of the towers based on the design specifications developed. The tower supplier selected would also supply 157 steel towers for GTC's thirty-eight (38) miles of Thomson – Warthen 500kV Transmission Line Project.

After proposals for developing the design specifications from the consulting firms were evaluated, Black & Veatch was selected. In order to incorporate requirements for hot line and helicopter maintenance in design specifications, a large meeting was called for soliciting advice and recommendations from personnel of helicopter companies specialized in transmission line maintenance, transmission line construction contractors with extensive experience in 500kV transmission line construction, suppliers of hotline maintenance tools, and Southern Company and GTC maintenance. A detailed design specification was developed for use to solicit proposals from tower suppliers for design, analysis, detailing, testing and supply of latticed steel towers. Following suppliers were contacted initially for pre-qualification:

- |                               |                         |
|-------------------------------|-------------------------|
| - Fort Worth Tower Inc. – USA | - Locweld Inc. – Canada |
| - Falcon Steel Company – USA  | - Fabrimet – Canada     |
| - Thomas & Betts – USA        | - SAE Towers – Mexico   |

- Sisttemex, Inc. – Mexico
- Formet – Mexico
- KEC – India
- Kalpataru – India
- Mitas – Turkey

After reviewing information submitted by the tower suppliers in the pre-qualification, it was found that no American suppliers have engineering and detailing capability to undertake the project. An invitation for proposal was then sent to the remaining suppliers. The following suppliers submitted proposals:

- Thomas & Betts, Fabrimet and Comemsa
- SAE Towers
- Sisttemex, Inc.
- Formet
- Kalpataru

All bidders were evaluated commercially and technically by GTC and Southern Company. Evaluations included contract terms and conditions, engineering capability, pricing, and review of facilities. SAE Towers and Kalpataru were short listed for further evaluation. Their proposals and preliminary designs were further scrutinized, which included a numerical weighted evaluation, an exchange of additional information, and a formal interview conducted by conference calls. SAE Towers was finally selected as the winning bidder.

### TOWER MATERIALS AND DESIGN

Tower materials were required to be new and undamaged and conform to AISC (AISC, 2005) and ASTM standard specifications such as ASTM A36 or ASTM A572, ASTM A394 or ASTM A325. The use of different steel grades were considered in the design. The capacity of tension members are directly proportional to steel grade used while the capacity of compression member is dependant on slenderness ratio  $KL/r$ . For long and slender compression members, it is common to use base quality structural steel ASTM A36. In general, weight is the dominant factor in the cost of a latticed steel tower (EPRI, 1990). The design that weighs the least will in general cost the least. However, many other factors such as detailing, bracing schemes, fabrication, handling, shipping and erection needed to be evaluated. Another cost factor that needed to be considered was member duplication. Since fabrication of latticed steel tower is a production line type operation, time and labor spent on setup on the shearing and punching equipment for each member could well impact the bottom line of total costs. It was noticed in the evaluation that designs submitted by Kalpataru, India have significantly more pieces than designs submitted by other bidders or similar designs done by domestic consultants or tower suppliers. This could be because labor costs in fabrication and erection does not have significant impact on cost in the designs. Each piece in latticed steel towers must be handled a number of times during fabrication, shipping and erection, therefore the number of pieces in a tower design is a significant cost factor. In addition, any operation that requires hand work or individual inspection such as welding, drilling, or bending is more costly than the production operations of shearing and punching. These factors should be considered in the economic evaluations.

The bolt size and grade are critical factors in the structural strength and economics of

tower design. It is common practice in the United States to use only one diameter and grade of bolt in any single tower design. ASTM A394 Type 0 and Type 1 bolts are the most commonly used bolts for transmission line towers in North America. However, considering more and more transmission line towers are designed and/or supplied by overseas fabricators, it may be desirable to specify ASTM A307 and A325 bolts for transmission line towers. Because ASTM A307 and A325 bolts are widely used in steel structural joints of buildings and bridges, the ASTM A307 and A325 specifications are better known internationally. These bolts are more readily available and generally have better quality assurance and quality control process.

Transmission tower connections are designed as bearing type connections. Decision on the design of connections with threads included or excluded from the shear plane could have significant impact on costs. If the connections are designed with threads included, then all threaded bolts could be used to provide ease of construction. It would also eliminate concerns about possible mistake of installing bolt threads in the shear plane which could lead to significant strength reduction of the connection when the design called for excluding threads in the shear plane. However, connections designed with threads included would require more bolts in the connection and increase number of gusset plates used in the connections. Gusset plates are always expensive, and sometimes they will increase the eccentricities in the connections. In addition to the cost of furnishing, fabricating, handling and erecting the additional piece, each gusset plate usually requires a few extra bolts and fills or washers which contribute more adverse economic comparison (EPRI, 1990). It should be a major goal in design and detailing to minimize the number of gusset plates used in a tower.

It was required in the design specifications that the transmission line structures to be designed in accordance with the ASCE 10-97. The loads, configuration and electrical clearances were provided to the bidders in loading and configuration drawings. The structures furnished under the design specifications included a family of following latticed steel towers:

- DSS-T        50 – 125 ft, self-supporting tangent structure, 0°-5°
- DSS-HT      50 – 135 ft, self-supporting heavy tangent structure, 0°-5°
- DSS-SA      50 – 120 ft, self-supporting small angle structure, 5°-15°
- DSS-LA      50 – 120 ft, self-supporting large angle structure, 15°-30°
- DSS-DE1     65 – 125 ft, self-supporting deadend structure, 0°-45°
- DSS-DE2     65 – 125 ft, self-supporting deadend structure, 45°-115°
- DGM-T      50 – 125 ft, guyed mast tangent structure, 0°-5°
- DGM-HT     50 – 135 ft, guyed mast heavy tangent structure, 0°-5°

After reviewed the preliminary designs submitted by the bidders, it was found that the structure DSS-DE2 was extremely heavy because it was designed to accommodate a very large line design angle. Past experience in Southern Company and GTC 500kV transmission line designs shows it is very rare in line design that any structure would have line angle greater than 90°. Therefore it was decided to reduce design line angle of the structure DSS-DE2 to 90° and add another design of DSS-DE3 structure with line angle 90°-115°. This would provide more economic utilization of all structures.

It was expected that all bidders would put sufficient efforts on designing the lightest towers possible in their proposals. However, it is extremely important for the owner to keep in mind that an economical tower design is a compromise between tower costs and foundation costs. The basic guidance is that a narrower base will lead to a lighter tower, but larger foundation reactions. While a wider base will in general reduce the foundation reactions, but may require longer, more costly tower bracing members and lead to a more expensive tower.

After initial evaluation of design proposals submitted by the bidders, it was found that further design optimization would be necessary taking into consideration of foundation reactions and costs in the tower designs. Request for additional design information was made to the two short listed bidders. The two bidders redesigned three towers selected by GTC to provide information on tower weights and foundation reactions under various tower base widths. After receiving the information on the revised tower base width and foundation reactions, foundation designs using EPRI's CUFAD (Compression and Uplift Foundation Analysis and Design) were performed. A cost comparison for different widths of tower base taking into consideration of both tower and foundation cost was then carried out. The data used is summarized below.

- The foundation designs were based on two soil borings obtained in a project area where two 500kV transmission lines will be built in the near future. The first soil boring was categorized as "Good Soil" with a blow count  $N = 22 - 34$ , unit soil weight =  $120 - 125 \text{ lb/ft}^3$ , soil friction angle =  $32 - 37$  degrees and no water table. The second soil boring was categorized as "Average/Poor Soil". The top forty-seven feet soil has blow count  $N = 8 - 35$ , dry unit soil weight =  $115 - 120 \text{ lb/ft}^3$ , soil friction angle =  $30 - 32$ , water table depth at 10 feet.
- Tower base widths considered:
 

Tangent tower: 36 ft, 40 ft and 45 ft	
Large angle tower: 40 ft and 48 ft	Deadend tower: 46 ft, 50 ft and 52 ft
- Tower costs:
 

Tangent tower steel: \$0.843 / lb	Deadend tower steel: \$0.951 / lb
Large angle tower steel: \$0.910 / lb	Steel erection cost: \$0.900 / lb
- Concrete pier foundation cost was assumed to be \$600 per cubic yard, including concrete, reinforcement and contractor labor and materials.
- Uplift and compression foundations were designed differently for angle and deadend towers. The minimum foundation diameter considered was 3 feet and maximum burial depth was 40 feet. Under same loading and soil condition, a smaller diameter and deeper foundation is in general cheaper than a larger diameter and shallower foundation.

The cost comparison results were summarized in the table below.

**Table 1: Cost Comparison for Different Widths of Tower Base**

Tower Type		Tangent	Large Angle	Deadend		
Base Width Increase (ft)		36 to 40	36 to 45	40 to 48	46 to 50	46 to 52
<b>Cost (\$)</b>	<b>Steel &amp; Erection</b>	1339 (↑)	4468 (↑)	3244 (↑)	2701 (↑)	4081 (↑)
	<b>Foundation</b>	-720 (↓)	-1680 (↓)	-11160 (↓)	-11160 (↓)	-20400 (↓)
<b>Total Cost Difference (\$)</b>		<b>619 (↑)</b>	<b>2788 (↑)</b>	<b>-7916 (↓)</b>	<b>-8459 (↓)</b>	<b>-16319 (↓)</b>
<b>Cost (\$)</b>	<b>Steel &amp; Erection</b>	1339 (↑)	4468 (↑)	3244 (↑)	2701 (↑)	4081 (↑)
	<b>Foundation</b>	-1680 (↓)	-7680 (↓)	-25800 (↓)	-23040 (↓)	-33840 (↓)
<b>Total Cost Difference (\$)</b>		<b>-341 (↓)</b>	<b>-3212 (↓)</b>	<b>-22556 (↓)</b>	<b>-20339 (↓)</b>	<b>-29759 (↓)</b>

The cost comparison shows that increasing tower base width to reduce foundation reactions will result in total savings except for tangent tower in “good soil” area. The savings could be quite significant for large angle and deadend towers located in “average/poor” soil areas. It was found that the deadend tower with 46 feet base width would require the uplift foundations in “average/poor” soil area to be designed with a diameter of 10-11 feet and a burial depth of over 40 feet, which would be a very expensive and impractical construction.

A guidance to determine the width of tower base could be to set the slope of the post legs of tower so the theoretical intersection of their extensions is at the elevation close to the centroid of the horizontal loads of the worst and the second worst design loading conditions. This design would provide following advantages (EPRI 1990):

- The post legs of the tower body form almost a true “A” frame and the horizontal shear bracing will be minimal.
- Forces in the post legs will be fairly uniform from ground line to tower waist.
- Foundation reactions will be fairly constant from the shortest to the tallest tower.

## TOWER MODELING

It is a standard practice to model latticed towers as ideal elastic three-dimensional trusses with pin connection at joints. Tower members are considered as axially loaded tension or compression truss elements. Moment due to eccentricities is assumed to be small and is not calculated in the analysis.

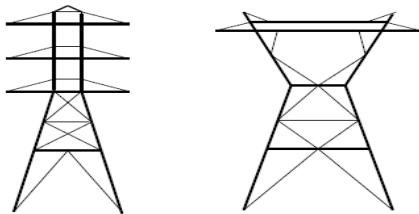


Figure 2 Beam Elements (Thick Lines)

PLS-TOWER is a specialized computer program for analysis of latticed transmission towers and is widely used by utilities around the world because of its compatibility to transmission line design software PLS-CADD. All computer programs used in analysis of

latticed transmission towers almost exclusively modeled the tower members as truss elements until recently, PLS-TOWER now recommends the use of beam elements to stabilize planar joints and mechanisms. PLS-TOWER recommends that all tower members be modeled as beam elements, except diagonals and single horizontal struts as shown in Figure 2 (PLS-TOWER, 2008).

PLS-TOWER emphasized that the main purpose of using beam elements is to stabilize planar joints and mechanisms. Beam elements, in addition to axial tension and compression can carry shears and moments, but they are not intended to be loaded in bending and there is no design check for moments and no moment report, except for the moment results table that can be generated using **“Model/ Results/ Moments for Angles Modeled as Beams”**. For design purposes, the beam members are still assumed to be loaded axially. The beam elements can be used to stabilize the model, but the model should still be triangulated (PLS-TOWER, 2008).

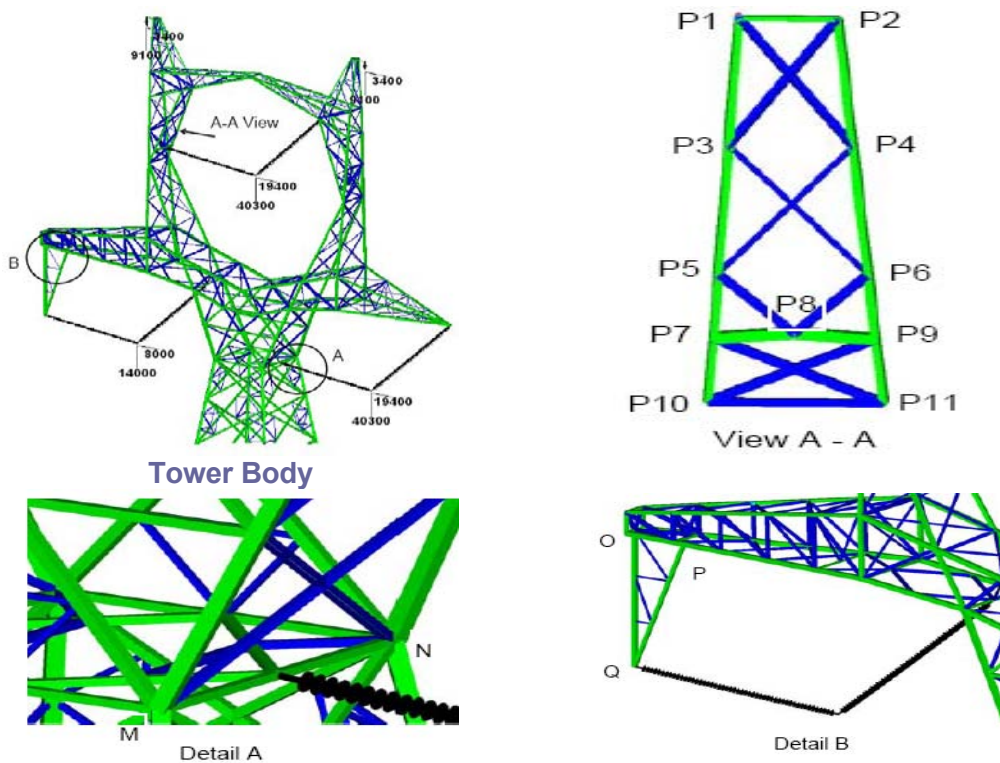


Figure 3 Tower Modeling Examples

Modeling examples in Figure 3 illustrate that it is extremely important for anyone using PLS-TOWER design latticed structures to have a complete understanding of the purpose of beam elements used in PLS-TOWER. It is equally important for anyone designing latticed structures to have understanding and knowledge of structural behavior when creating a valid model. Because beam elements in TOWER can carry shears and moments, and no design check for shears and moment is performed, mistakes of misusing beam elements in TOWER could be disastrous. It is an imperative to check the moment results generated in “**Model/ Results/ Moments for Angles Modeled as Beam**” and any other warnings in TOWER to ensure that no beam elements are carrying large moment.

Figure 3 shows an upper part of a small angle tower. Most members were modeled as beam elements. In “Detail A” the member MN (L3 x 3 x 3/16) was modeled as a beam element. The mid joint of the member is the insulator attachment point and has no support in vertical direction, which would generate significant moments in the member. Analysis of the member with significant moment is beyond the capabilities of TOWER. In “Detail B” members OQ (double angle L4 x 4 x ¼) and PQ (double angle L3½ x 3½ x 3/8) in the swing bracket were modeled as beam elements and attached to members that were modeled as beam elements as well. This model simulated the swing bracket as a rigid frame which was not what the design intended. It is obvious that the model had flaws and violated “the beam elements are not intended to be loaded in bending...” stated in the TOWER user’s manual. When the model was analyzed with TOWER in late 2007, the output showed that the member MN was loaded to 76% of its capacity and member PQ was at 56% of its capacity under the worst design loading. No warning

or any other message was given in the output. However, when the tower was tested in early 2008, both members MN and PQ failed prematurely.

The misuse of beam element shown in the examples of “Detail A” and “Detail B” are pretty obvious for someone with experience in tower design. But sometimes it can be quite intricate. In “View A-A” of Figure 3, horizontal and leg members were modeled as beam elements except members P10P11, X-bracing and V-bracing were modeled as truss elements. At the attachment point P8, two V-bracing at inside and outside panel was formed to provide support at all direction. The model was properly triangulated. No obvious flaw or violation to the recommendations and guidelines provided by the TOWER was found. However the result of modeling horizontal and leg members as beam elements is significantly different to the result when these members are modeled as truss elements. Table 2 shows the result of member force in term of its capacity.

**Table 2 Member Capacity Comparison: Beam Elements vs. Truss Elements**

	Member Force as % of Its Capacity										
	P1P2	P1P3 P2P4	P3P5 P4P6	P5P7 P6P9	P7P10 P9P11	P1P4 P2P3	P3P6 P4P5	P5P8 P6P8	P7P11 P9P10	P7P8 P8P9	P10P11
<b>Beam Element Model</b>	87	<b>48</b>	<b>36</b>	<b>57</b>	<b>97</b>	<b>83</b>	<b>91</b>	<b>33</b>	<b>21</b>	<b>57</b>	<b>33</b>
<b>Truss Element Model</b>	P1P2	P1P3 P2P4	P3P5 P4P6	P5P7 P6P9	P7P10 P9P11	P1P4 P2P3	P3P6 P4P5	P5P8 P6P8	P7P11 P9P10	P7P8 P8P9	P10P11
	238	<b>112</b>	<b>100</b>	<b>80</b>	<b>140</b>	<b>220</b>	<b>213</b>	<b>65</b>	<b>93</b>	<b>179</b>	<b>192</b>

The result in Table 2 shows that member design is within its allowable capacity in beam element model that simulates a rigid frame panel, whereas in truss element model majority of members are significantly overstressed. When the bracing is insufficiently stiff to provide proper support, the members modeled as beam elements shown carried moment and shear, but no design check for shear and moment is performed in TOWER. This had raised concerns about using beam elements in tower models, especially when the tower was modeled by someone with limited experience in modeling. The concerns were expressed to PLS in early 2008. Suggestions were made to PLS for adding a warning or a pop-up message when TOWER detects significant moments in members modeled as beam elements. The TOWER program released after April 2008 has an additional warning now listed when beam elements modeled are carrying significant moment. A graphic warning was also added in 2008. The graphic warning is a very helpful tool to ensure that the beam elements were used properly in TOWER. The tower designer should exercise extra caution and heed any warnings issued when beam elements are used in the tower model.

## DETAILING

The tower designer is responsible for ensuring structural integrity when the drawings are created by detailers. The drawings used for fabrication of tower should be consistent with the model. Moments due to framing eccentricities are generally not calculated in the design model. The detailer should minimize the framing eccentricities in detailing processes so that no significant moments would be generated. When framing eccentricities are unavoidable at some connections, proper design checks and calculations shall be performed to adjust the model and member selection accordingly.

Figure 4 shows a typical deadend tower body model. The "Detail A" shows detail of insulator attachment. The loads applied at point O will generate moments on member P and the bracing connected to the joint. Proper member design taking into consideration of moments due to eccentricities is necessary.

The quality of details is a major factor contributing to the strength of a tower. The designer and the detailer should continuously work together during the preparation of the fabrication drawings which would largely determine the economy of a design.

## TESTING

Full scale structural tests were performed for six out of nine towers designed. The other three towers (DGM-T, DGM-HT and DSS-DE3) will be tested later when they are used in a project. The tests were set up to conform to the design conditions and to validate the adequacy of the individual members and their connection designs to withstand the specified loading conditions. The tower tests perform as the acceptance checks. If there is no premature failure, the design is assumed to meet the minimum strength required.

Nine design loading conditions were specified for testing all six towers. The loading sequence for each tower test was determined so that the load cases having the least influence on the results of successive tests were performed first. Simplifying the testing operation was also considered in selecting the loading sequence. Testing loads were applied to 50, 75, 90, 95 and 100% of the factored design loads. At 50, 75 and 90% the load were held for two minutes, and at 95 and 100%, the loads were held for five minutes. All six towers were required to be tested to destruction at 115% of the factored design loads selected as the last testing load. Five towers tested passed 115% of the worst loading case selected. One tower failed at approximately 110% of the worst loading case selected. It was learned that five to six test loading conditions should be sufficient to validate the towers designed, and the nine loading conditions specified were not necessary for the tests of single circuit latticed steel towers.

It was required the test structure be constructed of the same material and by the same type of fabrication as in the production run. The maximum yield for ASTM A572/A572M Steel (Grade 50) members used in the test structure was 58 ksi. At the time of preparing the material for the test structures, the tower supplier was reportedly unable to find material for some tower members with a maximum yield lower than that specified. It was agreed that as a minimum, the requirement of a maximum yield of 58 ksi for ASTM A572/A572M Steel (Grade 50) shall apply to the members designed for only tension loading, and compression members with  $KL/r$  less than 120, and the members were designed to a stress over 80% of their capacity.

In all six towers tested, the first two tangent towers passed the tests with no premature

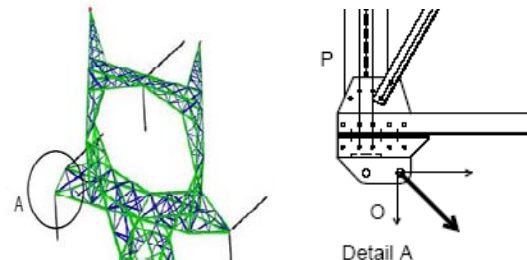


Figure 4

failure. Over a dozen premature failures occurred in the tests of next four towers, which were more than it would expect normally. All failures can be attributed to either detailing or modeling errors. Detailing errors occurred when double angles were used in the analysis, but not properly detailed contributed to several failures.



Figure 5

Figure 5 shows one failure where V-bracing was designed with back-back double angles, but the detail in View A-A did not properly design the sufficient bolts at connections between the V-bracing and the gusset plates. There was also a premature buckling failure when double angles were used in X-bracing, but only a single angle was shown on the drawings. Detailers should pay special attention when double angles are used. The tower designer should work closely with the detailers and perform a thorough review of all details when they are completed.



Failure at Tower Waist – Connection A



Failure at Connection B

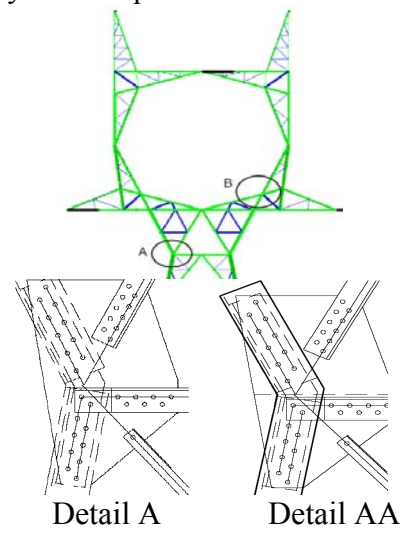


Figure 6

Figure 6 shows two failures occurred at two different connections when testing a deadend tower. The failed bolts in Connection A showed clear cut-off surfaces at the shear plane, which indicates the connection was significantly under designed. The connection was designed using AISC method for eccentric loads on fastener groups assuming each bolt group would withstand the force that connected to the member. Since the leg member was not continuous at the waist (see Detail A), the above assumption was not accurate. The combined forces from different members on each bolt group should have been considered. Detail AA shows an improved detailing with leg continuous above the tower waist.

The failure occurred in Connection B was quite different. The failed bolts showed clear necking at the failed surface. Deformation at shear planes was observed, which could be due to lack of hardness of the bolts used, or the shear planes slipped significantly when the test loads applied. The failure appeared to be tension failure due to prying action. Tower connections are designed as bearing type connection. To avoid prying action at connection, it would be a good practice to use high strength bolts in connections that connect high strength steel and are heavily loaded.

## SUMMARY

The proliferation of demands for reinforcing extra high voltage transmission line networks in recent years and for complying with updated codes and standards requires many utilities in the United States to develop new families of latticed steel structures. Design of latticed steel transmission towers is a challenging task which involves lengthy modeling and detailing of significant amount of steel members and connections. There are very limited resources in the United States capable of carrying out the detailing and design of latticed steel towers. Selecting experienced designers and detailers are critical for the success and economy of the project.

An economical tower design is a compromise of tower and foundation costs. The foundation costs should be considered when developing tower designs. It is extremely important to thoroughly understand the capability of the software used in the design and modeling of the structures, and to have knowledge of structural behavior. It is the responsibility of tower designer and detailer to ensure structural integrity of the towers designed. Full scale tower tests provide an indispensable tool to validate the adequacy of the structures designed, particularly when the structures were designed by someone with limited experience in the subject.

## REFERENCES

1. AISC, (2005), "Steel Construction Manual", Thirteenth Edition, American Institute of Steel Construction Inc.,
2. ANSI/ASCE 10-97, (2000), "Design of Latticed Steel Transmission Structures", American Society of Civil Engineering, Reston, Virginia.
3. ASTM A394-07, (2007), "Standard Specification for Steel Transmission Tower Bolts, Zinc-Coated and Bare", ASTM International, West Conshohocken, Pennsylvania.
4. EPRI, (1990), "Considerations for the Structural Design of a Lattice Steel Electrical Transmission Tower", Research Report RLMRC-89-R6, Haslet, Texas.
5. EPRI, (2003), "Foundation Analysis and Design (FAD)", Haslet, Texas.
6. PLS-CADD, (2008), Power Line Systems – Computer Aided Design and Drafting, Power Line Systems, Inc., Madison, Wisconsin.
7. TOWER, (2008), Analysis and Design of Steel Latticed Towers Used in Transmission and Communication Facilities, Power Line Systems, Inc., Madison, Wisconsin.
8. RCSC, (2000), "Specification for Structural Joints Using ASTM A325 or A490 Bolts", Research Council on Structural Connections, Chicago, Illinois.

## Lessons Learned on Mega Projects

Michael E. Beehler, P.E.

Burns & McDonnell Engineering Co., Inc., Transmission & Distribution Division, 9400 Ward Parkway, Kansas City, MO 64114; PH (816) 822-3358; FAX: (816) 822-3296; email: [mbeehle@burnsmcd.com](mailto:mbeehle@burnsmcd.com).

### Abstract

The electric transmission industry is booming. Several billion dollar scale mega projects are being routed and permitted, some are nearing start of construction and some are complete. Asset owners have struggled with engineering, material and contract labor resource availability and, as a result, have discovered several new methods of delivering these major projects. This paper will examine several major projects and discuss the lessons learned on each of the project delivery methods that were selected to deliver these billion dollar scale transmission projects. The common methods of delivering major projects (programs) are design/bid/build, design/build (EPC) and program management.

### **Design/Bid/Build Approach**

The Design/Bid/Build process is often referred to as the traditional approach or the multiple-contract approach in which multiple construction contracts are bid and awarded as lump sum projects based on plans and specifications prepared by an engineer. The project owner hires the design engineer, purchases equipment directly, and hires one or more contractors to perform the construction under separate contracts. The contracts are structured to allow multiple specialty contractors to perform the specific trade-related work in an effort to minimize sub-contracting and reduce contractor markups. The engineer may help to pre-qualify contractors and may make recommendations as to contractor selection.

### **Advantages of Design/Bid/Build Approach**

1. The owner can select an engineer that has its trust and confidence and is separate from the construction process. The owner works directly with the engineer to implement the utility's design philosophies and standard practices into the design.
2. The owner can have input as the design progresses and up to the time the plans and specifications are issued for bid without incurring costly change orders. It is not necessary for the owner to identify all its requirements at the beginning of the project.
3. Designs and bid evaluations can be performed to account for the life cycle costs of design decisions instead of just the initial capital cost.
4. The contracts can be structured to minimize the amount of subcontracting by prime contractors minimizing contractor markup. Equipment is purchased directly from the supplier eliminating contractor markups. Since the

construction contracts are smaller and more specialized a larger number of qualified contractors may be available to bid the work resulting in lower project costs.

5. The owner controls the contingency pool for the project.
6. The owner has direct control over the selection of material vendors and contractors for the project.

### **Disadvantages of Design/Bid/Build Approach**

1. The owner is responsible for controlling the interfaces and coordination among all the equipment and materials suppliers and the various construction contractors. This may be overwhelming and result in delayed schedules or in increased costs.
2. Total project costs cannot be confirmed until the final construction contract is completed.
3. Delays in completion of one contract may impact other contracts, resulting in potential additional project delays and/or costs to the owner.
4. There is no single responsible party to guarantee project cost, schedule, and performance.
5. Owner manpower and costs to coordinate and manage the interfaces among the construction contracts is increased over approaches that have a single contractor to handle such interfaces.
6. The owner is exposed to multiple contractor claims for impacted productivity, late delivery of owner-furnished materials, weather delays and labor disputes.
7. The owner is responsible for errors and omissions in design.
8. The owner has ultimate responsibility for site safety.

### **Design/Build Approach**

The terms Design/Build, EPC (engineer, procure and construct), and turnkey are generally synonymous and used to describe a project delivery approach in which the owner defines the project and then hires a contractor with total responsibility for the detailed engineering, procurement, construction, and coordination of all the project work. The owner carefully pre-qualifies bidders based on related project experience, bonding capability, safety record, etc. The owner prepares a specification for bid by three to five pre-qualified Design/Build teams. The bidder performs conceptual design and preliminary engineering to estimate the material quantities required for the project and obtains prices for equipment from suppliers. Construction pricing may be from the contractor's own experience or from quotations from potential subcontractors. The Design/Build contractor selects the equipment and construction subcontractors who provide the best value to the project from the Design/Build contractor's perspective while still meeting the requirements of the owner.

The Design/Build contractor self performs the detailed design or subcontracts it to an engineering firm. The Design/Build contractor is the general contractor. Typically, the contractor's strategy is to purchase equipment and material directly from the supplier eliminating subcontractor markups. The Design/Build contractor will contract directly with specialty contractors for the construction work not performed

by its own personnel. The scope of each subcontract is defined as clearly as possible to reduce the likelihood of change orders for the Design/Build contractor. The final project cost from the Design/Build contractor to the owner will include fees and expenses for providing the overall project management, accepting and managing project risks, and recovering the substantial cost of preparing the initial Design/Build proposals to the owner. In some cases, the markups and the fee can make the Design/Build contract more expensive than the Design/Bid/Build approach.

### **Advantages of Design/Build Approach**

1. The project cost and schedule can be defined very early in the project.
2. If the scope is well defined and the owner identifies its requirements in the Design/Build contract, there should be few, if any, change orders.
3. The owner can obtain guarantees on cost, schedule, and performance from a single responsible party.
4. Owners with limited staff to dedicate to the project can rely on the Design/Build contractor to coordinate each phase of the project. The owner can use its limited staff to monitor the contractor to confirm that the project meets the requirements of the contract.
5. The project schedule can be reduced due to close coordination of the design, procurement and construction activities by the Design/Build contractor allowing the owner to better define the project prior to issuing EPC bid documents.
6. Design/Build contractors may have innovative approaches that are less costly than the owner's standard practices and may meet the owner's requirements at a reduced cost.
7. All contractual disputes between the Design/Build contractor and the subcontractors are the direct responsibility of the Design/Build contractor.
8. Relatively large penalties in the form of liquidated damages can be established to motivate the Design/Build contractor to complete the project on schedule.
9. Lower material and equipment costs may be passed through to the owner during the bidding process due to the volume buying power of the Design/Build contractor.

### **Disadvantages of Design/Build Approach**

1. The Design/Build contractor receives an additional fee for managing and accepting project risks and higher exposure to risks lead to higher pricing.
2. The contingency included in a Design/Build price depends on the level of detail in the bid documents, project schedule, difficulty of construction and unknowns. To limit the amount of contingency in the Design/Build price most of the unknowns, such as subsurface or environmental risks, need to be defined prior to issuing the bid documents. Well-defined subsurface conditions also reduce owner exposure to change orders.

3. The owner generally does not select the equipment supplier. The Design/Build contractor will generally solicit bids from owner-specified vendors and select equipment with the lowest initial cost. Performance specifications that consider life cycle costs must be part of the initial bid package. Some owners may take bids on specialized equipment and then assign those contracts to the Design/Build contractor. This allows the owner to select this primary equipment and still obtain overall system guarantees.
4. Generally the owner is not involved in the detailed design decisions and has very limited time, if any, to review design drawings.
5. Scope and schedule need to be clearly defined very early in the project. Changes in scope or schedule after award will most likely cause the Design/Build contractor to revise the price of the project.
6. The owner will receive the contractor's standard drawing formats unless otherwise specified in the bid documents. The owner may also not receive detailed documentation, calculations, or manuals, since the engineer typically only produces those documents necessary for construction of the project.

### **Program Management Approach**

The Program Management approach provides for meeting all an owner's project delivery needs related to a large and complex effort involving the construction of multiple facilities over a several year period. The owner may choose to use internal resources for program management or, if the owner has limited resources, the owner may hire an outside resource as program manager. The program manager can be a construction general contractor or a consulting engineer, in which case, the program manager is commonly referred to as the owner's engineer. The program manager is an agent of the owner and serves as a single point of management for the entire process of completing the project(s).

The program manager provides detailed managerial support and added technical value to the owner and is normally involved in the earliest stages of a project. A program manager offers current planning methodologies, public involvement and testimony capabilities, design expertise, knowledge of construction methods and pricing, an understanding of competitive market conditions, and effective scheduling and cost control systems. Program management is successful when the project's planning, permitting, design and construction phases are effectively integrated into a single process. The program manager can deliver a project(s) with consistently successful results in several areas of measurement over the course of several years by developing an overall master plan for the project(s). The master plan might include such tasks as:

- Develop the program goals, objectives, and priorities.
- Provide for the integration of all program components and functions by responsibility, including administrative, regulatory, financial, architectural, engineering, construction, procurement and operations.
- Provide an organizational chart.
- Provide a directory of team members, with locations, telephone, and fax numbers.

- Describe the relationships between the program management staff and the owner as well as future consultants, contractors, construction managers, facilities users, government agencies, interveners and any other groups.
- Describe the key program management tasks and establish the procedural basis for executing program management functions.
- Establish state-of-the-art management controls to effectively manage time, quality, costs, and resources to achieve a high level of performance.
- Establish communications procedures, information document flow and data base management procedures.
- Define program-wide standards, policies, and procedures.
- Define program public information and coordination requirements.
- Identify the approvals and timing required.

Program management still requires that designs are completed, materials are procured and transmission lines and substations are built. The program manager may recommend either the Design/Bid/Build approach or the Design/Build approach for each individual project within the construction program.

### **Advantages of Program Management Approach**

1. This approach provides comprehensiveness and continuity of services for the owner with staff or a third party overseeing the entire process from project planning to project closeout.
2. The owner has more control of the design and construction processes throughout the project. The program manager provides timely cost and schedule information to the owner allowing informed decisions on cash flow and accurate information to executives, the public and regulators.
3. The owner can avoid hiring additional staff for specific project-related functions. The program manager can easily increase or decrease resources on the program applying specific resources when and where they are needed to maintain project objectives.
4. The program manager provides current knowledge of design and construction resources, material vendors and best practices. Program managers typically are involved in the largest, most complex projects in the country and the world. They bring a unique perspective and understanding to the owner.
5. Bid packages for engineering, materials and contracting can be staged based on project needs such as outage windows, financial objectives, seasonal weather, permitting requirements and environmental restrictions.
6. The program manager can be provided with penalties or incentives to maintain schedule and budget.

### **Disadvantages of Program Management Approach**

1. The program manager assumes no contractual responsibilities for design or construction. Contracts for engineering, materials and construction labor are held and maintained by the owner. Contract terms and conditions must contain strong enforcement language that allows the program manager to maintain budgets and schedules.

2. A strong working relationship between the owner and the program manager is paramount to success. Early involvement in the program develops trust and confidence between the program manager staff and the owner's staff. A keen understanding of the critical internal and external issues related to the project is fundamental for success.
3. The program manager must rely on the owner for key decisions that impact the project budget and schedule. Regular, documented communication is required.

### **Current Mega Project in the United States**

A mega project, or program, is defined by a capital cost over \$1 Billion and an implementation schedule of several years. Several programs meet these parameters to include: the Middletown-Norwalk Project, the New England East-West Solution Project, the TrAIL Project, the Susquehanna to Roseland Project, the Tehachapi Project, the Gateway West Project, the PATH Project, the Maine Reliability Project and the Baseload Project. Programs are underway or recently completed using the following delivery methods:

#### **A. Northeast Utilities (<http://www.nu.com/>) Middletown-Norwalk Project**

The Middletown-Norwalk Transmission Project involves construction of nearly 70 miles of new overhead and underground 345-kilovolt transmission line.

The project is among the largest transmission capital projects ever constructed and is the first project to include a program management role in the power delivery industry. It will use more 345-kilovolt cross-linked polyethylene (XLPE) underground conductor cable than has previously been installed on any other single project in the country.

This project is using Program Management under a Program Manager of Choice contract with Northeast Utilities. The successful PMOC was Burns & McDonnell ([www.burnsmcd.com](http://www.burnsmcd.com)). Burns & McDonnell is responsible for permitting, design, procurement, construction management, right-of-way acquisition, environmental issues, community relations, and document control. The project is energized and won the Utility Automation/ T&D 2008 Project of the Year and Engineering News Record's Energy Project of the Year.

#### **B. Northeast Utilities New England East-West Solution Project**

New England East-West Solution (NEEWS) is four related transmission projects developed by a working group of planners from Northeast Utilities, National Grid and ISO-New England.

The problems were identified by ISO-New England (<http://www.iso-ne.com/>) in its regional planning process. They are:

- Limitations to east-west movement of electricity on the New England power grid

- Weaknesses in transmission around Springfield, MA, a major interstate transmission hub
- Limitations to moving electricity across Connecticut, Massachusetts and Rhode Island
- Rhode Island's dependence on single transmission lines or autotransformers for reliability
- Limitations to the power that can flow from east to west within Connecticut

Each of these problems poses a threat to the reliability of electric power in southern New England and the region overall. These problems also negatively affect our ability to benefit from access to cleaner, competitively priced electric power.

This project is using Program Management under a Program Manager of Choice contract with Northeast Utilities. The successful PMOC is Burns & McDonnell.

#### C. Allegheny Power's TrAIL Project (<http://www.aptrailinfo.com/>)

The PJM board (<http://www.pjm.com>) has approved a five-year program designed to maintain the reliability of the transmission grid in the Mid-Atlantic region. The plan, includes construction of approximately 210 miles of 500-kV transmission lines within Allegheny's service territory.

Specifically, the plan calls for construction of a new 500-kilovolt (kV) line extending from southwestern Pennsylvania to existing substations at Mt. Storm, W.Va., and Meadow Brook, Va., and continuing east to Dominion Virginia Power's Loudoun Substation. The plan incorporates portions of Allegheny's proposal that was submitted to PJM as the Trans-Allegheny Interstate Line.

A preliminary estimate of Allegheny's portion of the expansion is in excess of \$850 million.

Line mileages by state: Maryland—10 miles, Pennsylvania—40 miles, Virginia—40 miles and West Virginia—120 miles.

The Trans-Allegheny Interstate Line (TrAIL) (<http://www.aptrailinfo.com/>) will extend from Southwestern Pennsylvania (37 miles) to West Virginia (114 miles) to Northern Virginia (28 miles). Dominion Virginia Power will build the line from an interconnection point east of Allegheny's Meadow Brook substation near Middletown, Va. to its Loudon Substation. About 36 miles of the 500-kV line in Southwestern Pennsylvania are needed to serve local demand in Greene and Washington counties.

This project is using an open book EPC delivery method with a management fee paid on milestones achieved through the life of the project. Successful contractor is Kinney Construction.

#### D. PPL's and PSE&G's Susquehanna to Roseland Project

In June 2007, PSE&G ([www.pseg.com](http://www.pseg.com)) announced plans to invest nearly \$1 billion to construct new transmission lines to keep up with increasing demand and to ensure continued reliability. The Susquehanna to Roseland line is the first of three proposed PSE&G projects to be approved by PJM. This new 500,000-volt line will run from PPL's Susquehanna substation near Berwick, Pa., to PSE&G's substation in Roseland, NJ. The entire line will be about 130 miles long. The New Jersey portion of the line will be 40-50 miles long.

On August 5, PSE&G selected the preferred route for the new Susquehanna-Roseland power line. This decision was based in part on a detailed study performed by a New Jersey-based siting contractor with national experience on projects such as this ([read the routing report](#)). PPL Electric Utilities (PPL) also announced the selection of this route as the best pathway for this new line. In addition to the placement of new towers and lines, PSE&G also will construct two new substations -- one in Jefferson Township, Morris County and another at its existing property in the Roseland/East Hanover area.

Based on a number of critical factors, PSE&G has determined that this route is the best choice for the project because it:

- Would be constructed entirely within an existing 230,000-volt (230kV) transmission right-of-way, which already contains transmission structures and wires, for its entire length in New Jersey. This minimizes the impact to the environment, requiring no construction on virgin right-of-way and minimal clearing of vegetation.
- Crosses the least amount of wooded wetlands and forested lands, and has the least potential to permanently alter these important habitats.
- Has the least impact on aesthetics where the line will be built and provides the least environmental, engineering and construction challenges.

On January 12, PSE&G submitted its application to the New Jersey Board of Public Utilities (<http://www.state.nj.us/bpu/>) to construct the Susquehanna-Roseland power line. PSE&G's partner in this project, PPL Electric Utilities, also filed an application for approval with the Pennsylvania Public Utilities Commission (<http://www.puc.state.pa.us/>). We expect that the BPU will issue a decision regarding this project later this year. The BPU process will include public meetings and hearings.

During the review period, PSE&G will conduct final design work to determine the location of each of the new structures and temporary access roads, as well as other construction details.

In addition to the BPU review process, the project will undergo environmental review by all government agencies with jurisdiction.

The line is expected to cost between \$1.2 billion and \$1.3 billion. The New Jersey portion will cost approximately \$750 million, which includes construction of new substations in Northern New Jersey. The cost will be shared by the 51 million electric customers in the PJM region, which includes 13 states and the District of Columbia.

The Pennsylvania portion of this project is using Program Management under a contract with PPL. The successful Program Manager is Burns & McDonnell. The New Jersey portion of this project is proposed for Program Management and PSE&G is in the process of evaluating proposals.

#### E. Southern California Edison's Tehachapi Project

Southern California Edison Company (SCE) ([www.sce.com](http://www.sce.com)) is proposing to construct the Tehachapi Renewable Transmission Project (TRTP) ([www.sce.com/PowerandEnvironment/Renewables/Wind/](http://www.sce.com/PowerandEnvironment/Renewables/Wind/)) to provide the electrical facilities necessary to interconnect new wind turbine based electrical generation in excess of 700 megawatts (MW) and up to approximately 4,500 MW from the Tehachapi Wind Resource Area (TWRA). The TWRA has been identified as the richest wind resource area in California. The proposed TRTP would consist of a series of new and upgraded high-voltage transmission lines (T/L) and substation facilities to deliver electricity from new wind farms in eastern Kern County, California, to the Los Angeles Basin.

The Tehachapi Renewable Transmission Project (TRTP) Segments 1 to 3 is a series of new and updated electric transmission lines and substations that will deliver electricity from new wind farms in the Tehachapi area to SCE customers and the California transmission grid. TRTP is a vital part of meeting California's renewable energy goals. The California Public Utilities Commission (CPUC) approved project Segments 1 to 3 in March 2007 and construction is now underway.

The proposed TRTP consists of eight segments enumerated as Segment 4 through Segment 11. Proposed Segments 4, 5, and 10 that would involve upgrading and expanding SCE's transmission system north of SCE's Vincent Substation in order to integrate TWRA wind generation to SCE's electric system. Proposed Segments 6, 7, 8, and 11 would involve upgrading and expanding SCE's transmission system south of SCE's Vincent Substation in order to deliver TWRA wind generation to SCE's load centers in the Los Angeles Basin. Segment 9 would involve building a new substation (Whirlwind Substation in Kern County), expanding two existing substations (Antelope and Vincent substations), and upgrading three substations (Gould, Mesa, and Mira Loma substations) (refer to Figure ES-1).

Southern California Edison (SCE) has chosen to use a modified form of Program Management called Owner's Agent for the TRTP 123 and TRTP 4-11. Unlike Program Management, the SCE version of Owner's Agent does not allow for right-of-way acquisition, the procurement major equipment or the performance of detailed design work. SCE has a significant staff and the services of several large A/E firms to support this effort. The successful Owner's Agent is Burns & McDonnell

#### F. Idaho Power's Gateway West Project

Idaho Power's ([www.idahopower.com](http://www.idahopower.com)) Gateway West project will supply present and future needs of customers and improve electric system reliability in the service territories of both companies. In addition, the project will enable delivery of new generating resources, including wind, to more customers in the region. Known as Gateway West, line segments are scheduled to be completed in 2014. At certain times of high customer demand, transmission lines reach full capacity. Idaho Power and Rocky Mountain Power are committed to ensuring reliable electric service to customers and respond to others requesting use of the transmission system. Work has begun to complete this project in the next five to seven years.

The companies are proposing to construct, operate and maintain approximately 1,150 miles of new 230 kilovolt (kV) and 500 kV electric transmission lines between the planned Windstar Substation near Glenrock, Wyoming to the planned Hemingway Substation near Murphy, Idaho.

This project is using the EPC method of project delivery. Power Engineers has been hired as the Owner's Engineer to prepare the EPC bid package.

#### G. AEP's PATH 765kV Project

AEP's ([www.aep.com](http://www.aep.com)) PATH project will employ advanced transmission technologies to make it the most reliable, efficient and environmentally sensitive project possible. Extra-high voltage transmission inherently costs less and requires less land to carry the same amount of power than other transmission designs, and new 765-kV designs reduce line losses 40 percent over older designs. That means the PATH line will transport electricity more efficiently and reduce the power generation necessary to meet electricity demand. Additional advancements in 765-kV and 500-kV conductor designs and new control technologies in the project's substations also will enhance the reliability and efficiency of the PATH lines compared with other transmission lines.

The PATH project includes approximately 244 miles of 765-kV extra-high voltage transmission from AEP's Amos substation near St. Albans, West Virginia, to Allegheny's Bedington substation, northeast of Martinsburg, West Virginia. Another 46 miles of twin-circuit 500-kV transmission will be constructed from Bedington to a new substation to be built near Kemptown, southeast of Frederick, Maryland. The total project is estimated to cost approximately \$1.8 billion. AEP's estimated share of the project is approximately \$600 million.

This project is using the design/bid/build method of project delivery. AEP is using internal design resources on the 765kV transmission and will contract for outside construction services once they obtain the needed permits to construct.

#### H. Maine Power Reliability Project

The Maine Power Reliability Program ([www.maine-power.com](http://www.maine-power.com)) includes a proposal to build a new, 345-kilovolt (kV) transmission line from Orrington, Maine (15 miles south of Bangor), to Newington, New Hampshire. The line will follow existing transmission corridors through nearly 80 Maine towns, including Detroit, Benton, Windsor, Lewiston, Yarmouth, Gorham, and Eliot. The program includes investments in new substations, upgrades to existing substations, and improvements to the 115-kilovolt (kV) electric system in central Maine.

The Maine Power Reliability Program began in January of 2007 with a study to project the region's future needs for electricity service. The first phase of the study, which was completed last summer, found that serious problems would emerge as early as 2012 without significant changes in demand patterns, transmission capacity, or new supply. The proposal includes transmission investments and recommendations to encourage alternatives to transmission, such as new generation, or programs to manage the growth in peak electricity demand.

CMP prepared its plan in conjunction with neighboring utilities in Maine and New Hampshire with oversight by ISO New England ([www.iso-ne.com](http://www.iso-ne.com)), the organization responsible for managing electricity supply and transmission for the New England states.

The preferred route calls for the construction of an additional 345kV transmission line following existing transmission corridors from Orrington to the Maine-New Hampshire interconnect in Eliot (Orrington-Detroit-Benton-Windsor-Lewiston-Gorham-Eliot-Newington, NH). CMP is also planning to build several new 115kV lines and upgrade others on existing corridors.

This project is using the Program Management approach. Central Maine Power (<http://www.cmpco.com/>) has very limited staff and has selected Burns & McDonnell as the successful Program Manager.

#### I. Progress Energy Florida's Baseload Project

Progress Energy Florida ([www.progress-energy.com](http://www.progress-energy.com)) is considering adding about 200 miles of transmission lines across nine counties to maintain reliability and to move energy efficiently to customers throughout the region and state. The lines would be 230 and 500 kilovolts (kV).

Transmission lines are planned in three main segments: from Levy County south to Hernando County, from Pinellas County east to Kathleen in Polk County, and from Levy County east to the Wildwood/Leesburg area. These proposed transmission lines could affect the counties of Citrus, Hernando, Hillsborough, Lake, Levy, Marion, Pinellas, Polk, and Sumter.

The transmission lines are expected to be built on two types of structures. Typically, the single steel poles are between 90 and 165 feet tall; the H-frame (two-pole)

structures about 120 feet tall. The structures would be spaced 700 to 1,300 feet apart, depending on the structure and terrain.

This project is using the EPC and Program Management approach. Progress has hired Patrick Engineering as an Owner's Engineer to prepare 500-kV standards and EPC bid packages. In addition, Progress plans to hire a Program Manager to handle construction management, inspection, budgeting, scheduling, public relations and more. The current plan is to allow the future Program Manager the opportunity to bid on the EPC work.

---

## 345 kV High Ampacity OH/UG Project

<sup>1</sup>Dana R. Crissey

<sup>1</sup>Oncor Electric Delivery, LLC, Transmission Line Engineering Department, P.O. Box 970, Ft. Worth, TX 76101-0970; (817) 215-6266; drcrissey@oncor.com

### ABSTRACT

When TXU Electric Delivery (now known as Oncor Electric Delivery) filed a CCN application with the Public Utility Commission of Texas (PUCT) in 2006 it planned to construct a new 345 kV line approximately 6.5 miles long on single pole structures. During the PUCT's review of the application the City of Dallas intervened in the process and requested that a portion of the line be constructed using UG technology.

The new line was necessary to provide additional capacity and reliability to the Dallas Central Business District. The circuit needed to be rated at 3400 Amperes. After much deliberation, the PUCT ruled that Oncor should construct a 0.7 mile segment of the line underground.

Thus began the first 345 kV underground project on the Oncor system. There are a number of 345 kV underground projects in service throughout the United States but none with a dynamic rating capability near the 3400 Ampere range required for this project. Selecting the correct technology and materials and developing a design to properly implement them has presented engineering (and political) challenges that Oncor will not soon forget.

The line is currently under design and will be constructed Spring through Fall of 2009.

### Background

In March, 2006 Oncor Electric Delivery filed an application for a Certificate of Convenience and Necessity (CCN) with the Public Utility Commission of Texas (PUCT) to construct the W. Levee-Norwood 345 kV line. The line would consist of two 345 kV circuits, with one circuit installed initially and the second as system needs dictated. The line would connect two existing major switching stations and was necessary to provide additional capacity and reliability to the area near downtown Dallas. As required in the filing Oncor had selected preferred and 10 alternate routes between the two existing stations.

During the PUCT review of Oncor's application a number of parties exercised their right to intervene and become a part of the regulatory process, including the City of Dallas. The City desired to modify the route of the line and also requested the PUCT to direct Oncor to construct a portion of the line using underground technology instead of overhead. The City contended that an underground line in the area near downtown would be more aesthetically pleasing and that a portion of the route was

subject to near term development plans due to the City's proposed Trinity River Project which had been approved by voters in a May 1998 bond election. The City of Dallas also offered to reimburse Oncor for 25% of the difference between cost of the installed underground line and what the overhead alternative would have cost.

The PUCT agreed with the City's proposal and directed Oncor by a 2-1 vote to construct a 0.7 mile section of the line underground. The remainder of the line would be constructed utilizing over methods but a large portion of the line would be built within the median of Irving Blvd., a major arterial street.

Thus began a process that is currently entering the construction phase and is scheduled to be complete by December 2009.

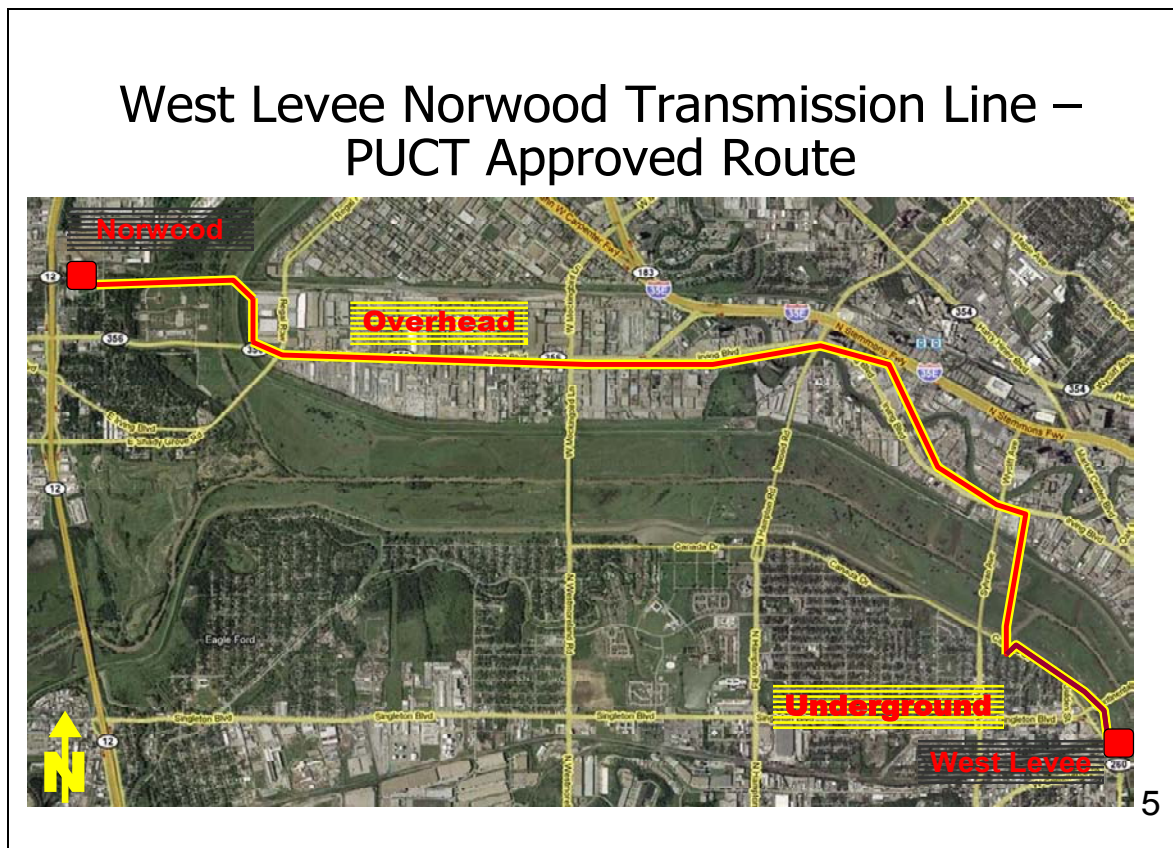


**Figure 1.** Project Route

#### **345 kV Underground Design Requirements**

As mentioned previously, the purpose for the construction of the line was to provide increased capacity and reliability to the area near downtown Dallas. The line was proposed to have a minimum dynamic rating of 3400 Amperes per circuit. This would not have been an issue if the line had been constructed by overhead methods. The overhead conductor, twin bundled 1590 kcm ACSR, Falcon, has a rating of 3412 Amperes based on Oncor's loading criteria.

In order to keep from having to de-rate the load transfer capability of the new circuit, the new underground circuits would need to provide the ability transfer the same load, 3400 Amperes.

Oncor has approximately 60 circuit miles of underground transmission line in its system, all at 138 kV. Industry contacts at other utilities and other sources identified a number of applications at 345 kV both in the United States and abroad but none at the 3400 Ampere capacity required for this project.

Oncor decided to seek outside engineering expertise to assist in the design and construction management areas of the project. Oncor developed a Request for Proposals from multiple firms qualified in this area of design. The RFP included an evaluation of the two most prevalent underground cable technologies, extruded cross link polyethylene (XLPE) solid dielectric cable systems and conventional high pressure fluid filled (HPFF) pipe type systems.

After a detailed and thorough evaluation of the proposals submitted by the design firms, Oncor selected Power Engineers, Inc. to provide design, material evaluation, construction management and support services for the project. The decision was also made to proceed with a conventional HPFF underground system. The decision was based primarily on the following items:

- The suitability and robust nature of the HPFF underground system for use on a high capacity (3400 A.) through flow transmission line like this project.
- Total installed cost analysis for this project, including associated pressurization systems and cathodic protection systems.
- Oncor's operating experience with existing HPFF underground systems on its transmission system.

## Materials

The various materials required for use on the underground line were evaluated with respect to the project design requirements. The major items selected for use on this project are listed below with a brief discussion of reasons for their selection:

- Conductor: 3-3500 kcm Copper, Compact Segmental PPP Laminate Insulated cables per phase
- Pipe: 10" ID steel with flared ends ASTM A523
- Coatings: Liberty Coating Pritrec 10/60 Extruded Polyethylene
- Dielectric Fluid: Polybutene Insulating Fluid ASTM D 1819 84
- Thermal Backfill: Fluidized Backfill RHO of 60 thermal ohms or less

## Design

The route of the underground section of the line was determined by the PUCT. It followed a path North from the W. Levee Sw. Station crossing under Singleton Ave., a major arterial street leading into downtown Dallas, and continued under the pavement of the South/West bound lanes of Canada Dr. The final design of the underground line section turned out to be approximately 0.9 mile in length.

This route posed two immediate problems (opportunities) for the designers. The first issue was to determine how to cross Singleton Ave. After consultations with the City it was determined that Singleton Ave. could not be closed continuously for term of construction activities in this area. It was decided that the use of directional drilling technology would be the best solution to install the UG circuits across this street.

The second issue was to determine how to install the circuits under Canada Dr. The City agreed that portions of Canada Dr. could be closed for periods of time adequate for conventional open-trench construction. This would allow the use of more readily available construction equipment and would also reduce the construction window significantly for that portion of the line.

Each cable trench is designed with a number of specific features. The HPFF steel cable pipes are located parallel and approximately 3 ft. on center. Each pipe is placed near the bottom of the trench on a sand bag cushion at a depth of approximately 4-4.5 ft. Each HPFF pipe has a 1" PVC temperature monitoring duct attached to the pipe surface. The trench also includes a 4" diameter oil supply line pipe and a 4" PVC communications duct. A 1 ft. protective layer of low compression strength Fluidized Thermal Backfill (FTB) material is placed around and over the steel pipes and ducts to aid in the transmission of heat away from the HPFF pipes. The FTB material contains a red dye to aid in the prevention of dig-ins after the underground lines are in-service. A 6" layer of 3000 psi concrete is then placed on top of the FTB material to further protect the underground system. The trench is then backfilled with layer of compacted native material to the elevation of the street sub-grade. A typical cross-section is shown below:

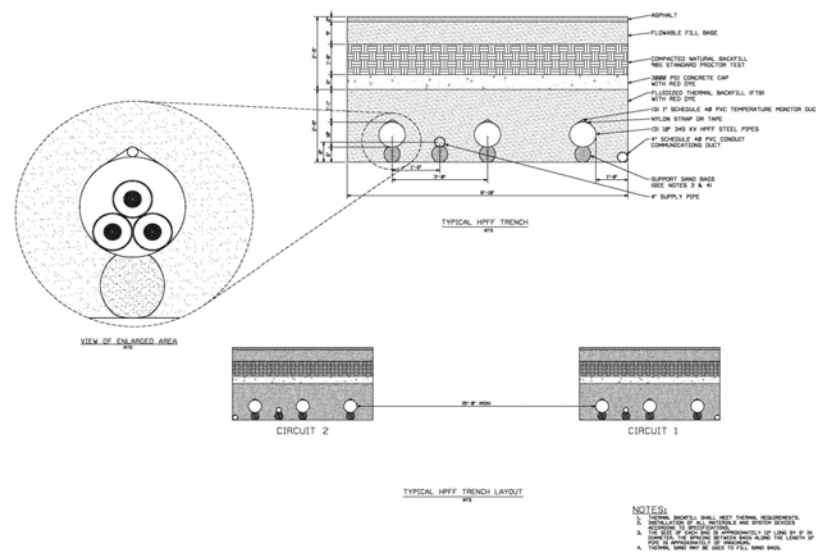


**Figure 2.** Pipe Layout in Trench

The proposed line has also been designed with a Dynamic Thermal Monitoring System (DTS) with the capability to continuously monitor the thermal characteristics of the entire line segment via fiber optic cable. This system provides Oncor the capability to dynamically rate the capacity of the line on a real time basis based on the changing thermal conditions of the line.

The line is also equipped with a leak detection system with the capability to continuously monitor and detect leaks as small 3 gallons per hour within a 24 hour period. The system also includes flow rate indicators, cumulative flow indicators, temperature data from the cable system and the earth, and load information from the substation feeder.

### Construction

The design of the underground section of the line was completed in September 2008 and Oncor issued a Request for Proposals from two potential contractors to construct the line and provide many of the required material including:

- UG Cable
- Pumping Plant and Pressurization Control System

In a move to ensure the availability of the specialized HPFF steel pipe required for this project Oncor had previously purchased the pipe and made arrangements to have the coating applied. Oncor also made plans to acquire the 18 overhead to underground terminations from G&W Electric Company due to the long lead time (30 week) for this product.

In October 2008 Oncor selected Prysmian Power Cables and Systems, LLC as the primary construction contractor for the project. Prysmian had a long working history with Oncor on many HPFF underground systems installed on its transmission system.

Construction began on the underground section of the line in February 2009 with the installation of six (6) directional drill bores, each approximately 600 ft. in length in the section under Singleton Ave. Construction of the open-trench section under Canada Dr. began in late April 2009 and continues at this time with a proposed completion date of October 2009.



**Figure 3.**

Directional Drill Section - 10" Pipe being lifted and aligned in preparation for back pull through bore hole.

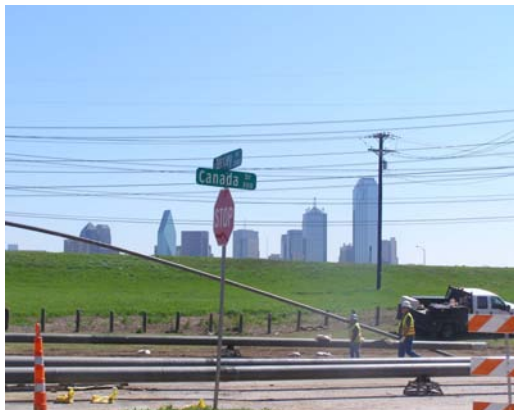


**Figure 4.**

Directional Drill Section - 10" pipe in final position. City of Dallas skyline in background.



**Figure 5.** 2 kV "jeep" testing of coated pipe.  
Searching for voids in coating



**Figure 6.**

Directional Drill Section – 10" HPFF and 4" Oil Supply Line Yoked for back pull through bore hole.



**Figure 7.**  
Directional Drill Section – Jetted rotating mandrel begins back pull through bore hole.



**Figure 8.**  
Transition Section – Directional Drill to  
Pipe in Trench Section



**Figure 9.**  
Transition Section – FTB Placement

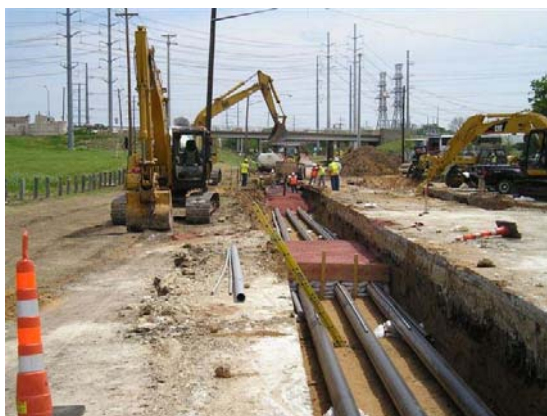


**Figure 10.**  
Pipe in Trench Section – FTB Placement



**Figure 11.**  
Trifurcating Manholes at Topeka

Telegram Channel: @Seismicisolation



**Figure 12.**  
Trifurcating Manholes at Topeka

### 345 kV Overhead Design Requirements

The overhead section of the W. Levee-Norwood 345 kV line is approximately 6.5 miles in length and is designed as a double circuit line is designed to have a minimum dynamic rating of 3400 Amperes per circuit. Only one 345 kV circuit will be installed initially. The line is designed to utilize twin bundled 1590 kcm ACSR, Falcon conductor per circuit with one 7/16" EHS Steel 7 Strand shield wire and one 24 Fiber OPGW fiber-optic ground wire. The majority of the line is supported on double circuit 345 kV structures with provisions for one future 138 kV circuit in an underbuilt position. The underbuilt 138 kV circuit will be installed in the line section to be built in the median of Irving Blvd. The 345 kV circuits are configured in a vertical position with the 138 kV circuit in a horizontal position.

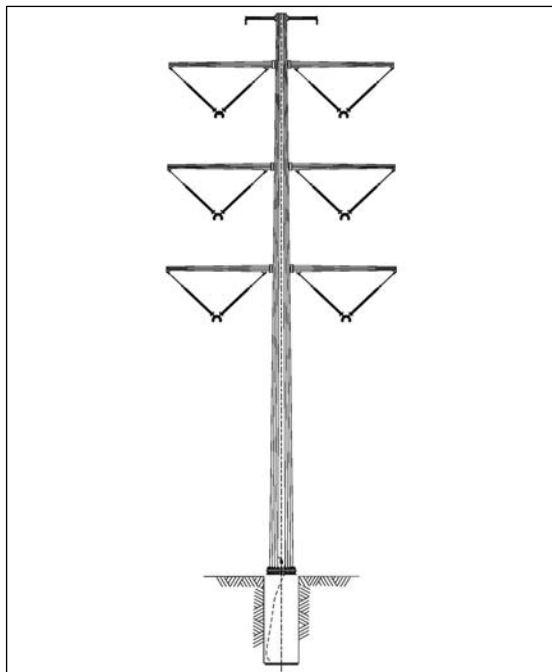


**Figure 13.**  
345 kV Double Circuit  
Tangent Structure

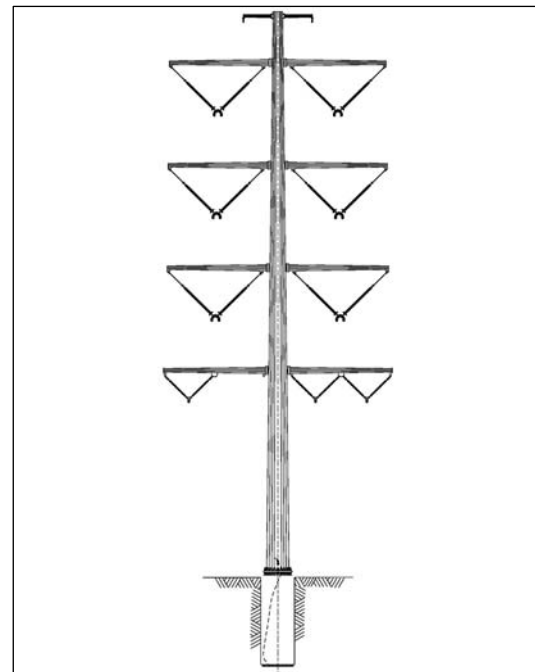


**Figure 14.**  
345 kV Tangent Structure  
w/138 kV Underbuilt Circuit

Due to the line route, structure heights and conductor loadings, galvanized tubular steel structures with base plates and anchor bolts were selected for use on this line.

### Line Design Issues

The route selected by the PUCT posed a number of challenges to the design and successful construction of the overhead section of the project:

- An approximate 2.1 mile segment of the Irving Blvd. route was designated as State Highway 356 and was under the control of the Texas Department of Transportation (TXDOT). TXDOT prohibits the placement of transmission line structures inside highway right-of-way.
- Approximately 1.2 miles of the line lie within the levee system of the Trinity River. This segment required permits from the US Army Corps of Engineers (USACE). These line segments also required an easement from the City of Dallas since the area inside the levees are designated as recreation area by the City.
- The entire 4.9 mile segment inside the median of Irving Blvd. required approval from the City for any modifications to the existing medians and street required to create a space to place the proposed transmission poles.
- The City of Dallas, TXDOT and the North Texas Tollway Authority (NTTA) were in the design phase of a new Sylvan Ave. bridge across the Trinity River and the new Trinity Parkway toll road parallel to the river. The new bridge is to be located approximately 160 ft. west and parallel to the proposed route of the new transmission line. The bridge construction will not take place until 2010-2012 and therefore required close coordination between Oncor, the City, TXDOT and NTTA to ensure proper structure placement to eliminate conflicts with the construction of the future bridge and parkway.
- There are three 138 kV lines that the new line is required to cross. One of these is located within the levee footprint and the existing structure can not be relocated and changed out or lowered to make a crossing easier to achieve.
- Although the vast majority of the overhead section of the line is located on public property, the route crosses four pieces of private property and will require the acquisition of easements from these owners.
- The route crosses one railroad and thus requires the acquisition of a crossing permit from the railroad.

A number of the pending issues were not of a design nature and Oncor was responsible for coordinating with the City of Dallas, TXDOT, NTTA and the USACE to reach a favorable resolution of those issues.

First, the City of Dallas and TXDOT began negotiations to transfer the ownership and thus the operating and maintenance responsibilities for the Irving Blvd. section of SH 356 to the City of Dallas. These negotiations also were expanded to include the City of Irving regarding a section of SH 356 that was located within the city limits of Irving. As it turned out when TXDOT and the cities reached agreement it was

discovered that the transfer would also require the approval of the Texas Attorney General and finally the Governor. These negotiations were successfully consummated in January 2009 when Texas Governor Rick Perry signed an order finalizing the transaction.

Oncor was required to prepare and submit a crossing permit to the US Army Corps of Engineers (USACE) for two crossings of the East Fork of the Trinity River. At these locations, all structures were designed to be outside of the USACE's "zone of concern" with respect to the levees. The USACE has heighted the review of structures that penetrate the footprint of the levees since Hurricane Katrina in 2005. At present time, the USACE's review of Oncor's submittal is in progress.

Oncor was also required to obtain an easement from the City of Dallas for the same Trinity River crossing since the City is the owner of the property and operates the Trammell Crow Park and Lake. Oncor prepared an easement submittal package and submitted it to the Dallas Park Board for their action. The Park Board held a public meeting and approved and forwarded their recommendation to the Dallas City Council for final action. The City Council approved the Park Board's recommendation and authorized granting the easement in June 2008.

### **Overhead Line Design**

Oncor engaged the services of M&S Engineering, Inc. to perform the line design, assist in the material evaluation, assist Oncor in the preparation of permit applications for submittal to the USACE, City of Dallas and the applicable railroad, design street modifications and assist in the construction management activities on this project.

M&S Engineering began to immediately address the remaining issues affecting the design of the line. They began working with the LIDAR data and began preliminary structure spotting followed by site visits to resolve conflicts with the numerous overhead utility crossings.

After preliminary structure locations were developed, meetings were scheduled with the City of Dallas to resolve issues where modifications to the road median would be required to enable the placement of a structure. The Public Works & Transportation Department of the City of Dallas worked with Oncor to finalize the design of the required street modifications. Final construction plans for the street modifications were approved by the City in June and construction is scheduled to begin in early July 2009.

The crossing of the three existing 138 kV lines was the next issue that had to be resolved. Two of the crossings were resolved by changing out existing double circuit structures with multiple shorter single circuit concrete poles and removing the shield wires in the crossing span. The third crossing was more of a problem. As stated previously, the existing structure was located within the levee template and could not be replaced by a new shorter structure. It was decided to design a replacement for the bottom conductor arm to support two phases and lower the top phase and shield wire

to the next lower arm positions. This work enabled the new 345 kV poles crossing the 138 kV line to be 20 ft. shorter and avoided the FAA requirement to install aviation lighting on structures.

The remaining line design issues were completed in early June 2009 and a pre-construction meeting for the project was held on June 17, 2009.

### **Construction**

The design of the overhead section of the line was completed in March 2009 and Oncor issued a Request for Proposal from potential vendors to provide the major items of material required for the line. The following is a list of the vendors selected and the items they are providing:

- FWT, Inc. - Tubular Steel Poles
- Southwire, Inc. – ACSR Conductor
- MacLean Power Systems, Inc. – Insulator Assemblies
- Hubbell Power Systems, Inc. – Insulator Assemblies
- Brugg Cables, LLC – Fiber Optic Cable

Oncor began geotechnical investigations for the structures located outside of the levee system in May 2009. The geotechnical investigations were conducted by TEAM Consultants, Inc. The USACE also approved the boring plan for the structures located inside the levees in late May. The geotechnical investigations at all accessible sites were completed in June 2009.

Oncor completed the design of the structure foundations for all accessible poles on June 24, 2009.

Oncor selected Chapman Construction Company as the primary construction contractor to construct the overhead segment of this line. Chapman began structure foundation construction in July 2009 and plans to begin the installation of structures during the Summer and conductor during the Fall 2009.

The project has a scheduled completion date of December 15, 2009.

## Integration of Optimum, High Voltage Transmission Line Foundations

Freeman Thompson, Nick Salisbury, Anwar Khattak, Aaron Hastings, Michael Foster

Thompson, Freeman, EIT, Design Engineer, Crux Subsurface, Inc., 16707 E. Euclid Ave., Spokane Valley, WA 99216; Phone (509) 892-9409, Fax (509) 892-9408, Email [fat@cruxsub.com](mailto:fat@cruxsub.com).

Salisbury, Nick, President, Crux Subsurface, Inc., 16707 E. Euclid Ave., Spokane Valley, WA 99216; Phone (509) 892-9409, Fax (509) 892-9408, Email [nick@cruxsub.com](mailto:nick@cruxsub.com).

Khattak, Anwar, PhD, Professor of Geotechnical Engineering, Gonzaga University, 502 E. Boone Ave., Spokane, WA 99258-0026; Phone (509) 313-3527, Fax (509) 323-5871, Email [khattak@gonzaga.edu](mailto:khattak@gonzaga.edu).

Hastings, Aaron, PE, Arroyo Engineering Consultants, Inc., 1328 Echo Creek, Henderson, NV 89052; Phone (702) 241-5339, Fax (702) 407-0531, Email [aec@aec-nv.com](mailto:aec@aec-nv.com).

Foster, Michael, PE, Supervising Transmission Engineer, Dashiell, LLC, 12301 Kurland Dr. Suite 400, Houston, TX 77034; Phone (713) 558-6660, Email [michael.foster@dashiell.com](mailto:michael.foster@dashiell.com).

### ABSTRACT

High voltage electric power transmission lines span various regions and geology, and with these variations in venue and subsurface conditions, comes the need for efficient foundation designs to control construction costs. In most locations conventional deep foundations prove to be economical for design and construction, and thus an optimum foundation system. In some locations, however, site conditions make conventional foundations too expensive or impractical, and micropile foundations become the prime solution.

Micropiles are often thought of as an emerging technology, even though they were conceived over 50 years ago and have been used in the United States for more than 30 years. The electric power transmission industry has recently discovered this “emerging technology” and is beginning to take advantage of it. As the need to transfer electricity from more remote locations continues to expand, the use of micropile foundations will become more common as a practical solution for the challenges encountered.

This paper will introduce and illustrate the basic advantages and disadvantages of both conventional and micropile foundations in this industry and how they are being integrated to provide design solutions. A brief history of the introduction of micropiles into this industry will also be discussed.

## INTRODUCTION

The paths of transmission lines include varying geographies: varying in terrain, subsurface conditions, environmental sensitivity, and accessibility. Approximately one third of the cost of each transmission tower/structure is beneath the ground surface and is never seen. The value of these foundations is of tremendous importance because remediation of a failed structure foundation incurs far greater cost than any other type of single-structure failure. Conventional deep foundations, which are cast-in-place drilled piers, are still the most economical solution for many structures, but when certain obstacles are encountered, micropile foundations become the most economical solution. These high costs, high values, and different foundation options elicit a closer look at this invisible portion of the structure.

## OBSTACLES

Efficient foundation design and construction are the major topics that will be discussed in this paper. One key to efficient design of proper foundations is the acquisition of accurate and adequate geotechnical and geological information of the tower sites, as this information greatly influences the foundation design requirements for each tower. An accurate geological survey requires quality survey data and supporting geotechnical information. A proper geotechnical investigation requires, among many things, access to critical locations on the site with small investigatory drills and associated equipment. Gaining such access is often an obstacle that can be very difficult and involve much more than will be discussed in this paper. It should be noted, however, that such access and permitting challenges will be similar or more stringent in the construction phase of the project, and the foundation design team should be aware of such obstacles.

Building transmission lines in remote areas brings about many constructability issues. Limited access can cause problems with getting equipment and material to the sites, which can increase time and cost. Some areas can be restricted such that no vehicular traffic is allowed to the structure sites at all. This can result in the need for hand digging foundations and/or blasting with explosives. This is where safety concerns increase tremendously in traditional construction techniques. Traditional foundations for deadend structures can extend to depths of 20 to 30 feet below grade. This introduces many safety concerns for hand-dug foundations. A typical 500-kV single circuit deadend structure can require up to 15 yards of concrete per leg. This requires approximately 60 helicopter trips with a single-yard concrete bucket. Clearly, this is both lengthy and expensive.

## INVESTIGATION

Geological and geotechnical investigation programs involve the study of the local terrain for stability and drainage, insitu tests such as standard penetration tests (SPTs), collection of disturbed and undisturbed soil samples, and pertinent laboratory

tests. Foundation design parameters are then estimated from the collected test data. The types of foundations chosen depend upon these geologic and geotechnical conditions identified, the tower loading, and various other factors, such as access constraints and environmental restrictions.

A limitation of typical geotechnical investigation programs is the number of locations that can be practically and economically explored during the design phase of the project. Typically, geotechnical borings are obtained at deadend locations and at least one per mile. This seems to be a commonly accepted practice, but leads to interpretation and conservatism in geotechnical properties to account for possible variations between boring locations.

After proper geological and geotechnical investigation programs have been performed and the respective reports and associated recommendations have been conveyed to the foundation designer, the final foundation design process begins. The final design considers the many different requirements and limitations, and finally produces foundations that satisfy all such controlling factors.

## CONVENTIONAL FOUNDATIONS

The design of conventional foundations (also called traditional foundations) often involves drilled-shaft-type deep foundations of sufficient size to support the specified structure loading in the worst expected geologic and geotechnical conditions identified or suspected in the geological and/or geotechnical reports and recommendations. These types of foundations are referred to as "conventional" (or "traditional") foundations for good reason: they have been effectively used for transmission structure foundations for the last century, and will continue to do so. Where both access is reasonable and subsurface conditions are favorable, conventional deep foundations are the optimum choice. An excepted limitation of a traditional foundation is that the loads supported by the foundation are usually too large to economically perform insitu testing to verify adequacy of the design. This causes additional factors of safety to be applied to the design to insure an adequate foundation. It also impedes the ability to streamline the design if soil conditions are better than expected.

## INTRODUCTION TO MICROPILES

Before discussing the benefits of micropile transmission structure foundations, the following is a brief introduction to micropile technology, which is still not well-understood by many and thus continues to be labeled as an "emerging technology."

Micropiles were conceived in Italy in the early 1950's, by Dr. Fernando Lizzi (Armour, T., et al., 2000). They were introduced into the eastern United States nearly 20 years later and have continued to grow in applicability and versatility for the last 30 years. A micropile is a small (about 4- to 12-inch-diameter) replacement pile -

versus a displacement pile, such as a driven pile. It is typically installed using a small drill (weighing 15- to 40-thousand pounds) and can be installed in virtually any geotechnical condition, from soft silts and clays to hard, igneous bedrock. During the drilling, the hole is stabilized (when necessary) using high grade steel tubing (casing), which is often extended behind the drill bit to the bottom of the hole. The drill steel and bit are then completely withdrawn from the fully-cased hole, a string of continuously-threaded rebar is inserted which extends the full length of the hole, and the hole is then tremie-filled with neat cement grout. The casing is withdrawn, exposing a portion of the micropile grout to the soil (this portion is called the bond zone), and leaving a portion of the casing in place around the upper portion of the micropile for connections and flexural performance. Figure 1 is an illustration of a typical composite micropile.

A typical composite micropile consists of these three main elements: a single strand of continuously-threaded rebar (bar) that extends the full length of the micropile in the center of the micropile; a design-specified length of steel tubing (casing) around the circumference that extends from the top of the micropile to a critical depth (about half the length of the micropile in Figure 1); and neat cement grout, encasing the bar, and bonding the micropile components together and to the geotechnical strata. Other ancillary components of the micropile include items such as couplers, which connect segments of bar to form a continuous element, and pvc centralizers, which position the bar in the center of the drill hole. Typical sizes of bar (nominal diameters) range from 1 to 3 inches, and typical strengths of such bar are 75,000 to 120,000 psi, minimum yield. Typical sizes of casing (outer diameter by wall thickness) range from 5 inches by 0.375 inches to 8-5/8 inches by 0.500 inches, with minimum yield strengths ranging from 45,000 to over 100,000 psi. Typical neat cement grout is composed of two primary elements: Portland cement and water, with 28-day unconfined compressive strengths ranging from 3,000 psi to more than 5,000 psi.

A single typical micropile can exhibit a capacity ranging from as little as 25 kips up to and exceeding 500 kips. While the lateral capacity of a single micropile is understandably limited, groups of appropriately arranged micropiles can support tremendous loading - both axially and laterally. The size, length, and configuration of micropiles are designed to accommodate the magnitudes and proportions of the different loading (axial loading, base shear, and overturning moment) on a project-specific basis.

Micropiles are not inexpensive foundation elements, nor is their cost as volatile as that of traditional foundations when limitations are imposed on access and/or construction procedures. Such limitations highlight the clearest benefit that micropiles can provide. The construction techniques for micropile installation are refined and controlled enough to satisfy many environmental concerns and still retain flexibility to meet higher, project-specific construction demands or limitations.

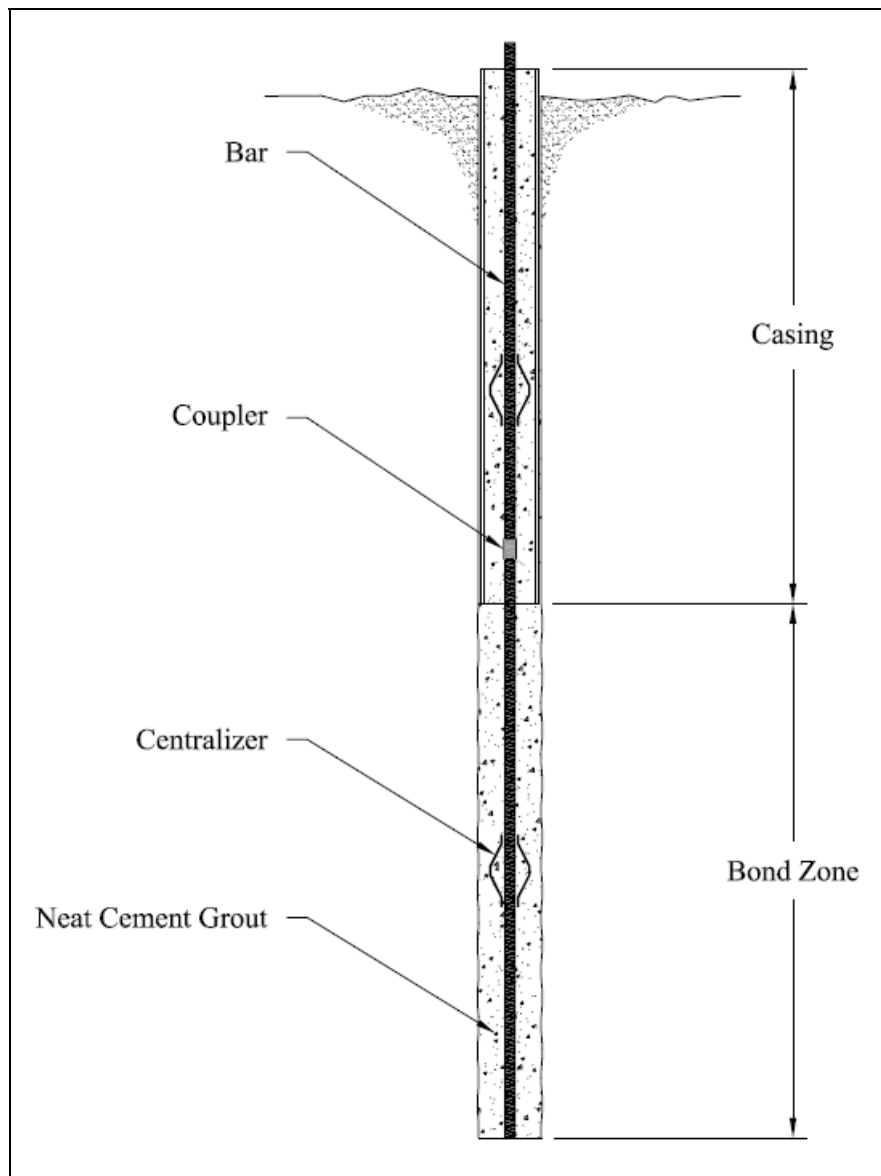


Figure 1: Typical Composite Micropile

## MICROPILE FOUNDATIONS

When factors such as access constraints and environmental restrictions become substantial obstacles, the advantages micropile foundations have over all other deep foundations, which are mostly construction-related, have significant effects on schedule and cost.

Micropiles can be installed through virtually any subsurface condition, from soft sediments and clays to hard, competent rock. This may seem counterintuitive to many, but in harder and more competent rock, the penetration rate for micropile installation typically becomes noticeably faster than in granular soils or less competent rock formations. Different subsurface conditions pose different obstacles, which will be highlighted in a few case histories.

Drill rigs used for micropile installation are small and light-weight (typically 15- to 40-thousand pounds). Specialized rigs are modular and sometimes even smaller, so mobilization of these rigs to limited access locations with medium-lift helicopters has become standard practice.

When subsurface conditions vary from those expected, the installation procedures for micropiles are flexible enough and have become streamlined to accommodate such variance by modifying the lengths, number, and/or configuration of the micropiles at each site. Such modification is part of design contingencies outlined in the construction documents in something called a decision tree or flow chart. With such a guidance tool, drill operators and inspectors have clear directives to follow in the event of such variant subsurface conditions.

Another unique quality of micropiles, because of their size and geometry, is their ability to be economically tested to validate their capacity. This ability reduces the need for additional conservatism and increased Factors of Safety - which are used to accommodate uncertainties in foundations that are not tested.

Health and safety are concerns in any type of construction, but the hazards present during micropile construction, while they do exist, are minor and are managed through regular, simple safety training protocols.

Other benefits of micropiles (which are not typically important in this industry) are the compact sizes of many micropile drills for use in restricted access and head space, as well as low noise and vibration emission.

Again, micropile foundations are not an inexpensive system, so they are not beneficial when a traditional foundation can be easily constructed, but the cost of micropile foundations do not escalate as rapidly as traditional foundations when various constraints and restrictions are imposed or adverse ground conditions are encountered.

## MICROPILES IN THIS INDUSTRY

The first micropile foundations for transmission structures in this industry involved triangular and rectangular micropile configurations with steel or concrete pile caps. The advent of radial micropile arrays has revealed numerous design and construction advantages. Radial-arrayed micropile configurations, installed with specialized equipment, can be completed with surprising accuracy and efficiency. In completely helicopter-supported site conditions, micropile foundation elements for all four legs of a 500-kV suspension tower have been installed in less than a day. In the same conditions, the same accomplishment for a 500-kV deadend tower has been achieved in under three days.

Both steel and concrete pile caps have been utilized for non-lattice structures. Concrete pile caps are currently the preferred choice for lattice towers, but advancements are continually being investigated and implemented for improved design and construction efficiency.

Even today, as constraints and restrictions grow and impede project advancement, micropile design and construction techniques continue to evolve to accommodate these increasing limitations. Some of these interesting evolutions and solutions will be illustrated in a few case histories.

The current state of practice for micropile foundations in the electric transmission industry is still developing as the industry leaders gain familiarity and comfort with this technology.

## INTEGRATION OF THE DIFFERENT FOUNDATIONS

**Kangley-Echo Lake Transmission Line (500-kV).** One of the first major attempts to implement micropiles as lattice transmission tower foundations was in part of the Kangley-Echo Lake 500-kV transmission line that extends through a protected watershed east of Seattle, Washington (Mathieson, W.L., et al., 2004). At that time (15 years ago), micropile construction techniques and efficient environmentally sensitive practices were still advancing, and only one tower was constructed using micropiles on this project.

**Swan-Tyee Intertie (138-kV).** This 138-kV line connects the Four Dam Pool Power Agency's hydroelectric facilities at Swan Lake and Lake Tyee. This 57-mile segment of line includes more than 250 structure locations with more than 350 foundations, all of which are supported by micropile foundations with steel pile caps. These structures consist of guyed single-shaft structures, guyed and un-guyed Y-structures, guyed H-structures, guyed 3-pole structures, and guyed A-frame structures for major water crossings. Lateral structure loading was supported via battered foundation micropiles and guy wires. Figure 2 is an example of one of these micropile foundations. This was the first micropile transmission line foundation project of this size, and micropiles were chosen because of the remote, mountainous terrain of the structure sites. This project was completely helicopter-supported. Another major variable encountered from site-to-site was the subsurface condition, ranging from 3-blow-count silt to 25,000-psi rock. With a foundation construction schedule of directions to follow, dependent on structure type and subsurface conditions encountered, micropile foundations were the only feasible approach to complete this project within the narrow seasonal window available.

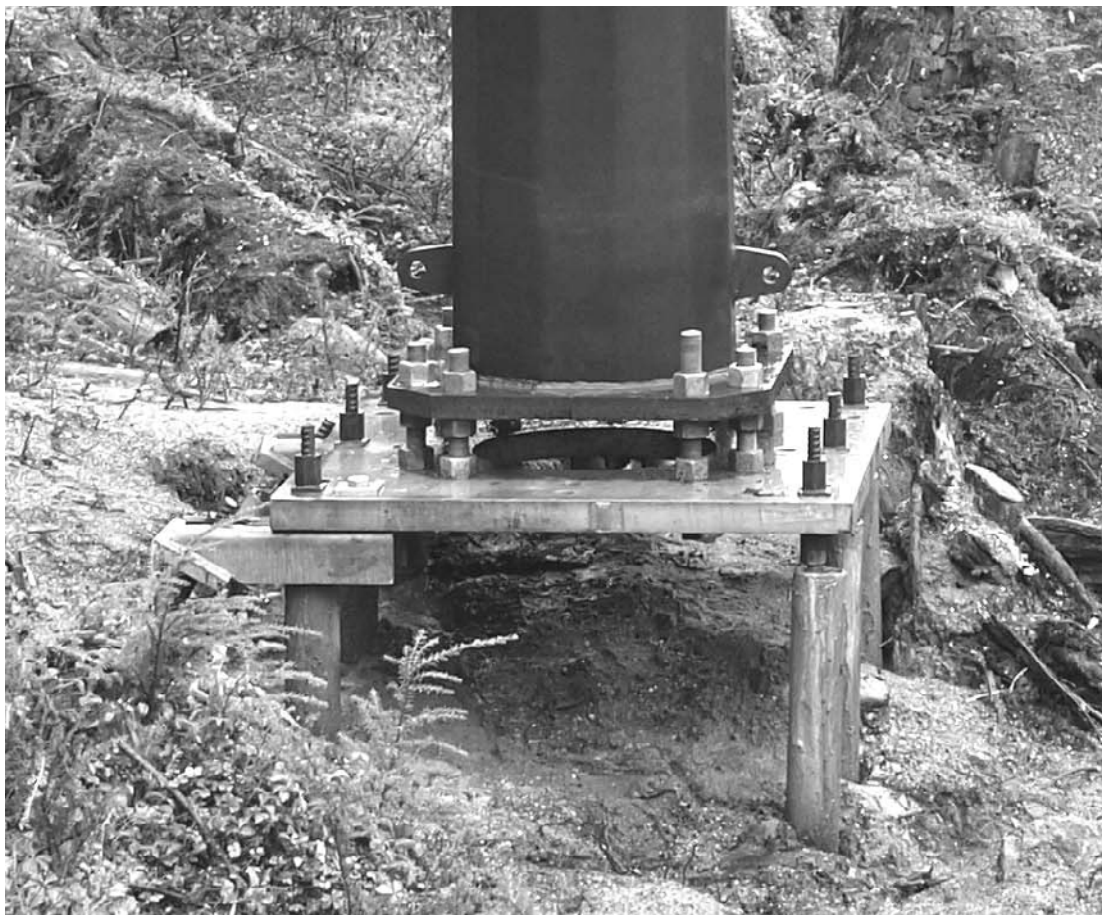


Figure 2 - Swan-Tyee Intertie Micropile Foundation

**Miguel to Mission Transmission Line (230-kV).** The construction of a new 230-kV transmission line on single-shaft self-supporting structures was proposed to address current and future overloads on existing 138-kV and 69-kV transmission lines. Several of these structures utilized micropile foundations, the construction of which satisfied various constraints, such as restricted access, environmental restrictions, and strict noise control requested by the community, which could not be efficiently satisfied with conventional foundations. Micropile foundations (with steel caps and concrete caps) were the solution. Figures 3 and 4 are photos of two such pile caps.



Figure 3 - Miguel to Mission Micropile Foundation with Steel Cap

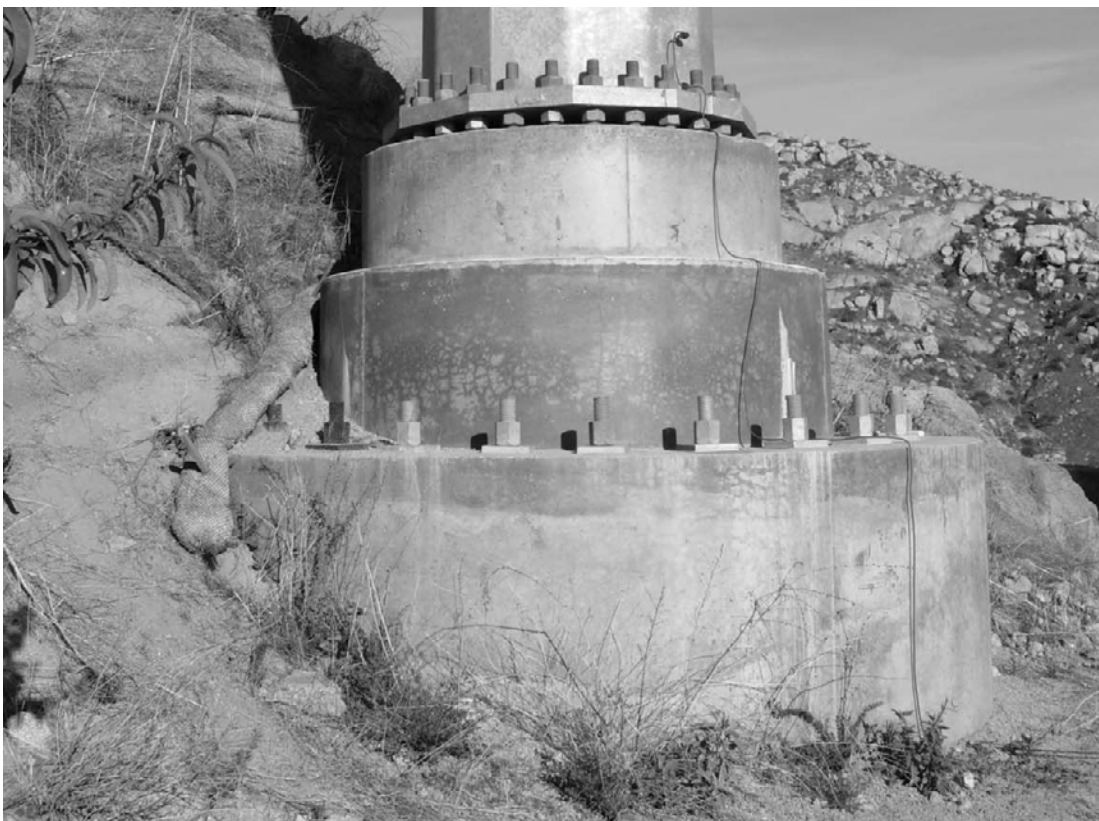


Figure 4 - Miguel to Mission Micropile Foundation with Concrete Cap

Telegram Channel: @Seismicisolation

**Ebey Slough (230-kV).** The rebuild of this 2.5-mile section of transmission line consisted of the replacement of 80 old wood poles with 15 new steel, single-shaft, self-supporting structures, carrying two 230-kV circuits. Of these 15 structures, the foundation construction for 10 was possible only with micropiles. These 10 structures are located in a sensitive estuary, having strict environmental restrictions, and silty, organic geotechnical material that simply could not support more than about 500 psf on the surface. Blow counts (N-values) for the first 50 to 75 feet of this material were between about 0 and 5 blows per foot. Directly beneath this material was the bearing unit of dense granular material. Because of these rare subsurface conditions, micropile lengths ranged from 70 to 120 feet. Special transportation vehicles, drilling equipment, and construction techniques were utilized to accommodate these unique challenges. High-capacity marsh buggies were assembled and used for transporting equipment, material, and crews to the structure sites; unique construction platforms were designed, assembled, and placed; and modular drill rigs were customized to drill these micropile foundations in a controlled, precise, and efficient manner. The suspension structures required 10 to 16 micropiles per structure, with a 9- to 10-foot-diameter concrete cap, and the one deadend structure in this section required 36 micropiles with an 18-foot-diameter concrete cap. This deadend foundation was designed to support a 15,000-kip-foot moment, and to exhibit less than three degrees of rotation. Figure 5 is a photo of this deadend foundation.



Figure 5 - Ebey Slough Micropile Deadend Foundation

**Tehachapi Renewable Transmission Project (TRTP) (500-kV).** This line is designed to carry 500-kV single-circuit bundled 2156 kcmil “Bluebird” conductor. The first 14 miles of Segment 1, Section 2 of this line traverses the Angeles National Forest, in which no new road construction was permitted. Most of the tower sites were, therefore, accessible only by helicopter. This portion of the section consisted of 60 lattice towers, 4 towers of which were accessible by existing road, and are supported by drilled shafts; the remaining 56 towers were accessible only by helicopter, and are supported by micropile foundations. The pile caps for these micropile foundations are of reinforced concrete, which accept the standard drilled-shaft stub angles. Construction techniques were understandably restricted, and a major influence on construction schedule was weather. Workable days were controlled by temperature, humidity, and wind, and their impact on assessed fire danger. The efficiency of micropile installation was unexpected by those new to micropile technology, and the short schedule was maintained. These footings consisted of between 3 and 8 micropiles, in a radial array ranging from 3 to 4 feet in diameter, all battered at 10 degrees out from the center of the array. Tangent towers had footings with as few as 3 micropiles each, and deadend towers had footings with as many as 8 micropiles each. Reinforced concrete pile caps for these footings ranged in diameter from 4.5 to 6.5 feet, and cap heights were between 4 and 6 feet. Figure 6 is a typical micropile suspension tower footing on this project.



Figure 6 - TRTP Micropile Suspension Tower Leg Foundation

## CONCLUSION

In this industry, traditional foundations are practical, trusted, and often the most economical choice for transmission structures; however, when varying obstacles and restrictions present themselves, threatening budget and schedule, micropile foundations can provide solutions that are being realized by the industry.

## REFERENCES

Armour, T., Groneck, P., Keeley, J., and Sharma, S. (2000). *Micropile Design and Construction Guidelines Implementation Manual*, 1.5-1.6.

Mathieson, W. L., Mitchell, C. L. B., Robertson, C. A., and Rustvold, J. (2004). “Micropiles to Support Electric Power Transmission Towers.” *Proceedings of the 29<sup>th</sup> Annual Conference on Deep Foundations, 2004, Vancouver, British Columbia, Canada*, 123-136.

# Geotechnical Investigations For A Transmission Line Are More Than Drilled Borings

Kristofer Johnson PG, CEG

Kleinfelder, 4670 Willow Road, Suite 100, Pleasanton, California, 925-484-1700,  
Fax 925-484-5838, email: [kjohnson@kleinfelder.com](mailto:kjohnson@kleinfelder.com)

## **Abstract**

With increasing need for design support on transmission lines, engineers need to be comfortable in evaluating limited geotechnical foundation design data spread out over long distances.

This report will show that through merging engineering geology and geotechnical engineering evaluations, data can be grouped into sections comprised of different design parameters along the length of a transmission line. The goal of this merger is to create a better characterization of the foundation design data along an entire alignment. Some tools and methods used by others are presented for consideration. When done well an engineer can better understand the nature of the foundation conditions along the alignment and why/where the geotechnical design parameters should be used and changed as a result of how they are grouped around similarities in geologic conditions.

## **Introduction**

To understand the needs and considerations necessary to design foundations for a transmission line both the engineering geology and overall geotechnical conditions must be combined. Often there is too much of an emphasis on drilled borings located at a predetermined distance and drilled to specified depths. Instead it is important to look for trends expressed through changes in geology. Such changes then need to be confirmed by geotechnical sampling at a frequency that matches the needs of a project. These trends in data must then be presented so that they may be reviewed and implemented into the design process.

## **Different Types of Geotechnical Guidelines for Investigation**

Most geotechnical guidelines for a transmission line have some form of required evaluation and investigation that include:

### Geologic Research and Reconnaissance

- Stereographic aerial photograph review
- Review of geologic maps
- Geologic reports and papers

### Geotechnical Investigation

- Subsurface investigation

[Telegram Channel: @Seismicisolation](#)

- Geophysical investigation
- Testing of soil and rock for strength and index tests
- Geotechnical design recommendations

Geotechnical investigation guidelines are often established for transmission line projects by utility companies, power administration agencies, and power delivery design firms. These guidelines differ quite a bit. The differences often are driven by a strong engineering focus or through requirements established in the planning and permitting process. However, in the end the guidelines can not dictate the geotechnical recommendations such that the results miss the key geologic conditions controlling the engineering needs of a transmission line project.

Some examples of guidelines that are currently in use include the following differences in how subsurface data is collected:

Entity	Required Boring Depth	Drilled Boring Locations	Required Depth to Core Into Bedrock	Sampling Intervals Within a Boring	Environmental Sampling Requirement	Unique Requirement
Utility Company	50', 70' if blow counts are 15 or less at 50'	Every tower with one boring * <sup>1</sup> At angle points > 3.99 degrees	Complete full depth to 50'	Sample 2', 5', 7' and 10' intervals using Mod. Calif. Sampler * <sup>2</sup>	Full suite of hazardous material tests at 2', 5' & 7'.	Requires use of <i>Design Summary Report</i>
Power Delivery Design Firm	30'	1 boring every 1/2 mile or angle points, dead ends, changes in geology, and roads	10'	Sample every 2.5' in upper 10', then every 5'.	None	None
Power Administration	30'-45' dependent on structure type	1 boring every mile or angle points, dead ends, 3 degree change in alignment, changes in geology	20'	Continuous coring using HQ3 wire line system for rock.	None	On boring log plot graph of SPT blow counts as representation of penetration resistance for soil and weathered rock.

\*<sup>1</sup> - Where slope stability information is needed and where changes in geologic formations occur.

\*<sup>2</sup> - At 15' and every 5' intervals after, use standard penetration test (SPT) sampler to full depth.

As shown each entity has a different way to obtain the geotechnical data needed for designing the foundations for a transmission line. Each of these entities may use their guidelines in the same state so there is no real geographical reason for the differences. Instead each is defined by their desired level of risk with some influence from the planning and permitting process. Although each acknowledges the need for description of geologic information in their guidelines the main topic by far is obtaining subsurface geotechnical engineering data.

These specifications often put a lot of weight on an 8 to 10 inch diameter boring that represents one location that is extrapolated to represent a one half mile to 1 mile of geotechnical conditions. Since lab data or boring log data by itself is risky to use, the engineer then has to evaluate the geologic conditions to fill in the gaps of information. This should be done in a way that associates key geotechnical changes with changes in the engineering geologic conditions along the alignment.

### ***Associating Geologic Conditions to Geotechnical Issues on a Project***

In preparing for a geotechnical investigation on a new transmission line, it is important to first evaluate and observe the geologic nature and topographic expression of land forms along the alignment. Such features as sharp or rounded ridge lines, erosion scars, presence of landslides, and expression of alluvial or bedrock structures will indicate how good subsurface conditions may be or how geologic hazards may impact a transmission line over time. It is recommended that one obtain enough subsurface data to understand each change in geology along an alignment. Understanding how these geologic conditions impact the geotechnical recommendations is key to having an overall understanding of the foundation needs of a project.

A feature like a sharp ridge line or high mountain range may indicate the presence of very strong bedrock like granite or metamorphic gneiss. Rounded hill sides with shallow and deep landslide features can indicate the presence of weak bedrock or poor soil conditions. Noting these features will help one evaluate the type of geotechnical conditions to be encountered as well as the type of investigation equipment that may be needed.

Considerations needed to make in planning a geotechnical investigation include:

Evaluating Geologic Hazards

- Landslides
- Fault crossings
- Liquefaction
- Seismic motions
- Erosion problems

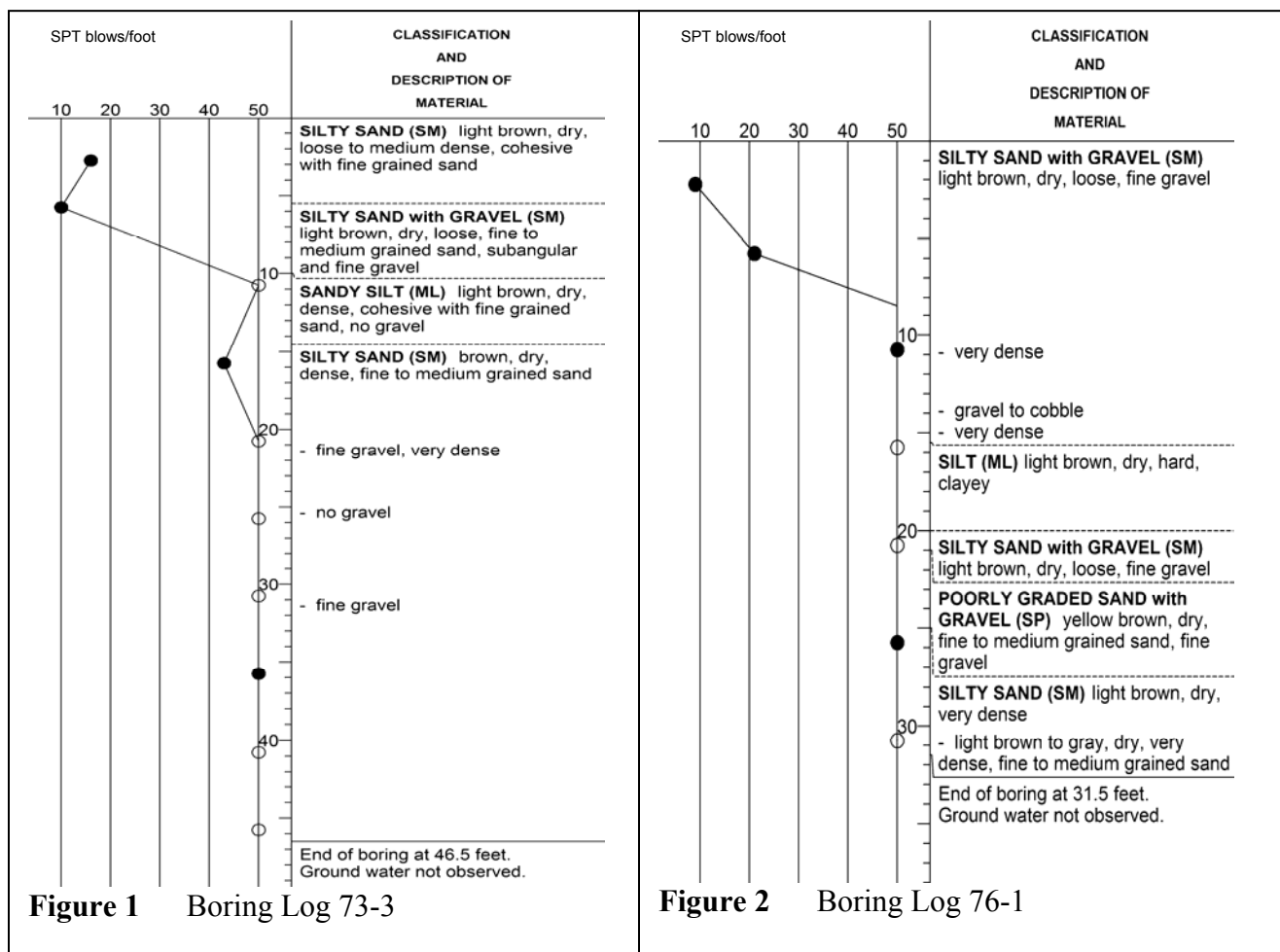
Design Data Needed

- Soil shear strength, density and deformation characteristics
- Compressibility
- Rock mass shear strength, density and deformation characteristics

Constructability Issues

- Caving or collapsing soil
- Running sands
- Hard rock

Often what one is looking for are trends in geologic and geotechnical conditions that are similar so that foundations can be constructed using the same general parameters to keep design and construction consistent over long line lengths. In Figure 1 and 2 the boring logs indicate very similar conditions as reflected by the SPT blow count graph where near surface conditions having blow counts from 10 to 20/ft and below 10 feet blow counts are above or greater than 50/foot. This example represents a segment of a power line that covers 6 miles. The similarity of SPT blow counts is matched to the same geologic formation present through out that distance. Such similarities allow the engineer to group the entire distance under the same foundation design recommendations. Outside of the grouped sections there is a need to focus on those few locations where there are significant differences in either geology or line loads.



In many cases one has to perform subsurface investigations at unique geologic features along a transmission line alignment to evaluate potential risks. Although some project alignments may appear to be located within nearly homogeneous geologic terrain, that is not often the case. Usually there may be one or two unique geologic conditions that provide significant risk to a power line project because they are hidden by erosion of the ground surface.

Figure 3 shows an alluvial plain (top portion of Figure 3 starting at 36/4) that is made up of medium dense to dense sediments adjacent to some hills (bottom portion of Figure 3) consisting of highly weathered poorly cemented silt stone and sandstone. One might expect subsurface conditions to be continuous in the alluvial area, but the presence of a dry creek required further investigation. There is a small dry creek (just below location 36/2) that crosses the power line alignment. A few transmission towers (36/2, 36/3, and 36/4) are located within the creek drainage. The basin that the creek drains is made up of siltstone that is eroded during flash floods. These silts do not consolidate easily in this arid region and were found to have low densities to much deeper depths than the adjacent soil material found at and in the direction above tower location 36-1. In Figure 4 the area showing a stippled pattern shows the problem area. Normally a geotechnical investigation may only pick up the angle point at 36/3. In this case more borings need to be drilled to evaluate the extent of the problem as indicated by the subsurface conditions. SPT blow counts are shown for towers 36/2 and 36/3 in a graphic representation of density on the boring logs that define where one side of the changes in soil conditions were located (see Figure 5 and 6).

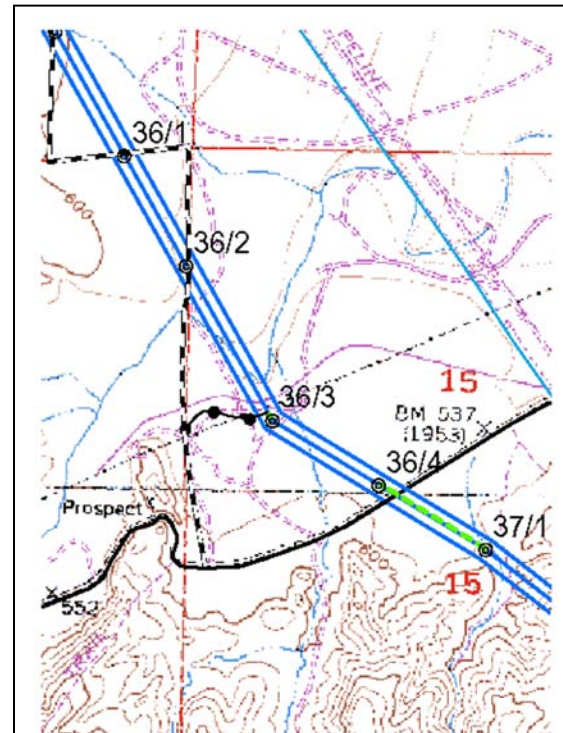


**Figure 3** Topographic Map

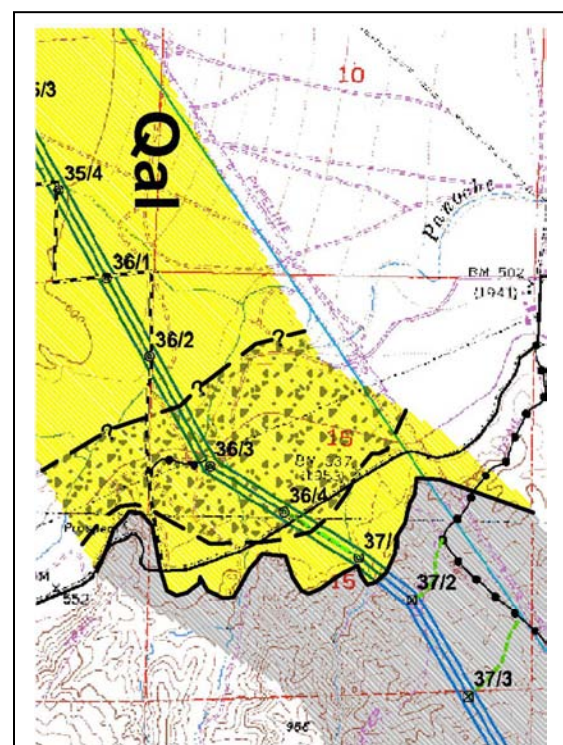
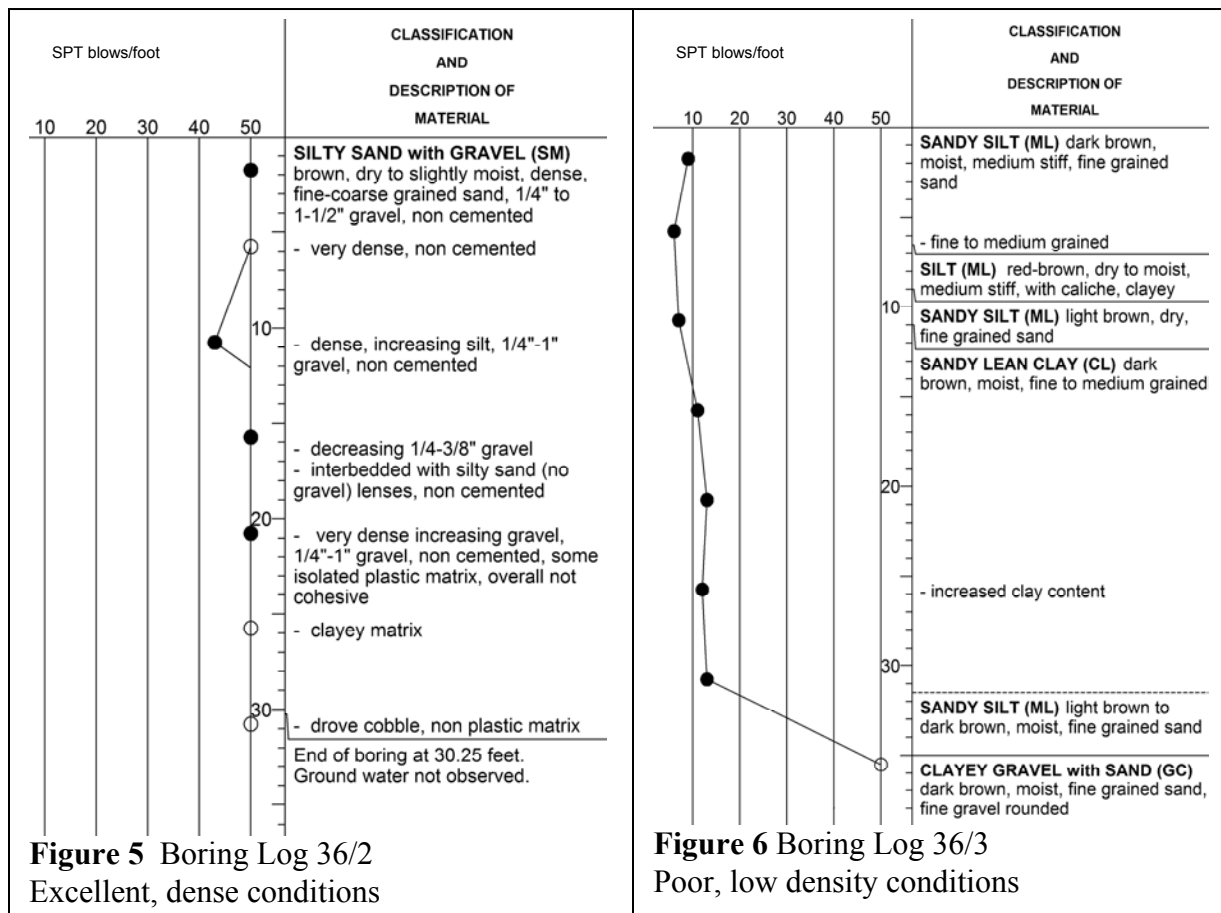


**Figure 4** Geologic Map



### **Benefits of Different Forms of Subsurface Investigation**

In every geotechnical investigation for a transmission line subsurface samples need to be obtained to confirm the design parameters that will be used for selected foundations. Soil and rock conditions do vary considerably and as a result many different types of equipment have been developed to get representative data.

Typically methods to obtain subsurface samples include:

- Back hoe or excavator test pits
- Hollow stem auger borings
- Diamond core drilling
- Rotary wash borings
- Cone penetrometer data
- Air rotary drilling
- Vibro-core drilling
- Standard Penetration Test (SPT)
- Pressure Meter

These methods are used to obtain the most representative data available for the subsurface conditions being investigating. The following summaries present the benefits and disadvantages of using these investigation methods:

#### Back Hoe and Excavator Test Pits

- Good for quick and shallow subsurface investigations

- Helps define geologic structure
- Can define the presence and extent of a landslide

#### Hollow Stem Auger Borings

- Widely available
- Typically lower in cost
- No drilling fluids and cuttings disposal less difficult
- Erroneous blow counts in saturated sands

#### Rotary Wash Borings

- Widely available
- Higher cost than hollow stem auger
- Drilling fluids used, so water source is required
- Higher accuracy in sampling saturated sands or soft clays
- Combine with Nx Core barrel for rock coring

#### Cone Penetration Rig

- Available in many areas where soft sediments are present
- Faster than soil borings and cheaper in many cases
- No soil cuttings generated
- Electronic data collected at 2 inch intervals (versus 5 ft in drilled borings)
- Limited soil sampling
- Some difficulties differentiating silty clay /silty sands

#### Limited Access Rigs (Any location is possible)

- Can generally provide any drilling method
- Drill rigs are mounted on 4x4, balloon tires, barges, tracks or placed on a platform delivered via helicopter (Figure 7).

#### Air Rotary

- Best for hard rock, reduces rock to chips, sampling is not generally available
- Rigs not commonly used as an investigation method

#### Vibro-Core

- Good for soil or rock. Collects complete sample but vibration fractures the samples. Rigs are hard to find and not commonly available.

#### Standard Penetration Test

- Good standardized blow count method indicating density and strength.
- Blow count data can be extrapolated into strength parameters.

#### Pressure Meter

- Pressure meter testing (PMT) can be used to reduce conservatism in design methods. The PMT measures the subgrade modulus in the field. This method is a highly accurate in situ strength test. Doing PMT is time consuming in the field. The test is most applicable for projects with long stretches of similar



Helicopter positioned limited access rig  
**Figure 7**

soil where higher modulus values can reduce the foundation size and associated project costs.

## Benefits of How Geotechnical Data is Presented

When delivering geotechnical design recommendations for a transmission line project, consultants need to think about how that data is to be presented and will be used. There are a number of report formats used that aid in communicating the geotechnical conditions more clearly and help make the information more supportive to the designers needs. Often a power line project is starting to be constructed at the same time the geotechnical report is being finished. The data needs to be delivered quickly and in an easy to use format that communicates to the design engineers where the concerns and constructability issues are located. Using a geotechnical report format generally used for a building would make the information hard to find and too time consuming to easily utilize. Some formats for data presentation are

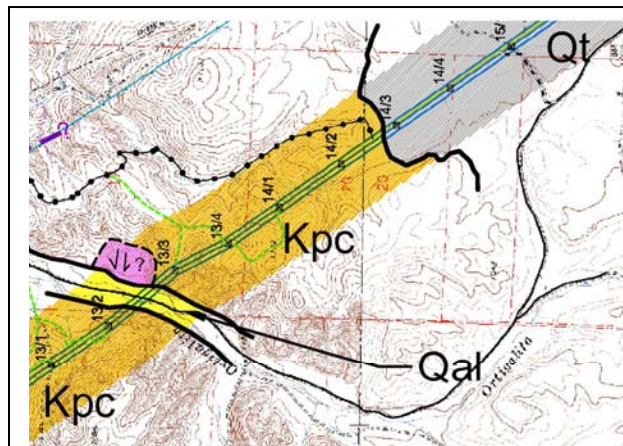


Figure 8 Geologic Strip Map

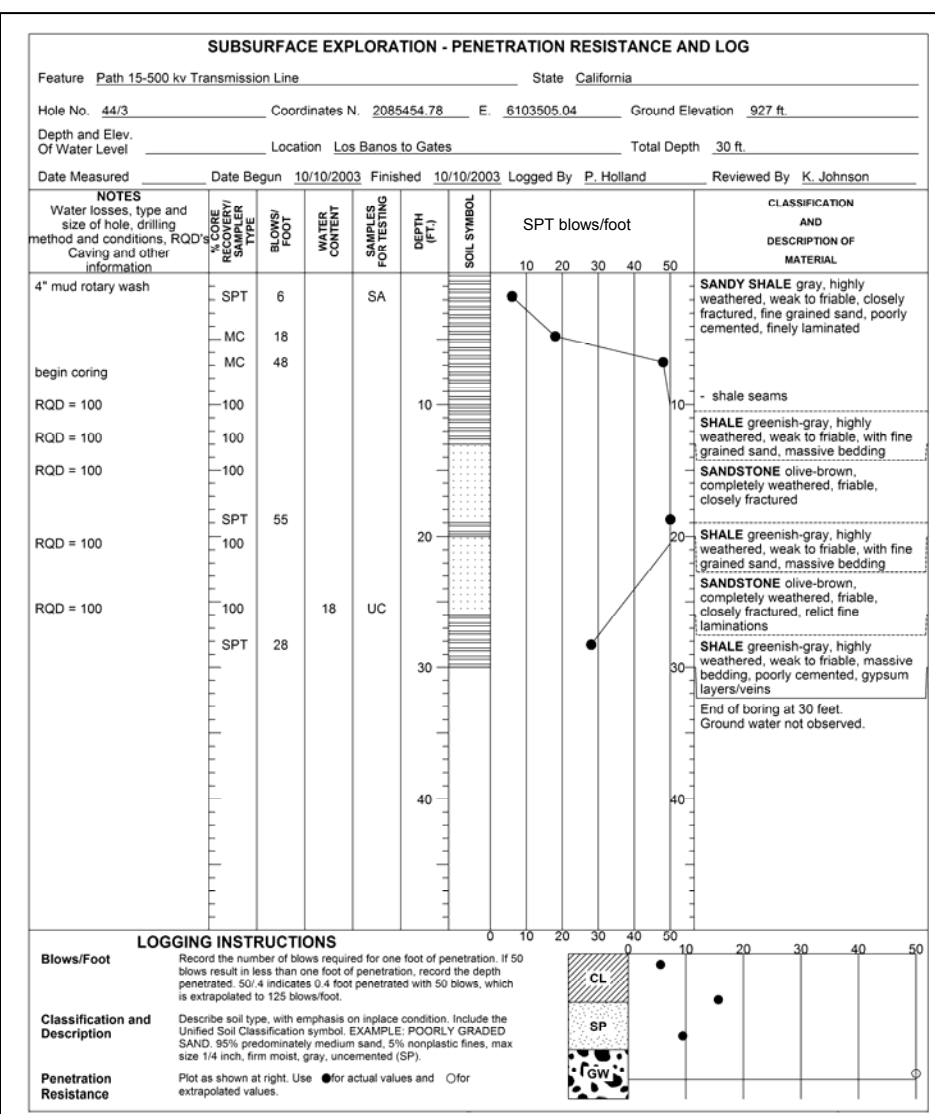


Figure 9 WAPA Boring Log Sheet

presented here for consideration as a way to make geotechnical data and recommendations more user friendly.

A geologic strip map (Figure 8) is often used to show only those aspects of the geology adjacent to a power line right of way. This map is a great way to show changes in geologic conditions which have impact on the power line. The map shown indicates the presence of an ancient landslide, topographic conditions, stream locations, presence of faults, and changes in geologic formations associated with the transmission line location.

One method to represent standardized geotechnical data is a boring log format (Figure 9) required on Western Area Power Administration projects. Their boring log format shows a graph of the changes in Standard Penetration Test (SPT) blow counts with depth.

This plot of penetration resistance makes it easy to tell how subsurface conditions and geotechnical densities change with depth. From there one can then group horizontal segments of a power line that have similar graphs and apply similar design parameters for foundations designed for those segments. In addition, the log form

GEOTECHNICAL DESIGN SUMMARY SHEET								
<b>PROJECT INFORMATION</b>								
Segment:	Boring No.:	Total Depth (ft):	Drilling Company:	Tower No.:	Date Drilled:	Depth to G/W (ft):	Drill Rig Type:	Tower Type:
Boring Coordinates (NAD 83) 7.5' Topographic Map Quad:				Logged By: _____ Boring Diameter: _____ Latitude: _____ Longitude: _____				
<b>SEISMIC PARAMETERS</b> Faulting Closest Fault: _____ Design Fault: _____ Distance to Fault: _____ (mi) Fault Type: _____ Expected Magnitude (Mw): _____ Primary Movement: _____				2007 CBC (ASCE 7-05) Seismic Parameters Seismic Category: _____ Reference Table 1613.5.6 Seismic Class: _____ Maximum Considered Earthquake MCE Ground Motion Short Period Spectral Response S <sub>1</sub> : _____ g Table 1613.5 1 second Spectral Response S <sub>1</sub> : _____ g Table 1613.5 Site Coefficient, F <sub>s</sub> : _____ Table 1613.5.3(1) Site Coefficient, F <sub>p</sub> : _____ Table 1613.5.3(2) Design Earthquake Ground Motion Short Period Spectral Response S <sub>0.5</sub> : _____ g 1 second Spectral Response S <sub>0.5</sub> : _____ g				
<b>GEOLOGIC/SEISMIC HAZARDS</b> Y / N Mapped Fault Hazard Zone <sup>1</sup> : _____ Fault Rupture Potential: _____  Mapped Liquefaction Zone <sup>2</sup> : _____ Potential Liquefaction Hazard: _____				Landslide/Slope Instability Y / N Mapped Landslides <sup>2</sup> : _____ Unmapped Landslides: _____ Seismic Slope Stability <sup>3</sup> : _____ Tsunami / Seiches: _____ Erosion / Surficial: _____				
<small>Notes: 1) Formerly known as Alquist-Priolo Fault Hazard Zones 2) From published Geologic Maps (see References) 3) CGS or County designated seismic hazards zones (see references)</small>								
<b>Foundation Design</b>								
<b>LPILE INPUT PARAMETERS</b>								
Layer	Depth to bottom of layer (ft)	Soil/Rock Type (USCS)	Unit Weight (pcf)	Ave. Blow Counts (blows/ft)	Friction Angle (degrees)	Cohesion (ksf)	Strength Reduction Factor	Soil Modulus K (ksf)
1								
2								
3								
4								
5								
6								
<b>Additional Data - SHAFT PARAMETERS</b>								
Layer	Depth to bottom of layer (ft)	SAND		Clay		Gravels & Rock		
1		K <sub>c</sub>	Beta	N <sub>c</sub>	Alpha	Poisson's Ratio	Young's Modulus (psf)	Socket Diameter (m)
2								
3								
4								
5								
6								
<b>Chemical Analysis</b>			<b>Depth to ignore</b> (ft)					
Sulfates	[ppm]							
Chlorides	[ppm]							
Resistivity	[ohm-cm]							
pH	_____							
<b>Caving Potential</b>								
Slight      2      3      4      Heavy								
Page: _____								

Figure 10 Southern California Edison Design Sheet

allows for the addition of subsurface descriptions, lab test results where obtained, and moisture content. The SPT log helps determine where the blow counts transition from soil into bedrock. One can also see that the bedrock has much lower blow counts than might be anticipated for rock where the deepest shale is encountered. The presence of blow counts in bedrock show that it is highly weathered and has the consistency of dense sand or clay. Hard bedrock would be cored and blow counts would indicate refusal conditions.

Another format used with Southern California Edison makes use of a *Geotechnical Design Summary Sheet* shown in Figure 10. This form recognizes the importance of active faults throughout Southern California on a foundation design. With this form a geotechnical engineer can give design parameters on a per tower basis. This data can then be easily considered in preparation of LPILE input parameters and other shaft parameters necessary for the design of drilled pier foundations. The form even allows for recognizing corrosion potential of subsurface conditions, surface depths to ignore and caving potential. This type of reporting format may seem time consuming initially but readily provides data necessary for foundation design that is often discussed in several pages of a standard geotechnical report.

## **Design Recommendations**

Taking into account the design methods to be used during foundation engineering is important when grouping engineering geology and geotechnical data. Drilled piers are the predominant foundation type for lattice towers and monopoles. Foundations designers can use geotechnical data in a number of different design methodologies. One common design method used for the drilled piers on transmission lines is LPILE (Ensoft Inc.).

LPILE is a method that analyses pile movement due to lateral loads. The software models soil behavior with data from p-y curves (Figure

<b>p-y Curve Criteria</b>			
Soil Modulus Parameter k			
Soil Strain Parameter E50			
E50 = Strain at 50% Stress Level of Clay			
<b>p-y Curve Criteria</b>			
These criteria are used by LPILE1 to calculate p-y curves internally:			
Option 1 – Soft Clay (Matlock, 1970) Option 2 – Stiff Clay Below the Watertable (Reese et al., 1975) Option 3 – Stiff Clay Above the Watertable (Reese & Welch, 1975) Option 4 – Sand (Reese et al., 1974)			
<b>Soil Modulus Parameter k for Clays</b>			
<b>Average Undrained Shear Strength</b>		<b>Static</b>	<b>Cyclic</b>
Soft Clay	c = 1.74 to 3.47 psi 250 to 500 psf 12 to 24 KPa	30 pci 8,140 KPa/m	-- --
Medium Clay	c = 3.47 to 6.94 psi 500 to 1000 psf 24 to 48 KPa	100 pci 27,150 KPa/m	-- --
Stiff Clay	c = 6.94 to 13.9 psi 1000 to 2000 psf 48 to 96 KPa	500 pci 136,000 KPa/m	200 pci 54,300 KPa/m
Very Stiff Clay	c = 13.9 to 27.8 psi 2000 to 4000 psf 96 to 192 KPa	1000 pci 271,000 KPa/m	400 pci 108,500 KPa/m
Hard Clay	c = 27.8 to 55.6 psi 4000 to 8000 psf 192 to 383 KPa	2000 pci 543,000 KPa/m	800 pci 217,000 KPa/m
<b>Soil Modulus Parameter k for Sands</b>			
<b>Relative Density</b>		<b>Loose</b>	<b>Medium</b>
Submerged Sand		20 lb/in <sup>3</sup>	60 lb/in <sup>3</sup>
Submerged Sand		5,430 KPa/m	16,300 KPa/m
Sand Above WT		25 lb/in <sup>3</sup>	90 lb/in <sup>3</sup>
Sand Above WT		6,790 KPa/m	24,430 KPa/m
<b>Dense</b>			
		125 lb/in <sup>3</sup>	33,900 KPa/m
		225 lb/in <sup>3</sup>	61,000 KPa/m

**Figure 11 –p-y Curve Criteria**

11) that are internally generated for standard soil types. It takes into account the lateral modulus of subgrade reaction ( $k$ ) to evaluate pier dimensions.

Given the similarity of the subsurface conditions as represented in Figures 1 and 2 earlier, design data was prepared and grouped as shown in Example #1 and Table 1. The data represents a 6 mile span of distance along a transmission line. Looking for such opportunities to group data simplify the presentation of the geotechnical design parameters for a project.

***Example #1- Engineering Parameters (Geotechnical L Pile Design Parameters Tower Locations 70/4 to 76/1 – Older Alluvial Soil)***

- *Older Uplifted Alluvial Soil Deposits. The soil is loose to very dense, comprised mostly of silts and sandy silts that are locally clayey. At the surface, these soils are dry and very loose.*
- *These granular soil deposits may be susceptible to sloughing. The contractor should be prepared to case these holes if needed during pier drilling.*
- *Recommend that the strength contribution from the upper five feet of soil be neglected. Vertical pressure due to weight of this layer on underlying layers need not be neglected.*
- *Design for lateral loads should be for a primarily non-cohesive soil.*

**TABLE 1**

Layer No.	Layer Thickness (ft)	Effective Weight of Soil (pcf)	Friction Angle (degrees)	Cohesion (psf)	Ultimate Bearing Capacity (psf)	Ultimate Skin Friction Compression (psf)	Ultimate Skin Friction Uplift (psf)
1	5	105	-	-	-	-	-
2	10	120	36	-	12,000	750	550
3	30	120	40	-	20,000	1,500	1,150

Note: Cells with no data indicate zero strength or zero capacity for the soil layer.

*The adjacent photo (Figure 12) shows similar surface conditions found between towers 70/4 to 76/1. In this area there were also uniform subsurface geologic formations allowing for grouping of the design parameters used for the foundation piers.*

### **Conclusion**

This paper suggests that a geotechnical investigation for a transmission line should be performed so that geologic engineering is an integral part to the geotechnical engineering evaluation. Several field data and report format methods can be incorporated that bring more clarity in the similarities to the design data of a



Towers 70/4 to 76/1  
**Figure 12**

project alignment. When done well an engineer can better understand the nature of the foundation conditions along the alignment by grouping the engineering parameters around these similarities and changes in geologic conditions.

## References

- Black & Veatch Corporation, (2004). *Geotechnical Engineering Services Specification, Geotechnical Services, Exploration Borings and Laboratory Tests*.
- Kleinfelder, (January 2004), *Summary Geotechnical Investigation Report, Path 15 500 Kv Transmission Line, Gates – Los Banos, California*.
- Southern California Edison (SCE). (2008). *Guideline for Geotechnical Investigation For Transmission Line Projects*, Transmission and Distribution Business Unit Civil/Geotechnical Engineering Group, Rosemead, California.
- Kondziolka, R., E., and Rojas-Gonzales, L., F., (1991), *Case History of a Cost Effective Design Approach for Laterally Loaded Drilled Shafts*, IEEE Xplore.
- Western Area Power Administration (WAPA). (2008). Geotechnical Investigation Statement of Work, Sacramento Voltage Support.
- Dembowski, Scheffield and Smith, “A Foundation Cost Comparison: Alternate Methods of Specifying Loads for the Design of Rigid Base Tower Foundations.”

## **TRANSMISSION POLE FOUNDATIONS: ALTERNATE DESIGN METHODS FOR DIRECT-EMBEDDED ROUND, WOOD TRANSMISSION POLES**

**Cassie McNames, PE, MS<sup>1</sup> and Sivapalan Gajan, Ph.D.<sup>2</sup>**

<sup>1</sup>Ulteig Engineers, Inc., 3350 38<sup>th</sup> Avenue South, Fargo, ND 58104; PH: (701) 280-8636; FAX: (701) 280-8739; email: Cassie.McNames@Ulteig.com

<sup>2</sup>North Dakota State University, Department of Civil Engineering, 1410 14<sup>th</sup> Avenue North, Fargo, ND 58105; PH: (701) 231-5648; email: S.Gajan@ndsu.edu.

### **ABSTRACT**

Although close attention is paid to the design of transmission poles, many times the design of the foundation is left up to a “rule of thumb” method. Reliable and established methods for analyzing laterally loaded piles have been incorporated into the current study to calculate the required depth of embedment for transmission poles, and the results are compared to the current methods. The results show that the current methods for determining embedment depths for direct-embedded transmission poles significantly underestimate or overestimate the required embedment depth depending on the soil conditions. Recommendations are made for alternate design methods for transmission pole foundations. A case study is presented where direct-embedded wood transmission poles fell over due to inadequate foundation design. The results of the case study are compared to the methods presented in this paper. It is concluded that the alternate design methods will generate more accurate results than the current methods.

### **INTRODUCTION**

Tangent transmission structures endure lateral loads due to wind pressures on the conductors and the structure itself. The lateral loads are resisted by the soil along the depth of the pole below grade. The industry standard is to embed the pole a depth of 10% of the total pole height plus 0.61 m (2 ft) below grade, which does not take into account the pole or soil properties. In 2002, Mehran Keshavarzian studied the current methods for foundation design and found “that no equation in the form of a rule of thumb or a single chart is likely to be found to yield consistently reliable pole foundations in all soil types and for all possible pole classes, lengths, species, and pole loading scenarios” (Keshavarzian, 2002, p. 155). Although few studies have been performed on transmission poles specifically, several researchers have studied lateral loaded piles. These concepts have been adopted in this literature to determine more accurate embedment depths for round, wood transmission poles. Using the information presented in this study, the designer will be able to generate more reliable foundation designs for round, wood transmission structures.

## MATERIALS

Wood transmission poles are classified based on the American National Standards Institute (ANSI) O5.1 (ANSI, 1987). The poles are classified by a predetermined ultimate load that the pole must support for a given pole diameter (ANSI, 1987). The pole classifications investigated in this paper include class 2, 1, H1, H2, and H3 with heights ranging from 12.2 m (40 ft) to 36.6 m (120 ft). The species of wood used in this study is Western Red Cedar. Since the applied load on a transmission pole will vary greatly between projects, the loading used to determine the required embedment depths was based on the ultimate loads found in the ANSI O5.1 standard (ANSI, 1987).

The soils analyzed include homogeneous cohesive and cohesionless soils. Undrained shear strengths,  $c_u$ , ranging from 5 kN/m<sup>2</sup> (100 psf) to 192 kN/m<sup>2</sup> (4000 psf) were used to calculate embedment depths in cohesive soils. Based on research by the authors, it was determined that the undrained shear strength of the soil plays a large role in determining the required embedment depths for cohesive soils, especially for poles placed in poor soils. As the undrained shear strength increases, the embedment depth required decreases. Therefore, the authors assembled a soil classification system based on the results of this study for cohesive soils which is listed in Table 1.

**Table 1. Soil Classification Summary for Cohesive Soils (Adapted from McNames, 2008)**

Soil Classification	$c_u$ , kN/m <sup>2</sup> (psf)
Very Poor Clays	5-23 (100- 499)
Poor Clays	24-47 (500-999)
Average Clays	48-95 (1000-1999)
Good Clays	>96 (2000)

Both saturated and unsaturated conditions were analyzed for the case of cohesionless soils. Friction angles,  $\phi$ , varying from 20° to 40° were selected for the analysis of poles placed in cohesionless soils. The passive earth pressure coefficient,  $K_p$ , was determined using Rankine's method where  $K_p = \tan^2(45 + \phi/2)$ . Small differences in the effective unit weight, 3.1 kN/m<sup>3</sup> (20 pcf), do not have a significant impact on the embedment depth required, which is how the classification system shown in Table 2 was derived. Average values for the unit weight of cohesionless soils were taken as 17.3 kN/m<sup>3</sup> (110 pcf) for the moist unit weight and 7.4 kN/m<sup>3</sup> (47 pcf) in the case of fully saturated soils.

**Table 2. Soil Classification Summary for Cohesionless Soils (Adapted from McNames, 2008)**

Soil Classification	$\phi$ , degrees
Poor Sands	20-29
Average Sands	30-39
Good Sands	>40

## EXISTING DESIGN METHODS FOR LATERALLY LOADED PILES

It is assumed that the embedded portion of the transmission pole behaves as a short-rigid body. Since the stiffness of the pole itself is typically greater than the surrounding soil, it is assumed that the soil will yield before the pole. It has been noted in research by Fan and Long (2005) that the stiffness of the pile does not have a significant effect on the lateral resistance of the pile (Fan and Long, 2005). Well-known methods for determining the lateral capacity of short-rigid bodies embedded in cohesive and cohesionless soils were customized for the purpose of determining the necessary embedment depth of transmission poles. Two methods were chosen to analyze the embedment depth of round, wood poles placed in cohesive soils: Broms (1964b) and Fleming et al. (1992). Three methods are presented for analyzing transmission poles set in cohesionless soils: Broms (1964a), Fleming et al. (1992), and Prasad and Chari (1999). The lateral pressure distribution assumed along the depth of a round, wood pole for each method is shown in Figure 1.

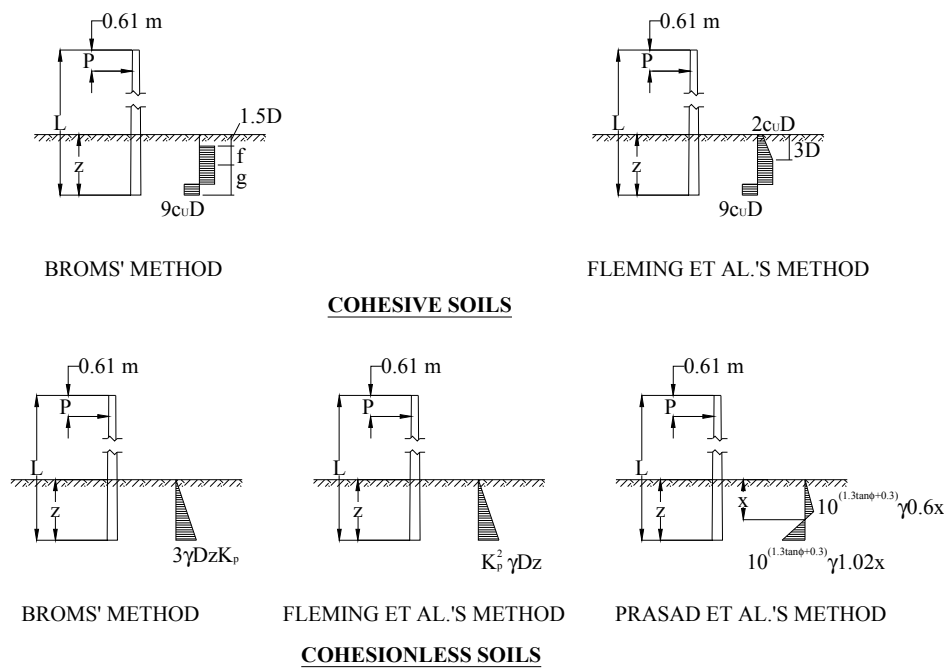


*Figure 1. Soil pressure distribution for cohesive and cohesionless soils. (Adapted from McNames, 2008)*

**Cohesive Soils.** The pressure distribution for Broms (1964b) method for cohesive soils is shown in Figure 1. Based on this pressure distribution, the required embedment depth,  $z$ , is determined by solving the following equation for  $y(z) = 0$ ,

$$y(z) = 1.5D + \frac{P_{app}}{9c_u D} + \sqrt{\frac{P_{app}(L - 0.61 - z + 1.5D + \frac{P_{app}}{9c_u D})}{2.25c_u D}} - z, \text{ where } P_{app} \text{ is the}$$

applied lateral load,  $L$  is the length of the pole, and  $D$  is the groundline diameter of the pole as determined by ANSI (McNames, 2008). Fleming et al.'s (1992) assumed pressure distribution is also shown in Figure 1. The required embedment depth is determined from this distribution by solving the following equation for  $y(z) = 0$ ,  $y(z) = 1.2(4.5c_u Dz^2 - 10.5c_u D^2z + 10.5c_u D^3 - P_{app}(L - 0.61))$  (McNames, 2008).

**Cohesionless Soils.** Using the pressure distribution shown in Figure 1 for Broms' (1964a) method, the required embedment depth is calculated as

$$z = \sqrt[3]{\frac{2 \cdot P_{app} \cdot (L - 0.61)}{K_p \cdot \gamma \cdot D}}, \text{ where } \gamma \text{ is the unit weight of the soil } (\gamma \text{ when water table is}$$

below the pole and } \gamma' \text{ where the water table is present along the length of the pole) (McNames, 2008). Fleming et al. (1992) suggest that the pressure distribution is linear as Broms proposed in 1964, however, the pressure is directly proportional to } K\_p^2 \text{ rather than } K\_p \text{ based on tests performed by Barton in 1982 (as cited in Fleming et al., 1992). The required embedment depth is calculated as } z = \sqrt[3]{\frac{6 \cdot P\_{app} \cdot (L - 0.61)}{K\_p^2 \cdot \gamma \cdot D}}

(McNames, 2008). Based on the distribution proposed by Prasad and Chari (1999), the embedment depth is determined to be equal to

$$z = 1.588x - \frac{P_{app}}{0.408 \cdot [10^{(1.3 \tan \phi + 0.3)}] \cdot \gamma \cdot D \cdot x}, \text{ where } x \text{ is the distance from the}$$

groundline to the point of rotation as shown in Figure 1 (McNames, 2008).

## CURRENT DESIGN METHODS

The 2004 RUS *Bulletin 1724E-200* recommends a “rule of thumb” for determining the required embedment depth for “most wood pole structures in good soils and not subjected to heavy loadings” (RUS, 2004, p. 12-3) as  $z = 0.1L + 0.61$  (rule of thumb), where the constant 0.61 is in meters. The RUS (2004) also includes an equation found in the *Wood Preserving News* (as cited in RUS, 2004) for determining appropriate embedment depths for round, wood poles as

$$P = \frac{S_e z^{3.75}}{L - 0.61 - 0.662z} \text{ (RUS equation), where } S_e \text{ is the soil constant: 140 for good soils, 70 for average soils, and 35 for poor soils (RUS, 2004).}$$

## ALTERNATIVE DESIGN METHODS

The existing design methods for short-rigid bodies were adopted for use in the design of foundations for direct embedded transmission poles. These methods were compared to the current design methods for direct embedded transmission poles. The research found that the current methods tend to over and under estimate the required embedment depth as illustrated in Figure 2-3 for cohesive soils and Figure 4-6 for moist cohesionless soils. It was determined that the embedment depths found using Broms' (1964b) and Fleming et al.'s (1999) methods for class H3 poles are typically 21%, 16%, 10% and 5% greater than class 2, 1, H1, and H2 embedment depths respectively for cohesive soils. For the case of cohesionless soils, class H3 embedment depths are 15%, 11%, 7%, and 3% greater than class 2, 1, H1, and H2 poles respectively for all three cohesionless soil methods presented in this paper.

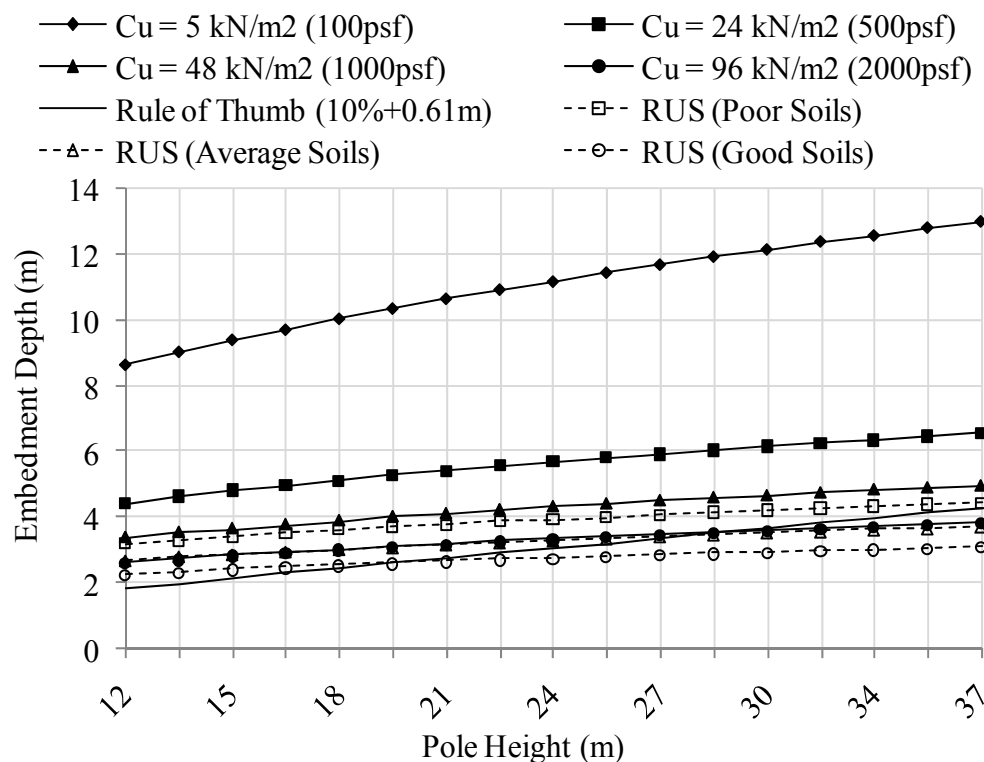


Figure 2. Required embedment depths for Broms' method for cohesive soils (class H3 poles). (Adapted from McNames, 2008)

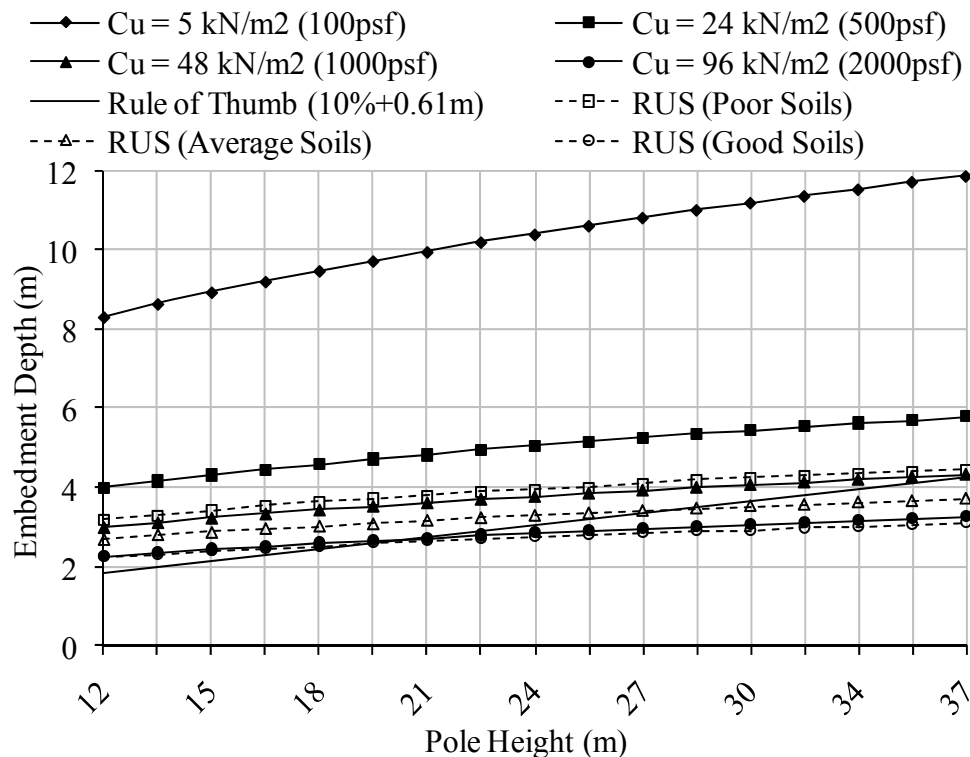


Figure 3. Required embedment depths for Fleming et al.'s method for cohesive soils (class H3 poles). (Adapted from McNames, 2008)

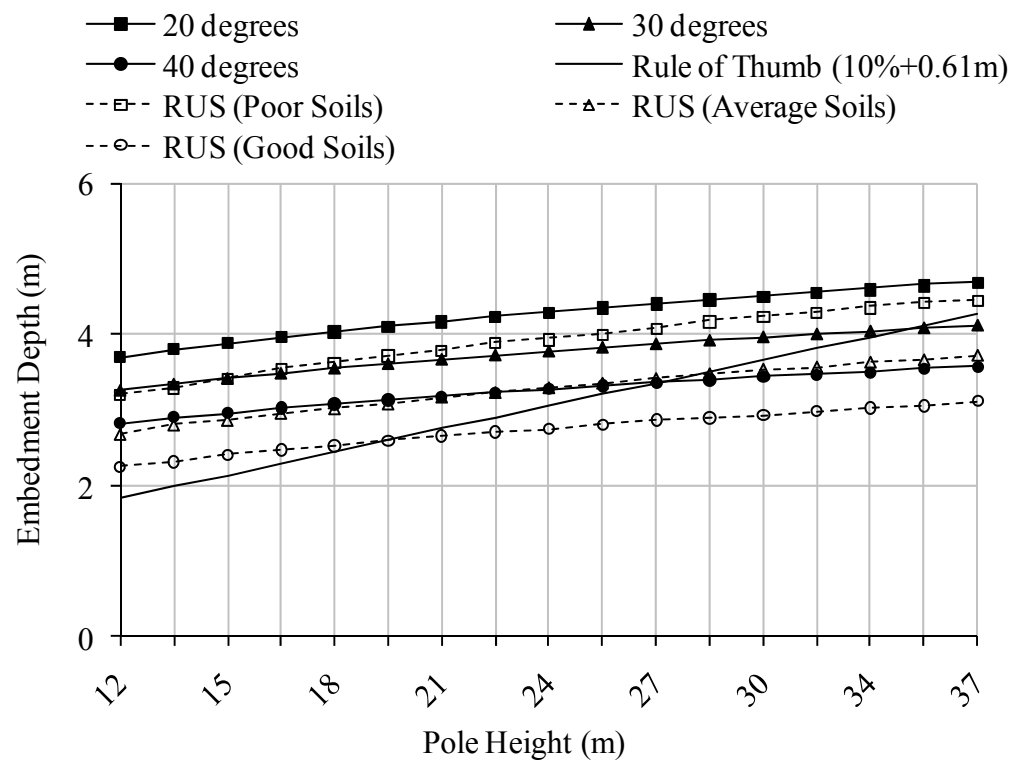


Figure 4. Required embedment depths for Broms' method for moist cohesionless soils (class H3 poles). (Adapted from McNames, 2008)

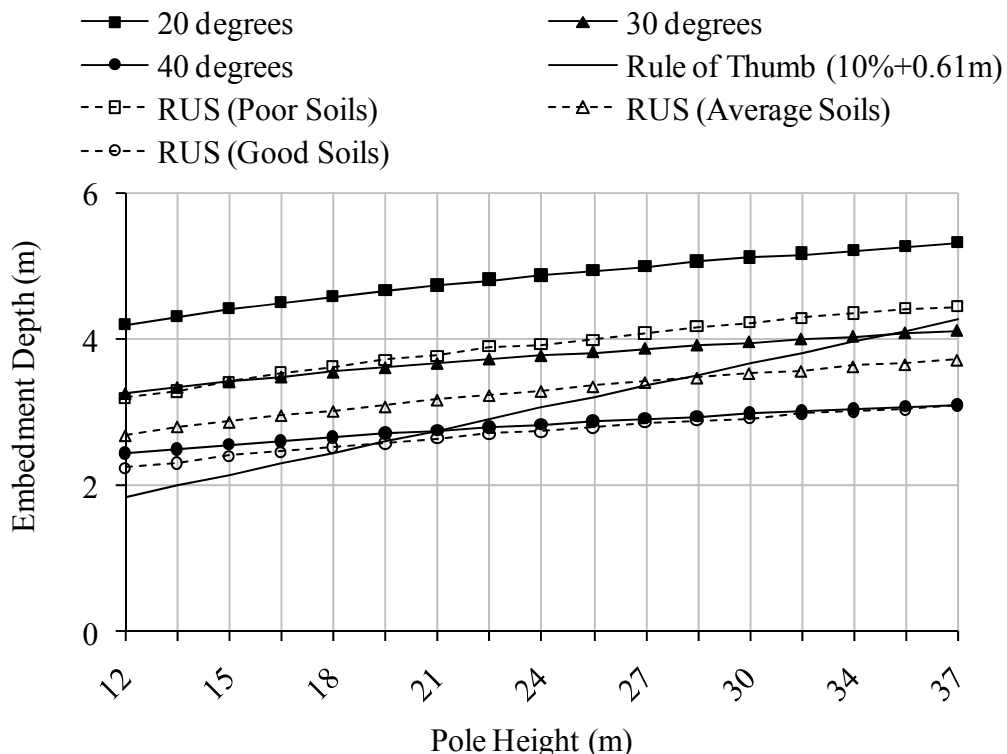


Figure 5. Required embedment depths for Fleming et al.'s method for moist cohesionless soils (class H3 poles). (Adapted from McNames, 2008)

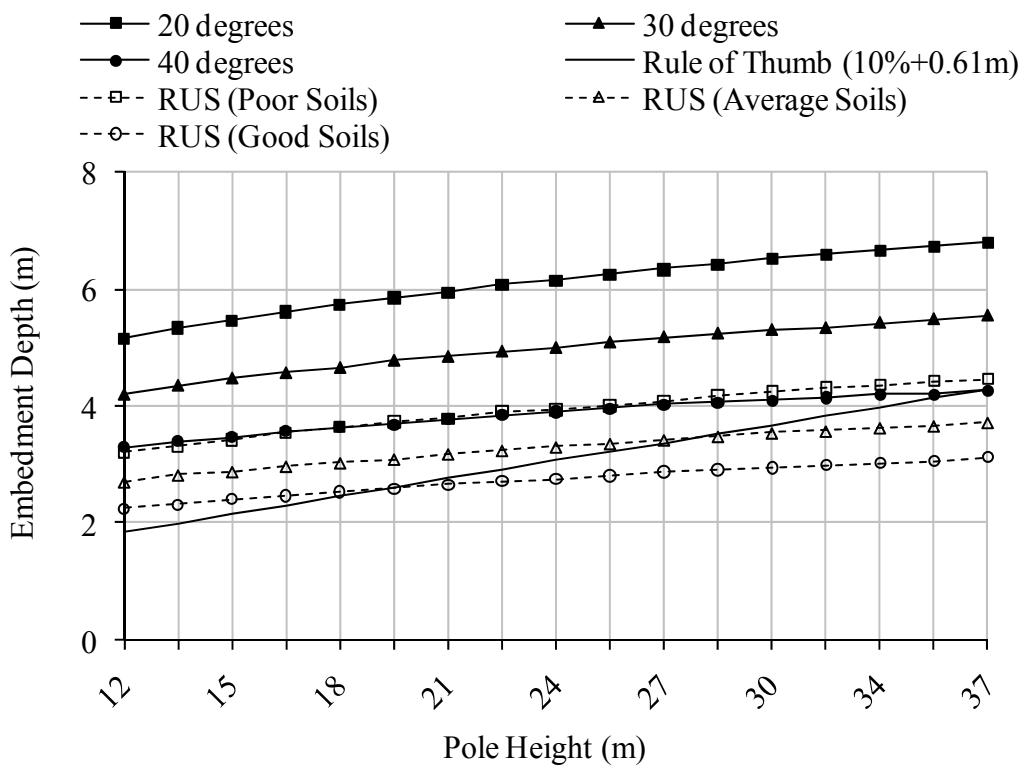


Figure 6. Required embedment depths for Prasad et al.'s method for moist cohesionless soils (class H3 poles). (Adapted from McNames, 2008)

**Linear Curve Fitting for Cohesive Soils.** It was determined that the results for Broms' (1964a) and Fleming et al.'s (1999) methods tend to follow a linear curve. Therefore, linear equations for each method were generated using the soil classifications listed in Table 1. The purpose of providing the linear equations is to give the designer a method similar to the traditional "rule of thumb". To simplify the amount of equations, the results for class H3 poles and the lower limit of the undrained shear strength (Table 1) were used to generate the linear equations. As was noted earlier, embedment depths for class H3 poles are typically 21%, 16%, 10% and 5% greater than class 2, 1, H1, and H2 respectively. Therefore, the linear equations presented will provide conservative results for pole classes smaller than H3. The linear equations and the coefficient of reliability,  $R^2$ , associated with each equation are listed in Table 3 for cohesive soils.

**Table 3. Summary of Linear Equations for Cohesive Soils (Adapted from McNames, 2008)**

Method	Soil Classification	Linear Equation	$R^2$ Value
Broms	Very Poor Clay	$z \text{ (m)} = 0.18*L + 6.7 \text{ m}$	0.990
	Poor Clay	$z \text{ (m)} = 0.09*L + 3.4 \text{ m}$	0.972
	Average Clay	$z \text{ (m)} = 0.06*L + 2.7 \text{ m}$	0.966
	Good Clay	$z \text{ (m)} = 0.05*L + 2.1 \text{ m}$	0.964
Fleming et al.	Very Poor Clay	$z \text{ (m)} = 0.15*L + 6.7 \text{ m}$	0.999
	Poor Clay	$z \text{ (m)} = 0.07*L + 3.4 \text{ m}$	0.979
	Average Clay	$z \text{ (m)} = 0.05*L + 2.4 \text{ m}$	0.953
	Good Clay	$z \text{ (m)} = 0.04*L + 1.8 \text{ m}$	0.989

It was revealed that embedment depths for transmission poles placed in cohesive soils can easily be determined from normalized plots using the quantity  $c_u D L^2 / M_{app}$  as shown in Figure 7. This quantity was chosen because all of these properties play a large role in determining the required embedment depth, and are parameters that can be easily obtained. This is also the normalization that gives the best fit for the data collected for each method. Some advantages of using the normalized plots rather than the linear equations include: more accurate embedment depths because all of the data gathered in the research is incorporated to the normalized plots, the applied loads can be tailored to fit a specific pole scenario, and the factor of safety is left up to the discretion of the designer.

It should also be noted that both methods provide unstable results for values of  $c_u D L^2 / M_{app}$  near 3.2. This occurs when heavily loaded poles are placed in soils with very low undrained shear strengths. To account for this, a lower limit of 3.2 has been set for both of the methods, and the data points below this limit have been removed to generate the curves shown in Figure 7. The upper and lower limits of the "rule of thumb" are also plotted along with the power curves to illustrate the limitations of the current method. Based on the data shown in Figure 7, it can be concluded that the "rule of thumb" will most often generate unconservative embedment depths.

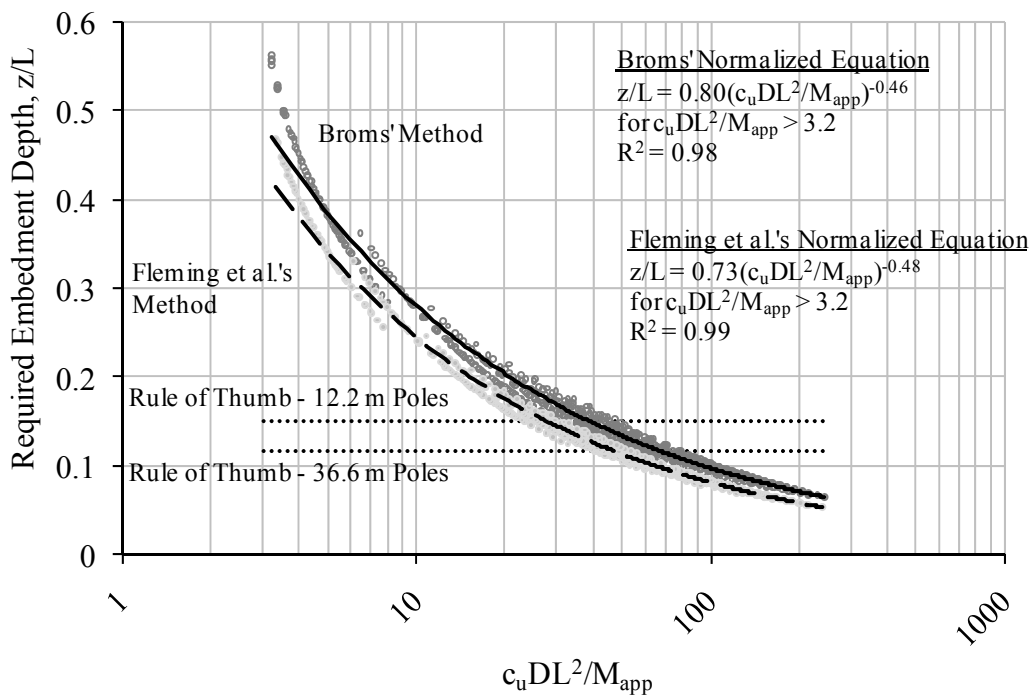


Figure 7. Normalized summary plots for laterally loaded transmission poles embedded in cohesive soils. (Adapted from McNames, 2008)

**Linear Curve Fitting for Cohesionless Soils.** Broms' (1964a), Fleming et al.'s (1992), and Prasad and Chari's (1999) methods for short-rigid laterally loaded piles were adopted for use in determining the required embedment depths for direct embedded transmission poles. It was determined that for nearly all pole classes, pole heights, and soil types; the embedment depths calculated by the existing methods provide unconservative results.

Based on the research, it was discovered that when plotted the data trends are nearly linear for all three methods studied. Therefore, linear equations were fit to each method based on the soil classifications listed in Table 2 using the lower limits of the friction angle for each classification and the data gathered for class H3 poles. The linear equations are shown in Tables 4 and 5 for moist and fully saturated cohesionless soils respectively. The embedment depths obtained using these equations will be conservative for class 2, 1, H1, and H2 poles. As was noted earlier, the embedment depths for class H3 poles are 15%, 11%, 7%, and 3% greater than class 2, 1, H1, and H2 poles respectively.

**Table 4. Summary of Linear Equations for Moist Cohesionless Soils (Adapted from McNames, 2008)**

Method	Soil Classification	Linear Equation	R <sup>2</sup> Value
Broms	Poor Sand	$z \text{ (m)} = 0.04*L + 3.4 \text{ m}$	0.974
	Average Sand	$z \text{ (m)} = 0.03*L + 3.0 \text{ m}$	0.981
	Good Sand	$z \text{ (m)} = 0.03*L + 2.4 \text{ m}$	0.953
Fleming et al.	Poor Sand	$z \text{ (m)} = 0.05*L + 3.7 \text{ m}$	0.988
	Average Sand	$z \text{ (m)} = 0.03*L + 3.0 \text{ m}$	0.984
	Good Sand	$z \text{ (m)} = 0.03*L + 2.1 \text{ m}$	0.968
Prasad and Chari	Poor Sand	$z \text{ (m)} = 0.06*L + 4.6 \text{ m}$	0.986
	Average Sand	$z \text{ (m)} = 0.05*L + 3.7 \text{ m}$	0.974
	Good Sand	$z \text{ (m)} = 0.03*L + 3.0 \text{ m}$	0.944

**Table 5. Summary of Linear Equations for Fully Saturated Cohesionless Soils (Adapted from McNames, 2008)**

Method	Soil Classification	Linear Equation	R <sup>2</sup> Value
Broms	Saturated Poor Sand	$z \text{ (m)} = 0.06*L + 4.3 \text{ m}$	0.962
	Saturated Average Sand	$z \text{ (m)} = 0.05*L + 3.7 \text{ m}$	0.976
	Saturated Good Sand	$z \text{ (m)} = 0.04*L + 3.4 \text{ m}$	0.990
Fleming et al.	Saturated Poor Sand	$z \text{ (m)} = 0.06*L + 4.9 \text{ m}$	0.990
	Saturated Average Sand	$z \text{ (m)} = 0.05*L + 3.7 \text{ m}$	0.979
	Saturated Good Sand	$z \text{ (m)} = 0.04*L + 2.7 \text{ m}$	0.988
Prasad and Chari	Saturated Poor Sand	$z \text{ (m)} = 0.09*L + 5.8 \text{ m}$	0.992
	Saturated Average Sand	$z \text{ (m)} = 0.07*L + 4.9 \text{ m}$	0.978
	Saturated Good Sand	$z \text{ (m)} = 0.06*L + 3.7 \text{ m}$	0.970

The methods presented in this paper for cohesionless soils can also be normalized based on the quantity  $(\tan\phi)^{1.5} \gamma DL^3/M_{app}$ . Each of these parameters plays a role in determining the embedment depth and is a parameter that can easily be obtained by the designer. The data for each method has been fit to a power trendline with the results shown in Figure 8 for cohesionless soils. These results are compared to the “rule of thumb”, and it can be seen that the “rule of thumb” is unconservative for most conditions when compared to the alternative methods.

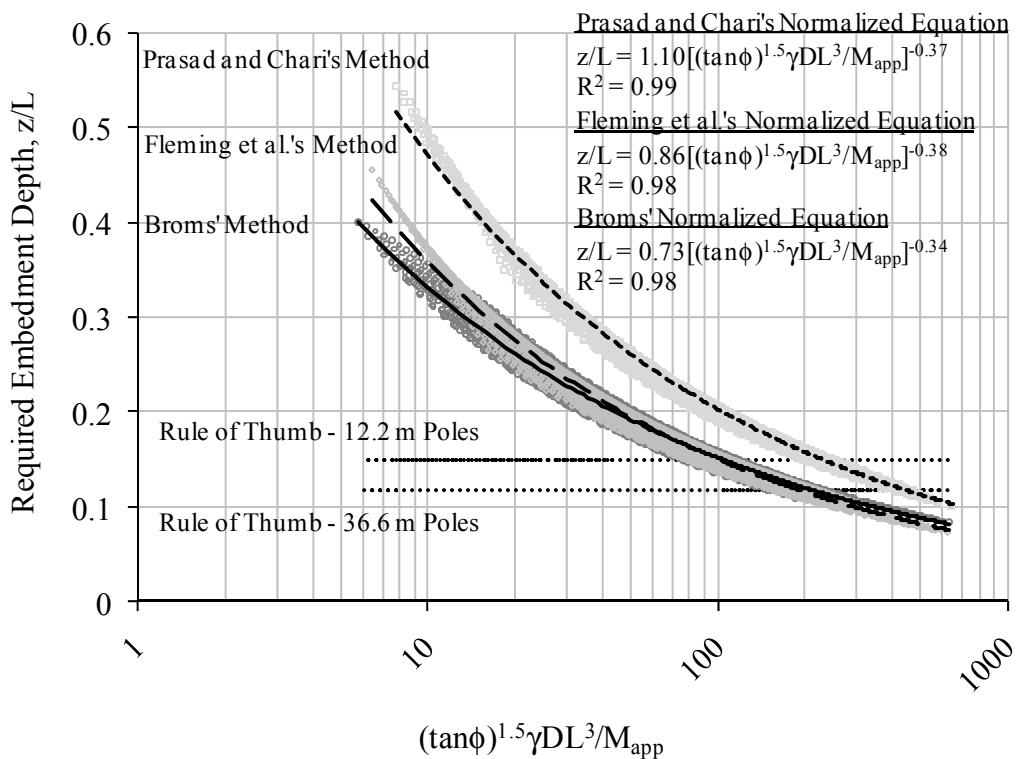


Figure 8. Normalized summary plots for laterally loaded transmission poles embedded in cohesionless soils. (Adapted from McNames, 2008)

## CASE STUDY

**Hancock 34.5 kV Windfarm Line (Wen, 2004).** In early 2004, several round, wood structures used to support a double circuit 34.5 kV transmission line fell over in Hancock County, Iowa after a storm left the ground saturated (Wen, 2004). Henry Wen was asked to investigate the cause of the failure, and found that the foundations were undersized when analyzed for the design loads using the soils found at the site. The poles used on the line were Western Red Cedar, 16.8 m (55 ft), class H1 poles. The embedment depth used in the original design was based on the “rule of thumb”, such that the poles were embedded in the ground 2.3 m (7.5 ft) (Wen, 2004).

Based on soil borings performed in the area, Wen (2004) determined that the poles should have been embedded in the ground up to 6.1 m in some areas (Wen, 2004). The PLS-Caisson (2002) program distributed by Power Line Systems (PLS, 2002) was used by Wen (2004) to determine the proper embedment depths for the poles. The PLS-Caisson (2002) program uses a modified version of Broms’ method (1964a&b) to determine proper embedment depths of transmission poles embedded in layered soils (PLS, 2002).

**Comparison with Alternate Design Methods.** Using the design loads and soil borings found in the report assembled by Henry Wen (2004), the alternative design methods included in this paper were compared to the PLS Caisson (2002) results determined by Wen. Since the soils found at the site consisted of layered cohesive soils, a weighted average for the undrained shear strength ( $c_u^*$ ) was calculated along the depth of embedment. (Additional information regarding the soils found at the site can be found in McNames, 2008.)

Wen (2004) determined that the poles placed near Boring #4 should have been embedded in the ground a total of 5.9 m (19.37 ft) with the PLS-Caisson (2002) program using an average diameter of 0.44 m (1.45 ft), pole height of 16.8 m (55 ft), applied moment of 257.7 kN-m (189.5 k-ft), and weighted average undrained shear strength of 12.2 kN/m<sup>2</sup> (255 psf) (Wen, 2004). The linear equations presented in this paper for Broms' (1964b) and Fleming et al.'s (1992) methods predict required embedment depths of 9.7 m (31.9 ft) and 9.2 m (30.25 ft) respectively. Wen's (2004) results are also compared to the normalized plots presented in this paper. The predicted embedment depths are 5.9 m (19.25 ft) and 5.2 m (17.1 ft) for Broms' (1964b) and Fleming et al.'s (1992) methods respectively.

The design parameters Wen (2004) used for Boring #5 are as follows: 0.44 m (1.45 ft) pole diameter, 16.8 m (55 ft) pole height, 257.7 kN-m (189.5 k-ft) applied moment, and an average undrained shear strength of 29.1 kN/m<sup>2</sup> (607 psf) (Wen, 2004). Based on these parameters, Wen (2004) determined that the embedment depth required is 3.8 m (12.37 ft) from the PLS-Caisson (2002) program (Wen, 2004). When these parameters are used with the linear equations presented in this paper, the predicted embedment depth is 4.9 m (15.95 ft) for Broms' (1964b) method and 4.5 m (14.85 ft) for Fleming et al.'s (1992) method. The normalized methods produce embedment depths of 4.0 m (13.2 ft) and 3.5 m (11.55 ft) for Broms' (1964b) and Fleming et al.'s (1992) methods.

**Conclusion.** When compared to the existing rule of thumb, the simplified linear equations generated conservative values for the embedment depth. This is due to the fact that the linear equations presented are generated using the ultimate moment capacity and geometry of class H3 poles, and are based on the lower limits of the soil parameters presented in Table 1.

As can be seen in the previous examples, the normalized plots provide embedment depths within 12% of those calculated by the PLS-Caisson (2002) program. The rule of thumb that was used in the original design of the foundations in question underestimated the embedment depth by as much as 61% in some locations. The normalized plots predict a much improved and more reliable design compared to the traditional rule of thumb method. The method of using a weighted average for layered cohesive soils proved to be fairly accurate, although it should be tested with additional soil types.

## SUMMARY AND CONCLUSIONS

When the results of the alternate methods presented in this paper are compared to the current design methods: RUS (2004) and “rule of thumb”, it is evident that the current design methods can greatly underestimate and overestimate the required embedment depth depending on the applied load, pole class, pole height, and soil properties. This is due largely to the fact that the pole and soil properties are not fully analyzed in the current methods. The embedment depth is a function of the pole diameter, pole height, applied load, and soil parameters (unit weight, friction angle, and undrained shear strength). All of these properties should be considered when determining the proper embedment depth for a transmission pole.

Alternative design methods have been presented for determining the necessary embedment depths of round, wood transmission poles. Simplified linear equations are presented in a similar format as the “rule of thumb”. It was shown that this method will provide results that are conservative compared to the current methods. The normalized plots and equations provide the designer with additional flexibility, such that the loading and factor of safety is determined by the designer.

To determine the accuracy of the proposed methods, the alternate design methods were compared to a case study where several poles fell over due to inadequate foundation design. It was determined that the normalized methods presented in this paper predict embedment depths similar to the PLS-Caisson program (2002). Based on comparisons with the results obtained in the case study by Wen (2004), it was concluded that the simplified linear equations will provide the designer with more conservative embedment depths unlike the current methods.

## REFERENCES

- American National Standards Institute (ANSI), Inc. (1987). “American National Standard for Wood Poles – Specifications and Dimensions,” *ANSI O5.1*, American National Standards Institute, New York.
- Broms, B. (1964a). “Lateral Resistance of Piles in Cohesionless Soils,” *Journal of the Soil Mechanics and Foundation Division*, ASCE, Vol. 90, No. SM3, pp. 123-156.
- Broms, B. (1964b). “Lateral Resistance of Piles in Cohesive Soils,” *Journal of the Soil Mechanics and Foundation Division*, ASCE, Vol. 90, No. SM2, pp. 27-63.
- Fan, C.C., and Long, J.H. (2005). “Assessment of Existing Methods for Predicting Soil Response of Laterally Loaded Piles in Sand,” *Computers and Geotechnics*, Vol. 32, pp. 274-289.
- Fleming, W.G.K., Weltman, A.J., Randolph, M.F., and Elson, W.K. (1992). *Piling Engineering*, 2<sup>nd</sup> Edition, Blackie & Son Ltd, New York.
- Keshavarzian, M. (2002). “Self-supported Wood Pole Fixity at the ANSI Groundline,” *Practice Periodical on Structural Design and Construction*, Vol. 7, No. 4, pp. 147-155, Nov. 1.

- McNames, C. (2008), "Improved Design of Embedment Depths for Round, Wood Transmission Poles Subject to Lateral Loading" MS Paper, North Dakota State University, August 2008.
- Power Line Systems, Inc. (PLS) (2002). *Caisson*, Version 4.91.
- Prasad, Y., and Chari, T. R. (1999). "Lateral Capacity of Model Rigid Piles in Cohesionless Soils," *Japanese Geotechnical Society: Soils and Foundations*, Vol. 39, No. 2, pp. 21-29.
- Rural Utilities Service (RUS) (2004). "Design Manual for High Voltage Transmission Lines," *RUS Bulletin 1724E-200*, U.S. Department of Agriculture.
- Wen, H. (2004). "Hancock 34.5 kV Windfarm Line," *A Memorandum to Bob Vosberg*, July 12. (Line Failure Study Report emailed to the author by H. Wen.)

## **Assessment and Repair of Steel Tower & Steel Pole Foundations**

Nelson G. Bingel III<sup>1</sup> and Kevin D. Niles<sup>2</sup>

<sup>1</sup>Osmose Utilities Services, Inc., 215 Greencastle Rd., Tyrone, GA 30290-2944; PH (770) 632-6703; email: nbingel@osmose.com

<sup>2</sup>Osmose Utilities Services Inc., 980 Ellicott St., Buffalo, NY 14094-2398; PH (716) 319- 3404; email: kniles@osmose.com

### **Abstract**

During the course of their service-life steel pole and lattice tower foundations are subjected to significant environmental forces that can have a detrimental impact on their service life. Foundations are critical components of all transmission systems and therefore are crucial to the national power grid.

Deterioration identified in these foundations during regular inspections and assessment should be categorized into specific levels of structural severity. Each should be addressed accordingly by a varied regimen of mitigation and repair options.

Coatings and anode installation are most commonly used to help prevent deterioration. Repair options include but are not limited to: bolted steel repairs, welded steel repairs, reinforced concrete encasement of concrete foundations and direct member replacement.

This paper will address assessment and repairs specific to steel tower and steel pole foundations inclusive of structural durability, corrosion issues and standard repair methods.

### Steel Transmission Structures

Regardless of their construction, steel transmission structures are composed of two basic components: the foundation which provides basic structural support for the entire structure and the structure itself, which creates clearance and provides support to the overhead electric conductors, ground wires and their associated hardware.

Most steel transmission structures can be separated into five distinct groups:

- Self Supporting Steel Lattice Towers – which are typically constructed by mechanically joining multiple steel members together to form a supporting lattice space truss.
- Guyed Steel Lattice Towers – similar to the self supporting steel lattice structures described above, guyed towers are distinctly different because of their reliance on multiple guys to provide structural stability.
- Self-Supporting Steel Poles – which are usually constructed of only a few large components welded together to form a tapered hollow “pole”.
- Guyed Steel Poles – similar to self-supporting steel poles, guyed steel poles rely on multiple guy wires to provide stability.
- Tubular Steel H-Frames – consisting of two steel poles placed adjacent to each other with a steel cross arm spanning the distance between the two.

### Foundation Types

All steel structure types require an adequate foundation to support the loads imposed on the structure. Because of the varying types of environments and soil conditions where these structures may be located, it is necessary to utilize different types of foundations in order to provide a stable platform for the structure. These include:

- Direct-embedment, which can be utilized for both steel poles and steel grillage, involves the excavation of a foundation hole in the earth by means of a drill rig or similar equipment. Excavations are made to accommodate the tower leg and grillage, which are set into the excavation and backfilled with either native soil, compacted gravel, crushed stone or concrete.

Direct embedment of steel poles and steel grillages may sometimes be preferred over other foundation options due to their typically lower cost and ease of installation. However, they are usually not used where shallow rock and ledge are present or in areas where soil stability is a concern due to sandy soil conditions or in soil weakened by the influence of water.

- Concrete foundations can encompass a wide range of variations depending on the application they are being utilized for. Two of the most common types are:
  - Drilled shafts –also called caissons, which are probably the most widely used concrete foundation type. These foundations are installed by drilling holes with a large auger and then filling them with concrete and reinforcing steel.

In some cases a “belled” drill shaft is used instead of a straight shaft to help provide additional capacity. A belled hole is created in the same way as a regular drilled shaft but with a distinct modification. The bottom portion of the hole is hollowed out creating a type of anchor or “bell” at its base.

- Pier slabs (pads) – encompass a wide range of applications and can either be pre-cast or formed and poured in place. Typically, these foundations are relatively shallow in comparison to drilled foundations, with most set at an average depth of approximately 10' or less. This usually entails the excavation of large foundation holes and a significant amount of non-native backfill which is compacted in place over the foundations. These foundations rely on their large surface area and weight of backfill to provide stable support for the structure and resistance to uplift.

One of the most significant advantages of reinforced concrete foundations is that the structural steel members are protected from the environment by the concrete, which limits their exposure to corrosion and significantly increases their service life.

#### Base Plates, Anchor Bolts and Stub Angles

When utilizing drilled shaft or pier slab foundations it is necessary to have a reliable interface connection between the steel and concrete.

Three of the most common connections are

- Base Plate and Anchor Bolts – Lattice towers and steel poles have used both base plates and anchors bolts of various designs to anchor the upper support structure to the foundation.
- Stub Angles – usually a short piece of angle steel with shear connectors, which is set directly into the concrete.
- Pin Bases – several designs have been engineered to create a pin connection between a tower and its foundations. These are normally used with guyed structures such as guyed vee's.

### Reasons to Inspect

It is important to understand that with all structures there is a need for periodic inspection to ensure structural integrity and public safety. Steel structures and their foundations are no exception, as these structures are sometimes placed in environments that are less than ideal relative to the longevity of their structural components.

Environmental conditions can have a dramatic impact on the structural integrity of steel and concrete over relatively short periods of time. Detrimental influences such as agricultural activity, changes in soil elevation from construction and emissions from manufacturing facilities can all contribute to the degradation of structural components. These effects can be compounded by unseen defects in structural members, coatings and concrete at the time of construction.

Often these environmental influences combine to create active corrosion cells which are detrimental to steel structural components.

### Definition of a Corrosion Cell

The basic electrochemical corrosion cell consists of four components; a cathode, an anode, an electrolyte and a metallic path. Corrosion within the cell exists because of the flow of electrons and ions between these components.

- Anode – the point where corrosion takes place within the cell due to the flow of positively charged ions away from it.
- Cathode – negatively charged ions migrate from the cathode, which creates a polarization helping to protect the cathode from corrosion.
- Electrolyte – is a substance or solution capable of conducting electricity.
- Metallic path – conducts negatively charged electrons from the anode to the cathode.

With a corrosion cell on steel towers and steel poles, the electrolyte is represented by the soil the structure is buried in. The metallic path is the metal of the structure and the cathode and anode can either be between the different legs of a steel tower or along the surface of a steel pole where there is a difference of corrosion potential between two points.

### Development of Corrosion Inspection

Some of the earliest studies into corrosion took place in England during the mid to late 1800s, with additional detailed testing to come in the early 1900s. This early research into the chemistry of corrosion developed the fundamentals of research and inspection that are still in use today.

Mainly used in gas, petroleum and other similar industries, corrosion inspection is a proven science with a long history of success. Inspection procedures and equipment have been developed and refined over many years, even though some of their basic principles have not changed.

In recent years, inspection methods and mitigation technology have been adopted by many other industries, both public and private, which have an economic interest in protecting their infrastructure. Electric utilities are no exception and have begun to recognize the necessity for integrating corrosion inspection and mitigation efforts into their regular maintenance programs.

### Direct Inspection Procedures

A large majority of corrosion inspection is conducted through visual and physical assessment. These inspection methods include:

- Visual assessment – by utilizing various grading criteria from recognized experts in the industry, corrosion on metal can be quantified by various grades. A standard method for this purpose is the “SSPC VIS2 Standard Method for Evaluating Degree of Rusting on Painted Steel Surfaces”, developed by the Society for Protective coatings. This allows the inspector to compare existing surface corrosion to samples in the standard so the corrosion can be classified by both type and severity.
- Physical measurements – allow the inspector to measure the different components of a structure to help determine the amount of section loss caused by corrosion. The most common hand devices for these measurements are calipers, micrometers and pit gauges. Photos are sometimes also used to support the physical measurements recorded in the field.
- Excavation – because steel towers and steel poles may be buried in soil it is often necessary to make shallow inspection holes. The excavation extends the visual assessment and physical measurements through the initial transition area of the steel to soil interface. Usually inspection excavations are limited to a depth of 18” – 24” but can occasionally be deeper if necessary to determine the extent of visible corrosion.
- Ultrasound measurements – when visual inspection and physical measurements are limited due to a structures design or location, ultrasound

can be successfully utilized in certain applications to help further assess a structures condition.

- Electromagnetic Acoustic Transducer (EMAT) technology has expanded the use of ultrasonic testing from rudimentary lateral scans reading through the structure to longitudinal scans along the length of its surface. This process can detect below ground corrosion on steel structures.

### Indirect Inspection Methods

Environmental factors have a significant affect on the corrosion process. Indirect inspection methods have been developed to quantify their influence at specific locations. Several of these methods have become standard procedures in the pipeline industry and have been adapted for use in evaluating the environmental conditions surrounding steel structures.

- pH – probably one of the most easily understood environmental influences, the pH measurement of soil surrounding a tower determines how acidic the soil is and helps to define its potential influence in the corrosion process. Measurements of a pH around 7 show a relatively neutral environment while measurements of 5.5 or less are considered to be acidic. A pH reading of 8.0 or more usually indicates an alkaline environment and is typically less of a concern as it usually has little corrosive effect on steel.
- Redox – otherwise known as the measurement of oxygen reduction, redox measures the dissolved oxygen content in the soil. Distinct differences in oxygen content in the soil surrounding a buried steel structure can indicate the potential influence of microbial activity on corrosion.

Although bacteria itself does not typically attack metals directly, various bacteria develop in certain Redox environments which can influence the corrosion process by creating corrosive byproducts. Environments free of oxygen support the presence of anaerobic bacteria, while oxygen rich environments tend to support aerobic bacteria. Environments that exist somewhere in the middle of the scale are relatively neutral and tend not to support microbial activity detrimental to steel. Redox measurements collected in close proximity to the structure can help to determine whether a structure is at risk from microbial influence.

Redox measurements of less than 100 mV can indicate the presence of aerobic bacteria and an increased potential for corrosion activity. While redox measurements between 100 and 350 mV which tend to support more anaerobic activity tend to be more neutral.

- Soil Resistivity - is a significant indicator in determining how corrosive a soil environment is. Soils with low resistivity allow for the easy flow of current

between an anode and cathode creating a higher level of corrosion activity. Soils with a resistivity of 1000 ohm-cm or less tend to be very corrosive, while soils with a resistivity of 10,000 ohm-cm are considered much less of an influence to corrosion.

- Half –Cell Measurements – measure the structure to soil potential within the environment. Typically, this is done utilizing a digital or analog potential meter. The more negative the measurement is ( $< -.850$  mV), the more likely it is that the structure will have a reduced potential for corrosion. The less negative the measurement ( $> -.400$  mV), the more likely it is to corrode.

### Corrosion Rating

The factors previously discussed are only indicative when considered alone. They must be evaluated as to how they relate to each other in a specific environment. To do this an algorithm was developed to measure these factors together in order to determine a structures potential for corrosion or its “corrosion rating”.

These ratings are divided into specific categories quantifying each structure’s potential for future corrosion, as listed below:

- Low – the potential for corrosion is low and no further action is necessary at this time. Typically the recommendation for these structures is to re-inspect in another ten years.
- Mild – the potential for corrosion is slightly elevated and, while it may not be visually evident, it is possible that minor corrosion activity is present. Similar to the structures rated as low, it is recommended to re-inspect these structures in another ten years
- Moderate – structures rated as moderate usually show positive indicating factors for corrosion even though only minor corrosion may currently be visible. This corrosion may appear as minor surface corrosion or pitting. Structures in this condition should have mitigation efforts put in place soon to help avoid further corrosion degradation. Once these measures are put in place, these towers should be re-inspected within ten years.
- Severe – these towers are significantly corroded and show signs of metal loss such as large pitting, edge loss and thinning. In severe cases large perforation of structural members are present.

### Mitigation Alternatives

Similar to inspection methods, corrosion mitigation methods have been used in gas, petroleum and other industries for many years. As such, many of these products can be readily adapted for use in similar applications.

The most common and practical mitigation efforts available are the application of protective coatings. Coatings protect the steel from exposure to its surrounding environment, providing a barrier against moisture and other corrosive mechanisms.

A good coating application program involves an extensive excavation and a thorough surface cleaning of the structure prior to application of the coatings. These surface preparations are critical to the overall performance of the coating system and are covered by a number of ASTM and NACE standards. Coatings are available in several different types for a variety of applications. It is very important that the correct material is used with the recommended application procedure to achieve the desired level of protection.

When coatings alone are not sufficient to protect structures from the effects of corrosion, an additional measure of protection that can be applied is sacrificial anodes.

Sacrificial galvanic anodes give up of themselves to protect steel structures from corrosion by means of the galvanic reaction that takes place between the steel and the anode. Because the anode is higher in the galvanic series than steel, when it is put in direct contact with the steel structure the loss of negatively charged ions is transferred from the steel to the anode so that the anode corrodes in place of the steel.

Anodes are usually applied by placing them into trenches or augured holes in close proximity to the structure. The anodes are then connected directly to the steel structure by means of a conductive wire.

Because of the varying amount of steel exposed in the ground on various structures, protective anode systems, or beds, are designed specifically for the structure they are to protect. A misapplication of anodes will usually result in inadequate protection for the structure and will likely lead to an early failure of the anode system.

### General Repairs

Structures that have deteriorated beyond the protective capabilities of coatings and anodes usually are significantly weakened by section loss of their supporting structural members or foundations. In most cases, in-place repairs can be individually engineered for these structures in order to avoid the high cost of replacing the entire structure.

### Concrete Foundation Repairs

Concrete foundation repairs can usually be achieved by simply encasing the degraded foundation in new concrete. This usually involves excavating around the foundations to an adequate depth to remove any loose or broken concrete and then placing forms

in place to accommodate the new concrete. Once the concrete is poured and hardened sufficiently the forms are removed and the new foundation is backfilled.

### Steel Repairs

Weakened structural steel members must either be replaced or reinforced to continue to provide adequate support to the structure. There are a number of different ways for this to be done:

- Complete Member Replacement – removing and replacing a complete member involves the temporary bracing of the structure to provide interim support for the tower while repairs are taking place. Once braced, the weakened member can be removed, in most cases, by simply unbolting it from the surrounding structure and replacing it with a member identical to its original design, which can be bolted back in place. Once repairs are complete the bracing can be removed.
- Bolted Member Section Replacement – similar to the entire section replacement, the tower is typically braced during the repair. However instead of replacing the entire member only the weakened section of the member is removed. That section is then replaced by drilling and bolting a new piece of steel of similar dimensions in place by drilling and bolting. Usually, there is a good amount of overlap of the section being replaced to accommodate the application of the bolts.
- Welded Member Section Replacement – in this repair the tower is temporarily supported and the weakened section is removed, however instead of bolting the new section in place the replacement piece of steel is usually butted up to the cut ends of the original member and butt-welded into place.
- Member Encasement – in this repair, instead of being removed the weakened piece of steel is encased in concrete.
- Bolted Splice Repair – this repair leaves the weakened member in place similar to the encasement repair. However, in this repair the weakened member is sandwiched between two similarly sized pieces of steel, which are drilled and bolted in place effectively transferring the load of the weakened member to the two new pieces of steel.

### Summary

Because of the aging infrastructure in the United States relative to the national power grid, it is important to bring to light practices and methodologies to the electric industry that help to improve practical economic decisions concerning its long term durability.

In this paper, some of the most common assessment and repair techniques and procedures available specific to steel tower and steel pole foundations were addressed.

It is hoped that this information generates further investigation into practical economic solutions that will maintain the national power grid through the responsible use of appropriate maintenance programs.

### References

- P.R. Roberge, “Scope of language and Corrosion” Corrosion Basics: An Introduction, Second Edition NACE (2006): pp. 15–19.
- H.H. Ulig, “The Cost of Corrosion in the United States,” Chemical and Engineering News 27 (1949): pg 2764.
- G.H. Koch, M.P.H. Brongers, N.G. Thompson, Y.P. Virmani, J.H Payer, “ Costs of Corrosion and Preventative Strategies in the United States,” National Technical information Services, FHWA-RD-01-156, Springfield, VA, Sept. 30, 2001.
- NACE Publication 3C149, “Economics of Corrosion” (Houston, TX: NACE, 1994).
- R.D. Gundry, Corrosion/93 Plenary & Keynote Lectures (Houston, TX: NACE International, 1993).
- W. Lynes, “Some Historic Developments Relating to Corrosion,” Journal of the Electrochemical Society 98 (1951): pp. 3C – 10C.
- S.D. Cramer, B.S. Covino, G.R. Holcomb, M. Ziomek-Moroz, “Information Sources and Databases for the Corrosionist,” in vol. 13A, Corrosion: Fundamentals, Testing, and Protection, eds. D.S. Cramer, B. S, Covino (Metals Park, OH: ASM International, 2003), pp.999-1001

## Substation Bus Design: Current Methods Compared with Field Results

Keith Malmedal Ph.D. P.E. P.Eng.<sup>1</sup> and John Wendelburg P.E.<sup>2</sup>

<sup>1</sup> NEI Electric Power Engineering, President, Box 1265, Arvada, CO 80001; PH (303) 431-7896; Fax (303) 431-1836; email: [kmalmedal@neiengineering.com](mailto:kmalmedal@neiengineering.com)

<sup>2</sup>NEI Electric Power Engineering, Project Manager, Box 1265, Arvada, CO 80001; PH (303) 431-7895; Fax (303) 431-1836; email [jwendelburg@neiengineering.com](mailto:jwendelburg@neiengineering.com)

### ABSTRACT

Current standards define accepted methods of substation bus design. These standards also require certain strength and deflection criteria. This paper will examine commonly proscribed rigid bus design methodologies and compare them with actual field experience in the design of a 500kV switching station. Special attention will be given to required deflection criteria, methods commonly used to achieve these criteria, and results actually measured in the field.

### INTRODUCTION

The bus work in a substation are the structures that carry the electrical current. They are usually made of aluminum pipe or cable and are supported by porcelain or polymer insulators which are in turn supported by steel supports on foundations. Since the buses are typically energized at high voltages they must be separated from each other by distances that increase as the voltages increase. The air between the buses serves as the insulation between the voltages on each bus preventing electrical arcs from developing between the buses which would cause their destruction. This paper will consider the bus types used in this type of typical air-insulated substation using aluminum pipe bus. Gas insulated substations or substations using cable or materials other than aluminum will not be discussed.

Several forces, some electrically produced and some resulting from environmental effects, must be resisted by the bus design. Short circuits occurring either near or remote from the substation cause high current flows for short periods of time in the buses. These high currents cause high magnetic fields between the buses which produce large forces that must be considered in design. Buses must also be designed for gravity forces, including the weight of ice during icing conditions, wind, and seismic forces.

The approach normally taken in design is to choose a minimum bus diameter dependent upon current carrying ability and corona limitations and then determining the maximum span between bus supports dependent upon both deflection and strength limits of the aluminum pipe used. Bus diameter may need to be adjusted due to required span lengths between bus supports. After an adequate span and bus

diameter are chosen, the necessary cantilever strength of support insulators is calculated and insulator types are chosen. If sufficiently strong insulators are not available, or are determined to be too costly, additional supports may be added to reduce maximum bus spans.

### BUS SIZE DUE TO AMPACITY REQUIREMENTS

Bus ampacity (the amount of current a bus can safely carry) sets the lower limit for bus size. Every substation must carry a certain maximum amount of current and the bus work must be large enough to carry this current. As the amount of current a conductor carries increases, the temperature of that conductor will increase. Aluminum may be safely operated continuously at a temperature of 90°C; however, to prevent excessive oxidation this is usually limited to 70°C. There are two aluminum alloys available for pipe bus, 6061-T6 (with a conductivity of 40%) and 6063-T6 (with a conductivity of 53%). If the bus work needs to be designed for maximum ampacity, then 6063-T6 should be the choice. 6063-T6 allowable stress is somewhat less than 6061-T6, so the higher conductivity is counterbalanced by the need to provide more frequent supports. If minimizing the number of bus support points is the most important criteria, then 6061-T6 should be chosen. The current carrying capacity of the aluminum is also affected by the emissivity of the material. For both alloys the emissivity may be taken as 0.5.

Certain ambient conditions must be assumed. Conservatively, full sun and no wind (or very small wind) may be used. IEEE Std. 605 contains equations which may be used to determine bus ampacity under nearly any condition, but using the above assumptions (full sun, emissivity = 0.5, no wind, maximum temperature rise of 30°C at 40°C ambient resulting in a maximum temperature of 70°C) Table 1 may be used to choose the minimum bus size required based on ampacity.

**Table 1: Pipe bus Ampacity 30° rise over 40° ambient.**

Nominal Bus Size (in)	6063-T6		6061-T6	
	Schedule 40 Ampacity (Amps)	Schedule 80 Ampacity (Amps)	Schedule 40 Ampacity (Amps)	Schedule 80 Ampacity (Amps)
1.0	572	650	510	580
1.5	805	930	718	830
2.0	991	1161	884	1037
2.5	1314	1507	1173	1345
3.0	1582	1833	1412	1637
3.5	1796	2092	1603	1868
4.0	2015	2358	1800	2105
5.0	2474	2912	2009	2532
6.0	2943	3547	2628	3167
8.0	3830	4556	3420	4068

## CORONA EFFECTS ON REQUIRED BUS SIZE

Corona is a physical condition caused by the ionization of air near an energized conductor. It results in energy loss, noise, and light emissions. Its major effect is radio interference. Corona must be minimized to prevent excessive electromagnetic interference (EMI). Corona discharges increase as the voltage on a bus increases or its diameter decreases. Corona will also increase on sharp edges or at corners. Bus size must be chosen to keep corona below allowable levels. Typically, corona only becomes a concern when station voltages equal or exceed 230kV line-to-line. IEEE Std. 605 contains methods to determine the minimum bus size necessary to prevent excessive corona. Assuming typical bus configurations, spacing, and heights given in IEEE Std. 1427, Table 2 gives the minimum bus diameters which may be used at various altitudes.

**Table 2: Minimum allowable bus diameter (in.) to minimize corona discharge.**

System Voltage (kV)	Altitude above sea level (ft)										
	0	1,000	2,000	3,000	4,000	5,000	6,000	8,000	10,000	15,000	20,000
230	1.5	1.5	1.5	1.5	1.5	1.5	2	2	2	2.5	2.5
345	2	2.5	2.5	3	3.5	3.5	3.5	4	4	5	5
500	3.5	4	5	5	5	6	6	8	8	8	8
765	8	8	8	8	>8	>8	>8	>8	>8	>8	>8

## FORCES ON SUBSTATION BUSES

After the preliminary bus size is chosen using ampacity and corona criteria, the forces on the bus can then be calculated with the objective of determining the required spacing between support structures. This distance is typically limited by deflection but may also be limited by strength considerations of the bus type or the supporting insulators.

Three forces must be computed.

1. Gravitational = bus weight+ice load weight+damping conductor weight
2. Short circuit forces
3. Wind forces

Ice loading for any location in the U.S. may be determined from IEEE Std. C2 or ASCE 7-05. Ice weight per foot may then be found using equation 1.

$$W_i = 1.24r(d + r) \quad [1]$$

Where:

- $W_i$  = Ice weight (lb/ft)  
 $r$  = radial ice thickness (in)  
 $d$  = bus diameter (in)

Weight of bus of varying diameter may be found in Table 3.

**Table 3: Unit weight and section modulus of aluminum bus.**

Nominal Bus Size (in)	Schedule 40			Schedule 80		
	Unit Weight (lb/ft)	Section Modulus (in <sup>3</sup> )	Moment of Inertia (in <sup>4</sup> )	Unit Weight (lb/ft)	Section Modulus (in <sup>3</sup> )	Moment of Inertia (in <sup>4</sup> )
1.0	0.581	0.1328	0.0873	0.751	0.1606	0.1056
1.5	0.94	0.3262	0.3099	1.256	0.4118	0.3912
2.0	1.264	0.5606	0.6657	1.737	0.7309	0.8679
2.5	2.004	1.064	1.530	2.65	1.339	1.924
3.0	2.621	1.724	3.017	3.547	2.225	3.894
3.5	3.151	2.394	4.788	4.326	3.140	6.281
4.0	3.733	3.214	7.232	5.183	4.272	9.611
5.0	5.057	5.451	15.16	7.188	7.432	20.67
6.0	6.564	8.498	28.15	9.884	12.227	40.501
8.0	9.878	16.813	72.51	15.008	24.520	105.743

Bare aluminum conductors may be installed inside tubular bus to attenuate wind induced vibrations. Typically these conductors are chosen to have a unit weight equal 10%-30% of the bus unit weight. Vibration damping conductors should be installed if maximum span lengths exceed those shown in Table 4.

**Table 4: Maximum span length allowed without vibration damping conductors.**

Nominal Bus Size (in)	Maximum Span Length Without Vibration Damping
1.0	5'
1.5	7'
2.0	9'
2.5	10'-9"
3.0	13'-3"
3.5	15'-3"
4.0	17'
5.0	21'-3"
6.0	25'-3"
8.0	28'

When a short circuit occurs inside or outside the substation currents will flow through the buses which may be orders of magnitude higher than normal current. These high currents produce magnetic fields surrounding the buses which will try to either force the buses toward or away from each other depending upon the direction of current flow. These forces must be computed and resisted by the buses and their supports. The Design Guide for Rural Substations (RUS 2001) gives Equation 2 for calculating the maximum short circuit forces which will occur on evenly spaced buses.

$$F_{sc} = (37.4 \times 10^{-7}) 0.67 \frac{i^2}{D} \quad [2]$$

Where:

- $F_{sc}$  = Short Circuit Forces (lb/ft)  
 $i$  = Short Circuit Current (Amps rms)  
 $D$  = Centerline-Centerline spacing of buses (in.)

Wind loading may be calculated using pressures derived from ASCE 7-05 or from IEEE Std. C2. When ASCE 7-05 is used there are three loading cases that must be considered and two wind values are needed. The three loading cases are:

1. Extreme wind on bus without ice.
2. Coincident wind on bus including ice.
3. Extreme ice no wind.

The first load case requires determining the fastest possible wind for the location in question. The second load case requires the value of wind shown coincidental with the worst icing conditions. The wind force is then calculated using the first value on a bus diameter without ice and the second value on a bus diameter including ice. The third case is a vertical load only. The largest resultant force is then used in the design. If IEEE Std. C2 is used, only one calculation is needed (unless the bus is over 60 feet above ground level) based upon the value for wind pressure given for the loading district (light, medium or heavy) at the location. In either case Equation 3 is then used to calculate the force per unit length on the bus.

$$F_w = 0.083 P_w d \quad [3]$$

Where:

- $F_w$  = Wind loading (lb/ft)  
 $P_w$  = Wind pressure ( $\text{lb}/\text{ft}^2$ ) from ASCE 07 or IEEE Std. C2  
 $d$  = Outside diameter of the conductor including ice if needed (in.)

The total bus loading  $F_T$ , in lb/ft may then be determined using Equation 4 where  $W_C$  is the sum of the bus and the dampening conductor weight in lb/ft.

$$F_T = \sqrt{(F_{sc} + F_w)^2 + (W_C + W_i)^2} \quad [4]$$

If wind loads were computed using ASCE 7, then Equation 4 must be solved three times. The first case will include wind without ice in which case  $W_i$  is not included. The second case will be coincident wind with ice. The third case is ice only and  $F_w$  is not included. In all cases short circuit forces  $F_{sc}$  should be included. The worst total  $F_T$  will then be used to determine the maximum bus support spacing. If wind loads

are computed using IEEE Std. C2, then Equation 4 applies both wind and ice loads simultaneously for the appropriate loading district. However, IEEE Std. 605 suggests applying lateral and gravity loads individually and calculating  $F_T$  first with only maximum wind and then with only maximum ice and then using the largest value of  $F_T$ . If the bus height were to exceed 60 ft. then IEEE Std. C2 would also require an additional computation for the extreme wind condition in which case Equation 4 must be solved again using the extreme wind pressure but no ice load. RUS 1724E-300 takes a more conservative approach and suggests extreme wind be considered for all bus designs no matter their height. So, while the design standards are not completely consistent, it would seem prudent to consider the following load cases for  $F_w$  and  $W_i$  when solving Equation 4.

1. Simultaneous NESC wind and ice for district loading.
2. Extreme wind (taken from ASCE 7 or IEEE Std. C2) and no ice.
3. Coincident wind and ice (taken from ASCE 7 or IEEE Std. C2).
4. Extreme ice (taken from ASCE 7 or IEEE Std. C2) and no wind.

### CALCULATING MAXIMUM DISTANCE BETWEEN BUS SUPPORTS

After all forces are determined, the maximum allowable distance between bus supports may be calculated. Strength criteria and then deflection criteria will be used to determine a maximum possible bus length between supports for each case. Then the shorter of the two distances will be used. The RUS suggests Equation 5 to determine the maximum allowable bus span considering strength criteria only.

$$L_M = \sqrt{K_{SE} \left( \frac{F_B S}{F_T} \right)} \quad [5]$$

Where:

- $L_M$  = Maximum bus support spacing (ft)
- $K_{SE}$  = Multiplying factor from Table 5
- $F_B$  = Maximum allowable fiber stress ( $\text{lb/in}^2$ )
  - 28,000  $\text{lb/in}^2$  for 6061-T6
  - 20,000  $\text{lb/in}^2$  for 6063-T6
- $S$  = Section modulus of the bus ( $\text{in}^3$ ) from Table 3.
- $F_T$  = Total conductor loading ( $\text{lb/ft}$ )

**Table 5: Values of  $K_{SE}$  and  $K_{DE}$  to be used in Equations 5, 6, 7 and 8.**

Bus System	$K_{SE}$	$K_{DE}$
Fixed Both Ends	1.0	4.5
Fixed-Simply Supported	0.82	9.34
Simply Supported Both Ends (single span)	0.82	22.5
Simply Support (two equal spans)	0.82	9.34
Simply Supported (three or more equal spans)	0.88	11.9

The RUS gives Equation 6 for calculating vertical bus deflection and recommends limiting deflection to L/200 including the effects of ice. IEEE Std. 605 however, suggests limiting deflection to a maximum of L/150 while not including ice in the calculation.

$$y = K_{DE} \frac{(W_C + W_i)L_D^4}{EI} \quad [6]$$

Where:

$y$  = Maximum bus deflection (in)

$K_{DE}$  = Multiplying factor from Table 5

$E$  = Modulus of elasticity =  $10 \times 10^6$  lb/in<sup>2</sup>

$I$  = Moment of inertia (in<sup>4</sup>) from Table 3

$L_D$  = Bus Support spacing (ft)

The maximum allowable length (ft) between supports using IEEE Std. 605 deflection limits would then be calculated from Equation 7.

$$L_D = 92.8 \sqrt[3]{\frac{I}{K_{DE} W_C}} \quad [7]$$

The maximum allowable length (ft) between supports using RUS deflection limits would be calculated using Equation 8.

$$L_D = 84.3 \sqrt[3]{\frac{I}{K_{DE}(W_C + W_i)}} \quad [8]$$

The calculation of deflection requires that the fixity of both ends of the span in question be determined. No end conditions will produce either completely fixed or simply supported, and the condition becomes more difficult to determine when some bus work is welded at the supports and some is not. One common condition is that a bus span is continuous on one side and supported by several supports over a long length, and simply supported on the other side. IEEE Std. 605 suggests a bus span of this type should be considered fixed on the continuous end and pinned on the other end. The RUS suggests, as may be seen in constant  $K_{DE}$  from Table 5, that the continuous end should not be considered entirely fixed.

The final factor limiting the allowable distance between bus supports is the strength of the insulators supporting the bus. The RUS recommends Equation 9 for determining the maximum allowable bus support spacing governed by the support insulator cantilever strength. This equation includes a suggested safety factor of 2.5 so the insulators working load will be approximately 40% of the rated cantilever strength.

$$L_s = \frac{W_s}{2.5(F_{sc} + F_w)} \quad [9]$$

Where:

- $L_s$  = The average of the two adjacent span lengths, or the span length if equal spans (ft)
- $W_s$  = Rated insulator cantilever strength (lbs)

The maximum bus span length can now be determined by finding the smaller of  $L_s$ ,  $L_D$ , and  $L_M$ .

## DESIGN EXAMPLE

In a recent switchyard design a critical long span (60 ft) was included which was needed to cross a service road. This span was critical because it was highly visible and for aesthetic reasons the owner wanted a strict L/150 limitation on the bus deflection. The span in question was supported as shown in Figure 1. It was continuous on one side and supported by more than three supports to which the bus was welded, and simply supported on the other side where it made a connection to an expansion fitting and a switch. Six-inch schedule 80 bus was used. A problem was encountered when the calculated deflection was compared to the actual results after construction was completed.

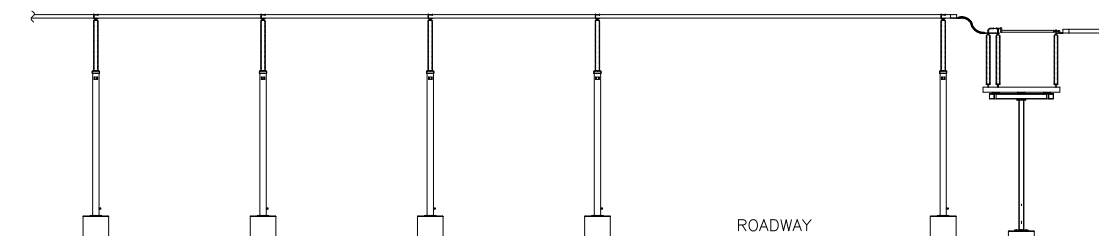


**Figure 1: Bus system with supports.**

The suggestions given in IEEE Std. 605 for fixity, deflection limits, and ice loading were used in the deflection calculations resulting in assuming a fixed-pinned condition without ice load. Using Equation 6 (and adding 30% to the bus weight due to the addition of the installed damping conductor) the maximum deflection should have been 3.94 inches which is well within the L/150 deflection limit (4.8-inches). A photograph of the bus in question is shown in Figure 2. After construction was complete the deflection was field measured and determined to be approximately 4.7 inches, which is much greater than expected and just barely within the 4.8 inches required. After creep the deflection would likely exceed the deflection criteria. The discrepancy between calculated and measured results is due to the inexactness of the fixity assumption. The continuous end of the span does not perform as perfectly fixed.



Figure 2: Deflection in 60 ft. bus span.

Assuming the span was a simply supported single span Equation 6 predicts a deflection of 9.51 inches which is far too large. Using the more exact assumption of three or more spans simply supported the calculated deflection becomes 5.03 inches which is slightly too large but close to the measured result. It is clear that none of the fixity assumptions contained in the RUS or IEEE Std. 605 design guidelines produces exact results for this condition and using the fixity suggestion contained in IEEE Std. 605 results in calculating a deflection that is much less than the installed condition. A far more exact and conservative result is produced by assuming all the spans are simply supported and using the value of  $K_{DE}$  from Table 5 for multiple simply-supported spans even though in the case considered the spans were not of equal length.

## CONCLUSION

Methods have been described which are commonly used to design bus systems. Only tubular aluminum materials were considered and no point loads were included in the methods described. In some spans point loads will exist, such as when high-bus is supported by a span of low-bus. These point loads must also be considered for the critical spans in question. The introduction of expansion joints is another condition to be considered for critical spans.

It may be seen that the methodology and assumptions included in RUS sources and IEEE sources may not always completely agree, and the engineer must

choose which assumptions best fit their design. Special consideration should be given to deflection calculations. Deflection in a substation bus design is typically not critical from a performance or structural standpoint but may become important for aesthetic considerations. However, when deflection does become critical, the fixity assumptions suggested in some standards were found to be somewhat in error and in the case of those in IEEE Std. 605 were non-conservative. In the case considered here, with a continuous bus on one side of the span and a pinned support on the other side of the span, the results using the assumptions for multiple simply-supported spans given in the RUS documents produced the most accurate results when compared with actual measured deflections, and the suggestions contained in IEEE Std. 605 resulted in considerable error when compared to field measured results.

## REFERENCES

- IEEE Std. 605-1998. *IEEE Guide for Design of Substation Rigid-Bus Structures*. IEEE , New York, NY.
- IEEE Std. 1427-2006. *IEEE Guide for Recommended Electrical Clearances and Insulation Levels in Air Insulated Electrical Power Stations*, IEEE New York, NY.
- IEEE Std. C2-2007. *National Electrical Safety Code*. IEEE New York, NY.
- RUS Bulletin 1724E-300. (2001). *Design Guide for Rural Substations*. Rural Utilities Service, U.S. Department of Agriculture. Washington D.C.
- ASCE Standard No. 7-05. (2006). *Minimum Design Loads for Buildings and Other Structures*, American Society of Civil Engineers, Reston, VA.

### 3D Automated Design of Substations

D.R. Lemelin<sup>1</sup>, C. Bégel<sup>1</sup>, C. Benavides<sup>1</sup>, C. Lacroix<sup>1</sup>, Y. Drolet<sup>1</sup>

<sup>1</sup>Hydro-Québec, Direction Ingénierie de Transport, Génie civil de Postes  
855 Ste-Catherine E., Montreal, Quebec, Canada, H2L 4P5  
email : [lemelin.denis.r@hydro.qc.ca](mailto:lemelin.denis.r@hydro.qc.ca)

## ABSTRACT

This paper reveals a new approach to the design of civil engineering components of a substation. A design pattern is presented that enables the engineer to design and generate 3D structures, foundations, oil containment devices and soil cut and fill of a substation. The process is automated for minimum user operations and the final product is a 3D model of the entire substation. For the client, the outcome is cost reduction, better quality control, overall lifecycle project time reduction and a virtual realistic representation of the substation that can be looked at from different angles and directions. Quantities for cost estimation by the project engineer are readily available from the 3D model. This paper also portrays the 3D model of a substation as a virtual tool that embraces all aspects of the lifecycle of a substation project.

## INTRODUCTION

Numerous 3D computational tools are available to calculate the many aspects of civil engineering of substations. However, the engineering process of a substation project still relies on 2D information. The electrical department prepares 2D drawings showing plan and elevation views by voltage levels. These drawings are then submitted to the civil engineer who produces its own 2D drawings showing infrastructures with drainage, foundations layout and details, steel structures layout and details as well as oil spill containment devices and fire/noise wall protection. This process is cumbersome and needs constant interaction between the disciplines to ensure that changes are taken into account from both sides. A new approach based on a 3D design pattern is presented below where advantages are foreseen in the lifecycle of a project from design to delivery to the client as shown in Figure 1. Catia V5 and Smarteam from Dassault Systemes company are respectively the 3D CAD (Computer-Aided Design) and PLM (Product Lifecycle Management) database softwares used to develop the automated solutions described in this paper.

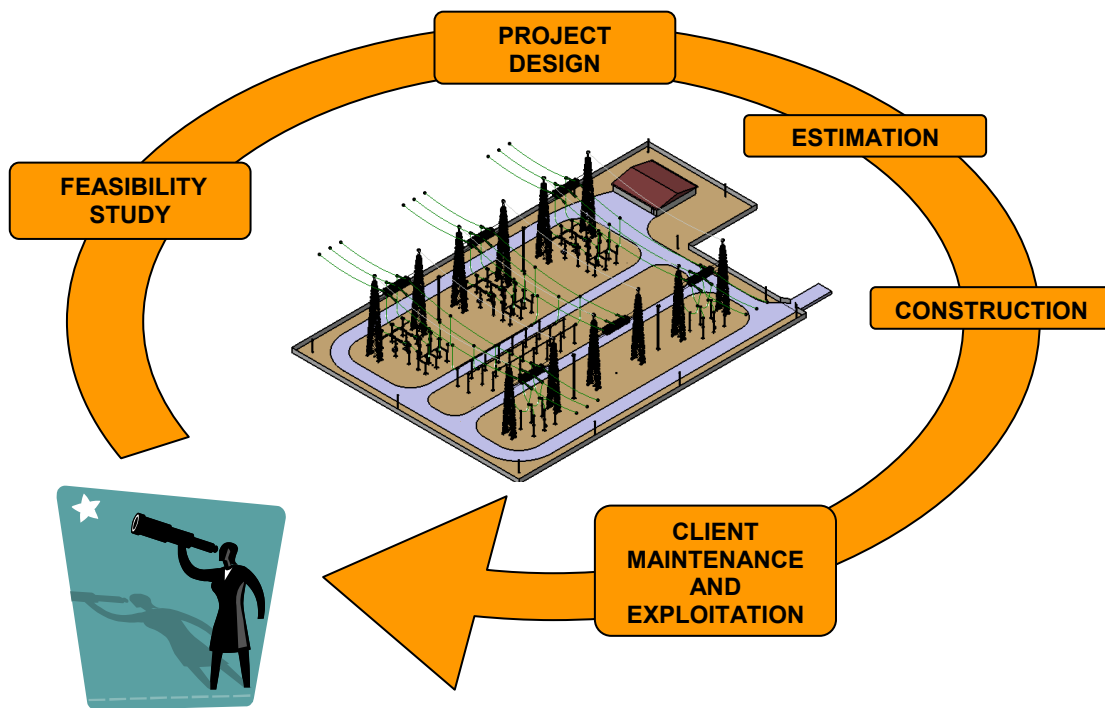


Figure 1. Lifecycle of a substation project in a 3D environment.

#### FROM 2D PAPERS TO ONE 3D VIRTUAL SUBSTATION

The new approach relies on a simultaneous flow of information between electrical and civil engineering groups. No more drawings need to be printed and any changes can be looked at in real time. As soon as the electrical equipment locations are available, the civil engineering components are generated through a design pattern that involves “intelligent assemblies”. Thus, the substation becomes the summation of all intelligent assemblies representing the electrical equipment groups. Each assembly contains parametric parts chosen from a catalogue or specifically created. They have particular design data and material characteristics allowing the output of bill of quantities.

## DESIGN PATTERN WITH INTELLIGENT ASSEMBLIES

Creating 3D models of civil engineering elements in order to gather them in a detailed mock-up of a substation can be a very fastidious process. To take benefit of 3D tools to reduce design lifecycles, 3D design need to be re-usable. For instance, an electrical equipment steel support can be re-used as often as necessary in a specific mock-up or in any other one. This way is appropriate when using normalized components that can be gathered in 3D catalogues. However, civil engineers face the need to design 3D models that are similar from one project to another but not exactly the same. For example, reinforced concrete foundations may be designed with customized dimensions and characteristics depending on soil nature and applied loads. In this case, it is not always possible to re-use an existing 3D model as it is. In such cases, designers have to go a step forward aiming at a more generic approach.

In practice, similarities of different designs are identified in order to build generic 3D models that can take into account options and variants. Such generic 3D models are also called design patterns that include parameters (mainly geometrics) as input. For a substation reinforced concrete foundation, a single 3D model becomes adaptable to represent either a massive foundation or a foundation with one, two, three or more pilasters with one or many footings. Elaborating such design patterns are required to be competitive using 3D design processes. The explanation on how the design pattern is built falls within an art to correctly identify similarities in designs in order to gather them in a single and stable 3D model. It is more convenient to build 3D models by putting together independent smaller 3D parts that are federated at the end into the complete 3D model. For instance, a pilaster, a footing and a low wall represent three different 3D stand-alone parts of the 3D foundation model. With this modular approach where each 3D part is also called a 3D module, a complex 3D intelligent assembly can easily be maintained and can evolve to account for future needs.

The design pattern also bridges engineering criteria and analyses tools with 3D generated intelligent assemblies and parts. These make up the 3D model of the substation as shown in Figure 2 where all the civil engineering components are included. The assembly of the shunt capacitors depicted in the top right of Figure 2 is enlarged in Figure 3 along with the total bill of quantities of granular backfill, concrete foundations volume, steel reinforcement and structural steel. When the 3D model evolves, assemblies move accordingly and data are automatically updated. For estimation purposes, any part can be selected to obtain the corresponding information as shown in Figure 4.

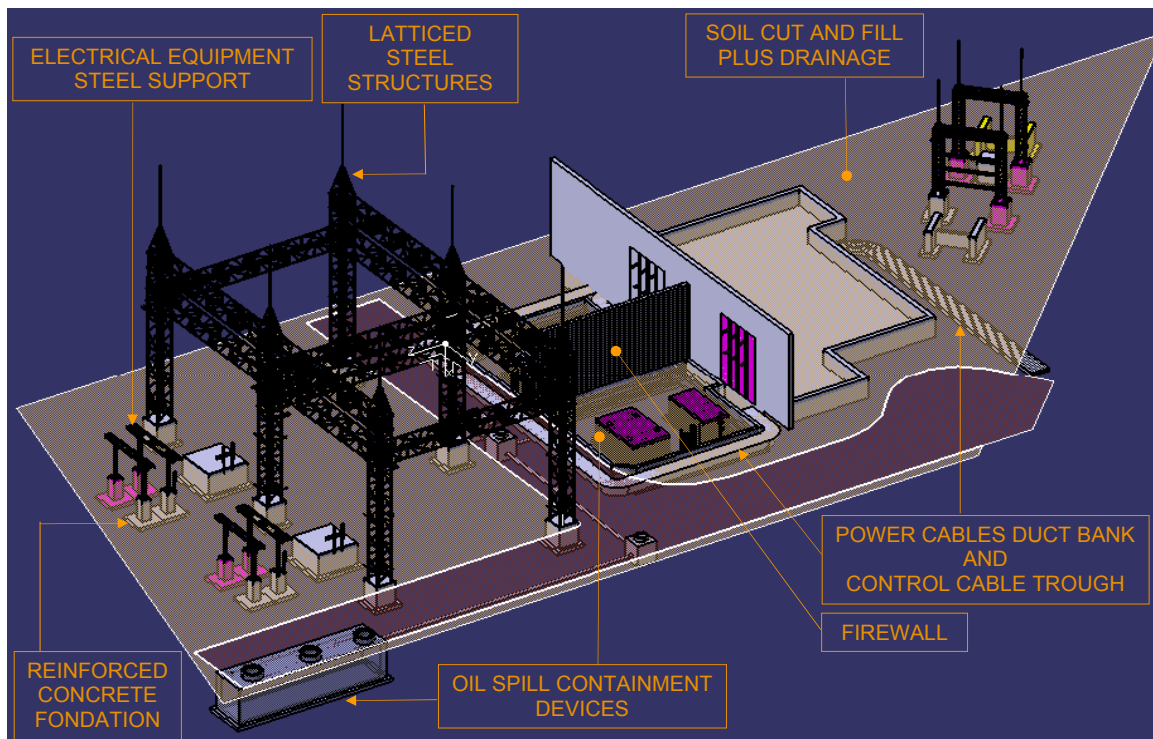


Figure 2. Catia V5 3D model of a substation.

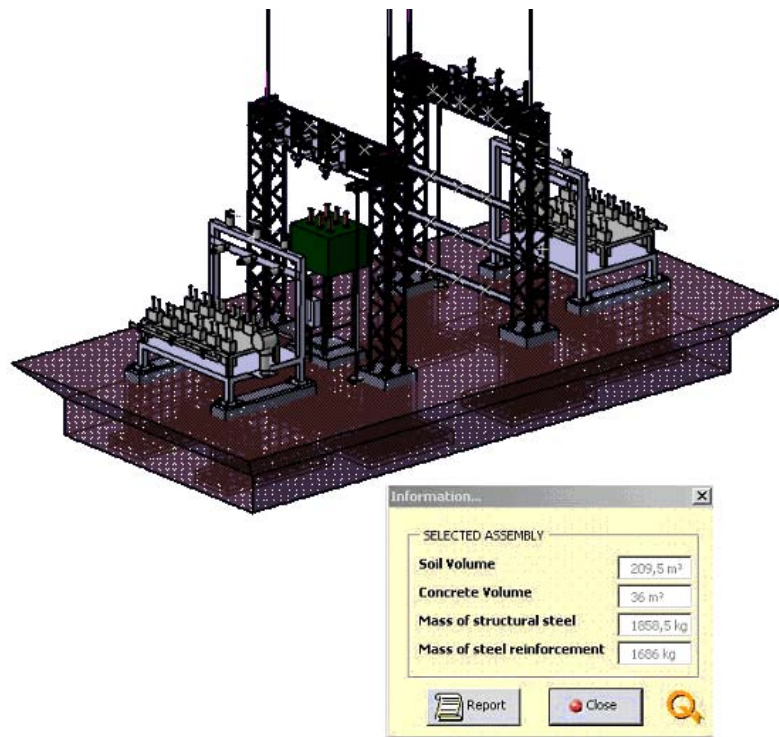
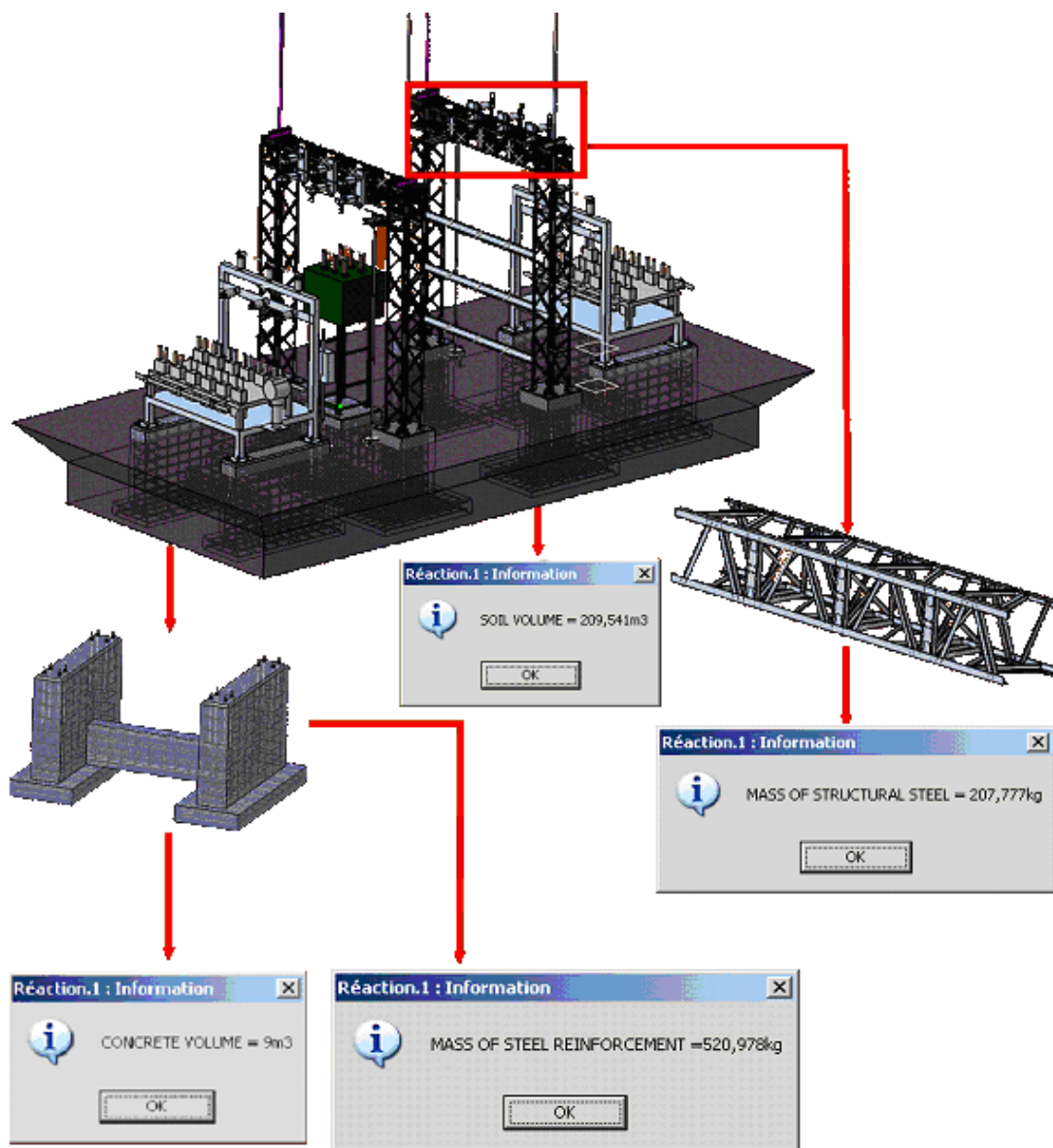


Figure 3. Shunt capacitors arrangement.

Telegram Channel: @Seismicisolation



**Figure 4. Detailed parts for estimation purposes.**

Design of different parts included in the intelligent assembly is facilitated with an automated process to conveniently transfer the results of computational tools into Catia V5 for 3D design of parts with all engineering and material properties. This principle is illustrated in Figure 5 to design the shunt capacitor foundation. The design pattern is also well suited to choose the most appropriate site of the substation among several possible locations. Earthworks and drainage design are easily performed in Catia V5 as illustrated in Figure 6.

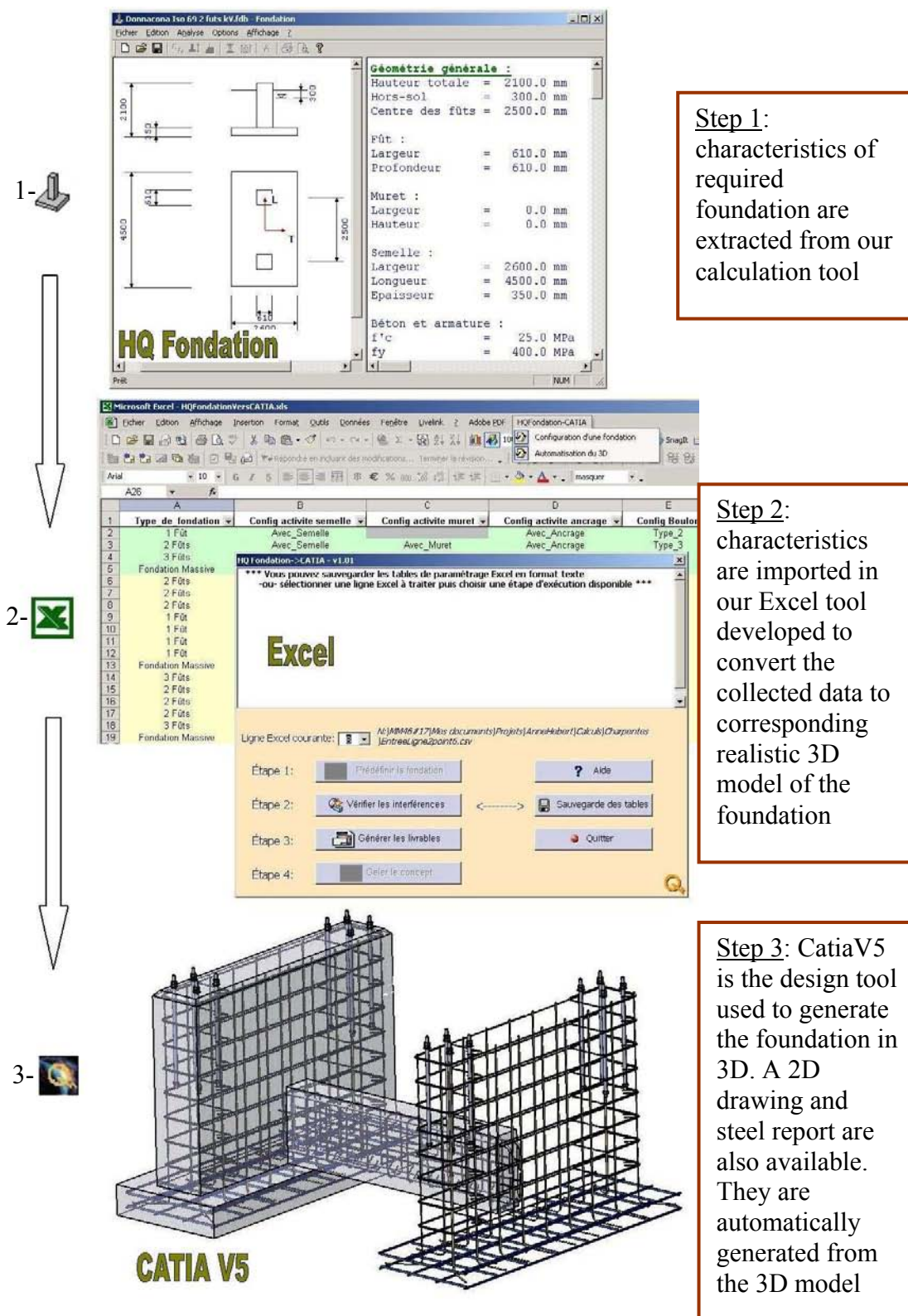
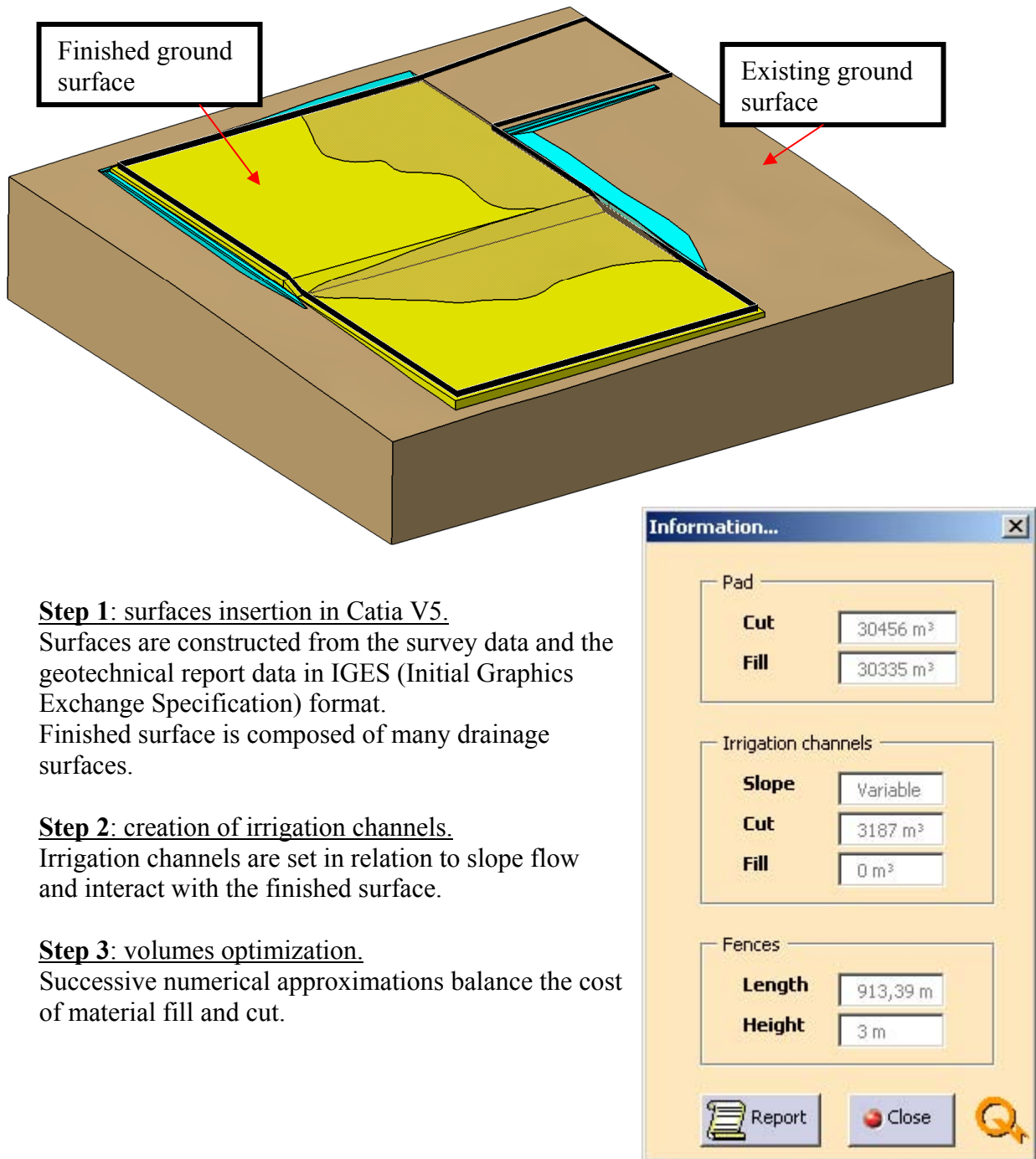


Figure 5. Automated foundations 3D design process for substations.

Telegram Channel: @Seismicisolation



**Figure 6. 3D earthworks and drainage of a substation site.**

## CONCLUSION

The approach of design pattern using Catia V5 to generate a 3D model of a substation is very well suited with engineering activities that evolve starting from the feasibility study and ending with the final design project. Bill of quantities are generated automatically and adjusted when changes appear. The benefits of the design pattern approach with Catia V5 also include :

- engineering efficiency and cost reduction through optimization capabilities and standardization
- the 3D model becomes the common denominator of engineering fields
- all data are gathered in a main catalogue
- “green engineering” as of the progressive elimination of paper drawings
- virtual substation allowing easy understanding during public hearings
- simulation of interferences and construction sequences
- improved quality control

## REFERENCES

Alexander C. (1977). “A Pattern Language: Towns, Buildings, Construction.” Oxford University Press, USA.

Judson S.R. et al. (2003). “A Metamodeling Approach to Model Refactoring.” IEEE Computer Society.

## Seismic Design of Substation Structures

E. Bazán-Zurita<sup>1</sup>, J. Bielak<sup>2</sup>, A M. DiGioia, Jr.<sup>1</sup>, S. Jarenprasert<sup>1</sup>

<sup>1</sup>DiGioia, Gray and Associates, LLC, 570 Beatty Road, Monroeville, PA 15146; PH: 412-372-4500; FAX: 412-372-1972; [enrique@digioiagray.com](mailto:enrique@digioiagray.com)

<sup>2</sup>Department of Civil and Environmental Engineering, Carnegie Mellon University, Pittsburgh, PA 15213; PH: 412-268-2958; FAX: 412-268-7813; [jbielak@cmu.edu](mailto:jbielak@cmu.edu)

### ABSTRACT

The 2008 Edition of ASCE Manual 113, "Substation Structure Design Guide," devotes several sections to criteria and procedures for the seismic design of structures and components of electric substations. This paper describes concepts that interpret and supplement the seismic provisions of Manual 113. Among the issues discussed are: definition of seismic design spectra, simultaneous occurrence of ground motion in three mutually perpendicular directions, incorporation of soil-structure interaction effects and estimation of deflections under seismic loading. Numerical examples are presented to illustrate some concepts, and recommendations are given to implement them in practice.

### INTRODUCTION

Electrical substation structures support sensitive and costly equipment that could be damaged by earthquakes. In the United States, the reference document for the design of substation structures and components is ASCE Manual 113, "Substation Structure Design Guide." The 2008 edition of this document devotes Sections 3.1.7, 5.6.2.1 and 6.7 to criteria and procedures for seismic design. In this paper we review, interpret and supplement the seismic provisions of Manual 113. To this end, we have conducted parametric studies and have reviewed related documents including IEEE 693-2005, ASCE 7-05, and ASCE 4-98 to identify appropriate procedures and guidelines.

### SEISMIC INPUT

The seismic demand can be defined as one of the following options:

- A seismic coefficient that applied to the weights of the structural members and the supported equipment provides static lateral forces.
- Design spectrum, i.e., a table of maximum pseudo-acceleration versus period or frequency, as input in a modal spectral analysis.
- Acceleration time histories for linear or nonlinear step-by-step analyses.

Seismic coefficients and design spectra are provided by local or national codes, or can be developed via site specific seismic hazard analyses. In the United States, elastic design spectra are prescribed in Standard ASCE 7-05 and are based in seismic hazard maps developed and published by the USGS, most recently in 2008. This information is used to calculate design spectra with a shape similar to that given in Fig. 1.

Section 3.1.7 of Manual 113 defines the seismic design spectrum in its Eqs. 3-8 and 3-9, based on the USGS spectra which correspond to 5% of critical damping. To convert a

5%-spectrum to other damping ratios, Manual 113 provides Fig. 5.2 with normalized spectra for damping ratios of 2%, 5% and 10%, reproduced in Fig. 1. The USGS spectra correspond to rock sites. Thus, to account for flexible subsurface layers, Tables 3-12 and 3-13 of Manual 113 adopt the site modification factors from the ASCE 7-05 Standard.

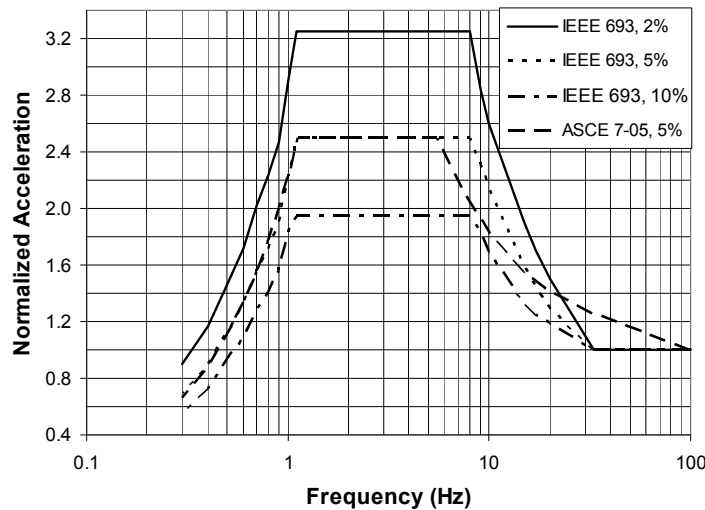


**Figure 1. Comparison of IEEE and ASCE Design Spectra.**

The seismic analysis can also be performed by numerical integration of the equations of motion. The input usually consists of actual records modified to match prescribed design spectra. Elastic step-by-step analysis normally uses a single time history; however, suites of earthquake records are required for nonlinear dynamic analyses.

Multiple components of ground motion must be considered in all analysis options. Generally, the horizontal design spectrum represents the ground motion in any horizontal direction and two perpendicular directions are considered. The vertical ground motion is usually defined with reference to the horizontal spectrum. Manual 113 specifies vertical accelerations equal to 80% of the horizontal and requires consideration of combined horizontal and vertical motions. For static analysis, Manual 113 specifies that the vertical accelerations be combined with the horizontal accelerations that produce the most severe stresses. We interpret that this requirement is satisfied by conducting the seismic analysis for two orthogonal horizontal directions and for the vertical direction, and then combining the results with rules described later in this paper.

Most static and dynamic seismic analyses consider elastic behavior. However, under severe events structures can undergo significant nonlinear deformations. Thus, design codes stipulate materials, structural layouts and details that promote nonlinear energy dissipation. On account of this beneficial inelastic behavior, the elastic response is reduced by a factor R. Following the format of ASCE 7-05, Section 3.1.7.3 of Manual 113 prescribes the R values given in Table 1 for use in ultimate strength design (USD). In reality, R depends on the natural frequency of the structure and for very high frequencies, R=1, regardless of the nonlinear structural characteristics. We understand that this is the basis for R being 1.3 for structures with natural frequency equal to or larger than 25 Hz in Table 1. In our opinion, it is preferable to define the reduction as a

function of frequency,  $R(f)$ , that varies smoothly between 1 at say 33 Hz and remains constant for frequencies smaller than or equal to a characteristic value  $f_R$ , for instance:

$$R(f) = R \quad \text{for } f \leq 8 \text{ Hz} \quad (1)$$

$$R(f) = 1 + (R - 1) [(33 - f)/25]^{2.6} \quad \text{for } 8 \leq f \leq 33 \text{ Hz} \quad (2)$$

$$R(f) = 1, \quad \text{for } f > 33 \text{ Hz} \quad (3)$$

$f$  = natural frequency in Hz

These equations correspond to  $f_R = 8\text{Hz}$ . Resulting reduced spectra are shown in Fig. 2 for a damping ratio of 5%.

**Table 1. Structure Response Modification Factor, R.**

Structure or Component Type	R for USD
Moment-resisting steel frame	3.0
Trussed tower	3.0
Cantilever support structures	2.0
Tubular pole	1.5
Steel and aluminum bus supports	2.0
Station post insulators	1.0
Rigid bus (aluminum and copper)	2.0
Structures with natural frequency $\geq 25$ Hz	1.3

$R$  can also vary with the direction of motion because different structural systems can be used to resist lateral forces in different directions. In addition, the systems that resist vertical seismic accelerations are frequently different than those resisting horizontal forces. Gravity can lead to asymmetric hysteresis loops for vertical vibratory loads, diminishing the ability of the structure to dissipate inelastic energy and thus decreasing  $R$ .

## SEISMIC ANALYSES OF SUBSTATION STRUCTURES

Seismic analyses provide estimates of stresses and deflections, for use in load combinations that include seismic effects in the verification of the adequacy of members or components. Current seismic analysis methodologies are classified as static, modal response spectrum analysis, and time history (step-by-step) analysis.

### Static method

The static method is applicable to structures or components with a dominant mode, and uses as seismic coefficient the spectral value corresponding to the fundamental frequency. Following Standard IEEE 693-2005, Manual 113 requires that the seismic coefficient be multiplied by 1.5 when higher vibration modes could contribute significantly to the seismic response. Static seismic forces on each component or equipment are calculated by multiplying their mass by the seismic coefficient in each direction of motion, and are applied at their centers of mass.

Since seismic vertical and horizontal ground motions occur at the same time, codes require simultaneous consideration of seismic forces in both directions. Considering that spectra are maximum responses that are unlikely to occur simultaneously in the three

directions, Section 5.6.2.1 of Manual 113 allows estimation of the combined response as the square root of the sum of squares (SRSS) of the responses to each direction of ground motion. Another rule combines 100% of the response to one direction of motion with 40% of the responses to the motion in the other two directions (100, 40, 40 rule). ASCE 4-98 Standard describes the use of these rules.

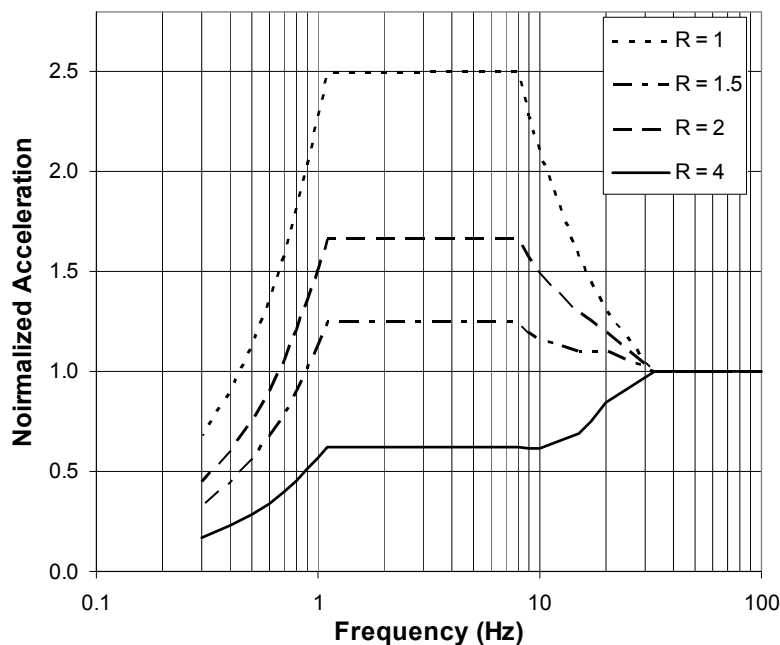


**Figure 2. Spectra for Different Reduction Factors R.**

### Modal response spectrum analysis

A modal response spectrum analysis uses a finite element model to obtain the natural vibration properties of the structure. The model represents the stiffness and mass distributions and damping properties of the structure and supported equipment. Real frequencies and modes of vibration are calculated and the seismic input for each mode is determined from the design spectrum for each direction of analysis. Only a limited number of modes are included in the spectral analysis, neglecting high frequency modes that have a small participation in the total response. On the other hand, sufficient modes must be included to obtain an accurate estimate of the total seismic response. Section 5.6.2.1 of Manual 113 specifies that the number of considered modes should render a total response that does not increase by more than 10% with additional modes. Other standards, such as IEEE 693, require a number of modes such that the cumulative participating mass is at least 90% of the total mass. This requirement is more restrictive than Manual 113 and, in our opinion, must be fulfilled.

Earthquake dynamic analysis using a response spectrum is required by Manual 113 for flexible structures, defined as those with a first natural frequency smaller than 33 Hz. Manual 113 defines a design spectrum with the shape displayed in Fig. 1, with a flat value equal to the peak ground acceleration (PGA) at frequencies of 33 Hz and higher.

This reflects past practice in the nuclear industry that considered no amplification of the PGA for frequencies equal to or higher than 33 Hz. Recent ground motion models for Eastern North America (Atkinson and Boore, 2006), however, indicate that the seismic response at frequencies higher than 33 Hz can be significantly above PGA. The issue is less relevant when nonlinear behavior is anticipated since the reduced spectra are flatter.

Flexible soil layers modify the ground motion. Typically, these site-effects are quantified with one-dimensional wave propagation analyses that account for the stiffness and damping properties of the soil/rock layers. ASCE 7-05 adopts a simpler approach where sites are assigned a Class A to F based on shear wave velocity, standard penetration blowcounts, and/or undrained shear strength. Then, two modification site coefficients are tabulated for each site class in terms of the spectral amplitude at rock. This approach is adopted by Manual 113 and is sufficient for most substation projects. If necessary, wave propagation analysis can be conducted with linearized procedures (Schnabel et al., 1972). The most important task is the determination of shear modulus and viscous damping that properly represent the dynamic nonlinear response of the soil layers.

For combining modal responses, Section 5.6.2.1 of Manual 113 allows the SRSS method when the relevant natural frequencies differ more than 10 percent. Otherwise, a complete quadratic combination (CQC) method must be used. Since CQC rules can be easily implemented in computer codes, there is no reason to use the SRSS method.

Three modal analyses are conducted with spectra for three orthogonal directions of ground motion. In each analysis, the total response is a CQC combination of modal responses. These three responses are combined with the SRSS or the 100-40-40 rules.

### Time history (step-by-step) analysis

The time history analysis consists of numerical integration of the differential equations of motion in small time steps. For linear systems, the time history is simplified because the mass, damping and stiffness matrices remain unchanged. The analysis must consider only the modes with larger participation, and the input consists of three accelerograms matching the design spectra in each direction of ground motion. Uncorrelated records can be input simultaneously, considering all combinations of positive and negative signs to capture the most unfavorable effects on each component. For correlated records, the analysis is performed independently for each ground motion direction and the results are combined with the SRSS or the 100-40-40 rules. Linear time history analyses also have to consider nonlinear effects. One possibility is to develop time histories that match the reduced spectra, but it is preferable to perform the actual nonlinear analyses. Linear step-by-step analysis constitutes a convenient option for systems with non-proportional damping that have complex modes and frequencies; otherwise, the modal response spectrum approach is sufficiently accurate.

Spectral matching must satisfy several requirements. In addition to enveloping the design spectrum, a time history must contain sufficient energy in all relevant frequencies. Typical frequency content, duration and matching requirements are given in Appendix A of IEEE 693. Time histories also must reflect site conditions, usually by means of one-

dimensional wave propagation analysis (Schnabel et al., 1972); however, more accurate two and three-dimensional formulations have been developed by Bielak et al. (2003).

Time history analysis is unavoidable if one needs to take into consideration nonlinearities in components or equipment. Appropriate constitutive models must be identified to capture the main nonlinear structural characteristics under cyclic loading. Since the nonlinear response can vary significantly under different input time histories, sufficient earthquake records must be selected to represent the potential seismic events at the site. An added complication is the need to incorporate all combinations of signs and directions of seismic input. Owing to these difficulties, nonlinear analyses are rarely conducted, except for seismic qualification of equipment excessively large to be qualified by testing.

### EFFECTS OF DAMPING RATIO ON DESIGN SPECTRA

As prescribed in current codes, R values are applicable to structures with 5 percent of critical damping, usually appropriate for buildings. Different damping ratios, say 2%, may be adequate for substation components. The design seismic coefficient or spectrum can be adjusted using Fig. 1. However, based on the IEEE 693 equations, the spectrum for a prescribed percent damping ratio, d, is obtained by multiplying the 5-percent spectrum by  $F_d$ , as follows:

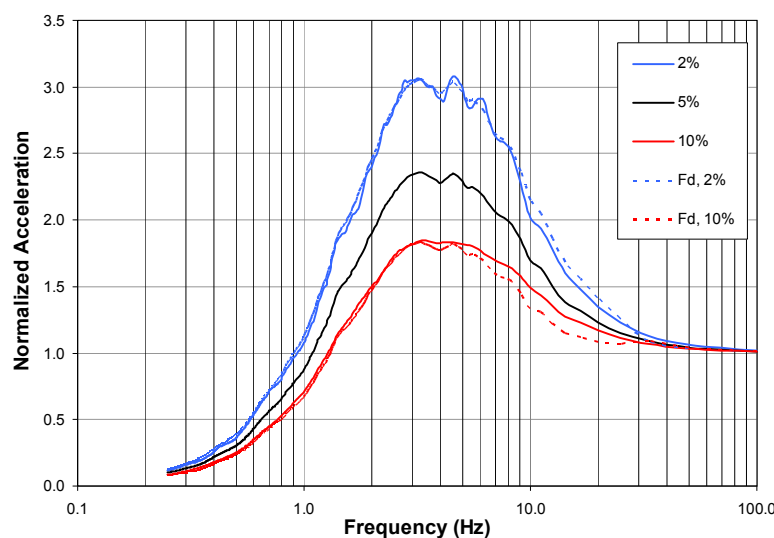


**Figure 3. Calculated and Approximate Spectra (IEEE approach).**

$$F_d = \beta, \quad \text{for } 0 \leq f \leq 8 \text{ Hz} \quad (4)$$

$$F_d = 1 + 0.04 (\beta - 1) (33 - f), \quad \text{for } 8 \leq f \leq 33 \text{ Hz} \quad (5)$$

$$F_d = 1, \quad \text{for } f > 33 \text{ Hz} \quad (6)$$

$$\beta = 1.5173 - 0.3213 \ln(d) \quad (7)$$

d = percent of damping ratio

To examine the accuracy of  $F_d$  we analyzed elastic single-degree-of-freedom systems excited by a set of 87 Californian earthquake records from stiff to medium stiff sites. The records were normalized to have the same Arias Intensity and to yield average peak ground acceleration equal to that of gravity. We considered damping ratios of 2, 5 and 10

percent. Fig. 3 shows that the average spectra (continuous lines) resemble design spectra and indicates an excellent agreement with spectra calculated with Eqs. 4 through Eq. 7. We have developed a similar approach where the 5-percent spectrum is multiplied by a factor  $\alpha$ , as follows:

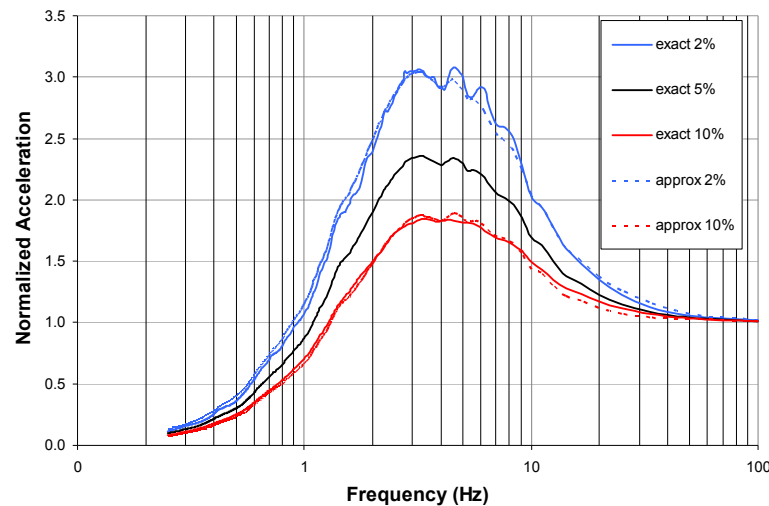
$$\xi = 0.3 + 0.01d \quad (8)$$

$$\delta = (5/d)^{\xi} \quad (9)$$

$$\alpha = 1 + (\delta - 1) \exp(-0.05 f) \quad (10)$$

$d$  = percent of damping ratio

$f$  = frequency in Hz



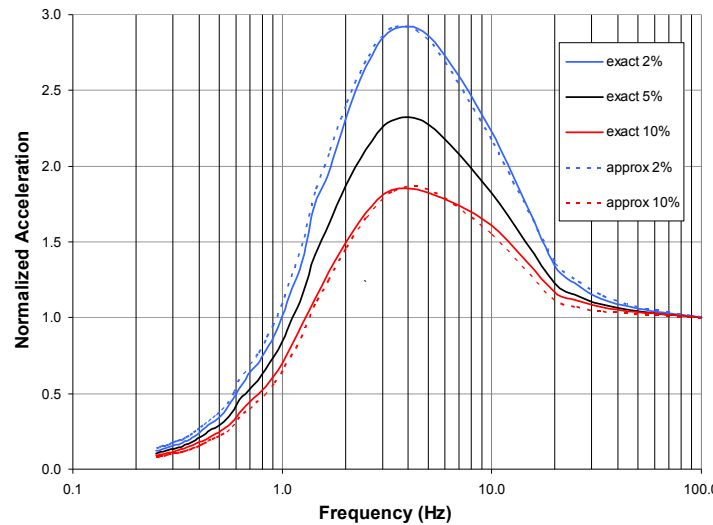
**Figure 4. Calculated and Approximate Spectra (This paper approach).**

Fig. 4 shows that the spectra (dashed lines) resulting from Eqs. 8 to 10 are in slightly better agreement with the average spectra that the IEEE approach. The advantage of our approach is that it has been extended to adjust spectra reduced due to nonlinear behavior. Indeed, substation structures are designed anticipating inelastic behavior under strong earthquakes with energy dissipation from viscous as well as hysteretic damping. The viscous damping contribution decreases with larger nonlinear energy dissipation. Thus, we have also analyzed single-degree-of-freedom systems with bilinear hysteretic force-displacement curves. The second slope of the curves equals 2 percent of the initial slope. The seismic coefficient is the yield strength,  $F_y$ , divided by the weight of the system. The ductility demand,  $\mu$ , is the maximum displacement divided by the yield displacement.

Figs. 5, 6 and 7 present the average spectra (solid lines) for  $\mu=1, 2$  and  $4$ . Note that the spectra for different damping ratios become closer as  $\mu$  increases, confirming that higher inelastic energy dissipation diminishes the role of viscous damping. Figs. 5, 6 and 7 also show (dashed lines) spectra obtained multiplying the 5-percent spectrum by  $\alpha$ , defined by Eq. 10. Reflecting the influence of  $\mu$ , the parameter  $\xi$  is calculated as:

$$\xi = (0.3 + 0.01 d) / \mu^{0.55} \quad (11)$$

$\mu$  = average ductility demand



**Figure 5. Spectra for Average Ductility Demand  $\mu = 1$ .**

Again, the closeness between continuous and dashed lines in Figs. 5, 6 and 7, demonstrates the accuracy of Eqs. 9, 10 and 11 for estimating spectra for damping ratios between 2 and 10 percent. Note that for  $\mu = 1$ , Eqs. 8 and 11 yield the same value.

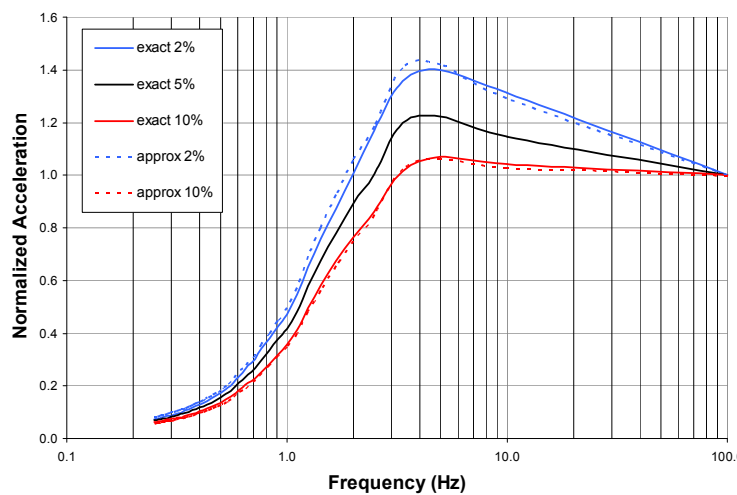


**Figure 6. Spectra for Average Ductility Demand  $\mu = 2$ .**

## SOIL STRUCTURE INTERACTION

Section 3.1.7 of Manual 113 states: “Designers should be aware of unusual soil conditions, soil structure interaction, and the potential of modified response due to an intermediate structure.” Soil-structure interaction (SSI) can appreciably change vibration frequencies, increase damping, and increase displacements. SSI effects can be included using springs with constants,  $K$ , and dashpots with damping coefficients,  $C$ , that represent

the flexibility and energy dissipation characteristics of the soil/foundation system. Up to six values of K and C can be calculated corresponding to the six degrees of freedom of the foundation: two translations in horizontal orthogonal axes, one vertical translation, and three rotations (two rocking and one twisting) about these three axes.

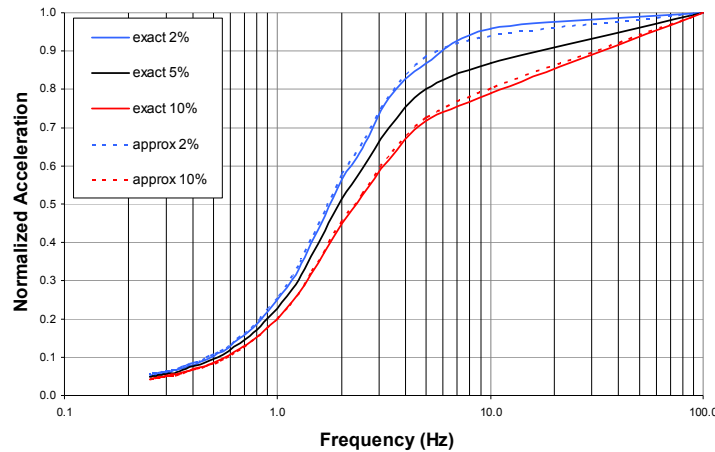


**Figure 7. Spectra for Average Ductility Demand  $\mu = 4$ .**

Following pioneering work by Jennings and Bielak (1973), Gazetas (1991) developed formulas for K and C representing shallow foundations in homogeneous soil and considering the plan shape of the foundation and its embedment depth. Procedures for analyzing pile foundations under dynamic loads are presented in Puri and Prakash (2007). The soil-pile behavior under earthquake loading is generally non-linear, which is accounted for by defining soil-pile stiffness in terms of strain dependent soil modulus. In addition to the foundation geometry, these procedures require estimates of the geotechnical properties of subsurface materials, including shear modulus (G), Poisson ratio ( $\nu$ ) and unit weight ( $\gamma$ ). While some properties, such as  $\nu$  and  $\gamma$ , exhibit limited variability, others, such as G, can vary significantly from site to site (even within a site) and with the level of deformations. Thus, it is important to identify the subsurface characteristics at the site by means of geotechnical investigations, laboratory testing and judicious use of correlations and presumptive values. Cantilever support structures, tubular poles and similar systems, can experience increased displacements due to SSI flexibility inducing larger P-delta effects.

SSI springs and dashpots can be readily incorporated in structural models. In static analyses, the most significant impact is increased displacements. In dynamic analysis, the natural vibration frequencies become smaller and the spectral acceleration can change. Indeed, an accurate indicator of the relevance of SSI is the percent of decrease in the fundamental frequency of vibration. A modest decrease indicates negligible SSI effects and vice versa. In any event, SSI stiffness and damping parameters should be calculated and included in the calculation of modes and frequencies of vibration.

Saturated granular loose soils are susceptible to liquefaction during earthquakes. Dramatically settled and tilted structures have been manifestations of this phenomenon in past earthquakes. A recent monograph by Idriss and Boulanger (2008) presents updated methodologies to assess liquefaction potential and to mitigate liquefaction hazards. It

should be kept in mind that piles could experience excessive lateral displacements and bending moments in liquefied soils. A possible solution is the used of drilled shafts embedded into deeper non liquefiable soils or in rock.

## DISPLACEMENTS

Section 5.2 of Manual 113 highlights the importance of accurately estimating displacements in substation components, warning that “A structure designed for strength may have excessive deflections.” By contrast, Section 3.1.11.3 of the Manual states that loads from “earthquakes should not be considered in deflection analysis. It is argued that nonlinear dynamic analyses can be difficult and unreliable. However, seismic regulations, such ASCE 7-05, accept that linear analyses along with structural-response modification factors, is sufficiently reliable for estimating stresses and displacements under seismic loads. Most of the uncertainty in seismic response estimates resides in the assessment of seismic activity, rather than in structural analyses methodologies,

The static and the modal spectral seismic analyses produce estimates of the displacements at any point of a structure. Since the linear analyses use forces reduced by a factor R, on account of nonlinear behavior, the ensuing displacements are also reduced and have to be increased to estimate the inelastic deformations. To this end, seismic regulations stipulate amplifications factors for R-reduced displacements. For instance, ASCE 7-05 requires that displacements be amplified by a factor  $C_d$  tabulated along with R. Manual 113 does not provide values for  $C_d$ . Upon examination of Table 12.2.1 of ASCE 7-05, we propose that  $C_d$  be equal to R.

## EXAMPLES

The following examples are based on the Dead-End Structure example of Section 3.6.1 and Fig. 3.5 of Manual 113. Cantilever support poles constitute the structural system in one horizontal direction. We understand that 5 percent damping was considered in this example. Manual 113 considers a Site Class D and provides the following information:

$$\begin{aligned} F_a &= 1.33, S_S = 0.590, F_v = 2.06, S_1 = 0.186 \\ S_{DS} &= 2/3 F_a S_S = 2/3 \times 1.33 \times 0.590 = 0.523, \text{ assumed to control.} \end{aligned}$$

Manual 113 assumes R=2 and importance factor  $I_{FE}=1.25$ . Thus, the seismic design force,  $F_E$ , is equal to  $(S_a/2) \times 1.25W = 0.33W$ . For the other direction, we assume that the structural system is a moment-resisting steel frame. Now R=4 and  $F_E = (S_a/4) \times 1.25 W = 0.17 W$ , if all other data remain the same. In the vertical direction, lacking any other guidance, we would use  $F_{EV}$  equal to 0.8 times the larger horizontal force, i.e.,  $F_{EV} = 0.8 \times 0.33 W = 0.26 W$ .

Now let us consider that a damping ratio of 2 (rather than 5) percent is appropriate. Using Figure 5.2 of Manual 113, or Eqs. 6 and Eq. 7, the amplification in the flat region of the design spectra (say at a frequency of 7 Hz), the factor equals  $3.25/2.5 = 1.3$ . However, using equations 9 and 11, with  $\mu = R = 2$ , and  $d = 2$ , we have:

$$\begin{aligned}\xi &= (0.3 + 0.01 d) / 2^{0.55} = 0.22 \\ \delta &= (5/d)^{0.22} = (5/2)^{0.22} = 1.22 \\ \alpha &= 1 + (\delta - 1) \exp(-0.05 \times 7) = 1.16\end{aligned}$$

In the other direction ( $R=4$ ) the adjustment for a 2 percent damping ratio is:

$$\begin{aligned}\xi &= (0.3 + 0.01 d) / 4^{0.55} = 0.15 \\ \delta &= (5/d)^{0.15} = (5/2)^{0.15} = 1.14 \\ \alpha &= 1 + (\delta - 1) \exp(-0.05 \times 7) = 1.10, \text{ while the Manual 113 value is still 1.3.}\end{aligned}$$

## CONCLUDING REMARKS

ASCE Manual 113 is a welcome addition to the technical literature on the design of substation structures and foundations. The specifications of Manual 113 provide a balance between having sufficient criteria available to achieve acceptable uniformity in the seismic design while allowing designers to exercise their experience and judgment. In this paper we have presented our opinions on interpretation of the seismic provisions of Manual 113. We recommend that modal spectral analyses be used for the seismic design of substation structures. The development of required finite element models is facilitated with the variety of available software. The number of modes included in the analyses should ensure that the sum of effective masses equals at least 90 percent of the total mass. A CQC modal combination rule should always be used. These rules are incorporated in most commercial finite element programs.

Both static and dynamic procedures can be simplified. A frequent simplification consists in using two-dimensional models. However, current software facilitates the construction of three-dimensional (3D) models, rendering such simplifications unnecessary. The same model is used for calculating the response to the three components of ground motion, since all three-dimensional features are already represented. The calculation of natural 3D frequencies and modes of vibration is also relevant in the assessment of the structural response to non-seismic dynamic loads. The number of modes included in the analysis should result in a cumulative participating mass of at least 90% of the total mass. The calculation of displacements should reverse the reductions associated with the use of R-reduced design spectra, since these reductions were introduced originally to account for nonlinear hysteretic behavior. Such behavior is undesirable in substation structures. Finally, the response to simultaneous ground motion in three orthogonal directions can be calculated with the square root of the sum of the squares or the 100-40-40 rules.

We recommend that soil-structure interaction (SSI) be always modeled in the seismic analysis. The added complexity in the finite element model is minimal while the benefits can be significant: a more accurate estimation of natural frequencies, which can modify the spectral amplitudes; and more accurate estimates of stresses and displacements.

An original contribution of this paper is the development of an improved approach for adjusting 5-percent damped design spectra to other damping ratios. The procedure of

Standard IEEE 693, adopted in Manual 113, is adequate for modifying elastic spectra. However, substation structures are designed anticipating inelastic behavior with energy dissipation occurring via viscous as well as hysteretic damping. Using inelastic nonlinear analyses of single-degree-of-freedom systems we have verified that viscous damping is less effective when higher hysteretic energy dissipation occurs. This implies that the required modification of the design spectrum due to a change in the damping ratio decreases when the target ductility demand increases. Equations 9, 10 and 11 have been developed herein to calculate spectral adjustment factors for damping ratios between 2 and 10 percent, considering average ductility demands between 1 and 4. These factors correctly approach unity at high frequencies.

## REFERENCES

- Atkinson, G.M. and Boore, D.M. (2006). "Earthquake Ground-Motion Prediction for Eastern North America." *Bulletin of the Seismological Society of America*, 96(6): 2181-2205.
- ASCE (2000). "Standard ASCE 4-98: Seismic Analysis of Safety-Related Nuclear Structures." Reston, VA.
- ASCE (2006). "Standard ASCE/SEI 7-05: Minimum Design Loads for Buildings and Other Structures." Reston, VA.
- ASCE (2008). "Manual 113: Substation Design Guide." Edited by L. Kempner Jr. Reston, VA.
- Bielak, J., Loukakis, K., Hisada, Y., and Yoshimura, C. (2003). "Domain reduction method for three-dimensional earthquake modeling in localized regions part I: Theory. *Bulletin of the Seismological Society of America*, 93(2): 817-824.
- USGS (2008). "United States National Seismic Hazard Maps." <http://earthquake.usgs.gov/research/hazmaps/>
- Gazetas, G. (1991). "Chapter 15: Foundation Vibrations." *Foundation Engineering Handbook*, Edited by H-Y Fang, Van Nostrand, New York.
- Idriss, I.M. and Boulanger, R.W. (2008). "Soil Liquefaction During Earthquakes." Earthquake Engineering Research Institute, Oakland, CA.
- IEEE (2006). "IEEE Standard 693: Recommended Practice for Seismic Design of Substations," American National Standards Institute.
- Jennings, P.C. and Bielak, J. (1973). "Dynamics of building-soil interaction." *Bulletin of the Seismological Society of America*, V. 63, No. 1, pp. 9-48.
- Prakash, S. and Sharma, H.D. (1990), "Pile Foundations in Engineering Practice," John Wiley and Sons, New York.
- Puri, V. K. and Prakash, S. (2007). "Foundations under Seismic Loads." 4th International Conference on Earthquake Geotechnical Engineering. Paper No. 1118. Thessaloniki, Grece.
- Schnabel, P.B., Lysmer, J. and Seed, H.B. (1972). "SHAKE: A computer Program for Earthquake Response Analysis of Horizontally Layered Sites." Report UCB/EERC 72/12. University of California, Berkeley, CA.

## Analytical Techniques to Reduce Magnetic Force from High Fault Current on Rigid Bus

T.A. Amundsen<sup>1</sup>, J.L. Oster<sup>2</sup> and K.C. Malten<sup>3</sup>

<sup>1</sup>PE, SE, Member ASCE, Manager, Sargent & Lundy LLC, 55 E Monroe, Chicago IL 60603, Email: [thomas.amundsen@sargentlundy.com](mailto:thomas.amundsen@sargentlundy.com), Phone: 312-269-2637.

<sup>2</sup>EIT, Associate Member ASCE, Associate, Sargent & Lundy LLC, 55 E Monroe, Chicago IL 60603, Email: [jesse.oster@sargentlundy.com](mailto:jesse.oster@sargentlundy.com), Phone: 312-269-2623.

<sup>3</sup>PE, SE, Fellow ASCE, Senior Manager, Sargent & Lundy LLC, 55 E Monroe, Chicago IL 60603, Email: [kenneth.c.malten@sargentlundy.com](mailto:kenneth.c.malten@sargentlundy.com), Phone: 312-269-6486.

### ABSTRACT

Fault currents are increasing on existing and new substations due to system additions and modifications. Bus designs are typically based on the circuit breaker rating of 40kA to 80kA. Phase spacing is no greater than that required by insulation level, thus for configurations in the 115kV to 138kV range, magnetic forces over 100 pounds per foot are not uncommon when computed per IEEE 605 methods.

The magnetic force calculation in IEEE 605 is proportional to the decrement factor squared and 1.6 is the default decrement factor. The first reduction strategy is to calculate the actual decrement factor. The decrement factor is a function of fault clearing time, system reactance and system resistance. Typical system reactance to resistance ratios (X/R) can reduce magnetic force 12 to 18 per cent for a two cycle breaker. More reduction is available with greater clearing times.

The second force reduction strategy is to compare the natural frequency of the bus to the forcing function frequency. This paper presents a simplified generalized coordinate method to determine the frequency based response of the bus to the magnetic field.

The paper will also review the cost savings as a result of applying these techniques.

### DECREMENT FACTOR

**Decrement factor defined.** The purpose of the decrement factor is to account for the momentary peak effect of the AC and decreasing DC components of the short-circuit current during the first half-cycle of the fault, where the DC component is at a maximum. A full explanation of the theory behind the decrement factor is outside the scope of this document – see section 10.2 of IEEE Std. 605-1998 for further explanation.

**Influence of the decrement factor.** The following equations show that the short-circuit force is proportional to the square of the decrement factor (See Equation 12 IEEE Std. 605-1998).

$$F_{SC} = K_f \frac{C \cdot \Gamma \cdot (D_f \sqrt{2} \cdot I_{SC})^2}{D} \quad (1)$$

where

$F_{SC}$  = short - circuit force, lbf/ft

$K_f$  = mounting - structure flexibility factor usually taken as unity

$C = 5.4 \times 10^{-7}$  for USCS units

$D_f$  = decrement factor as given in the equation shown below

$I_{SC}$  = symmetrical short - circuit current, A

$D$  = conductor phase spacing center - to - center, in

$$D_f = \sqrt{1 + \frac{T_a}{t_f} \cdot \left( 1 - \exp\left(\frac{-2 \cdot t_f}{T_a}\right) \right)} \quad (2)$$

where

$$T_a = \frac{X}{R} \frac{1}{2 \cdot \pi \cdot f} \quad (3)$$

and

$t_f$  = fault current duration, sec

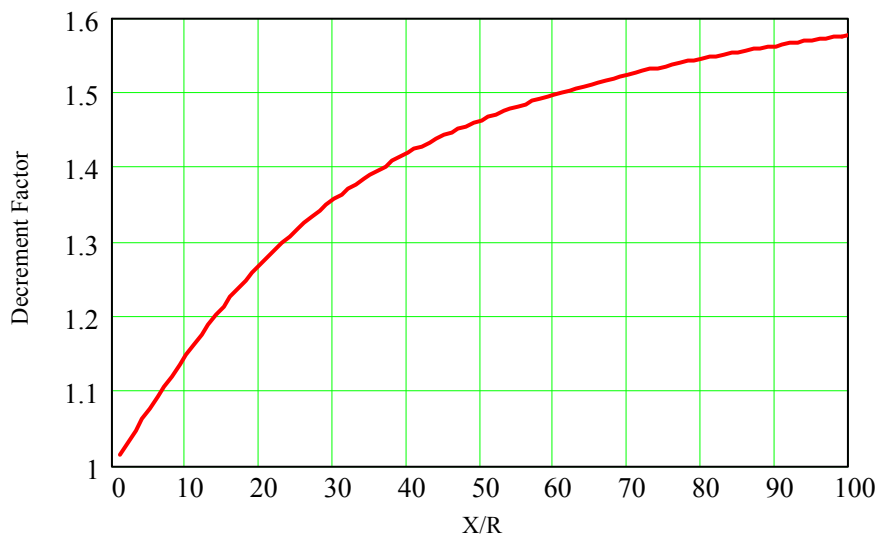
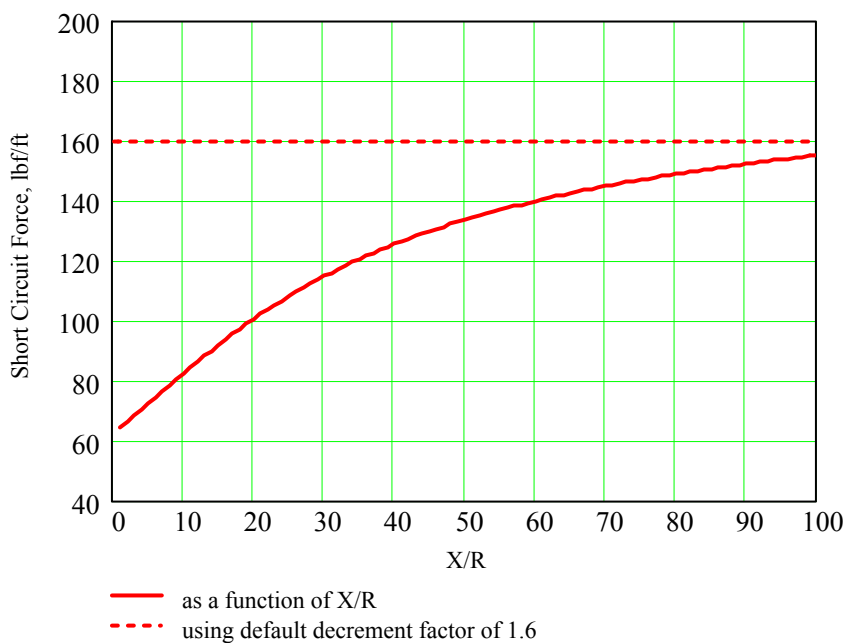
$X$  = system reactance

$R$  = system resistance

$f = 60$  Hz

Figure 1 plots the decrement factor for a common 5 cycle clearing time,  $t_f = 0.083$  sec, at a fault current of 80 kA over a range of (X/R) ratios with a common 138 kV phase spacing of 8'-0". Note that even for very high X/R ratios the calculated values approach but do not reach the default maximum decrement factor of 1.6.

Figure 2 plots the corresponding short-circuit force using Equation 1. Note that only for very high X/R ratios do the calculated values approach 160 lbf/ft maximum short-circuit force using the default 1.6-decrement factor.

**Figure 1. Decrement factor vs. X/R ratio****Figure 2. 138 kV short – circuit force vs. X/R ratio**

**Force Reduction.** The figures above show the effect of the decrement factor on the short-circuit equation for a wide range of X/R ratios. However, most substations will have an X/R ratio less than 30. Therefore, one can expect marginal to significant reductions in the short-circuit force for most substations compared to the default maximum short-circuit force using the 1.6 decrement factor. It is important to note that calculating the decrement factor requires little computation time and only

requires two additional electrical design inputs - the X/R ratio and the fault clearing time.

## DYNAMIC RESPONSE OF BUS

**Introduction.** The short-circuit force is dynamic in nature. Consequently, the dynamic response of a given span of rigid bus is highly dependent on the natural frequency of that span in relation to the frequency of the forcing function. The standard method of calculating the short-circuit force does not account for the dynamic response of the rigid bus to the short-circuit-forcing function and often leads to overly conservative results.

IEEE recognizes this and even states that for certain natural frequencies the rigid bus “will have fault current forces of less than one half the calculated first quarter-cycle force when the conductor span reaches full deflection” (IEEE Std. 605-1998). In fact, the standard equation computes the equivalent static force on the bus assuming the bus has fully deflected at the same time the forcing function reverses direction. However, such a condition is extremely unlikely considering that the natural frequency of a common rigid bus span is significantly different from the frequency of the forcing function (60 Hz) – see Figure 3 below.

Most utilities account for the conservatism with an overload factor around 1.0 applied to short-circuit forces for insulator design, compared to the much higher factor applied to wind and dead loads of approximately 2.0. Note that the smaller overload factor for insulator design no longer applies with a more accurate estimate of the short-circuit load; an overload factor similar to that for wind is instead appropriate.

The following sections explain the effect of the natural frequency on the dynamic response of the bus to the short-circuit forcing function. Also presented is a simplified method for determining the dynamic response of rigid bus to the short-circuit forcing function.

**Assumptions.** The following common rigid bus assumptions and materials provide the basis for the dynamic analysis method for reducing the short-circuit force.

- Assume only the first mode of vibration
- Conservatively assume no damping
- Assume rigid bus spans behave independently
- Assume insulators act as structurally fixed supports corresponding to rigid or slip bus support fittings.
- Treat beams as a distributed mass systems
- Spans range from 15' to 40'
- Use 5" Schedule 40 6061-T6 aluminum bus ( $E = 10^4$  ksi,  $I = 20.7 \text{ in}^4$  and a self weight of 7.19 lbf/ft)
- Frequency of the short-circuit-forcing function, hereafter referred to as the “forcing function” is  $f = 60$  Hz.

Note that one can apply this simplified method for rigid bus arrangements with rigid connections between the high and low bus using structural modeling software capable of dynamic analysis.

**Common natural frequencies.** This section computes the natural frequencies for a range of realistic rigid bus spans using the aforementioned assumptions and materials. The standard equation for the natural frequency of a fixed-fixed beam is:

$$f_n = \frac{3.52}{\sqrt{\frac{wL^4}{384EI}}}$$

where

$f_n$  = natural frequency of the rigid bus span, Hz

w = self weight of bus, kip/in

L = span length, in

E = modulus of elasticity, ksi

I = moment of inertia, in<sup>4</sup>

Plotting the above function for the previously defined range of span lengths produces Figure 3 shown below.

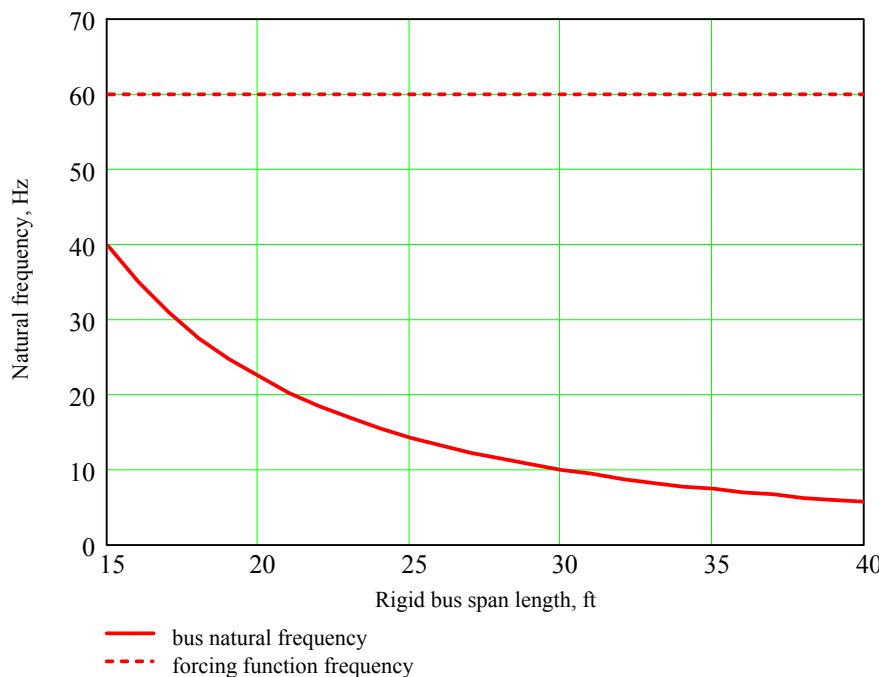


**Figure 3. Natural frequency of fixed-fixed simple bus spans vs. length**

The results shown in Figure 3 indicate that, even for very short and stiff rigid bus spans, the natural frequency of a rigid bus span is significantly less than that of the forcing function. For example, the highest natural frequency shown in Figure 3 (15' span) is 39.6 Hz which is only  $36.9/60 = 0.66$  times the forcing function frequency. Thus, the natural frequency of the rigid bus is usually significantly less than that of the forcing function, which corresponds to a similarly reduced dynamic response and equivalent static short-circuit force than that calculated using the default equation.

**Overview of method.** A discussion of the structural response of beams subjected to uniformly distributed load is outside the scope of this document. However, the method presented below follows the distributed mass – undamped system response to a uniformly distributed harmonic loading using the generalized single-degree-of-freedom methods presented in sections 2-7 and 4-1 of the “Dynamics of Structures” textbook (Clough 1975). The required steps and simplified equations are as follows:

1. Choose a shape function representing the deflected shape of the beam  $\psi(x)$ . For example, one could use the standard equation for the deflection of a fixed-fixed beam setting the distributed load equal to unity.
2. Calculate the first and second derivatives of the shape function.
3. Calculate the generalized mass of the beam:

$$m_G = \frac{w}{g} \int_0^L [\psi(x)]^2 dx \quad (4)$$

where

$m_G$  = generalized distribution of mass along the beam, lb/in

$w$  = weight per foot of the rigid bus span, lbf/in

$g$  = gravitational constant = 386 in/sec<sup>2</sup>

$\psi(x)$  = shape function previously defined

$L$  = length of the beam, in

4. Calculate the generalized beam stiffness using:

$$k_G = EI \int_0^L [\psi''(x)]^2 dx \quad (5)$$

where

$k_G$  = generalized beam stiffness, lb/(in·sec<sup>2</sup>)

$E$  = modulus of elasticity of the beam, psi

$I$  = moment of inertia of the beam, in<sup>4</sup>

$L$  = length of the beam, in

$\psi''(x)$  = second derivative of the shape function

5. Calculate the natural circular frequency of the beam (rad/sec) with the following equation with the generalized mass and stiffness defined above.

$$\omega_n = \sqrt{\frac{k_G}{m_G}} \quad (6)$$

6. Calculate the generalized short-circuit force for the shape function with:

$$F_G = F_{SC} \int_0^L \psi(x) dx \quad (7)$$

where

$F_G$  = generalized short-circuit force for the shape function, lbf/in

$F_{SC}$  = short-circuit force calculated using Equation 1 converted to units of lbf/in from lbf/ft

$\psi(x)$  = shape function previously defined

7. Noting that the deflection everywhere in the beam is at a maximum at the same time the deflection at midpoint is a maximum; use the general solution of the displacement at midspan with the following equation.

$$v_m(t) = \left[ \frac{F_G}{k_G} \frac{1}{1-\beta^2} (\sin \omega t - \beta \sin \omega_n t) \right] \psi_m \quad (8)$$

where

$v_m(t)$  = general solution of deflection at midspan vs. time, in

$F_G$  = generalized short-circuit force for the shape function, lbf/in

$\omega$  = circular frequency of the forcing function, rad/sec

$t$  = time (ranging from 0 to the fault clearing time,  $t_f$ ), sec

$\beta$  = ratio of the forcing frequency to the natural frequency =  $\omega/\omega_n$

$k_G$  = generalized beam stiffness, lb/ (in-sec<sup>2</sup>)

$\psi_m$  = is the deflection value of the shape function evaluated at

midspan =  $\psi(x=L/2)$

8. Plot the general solution for midspan deflection over the duration of the fault (from  $t = 0$  to  $t = t_f$ ) and locate the maximum midspan deflection ( $\Delta_{max}$ ).

9. Calculate the static component of the maximum midspan deflection using:

$$\Delta_{st} = \frac{F_G}{k_G} \psi_m \quad (9)$$

where

$\Delta_{st}$  = static component of the maximum midspan deflection, in

$F_G$  = generalized short-circuit force for the shape function, lbf/in

$\psi_m$  = is the deflection value of the shape function at midspan

$k_G$  = generalized beam stiffness, lb/ (in-sec<sup>2</sup>)

10. Calculate the dynamic maximum response (DMF) of the rigid bus span to the forcing function as shown below.

$$DMF = \frac{\Delta_{\max}}{\Delta_{st}} \quad (10)$$

where

$\Delta_{\max}$  = maximum total deflection at midspan from step 8, in

$\Delta_{st}$  = static component of the maximum deflection at midspan from Equation 9, in

11. Finally, compute the equivalent static short-circuit force applied to the bus with:

$$F_{SC\_EQ} = F_{SC} \cdot DMF \quad (11)$$

where,

$F_{SC}$  = short-circuit force calculated using Equation 1, lbf/ft or lbf/in

DMF = dynamic maximum response calculated above

12. Design the rigid bus and insulators the usual way with the equivalent static short-circuit force and an insulator overload factor of 2.0 to 2.5 applied to the short-circuit load.

Note that it is conservative to apply the resulting reduced short-circuit load,  $F_{SC\_EQ}$ , for the stiffest span to all rigid bus spans.

**Force reduction.** The amount of short-circuit force reduction is proportional to the dynamic maximum response factor, DMF, which will be less than 1.0 for normal rigid bus spans. The actual reduction depends on the rigid bus material, span length, support conditions, other loads (such as wind and ice) and the utility's overload factors for insulator design. The results of the hypothetical case study (see following section) provide reasonable estimates of the force reductions one can expect for common 138 kV rigid bus spans.

## COST SAVINGS

The cost savings associated with both the decrement factor and dynamic analysis methods to reduce the short-circuit load are dependent on many variables unique to each substation such as the rigid bus materials, insulator strengths, other rigid bus loads, span lengths, support conditions and the insulator overload factors. Therefore, this section of the paper uses the results from a hypothetical case study to provide reasonable estimates of the force reductions and cost savings one can expect for the typical 138 kV substation.

**Design inputs.** The following design inputs define the case study rigid bus geometry, support conditions, loads, fault current data and insulator overload factors.

- Controlling stiffest span is a rigid-slip (structurally fixed-fixed) span with  $L = 26' = 312''$ .
- The phase spacing is  $D = 8' = 96''$
- Use 5" Schedule 40 6061-T6 aluminum bus ( $E = 10^7$  psi,  $I = 20.7 \text{ in}^4$  and a self weight of 8.26 lbf/ft = 0.6883 lbf/in including the damping wire)
- Frequency of the short-circuit-forcing function, hereafter referred to as the “forcing function” is  $f = 60$  Hz.
- The X/R ratio is equal to 20 and the corresponding decrement factor is 1.27
- The fault clearing time is  $t_f = 0.083$  sec
- The fault current is  $I_{SC} = 50000$  A
- The extreme wind and short-circuit load case with  $V = 90$  mph controls.
- Extreme wind load on the bus is,  $F_w = 9.4$  lbf/ft
- Insulator overload factors are:
  - $K_1 = 2.5$  for wind load
  - $K_2 = 1.6$  for short-circuit load without dynamic reduction
  - $K_2 = 2.5$  for short-circuit load with dynamic reduction

**Short-circuit force reductions.** Table 1 below tabulates the resulting reductions in short circuit force using the decrement factor method and the dynamic analysis methods described in this paper.

**Table 1. Short circuit forces (lbf / ft) and corresponding reductions**

Load reduction method	Fsc	Reduced / Default	Percent reduction	See Equation(s)
Default with $D_f = 1.6$	62.4	1.00	0.0	1
Df reduced to 1.27	39.2	0.63	37.2	1 to 3
Dynamic analysis reduction with DMF = 0.23	14.4	0.23	76.9	10
Combining methods	9	0.14	85.6	-

**Total lateral force reductions.** The cost savings associated with reducing the short-circuit force is related to the total reduction in lateral load (wind and short-circuit). In addition, the insulator strength usually controls the allowable span length between support rather than bus stresses and deflection. Therefore, the total lateral load including insulator overload factors is the most important criterion when determining

cost savings. Table 2 below presents the effect of the both the decrement factor and dynamic analysis methods of short-circuit force reduction as well as a case combining both methods.

**Table 2. Total lateral loads including overload factors with corresponding reductions**

Load reduction method	K <sub>2</sub> F <sub>SC</sub> <sup>*</sup> (lbf/ft)	K <sub>1</sub> F <sub>w</sub> <sup>*</sup> (lbf/ft)	F <sub>T</sub> <sup>**</sup> (lbf/ft)	Reduced / Default	Percent reduction
Default with D <sub>f</sub> = 1.6	99.8	24	124	1.00	0.0
D <sub>f</sub> reduced to 1.27	62.8	24	87	0.70	29.9
Dynamic analysis reduction with DMF = 0.23	36	24	60	0.48	51.5
Combining methods	22.5	24	46.5	0.38	62.4

\* K<sub>1</sub> = 2.5 and K<sub>2</sub> = 1.6 or 2.5 for short-circuit load without and with dynamic reduction, respectively

\*\* F<sub>T</sub> = K<sub>1</sub>F<sub>w</sub> + K<sub>2</sub>F<sub>SC</sub>

**Estimated cost savings.** As mentioned earlier, the insulator strength generally limits the allowable rigid bus span lengths. Therefore, one can estimate the cost savings based on the ratio of default to reduced total factored lateral loads because the ratio applies to the number of bus supports required for a given bus run. For example, Table 2 above shows that, compared to using the default short-circuit force, one would only need approximately 38% as many bus supports (including insulators, fittings, support structures and foundations) after combining both reduction methods. Hence, the percent reduction column in Table 2 above represents the cost savings in insulators, fittings, support structures and foundations as a percentage of the default costs.

## CONCLUSIONS

- The short-circuit force is overly conservative when calculated using the default IEEE equations with a decrement factor of 1.6.
- One can significantly reduce the short-circuit force by calculating the actual decrement factor of the system and/ or performing a structural dynamic analysis of the rigid bus.
- Calculating the decrement factor is simple and only requires the system X/R ratio and fault clearing time.
- Performing a dynamic analysis is more difficult and time consuming.
- Use the standard short-circuit force insulator overload factor when using the decrement-factor reduction method.
- Use a higher short-circuit force insulator overload factor (2.0 to 2.5) when using the dynamic reduction method.

- One can expect the following cost savings for a typical 138 kV rigid bus design including insulators supports and foundations
  - 30% using a reduced decrement factor
  - 52% using a structural dynamic analysis
  - 62% combining both methods

## BIBLIOGRAPHY

Institute of Electrical and Electronics Engineers (IEEE). (IEEE Std. 605-1998). *IEEE*

*Guide for Design of Substation Rigid-Bus Structures*, New York, New York.

Clough, R.W. (1975). "Dynamics of Structures." McGraw-Hill, USA

## Wind Loading: Uncertainties and Honesty Suggest Simplification

Alain H. Peyrot, PhD, PE<sup>1</sup>

<sup>1</sup>

Emeritus Professor of Civil Engineering, Univ. of Wisconsin, Madison, WI,  
USA  
Past President (1992 to 2008), Power Line Systems, Madison, WI, USA  
[apeyrot@powline.com](mailto:apeyrot@powline.com)

### ABSTRACT

This paper discusses some of the recent wind loading procedures for the design of transmission lines (NESC, ASCE, IEC, CENELEC, etc.). It provides some detailed background behind their formulas for gust factors, span factors and gust response factors. It discusses the uncertainties inherent in each one of the parameters and assumptions behind the formulas: wind storm type, reference wind, terrain roughness, profiles, gustiness, time and spatial correlations, dynamic response, wind direction, drag coefficients, etc. It provides some examples to illustrate the current lack of consensus and to identify the important design parameters. The paper concludes that the complexity of most current wind design procedures is not justified. Instead, it provides the rationale for simplifying the entire wind design process and it offers specific recommendations for achieving that goal.

### 1. INTRODUCTION

The theoretical bases of the extreme wind provisions of some of the current generation of codes, standards or guides dealing with overhead transmission lines (NESC, 2007; CENELEC, 2001; IEC, 2003; UK NNA, 2004; ASCE Manual 74, 2008; ASCE Manual 113, 2008; etc.) were developed in the 1960's and early 1970's by a very small number of individuals with very sophisticated mathematical skills (Davenport, 1961 and later; Harris, 1963; Manuzio et al, 1964; Castanheta, 1970; Cojan, 1973; Armitt et al, 1975). We will refer to all the above-mentioned documents as "codes" even when they do not have that status. The mathematical bases of the wind models and associated structural responses borrowed from the random vibrations field (Crandall, 1963) and communication theory. For three decades, these provisions were published in draft documents and guides, but were not parts of legally binding documents. Therefore, they were mostly ignored. However, once the NESC in the US adopted Rule 250C in 2002, once the CENELEC document was finalized in 2001 and the IEC issued its Standard in 2003, it was no longer possible to ignore these provisions and they were finally tested by practicing engineers. This actual implementation revealed many problems and generated quite a few debates. In fact, the Europeans could never agree on a single approach and the CENELEC standard has an escape clause that allows each country to basically do what it wishes (i.e. publish a National Normative

Aspects, or NNA) as long as the general nomenclature is respected. This is what most of them do.

This writer is in a unique position to comment on the recent wind provisions as: 1) he has conducted academic research and taught graduate level and professional classes in wind engineering, reliability-based design and transmission line design, 2) he has been a member of some of the CIGRE (CIGRE, 1990) and ASCE (ASCE Manual 74, 1984, 1991, 2008) committees that developed the recent wind provisions, 3) he has worked as a transmission line consultant for many years and investigated line failures, and 4) he has participated in the implementation of the wind provisions of many international codes and standards in his company's design software (PLS-CADD & TOWER) that is used in over 100 countries. In doing so he has sometimes uncovered provisions that were simply untested, incomplete and confusing. Being confronted with so many ways of approaching the common problem of designing safe lines economically and practically, has led this writer to reflect on what we are doing, what is really justified and to suggest some simplifications. This is the rationale for writing this paper and hopefully convincing future generations that: 1) there is nothing sacred behind the current code procedures, 2) the complexity of the problem is not amenable to its description by fancy equations, and 3) simpler formulations should be considered.

Refining the wind loading equations has been part of the larger goal of improving design by what is now commonly known as Reliability Based Design (RBD). There was even some hope in the early days of RBD development, that given a sufficient amount of research and data collection, our industry would someday be able to quantify the probability of failure of a line (for example statistically determine the extent and number of failures of a line over a period of time). However, in part because of the uncertainties described in this paper, other uncertainties related to the size of the storms and the corresponding number of exposed structures, we will never be able to achieve this lofty goal. In spite of this shortcoming (inability to quantify the probability of failure), RBD is still a very valuable guide to develop consistent design procedures covering various combinations of loading events and materials (CIGRE, 1990 and 2006; ASCE Manual 111, 2006; Ghannoum, 2002; Mozer et al, 1984; Peyrot et al, 1984). Some concepts of RBD and simplicity are not incompatible.

## 2. TYPES OF WIND STORMS

For the proper understanding of the various engineering approaches to the determination of wind loads on transmission lines, it is imperative to have some knowledge of the various types of wind storms that may be damaging to our lines. Recommended reading on this subject are CIGRE Brochures 256 (2004), 344 (2008) and 350 (2008). Here we will limit our discussion to winds with gusts in the range of 40 to 60 m/s (about 90 to 140 mph) that cover at least two spans. Tornadic winds, while extremely violent, generally cover less than two spans and their peak velocity values are generally not considered in the statistics that form the basis of the "Basic/Reference Wind" maps produced around the world. While tornadic winds can be considered in design, for example as explained in ASCE Manual 74 (1991 and later), they will not be discussed in this paper.

## 2.1 Extra Tropical Cyclones/ Winter Storms

These storms are characterized by circulating winds around very low pressure zones: they are also referred to as cyclonic systems with very large diameters, say between 500 and 3000 km. They commonly occur in North America and Europe in winter. They are the most studied storms with a well-defined “boundary layer” behavior and have been the basis of the “Academic Winds” discussed in Section 2.5. While they are generally regarded as the storms that cause most transmission line failures in Western Europe, this is not the case in most other regions of the world.

For such winds, the motion of the air at heights above the boundary layer (at heights higher than the Gradient Heights generally considered to be higher than 250 m) is essentially parallel to the isobars and its velocity is referred to as the Gradient, Geostrophic or Synoptic Wind.

## 2.2 Tropical Cyclones

These are the well-known hurricanes/ typhoons/ cyclones that affect coastal areas during warm seasons. Very high winds exist near the low pressure center of the storm (the eye). Tropical cyclones can be very damaging to lines due to their extent, duration and propensity to carry debris.

## 2.3 Local Storms

These include a large variety of storms from the classical convective cell thunderstorms to the squall line winds and downbursts (macroburst and microburst) that occur near advancing cold fronts. To distinguish them from those due to Extra-Tropical or Tropical Cyclone winds, such winds have also been referred to as High Intensity Winds or HIW. While local storms are smaller in size than winter storms, they are more frequent, and according to several authors (Dempsey et al, 1996; de Oliveira, 2006), including the individual who produced the non-hurricane portion of the latest NESC and ASCE wind maps used in the US (Peterka, 1998 and 2005), and according to CIGRE Brochures 256 and 350 (CIGRE, 2004 and 2008), they are the cause of most wind failures in the USA, the central Canada, South America, South Africa and Australia.

## 2.4 Katabatic and Downslope Winds

Katabatic winds develop on the leeward side of mountains or ridges when the air approaching on the windward side is colder and flows downhill into warmer valleys due to its higher density. Downslope winds can also be caused by dry warm air forced down mountain sides by strong winds aloft. The various “Foen” winds of Europe and the “Chinook” wind in the USA are well-known examples of downslope wind.

## 2.5 Academic winds

Given the wide variety of storm types and the fact that no two storms are alike (and

that their characteristics may even be affected by global climate change), it is understandable that it will never be possible, even statistically, to accurately predict future occurrences of winds, including their spatial and temporal variations. However, some attempts have been made and we will refer to them as the “Academic Winds” to emphasize the big differences between real future storms and the elegant idealized equations that attempt to characterize them.

The academic winds that have been proposed for transmission lines can only be justified for winter storms and maybe tropical storms (Sections 2.1 and 2.2). An academic wind assumes that, for an averaging time period,  $T_{av}$ , of at least 10 minutes, and sometimes 1 hour, the wind velocity at height “ $z$ ” above the ground is the sum of a mean value  $V_m[z]$  (a single random variable) plus a zero-mean fluctuating value  $V_f[z,t]$  (the

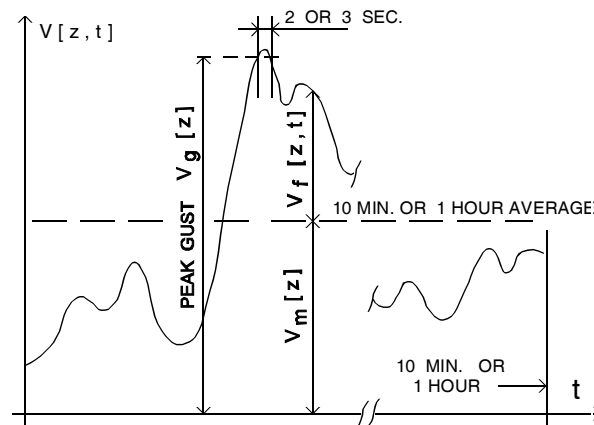


Figure 1 Wind over averaging period

turbulence) as shown in Fig. 1. The fastest wind value is the peak gust  $V_g[z]$ . Actually, given the precision of everything related to wind, the peak gust or the often quoted 2-sec or 3-sec gusts are equivalent and will simply be referred to as the “peak gust” or simply “gust” in this paper. The gust is the maximum wind that a structure or a very short span experiences. While Fig. 1 depicts the variation over time of the wind velocity at one point, it could also be interpreted as the spatial variation of the wind velocity along the centerline of a transmission line at one instant of time.

### 2.5.1 The mean value

In the context of a winter storm, it can be argued that if you are far enough above the ground (above the gradient height), there is very little turbulence and the wind velocity is not affected by the retarding effect of the roughness of the ground (i.e., when  $z$  is higher than the gradient height,  $V_f[z,t]$  is equal to zero and  $V_m[z]$  is constant and equal to the gradient speed). Based on experimental observations and considering the need for simplification, an academic wind assumes that, below the gradient height, the average wind velocity decreases following a well defined profile. Below the gradient height, the rougher the surface of the ground (upstream from the location where we are interested in the wind speed), the slower the average wind speed  $V_m[z]$  will be. Fig. 2 shows typical academic wind profiles, completely defined by the assumed reference wind speed  $V_{Ref}$  at 10 m above the ground and the ground roughness.

Profile equations proposed by three major international codes for Open Country or Reference category (called Category C by ASCE, Category B by IEC, and Category 2 by CENELEC) are:

ASCE/ NESC       $V_m[z] / V_m[10] = 1.42(z/275)^{1/9.5}$       Eq. 1

IEC       $V_m[z] / V_m[10] = (z/10)^{0.16}$       Eq. 2

CENELEC       $V_m[z] / V_m[10] = 0.19 \log [z/0.05]$       Eq. 3

At 40 m above ground, the above equations give increases in velocity of 1.16, 1.25 and 1.27, respectively (actually, Eq. 1 is applied to the gust even though its source implies an established wind over several minutes). Given that pressures are proportional to the squares of velocities, the pressure increase at 40 m over that at 10 m are 35%, 56% and 61% respectively. Nobody can really say that one of the prescribed increases is better

than the other, as in a real storm the values are quite variable. One of the few full scale tests conducted on power lines (Houle et al., 1991) during Winter Storms conditions, show a very high coefficient of variation (from 30 to 42%) for the exponent of the power laws in Eq. 1 and 2. These observations, coupled with the fact that terrain categories are somewhat arbitrary and difficult to assign in real situations, suggest that there is significant uncertainty in the assumed shapes of the profiles. In fact, as described in CIGRE Brochure 350 (CIGRE, 2008), even the general shapes of the profiles shown in Fig. 2 are totally inappropriate for local storms.

While the profiles described by Eqs. 1 to 3 are supposed to be valid for the mean velocity and extend to very high elevations (the gradient height), actual profiles of interest are generally limited to less than 60 m (except for river crossing towers).

### 2.5.2 The fluctuating value

The fluctuating value  $V_f[z,t]$  is assumed to be a stationary random process with invariant statistical properties over the averaging time period  $T_{av}$ . This assumes that during at least 10 minutes the storm properties do not change (stationarity). One can immediately see that this assumption is invalid for all local storms. Due to the retarding effect from the roughness of the ground, the turbulence increases from the gradient height down to the ground level, and is greater for rougher terrains (i.e. increasing from terrain Category D to Category A according to the ASCE

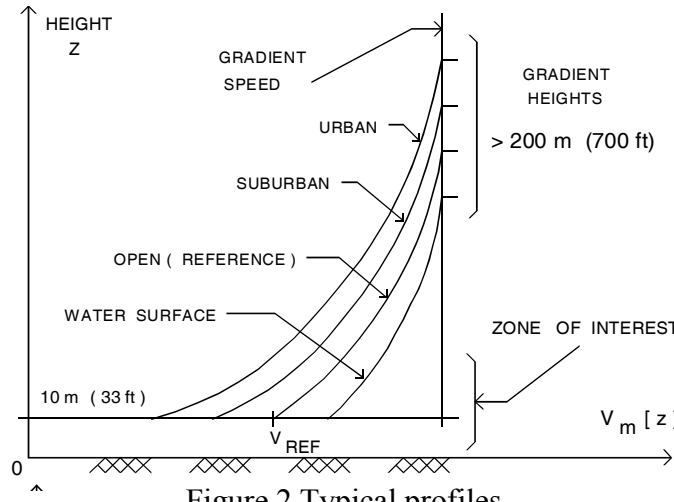


Figure 2 Typical profiles

classification, from Category A to Category D according to IEC classification and from Category 1 to Category 5 according to CENELEC classification). The turbulence has to be characterized by an auto-covariance and a cross-covariance function. The auto-covariance function  $C[z,lag]$  is a measure of the correlation between  $V_f[z,t]$  at time  $t$  and its value  $V_f[z,t+lag]$  at a later time  $t + lag$ . The cross-covariance function  $C[v,w,lag]$  is a measure of the correlation between the velocity  $v$  at one point in space (say one point on a transmission structure or along a span) and the velocity  $w$  at a second point (on the same structure or the same span, but a given distance away from the first point). The Fourier transforms of the auto-covariance function and the cross-covariance function are the Power Density Spectrum  $S(z,f)$  and the Cross-Spectrum  $S(z,f,distance)$  of the gust, respectively, where  $f$  is frequency.

The most used Power Density Spectra of the fluctuating wind referred to over and over again for the calculation of wind loads in the overhead line community (Cojan, 1973, Castanheta, 1970, Armitt et al., 1975; ASCE Manual 74, 1984, 1991 and 2008; NESC, 2007) are those suggested by Davenport (Davenport, 1961 and later). The Davenport spectra are “empirical” equations based on the average of measurements performed in strong winds, over terrains of different roughness, at different heights. The basic form is:

$$f S[f] = a x / (1+x)^{4/3} \quad \text{Eq. 4}$$

where  $x = 1200 f$  divided by the mean velocity at 10 m and “a” is a constant that includes the mean wind value at 10 m above the ground and a surface drag coefficient. Eq. 4 assumes the spectrum to be independent of height, which is really not the case.

Davenport later proposed another formula that included the height above the ground (Davenport, 1979):

$$f S[f] = b (f z)^{-2/3} \quad \text{Eq. 5}$$

where  $b$  is another constant.

Regarding assumed cross-spectra, there are very complicated equations and concepts: we will spare you the details.

#### 2.5.2.1 The Gust Factor

One important thing to know about the academic winds, is that their wind gusts are not related to measured values such as those that form the basis of the 3-sec gust ASCE map (ASCE, 2006), but are statistical estimates related to their mean. The relationship between the wind gust and the corresponding 10 min average (or other averages) is called the Gust Factor, GF, which is NOT to be confused with the Gust Response Factor, GRF discussed later in this paper. Fig. 3 shows IEC estimates of the ratio of the fastest wind averaged over a time period “t” to the 10 min. average (IEC, 2003). This is obviously extremely approximate and results in straight lines on a log-scale

paper between 2 sec. and 10 min., but it is being proposed to determine Gust Factors. ASCE Manual 74 uses a curve developed by Durst (Durst, 1960) to estimate GF's. CENELEC uses the following equation for the Gust Factor at height  $z$  to relate the peak gust  $V_g[z]$  to the 10-min average for Open Country:

$$GF[z] = 1 + 2.28/\log[z/0.05] \quad \text{Eq. 6}$$

For Open Country, the Gust Factor related to the 10 minute average is about 1.40 according to IEC (from Fig. 3), 1.43 according to Durst and 1.43 according to CENELEC. The fact that these three numbers are close to each other does not imply that for real storms there is a good relationship between a gust and the 10-min average: it simply means that all three documents are based on similar 1960's models. Actually, GF values for real storms vary wildly and one can assume that any proposed equation or graph for GF's can only be approximate. According to IEC, the Open Country GF related to the hourly average is  $1.4/0.88 = 1.59$

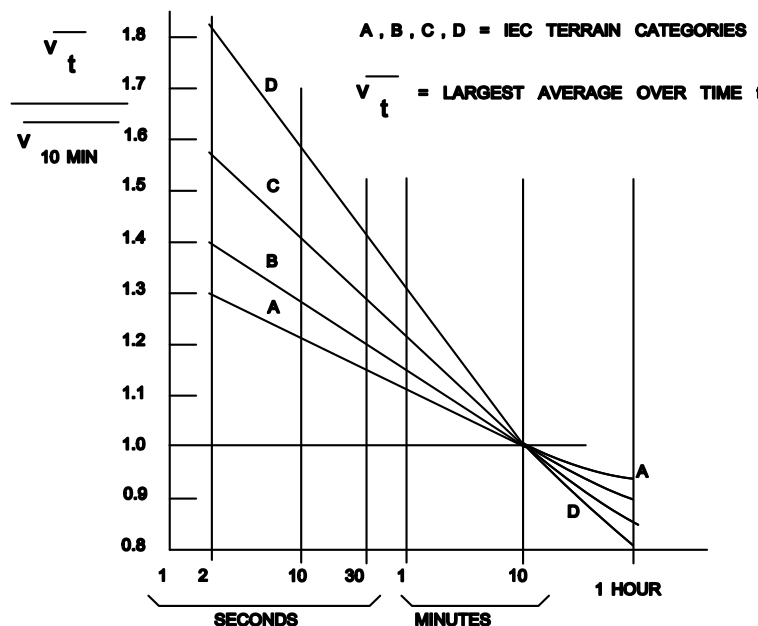


Figure 3 IEC velocity ratios for various averaging times

### 2.5.3 Can we trust the academic wind equations ?

This author developed some teaching material for an advanced graduate course on the dynamics of structures subjected to random loads such as wind and earthquakes and he used a well-developed textbook on the subject (Ghiocel et al, 1975). Based on this experience, it was concluded that some advanced knowledge of calculus, statistics and random processes, and several class hours were needed simply to understand the concepts and limitations behind the academic winds, their power spectra and cross-spectra, and the corresponding structural responses. The complexity of the formulations has intimidated many engineers and prevented them from questioning their validity.

In summary, the academic winds assume the following:

At the somewhat arbitrary gradient height there is a hypothetical wind with no

turbulence that remains constant over at least 10 minutes. However, due to the roughness of the ground, the mean wind is slowed-down by friction against the ground and turbulence is generated by that friction. The amount of turbulence depends on the roughness of the ground that is somewhat arbitrarily defined for 3 to 5 categories: smooth water surfaces such as coastal areas (ASCE Category D), slightly rough surfaces such as open country (ASCE Category C), rougher surfaces such as suburban areas (ASCE Category B), etc. Estimated gusts associated with academic winds are very approximate statistical outgrowth of the turbulence and are not a measured quantity.

Unfortunately, because of the impossibility of characterizing the almost infinite ways in which real winds can vary during a storm, their reduction to “academic winds” as described above (1960 and 1970 vintage models) has gained credibility due to: 1) the absence of alternatives, 2) the lack of understanding of the limiting assumptions, 3) the elegance of the formulations, and 4) the status acquired by their appearance in print. Our industry was grasping for something to quantify a basically unknowable phenomenon. Therefore, like with other parts of the wind loading equations that are discussed later in this paper, the “academic winds” spread like unchecked viruses in many codes, are often accepted as “facts”, and are unnecessarily complicating our design processes.

### **3. EFFECT OF TOPOGRAPHY**

It is well known that the presence of hills and valleys locally affects the wind velocity. The wind blowing over a hill ridge and perpendicular to that ridge has a higher velocity and different turbulence characteristics than the wind undisturbed by the hill. There are proposed solutions to that problem (Armitt et al., 1975; ASCE Manual 74, 2008), but it is generally not taken into account in transmission line design, probably because of the wide variation of topographic features along a line route and the need for standardization. However this is an important concept for building design where the topography is well known, the structure is custom designed and the need for precision is higher.

### **4. FROM WIND VELOCITY TO STRUCTURAL RESPONSE**

If a transmission structure or a span were just a small rigid body at a distance  $z$  above the ground, the maximum wind force on it would simply be:

$$F = q_g[z] C_d A \quad \text{Eq. 7}$$

where  $q_g[z]$  is the stagnation pressure (also called the dynamic wind pressure) equal to  $0.5 \times \text{mass density of air} \times V_g[z]^2$  (where  $V_g[z]$  is the gust velocity at height  $z$ ),  $C_d$  is the drag coefficient of the body, and  $A$  is its exposed area (perpendicular to the wind).

#### 4.2.1 Span Factor and Gust Response Factor

Unfortunately our transmission structures and our spans may not be small in size and,

as some have suggested, they may have some kind of resonant dynamic response to the wind. We will first deal with the “resonant response” concern and then with the “size effect”.

By resonant dynamic response, we are not talking about the pseudo static response of a line component that simply follows slowly increasing or decreasing winds, or the aeolian vibration (perpendicular to the wind velocity) that some spans and structural components experience under laminar wind, or the galloping of spans. We are talking about the possibility of some “along-wind” resonance, i.e. a resonant response in the direction of the wind due to the fact that the wind spectrum could have significant energy close to some natural frequencies of the system. Fortunately for us, along-wind resonance of transmission lines is NOT a concern. The majority of the wind loads come from the spans and when a span is subjected to extreme wind (blown out with non-uniform wind along its length) there is no conceivable mechanism or identifiable pendulum-type natural frequency that could be excited dynamically by the wind. As to some dynamic response of latticed towers, they have high natural frequencies at which the wind does not have energy. This is unlike some tall buildings that have much lower frequencies. Steel and concrete poles, if wires were not attached to them, could have some resonant along-wind response. However, with the wires attached, it is not possible for these structures to vibrate as they would do alone, both because of the restraint from the wires and the damping that they provide. Therefore, any attempt to include a possible resonant response factor in our transmission line design practice should be resisted vigorously as unfounded. This is similar to the attempt made by building designers to force our industry to include an earthquake loading case for transmission lines. Transmission lines, as shown during real earthquakes or theoretically, do not respond significantly to earthquakes as substation or building structures do.

Now let us discuss the “size effect”, also referred to as aerodynamic admittance. First consider a 40 m/s gust. In 3 seconds it will have covered a space of 120 m. Therefore, such a gust will envelope an entire transmission structure (except probably a river crossing tower) at once and also a very short span (certainly the span of a distribution line). Therefore, there should not be any size effect concern for most of our transmission structures if the velocity of the gust is the reference design value. However, for spans, it is very likely that when a gust hits a portion of a span, the rest of it is subjected to lesser wind velocities. This is because wind velocities are not fully correlated over longer spans. Therefore, this “size effect” can be taken advantage of by allowing a reduction of the unit wire design loads for long spans. This is usually handled by adding a Span Factor (SF) to Eq. 7 as shown in Eq. 8:

$$F = q_g[z] SF C_d A \quad \text{Eq. 8}$$

Codes that use Span Factors as shown in Eq. 8 normally neglect the “size effect” on structures and neglect all dynamic effects. Only the lack of correlation of the wind velocities along the span are considered.

Another approach to the handling of the “size effect” and the possible “resonant effect” is the Gust Response Factor (GRF) approach. The GRF approach consists of specifying a force  $F$ , which, if applied statically, would cause the system to reach its expected peak response. With the GRF approach, Eq. 8 is replaced by Eq. 9 where the stagnation pressure  $q_m[z]$  is now equal to  $0.5 \times \text{mass density of air} \times V_m[z]^2$  (where  $V_m[z]$ ) is the 10-min average, or longer, wind velocity):

$$F = q_m[z] \text{ GRF } C_d \text{ A} \quad \text{Eq. 9}$$

Codes that use Gust Response Factors traditionally consider both the “size effect” and the “resonant effect”, not only on spans but also on structures. The ASCE Standard 7-05 (ASCE, 2006) for buildings includes the resonant effect in its gust factors, but this standard is certainly not applicable to transmission lines.

There is sometimes some confusion in the naming of the factors: for example, CENELEC (CENELEC, 2001) in Art. 4.2.2.3 calls Gust Response Factor what is really the square of the Gust Factor (Gust Factor = ratio of peak wind to 10-min average) and it calls “Structural Resonance Factor” what is really as Span Factor. We also know of big mistakes that have been made when using 10-min mean wind values as input to equations such as Eq. 8 or gust values as input to equations such as Eq. 9. Depending on the formulation, SF and GRF may be a function of the height above ground “z”.

The derivation of the Gust Response Factor proposed by Davenport (Davenport, 1978 & 1979) that eventually found its way into the ASCE/ NESC equations is very elaborate and based on many assumptions, one of which is quite arbitrary. This arbitrary assumption simply says that the peak response of a span or a structure is equal to its response to the mean wind value (10-min average) plus a certain number (statistical factor) of standard deviations of the response. The statistical factor is suggested to be a number between 3.5 and 4. The standard deviation is calculated as the area under the power spectrum of the response. There are also approximations in the mathematics. For any wind that does not follow exactly the stationarity assumption and the power spectrum of the academic wind (as so many winds do), one has to question the validity of the proposed GRF.

Because Eq. 9 starts with the mean wind, the Davenport approach should end up with GRF's for small structures and short spans that are larger than 1. However, because the NESC/ASCE procedures are not using an average reference wind but a gust reference wind,  $q_g[z]$  replaced  $q_m[z]$  in Eq. 9 and the GRF's were decreased by the square of the gust factor.

#### 4.2.2 Wind direction

Whether one uses a design equation such as Eq. 8 or Eq. 9 for determining the wind force on a span, it is almost universally assumed, as a worst case hypothesis, that the

wind blows perpendicular to the spans. However, if the wind were to blow at a certain incidence angle from the normal to a span, the force would decrease by a factor that is equal to the square of the cosine of the incidence angle. For example, if the wind is at 45 degrees, the force goes down by a factor of 2. For any incidence larger than 18 degrees, the force will go down by more than 10%, i.e. for winds that are equally likely to come from any direction, there is an 80% chance that the force will be 10% smaller (and sometimes much less) than assumed by a design equation that applies the wind normal to the span. Since most design wind maps are statistics of wind velocities that do not consider wind direction, assuming that these wind will occur perpendicular to the spans as most codes require is quite conservative. For directional winds such as Downslope Winds, some lines will be much more vulnerable than others.

The wind direction effect is one of the major uncertainties when trying to estimate wire loads on a probabilistic basis. Some building and communication tower codes even include a “wind directionality factor” to account for the reduced probability of maximum wind coming from any direction.

#### 4.2.3 Center of pressure

There is the question about what value of “z” should be used in Eqs. 8 and 9. For structures, the NESC suggests using a single value at 2/3 the height of the structure and then using the resulting pressure over the entire height. Other codes expect the designer to break down the structure into sections at different heights and to compute a different pressure at each height based on the center of gravity of the area of the section. For spans, some codes require the use of the center of pressure for the conductor, which is approximated as 1/3 of the sag below the attachment points. One issue is whether to have a different “z” for each wire or to use some kind of average. Some codes suggest using the average attachment height of all wires or that of the highest wire. Calculated loads are certainly sensitive to these assumptions.

#### 4.2.4 Wire tensions

Wire tensions affect the transverse loads on all angle structures and all dead ends. They also affect the vertical loads on all structures with non-horizontal adjacent spans. So, the tension is not really due to the effect of the wind on the two spans adjacent to a structure, but the uncorrelated wind on all the spans in the tension sections (from dead end to dead end) where the structure is located. If this tension section includes many spans, no one will ever know what length to use for the calculation of the SF or the GRF, or even if the equations are valid for such a calculation.

#### 4.2.5 Drag Coefficient

ASCE Manual 74 (1984 and 1991) had quite a bit of information on published values of drag coefficients for cables, structural members and some assemblies.

While these ASCE documents and IEC suggest a drag coefficient of 1 for all wires,

international practice regarding this varies widely. Houle et al (1991) and ASCE Manual 74 show that, even for a given Reynolds number, there is a wide scatter of conductor drag coefficients.

For poles, drag coefficients close to 1 are generally recommended.

Regarding latticed towers, the NESC simply requires a combined drag coefficient of 3.2 (1.6 for the members of the front face plus 1.6 for the members on the back face) to be applied to the exposed area of the front face and a constant design pressure calculated at 2/3 the height of the tower. However for rectangular cross section towers, the IEC, CENELEC and ASCE all use the same formula for the combination of drag coefficient and exposed area. The formula is:

$$(1+0.2 \sin^2[2a]) (C_t A_t \cos^2[a] + C_l A_l \sin^2[a]) \quad \text{Eq. 10}$$

where "a" is the direction of the wind relative to the tower transverse axis,  $A_t$  is the area of the tower face exposed to pure transverse wind,  $A_l$  is the area of the tower face exposed to pure longitudinal wind and  $C_t$ ,  $C_l$  are drag coefficients based on the solidity ratios of the faces (these coefficients can vary from 4 to slightly less than 2). This is an example of a formula that spread like a virus from one code to the other as there is no real knowledge of what happens to a full size tower in a real storm. The formula is of no help to the designers of towers that have non-rectangular cross sections such as shown in Fig. 4 and is almost impossible to automate in a tower design computer program. The limitation of the formula was determined experimentally (De Oliveira et al, 2006).

The limited use of Eq. 10 prompted the latest ASCE Manual 74 (2008) to include a universal "wind on members" procedure as an alternate to the "wind on face" approach of Eq. 10. This alternate procedure conservatively ignores shielding (which is impossible to know for any configuration different from a perfectly rectangular section) and determines the wind force on each member independently, based on the relative orientation of the wind and the axis of that member. In the comparisons

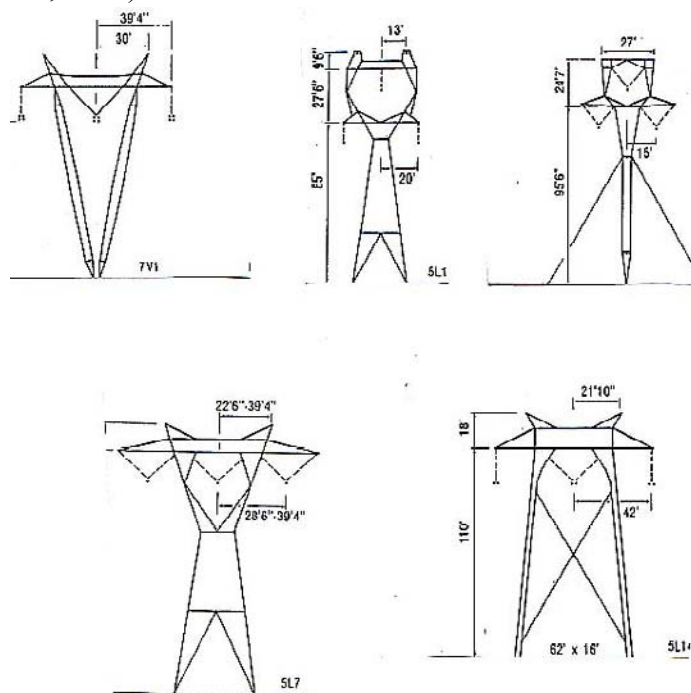


Figure 4 Typical tower configurations

of Section 6.2, we will refer to the ASCE 2008 method that uses the face as “ASCE 2008 F” and that handles each member separately as “ASCE 2008 M”.

In addition to its lack of universality, the formula of Eq. 10 requires that a tower be divided into sections, each section having its own solidity ratio and height above ground. The combination of having to micro-manage the solidity ratio together with the section height is another complexity (fortunately not required by the NESC) which cannot be justified by the uncertainties involved.

Micro-managing the wind load on a tower can be pushed to extremes as demonstrated by the UK-NNA (2004). This specification considers the probability that the maximum conductor loads are not fully synchronized with the maximum load on the tower itself, and therefore the two are not simply additive. Since the portion of the resulting force in a member due to the loads from the wires as opposed to wind loads directly on the structure varies depending on the type of member and its location (for example main leg member vs. diagonal), there is a factor that adjusts wind loads based on the relative sensitivity of the members to wire and tower loads.

#### 4.2.6 Wind on insulators

Some codes require that wind on insulators be calculated, including the effect of gustiness and increase of wind velocity with height. This is probably the epitome of un-necessary complexity as no-one knows the shielding effect of the structures on insulators on one side of a structure and the exposed area/ drag coefficient of an inclined insulator under extreme wind. Given the small contribution of the insulator load to the total structure load, this is certainly something that can be neglected as rightly done in the US.

### 5. CODES, STANDARDS AND GUIDES SELECTED FOR COMPARISONS

Three design methods that have received international attention are those of the ASCE/ NESC, CENELEC, and IEC. We will add to the list a fourth method, the UK NNA method, which is one of the many variants of CENELEC, but is based on a one hour average academic wind. All are loosely based on academic wind models developed more than 30 years ago by the few individuals cited in Section 1. Very few engineers on the current code committees even know the assumptions and complexity of the original mathematics. However, over the last 30 years, the three design methods have evolved somewhat independently due to the political and adaptation processes that eventually led to their official adoption since 2000.

All four methods start with the selection of a basic 50-year Reference Wind measured at the Reference Height of 10 m. Reference Winds are normally available from national wind maps. However, the type of Reference Winds and their averaging time are totally different. In IEC document, it is a 10-minute average wind. In CENELEC (depending on the NNA or method chosen), it can be a 2-sec gust, a 10-min average or even a 1-hour average as used in the UK NNA. In ASCE/ NESC, it used to be a fastest mile (which is close to a 1-min average), but it is now a 3-sec gust. Since gusts

are the velocities of importance in design, collecting and using “gust” data as the starting point (Reference Wind) is certainly the right thing to do, rather than counting on some loose statistical relationships between a gust or a peak structural response and the corresponding 10-min or 1-hour reference values. So we can certainly say that the adoption by the ASCE/ NESC of a 3-sec Reference Wind is a major move in the right direction. One of the common-sense features of the ASCE wind map is that measured gust data for the non-hurricane zones of the US were assembled from a number of stations in state-sized areas to decrease sampling error (Peterka, 1998). Then, based on the insufficient variations over the Eastern 3/4 of the lower 48 States to justify contours, a single zone of 40 m/s (90 mph) was adopted. This laudable simplification is in contrast to some unbelievable micro-zoning maps included in some other national codes. But it is understood that this simplification (harmonizing all winds into larger zones) has its inherent inaccuracies and has been challenged (Simiu, 2003).

One thing is clear though with the ASCE/ NESC maps: they do mix together data from large scale wind storms and local storms, as well as those from tropical cyclones, but they exclude winds from tornadoes. They are wind estimates at a point. However, the 50-year reference wind that would be needed for a better reliability estimation of a line should not include maximum winds at a point but maximum winds over the space of the line: but those data are rarely available.

All four methods use wind profiles (effect of height), and some combination of gust factors with span factors, or gust response factors, all of which are essentially only valid for the “academic winds”. In fact, the ASCE/ NESC procedure, which is using the best basis for the Reference Wind (3-sec), is still borrowing internally the mathematics of an academic wind. Now, let's think for a minute about what it is doing. It starts with a 3-sec gust which is related to measured data, but the academic wind theory says that we need an established wind over at least 10-minute for the theory behind the profiles and the GRF's to be valid. So the ASCE/ NESC procedure takes a good design value (the 3-second gust) and it reduces that value internally by a somewhat arbitrary number to get the corresponding 10-min wind so that it can salvage the academic wind basis of the profile and the vintage GRF. It makes very little sense to say that a measured gust of say 40 m/s is really the peak wind of an assumed 10-min wind of 28 m/s or an assumed 1-hour wind of 25 m/s.

This writer understands the huge amount of sincere efforts behind the development of the code procedures mentioned in this section. The negative comments throughout this paper are only meant to emphasize the underlying uncertainties, the unnecessary complexity and the lack of consensus.

For the design of buildings or other isolated structures as described in the ASCE Standard 7-05 (ASCE, 2006) one can possibly justify some refinements in the description of the nearby terrain roughness and topography, as well as the dynamic and shape characteristics of these structures. But transmission lines are totally different systems from buildings that are normally custom designed for a site. Buildings have volumes for which there are very important issues of local “force” coefficients that affect local pressures around the building and possible “dynamic”

behavior. Transmission lines and their supports, on the other hand, have “line like” components with insignificant along-wind resonant dynamics and where local “force” coefficients are irrelevant, but instead “drag” coefficients are needed. Transmission lines also benefit from some level of standardization and they can cover a wide range of terrain characteristics: their most important loads are span loads for which ground roughness, span length and wind incidence introduce considerable uncertainties. Therefore, design rules for transmission lines should be unique and not be imposed by regulating bodies or academic-types that deal with building structures.

## 6. SOME COMPARISONS

Very simple examples are presented in this section to demonstrate the combined effect of height and span length on wire loads and the combined effect of height and drag coefficients on structure loads with the goal of appreciating the sensitivity of these loads to some code assumptions and the corresponding lack of consensus.

### 6.1 Wire loads

The wire load examples all consider a Drake conductor sagged at 20% of ultimate after creep for various combinations of attachment heights, span lengths and code methods. For the five attachment heights considered, the span lengths were maximized so that they would have an 8 m clearance above ground at 115 deg C after creep as shown in Fig. 5 (a vertical to horizontal

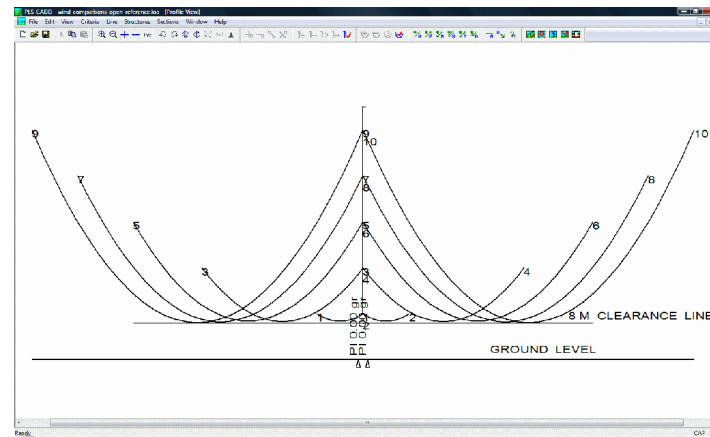


Figure 5 Span examples

scale ratio of 10/1 was selected for the display of the PLS-CADD models in Fig. 5 for clarity of presentation).

As a reference for our wire load examples, a 1 m long rod having the same diameter as the Drake conductor, located 10 m above the ground and subjected to a gust of 40 m/s would be subjected to a force of  $.613 \times 40 \times 40 \times 0.0281 = 27.6$  N/m. In the rest of this section, we will report the load per unit length of that same Drake conductor in the models of Fig. 5 when subjected to combinations of heights, span lengths and code assumptions as the rounded ratio (Wire Load Ratio) of the calculated code load divided by the Reference Load of 27.6 N/m. The ratio is rounded to two digits, as any other precision for our demonstration purpose would be meaningless.

For comparison with the old traditional US design methods, the ratios are also calculated for NESC Rule 250B (including the 2.5 load factor for wind and the ice thickness, if any). For example, the ratio is 0.93 (25.6 N/m divided by 27.6) for the

Heavy Loading District, 0.71 for the Medium District and 1.10 for the Light District.

For the various codes considered, the Reference Winds at 10 m above the ground were taken as follows:

NESC 2007	40 m/s gust (same as ASCE Terrain Category C)
ASCE 2008	40 m/s gust for ASCE Terrain Category C
IEC 2003	$40/1.40 = 28.6$ m/s 10-min av. for IEC Terrain Category B (Remember, 1.40 from Section 2.5.2.1 is somewhat arbitrary)
CENELEC 2001	40 m/s gust for CENELEC Terrain Category II
UK NNA 2004	$40/1.59 = 25$ m/s 1-hr av. for UK NNA Terrain Category 3 (Remember, 1.59 from Section 2.5.2.1 is somewhat arbitrary)

For the Reference Winds described above, Table 1 shows the Wire Load Ratios for the Open Terrain categories of various codes. For completeness, these categories are described below (the wording of the documents is purposely included to draw attention to the sensitivity of the answers to some imprecise definitions):

NESC 2007	No terrain category considered
ASCE 2008	Cat. C: Flat open country, farms, and grasslands.
IEC 2003	Cat. B: Open country with very few obstacles, for example airports or cultivated fields with few trees or buildings
CENELEC 2001	Cat. II: Farmland with boundary hedges, occasional small farm structures, houses or trees
UK NNA 2004:	Cat. III: Basic open terrain, typical UK farmland, nearly flat or gently undulating countryside, fields with crops, fences and low hedges or isolated trees.

In order to show how loads change when going from one loosely defined terrain category to the next rougher one, Table 2 shows Wire Load Ratios similar to those in Table 1 for the categories defined below:

NESC 2007	No terrain category considered
ASCE 2008	Cat. B: Urban or suburban areas, well wooded areas, or terrain with numerous closely spaced obstructions having the size of a single-family dwelling or larger.
IEC 2003	Cat. C: Terrain with numerous small obstacles or low height (hedges, trees and buildings)
CENELEC 2001	Cat. III: Suburban or industrial areas and permanent forests
UK NNA 2004:	Cat. IV: Farmland with frequent high hedges, occasional small farm structures, houses or trees.

Table 1 Wire Load Ratios for Drake conductor in Open Country

	Combinations of attachment heights and span lengths (m)				
	10-100	20-350	30-500	40-620	50-720
NESC 2007	0.80	0.78	0.80	0.83	0.85
ASCE 2008	0.80	0.78	0.80	0.83	0.85
IEC 2003	0.94	1.03	1.05	1.06	1.07
CENELEC 2001	0.92	0.99	1.05	1.10	1.13
UK NNA 2004	0.85	0.81	0.84	0.86	0.88
Old NESC 250B Heavy:	0.93				
Old NESC 250B Medium:	0.71				
Old NESC 250B Light:	1.10				

Table 2 Wire Load Ratios for Drake conductor for next rougher terrain category above Open Country

	Combinations of attachment heights and span lengths (m)				
	10-100	20-350	30-500	40-620	50-720
NESC 2007	Not used				
ASCE 2008	0.64	0.62	0.65	0.68	0.70
IEC 2003	0.76	0.85	0.88	0.89	0.90
CENELEC 2001	0.85	0.72	0.77	0.82	0.85
UK NNA 2004	0.69	0.75	0.78	0.81	0.83

One could be tempted to make comparisons between corresponding numbers in different rows within each of the two tables above, and say for example that NESC (2007) is not conservative because it sometimes gives conductor loads that are more than 20% lower than those from the IEC. However, such conclusions are meaningless as one calculation starts with a gust wind and the other with a 10-min average, and there is no fixed relationship between the two. But some useful conclusions can be drawn from the above tables as discussed below.

Looking at all the numbers across one row of Table 1 (i.e. over a very wide range of spans), one will notice that the maximum variation is only 6.6% for the NESC and ASCE, 13.5 % for IEC, 22.8 % for CENELEC, and 3.2 % for UK NNA. These percent numbers would be even smaller if we had accounted for the lower center of pressure for long spans, which some codes require to be 1/3 of the sag below the attachment points. This “relative insensitivity” of the wire loads to the combined height and span length parameters was also mentioned in a proposed change of the NESC (Kluge, 2005) and can be used as an argument for one of the proposed simplification in Section 7.3.4. Because long spans tend to be higher, the increase of the wind velocity with height is tempered by the lack of correlation of the gusts along

the span (the size effect), thus the “relative insensitivity” (a term we will use later in this paper) of the wire loads.

But looking at numbers in identical locations in Table 1 and in Table 2 will show much larger differences. For example, the fact that the number of trees or buildings may vary from “a few” to “numerous” will lower the IEC span loads by over 17%, which is more than the 14% variation due to the full range of heights and span lengths considered. This is a very significant contribution to the uncertainty of the calculated numbers when one considers that a line will most likely traverse terrains where the roughness and topography of the upwind surface varies.

## 6.2 Structure loads

To illustrate some of the complexities, variations and uncertainties of some code tower wind loads, we purposely selected a very tall tower (86 m) as shown in Fig. 6. That tower has a fairly simple geometry, so that Eq. 10 can be used on the 7 main sections of the tower whose important properties are summarized in Table 3. The arms at each of the three levels were modeled as three separate sections with transverse wind areas of 4.5, 4.5 and 5.8  $\text{m}^2$ , respectively.

Table 3 Tower Sections

Sect. #	Average Height (m)	Face Area ( $\text{m}^2$ )	Solidity Ratio (%)
1	81	6.2	37.1
2	70	9.4	39.6
3	57	8.2	23.7
4	46	6.1	14.4
5	35	9.1	9.4
6	21	8.9	8.3
7	8	10.4	6.1

We used the TOWER program to analyze the tower without conductor loads but with a transverse wind blowing on the tower, assuming in all cases a 40 m/s Reference Gust Wind at 10 m above the ground giving a Reference Pressure of  $.613 \times 40 \times 40 = 981 \text{ Pa}$ . Assuming that the Reference Wind is applied over the entire height of the tower, i.e. that there is no escalation with height, two Reference cases were

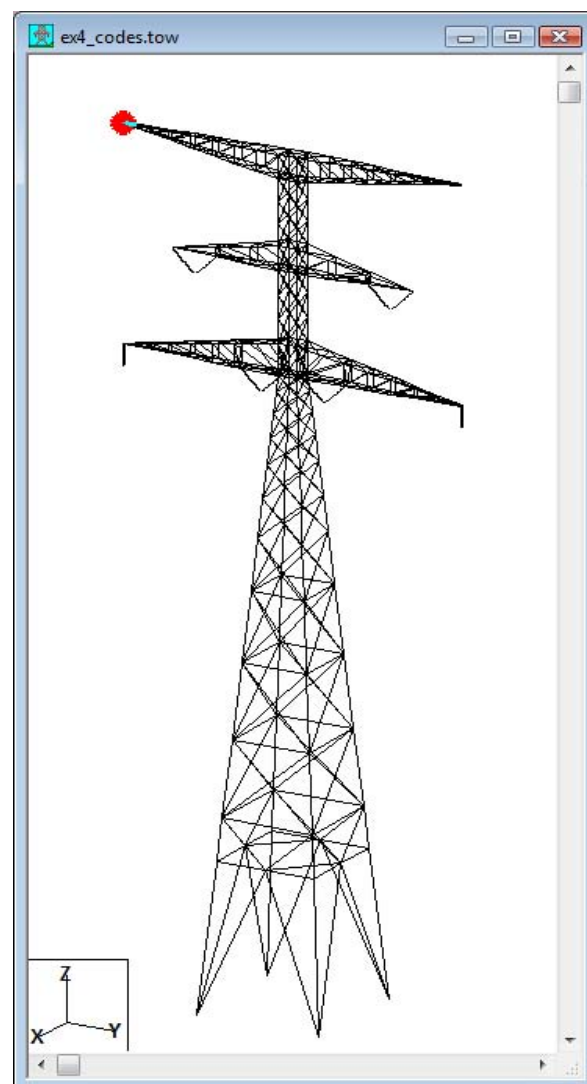


Figure 6 Tower example

considered. For the “Reference F” case, the reference pressure of 981 Pa was applied to the entire face of the tower assuming a drag coefficient of 3.2 for that face (similar to that required by the NESC): this is a “wind-on-face” approach. For the “Reference M” case, the reference wind of 40 m/s was applied on each individual member of the tower, assuming a drag coefficient of 1.6 for each member and letting the computer determine the wind load on each member based on the relative orientation of the wind velocity and the member axis: this is a “wind on members” approach.

For each of the two Reference Cases and for some codes, the overturning moments at the tower base were calculated as shown in Table 4. The overturning moment is the simplest and most important measure of the wind load and its demand on the tower. All the calculations in Table 4 assumed an Open Country (as was done for the wires in Table 1). Since ASCE 2008 allows two alternate methods (a “wind-on-face” approach and a “wind-on-members” approach), the two methods are included in the table and are designated as “ASCE 2008 F” and “ASCE 2008 M”, respectively. All other code methods use the “wind on face” approach. Where appropriate, Table 4 also includes the pressures and drag coefficients for 3 of the 7 sections.

Table 4 Tower Base Moment, Pressures and Drag Coefficients for selected sections (Open Country)

	Base Moment (kN-m)	Sect. 1 Press. CD (Pa)	Sect. 3 Press. CD (Pa)	Sect. 6 Press. CD (Pa)
Reference F	10,300	981 3.2	981 3.2	981 3.2
NESC 2007	11,700	1110 3.2	1110 3.2	1110 3.2
ASCE 2008 F	9,200	1190 2.2	1110 2.9	901 3.7
IEC 2003	10,500	1310 2.3	1300 2.8	1090 3.5
CENELEC 2001	13,000	1700 2.3	1580 2.8	1260 3.5
UK NNA 2004	11,300	1560 2.3	1390 2.8	1000 3.5
ASCE 2008 M	11,800	Velocity at height of member considered CD = 1.6 for all members ASCE GRF = 0.78 for 86 m tower included		
Reference M	10,500	40 m/s assumed at all member locations CD = 1.6 for all members		
		No GRF included		

Following are some comments regarding the numbers in Table 4.

NESC 2007 includes a 0.78 tower GRF (a surprisingly small number implying a significant lack of correlation of wind velocities along the height of the 86 m tower), it assumes a constant design pressure as that calculated at 2/3 of the total height of the structure and it uses a constant drag coefficient.

ASCE 2008 F includes a 0.78 tower GRF, it increases the pressure with height and it

varies the drag coefficient based on the solidity ratio of the face of the section.

The IEC, CENELEC and UK NNA formulae do not specifically isolate a GRF for the tower (even though the TOWER CENELEC calculations include the recommended “structural resonance factor” of 1.05), but they require varying pressures with height and varying drag coefficients.

The large differences in base moments when comparing the IEC, CENELEC and UK NNA (there are much greater variations with other European codes that we have not summarized in this example) were surprising given the supposed cross-pollination between these specifications. This is just one example of the lack of consensus which we have observed all over Europe.

Comparing the base moment for “Reference M” (which ignores the increase of wind velocity with height and the complexity of the “wind on face” approach and associated solidity ratio issues) to the moments from the other codes, suggests that the conservativeness of the “wind on members” approach somehow makes up for ignoring the other factors.

Although not shown here, there would be a substantial drop in the tower loads if the terrain category was changed to the next rougher category.

As with the wire loads, there is some “relative insensitivity” of the final tower load (measured by the base moment) to the tower height and other parameters. This is because the increase of velocity with height may be tempered by a built-in code “size effect” and section drag coefficients that are substantially smaller in the high portion of a tower than near its base. Another contributor to the insensitivity is the fact that short towers are often used on top of a hill where the wind velocity may be higher as opposed to taller towers used at lower elevations. Given that: 1) some “relative insensitivity” is observed for some code procedures, 2) tower wind loads are much smaller than the sum of the wire loads, 3) tower wind loads are not fully synchronized with the wire loads (lack of spatial correlation), and 4) large uncertainties related to the use of academic winds and terrain categories, one should wonder if the minutia of dividing a tower into sections is necessary.

## 7. NEED FOR SIMPLIFICATION

It has been suggested that, given that most lines are now designed by computers where complex code formulas are automated (PLS-CADD, TOWER, Etc.), complexity is not an issue. This writer totally disagrees with this argument for the two reasons discussed below.

### 7.1 Reason 1 - Honesty

Given that damaging winds can come from a wide variety of storms and given all the uncertainties discussed previously, it is basically dishonest to pretend that our wind designs will be better (better balance between costs and reliability) if one fine-tunes

the contribution of each of the many factors affecting the problem with some questionable equations. The multitude of the current factors that have to be accounted for increases the chance of errors and provides additional litigation opportunities to ignorant parties that will focus on minute irrelevant details rather than understanding what is important. As engineers, we should always favor common sense.

## 7.2 Reason 2 - Simplify the life of the designer.

One extremely useful concept often used in line design considers that a family of supports, for given supported wires and code criteria, has some allowable wind and weight spans. This concept is immediately invalidated by making wind loads dependent on structure height, conductor heights and span lengths. Another useful concept is that of designing a standard family of supports with the same top geometry but with different heights. For example, the upper portion of a tower and its shortest body is common to the entire family, with body and leg extensions taking care of the need for varying heights. Other issues that can plague the engineer when the wind loads vary with height and span length are the corresponding calculations of the wire tensions. Therefore, there are very good practical arguments for eliminating the dependence of wind loads on height and span length for most common design situations.

## 7.3 Suggested simplifications

### 7.3.1 Utilize the 3-sec gust as the Reference Wind

This simplification does not apply to the US where NESC/ ASCE already use gust as the reference wind speed. CENELEC also allows as an option the use of the gust. Since gust winds are those that destroy lines, starting the design process with the gust wind (Reference Wind) eliminates the large inherent uncertainty in some codes of going from mean wind velocity to gust through the Gust Factor or going from mean structure response to peak value through the Gust Response Factor.

The pressure caused by the Reference Wind is the Reference Pressure  $q_{Ref}$ . Some codes specify that pressure as the starting point of their wind calculations instead of the corresponding gust velocity.

### 7.3.2 Eliminate terrain categories

Since terrain categories have such an uncertain effect on wind gusts and are not amenable to clear definitions along a line, they should be eliminated. The reference Open Country category is the only one to keep. This is currently done by the NESC. A coastal or lake increase factor of about 20% might be appropriate for such exposures (current ASCE Category D or IEC Category A).

### 7.3.3 Abandon the concept of Gust Response Factor

As its name indicates, a Gust Response Factor is the ratio of a peak structure response divided by the average response due to the mean wind. As mentioned in Section 4.2.1, the GRF normally accounts for a possible resonant “dynamic effect” and a “size effect” (lack of correlation of wind gusts at distant points). But the “dynamic effect” is not a factor in transmission lines. The “size effect” is significant for wires, but not for their supporting structures. Therefore, the only contribution from the GRF should be a reduction of wire loads for longer spans, which is exactly what the concept of a Span Factor does.

Because: 1) there is no average structure response to apply a GRF to if one starts with a reference wind which is a gust, 2) there is no identifiable “resonant” response in transmission lines, 3) there is no significant “size effect” on transmission structures, and 4) the only components that can benefit from the “size effect” are the wires, the concept of GRF is inappropriate and should be replaced by a simpler Span Factor where there is a need to reduce unit loads on very long spans. This turns out to be the alternate “empirical approach” of CENELEC.

#### 7.3.4 Eliminate height and span length as variables for the majority of designs

For all structures with maximum height below a cutoff value (to be determined but certainly above 50 m) use the Reference Pressure  $q_{Ref}$  over the entire height of the structure and use a reduced pressure (suggested to be around 0.90  $q_{Ref}$ ), for all wires attached to the structures. The reduction factor accounts for the low probability of having winds perfectly perpendicular to the spans and having the span loads perfectly synchronized with the structure loads. Using a constant design value accounts for some of the “relative insensitivities” discussed in Sections 6.1 and 6.2.

For unusual situations (river crossing or very long spans), an increase of wind velocity with height and a Span Factor may be considered.

An obvious and even more justified extension of this recommendation would be to simply use the Reference Pressure  $q_{Ref}$  on all structures and wires within a substation (ASCE Manual 113, 2008).

#### 7.3.5 Use the same wire wind load for the determination of the lateral wire load transmitted to the supporting structure and for the determination of the wire tensions

This was discussed in Section 4.2.4, and if followed, this simplification will generally result in conservative values of mechanical tensions. However, since tension affects the loads on angle and dead-end structures and since these structures are normally designed to a higher reliability level than regular tangent structures, conservative tensions are desirable.

#### 7.3.6 Offer an alternative to the solidity ratio-based drag coefficients for towers

As discussed in Section 4.2.5, an alternate “wind on members” option is necessary to handle towers that are not appropriate for a “wind on face” approach. This is already included in the latest ASCE Manual 74 (ASCE, 2008).

One could conclude after reading this section that we are going backward. But, after many years of hoping for a better handle on wind loads through research and detailed procedures, we are forced to admit that: 1) we are confronted by an immense problem that is not amenable to precise quantification, and 2) some of the simpler ways of the past, calibrated by new knowledge, are more appropriate.

## 8. SUMMARY

The complexity of the current generation of procedures for the design of wind loads on transmission lines (and substation structures) is not justified by the uncertainties inherent in each parameter or equation that make up the design process: wind storm type, reference wind, terrain roughness, profiles, gustiness and underlying assumptions regarding time and spatial correlations, gust response factor, wind direction, drag coefficients, etc. Scientifically, one cannot prove that a line designed according to NESC, ASCE, IEC, CENELEC, or any of its NNA's, has a better balance of reliability vs. economy than one designed according to some simpler procedures such as those suggested. Therefore, rather than pursuing the illusion that better designs can be achieved through the precision of complex formulas that depend on a multitude of unknowable parameters, let's favor common sense, engineering honesty and design simplicity over pseudo science. It is hoped that after three decades of complicating our design equations we will come to our senses and work on simplifying them.

## REFERENCES

- Armit, J., Cojan, M., Manuzio, C. and Nicolini, P. (1975). “Calculation of Wind Loadings on Components of Overhead Lines”, Proceedings IEE, Vol. 122, No. 11, Nov., 1242-1252.
- ASCE Manual 74 (1984, 1991 & 2008). *Guidelines for Electrical Transmission Line Structural Loading*, Reston, VA, USA, 2006.
- ASCE Standard 7-05 (2006). *Minimum Design Loads for Buildings and Other Structures*, Reston, VA, USA.
- ASCE Manual 111 (2006). *Reliability-Based Design of Utility Pole Structures*, Reston, VA, USA.
- ASCE Manual 113 (2008). *Substation Structure Design Guide*, Reston, VA, USA.
- Castanheta, M.N. (1970). “Dynamic Behavior of Overhead Power Lines Subject to the Action of the Wind”, National Civil Engineering Laboratory, Ministry of Public Works, Lisbon, Portugal.
- CENELEC (2001). *European Standard EN 50341-1, Overhead Electric Lines Exceeding AC 45 KV, Part 1: General Requirements - Common Specifications*, European Committee for Electrotechnical Standardization, Brussels.
- CIGRE (1990). "Loading and Strength of Overhead Transmission Lines", Working Group 06 (Line Reliability and Security) of CIGRE Study Committee 22,

- ELECTRA, No. 129, March, 64-97.
- CIGRE Brochure 256 (2004). "Report on Current Practices Regarding Frequencies and Magnitude of High Intensity Winds", Working Group B2.16, Oct , 46 pages.
- CIGRE Brochure 289 (2006). "Reliability Based Design Methods for Overhead Lines - Advantages, Applications and Comparisons", Working Group B2.06, April, 106 pages.
- CIGRE Brochure 344 (2008). "Big Storm Events - What we have learned", Working Group B2.06, April, 167 pages.
- CIGRE Brochure 350 (2008). "How OHL Respond to Localized High Intensity Winds - Basic Understanding", Working Group B2.06.09, ELECTRA, June, 9 pages.
- Cojan, M. (1973). "Etude de l'Action du Vent sur les Conducteurs des Lignes Aerielles", Revue Generale de l'Electricite, Feb., Paris, France.
- Crandall, S.H. and Mark W.D. (1963). *Random Vibration in Mechanical Systems*, Academic Press, New York.
- Davenport, A.G. (1961). "The Application of Statistical Concepts of the Wind Loading on Structures", Proceedings of The Institution of Civil Engineers, London, Vol. 19, Aug., 449-472.
- Davenport, A.G. (1967). "Gust Loading Factors", Journal of the Structural Division, ASCE, June, 11-34
- Davenport, A.G. (1978). "Gust Response Factors for Transmission Line Loading", Proceedings, Fifth International Conference on Wind Loading, Colorado State University, Fort Collins, CO, July - also Research Report submitted to Pennsylvania Power and Light Company and Electric Power Research Institute
- Davenport, A.G. (1979). "Loading of a Transmission Line due to Turbulent Wind", CIGRE 22-79 (WG06) 05.
- Dempsey, D. And White H.B. (1996). "Wind Winds Wreak Havoc on Lines - The cause of most transmission structure outages in many areas of the world is high intensity wind", Transmission and Distribution World, June.
- De Oliveira E Silva, A., de Medeiros, J.C.P., Loredo-Souza, A.M., Rocha, M.M., Rippel, L.I. and Carpeggiani, E.A. (2006). "Wind Loads on Metallic Latticed Transmission Line Towers", CIGRE Paper B2-202.
- Durst, C.S. (1960). "Wind Speeds over Short Periods of Time," Meteorological Magazine, Vol. 89, 181-186.
- Ghannoum, E. (2002). "Evolution of IEC 60826 -Loading and Strength of Overhead Lines", Electrical Transmission in a New Age, ASCE/SEI Conference, Omaha, Nebraska, Sept., 59-73.
- Ghiocel, D. and Lungu D. (1975). *Wind, Snow and Temperature Effects on Structures Based on Probability*, Abacus Press, England.
- Harris R.L. (1963). "The Response of Structures to Gusts", International Conference on the Wind Effects on Buildings and Structures, National Physics Laboratory, Teddington, Middlesex, June.
- Houle, S., Hardy, C. And Ghannoum, E. (1991). "Static and Dynamic Testing of Transmission Lines Subjected to Real Wind Conditions", Paper No. S 33-91, CIGRE Symposium, Leningrad, Russia.
- IEC (2003), *Design Criteria of Overhead Transmission Lines, Standard IEC 60826*, IEC, Geneva, Switzerland.

- Kluge, R.O. (2005). "Change Proposal CP2718 for Rule 250C of the 2007 Edition of the National Electric Safety Code", on behalf of Wisconsin Utilities Association.
- Manuzio, C. and Paris, L., (1964). "Statistical Determination of Wind Loading Effects on Overhead Conductors", CIGRE Report 231, Paris, France.
- Mozer, J.D., Peyrot, A.H. and DiGioia, A.M. (1984). "Probabilistic Design of Transmission Lines", J.of Structural Engineering, ASCE, Vol. 110, No. 10, Oct., 2513- 2528.
- NESC/IEEE (2007). *National Electrical Safety Code*, Standard C2-2007, IEEE, New York.
- Peterka, J. and Shahid, S., (1998). "Design Gust Speeds for the United States," J. Of Structural Engineering, ASCE, 124 (2), 207-214.
- Peterka, J. (2005). "Comment in Support of Change Proposal CP2718 for Rule 250C of the 2007 Edition of the National Electric Safety Code", Cermak Peterka Petersen, Inc., Fort Collins, CO 80524
- Peyrot, A.H. and Dagher, H.J. (1984). "Reliability Based Design of Transmission Line Structures", J. of Structural Engineering, ASCE, Vol. 110, No. 11, Nov., 2758 2777.
- PLS-CADD, A Computer Program for the Analysis and Design of Overhead Electric Lines, Power Line Systems, Madison, WI, USA.
- Saul, W.E., Jayachandran P.M. and Peyrot, A.H. (1976). "Response to Stochastic Wind of N-Degree Tall Buildings", J. of the Structural Division, ASCE, Vol. 102, May.
- Simiu, E. (1973). "Gust Factors and Along-Wind Pressure Correlations", J. of the Structural Division, ASCE, April, 773-783.
- Simiu, E. et al. (2003). "Wind Speeds in ASCE 7 Standard Peak-Gust Map: Assessment", J. of Structural Engineering, ASCE, April.
- TOWER, A Computer Program for the Analysis and Design of Steel Latticed Towers, Power Line Systems, Madison, WI, USA.
- UK NNA (2004). "UK Normative Aspects (UK NNA), European Standard EN 50341-13-9," Issue 3, CENELEC, European Committee for Electrotechnical Standardization, Brussels

## Review of Span and Gust Factors for Transmission Line Design

Roberto H. Behncke, Ph.D.<sup>1</sup>

T. C. Eric Ho, Ph.D., P.Eng.<sup>2</sup>

<sup>1</sup> Senior Project Engineer, POWER Engineers, Inc., Meridian, Idaho 83642; Tel: (208) 288-6499; E-mail: rbehncke@powereng.com.

<sup>2</sup> Director, The Boundary Layer Wind Tunnel Laboratory, University Of Western Ontario, London, Ontario N6A 5B9; Tel: (519) 661-3338; E-mail:ericho@blwtl.uwo.ca.

### ABSTRACT

Current criteria for the calculation of synoptic wind load effects on transmission line components are based on Davenport's gust response factors, which take into account the different response of structures and long spans of wires to turbulent wind. The gust factors include resonant components that imply possible dynamic amplifications of the wind effect on the structures and wires, although the wire resonant response is generally ignored because of high aerodynamic damping.

Although the gust response factor equations were derived for 1-hour mean wind records, the factors are being applied for winds with different sampling intervals but with reference to 10-minute winds. The conversion is based on Durst's velocity ratio curve, which was not derived from records of extreme winds but from low velocity storms. Due to these differences, and also other simplifications, there could be errors in calculated line or component reliability of at least one order of magnitude.

While line design weather loading conditions are derived from synoptic wind records, it is well known within the industry that most line or structure failures are induced by non-synoptic storms, such as downdrafts or tornadoes generated by thunderstorms. Field evidence from these storms indicate that the 1-hour mean factors, even when extrapolated to very short-interval gusts, do not explain the observed effects and therefore new span and gust factors are needed for design.

The paper reviews the basic concepts and history of span and gust factors and the impact of some of the current assumptions and simplifications. It also focuses on recent research on the actual effects of non-synoptic storms and the new factors that are derived from these experiences.

### INTRODUCTION

Current transmission line design codes such as ASCE (1991, 2006), NESC (2007), IEC (2003) and BSI (1986) are based on winds measured within the atmospheric boundary layer by anemometers mounted on masts, usually at airports and airfields. These are large-scale air movements or pressure gradients generated by global atmospheric instability as determined by seasonal patterns in temperate climates. The 10-minute or 1-hour or fastest-mile mean wind records are then normalized to a common surface roughness and height above ground and, using statistics of extremes,

design wind speeds are established usually for a 50-year return period. In the U.S. 50-year, 3-second gust design wind speeds outside of the hurricane regions are in the order of 85 to 90mph (~ 40m/s.)

As the wind speed at any point within the turbulent boundary layer is not uniform but a random function of time and space, the instantaneous velocity and spatial variations of wind can be described only in statistical terms involving mean values, turbulence intensity (root mean square fluctuations about the mean), spectrum of turbulence and correlation functions. The resistance or response of structures within a flow of turbulent wind, on the other hand, includes drag effects, inertial reactions due to the acceleration of the structure, and structural damping.

In the case of a transmission system, the probability that a high-speed wind gust or front can envelope the line and act simultaneously on all points of a medium to long span of wires is very low, but at the same time most points of a structure are likely to be affected by a single gust. The response of towers and conductors to turbulent wind is also different, as they have different along-wind dimensions, shapes and inertial properties.

In recognition of this most line design standards have usually incorporated factors that adjust the effects of the turbulent wind on the different system components, primarily wires and structures. These factors are known in the industry as span, gust or, more recently, gust response factors.

The first reference that the authors could find on the subject of wire response as a function of span is a CIGRÉ paper by Manuzio and Paris (1964), which introduces an analytical approach for the determination of wind effects on conductors based on statistical theory.

Subsequently, Castanheta (1970) defines the ground roughness and the span length as the most important factors influencing the conductor response, and introduces a “spatial coefficient of reduction” for wind forces on long cables. However, the paper focused more on the effect of anemometer response, as it represented the bulk of the uncertainties at the time when local meteorological data were unreliable and the measurement methods were not standardized.

Armitt et.al. (1975) summarizes the research work carried out by a European working group for the determination of design loads on transmission systems. Armitt's description of the span factor is based on local anemometer and terrain conditions with a 2-second averaging time. Three sets of curves were given for the three terrain conditions studied, but with no specific instructions on the available options from them.

All these early investigations made reference to the statistical description of natural winds by Davenport (1960, 1961) and its relationship to the wind loading on structures, Davenport (1969.) The same statistical description of the wind was used in

the development of the gust loading factor for line-like structures by Davenport (1967) suitable for general code use.

## GUST RESPONSE FACTORS

Based on the statistical methods discussed above, Davenport (1979) developed simplified gust response factors (GRF) for transmission line structures and wires. The concept was to develop design loadings from turbulent wind acting simultaneously on the wires and the structure, recognizing firstly that high speed gusts would not envelope a large span of conductors, and secondly that wind fluctuations at frequencies near the critical values could result in dynamic amplification and potential damage due to structure resonant response. The development of the GRF equations and their application is well documented, Davenport (1979), ASCE (1991, 2006), NESC (2007). Only the basic concepts will be briefly reviewed here.

The peak response  $\hat{R}$  of a structural system to fluctuating winds, in terms of bending, shear or displacements, can be separated into a constant mean component  $\bar{R}$  and a dynamic component  $\sigma_R$  that fluctuates randomly about the mean. The fluctuating component can be subdivided into a background response that varies slowly in time, and a sinusoidal resonant component cycling at the natural frequency of the structure. Following Davenport (1979), the gust response factor is developed based on the peak response or load effect  $\hat{R}$  in the tower, given by the following:

$$\hat{R} = \bar{R} + g\sigma_R \quad (1)$$

in which  $g$  is a statistical peak factor relating the contribution of the fluctuating component to the peak response. The mean wind effect  $\bar{R}$  on the structure and wires is proportional to the square of the mean velocity and is also influenced by the tower and conductor drag force components.

Because of differences in spatial description and natural frequencies and damping, the loading in the wires and the towers can be largely treated independently. This means that the tower oscillations in the wind would not have an effect on the conductors, and that the conductor forces can be assumed as quasi-static loads acting on the tower. This allows the mean square fluctuating response of the structure to be expressed as:

$$\sigma_R^2 = B_c + R_c + B_t + R_t$$

where the  $B_t$  and  $B_c$  components are the mean square responses to the background wind loads acting on the tower and conductors in the low frequency range, and the  $R_t$  and  $R_c$  components are the mean square responses to the wind acting on the tower and conductors at frequencies near to critical.

The critical parameters for the wire gust response factor are ground roughness and span length. For the tower loading the critical parameters are ground surface roughness, height to center of pressure and natural frequency of the tower. The responses are not sensitive to other parameters and for the purpose of generating a

simple loading model the variability of the other parameters may be ignored. Solving Equation (1) for the above conditions and the external parameters, the peak tower response  $\hat{R}$  can then be expressed as follows:

$$\hat{R} = \theta_{tc} p_c GRF_c + \theta_{tt} p_t GRF_t \quad (2)$$

where the terms  $\theta$  are influence functions for the tower response due to the conductors and tower loads; terms  $p$  are the mean wind forces acting at the effective height of conductors and tower, and the  $GRF$  terms are the gust response factors of conductors and tower, both adjusted for effective height and ground surface roughness. As the aerodynamic damping in the wires is significant, the dynamic amplification  $R_c$  due to resonance in the wires can be ignored. The reduction in wind loading in the conductor gust response factor is then due only to the lack of spatial correlation of the wind gust along the line. The gust response factors are as indicated below.

$$GRF_c = 1 + g\varepsilon E \sqrt{B_c} \quad (3)$$

$$GRF_t = 1 + g\varepsilon E \sqrt{B_t + R_t} \quad (4)$$

in which  $\varepsilon$  is a load coincidence coefficient ranging from 0.7 to 1.0 that accounts for the non-simultaneous occurrence of peak tower and conductor loads, and  $E$  is an exposure factor equal to two times the turbulence intensity  $I_u$ . The gust factor given above for each line component is the ratio of the peak response, given by the sum of the mean and the fluctuating responses, with respect to the mean system response.

## DISCUSSION ON GRFs

This approach proposed by Davenport (1979) is now part of most line design codes, especially ASCE (1991, 2006) and NESC (2007.) GRFs for 1-hour mean and other sampling intervals have been developed for approximately equivalent wind speeds and are included in Table 1. The comparison is made for a 125ft (38m) tall structure in open country terrain, with conductors and tower effective heights of 115ft (35m) and 85ft (26m), respectively. The tower GRF includes a 1% damping coefficient and a critical frequency of 2 Hz for  $R_t$ .

**Table 1:** GRFs for different sampling intervals

Sampling Interval	1-hour Davenport (1979)	Fastest Mile ASCE (1991)	3-second ASCE (2006)
Equivalent Wind Speed (mph)	60.0	75.0	90.0
GRF <sub>c</sub>	1.34	0.80	0.56
Peak Response Conductor (psf)	17.8	16.6	15.6
GRF <sub>t</sub>	1.97	1.20	0.87
Peak Response Tower (psf)	24.2	22.8	22.1

These results show that the calculated wind pressures are consistent for all the sampling intervals. The conductor GRF for each reference velocity has a mean plus dynamic proportion of approximately (1+0.3), and the tower GRF has a proportion of approximately (1+1.0), thus indicating that the fluctuating wind adds a load effect equivalent to 30% of the mean wind to the conductors, and doubles the mean wind effect on the tower.

The square root of the conductor GRF can also be interpreted as a wind gust effect factor that adjusts the reference velocity of each sampling interval to an equivalent 2- to 5-minute wind, thus slow enough to affect the entire span length. Similarly, the square root of the structure GRF can be interpreted as a gust factor that adjusts the reference velocity to approximately an equivalent 10-second wind gust that is large enough to envelope a complete structure.

There has been a tendency to disregard the tower dynamic response in design, as lower voltage structures would have little resonant response. The use of a 3-second gust dynamic pressure without any reduction or amplification, with approximately a 10-second equivalent gust response as discussed above, would be sufficient for these shorter towers. However, the structure dynamic response factor  $R_t$  should not be systematically ignored for taller towers, as in very high voltage lines or river crossings.

Although comprehensive, the gust response factor approach contains several assumptions and simplifications. For example the statistical factor  $g$  for 1-hour mean winds in Equations (3) and (4) is in the range of 3.5 to 4.0, or a 15% variation. The load coincidence factor  $\epsilon$  is estimated at a range of 0.7 to 1.0, depending on the relative span to structure contribution to the load effect, thus with a 40% variation.

For the application of the GRF approach to different sampling intervals the GRFs have to be adjusted by the ratio of velocities  $k_V$  squared. Normally this is done using the conversion curve proposed by Durst (1960), who based his analysis on wind speeds of no more than 40-50mph. Sissenwine et.al. (1972) has shown that the velocity ratio, or gust factor,  $k_V$  is not the same for low and for high wind speeds. Further, the authors note that the GRF equations in ASCE (1991, 2006) and NESC (2007) estimate the  $k_V$  gust factor with respect to a 10-minute reference velocity, and not 1-hour mean as in the original GRF development by Davenport (1979.) This systematically introduces a 15% difference in the GRF calculations using these codes.

The load variations due to the above discrepancies may have a minor impact on the calculation of wire or structure loads. But these differences are important if what is needed is an estimation of the reliability of the system. As we know, the doubling of the return period for winds with a COV of 15-20% adds approximately 15% to the calculated loads. Even if a reference 50-year wind speed could be established with reasonable approximation for a point in a line, the introduction of any of the variances described above, or their combination, would result in an error in the reliability

estimation of at least one order of magnitude, which invalidates any reliability based theory for transmission line design. Changes in line reliability can still be calculated, but only relative to a reference level, as suggested by Behncke et.al. (1994.)

## GUST AND SPAN FACTORS

A different approach that has been used in the past for the determination of wind loads on line components consists of two separate factors, namely a gust factor that addresses the time variations of the wind, and a span, or gust extent factor that accounts for the space variations of gusts. In this case the conductor dynamic response can be omitted.

The gust factor is calculated as the ratio of the gust wind speed to the mean wind speed, usually 5-second to fastest mile or 1-hour wind. The gust factor is then adjusted for height above ground, as the wind turbulence decreases with height. Using the same  $k_V$  velocity ratio based on Durst (1960), the following expression for the reference gust factor is obtained for fastest mile records,  $V_{FM}$ , after EPRI (1987.)

$$G_{Fo} = 1.13 + 5.5/V_{FM}$$

The total multiplier to calculate the design peak velocity at the effective height  $z_h$  is as follows:

$$G_{Fh} = G_{Fo} (z_0/z_h)^{1/\alpha}$$

where  $z_0$  and  $z_h$  are the reference and effective heights respectively,  $\alpha$  is the power load exponent as a function of ground surface roughness, and the total design gust wind is thus ( $V_{FM} G_{Fh}$ ). This concept is used in a report by IEEE (1977), where a reference gust factor  $G_{Fo}$  of 1.3 is suggested.

The span factor is defined as the ratio of the effective gust wind load on the wires to the fully correlated gust wind load on the entire span. While the background component of the wire load represents the reduction due to spatial correlation, the relationship between the span factor and the gust response factor can be considered as an equivalent span factor, as follows:

$$\text{Equivalent Span Factor} = (1 + 2\epsilon g I_u \sqrt{B_c}) / (1 + 2g I_u) \quad (5)$$

where the denominator is the fully correlated loading relative to the mean velocity, and  $I_u$  is the turbulence intensity. This span factor equation is the same as that proposed by Holmes (2008) except the load coincidence factor  $\epsilon$ . Holmes considered the spatial correlation in the wind, but omitted the non-coincident occurrence of the gust effects of the wind loads from the tower and the wires. It can be shown that, for the case when the response ratio is in the order 0.1, i.e. the load effect from the tower load is 10% of the load effect from the wire load, the coincidence factor  $\epsilon$  for a typical span length can be as large as 0.8. The omission of the load coincidence factor may lead to a conservative specification by about 10%. A value of 0.75 is recommended for the load coincidence factor  $\epsilon$ .

Holmes (2001, 2008) proposed the following expression for synoptic wind span reduction factor (SRF) valid both for open country and semi-urban ground roughness, in which  $L$  is the span length in ft:

$$SRF = 0.59 + 0.41 e^{-(L/690)} \quad (6)$$

Figure 1 shows the comparison of the span factor  $SRF$  for synoptic winds from Equation (6) as proposed by Holmes (2008) and that implied by the specification of the conductor GRF, calculated from Equation (5) for open country terrain and conductor effective height of 115ft (35m.) It can be seen that they are equivalent quantities.

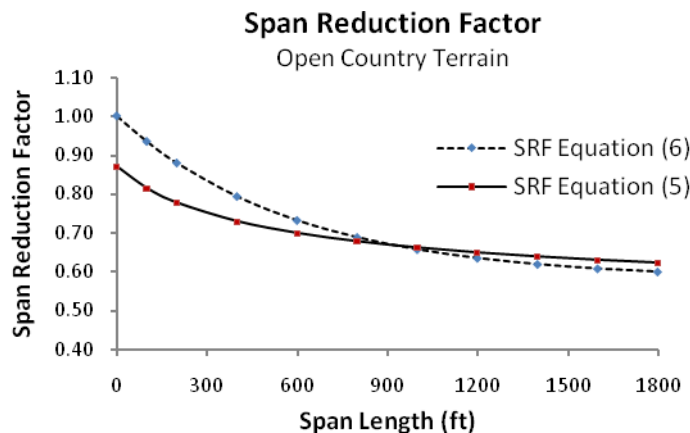


**Figure 1:** Comparison of span factors – synoptic wind

It is clear from the above concepts that the gust multiplier is applied to the mean wind velocity to estimate the faster gusts loading the tower and conductors, while the span factor is applied to the gust wind pressure on the conductors, as it would not be uniformly distributed over the entire span length.

## HIGH INTENSITY WINDS

Other wind types should also be considered for transmission line design. Hurricanes (also known as typhoons in the Pacific region and cyclones in Australia) are large-scale tropical cyclonic systems with similar temporal and spatial wind characteristics as the synoptic winds we have just examined. Generally, current wind maps provided in national codes already include design wind speeds for coastal regions, and the design of transmission systems for hurricane winds should follow the same approach as presented above.

Local convective downbursts and tornadoes generated by thunderstorms are generally classified as high intensity winds (HIW), and they are characterized by their short duration and very high wind speeds. Although the spatial extent of HIW storms is small compared to synoptic weather systems, in certain cases the spatial effects on the design wind loads may be larger, as discussed below.

Downburst, a type of high intensity wind spawned by severe thunderstorms, is a falling mass of evaporating air generally driven by hail and heavy rain. When the falling mass of air impinges on the ground it generates strong, short duration surface winds in all directions. Recent research by Holmes (2008) shows that downburst winds have much higher spatial correlation over a typical span of a transmission line when compared to that found in synoptic winds. Based on an analysis of the wind speed data from an array of towers at Lubbock-Reese Air Force Base, TX, during a downdraft in 2002, Holmes et.al. (2008) suggested the following span factor for downburst-type winds, where  $L$  is the span length in ft.

$$SRF = e^{-0.00009235L} \quad (7)$$

Following the basic formulation of Davenport's GRF described in this paper, the effect of the high spatial correlation in a downburst can be represented by a large integral length scale  $L_S$ , which approximates the size of the correlated wind gust. Figure 2 shows a comparison of Holmes' suggested span factor in Equation (7) with the equivalent span factor derived from the GRF formulation in Equation (5), with an integral length scale  $L_S=1,500\text{ft}$  and for a conservative load coincidence factor  $\varepsilon=1.0$ . The higher coincidence factor recognizes the more dominant effect of the wires due to the higher spatial correlation in downdraft winds.

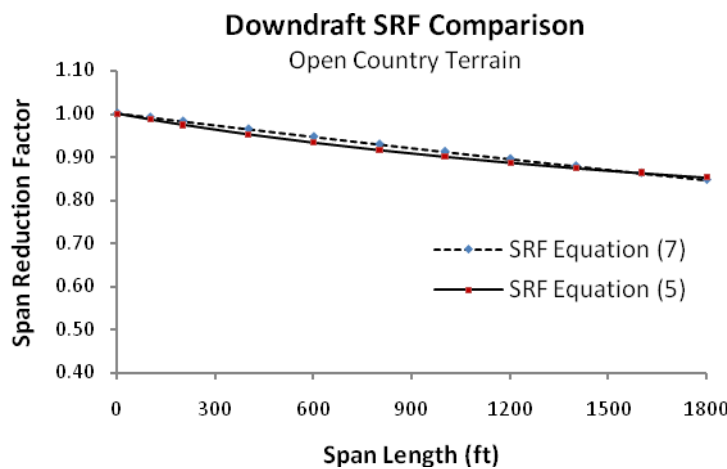


**Figure 2:** Comparison of equivalent span factors – downdraft wind

As in the case of downdrafts, the origin of tornadoes is related to low level warm and moist air interacting with a dry and cool mass of air above it, as well as a fast jet stream above the dry air. This interaction often produces a falling mass of evaporating air accompanied by hail and rain that can generate tornadoes.

Tornadoes are relatively small, short duration systems that can have very high wind speeds. Statistics of tornado frequencies in the U.S. given in ASCE (2006) and Banik et.al. (2008) show that approximately 85% of all observed tornadoes can be classified as F2 or lower in the F-scale, Fujita (1973), thus with velocities ranging from 125 to 150mph (200 to 240kph.) Further, statistics of the relationship between tornado intensity and damage path show that the mean width of an F2 tornado is in the order of 300ft (100m), Banik et.al. (2008.)

Behncke and White (1984), Behncke et.al. (1994) and Ishac and White (1995) among others have studied the effects of strong tornado winds on transmission lines. It was observed that the windward masts of guyed structures were invariably overwhelmed by bending and P- $\delta$  effects generated by the increased wind pressure. In self-supporting structures the primary failure due to a tornado wind occurs in the lateral bracings of the structure, which then induce the collapse of the main chords as a secondary effect. As tornado winds are highly localized, extreme wind speeds along the tornado path are often accompanied with little or no wind a short distance away, thus suggesting that the failure is related to a more or less direct impact on the tower, as the load effect on wires would not be significant.

Based on the statistics mentioned above it was initially proposed that a load equivalent to F2 wind in the F-scale be applied on the towers alone, with both the velocity pressure exposure coefficient and the structure gust factor equal to 1.0, which reflected the lack of knowledge on the vertical profile of HIWs. The F2 wind intensity was not based on any risk or return period calculation, but solely on the basis that it represents the majority of extreme winds expected to intercept a line, it requires small additions of strength to the structures, and the modeled behavior of towers under the full range of F2 load as a minimum closely resembles the observed field effects.

Recognizing that even a narrow-front tornado would have some effect on the wires, Behncke and White (2006) subsequently proposed a span reduction factor for tornado wind, given by the following expression:

$$SRF = W_G (1 - 0.25W_G/L)/L$$

where  $L$  is the average span length and  $W_G$  is the tornado gust width. Figure 3 shows the proposed span ratio for tornadoes, assuming a 300ft gust front.

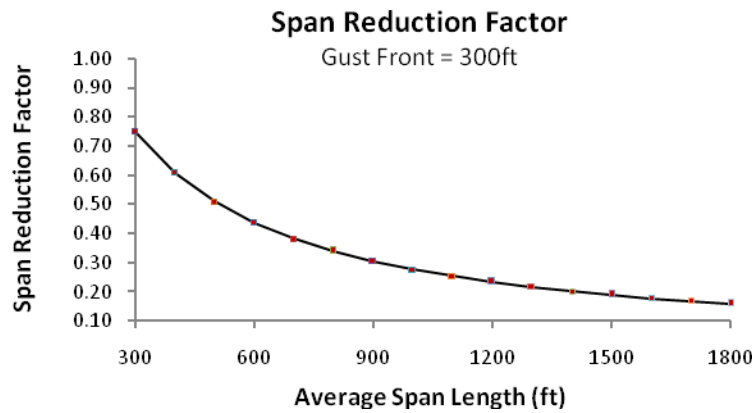


**Figure 3:** Span reduction factor for tornado winds

This proposed span reduction factor developed for F2 tornado winds is based on a patch loading approach where, as mentioned, wind loads are generated only over the width of the gust front. In this case, the general formulation of the GRF does not

apply since it assumes that the entire span would receive mean and background dynamic wind loading.

## CONCLUSION

The development and evolution of span and gust factors for transmission line design has been examined. The initial approach of two separate factors, namely a wind velocity ratio and a span reduction factor applied to conductors, has been replaced in design codes by a single tower peak response concept that takes into account both the temporal and spatial variations of wind gusts, as well as the dynamic responses of the line components at their characteristic frequencies and according to their inertial properties.

These factors are applicable to the near-the-ground turbulence generated by synoptic winds, in the order of 90mph (40m/s) in the U.S., which are well documented from records at typical weather stations. Although this approach provides a good basis for line component design, experiences with long transmission lines in many countries have demonstrated that structures usually fail due to non-synoptic winds. For example, a CIGRÉ (1996) survey shows that nearly 65% of the reported line failures had been triggered by high intensity winds in the form of downdrafts or tornadoes generated by local atmospheric thermal instability.

Although the wind speed in convective downdrafts is in the range of F0 or F1 in the F-scale, their large spatial correlation over the typical length of line spans results in greater loads on the conductors. Results from field investigations on downdrafts show that span reduction factors for these storms should be between 40 and 50% greater than those for synoptic winds, as shown in Figures 1 and 2. In view of the uncertainties related to proper identification and analysis of thunderstorm winds in the meteorological data, it would be also prudent to take a more conservative approach in specifying the corresponding gust response factor for the conductors.

In the case of tornadoes, experience shows that failures caused by direct wind impact on the tower, excluding projectiles, can be reasonably modeled by the application of a narrow-front wind with intensity F2 in the F-scale, as this intensity represents the majority of observed tornadoes. The proposed smaller span factor in Figure 3 corresponds to the reduced gust effect on the conductors. The designer should select the maximum wind velocity within the F2 range based on the local indications of tornado occurrence.

In considering the design wind loads for transmission line systems, wind loads due to different types of storms can be considered independently. Although the general specification of the design wind speeds inherently includes the convective wind storms such as thunderstorms and downbursts, in many of the areas the synoptic winds would be the dominant component in these combined wind speeds. Applying the higher GRF or span factor for thunderstorm or downburst winds with these wind speeds would be overly conservative.

An appropriate design procedure may include the use of the specified combined (synoptic and thunderstorm) wind speed with the GRF or span factor for synoptic winds and then perform a design check using the higher GRF or span factor with a separately specified thunderstorm wind map that needs to be developed. For tornado winds, the design wind speed is dependent on the probability of occurrence per unit area. Design wind maps should be developed based on this probability as well as the overall length of the transmission line system under consideration.

## REFERENCES

- Armitt, J., Cojan, M., Manuzio, C. and Nicolini, P. (1975) *Calculation of Wind Loadings on Components of Overhead Lines*, Proc. IEE, Vol. 122, No 11.
- ASCE (1991) *Guidelines for Electrical Transmission Line Structural Loading*, ASCE Manuals and Reports on Engineering Practice No. 74, American Society of Civil Engineers, New York, 139 pp.
- ASCE (2006) *Guidelines for Electrical Transmission Line Structural Loading*, ASCE Manual 74, Peer Review Draft, ASCE Manual 74 Committee.
- Banik, S.S., Hong, H.P. and Kopp, G.A. (2008) *Assessment of tornado hazard for spatially distributed systems in southern Ontario*, Journal of Wind Engineering and Industrial Aerodynamics, 96. pp 1376-1389.
- Behncke, R.H. and White, H.B. (1984) *The Alicurá 500kV Transmission System*, Paper 22-02, CIGRÉ International Session, Paris.
- Behncke, R.H., Milford, R.V and White, H.B. (1994) *High Intensity Wind and Relative Reliability Based Loads for Transmission Line Design*, Paper 22-205, CIGRÉ International Session, Paris.
- Behncke, R.H. and White, H. B. (2006) *Applying Gust Loadings to Your Lines*, Proceedings of the 9th International Conference on Overhead Lines. Fort Collins, Colorado.
- BSI (1986) *BS 8100-1 Lattice Towers and Masts – Part 1: Code of Practice for Loading*, British Standards Institution.
- Castanheta, M.N. (1970) *Dynamic behaviour of overhead power lines subject to the action of the wind*, Paper 22-08, CIGRÉ International Session, Paris.
- CIGRÉ (1996) *Review of IEC 826: Loading and Strength of Overhead Lines. Part 3: Analysis of Recent Transmission Line Failures*, SC-22 WG22-06.
- Davenport, A.G. (1960) *Rationale for determining design wind velocities*, Journal of the Structural Division, Proceedings of the American Society of Civil Engineers, Vol. 86, ST5, pp 39-68.
- Davenport, A.G. (1961) *The spectrum of horizontal gustiness near the ground in high winds*, Quarterly Journal of the Royal Meteorological Society, Vol. 87, No. 372, pp194-211.
- Davenport, A.G. (1967) *Gust loading factors*, Journal of the Structural Division. Proceedings of the American Society of Civil Engineers, Vol. 93, ST3, pp 11-34.
- Davenport, A.G. (1969) *The application of statistical concepts to the wind loading of structures*, Proc. Inst. Civil Engrs. 19, pp. 449-472.

- Davenport, A.G. (1979) *Gust response factors for transmission line loading*, Wind Engineering, Proceedings of the 5<sup>th</sup> International Conference on Wind Engineering. Colorado State University, Ed. J.E. Cermak. Pergamon Press.
- Durst, C.S. (1960) *Wind Speeds over Short Periods of Time*, Meteorological Magazine, Vol. 89, pp. 181-186.
- EPRI (1987) *Reliability Based Design of Transmission Line Structures: Final Report, Volume I: Methods*, Electric Power Research Institute, Project 1352-2.
- Fujita, T.T. and Pearson, A.D. (1973) *Results of FPP Classification of 1971 and 1972 Tornadoes*, 8th Conference of Severe Local Storms, American Meteorological Society, Boston, Mass. pp. 142-145.
- Holmes, J.D. (2001) *Wind Loading of Structures*, Spon Press, London, U.K.
- Holmes, J.D. (2008) *Recent Developments in the Specification of Wind Loads on Transmission Lines*, Journal of Wind and Engineering of the Indian Society of Wind Engineering, Vol. 5 No.1.
- Holmes, J.D., Hangan, H.M., Schroeder, J.L. and Letchford, C.W. and Orwig, K.D. (2008) *A forensic study of the Lubbock-Reese downdraft of 2002*, Wind and Structures, Vol. 11, No. 2, pp 137-152.
- IEC (2003) *Design Criteria for Overhead Transmission Lines*, International Standard IEC 60826, International Electrotechnical Commission, 3<sup>rd</sup> Edition 2003-10.
- IEEE (1977) *Loading and Strength of Transmission Line Systems, Part 2: Designing for Wind Loads*, Task Group of Line Loading and Strength of Transmission Line Structures, Paper PES A 77 229-8.
- Ishac, M. and White, H.B. (1995) *Effect of Tornado Loads on Transmission Lines*, IEEE, Transactions on Power Delivery.
- Manuzio, C. and Paris, L. (1964). *Statistical determination of wind load effects on overhead line conductors*. CIGRE, Paper 231.
- NESC (2007) *National Electrical Safety Code*, National Bureau of Standards, Washington, D.C.
- Sissenwine, N., Tattleman, P., Granthan, D.D. and Gringorten, I.I. (1972) *Extreme Wind Speeds, Gustiness and Variations with Height*, Air Force Cambridge Research Laboratories, Technical Report 73-0560, Aeronomics Laboratory, Project 8624.

## Wind Load Methodologies for Transmission Line Towers and Conductors

Leon Kempner Jr<sup>1</sup>

<sup>1</sup>Principal Structural Engineer, Bonneville Power Administration, P.O. Box 61409 (TEL-TPP3), Vancouver, WA, 98666-1409; email: lkempnerjr@bpa.gov.

### ABSTRACT

This paper discusses ASCE 74, IEC 60826, and NESC (Rule 250C) extreme wind load methodologies applied to transmission line towers and conductors. The application of these methods can result in varying loads applied to towers and conductors. The wind parameters used and some of the differences between these wind loads methods will be discussed. This information will help utilities to better understand the limitations and assumptions used to determine design wind loads on transmission line conductors and towers. Comparison of wind load results performed by the CEATI International, Inc., using the ASCE 74, IEC 60826, and the NESC methods are presented. Also presented are issues that should be investigated to develop or enhance future wind load methods.

### INTRODUCTION

Where did the transmission line industry start concerning the determination of tower/conductor wind loads? A review of old technical papers would suggest that we started from the wind load performance of wind mill towers. Scholes (1908) states that transmission line tower wind load criterion was calibrated using the wind load performance of wind mill structures. The early NESC documents started with the base concurrent loading case of  $\frac{1}{2}$  inch [1.27 cm] glaze ice (57 pounds per cubic foot weight [8.96 KN/m<sup>3</sup>], and 8 pounds per square foot [383 N/m<sup>2</sup>] wind (40 mph [17.9 m/s] on a 1 inch [2.54 cm] diameter conductor). The resulting forces were adjusted by load (overload) factors. The basis of this loading case is discussed in a paper by Worcester (1912). The application of these loads to the towers and conductors used a simple equation: Pressure = Constant \* [Velocity]<sup>2</sup>, with no adjustments for the characteristics of the wind (such as increased wind with height) or topographical features.

Today the determination and application of wind to structures has become more complex compared to the "The Old Days." The basis of this additional complexity is the advances made in understanding the characteristics of wind, topographical features, and how structures respond to the resulting loads. Engineers have better knowledge of the parameters for determining the wind loads today than in the "beginning." With this knowledge transmission line engineers can make more informed decisions when determining the wind loads on transmission line towers and conductor systems.

The advancements made in Wind Engineering are presented in the ANSI Standard ASCE-7, "Minimum Design Loads for Buildings and Other Structures." This Standard provides information on the basic wind parameters and their application to buildings and other structures. Another significant document that defines the application of wind to transmission line towers and conductors was published by Dr. Alan Davenport, (1979). This paper presents the application of a wind load methodology to a transmission line system (towers and conductors). These two documents are the basis of the wind load procedure in the current ASCE Manual 74, "Guidelines for Electrical Transmission Line Structural Loading," and the National Electrical Safety Code (NESC) Rule 250C. These documents provide a method for determining the gust response factors and the application of wind to towers and conductor systems. The ASCE-7 wind methodology is also used in the latest edition of the ANSI Standard TIA-222-G, "Structural Standard for Antenna Supporting Structures and Antennas."

Another significant document that provided advancements in the determination and application of transmission line wind loads is the International Electrotechnical Commission Standard (IEC) 60826, "Design Criteria for Overhead Transmission Lines." This document uses similar basic wind parameters except that a different equation is used for the determination of the gust response/gust effect factors. The author has been told that one source of information for the IEC wind load application to the transmission line towers and conductors was obtained from the work completed at the Hydro Quebec's Iles-de-la-Madeleine experimental test line. Houle (1991) presents some of the results of the significant research performed at this test station. The IEC 60826 wind load method is currently used by the National Standard of Canada, CAN/CSA-C22.3, "Design Criteria of Overhead Transmission Lines."

The discussion in this paper will be limited to winds generated by large moving pressure systems, typically called synoptic or continental winds. Transmission lines are subjected to other wind storm types such as hurricanes, tornadoes, and downburst. The last two wind types are called High Intensity Winds (HIW). High Intensity Winds (HIW) are generated by intense thermal activity, which can produce tornados, microbursts, and downbursts that frequently accompany a thunderstorm or squall line. CIGRE has published a number of technical brochures, CIGRE 256 (2004) and 350 (2008), addressing HIW winds.

The importance of wind loads on transmission line systems can be demonstrated by few recent extreme wind storms (not hurricanes). The CIGRE Technical Brochure 344 describes two major wind storms experienced in Belgium (1990) and France (1999).

A comparison of the extreme wind load forces obtained using ASCE 74, NESC Rule 250C, and IEC 60826 documents will be presented in a following section of this paper. But first a brief discussion of wind parameters will be discussed so that the reader understands the terminology used.

## WIND LOAD PARAMETERS

The basic Wind Force Equation is typically expressed as follows:  $W_F = Q * k_z * K_t * K_d * V^2 * I * G_{RF} * C_d * \text{Area}$  (Pounds, Newtons, kg). Individual terms are discussed in the following paragraphs.

The Air Density Factor ( $Q$ ) converts kinetic energy of moving air into potential energy of pressure. The value of  $Q$  can be determined from  $Q = \frac{1}{2} \rho$ , where  $\rho$  = mass density of air. The typical recommended value of the air density factor, 0.00256 [0.613 N/m<sup>2</sup>], is based on the specific weight of air at 59° F [15° C] at a sea level pressure of 29.92 in. [76 cm] of mercury, and the units for the wind speed in miles per hour (mph) [m/s] and pressure in pounds/foot<sup>2</sup> (psf) [N/m<sup>2</sup>]. The air density varies with temperature and atmospheric pressure. ASCE 74 provides a table of values for the air density factor as a function of air temperatures and pressures (elevations above sea level). The use of an air density factor value other than that recommended by an appropriate design code/guide should be based on good engineering judgment with sufficient weather data available to justify a different value for a specific design application.

The Basic Wind Speed ( $V$ ) averaging period can vary depending on the use of the data. Averaging periods below 5 minutes is typically used to determine the gust speed wind, such as the 3-second gust wind speed used by ASCE 7, ASCE 74, and the NESC Rule 250C. The Basic 3-second gust wind speed, mph at 33 ft. (10 m) above ground with an annual probability of 0.02 (50 year return period) is provided by ASCE-7. Averaging period of 10 minutes is used in IEC 60826 and CSA C22.3.

It is recognized that wind speed values depend on the averaging time. Shorter averaging time corresponds to a higher wind speed magnitudes, while a longer averaging time would give a lower wind speed value. It is often necessary to obtain equivalent wind speeds from different averaging periods. Conversion between averaging periods can be accomplished using the Durst approach presented in ASCE 74. Table 1 shows some converted wind speed values for typically used averaging periods.

Table 1. Wind Speed Conversions (mph)

3 Sec. Gust	Fastest-Mile	10 min. avg	Hourly mean
90	75	62	60
100	80	69	66

[1 mph = 0.447 m/s]

A term not used in the above basic wind force equations, but should be discussed, is the "Gust Factor." The gust factor is the ratio of the gust wind speed at a specified short duration, e.g., two seconds, to the mean wind speed measured over a specified averaging time, e.g., ten minutes,  $GF = V_{2\text{-sec}}/V_{10\text{-min}}$ . The gust factor modifies the "mean" wind speed, as shown in the following equation, Gust Wind Speed =  $(GF * V_{avg})^2$  or  $[GF^2 * V_{avg}^2]$ , to account for peak fluctuation about the mean value. In the "beginning" this was the method used to obtain the gust wind speed. Typically, mean wind speeds are averaged over a 10 – 60 minute period. The Gust Factor only takes into account the dynamic characteristic of the wind. The Gust

Response Factor, discussed below, takes into account the structure's response to the dynamic characteristic of the wind. Gust Factors have values greater than 1.0.

The Gust Response Factor ( $G_{RF}$ ) is the ratio of the peak gust load effect on the structure or cables to the mean load effect corresponding to the mean wind speed. The gust response factor accounts for the additional load effects due to wind turbulence and dynamic amplification of flexible structures and cables. The gust response factor represents the cumulative effect or integration of the gusts and lulls of the wind over the range of span lengths of typical transmission lines, as well as the effect of the wind on the supporting structures. The IEC, ASCE 74, and NESC provide equations for determining the Structure and Conductor gust response factors. The IEC refers to this factor as the Combine Wind Factor. ASCE-7 calls this parameter the Gust Effect Factor. The Gust Response Factors have values that are typically 1.0 or less, depending on the basic wind averaging period.

It should be noted that the recommended Gust Response Factor in ASCE 74 is modified from that presented in Davenport, 1979. The original Davenport equation accounted for the structure/conductor "background" and "dynamic" wind response. The recommended ASCE 74 Gust Response Factor does not account for the dynamic component. It was decided by the original ASCE 74 committee that the dynamic component did not represent the actual behavior of a transmission system to applied winds.

The Velocity Exposure Coefficient ( $k_z$ ) accounts for the increase wind with height, including the effects of the terrain category. The basic wind speed values are typically measured at 33 ft [10 m] above the ground. The wind speed will increase with height up to the gradient wind height. The gradient height is where the wind speed is assumed to be constant above the ground surface. The variation of wind speed with height is caused by ground friction that varies with ground roughness. The height of the gradient wind varies with terrain category. An exception to increased wind speed with height has been noted during certain high intensity wind (HIW) conditions.

Two equations are used to represent the wind distribution with height: Power Law [ $V(z) = V_h (z / z_h)^{1/\alpha}$ ] and the Logarithmic Law [ $V(z) = (1/k) V^* \ln(z / z_0)$ ]. Where:  $V(z)$  = Velocity at height  $z$  above the ground,  $V_h$  = Measured wind speed at a reference height  $z_h$ ,  $z_h$  = Measured reference height,  $\alpha$  = Power Law Coefficient,  $V^*$  = Shear velocity or friction velocity  $= (\sqrt{\tau_0 / \rho})$ ,  $\tau_0$  = stress of the wind at ground level,  $\rho$  = air density,  $k$  = von Karman constant, approx. 0.4, and  $z_0$  = roughness parameter of the ground. The parameters used in these equations are determined by the terrain exposure categories. ASCE 74, NESC, and IEC use the power law equation to increase the wind speed with height (see Figure 2a).

Wind effects are influenced by the terrain roughness. The greater the roughness, the more turbulent and slower the wind is at lower ground levels. There are four basic terrain exposure categories shown in Table 2. It should be noted that ASCE 74 and IEC 60826 reverse the categories. The NESC only uses one category, C. Wind characteristic parameters for the different terrain exposure categories are listed in Table 3. It should be noted that the " $\alpha$ " used in the Power Law changes based on the averaging period of the basic wind speed.

Table 2, Terrain Exposure Categories

US	Characteristic of the terrain crossed by a line	IEC 826
A*	Large Cities	-----
B	Suburban areas or terrain with many trees	D
B	Terrain with numerous small obstacles of low height (hedges, trees, and buildings)	C
C	Open country with very few obstacles, for instance moorlands or cultivated field with few trees or buildings	B
D	Large stretch of water up-wind, flat coastal area, flat dessert	A

\* Terrain Exposure Category A is no longer referenced in ASCE 7 and ASCE 74

Table 3, Power Law, Gradient Height, and Terrain Roughness Parameters

Exposure	Power Law ( $\alpha$ ) 3 sec. Wind ASCE 7	Power Law ( $\alpha$ ) Fastest-Mile	Power Law ( $\alpha$ ) 10 min. IEC 826	Gradient Height (ft)	Terrain Roughness $z_0$ (in)
A*	5.0	3.0	3.6	1500	31.5 – 39.4
B	7.0	4.5	4.5	1200	7.9 – 11.8
C	9.5	7.0	6.3	900	1.4 – 2.0
D	11.5	10.0	9.1	700	0.3 – 0.4

\* Terrain Exposure Category A is no longer referenced in ASCE 7 and ASCE 74

[1 mph = 0.447 m/s, 1 ft = 0.3048 m, 1 in. = 2.54 cm]

Table 4, Typical Basic Wind “Load” Importance Factor vs. Return Period

Relative Reliability	Return Period Rp (years)	Wind Load Importance factors applied to $W_{50}$
0.5	25	0.85
1	50	1.00
2	100	1.15

The Importance Factor (I) is typically used to adjust the resultant wind load determined from the basic wind speed for different design reliabilities. Extreme value distributions can be used to determine the extreme wind speed that can be expected in an N-year return period. The typical return period recommended for transmission line design is 50 years. The appropriate selection of a return period is the responsibility of the Utility. The loads derived from extreme value wind speed maps can be adjusted to other return periods using Importance Factors similar to those shown in Table 4. The factors in Table 4, which are applied to the extreme wind load, were derived from the Gumbel extreme type 1 distribution. The Importance Factors in Table 4 show that increasing the design wind load by 15-percent doubles the return period. Table 5 shows the probability of exceeding the return period design value for a given service life of the structure.

Table 5, Probability of Exceeding Design Values During Service Life

Return Period	Service Life Period n(years)					
	1	5	10	25	50	100
25	0.04	0.18	0.34	0.64	0.87	0.98
50	0.02	0.10	0.18	0.40	0.64	0.87
100	0.01	0.05	0.10	0.22	0.40	0.64

The Wind Directionality Factor ( $K_d$ ) can be used to account for the variation in extreme wind direction that is potentially applied on a structure. The wind direction that a structure/transmission line experiences during its service life can be a significant design parameter. Wind direction distributions are typically not readily available to the design engineer. Some design codes provide a wind directionality factor to be used with the design assumptions provided within the particular design code. Representative values for the wind direction factor can range from 0.85 to 0.95 (ASCE 7). For transmission line design this factor is typically assumed to be 1.0.

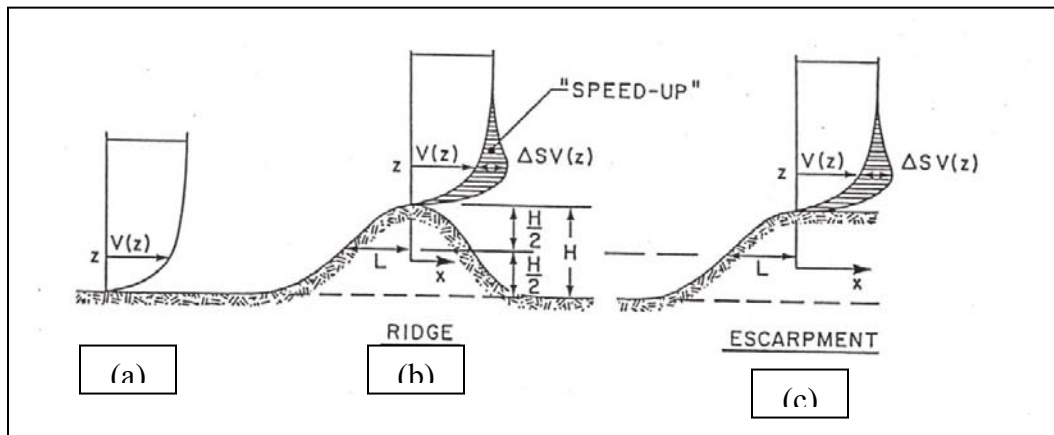


Figure 2, Terrain Effects, Hills and Escarpments (ASCE 7)

The Topographic Factor ( $K_t$ ) is used to account for unique terrain features, such as a ridge or escarpment (Figure 2), which can increase wind speeds over these features. Studies have confirmed wind velocity 'speed-ups' of up to 1.30 to 2.0 times, or higher, than the basic wind speed. It is therefore important when locating structures that consideration is given to the increased loading that can occur when structures need to be sited on exposed hills and other prominent topographical features. The application of this factor could be used to check site specific loads.

The Force Coefficient ( $C_d$ ), also referred to as Drag Coefficient or Shape Factor, is used to account for the effect of the object's shape that the wind is applied to. The structural member force coefficient accounts for the effects of a member's characteristics (shape, size, orientation with respect to the wind, solidity, shielding, and surface roughness) on the resultant force. The force coefficient is the ratio of the resulting force per unit area in the direction of the wind to the applied wind pressure. A typical value for a structural shape, such as an angle, would be 1.6. The conductor force coefficient is typically referred to as the Drag Factor. Test data, such as that shown in Figure 3, shows that conductor drag values, as a function of the Reynolds

Number ( $Re$ ), have significant variations,  $C_d$  ranges from 0.7 to 1.4, between  $Re$  values of  $3(10)^3$  to  $3(10)^5$ . The conductor drag is typically assumed to be 1.0.

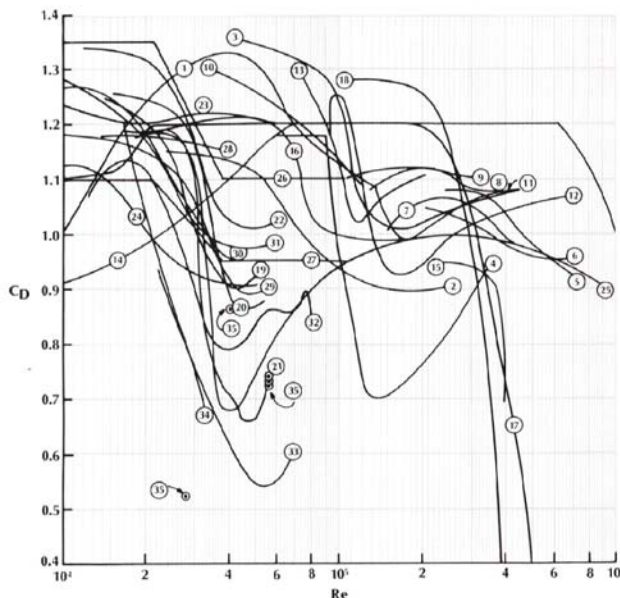


Figure 3, Conductor Drag,  $C_d$  vs. Reynolds Numbers (ASCE 74)

## WIND LOAD APPLICATION

Once the wind speed is determined from the basic wind parameters it can be used to calculate the wind forces to be applied to the tower and conductor system. Adjustments to these wind forces should consider the following issues.

When two members or frames of a member assemble are placed in line with the wind, such as in lattice tower structures, the leeward frame is partially shielded by the windward frame. The Shielding Factor is defined as the ratio of the force coefficient of the shielded frame to the force coefficient of the unshielded frame. The wind shielding is influenced by the solidity ratio, spacing between frames, and the wind yaw (skewed) angle to the plane of the frame. The solidity ratio is the ratio of the wind frontal area of all members in the windward face, of the frame, to the area of the outline of the windward face of the frame. The design engineer needs to decide if the tower faces are far enough away to apply the full wind on both faces (Whitbread, 1979).

Skewed (Yawed) Wind is used to describe winds whose angle of incidence with a shape is other than perpendicular (normal). The angle of yaw is measured in a horizontal plane. For square shaped lattice towers the maximum wind effect on the tower is at a yaw angle, measured normal to the windward face, of approximately 26 – 30 degrees. Both IEC and ASCE 74 provide equations to account for the skew wind case.

Wind forces applied on the tower from the wires can be modified by a Span "Reduction" Factor or Wind Effectiveness Factor, also referred to as the Span Factor. The span reduction factor takes into account the non-uniform wind forces integrated

along the spans. The Span Factor is applied to the wire wind force. The wind speed varies not only with time and distance above ground level, but also horizontally over a front normal to the wind flow, Figure 4. The actual wind pattern is of a turbulent nature where the wind speed is non-uniformly distributed over the transmission line span. It is generally accepted that in most instances a wind gust will not impact more than a fraction of the transmission line span.

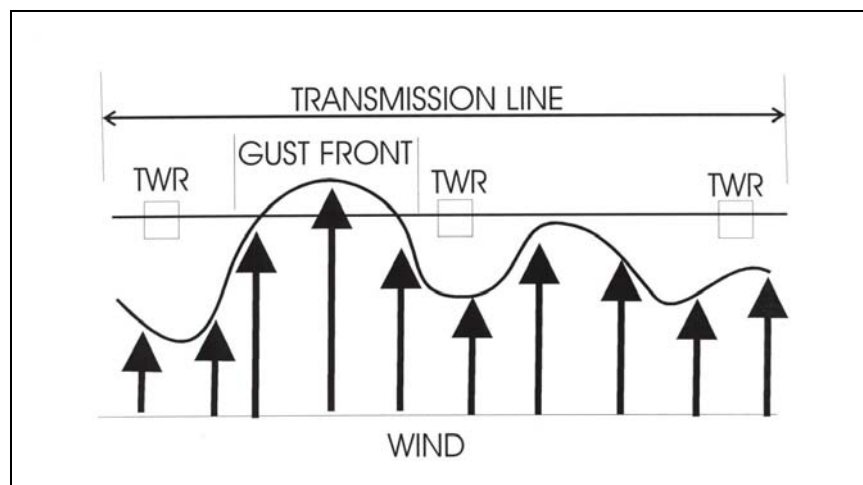


Figure 4, Spatial Distribution of Wind Speed Gust Front

Variables that influence the Span Factor are terrain, height above ground, wind speed, wind direction, and transmission line span length. The Span Factor typically decreases with increase in span length, wind speed, and terrain roughness. The mean wind speed-averaging period will influence the Span Factor. A smaller value would be used with a 3-second wind than with a 1-minute wind. The span factor increases with height to a constant value of 1.0 at a height where the gust turbulence approaches zero. Published Span Factor values range from 0.5 to 1.0. Transmission line spans over special 'terrain features such as river channels, large bodies of water and canyon crossings will most likely be exposed to uniform wind and a span reduction factor of 1.0 is commonly used.

Transmission lines are distributed system versus a single "point" structure such as telecommunication towers or the structures of a switchyard. Typically, maps of extreme wind values are collected at points. Projections of point data by Gumbel distribution to determine N year return period values will produce extreme event values appropriate for the design of point structures. However, a transmission line has length (distributed structures) and thus has exposure to a larger number of event locations than any single structure. Therefore, a transmission line has a greater likelihood of experiencing an extreme wind load than a point structure. Distributed system will have a lower N year return period than a point structure designed for the same extreme wind value. The distributed system effects are the same for ice loads. A CEATI report (2003) that discusses spatial factors for wind and ice mentions that the CSA standard for overhead lines specifies a Spatial Factor of 1.5 to be applied to the mapped 50-year point ice thicknesses. In the US, the spatial effect is discussed in the ASCE-7 standard, but no Spatial Factor is specified. Future design standard and

guidelines may provide a wind load adjustment “Spatial” Factor to account for the vulnerability of a transmission line based transmission line length.

## COMPARISON OF ASCE 74, NESC, AND IEC 60826

The Canadian Electric Association Technology International (CEATI), Inc., Montreal, Canada, completed a study of the comparison of the ASCE 74 (2005 Draft), IEC 60826 (2003), and NESC (Rule 250C, 2002) wind load methods. The study, Report T053700-3324 was commissioned by the CEATI Overhead Design Issues and Wind & Ice Storm Mitigation Interest Group (WISMIG). The principal investigator was Mr. Elias Ghannoum. The report also included a comparison with the European Standard CENELEC EN 50341-1-2001 and CSA C22.3 No. 1-01, but these results are not presented herein.

The purpose of this study was to identify the similarities and difference between the wind load methods. Key wind load parameters, assumptions, and limitation were presented. For comparison of the calculated wind loads a simple structure with varying parameters was used. The tower heights used were 82, 98, 115, 131, and 164 ft. The unique heights listed are the result of the conversion from meters to feet. The report used SI units. The towers were assumed to be lattice structures with an average solidity ratio of 0.40, and the conductors at one level, flat configuration.

In general, the ASCE 74 and NESC methods are similar, whereas the IEC 60826 and CSA C22.3 methods are similar. For the purposes of this paper, comparisons between ASCE 74, NESC, and IEC 60826 for normal wind to the tower and conductors will be discussed.

Some of the major differences between the ASCE, NESC, and IEC documents are presented. The first is the basic wind speed averaging period. ASCE uses the 3-second gust wind speed. The IEC uses the 10-minute average wind speed. ASCE uses equations to determine the structure and conductor Gust Response Factors, where IEC uses a graph to determine the Combine Wind Factors (Gust Response Factors). Both ASCE and IEC use the 50-year return basic wind speed as the design level. Other recommended return periods are different in these two documents. ASCE used 50, 100, 200, and 400 year return periods, whereas IEC uses 50, 150, 500 year return periods. Both these documents use the power law to vary wind speed with height. The wind parameters use in the power law equations are different because of the different wind speed averaging periods used by the two documents. The IEC has a separate factor to account for the Span Factor ( $G_L$ ). The author has been told that the Davenport Gust Response Factor accounts for the span factor affect. There are some other differences in the determination and application of the wind loads and these will not be discussed here. The following comparisons were made using a terrain category of C (ASCE/NESC) and equivalent B (IEC). The basic wind speed was converted to be equivalent for the method used.

Table 6 show the comparison of the effective wind pressure (psf) [ $N/m^2$ ] on conductors. This is the pressure that includes all the adjustment factors due to height, gust response factor, span factor, etc. These values show that ASCE/NESC values are 20% less than that obtained from the IEC method.

Table 6, Comparison of the Effective Wind Pressure on the Conductors

Structure Height (ft)	IEC (psf)	ASCE/NESC (psf)
82	23.7	18.8
98	24.4	19.4
115	25.0	19.9
131	25.6	20.4
164	26.5	21.2

Note: 96 mph, 3-second gust wind speed, 1312 ft level span  
 $[1 \text{ ft} = 0.3048 \text{ m}, 1 \text{ psf} = 47.9 \text{ N/m}^2]$

Table 7 show the comparison of the wind forces on the structure (pounds). These forces include all the adjustment factors due to height, gust response, span factor, shielding, and force coefficient. These values show that ASCE forces are 10% less than that obtained from the IEC. The NESC values are higher, average 45%, because the shielding factor is 2.0, giving a force coefficient of 3.2. The ASCE and IEC use a variable force coefficient that depends on the solidity ratio of the windward face.

Variations of conductor wind pressure with span length, to assess span effect, are compared in Table 8. The effective wind pressure on conductors has been calculated for each span length using a constant height of 98.4 ft [300 m]. This data confirms that the effective wind pressure decreases with increasing spans. The data shows that the pressures decrease at, almost, the same rate, meaning the “span factor” effect is almost the same in IEC and ASCE/NESC. In order to check this assumption, the “span factor” was computed in each practice as a ratio of the effective wind pressure for a span length to the pressure for a base span length (span factor =1) of 656 ft [200 m]. The results are shown in Table 8.

It can be seen from the table above that the effective “span factor” reduction is quite similar in the IEC, ASCE, and NESC. For example, the ratio of the effective conductor wind pressures computed using a 1312 ft [400 m] span to a 656 ft [200 m] span varies from 93% to 94%.

Table 7, Comparison of Wind Forces of Structure

Structure Height (ft)	IEC (Kips)	ASCE (Kips)	NESC 250C (Kips)
82	27.6	25.3	40.9
98	33.8	30.9	49.9
115	40.4	36.9	59.0
131	47.3	42.8	68.3
164	61.5	54.8	87.3

Note: 96 mph 3-second gust wind speed, 1312 ft level span, 1 Kip = 1000 pounds  
 $[1 \text{ Kip} = 4.448 \text{ KN}, 1 \text{ ft} = 0.3048 \text{ m}, 1 \text{ mph} = 0.447 \text{ m/s}]$

Table 8, Relative variation of wind pressure with span length (Const. Ht = 98.4 ft)

Span (ft)	IEC (psf)	IEC	ASCE/NESC (psf)	ASCE/NESC
656	25.9	100%	20.8	100%
820	25.6	99%	20.3	98%
984	25.2	97%	19.9	96%
1148	24.8	96%	19.6	94%
1312	24.2	94%	19.3	93%
1476	24.0	93%	19.1	92%
1640	23.6	91%	18.9	91%

[1 ft = 0.3048 m, 1 psf = 47.9 N/m<sup>2</sup>]

## FUTURE NEEDS FOR TRANSMISSION LINE WIND LOAD METHODS

This author believes that the advancements in wind load methodology applied to transmission line systems are necessary so that design engineers understand the characteristic parameters and limitations used to determine tower and conductor wind forces. This knowledge allows the engineer to make decisions on wind loads that directly affect the reliability of the transmission line. The advanced information is also important when an engineer is conducting a failure investigation of a tower after an extreme event wind storm. Also, the utility engineer can use the advanced methods to calibrate a simpler in-house procedure. Site specific evaluation of a transmission line tower requires the information from an advanced method to determine the adequacy of the structure.

The difference between the IEC and ASCE 74 are more readily acceptable when detailed information is presented on their development. The design engineer should remember that the wind characteristic parameters and extreme wind speeds are not exact representations of what the actual transmission line may experience. Utilities need to decide the complexity level of the wind load methodology that provides adequate transmission line performance. It should be remembered that short term performance, such as less than 50 years experience, by its self, does not justify acceptable performance. The advanced wind load methodologies will help the Utility engineer to make the best decisions with respect to the appropriate wind load method, be it a simple method or a more complex method.

The IEC and ASCE 74 committees should work together to present a common and consistent wind load methodology. This would benefit the US and World transmission design communities. The new research in HIW will soon provide an additional wind methodology that may control in some regions future tower designs. The transmission line engineer should be fully engaged in this research effort. Both CIGRE ([www.cigre.org](http://www.cigre.org)) and CEATI ([www.ceati.com](http://www.ceati.com)) are active in wind load research.

## REFERENCES:

ANSI/TIA 222 G (2005), "Structural Standard for Antenna Supporting Structures and Antennas," Telecommunication Industry Association, Arlington, VA

- ASCE 74 (2002), Guidelines for Electrical Transmission Line Structural Loading, Draft, Reston, VA
- ASCE 7 (2005), Minimum Design Loads for Buildings and Other Structures, SEI, American Society of Civil Engineers, Reston, VA
- CEATI (2003), Spatial Factors for Extreme Ice and Extreme Wind: Task 1 Literature Review on the Determination of Spatial factors, Report T053700-3324, Canadian Electrical Association Technology International, Inc., Montreal, Canada
- CEATI (2005), Comparison of Wind Load Methodologies for Lattice Transmission Line Towers, Report T053700-3324, Montreal, Canada
- CIGRE 256 (2004) Technical Brochure, Report on Current Practices Regarding Frequencies and Magnitude of High Intensity Winds, Working Group B2.16, International Council on Large Electric Systems, Paris, France
- CIGRE 334 (2008) Technical Brochure, Big Storm Events, What We Have Learned, Working Group B2.06, Paris, France
- CIGRE 350 (2008) Technical Brochure, How Overhead lines Respond to Localized High Intensity Winds, Basic Understanding, Paris, France.
- CSA 22.3 (2006), Design Criteria of Overhead Transmission Lines, Canadian Standards Association, Mississauga, Canada
- Davenport, A.G. (1979), "Gust Response Factor for Transmission Line Loading," Fifth International Wind Engineering Conference, Fort Collins, CO
- Houle, S., Hardy C., Ghannoun E., (1991), Static and Dynamic Testing of Transmission Lines Subjected to Real Wind Conditions, Paper S33-91, CIGRE Symposium, Leningrad, Russia
- IEC 60826 (2002), Design Criteria of Overhead Transmission Lines, International Electrotechnical Commission, Geneva, Switzerland.
- NESC (2002), National Electrical Safety Code C2, Institute of Electrical and Electronics Engineers, Inc., New York, NY
- Scholes, D.R. (1908), Fundamental Considerations Governing the Design of Transmission-Line Structures, American Institute of Electrical Engineers, Atlantic City, NJ
- Whitbread R.S. (1979), "The Influence of Shielding on the Wind Forces Experienced by Arrays of Lattice Frames," Proceedings, Fifth International Conference on Wind Engineering, Pergamon Press, New York, NY
- Worcester, T.A. (1912), Some Mechanical Considerations of Transmission Systems, American Institute of Electrical Engineers, Atlantic City, NJ

## The Effects of Ice Shedding on a 500 kV Line

Alan B. Peabody<sup>1</sup> and Ron Carrington<sup>2</sup>

<sup>1</sup>Construction Management Department, University of Alaska Anchorage, 3211 Providence Drive, Anchorage AK 99508-4614; PH (907) 786-1323; email: afabp1@uaa.alaska.edu, member ASCE

<sup>2</sup>Power Engineers, Inc., 3900 S. Wadsworth Blvd. Suite 700, Lakewood, CO 80235; PH: 970.226.3706; email: rcarrington@powereng.com

### Abstract

Ice shedding and the subsequent conductor jump have been of interest to transmission and distribution designers since the early 1900's. Some of the factors that affect the height of the jump and the transverse movement of the conductor are ice thickness, ice density, phase to phase and span to span patterns of ice loading, the pattern of ice shedding within the span, the wind speed, conductor size and stranding, line angle, structure type, span, and elevation differences between supports. This paper reports the results of finite element dynamic modeling of ice shedding from a 500 kV single circuit tubular steel transmission line. Ten spans of line were modeled including all three phases and two shield wires. The structures and insulators and shield wire hardware were also modeled. All simulations were performed using the commercial finite element program ADINA.

### Introduction

Ice shedding and the subsequent conductor jump have been of interest to transmission and distribution designers since the early 1900's (Greisser 1913). Problems with ice and snow shedding have been reported in many countries, including Austria (Schauer and Hammerschmid 1983), China (Fuheng and Shixiong 1988) and Slovenia (Jakse et al. 2001).

Full scale tests of ice shedding were performed in 1930 in Switzerland (Oertli 1950), in Great Britain in 1964 (Morgan and Swift 1964), in Germany in 1981 (Freitag and Brandt 1981) and in the US by EPRI in the 1970's (Power Technologies 1978; Stewart 1983). Model ice shedding tests were performed relatively recently in Canada (Jamaleddine et al. 1996).

In this study, the effects of ice shedding were simulated with dynamic finite element models using the computer program ADINA from ADINA R&D, Inc. This finite element dynamics program has been used many times for analysis of both broken wires (McClure 1989; McClure and Lapointe 2003; McClure and Tinawi 1987; 1989; Peabody 2004) and ice shedding (Jamaleddine 1994; Jamaleddine et al. 1996;

Jamaleddine et al. 1993; Kálman et al. 2007; Roshan Fekr 1995; Roshan Fekr and McClure 1996; Roshan Fekr and McClure 1998; Roshan Fekr et al. 1998).

Oertli, Freitag, Morgan and Swift and PTI all assumed that the worst case jump height occurred with one loaded span surrounded by bare spans. Jamaleddine's model tests showed that this is not the case. In his two span model, the jump height was higher when the neighboring span was loaded.

Roshan-Fekr's study using the ADINA software showed that changes in elevation (within the bounds of his study) had a minor impact on the jump height of the cables. Ice shedding in the center 1/3 to ½ of the span is more important than ice shedding from near the supports. None of the tests and studies addressed the question of the affect of multiple loaded spans adjacent to the span shedding.

Greisser, Oertli and Jakse all indicated that in areas of heavy icing, double circuit structures need, not only horizontal offsets between the middle phase and the top and bottom phases, but also horizontal offsets between the top and bottom phases.

For tangent sections of line with no wind, the cables jump almost completely vertically with practically no transverse motion. This was observed and reported for the tests performed by Oertli, Morgan and Swift, and PTI. Oertli's tests showed that substantial lateral movement can result when ice sheds from spans ending in I-string running angle insulators. Oertli's tests also showed that wind may be a factor in causing substantial transverse motion when a cable sheds ice.

The tests with suspension insulators all were carried out on lattice steel towers which are very stiff compared to tubular steel structures. The flexibility of the supports, particularly in the transverse direction, had not been adequately studied to date.

The tests and simulations noted above were typically made on lower voltage lines with relatively stiff lattice steel towers. This study extended the range of previous studies to a 500 kV line using relatively flexible tubular steel structures.

There are relatively few reported field observations of ice shedding. Several of the papers reviewed here have noted the tendency of ice to slide towards the low point of sag and accumulate there—even to the extent of damaging suspension clamps in side-hill spans. Laforte et al. observed this sliding assisting in the removal of ice by collisions between chunks of ice. The significant patterns studied have included full spans shedding, and ice concentrated near the low point of sag shedding.

### **Finite Element Models**

Both 2D and 3D models were used. The 2D models were used to explore the effect of the span length and number of loaded spans on the jump of the conductor after ice shedding. They were also used to examine the effect of various patterns of ice loading on the height of jump.

The 2D models used single Bluebird conductor. In the 3D model, the 2-bundle Bluebird ACSR conductor was modeled as a single conductor with the mass, stiffness, loads and damping equivalent to the twin bundle. This assumption reduces the number of nodes and elements by approximately one-half which reduces the amount of time to perform the analysis. The only limitation imposed by using an equivalent single conductor is that shedding from only one of the two sub-conductors cannot be modeled. The 3D model also used ½ inch EHS shield wire. Catalog properties were used with moduli of elasticity of 9,020,000 psi and 25,000,000 psi, for the conductor and shield wire respectively.

The wires were divided into pin-connected truss elements 10 to 15 ft long. The conductor and shield wire were modeled using horizontal tensions at 32° F final tension including creep. Table 1 shows the horizontal tensions.

**Table 1 Conductor and Shield Wire Horizontal Tensions**

Ruling Span	Conductor (lb)	Shield Wire (lb)
900	11,390	-
1200	11,716	-
1500	11,934	3,642

The internal damping of the wires was modeled as the axial viscous damping of a rod. The critical axial viscous damping for a rod is given in the following equation where  $c_{cr}$  is the critical damping constant,  $A$  the area of the rod,  $E$  the modulus of elasticity and  $m$  the unit mass. Axial damping of 0.5% of critical was used.

$$c_{cr} = 2\sqrt{AEm}$$

Aerodynamic damping is due to the motion of the conductor relative to the air. In still air, the aerodynamic damping force is given by Equation 2 (Dyrbye and Hansen 1996, p. 76).

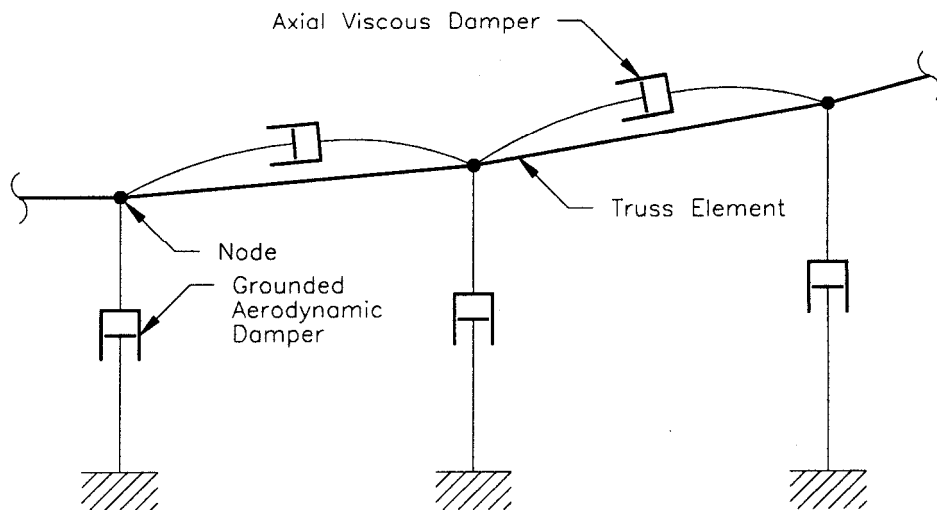
$$F_d = \frac{1}{2} \rho V_r^2 C_d A_p$$

Where  $F_d$  is the damping force,  $\rho$  is the air density and  $V_r$  is the velocity relative to the air,  $C_d$  is the drag coefficient and  $A_p$  is the projected area.  $C_d$  depends on the Reynolds number (following equation) where  $d_w$  is the conductor diameter and  $\mu$  is the viscosity of air.

$$Re = \frac{\rho V_r d_w}{\mu}$$

For smooth circular cylinders,  $C_d$  is between approximately 0.9 and 1.2 for Reynolds numbers between 200 and 100,000 (Binder 1973; Eisner 1931). As the relative velocity is reduced below a Reynolds number of 200,  $C_d$  steadily increases to over 50 at a Reynolds number of 0.1. A  $C_d$  of 1.25 was used for the calculations as relatively low velocities were expected.

Fig. 1 shows a 2D conductor model. When 3D models are used, additional horizontal dampers are added at each node to damp the transverse motion of the conductor. With no wind, the aerodynamic dampers are identical in placement and number as the vertical dampers.

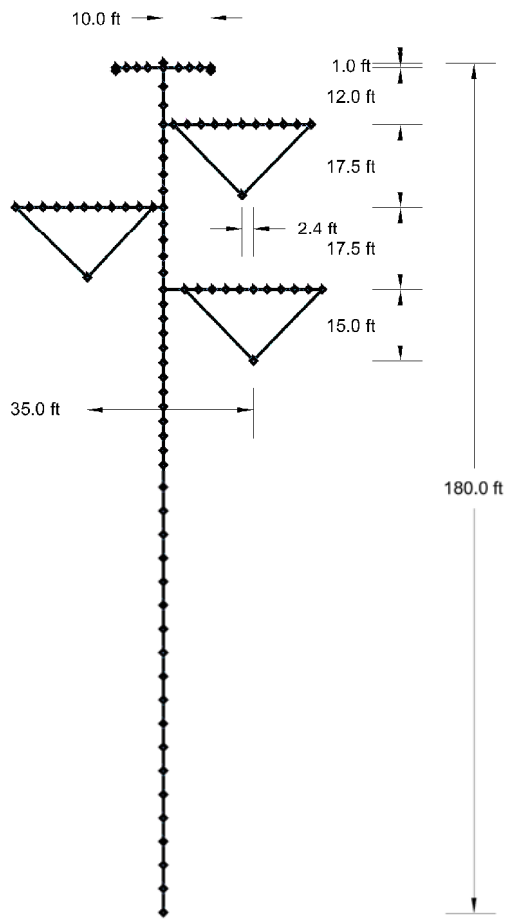


**Fig. 1 Conductor Model**

2D models were used to examine the variation of ice jump for different patterns of load, numbers of spans and length of span. These models consisted of 14 ft long I-string insulators with fixed attachment points suspending a single Bluebird ACSR conductor. The fixed attachment points are equivalent to extremely stiff lattice steel towers.

#### ***Modeling a Complete Line Section***

In order to examine the effect of the flexibility of tubular steel towers on the conductor during ice shedding, a nine span model was used which included the tubular steel towers, both shield wires and three phases (single conductor equivalent to the twin Bluebird). Fig. 2 shows the finite element model of the tubular steel tower.

**Figure 2 Tower Finite Element Model**

Details of the pole shaft and arms are shown in Tables 2 and 3 (Arm lengths are from face of pole).

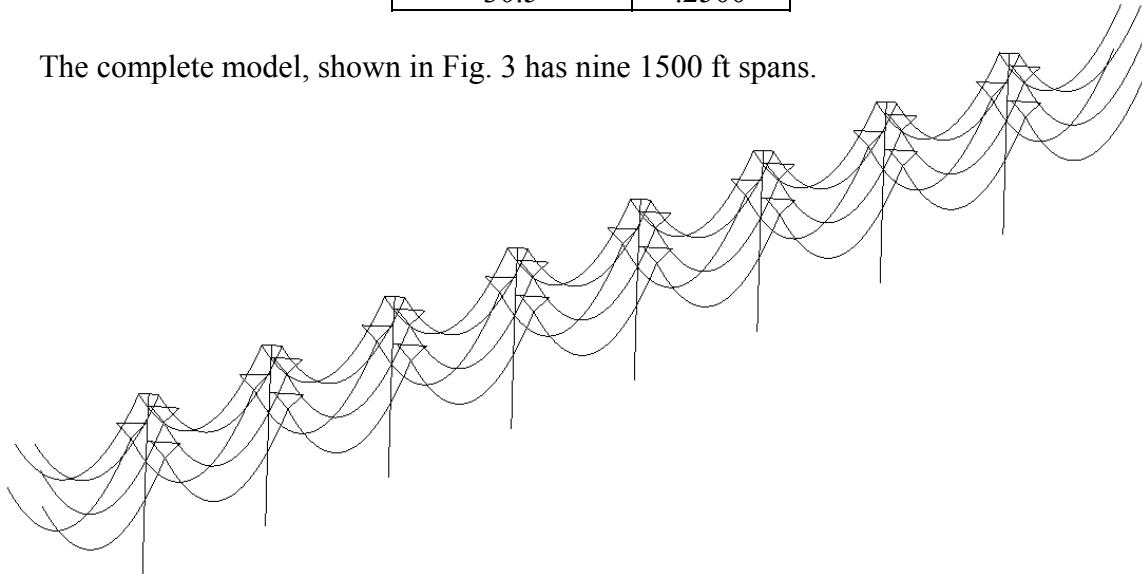
**Table 2 Tubular Steel Tower Dimensions**

Component	Length (ft)	No of Flats	Wall Thickness (in)	Base Diameter (in Flat to Flat)	End Diameter (in Flat to Flat)
Pole	180	12	Table 3-1	69	24
Shield Wire Arms	12	6	0.250	12	6
Upper and Middle Xarms	30	6	0.375	22	12
Lower Xarm	32	6	0.375	22	12

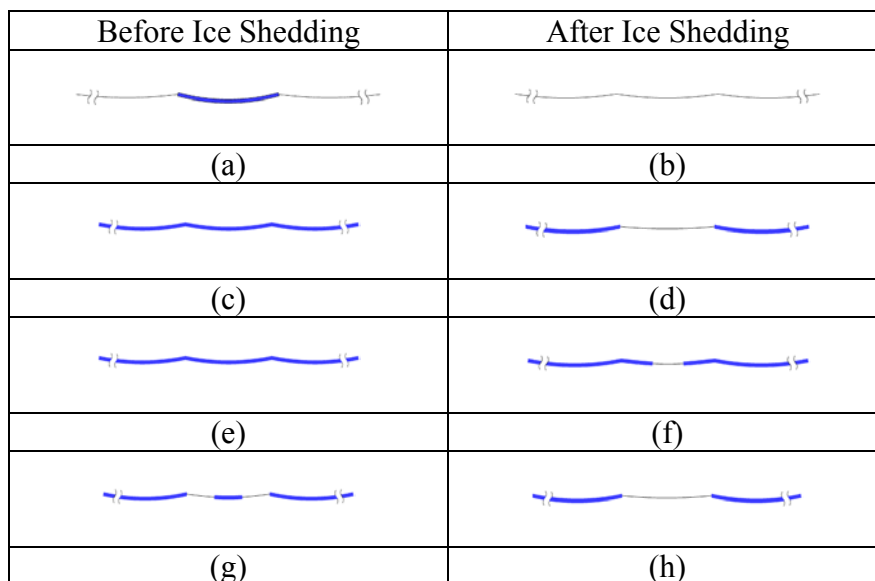
**Table 3 Main Shaft Thicknesses**

Length (from base up) (ft)	Wall Thickness (in)
95.0	.4375
54.5	.3750
30.5	.2500

The complete model, shown in Fig. 3 has nine 1500 ft spans.

**Fig. 3 Nine Span Line Model**

The four ice shedding scenarios shown in Figure 4-1 were simulated using 2D finite element models.

**Fig. 4 Ice Shedding Scenarios, 2D**

Figures 4(a) and (b) represent the last span loaded in a section shedding its ice from the full span. Figures 4(c) and (d) show a span in the center of a fully loaded section that sheds all of its ice at once. Figures 4(e) and (f) show only the 500 ft in the center of a span shedding its ice in a section with all the spans fully loaded. Figures 4(g) and (h) show the center 500 ft shedding its ice in an otherwise fully loaded section. This would typically take place after the center of the span has already shed its ice and the ice in the sides of the span slides down to reload the center of the span.

Figure 5 compares the effect of the different loading patterns shown in Figure 4. All the curves are based on the center span of nine 1500 ft spans with an ice load of 1.0 radial glaze ice equivalent.

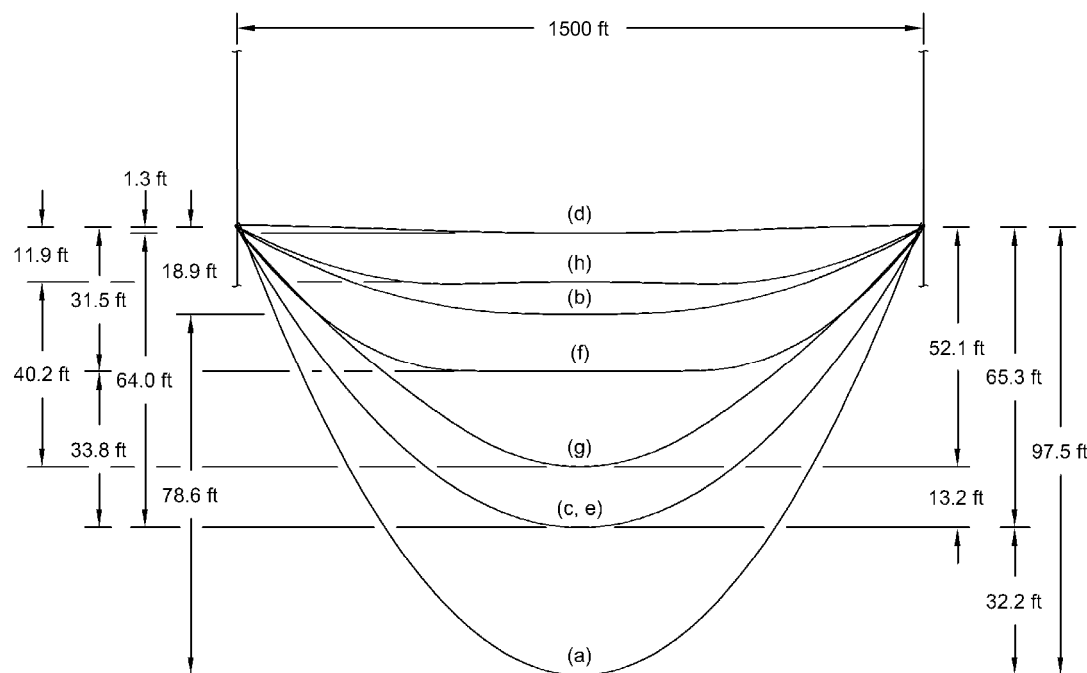


**Fig. 5 Effect of Ice Shedding Patterns (Scale 10V:1H)**

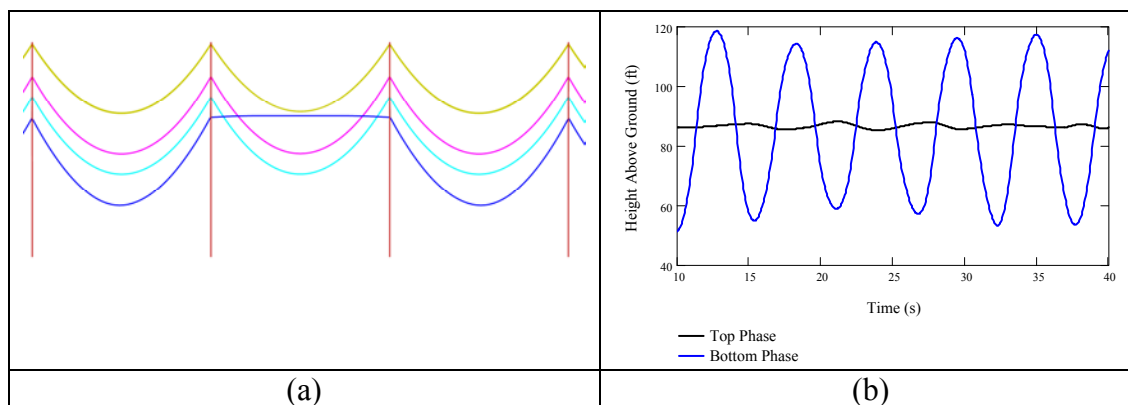
Table 4 summarizes the results of the analyses of the 2D nine span line sections simulated. The middle 500 ft of the center span was loaded for all of the “partial” lower span loads. The upper span sag is the ruling span sag for the span and radial ice thickness listed. The vertical gap and overlaps are based on a phase spacing of 37.5 ft.

**Table 4 Summary of Nine Span Results  
37.5 ft Vertical Phase Spacing**

Span (ft)	Radial Glaze Equiv. (in)	Lower Span Loading	Upper Phase Sag (ft)	Lower Phase Starting Sag (ft)	Lower Phase Jump Sag (ft)	Jump (ft)	Vertical Gap (ft)	Overlap (ft)
900	0.50	Partial	24.3	22.8	10.0	12.8	23.2	
1,200	0.50	Partial	40.9	36.9	19.2	17.7	15.8	
1,500	0.50	Partial	61.8	54.5	32.4	22.1	8.1	
900	1.00	Partial	26.6	24.0	0.7	23.3	11.6	
1,200	1.00	Partial	43.8	36.7	4.9	31.8		1.4
1,500	1.00	Partial	65.1	52.1	11.9	40.2		15.7
900	0.50	Full	24.3	24.3	8.7	15.6	21.9	
1,200	0.50	Full	40.9	40.9	15.4	25.5	12.0	
1,500	0.50	Full	61.8	61.8	25.1	36.7	0.8	
900	1.00	Full	26.6	26.6	-1.6	28.2	9.3	
1,200	1.00	Full	43.8	43.8	0.0	43.8		6.3
1,500	1.00	Full	65.1	65.1	1.3	63.8		26.3

### 3D Structure and Wire Model Results

The 3D model of a complete line section (Fig. 3) consists of nine 1500 ft spans of wire with eight 180 ft tubular steel towers. One load shedding event was simulated, 1.0 inch radial glaze ice equivalent shedding from the entire center span of the lower conductor. Figure 6a shows a profile of the center three spans with the bottom phase at the peak of its jump. All other spans of wire are loaded with ice. Note that bottom phase jumps above its attachment point overlapping with the top phase and nearly reaches the height of the shield wire's low point of sag. The total jump is 67 ft, which is over three ft higher than the conductor jumps with rigid insulator attachment points.



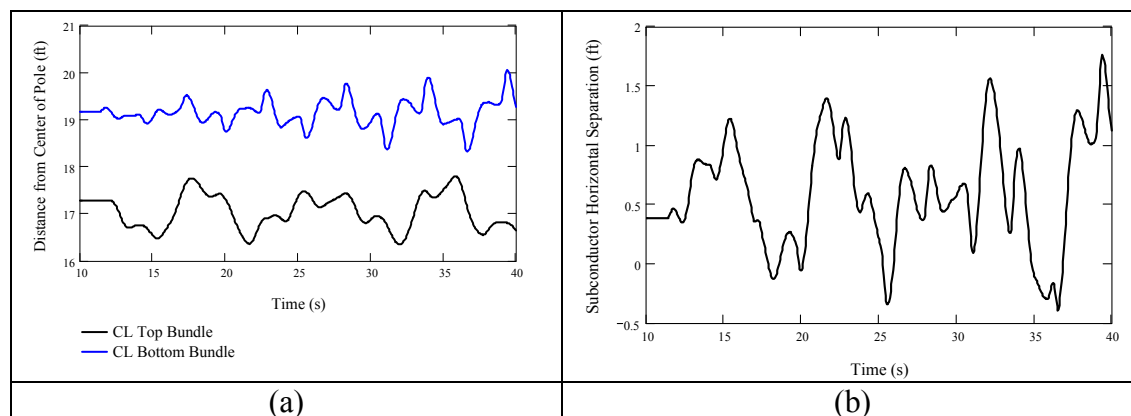
**Fig. 6 3D Model Results**

Figure 6b compares the time histories of the vertical positions of the center points of the top and bottom phases. With this long span, there is substantial overlap continuing for the entire 30 seconds simulated.

Fig. 7a compares the time histories of the horizontal positions of the center of the span at the mid point between the two subconductors. Note that the horizontal displacements of both phases are increasing at the end of the 30 second simulation.

The transverse motion of the conductor is caused by the motion of the tubular steel structures when the ice sheds. Before the ice sheds, the structures deflect towards the side with two phases due to their being balanced by only one phase on the other side of the structure. When the ice sheds, the bending load is reduced and the structures rebound swaying back the other way inducing transverse vibrations in the structure which are coupled to the conductors through the insulator strings.

Fig. 7b is the difference between the time histories shown in Fig. 7a. In addition, the difference has been reduced by 1.5 ft to take into account an 18 inch bundle spacing. This figure shows that the sideways motion causes the horizontal paths to also overlap slightly based on the 2.4 ft static offset of the structures modeled.



**Fig. 7 Time Histories of Horizontal Movement**

In summary, using tall flexible tubular steel pole structures increases the height that the conductor jumps during ice shedding and also adds horizontal motion that may increase the offset needed.

## Conclusions

The simulations of ice shedding performed in this study have shown that conductors shedding ice have the potential to jump to heights above their insulator attachment points, even with a stiff, heavy Bluebird conductor. Smaller conductors may jump higher than the Bluebird conductor under the same icing conditions.

It is important to remember that transmission lines in the “real world” consist of nearly infinite combinations of span lengths, structure heights, phase spacing, elevation differences and tension sections with different conductor tensions, temperatures and ice and wind loading. Even though powerful computer modeling tools are available, to obtain meaningful and understandable results, simplifying

assumptions must be made. In this paper, the assumed ice distributions have been reduced to a few simple patterns. The lines studied have also been simplified to sections with even spans and wire attachment elevations. The results of the study cannot provide definitive guidance, but mainly serve to enhance our engineering judgment when designing lines in icing areas.

When ice and snow begin falling from a line, distortions of the wire system will occur. When a span is more heavily loaded than the spans around it, its sag increases (see Fig. 5 curve "a") in comparison with the calculated sag (based on evenly loaded line sections). Modern line design software has some capability for determining the static position of the wires for different assumed loading patterns while also considering the movement of the insulators and supporting structures. Large distortions of the wire system have been observed in Alaska after snow has shed partially or fully from some spans while others remained more heavily loaded. In areas with very localized in-cloud icing, similar distortions can be expected when spans loaded with rime are adjacent to spans that are not. When ice sheds suddenly from a lower phase, there may already be an existing imbalance in ice loads that has reduced the phase to phase vertical clearance.

When designing a new line, areas where icing can be expected should be identified and the type and amount of ice estimated. A static analysis considering uneven loading, insulator movement and structure deflection should be considered when phases are placed one above the other.

Structures are typically designed with clearances for switching surges in everyday conditions and during moderate winds. An additional criterion may be added to maintain 60 Hz clearances during extreme winds. Similarly to extreme wind events, 60 Hz clearances should be maintained during ice shedding to avoid flashovers.

The studies and analyses described in this report show that the risk of flashover due to vertical jump during ice shedding is relatively small for phases directly above one another (37.5 ft spacing) for spans under 900 ft. The risk of flashover increases both with span length and with the amount and pattern of ice. For spans longer than 900 to 1000 ft, offsetting the adjacent phases horizontally is recommended when rigid towers, e.g. wide base, 4-legged lattice steel towers, are used. If flexible structures are used, e.g. tubular steel pole steel structures, the horizontal offset should be increased to account for the lateral motion of the conductor due to the motion of the tower.

### Acknowledgements

The authors are grateful for Southern California Edison's support of this work.

### References

- Binder, R. C. (1973). *Fluid Mechanics, Fifth Edition*, Prentice-Hall, Inc., Englewood Cliffs, NJ.

- Dyrbye, C., and Hansen, S. O. (1996). *Wind Loads on Structures*, John Wiley & Sons, Ltd, Chichester, GB.
- Eisner, F. (1931). Das Widerstandsproblem. In *Proceedings of the 3rd International Congress for Applied Mechanics, Stockholm 24-29 August 1930*, edited by C. W. Oseen and W. Weibull. AB. Sveriges Litografiska Tryckerier. Stockholm. 23-42.
- Freitag, A., and Brandt, E. (1981). "Dynamische Beanspruchungen von Mittelspannungs-freileitungen beim Abwurf von Eislasten (Dynamic Loads During Release of Ice Loads from Medium Voltage Overhead Lines) in German." *Elektrizitätswirtschaft*, 80(19), 668-676.
- Fuheng, S., and Shixiong, J. (1988) "Icing on Overhead Transmission Lines in Cold Mountainous District of Southwest China and its Protection." *Proceedings of the Fourth International Workshop on the Atmospheric Icing of Structures*, Paris, France, 354-357.
- Greasier, V. H. (1913). "Effects of Ice Loading on Transmission Lines." *Transactions of the AIEE?? Check*(June 27, 1913), 1829-1844.
- Jakse, J., Al Harash, M., and McClure, G. (2001) "Numerical modelling of snow-shedding effects on a 110 kV overhead power line in Slovenia." *ISOPE-2001: Eleventh (2001) International Offshore and Polar Engineering Conference*, Stavenger; Norway, 690-694.
- Jamaleddine, A. (1994). *Effets Statiques et Dynamiques du Délestage de la Glace sur les Lignes Aériennes de Transport D'Énergie Électrique (Static and Dynamic Effects of Ice Shedding from Overhead Electric Transmission Lines)* in French, PhD, Génie Mecanique (Mechanical Engineering), Université de Montréal, École Polytechnique, Montreal.
- Jamaleddine, A., Beauchemin, R., Rousselet, J., and McClure, G. (1996) "Weight-Dropping Simulation of Ice-Shedding effects on an Overhead Transmission Line Model." *Proceedings of Seventh International Workshop on Atmospheric Icing of Structures*, Saguenay—Lac-Saint-Jean, Québec, Canada, 44-48.
- Jamaleddine, A., McClure, G., Rousselet, J., and Beauchemin, R. (1993). "Simulation of Ice-shedding on Electrical Transmission Lines Using ADINA." *Computers and Structures*, 47(4, 5), 523-536.
- Kálmán, T., M., F., and McClure, G. (2007). "Numerical analysis of the dynamic effects of shock-load-induced ice shedding on overhead ground wires." *Computers and Structures*, 85, 375-384.
- McClure, G. (1989). *Interactions Dynamiques dans les Lignes Aériennes de Transport d'Électricité Soumises aux Bris de Câbles (Dynamic Interactions in Overhead Electrical Lines from Broken Wires, in French)*, Ph.D. Thesis, Département de Génie Civil (Department of Civil Engineering), Ecole Polytechnique de Montréal, Montreal.
- McClure, G., and Lapointe, M. (2003). "Modeling the Structural Dynamic Response of Overhead Transmission Lines." *Computers and Structures*, 81(8-11), 825-834.
- McClure, G., and Tinawi, R. (1987). "Mathematical Modeling of the Transient Response of Electric Transmission Lines Due to Conductor Breakage." *Computers and Structures*, 26(12), 41-56.

- McClure, G., and Tinawi, R. (1989). "Comportement dynamique des lignes aériennes de transport d'électricité dû aux bris de câbles. II. Problèmes numériques associés à la modélisation mathématique. (Dynamic Behavior of Overhead Electric Transmission Lines Due to Broken Cables. II Numerical Problems Associated with the Mathematical Modeling)." *Canadian Journal of Civil Engineering*, 16(3), 354-374.
- Morgan, V. T., and Swift, D. A. (1964). "Jump Heigh of Overhead-line Conductors after the Sudden Release of Ice Loads." *Proceedings of the Institution of Electrical Engineers*, 111(10), 1736-1746.
- Oertli, H. (1950). "Oscillations de Câbles Électriques Aériens après la Chute de Surcharges (Vibration of Overhead Electric Cables after Dropping Surcharge Loads, in French)." *Bulletin de L'Association Suisse des Electriciens (Bulletin of the Association of Swiss Electrical Engineers)*, 41(13), 501-511.
- Peabody, A. B. (2004). *Applying Shock Damping to the Problem of Transmission Line Cascades*, Ph.D. Thesis, Dept. of Civil Engineering and Applied Mechanics, McGill University, Montreal.
- Power Technologies, I. (1978). *Transmission Line Reference Book 115-138 kV Compact Line Design*, Electric Power Research Institute, Palo Alto.
- Roshan Fekr, M. (1995). *Dynamic Response of Overhead Transmission Lines to Ice Shedding*, Master of Engineering, Dept. of Civil Engineering and Applied Mechanics, McGill University, Montreal.
- Roshan Fekr, M., and McClure, G. (1996) "Numerical Modelling of the Dynamic Response of Ice Shedding on Electrical Transmission Lines." *Proceedings of Seventh International Workshop on Atmospheric Icing of Structures*, Saguenay—Lac-Saint-Jean, Québec, Canada, 49-54.
- Roshan Fekr, M., and McClure, G. (1998). "Numerical Modeling of the Dynamic Reponse of Ice-Shedding on Electrical Transmission Lines." *Atmospheric Research*, 46(1), 1-11.
- Roshan Fekr, M., McClure, G., and Hartmann, D. (1998) "Investigation of Transmission Line Failure Due to Ice Shedding Effects using Dynamic Analysis." *Proceedings of the Eighth Intenational Workshop on Atmospheric Icing of Structures*, Reykjavík, Iceland, 11-16.
- Schauer, H., and Hammerschimd, W. (1983) "Experience Concerning Ice Loads on Overhead Lines in Austria." *Proceedings of First International Workshop, Atmospheric Icing of Structures, CRREL Special Report 83-17*, Hanover, New Hampshire, USA, 333-340.
- Stewart, J. R. (1983) "Ice as an Influence on Compact Line Phase Spacing." *Proceedings of First International Workshop, Atmospheric Icing of Structures, CRREL Special Report 83-17*, Hanover, New Hampshire, USA, 77-82.

## Fact or Fiction – Weathering Steel Can Provide Effective Corrosion Protection to Steel Structures

C. Jerry Wong

DHW Engineering, 7981 Fairway Lane, West Palm Beach, Florida 33412; PH(561) 694-4877; email: ChungJWong@aol.com

### Abstract

The electrical utility industry has been using weathering (COR-TEN™) steel products for nearly 40 years. Along with the cost advantages to utility owners, it also provides more flexibility for pole manufacturers. Thus, the whole industry, from structural designers to construction workers, can benefit greatly if its unique characteristics are fully recognized and utilized.

However, weathering steel cannot be used in a carefree manner. Like all other materials, regular inspections and maintenance work needs to be performed in order to prolong its service life. What activities are required in order to achieve an efficient and effective assessment? Are most inspection programs adequate enough to find potential problems? What exactly are these ‘potential problems’? What long-term maintenance activities are required?

Performance-wise, are weathering steel poles really a time-bomb waiting to be ignited as some have claimed? Or is the bad reputation of weathering steel simply the result of misunderstanding and misuse?

Also, what about the use of weathering steel in other industries? It was fashionable to use weathering steel in the building and bridge industries during the 1970s. Do those industries face the same concerns? Do they now face the same exposure? Is there anything we can learn from them?

This article attempts to provide basic background on these questions and hopes to stimulate further study and discussion in this area from the utility industry.

### Historical Development

Weathering steel, best-known under the trademark COR-TEN™ steel, generally refers to a group of steel alloys that, due to their chemical compositions and under ideal conditions, exhibit better resistance to atmospheric corrosion as compared to normal structural steels.

In the early 1900's, research was done in an attempt to fulfill the market need for a high-strength steel. As part of the investigation, it was discovered, quite accidentally,

that a relatively high copper content could contribute to the formation of a dense oxide coating (patina) at the surface of the material. The research results indicated that, although these steels initially corrode at the same rate as plain carbon steel, they soon exhibit a decreasing corrosion rate. After a few years, under favorable environments, the continuation of corrosion is practically nonexistent. The adherent, protective films on high-strength low-alloy steels would essentially seal the surface against further penetration of water and delay the progression of metal corrosion. This tough adherent oxide layer would stabilize and act as a tightly adhered barrier coating, preventing future atmospheric corrosion.

Interestingly enough, the "corrosion resistance" aspect of this steel alloy's performance was almost unnoticed under the shadow of its high strength attributes. Indeed, this aspect was largely ignored until the mid 1960's. At that time, with maintenance costs rapidly escalating under the combined effects of inflationary labor price, high cost exotic coating materials, and greater environmental awareness of general public, the "natural" corrosion resistance properties of the material caught the attention of some marketing personnel at major steel suppliers. Weathering steel was portrayed as the final solution to all corrosion problems in advertising campaigns. It was marketed for such diverse applications as office buildings, bridges, utility structures, light poles, highway guide rails, and, unsurprisingly, a few unusual architectural applications.

## Metal Corrosion

Corrosion is the result of an interaction of metal with its surrounding environment that adversely affects the metal's properties. It is an undesirable deterioration of metal, as it impacts the structural integrity.

Corrosion of metals is an electrochemical process. It involves both the flow of electrons and chemical reactions. The basic electrochemical reaction that drives the corrosion of metals is galvanic action. Galvanic corrosion normally occurs when two dissimilar metals are placed in contact with each other in the presence of an electrolyte or a conductor such as water, acids, or salts. A galvanic cell can also be formed if the same metal is exposed to two different concentrations of electrolyte. Consequently, a current is generated internally by physical and chemical reactions occurring among the components of the cell. The resulting electrochemical potential then develops an electric current that dissolves the less "noble" material.

Copper, brass, bronze, and nickel are more "noble" materials, and will act as auxiliary cathodes to the steel and accelerate its anodic dissolution. Magnesium, aluminum, zinc and zinc-base alloy are nearly always less noble, and tend to divert the attack. They have a greater tendency to lose electrons.

From a thermodynamic perspective, the tendency to reduce internal potential energy is the main reason for the corrosion of metals.

The actual corrosion process that takes place on a piece of bare mild steel is very complex due to factors such as variations in the composition of the steel, the presence of impurities, uneven internal stress, or exposure to a non-uniform environment. In addition, the rate at which metals corrode is also controlled by numerous other factors such as the electrical potential and resistance between anodic and cathodic areas, the pH value of the electrolyte, temperature, and humidity. The combination effects can be complicated and complex.

To simplify the discussion, four (4) elements contribute to the basis of corrosion and corrosion prevention. They are the anode, cathode, electrolyte, and the return current path. Removing any one of these elements will stop the current flow and corrosion will not occur. The firmly adhered patina layer on weathering steels could essentially seal the steel member surface against further penetration of water, effectively removing the electrolyte, thus stopping the corrosion of the inner material.

### **Weathering (COR-TEN™) Steel**

The United States Steel Corporation (U.S. Steel) holds the registered trademark on the name COR-TEN™.

High strength steels can be produced under ASTM A-242, A-588, and A-871 specifications for atmospheric corrosion-resistant steels intended principally for applications requiring durability. They reduce the overall structure weight; minimize maintenance work, and lower initial costs.

The corrosion-retarding effect of the protective layer is produced by the alloying elements. Several compositions of weathering steels have been developed for atmospheric corrosion resistance properties. Relatively small amounts of copper, chromium, nickel, and silica, will result in a tenacious oxide film that improves atmospheric corrosion resistance if the surfaces are allowed to dry periodically in normal service. Copper is the key alloying element, but others enhance the beneficial effects of copper.

Even with the improved metallurgical compositions, the “weathering” characteristics of these steels can only be developed in favorable environments. When used outside of these suitable conditions, weathering steel is still vulnerable to extensive corrosion. A better understanding of these limitations is needed to allow for appropriate usage of this material.

To begin with, complete wet and dry cycles are essential for the development of a uniform patina layer to function as an effective corrosion barrier. The rapidity at which the protective film can be formed is highly dependent on the frequency with which the surface is made wet by dew or rainfall and dried by sun or wind. The oxide layer can only be formed through exposure to “sufficient cycles” of wetting and

complete drying of the steel surface. At first, the oxidation rate and its process is similar to that of carbon steel. However, if the protective patina layer forms properly, the process slows such that the corrosion of the steel is greatly diminished. In 1975, R.L. Brockenbrough and R.J. Schmitt of U.S. Steel<sup>1</sup> issued a paper establishing certain guidelines for the design of structural steel transmission towers. The authors state that "Alternate wetting and drying is necessary for the formation of the protective oxide film. Should the corrosion-resistant high-strength low-alloy steel remain wet for prolonged periods, they will corrode at the same rate as carbon steel."

This caution is not only limited to the atmospheric wetting and drying of the general surrounding for the entire structure. Localized details within the structure also need to be addressed. Due to design flaws or improper maintenance, certain parts of a structure can accumulate debris such as sand, dirt, pine needles, leaves, bird nests, animal remains, etc., which, when wet, will remain constantly moist for a prolonged duration of time. The resulting localized corrosion can become catastrophic. This issue has also been discussed in the Brockenbrough report: "The design of the structure should minimize ledges, crevices, and other areas that can hold water or collect debris. Details should be self cleaning if possible. Because it may not be readily apparent that abnormal conditions which can accelerate corrosion of bare COR-TEN™ steel structures are occurring, periodic inspections of towers should be made to determine if such conditions exist. Attention should be given to determining if 1) vegetation is causing corrosion damage, and 2) debris is present on ledges and causing corrosion."

As stated, proper steps should be taken during the design stage to minimize the retention and collection of moisture. Weathering steel is not rustproof in and of itself. If water is allowed to accumulate in pockets, those areas will experience accelerated corrosion rates. Structural details are a primary concern in order to achieve satisfactory, long term performance.

Weathering steel structures that are enclosed or covered by vegetation have similar corrosion concerns. Over-grown vegetation prevents air circulation and maintains a high moisture environment around the steel. Structure members or portions that have experienced constant damp surroundings will not be able to form a dense patina layer and will have metal loss at a rate consistent with bare carbon steel. Obviously, there is also the concern of deep pitting from the root systems of certain vegetation species.

Weathering steel is also sensitive to salt-laden air environments. These include exposure to salt water, salt spray, or even salt fog. In such environments, it is possible that the protective patina may not stabilize, but instead continue to corrode. In the previously mentioned paper, the authors also warn that, "It should be recognized, however, that the steel is not capable of performing satisfactorily under some conditions. One such condition is exposure to the seacoast where recurrent wetting by salt spray can occur. Another condition is exposure to chemical environments heavily contaminated with corrosive substances." The paper then goes on to state, "Where it is known that heavy localized chemical contamination or

concentrations of airborne particulate matter exists, periodic inspections should be made to determine whether there is a need for supplemental protection by painting."

Examples of airborne chemicals may include crop dusting, fertilizing, and other similar activities. The degree and type of contamination present will influence the formation of patina. Since the degree of contamination and severity of the chemicals can widely differ from location to location, and even from season to season, any pole located in or near these environments may require special considerations.

Even for structures located in favorable environments, there are potential traps such as corrosion at faying surfaces or at load carrying joints. The normal action of wind, loading, and temperature variations may cause constant movement at faying surfaces or at structural joints. If the weathering steel is subjected to this type of friction conditions, the patina layer may never fully develop under the constant motion of structural members. The corrosion by-product which accumulated at the faying connections is typically a porous medium with a coarse surface that readily absorbs moisture. In combination with oxygen, it can cause additional corrosive propagation. In other words, not only does the corrosion process not stabilize, it could actually accelerate.

Thick, non-uniform, stratified, deep pits have also been observed in the metal underneath. The pack-out formation could possibly result in higher stresses at a magnitude capable of distorting the steel members or exceeding the tensile strength of the connection bolts. With time, pressure between bolted members could increase due to pack out and pop connection bolts. It could ultimately cause structural failure.

Brockenbrough's paper in 1975 recommends details for joints and suggests increasing clamping pressure. Edge and pitch distances were reduced to generate a compact bolting pattern and keep the joint tight. The whole intention is to discourage moisture from entering the joints.

Many other issues exist (such as weld specifications, hardware/fastening material, vent or drain, foundation types, storage) and should be investigated to ensure successful long-term services.

## Applications in Other Industries

Weathering steel (Cor-Ten™) products have been utilized in a variety of ways throughout the world. Its widespread use is due to the benefits it offers in terms of corrosion resistance when it is situated in favorable environments. Using weathering steel also eliminates the need to paint a structure, as it develops a rust-like appearance over time.

The U.S. Steel Tower (Picture 1) in downtown Pittsburgh, Pennsylvania was constructed by U.S. Steel in part to showcase Cor-Ten™ steel. Many other weathering steel buildings in several major metropolitan areas have successfully served their needs over the years.

There are unfortunate examples as well. The former Omni Coliseum, built in 1972 in Atlanta, Georgia never stopped rusting. In fact, the deterioration rate noticeably accelerated. This structure was eventually demolished after only 25 years of service because large rusted holes had appeared in the surface of the structure.



Picture 1 U.S. Steel Tower

Under the leadership of the Federal Highway Administration (FHWA), more historical data and study reports are available in the bridge industry. Engineers have utilized weathering steel in the design of bridges since 1964. In fact, thousands of bridges in the United States have been built with this material over the years. Yet the widespread application of weathering steel in bridge industry has not been without controversy.

The first weathering steel bridge was built over the New Jersey Turnpike. About the same time, the Eight Mile Road Bridge was built in Wayne County, Michigan. Interestingly, while the agency in New Jersey was pleased with the performance of its weathering steel bridges, administrations in Michigan found this material performed poorly, specifically in the Detroit Metropolitan Area. The poor performance of weathering steel bridge in Detroit area led the State of Michigan to issue a moratorium (May 2, 1979) on the use of weathering steel for highway bridges of all types throughout the State. Similarly, weathering steel is prohibited for bridge construction in Germany.

It has also been reported that weathering steel bridges located in the northwest portion of the United States, west of the Cascade Mountain range, and southeast Alaska, have not performed satisfactorily and needed repairs soon after construction.

Under the guidance of the FHWA, long-term research projects were established to address issues related to the suitability of using weathering steel in highway bridge construction. The studies were conducted with help from American Iron and Steel

Institute (AISI) and Steel Structures Painting Council (SSPC) to address technical concerns and develop guidelines. Several reports and technical advisories were issued.

In short, the results of these studies demonstrated that:

- Uncoated weathering steel bridges designed and detailed in accordance with the recommendations outlined in the FHWA Technical Advisory will perform well under the favorable environments.
- There are “micro-environmental” material concerns in many of the bridges inspected. The “micro-environmental” concerns also include the build-up of debris, chemical, salt water spray, unprotected contact surface, and industrial waste.
- Bridge structures utilizing COR-TEN™ steel should be periodically inspected to ensure that all joints and surfaces are performing satisfactorily.
- Bare COR-TEN™ steel is not a maintenance-free material.

It is important to note that the FHWA recommends caution in employing weathering steels in areas where the material could remain wet for extended periods of time due to high levels of rainfall, humidity, or fog. The technical advisory (FHWA T5140.22, October, 1989) recommends evaluating these conditions using ASTM G 84 “Time of Wetness Determination (On Surfaces Exposed to Cyclic Atmospheric Conditions).” This advisory suggests that caution should be used if the average time of wetness exceeds 60%. Not many utility companies consider this type of guideline when determining what type of structural material to use.

## Discussion

Like all structural materials, weathering steel has its applications as well as its limitations. A comprehensive understanding of these limitations is absolutely necessary to effectively utilize the material. When utilized within these limitations, weathering steel structures could last an extended period of time.

Using weathering steel in construction presents several unique challenges. None of these challenges is more critical than recognizing the environment in which these structures will reside and providing adequate structural details to avoid water accumulation.

From an engineering perspective, the debate of having additional thickness to compensate for the surface deterioration will always exist. Many European countries have related regulations. Even the States of Louisiana and Texas have guidelines to address this issue. Most of these requirements are specified by authorities in the bridge industry. They have better records on the performance of this structural material and have conducted more research works in order to develop effective preventative measures.

Weathering steel is not a type of material that engineers can simply “put out there and forget about it”. Methodical inspection and maintenance activities are still needed. Indeed, inspection and maintenance programs must be written specifically to address the unique characteristic of weathering steel. A recent survey indicates that only 12.5% of the 56 companies have ever conducted corrosion surveys, such as plate thickness measurements, on their structures. This number is considered to be too low in author’s opinion. Well-planned inspection techniques and maintenance programs that prevent degradation of material should be implemented and could extend the useful service life of the structure.

#### Reference

- <sup>1</sup> Brockenbrough, R.L. and Schmitt, R.J., “Considerations in the Performance of Bare High-Strength Low-Alloy Steel Transmission Towers” IEEE C75 041-9, January 1975.

## Large Catenary Structures for High Voltage Transmission Lines

P. G. Catchpole, P.Eng.<sup>1</sup> and E. A. Ruggeri, PE<sup>2</sup>

<sup>1, 2</sup>POWER Engineers, Inc., P.O. Box 1066, Hailey, ID 83333; PH (208) 788-3456; FAX (208) 788-2082; [email: pcatchpole@powereng.com](mailto:pcatchpole@powereng.com); [email: eruggeri @powereng.com](mailto:eruggeri@powereng.com)

### ABSTRACT

Transmission Line Catenary structures are steel cable structures from which transmission circuit conductors are suspended. The objective is to keep the entire support structure above locations of high avalanche risk where other structure types have little chance of surviving. The world's first Catenary was built in 1955 in British Columbia, Canada. The authors have engineered and provided construction management for the installation of the world's second and slightly larger Catenary. It was installed 1,000 meters north of the first. The authors have also installed a smaller Catenary and done preliminary engineering for thirty four other Catenaries, all in British Columbia. This paper discusses transmission line Catenaries in general and will describe the 2007-2008 engineering and installation of Catenary 2 in detail.

### INTRODUCTION TO CATENARIES

A cable of uniform weight along its length suspended between two points and subjected to gravity forces forms a shape called a catenary. In the small community of people who have engineered, built and maintained a transmission line structure made entirely of long cables, this same word has become the identifying label for the structure type. Before the world's second large transmission line Catenary was built in 2008, the first Catenary was simply known as "the Catenary." They are now called Catenary 1 and Catenary 2 since they are both on the same line. These names were quickly shortened to Cat 1 (also called the 1955 Catenary by those with a sense of history) and Cat 2.

Cat 1 was conceived and engineered by H. Brian White in 1955 in response to the wiping out of three structures on two parallel single circuit lines that were placed in the belly of a mountain cirque on their way from a near sea-level river valley to a high elevation Pass and on into the adjoining valley. Brian's design used two 76 mm (3 inch) diameter galvanized steel rope cables each 1,158 m (3,800 ft) in length. The cables were essentially parallel, about 100 meters apart and oriented perpendicular to the

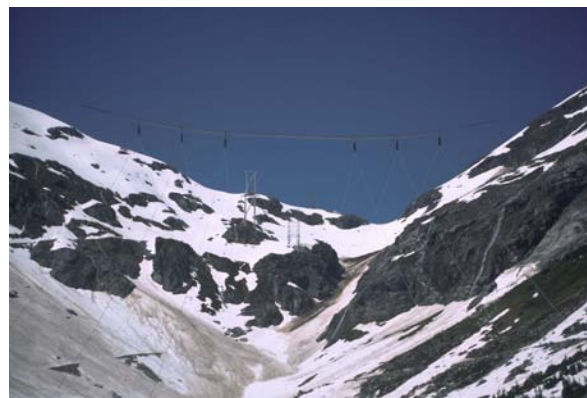


Figure 1 Catenary 1 against the sky, looking up towards the Pass

transmission line direction. Each cable was anchored into the high rock walls of the cirque and suspended high above the two 300 kV transmission circuits below. The 122 m (400 ft) middle segments of the cables over the circuits below were brought to a separation of 914 mm (3 ft) by yoke plates. Along the middle segment, a catwalk was suspended using the two cables as handrails and six large suspension insulator assemblies were also suspended there to carry the conductors that pass beneath the cables.

The ahead and back spans of the conductors suspended from the Catenary are 760 meters (2,500 ft) and 1,220 meters (4,000 ft) respectively with a weight span of about 1,000 meters (3,300 ft). The design load is 60 kg/m (40 lb/ft) and the conductor itself is a 3,364 kcmil ACSR 108/37 "Emu" weighing 7.08 kg/m (4.76 lb/ft). Access to the catwalk section of the Catenary is by helicopter to a small helipad mounted on the cables between the circuit attachments. The helipad is 135 m (450 ft) above the ground below. The structure's dimensions and forces on it are large. It is a dramatic structure in a dramatic location. For 53 years, this structure stood alone as a proud achievement that some consider as the safest structure on the 80 km (50 mile) transmission line.

In the 53 years since the Catenary was installed, the transmission line has been battered and damaged in several locations at several different times by large avalanches. The most problematic location was the next structure north of the Catenary on one of the two circuits where the lines rise up towards the Pass. Here, the original 35 ton latticed steel tower was harmed in a 1988 avalanche event and crumbled to the ground in late 1992 by a powder avalanche event. Its identical replacement tower was wiped from the face of the earth by a large, wet snow avalanche in March, 2007. These two circuits are a singular lifeline to the viability of the owner's facilities. These lines' service was very expensive to reinstate because the work occurs in the heart of the winter in BC's coastal mountains, by definition. Revenue losses are extraordinary and the owner's ongoing facility operations are put at serious risk. To the owner's question, "Can we build a Catenary in this location and stop this from happening again?" we answered 'yes' after a brief review of the site's terrain.

## OTHER CATENARIES

In the years immediately after the 1992 tower failure, the author provided preliminary engineering for a Catenary to be located a few miles away in the valley north of the above-mentioned Pass. There, a tower had been lost in 1985 and a study by avalanche experts had identified a whole series of at-risk towers along the valley floor in that area. The 1955 Catenary replaced six original structures in the floor of the cirque. This proposed Catenary used a similar two-cable/four anchor configuration. In the overall, it was to be much larger. The cables were 86 mm (3.375 inches) in diameter, over 1,500 meters (5,000 ft) long and the conductors' weight span was near 2,100 meters (7,000 ft). The helipad access on the cables was about 330 m (1,000 ft) above the ground below and the Catenary structure was to replace a total of nine original structures on the two circuits below. This Catenary remains in the drawer, waiting to see the light of day.

Concurrently, proactive action was taken at the site of the 1992 tower loss. Here, a single cable Catenary was installed between the bedrock at the base of the tower that had failed and a point high on the mountainside to the southeast. This single cable was a 44.5 mm (1.75 inch) galvanized bridge strand 670 m (2,200 ft) in length. It was considered to be an insurance policy against any future failure of that tower. It was put in place such that, upon the tower's loss, the circuit could be re-instated within weeks rather than in the nearly three months as was the case after the 1992 event.

To one's delight/surprise/dismay – depending on who you were, the 2007 failure of the same tower put this small Catenary to work, as planned 13 years earlier. A very important lesson to learn for locations as rugged and wild as high up in the BC Coastal Mountains is that Mother Nature has a large bag of tricks and will surprise the engineer in you routinely. The temporary 'insurance' Catenary was used to support the circuit for a full year, summer 2007 to summer 2008. However, the 2007 avalanche event was very different from the 1992 event and our well laid plans based on the 1992 experience needed serious modification. The damage rendered to the circuit was far more extensive in 2007, even touching the 1955 Catenary as it was the adjacent structure. With the decision made to install a permanent Catenary in the location, this small, temporary Catenary became known as the KitiKat in recognition of its relative size to Cat 1 and Cat 2 and as a play on words for the name of the nearest town, Kitimat.

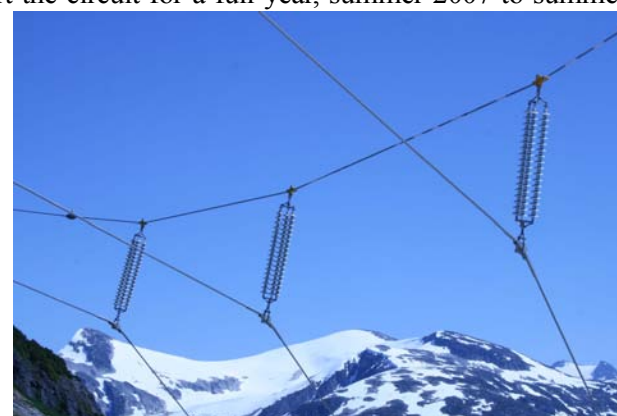


**Figure 2**The single cable KitiKat in use for one year

During the installation of Cat 2 in the summer of 2008, the owners of a proposed transmission line elsewhere in the province visited the site. After a tour of Cat 1, Cat 2 – under construction, the KitiKat and the site of the still shelved Catenary for the valley north of the Pass, the authors were asked to provide feasibility, preliminary designs and cost estimates for Catenaries – as needed for avalanche-prone sections of their proposed routes. On one route, seven Catenaries were proposed in series to cover a 12 km (8 mile) long, deep, narrow and steep walled valley without touching the valley floor. The lessons learned from the above-noted four Catenaries – three in existence and one engineered – lead to a proposed design for these Catenaries that is unique from all the rest.

## CATENARY 2

### The Design Constraints

The fundamental requirement of a Catenary structure is that it cannot be damaged by an avalanche. Unless the cable anchors can be placed out of the reach of avalanches, or rendered indestructible somehow, little is gained. Even though it can appear that the vast surface area of a mountainside would offer endless anchor location possibilities, this is not the case. The slope of the cables as they leave the anchor site out into the span can be as steep as 35° below the horizon. Anchor sites must have a slope in front that is steeper than this. It would be best if there was little avalanche threat above the site either by the absence of more elevation or by the shape of the slope above such as might direct a flow elsewhere. Above all, the anchor locations must allow cable load sharing that meets criteria; must be accessible for construction and must allow positioning the cables above the conductors' attachment points so that the line layout is served. Anchor locating can be a challenge. Finally the anchorage assembly must be low profile so as to not attract large impact forces when an avalanche does run over it.

If there are avalanches, there is snow. If there is snow, there is snow load. In this part of the world, the design loads for snow or ice on wires are substantial. It made no sense in this case to intentionally degrade the lines' original design load case of 60 kg/m (40 lb/ft) of snow/ice

weight on the conductors with a stress limit of 100%. For reference, this oddly stated load and stress limit combination translates into a span dependent and more typically stated load of about 37 kg/m (25 lb/ft) of load at 60% of conductor breaking strength. Since the structure itself is made of wires, it is impossible to rationalize not applying that load to the wire structure as well. This is a departure from our normal transmission structure line of thinking.

With loads this large on the wire structure, it is difficult to find other load cases of concern for its design. The two conditions that were monitored but in a near-qualitative manner were the cable's tensions for Aeolian vibration concerns and the bare wire, nice day tensions in place when construction and maintenance people are on the cables. Cable vibration damage must be mitigated and the factor of safety of the system components when personnel are on it must be acceptable. We sought a factor of safety of at least 5 whenever possible for the latter concern. This exceeds the factor of safety of a typical steel transmission support structure under these conditions but it honors the intent with mechanical cable system standards, even though it can be argued that a Catenary is not that.

We learned from the various events at this location that the Catenary can be asked to support a broken wire condition of very high tension. Although the Cat 2 conductor insulator assemblies are suspension types, they are also capable of carrying the breaking strength of the attached conductors, as is the Catenary itself. With the large ice load case and long weight span, it happens that the design load in suspension is nearly equal to the breaking strength of the conductors. How convenient!

If the entire assembly is intended to carry suspension or conductor tension loads, it must also be capable of significant articulation and large deflections that will occur as the forces on the Catenary change from intact cases to broken wire cases. Similarly, a very long span of cables will move in high wind. A very high wind over the Pass will strike Cat 2 transversely and push it a meter or two along line. The conductors will not be inclined to follow and will attempt to remain where they are. This will move the insulator strings out of plumb and they could interfere with the catwalk. If this differential displacement is not dealt with in the design details, conflict of parts and damage will occur.

The nature of the site defined the remaining design constraints. There is no road access within five kilometers (3 miles) of the site and all access and storage locations were at least that far away and 1.6 km (1 mile) below in elevation. In other words, everything and everyone could only be brought to the site by helicopters. Therefore, all materials and equipment had to transportable by helicopter. History told us that the S-64 SkyCrane and the 234 Boeing Chinook were generally available to us. We designed with these heavy lift machines in mind.

### **The Design Choices**

Catenary 1 was constructed by laying its large, heavy cables on the ground below their final position and raising them into place but pulling their ends towards the anchors with large winches set well below the anchor sites. Each of the two large



**Figure 3** The Boeing Chinook put 114 tons of material onto the mountain site in 6.5 hours from 12 miles away and one mile below. Here, three 6,000 lb cables reels go at once.

cables was made up of four segments up to 366 m (1,200 ft) long. The joints were poured zinc socket sets. Our decision with Cat 2 was to string the cables in place above the two operating circuits from one anchor site to its mate on the other side of the valley and to do this with jointless, single-length cable.

The cables of Catenary 1 and our general understanding of its design provided great initial design guidance. We knew that our cables might be slightly longer and might need to be a bit stronger. Its 3 inch steel rope cables are effectively made up of 6 one-inch cables helically wrapped around the central seventh. It would be impossible to lift long lengths of 3 inch cable to our work site and we had already envisioned the concept of assembling a cable “in situ” from a collection of seven smaller cables.

However one-inch diameter cables that would form an unwound 3 inch cable were going to be a bit heavy and require installation tensions larger than we wanted. Smaller cables were attractive but assembling them into a larger cable would require a second layer of 12 cables over the envisioned six for a total of 19 cables. Construction of that assembly was considered too unwieldy. We settled on an arrangement of 14 cables, each  $\frac{3}{4}$  inch (19 mm) in diameter and placed in two parallel sets of seven cables each. In this arrangement, we had a total of 28 –  $\frac{3}{4}$ ” cables that we expected would be up to 1,340 m (4,400 ft) in length. At this length, their on-reel weight would reach 2,700 kg (6,000 lbs) each and the stringing tension would be about 2,300 kg (5,000 lbs) each. These were acceptable values.

The comparable weight and strength comparisons of this cable set choice to Cat 1 cables was attractive. It was slightly heavier and slightly stronger allowing some freedom in establishing its four yet-to-be determined anchor sites. There was some attraction to having a pair of parallel 58 mm (2.25 inch) cables representing each of the two main cables. Given that marker balls would be required on the cables, a parallel set increased the construction cart configuration options.

### **The Design Process and Tools**

From a structural analysis and design perspective, the Cat 2 project offered a host of challenges that required the unconventional use of several common software programs. During the process of laying out the new Catenary, the objective was two-fold: to locate the best possible anchor locations using aforementioned criteria, and to increase the wire clearance to ground. This was done so that Cat 2 could be constructed well above the energized circuits, and upon completion, the wires could be lifted (almost) vertically to the new attachment points. This configuration also ensured that additional load would not be imparted on the existing structures. From the early design phases, the idea was to cross the two sets of cables so that the NE (‘A’) anchors shared cables with the SW (‘B’) anchors and the same with the SE and NW anchors (‘C’ and ‘D’ anchors, respectively) - keeping the wires close together in space to facilitate the construction of the catwalk by linemen in carts.

The design process began with a PLS-CADD model of the entire line section; extending from the southern dead-end towers (parked safely out of avalanche areas) to the dead-end towers at the top of

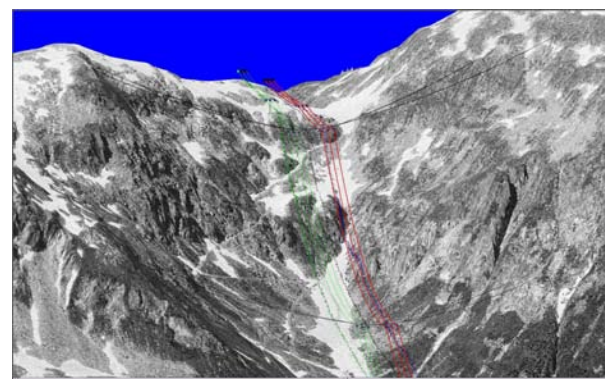


**Figure 4** The PLS-CADD model of the line section containing both Cat 1 and Cat2.

the Pass. The model also contained a detailed terrain model of the entire cirque. Using this model to identify preliminary anchor locations, the Catenary system coordinates (east/west yoke positions and assembly attachment points) and cable lengths were calculated using an Excel spreadsheet. This information was passed into PLS-TOWER in order to construct the Catenary structure. While TOWER is intended for 3-D lattice trusses with (4) anchors (legs) at typical spacings of 20' – 60', our application was a bit different: our TOWER model consisted of approximately 16,040' of cables and (8) anchor locations with a spacing of about 4000' between the east and west side anchors. The TOWER model's interaction with PLS-CADD required a coordinate transformation between a local structure coordinate system (TOWER) and the global coordinate system (PLS-CADD). This transformation was more complicated since the anchors sit almost 800' above and 2000' offset from the structure's centerline location.

Once the preliminary model was built, it was moved around and adjusted within the PLS-CADD file until the optimum anchor locations and conductor positions were achieved. Once the anchor positions were surveyed and field-reviewed, they were constructed in the summer of 2007. Upon completion, the anchor sites and saddle locations were surveyed in and passed into the model – essential information to determine the exact cable lengths. The cable lengths were calculated taking into account Cat 2's shape as well as the cable's pre-stress load and the offsets between the anchor points and the saddle. Finally, fourteen 3,673.80 ft reels were ordered for the A-B cables and fourteen 4,372.45 ft reels were ordered for the C-D cables.

While PLS-TOWER was useful and accurate for determining cable lengths and the structure's deformed shape under design loads, it could not provide all the details necessary for the design and construction. Initially, we exported the PLS-CADD file (with Cat 1 and Cat 2 structure models) into SAPS in order to satisfy ourselves that the Catenary would withstand a broken wire condition – the results of which are more accurate when all the conductors and support cables play a role in the calculation.

This model provided a more accurate depiction of the insulator assemblies. One hardware piece borrowed from Cat 1 was the suspension shoes and steel straps that connected the shoes to an assembly yoke plate. However, the Cat 1 design has different departure angles than those of Cat 2. Therefore, we had to adjust the strap lengths between the shoes and the yoke plates in order to guarantee that neither shoe contacts the yoke plate and that the load is shared well between the two shoes. This was done in SAPS by altering the uphill strap length accordingly and examining the deformed shape and strap loads.

Finally, the SAPS model assisted in determining the required conductor lengths adjustments for each phase and the attachment locations of each phase. The calculated values were verified in the PLS-CADD file using finite element analyses, and we provided the contractor with wire lengths to splice into each phase.

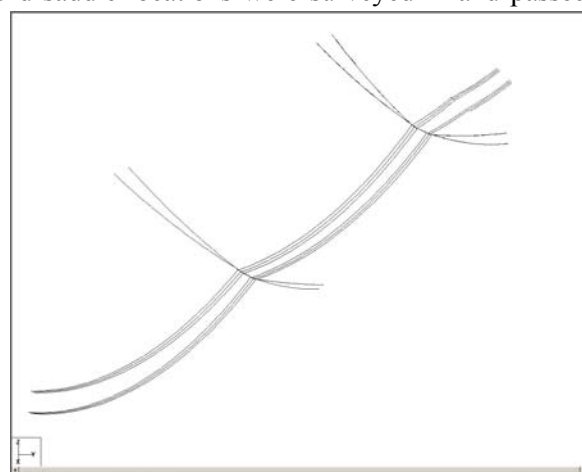


**Figure 5**The spider web of cables within the cirque as modeled in SAPS: 71,340' of conductor and steel cable!

The final portion of modeling work for Cat 2 had more to do with constructability. Given the rough anchor sites on the east side, the contractor was understandably concerned about what size winches and/or pulling equipment would be required to bring the two sets of cables together once the west yoke plate was installed. Therefore, we built a PLS-CADD model consisting of the four (4) bundled cables. The measured span lengths were a known quantity, as was the length of each cable which was the ‘conductor’ in this model. With this file, we were able to apply concentrated horizontal loads to the cables at the rigging point (15' east of the east yoke platform). This was done in an iterative process to determine the pulling tension required to bring the cables together. This model also allowed us to determine the additional sag in the support cables due to the carts themselves. It proved to be an instrumental tool in the construction plan development.



**Figure 6**SAPs played a fundamental role in determining the required strap lengths to keep the shoes from interfering with the yoke plate.

A survey of the completed Catenary showed that its position in space in the computer model and its actual as-built position in space agreed within about 10 cm (4 inches).

### The Construction Program

The 28 Cat 2 cables were to be strung anchor-to-anchor and assembled in place into four groups of seven above the operating circuits. Two sets of seven cables were arranged to cross over the other two sets and then these sets were to be drawn together near midpoint to form the catwalk-carrying section of the assembly. All of this type of activity had never been done before so a very detailed, step-by-step plan was essential. A plan was also essential because we knew that our construction season at the mountaintop elevation of our site was only mid-May to mid-September and weather was often not cooperative.

Our time on site would be sporadic and short. The risk of avalanches at several of our anchor sites would not be gone until mid-June. The depth of snow at other anchor sites would be as deep as 13 m (40 feet). If we moved in earlier than mid-May, we would spend most of our time moving snow. The construction plan also had to be as risk-free as possible considering the presence of the two



**Figure 7**A pulling trolley pulled all cables but the first, on which it rode. We put 40 miles on this rig making 26 round trips.



**Figure 9**Catwalk sections were flown to the men on the growing catwalk by an A-Star B2.

critical, operating circuits 240 m (800 ft) below the anchor sites.

The west side anchors were on the edge of the west side mountain top. They were about 150 m (500 feet) apart. The entire area was generally flat and this was our working site where we would store and stage materials and from which we would string cables to the east side. The east side anchors were well down that mountain slope and work space was very restricted.

We flew a 3,280 m (10,000 ft) long, 34,000 kg (75,000 lb) breaking strength pulling rope across the valley from west-side anchor B to east-side anchor A. There, it passed through a turning block and we returned its end to the west side where the puller sat about 100 m (300 feet) from the tensioner that payed out the cables. The first cable was pulled across over the circuits by this rope and pinned temporarily beyond its permanent anchor pins. This cable sat about 50 feet above its final sag. We placed a trolley on that cable and used the pulling rope and a haul-back rope attached to the trolley to pull the lead end of the 13 remaining cables across the valley. The use of the trolley greatly reduced the risk to the circuits below if some component of the pulling assemblage failed. The owner was adamant about that risk mitigation for obvious reasons. The entire pulling operation was then repeated for the other 14 cables between anchors D to C.

With four sets of seven cables strung across the valley in two parallel sets, the linemen in carts began to bundle each set of seven cables to form a single cable unit. This was done with specially sized Preform® wraps placed at 17 m (50 ft) intervals. Between the wraps, the seven cables were in contact but not bound to each other. It was expected that this loose arrangement would give the finished product considerable self-damping characteristics against Aeolian vibration. So far, this seems to the case.

The mid-section of the Catenary has a catwalk section over the circuit attachment area. At the catwalk ends, the cables were brought together and held in place with large aluminum yoke plates. Sets of cable clamps on the yoke plates gripped the cables against longitudinal slippage and had to resist lateral splitting loads caused by the cables' tensions and the angles turned by the cables as they were re-directed towards the anchorages. The yoke plates were set in place as the cables were rigged and pulled laterally by the men working on them. The west yoke plate was set first. With cables later pulled together at the east yoke plate site and now parallel between the yoke plate locations, the 28 catwalk sections – each 4.88 m (16 ft) in length were set in place from west to east. They were brought to the men on the Catenary by an A-Star helicopter, as was all of the attaching hardware.

There were 1 meter (3 foot) gaps in the catwalk at each of the six conductor insulator assembly points. This gap allows the insulator assembly to move along line without binding with the catwalk for the aforementioned reasons. When the catwalk installation passed the mid-point, the helipad was installed on the cables and access to the Catenary changed from necessary carts set out from the anchorages to helicopter drop-off. This expedited the work.



**Figure 8**Crews in Carts bundled the small cables into larger cables and rigged the parallel pairs towards each other at yoke plate positions

Once the Catenary itself was completed, the Chinook lifted the large equipment from the west side work site to below the Catenary and the business of moving the conductors off of their current structures to the Catenary began. The east (right) circuit was suspended on the KitiKat and the west (left) circuit was suspended on its original tubular aluminum 5-legged tower. The plan called for dropping the right circuit off the KitiKat, removing the KitiKat, adding a pre-determined length of new conductor into each phase and then lifting each phase the 150 m (500 ft) distance up to the Catenary and pinning it there. The planned outage was eight days if the weather held perfectly.

The plan for the left circuit was to follow immediately with a similar pattern although the dismantling of the aluminum tower required much more work than the removal of the KitiKat cable. The high cost of outages drove us to a very efficient plan of nine days for that event.

The overall project plan was for 55 days of work executed in an expected season of 110 days. The previous year offered us about 70% access time during the spring-summer season. We should make it. By the time we reached late August, we had worked non-stop 7-tens since mid-May but the weather had limited us to barely 50% access. Contingency planning was a daily topic of discussion. When we took the first, right circuit outage on August 27<sup>th</sup>, it was pouring rain and we just went for it as the outlook was reasonable. The right line transfer was completed in a nine day outage. But, the decision was made to hold off on the left outage and conductor transfer until the next year. We had run out of time since we could not trust the weather for the next two to three weeks of



**Figure 10** The nearly complete Catenary on a spooky day. The helipad is near the catwalk midpoint and the crew is finalizing the distant yoke plate assembly.

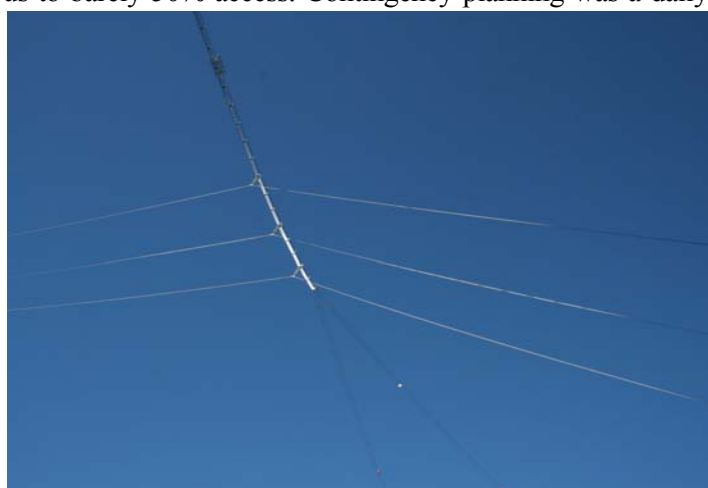


**Figure 11** The right circuit in place on the Catenary. Photographed from 500 ft below. Each bare wire phase weight is 10 tons.

September. Besides, the crew was beat. It was time to let them go home.

As of this writing, the 2009 plan for the relocation of the left circuit is underway and on schedule. The entire installation will be completed by July 2009. Other than routine inspections to ensure that the Catenary components behave as planned, there should be no more monumental and expensive service recovery events at this location in the years ahead.

## FUTURE CATENARIES

It is noted above that the lessons learned on each Catenary tackled have been insightful and very useful in developing the next.

The assembling of seven small cables into a larger cable on site has proven to be a workable idea with expected performance benefits. One of our Cat 2 anchorage designs was unique because the rock shape did not allow our planned configuration. However, it later became recognized as the better idea. As with any structures, whether they are buildings, bridges or transmission towers, ideas and methods are made attractive by the local and present circumstances. Certainly, this is the case with transmission line Catenaries. For example, the combination of constraints on this project leads us to believe that green field Catenaries – those not fit into existing lines – can be installed for half of the cost of this one, perhaps less.

The conditions that make a transmission line Catenary useful are rare but not unheard of. Recognizing the existence and constructability of such structures should remind us that the things that we think are genuine problems can be overcome when we apply our engineering and construction skills and are not stopped by conventional practices.

## References:

- PLS-CADD, (1992), *Power Line Systems – Computer Aided Design and Drafting*, Power Line Systems, Inc., Madison, Wisconsin
- TOWER, (1984), *Analysis and Design of Steel Latticed Towers Used in Transmission and Communication Facilities*, Power Line Systems, Inc., Madison, Wisconsin
- SAPS, (1984), *Structural Analysis of Power and communication Systems*, Power Line Systems, Inc., Madison, Wisconsin

## AESTHETIC MITIGATION – THE CHALLENGE CONFRONTING FUTURE EXPANSION OF TRANSMISSION LINES

Max Chau<sup>1</sup>, Archie Pugh<sup>2</sup>, and Scott Kennedy<sup>3</sup>

<sup>1</sup>American Electric Power, Transmission Line Projects Engineering, Director, 700 Morrison Road, Gahanna, OH 43230; (614) 552-1690; email: mchau2@aep.com

<sup>2</sup>American Electric Power, Project Management, P.O Box 2021, Roanoke, VA 24022; (540) 562-7055; email: adpugh@aep.com

<sup>3</sup>American Electric Power, Transmission Line Projects Engineering, P.O Box 2021, Roanoke, VA 24022; (540) 562-7295; email: skennedy@aep.com

### ABSTRACT

Transmission line construction during the early 1900s was primarily dictated by engineering issues with little devotion to mitigating visual impacts on the surrounding environment. Beginning in the 1960s and 70s, a new environmental ethic began to make its way into the planning process. As a result, heightened sensitivities to visual impact issues are now the norm on new transmission projects, thus making them a major objective on newer projects. This paper addresses the aesthetic challenges confronting future expansion of transmission lines, such as overcoming public objections, environmental stewardship and improving the appearance of transmission facilities.

The paper uses illustrations, photographs and case studies to review current solutions by American Electric Power (“AEP”) and other utility companies to reduce visual impacts on transmission projects. Current best practices revolve around route development, structure design, topographically sensitive siting techniques, off-site mitigation, accurate visual simulations, stakeholder input, construction management, and special structure and conductor finishes. Finally, the future of transmission line siting is discussed along with areas of needed research. These issues challenge the engineering team with the opportunity to provide innovative, creative solutions.

### INTRODUCTION

Future expansion of transmission lines is vital. The existing system is aging and insufficient to meet America’s long-term energy needs. Additionally, the existing grid was not designed to transmit the twenty-first century’s renewable energy, such as wind and solar power – that may be generated far from where it is needed. Nevertheless, the greatest challenge confronting future expansion of transmission lines is aesthetics and associated issues, such as overcoming public objections, and improving the appearance of transmission facilities.

The scenic landscape is a highly valued resource that enhances peoples’ lives and benefits society – it provides visual and sensory pleasure (USFS 1995). Aesthetic mitigation focuses on protecting the existing scenic quality and beauty, especially

natural-appearing landscapes (USFS 1995). A transmission project includes large steel structures, right-of-way (“ROW”) clearings, and conductors; clearly these man-made, linear features have the potential to contrast with a natural-appearing landscape. Even in unnatural developments, people do not want to see a transmission line in the backyard.

### ***Background***

For the first half of the 1900s, transmission line siting consisted of identifying the shortest and straightest route, even if it meant construction would take place over scenic mountains and rivers leaving lasting aesthetic impacts. Functionality and cost overshadowed aesthetic concerns and other environmental issues. Perhaps this past practice is the source of the heightened awareness and public opposition to transmission projects (fueled by aesthetic concerns) that strongly exists today.

An environmental awareness erupted, in the late 1960s and 1970s, resulting in passage of the National Historic Preservation Act of 1966, the National Environmental Policy Act of 1970, the Clean Water Act of 1972 and the Endangered Species Act of 1973. These federal policies and laws established a national framework to prevent environmental damage and protect endangered species (plant and animal), and contain action-forcing procedures to ensure these factors are taken into account (Bass and Herson 1993). At the state level, additional environmental protection laws and requirements were adopted; and state regulatory commissions, which have the authority to approve the construction and location of transmission projects, now require utilities to reasonably avoid adverse impact on the environment. Furthermore, to encourage environmentally responsive siting, the Federal Power Commission (1970) created the *Guidelines for the Protection of Natural, Historic, Scenic, and Recreational Values in the Design and Location of Rights-of-Way and Transmission Facilities*. In response, a new approach to transmission line siting emerged. Not only are function and cost considered today, the environmental consequences of a proposed action and its alternatives are carefully considered through environmental studies; wherein, aesthetic resources are a major component.

This paper shares AEP’s experiences mitigating aesthetic impacts during transmission line route development, engineering, and construction. The following mitigations are to stimulate discussion and are only a partial list, which could be ineffective or even impractical for some projects.

### **ROUTE DEVELOPMENT**

One of the best opportunities to mitigate aesthetic impacts is during route development – where potential alternatives are selected to avoid or minimize impacts to environmental resources. To this end, an environmental assessment and possibly an environmental impact statement are completed. Resources typically identified include, but are not limited to, the following: key observation points and managed vistas; local aesthetic preferences and values; conservation lands, recreation areas, existing and future land use; local zoning and comprehensive plans; transportation; major utilities; cultural features; topographic features; geology and soils; hydrology;

land cover; avian flyways; and endangered species. Though aesthetics is just one of many environmental resources, a major objective of route development is to avoid key and sensitive viewsheds while minimizing adverse impacts to other environmental resources (e.g., natural and cultural). A complete discussion of the environmental or aesthetic analyses employed by AEP is beyond the scope of this paper, yet the following are highlights that have proven beneficial in addressing aesthetic impacts during route development.

### ***Scoping and Stakeholder Input***

During the scoping process, it is critical to engage the public and identify their concerns, key viewsheds, and preferences. Input can be gathered through phone messaging (autodial) to reach citizens in immediate proximity (i.e., within 500 feet) of a study segment, press releases that alert the public of opportunities to provide input, public information workshops, written comments and direct interviews. Additionally, homeowner organizations, clubs and other local organizations should be contacted and a website established that includes general project information and a commenting forum.

Further stakeholder input from federal, state and local officials is collected through direct meetings and data request letters. These agencies should be involved early and throughout route development; their input and expertise are essential (e.g., endangered species, local future land use, and cultural and recreational resources). During field reconnaissance, input is validated and ground-truthed (e.g., critical viewsheds) and engineering constraints are also recorded.

The route development process should be iterative and collaborative with multiple opportunities for public input, agency review and participation, and route modifications as needed. During a recent 765kV project, lack of initial involvement from federal and state agencies hindered progress; however, once participation began and agencies shared critical insights concerning their resources, potential routes rapidly evolved. For example, by way of agency suggestion, a corridor developed that crossed a sensitive trail near an existing disturbed land use (an interstate highway). In the end, an acceptable route to all parties was approved.

### ***Key Observation Points***

Key observation points ("KOPs"), a U.S. Forest Service term (USDA 1995), are representative view points with an associated viewshed and could include residences, communities, parks, recreation, conservation areas, historical resources, trails, and scenic travelways (see Figure 1). They are identified through the initial scoping, public input, agency (federal, state and local) correspondence, websites, publications, electronic data, and aerial photography. Impacts to these valued and sensitive community viewsheds should be minimized to the extent possible during routing, thus it is important to define the KOPs' viewsheds. To accomplish this, a geographical information system ("GIS") viewshed analysis (ESRI ArcMap) is typically used.



**Figure 1:** Key observation point (KOP).

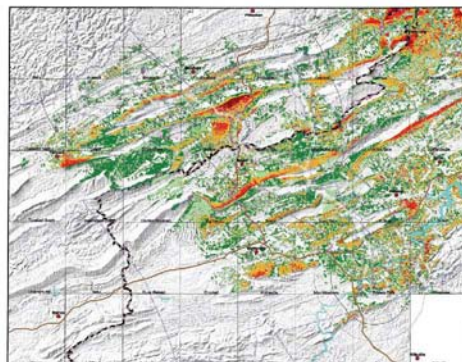


**Figure 2:** GIS Viewshed highlights sensitive areas to avoid. Generated from key observation points.

### ***GIS Viewshed Analysis***

GIS viewshed analyses are a major tool to mitigate aesthetic impacts during route development. The viewshed analysis uses three-dimensional terrain data to predict the area that can be seen from each KOP – its viewshed. Early visibility applications assumed a barren landscape. Arguments that a hurricane or other natural occurrence could affect existing vegetation are impractical and the concluding visibility is unbeneficial. Hence, existing vertical features such as trees and buildings should be included and draped on the terrain for meaningful results.

Knowing the most visible KOP areas provides the siting team with the opportunity to avoid them. For example, all KOPs located in a valley have views of a mountain peak; this peak clearly would need to be avoided. In the end, the viewshed analysis and mapping highlight the most visible areas by the study area's KOPs (see Figure 2). These results are combined with the KOP sensitivity level (scenic parkways have higher sensitivity levels than interstate highways), view distances (close-up views have higher impacts compared to background views), visual contrast levels (a residential area has higher visual contrast with a transmission line compared to an industrial area), and other visual analysis factors to avoid or minimize adverse impacts and develop alternatives and mitigations.

Furthermore, after alternatives are developed and structures preliminarily located, the area that a structure can see is generated – the structures' viewshed. In essence, eyeballs are placed on top of the structures. Running the analysis in reverse such as this, accounts for the structure height. For example, Structure No. 35 can see a historical resource, KOP No. 8, thus further analysis with visual simulations or line-of-sights would be justified and mitigations developed as practicable – such as modifying the structure location or point of observation screening.

Simply running the GIS viewshed from the proposed line without defining KOPs, provides inapplicable results and ignores the communities. For example, without KOPs and their analysis variables, a proposed line could be erroneously located in a densely, inhabited valley bottom, because the GIS viewshed area of the line appears low in the enclosed topography. This, however, would not happen if KOPs (parks,

residences, and other community features) are identified and considered. When used correctly, GIS viewshed analyses are valuable tools during route development.

### **Visualizations**

Visual simulations (see Figures 3 and 4), computer terrain models, and line-of-sight models illustrate degree of visual impacts, provide means to suggest mitigations, verify GIS viewshed analyses, and compare alternatives. Additionally, they are one of the best means of engaging decision makers, local officials and the public by showing them what the project will look like and dispelling exaggerated visions of the proposed project (IEA & LI 1995). For example, Figure 4 is a simulation used to show local officials what a proposed 161 kV line would like; it was helpful since the local officials believed the structure would be much larger. The project has progressed to completion.



**Figure 3:** Visual Simulation - used to analyze impacts and develop mitigations.



**Figure 4:** Existing view of a 69 kV line (left) and simulation of the proposed 161 kV line with distribution underbuild (right).



**Figure 5:** Helium-filled weather balloon at proposed structure location.

Occasionally, the public is skeptical of computer-generated visualizations and wants to see the proposal with its own eyes. For this reason, helium-filled weather balloons, flown at structure sites, can sometimes be more convincing (see Figure 5). This time-tested procedure was used extensively in Switzerland during the 1960s when poles had to be raised at the corners of proposed buildings so neighbors could envision the proposal (Schmid 2001). The negative aspect of visualizations (computer and balloon) is time and cost; nonetheless, this investment could avoid costly battles and mistakes later.

### **Existing Land Uses**

The route alternatives should be placed in compatible, existing land-uses to the extent practical. For example, few would complain about lattice towers in an industrial area (a compatible land use) where towers barely contrast with large buildings and smoke stacks; however, large structures near residential areas can result in a high degree of visual contrast (see Figure 6). We should note that residents are much more tolerant

of a transmission line when it pre-dates their development; see Figure 7, the existing 500kV line did not deter new residential development as shown.



**Figure 6:** Industrial land use (138 kV line) compared to a residential land use (500 kV line)

**Figure 7:** There is higher tolerance when the line pre-dates the development.

Additionally, utilizing existing farm, logging, jeep, and coal roads reduces access road development, resulting in less landscape scarring and aesthetic impacts. Hence, these land uses should be considered during routing.

### ***Paralleling***

Paralleling existing utility and non-scenic linear features such as natural gas lines, utility lines, railroads, roads and fence rows (see Figures 8 and 9) condenses aesthetic impacts to one corridor, reducing the before and after contrast as compared to a new line through an uninterrupted forest canopy. Paralleling, however, does have shortcomings. In Figure 8, the landscape could have absorbed one major line, but three have transposed the previous rural character into an industrial character. Other limitations include engineering code requirements and constraints (such as safety clearances), and reliability issues.

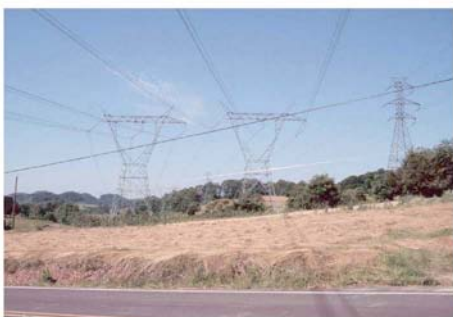


**Figure 8:** Utility corridor.



**Figure 9:** Low visual-quality, linear features (roads) should be paralleled or considered where possible.

### ***Offset Mitigation***

Offset mitigation is a creative way to reduce aesthetic impacts for the overall landscape at critical areas. There are various offsetting mitigation methods. On a new 765-kV transmission line, the removal of 17 miles of old transmission line and ROW is being phased in over a period of time, to partially offset impact to U.S. Forest Service lands. For another project (138kV line), a 69-kV line was retired and removed from the community's recreation area. Yet, another offset mitigation method is property exchange; for example, an equivalent property is exchanged to offset an impact of a proposed project. This type of mitigation is occasionally used

for conservation lands or forest resources. Hence, an impact is counter with a positive contribution to the overall landscape.

### ***Siting Team***

The siting team must digest the information and agree on acceptable routes that minimize not only aesthetic impacts but the many other competing environmental issues. This begins after data collection, stakeholder input, mapping, analyses, and field reconnaissance have concluded. At this point, the computer's job is over; people must ultimately site the routes – a computer cannot wear hiking boots nor comprehend beauty.

The siting team should consist of a diverse and experienced group of engineers (function), landscape architects (aesthetics), and ecologists (resource protection), and other as needed. Each member uses their expertise, best evaluation, and judgment to make difficult decisions. Often, they are faced with competing interests such as crossing of private lands as compared to state or federal lands, or visual impacts to scenic areas versus that to public or private properties.

### ***Corridors***

Initially, corridors (ranging from a minimum of 500 to 1,000 feet in width or more), not the final ROW, should be submitted for state regulatory approval. Later, a final ROW is sited within the corridor after completion of ground surveying, consultation with affected landowners, and final line design; this allows for one more opportunity to address engineering and environmental issues, constraints and impacts.

## **ENGINEERING**

Over the last hundred years AEP has built over 39,000 miles of transmission lines (including 2,100 miles of 765-kV lines). During this time, the new technologies and techniques that significantly reduce aesthetic impacts of transmission projects have developed. These advances include structure types, special structure and conductor finishes, conductor configurations, and maximizing the ROW.

### ***Structure Type - Flat Terrain***

For its 765-kV projects, a family of structures (four-legged lattice tower, guyed-v tower and tubular pole structure – depicted in Figure 10) has been developed. AEP draws from these designs to take advantage of each structure's individual characteristics to achieve the best fit with the visual landscape.

In flat terrain and in proximity to sensitive foreground (close-up) viewers (e.g., residences), the tubular pole structure is often favored by the public. Pole structures are a more accepted typology in residential and urban areas, being quite common in the urban distribution systems. See Figures 11, 12, and 13 for a comparison between pole and lattice structures.



**Figure 10:** AEP 765kV transmission structures: self-supporting lattice; guyed-v lattice; and tubular pole. Structure type is chosen based on topography, land use, land cover, and construction access.

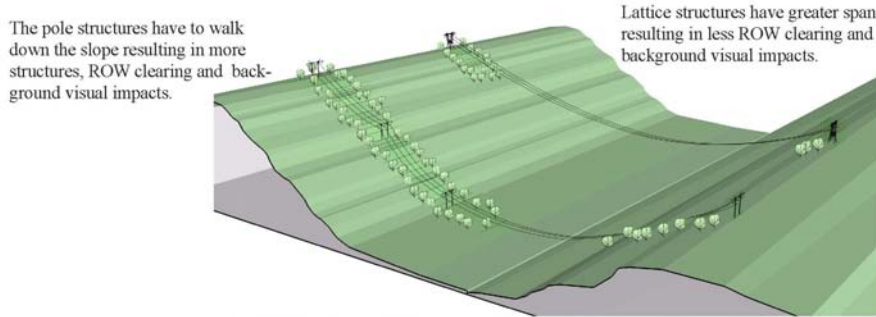


**Figure 11:** 765kV Lattice and H-Frame Pole Structure Comparison (Ridge and Valley Topography)



**Figure 12:** 765kV Lattice and H-Frame Pole Structure Comparison (Residential Land Use)



**Figure 13:** Visual simulations of 230kV (Double Circuit) Lattice and Pole Structure for Comparison.

### ***Structure Type - Mountainous Terrain***

The lattice structure is superior in mountainous terrain as compared to the pole. The lattice's long and high-span capability reduces structure numbers and ROW clearing (see Figures 11). In contrast, pole structures with short spans must walk down mountain slopes resulting in more structures, ROW clearing and aesthetic impacts.

Fewer structures reduces foreground to middleground visual impacts, while less ROW clearing reduces background impacts in mountainous terrain. Mountains rise

toward the sky making them iconic features carpeted with an uninterrupted forest canopy – due to the undevelopable slopes. To background views, the ROW clearing and shadow line appear as an unnatural slice through the forest, creating a high level of visual contrast (see Figures 14 and 15). Another advantage, the lattice's longer, higher spans provide the opportunity to minimize impacts on sensitive features like riparian areas, forest, scenic roads (see Figure 16), water courses and cultural sites.

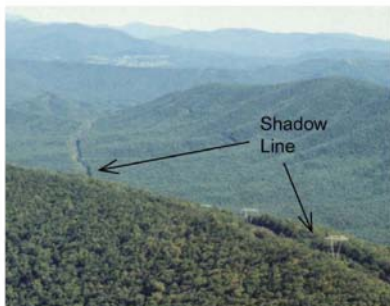


**Figure 14:** Lattice and tall structures should be utilized in unfragmented forest to reduce ROW clearing and shadow lines.

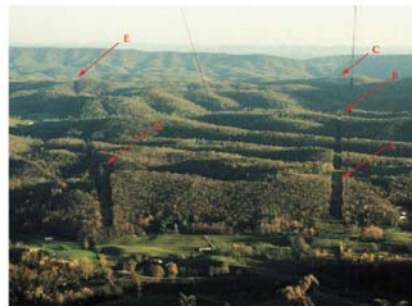


**Figure 15:** ROW visibility is the highest impact at background view distances.



**Figure 16:** Blue Ridge Parkway - a high span was utilized to avoid visual impacts on the scenic road.



**Figure 17:** Darkened steel structure.



**Figure 18:** Darkened steel and galvanized steel (left); non-specular conductor and typical conductor (right).

### ***Low-Reflectivity Materials***

Darkened or low-reflective materials (see Figures 17 and 18) for structures and conductors reduce the visual impact of transmission facilities. This is of particular benefit when the project is first constructed when it is most prominent; in contrast, the traditional shiny, galvanized finish appears synthetic at first, especially when contrasted with a natural landscape. The darkened effect is achieved by various treatments to the material surface during the fabrication process. Furthermore, dark and low reflectivity hardware, such as yoke plates, spacers, guy hardware and insulators can also reduce aesthetic impacts. There is, however, a premium associated with the low-reflectivity materials.

### ***Conductor Configuration***

New conductor configurations for extra high voltage (“EHV”) transmission lines reduce the audible noise produced by the corona on the conductors. Noise reduction reduces the transmission line presence and thus its visual attention. The new configuration, six-conductor bundle was used on AEP’s latest 765-kV line in West Virginia and Virginia to decrease noise level, particularly at higher elevations. In

practical terms, the new design cuts the audible noise level by half for a person standing 100 feet from the edge of the ROW. Furthermore, the use of a six-bundle configuration, as compared to a four-bundle configuration, reduces the individual conductor diameter (gauge), resulting in a lighter grey conductor and shadow and slightly less visibility.

### ***Maximizing the ROW***

Aesthetic impacts can be further reduced by maximizing the ROW with efficient designs. Modern EHV transmission lines have unparalleled performance and efficiencies, resulting in less environmental impact since fewer lines and less ROW need to be constructed. For example, one 765kV line requires 200 feet of ROW, while an equivalent number of 345kV lines requires 900 feet ROW (see Figures 19 and 20).

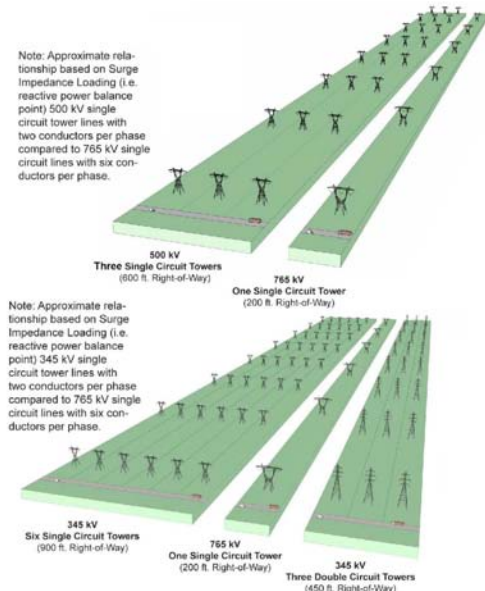


**Figure 19:** ROW width comparison between one 765kV structure and equivalent options



**Figure 20:** Visual impact comparison between one 765kV structure and equivalent 345kV (double circuit) option



**Figure 21:** Double circuit 138kV with distribution underbuild attached.

Another ROW maximizing technique is underbuilding and multi-circuiting. Underbuilding is when a new structure is engineered to include the proposed transmission and an existing distribution line (see Figures 4 and 21). The advantage

of this is when the existing distribution ROW and the proposed transmission ROW are co-located to minimize impact. Multi-circuiting is when transmission lines are combined on the same structure (see Figures 13, 21, and 28). For example, single lower-voltage regional circuits (230kV or less) can sometimes be combined onto one larger and taller structure. In very limited cases, a single EHV circuit (765kV or 500kV) can be combined with a single lower voltage regional circuit (230 kV or less); this, however, may require tower designs that have not been achieved to date. Two bulk transmission lines, such as 765kV and 500kV, should not be combined on the same structure due to reliability concerns.

## CONSTRUCTION

After the transmission line is sited, approved, and engineered, aesthetic attention should be integrated throughout construction. Much of this responsibility falls on the construction management team. During and after construction, the team should develop strategies to reduce construction impacts, monitor and address unforeseen aesthetic impacts, verify restoration and revegetation, and confirm cleanup. The following are mitigation examples during construction.

### *Vegetation Clearing Plan*

As repeated throughout this paper, minimizing ROW clearing is an important aesthetic mitigation. To this end, a vegetation clearing plan should be prepared to direct the clearing operations and to avoid over-clearing. Generally, trees in valleys and lower elevations, except for those locations where trees are tall enough to threaten the safety and reliability of the line, should not be cleared. Frequently, low-growing species such as redbud and dogwood are compatible with transmission line operations and left in the ROW in environmentally sensitive areas. Figures 22 and 23 are examples of selectively-cut ROWs. EHV lines are the exception due to their national importance and clearing procedures are often inflexible.



**Figure 22:** Low-growing and compatible vegetation should be preserved in ROW where practical.



**Figure 23:** Low-growing and compatible vegetation should be preserved in ROW where practical.

### *Minimizing Disturbance*

The construction management team should determine, mark, and enforce the limits of construction activity to prevent unnecessary impacts, and where appropriate, include mitigations in the construction specifications and contract(s). For example, all construction vehicle movement outside the ROW should be restricted to pre-

designated access, contractor-acquired access, or public roads. During clearing of trees and vegetation, activities should be limited to the ROW area and to dangerous trees located along the edge of the ROW, while trees not identified for removal should be protected to the extent practical. Furthermore, tree debris from ROW clearing should be scattered randomly onto non-seeding areas to maintain a more appropriate texture and low contrast with adjacent vegetation patterns. At sensitive or remote areas (i.e. federally designated roadless areas), helicopter erection could be a potential mitigation; this option can reduce construction road impacts, resulting in less aesthetic impacts.

### ***Feathering ROW Edges***

The United States Forest Service (“USFS”) occasionally suggests selected tree removal in graduated percentages outside the ROW edge to reduce the strong ROW shadows (USFS 2002). AEP experimented with this technique and concluded it is ineffective due to the dominating width of the ROW (see Figures 24 and 25). To be effective, an excessive quantity of mature trees would need to be removed, thus making the mitigation impractical and counterintuitive. Further research is needed to determine if ROW feathering could be effective on narrower ROWs such as 100 feet width or less. Nevertheless, this would be a rare mitigation used only at critical ridge crossings.



**Figure 24:** The 765kV ROW before feathering mitigation.



**Figure 25:** The ROW Feathering was unsuccessful - little effect due to the scale of the ROW and view distance.

### ***Natural Shapes***

Natural appearing shapes reduce visual contrast with the adjacent landscape. Hence, during construction, vegetation clearing for ROW, access roads, and staging yards should use curvilinear and natural appearing boundaries instead of straight lines to the extent practical and grading should be performed in a manner that minimizes erosion and conforms to the natural topography. Additionally, alignment of any access roads or cross-country routes should follow the landform contours to minimize ground disturbance and/or reduce scarring (visual contrast) of the landscape.

### ***Restoration***

Seeding and fertilizing (Figure 26) in areas of cut and fill disturbance speed revegetation, provide screening, reduce erosion, promote and maintain wildlife

habitat, reduce invasion pressure by non-native plants, reduce bird nest parasitism and predation, and restrict access by off-road vehicles. Material should be native, perennial, and compatible in color to the adjacent landscape and installed as soon as possible after grading.



**Figure 26:** 765kV ROW - Restoration and revegetation

## POST-CONSTRUCTION

### *Mitigation*

Occasionally, unpredicted aesthetic impacts occur during construction; these should be addressed proactively and in a timely manner. Figure 27 is an example of an unforeseen impact. At the request of residents in the immediate foreground views of the transmission line, vegetation buffers should be considered where effective and practical to limit views of the line. At critical visual areas (e.g., a greenway trail), new trees should be strategically grouped and planted either at the view point or near the transmission line, to break-up visibility of the line.



**Figure 27:** 765kV Line: Mitigation plan was developed during construction review.

### *Project Environmental Management System (EMS)*

An EMS should be established for each project's lands and ROW – a management strategy and operational framework to protect/restore habitats and ecosystems, which ultimately increases landscape health and aesthetics.

*Most EMSs are built on the "plan, do, check, act" model. This model leads to continual improvement based upon: Plan – planning, including identifying environmental aspects and establishing goals; Do – implementing, including training and operational controls; Check – checking, including monitoring and corrective action; and Act – reviewing, including progress reviews and acting to make needed changes to the EMS. (USEPA 2009)*

The EMS not only manages habitats, ecosystems, and vegetation but other issues such as ROW usage. As mentioned earlier, the ROW clearings, especially on mountains, can be a large impact to background views. Uses that encourage erosion scarring on mountain slopes such as all-terrain vehicles ("ATVs") should be restricted – barriers (access gates, woody material and tree slash, tank traps, and ditches) should be installed at strategic locations to discourage and prevent inappropriate use on the ROW. In contrast, for low voltage lines located in areas near communities, consider public ROW access such as trails (see Figure 28), recreation fields, or nature areas. These amenities benefit the community and offset impacts. For lands not owned in-fee simple, the EMS must be created with landowner cooperation and support. The final form of the EMS could include documents, plans, GIS, maps, inventories, and so forth.



**Figure 28:** Multi-circuit line and public ROW use (bicycle trails).

Furthermore, an EMS should build off of existing research and standards. For example, the Electric Power Research Institute (EPRI) has co-sponsored (with various utilities, academics and agencies) the development of integrated vegetation management (IVM) performance standards to provide a system for assessing the efficiency and effectiveness of the ROW vegetation management (EPRI 2006). IVM is an operational-level component of an EMS (Novak *et al* 2008). Continuing research, such as IVM standards, is needed to evaluate and determine the most effective strategies.

## CONCLUSION

New transmission lines are vital to update the current system and to make renewable energy sources accessible. The electricity delivery system in the United States is characterized by an aging infrastructure and largely reflects technology developed in

the 1950s or earlier (Edison Electric Institute 2009). Over seventy percent of transmission lines are 25 years or older (Center for Smart Energy 2005), yet Americans are using 13 times the electricity they used a half century ago (Tierney 2008). As a result, the system is being pushed to serve regional power markets and to perform functions for which it was not originally designed.

Additionally, access to domestic energy resources is vital to our national security and energy independence (Tierney 2008). An efficient, interstate transmission superhighway is required today to access America's clean, renewable generation. AEP's chairman, president, and CEO Michael Morris states "the Dakotas, Minnesota and Iowa have some of the very best wind generation resources in the United States, but the wind potential in this region cannot be developed unless we build a very efficient transmission superhighway to bring this clean, renewable generation to population and electricity load centers" (Morris 2008). "Transmission's role in solving these national challenges [i.e., development of domestic energy resources] is too often overlooked as the focus shines on power plants and demand-side measures. But inadequate attention to enhancing the nation's electric transmission system will undermine – if not prevent – our ability to satisfy our national economic goals while also addressing climate change and our needs for energy independence" (Tierney 2008).

To address the challenge of future expansion, not only are aesthetic mitigations for transmission projects needed, the industry will need to think out of the box. Bridges that were once considered eyesores are now considered architectural assets and engineering achievements. Perhaps, to a degree, the same can be true for transmission lines. Imatran Voima Oy ("IVO"), the largest utility company in Finland, is doing some motivating work with transmission structures. They are incorporating artistic features into their structures to break up the "monotony" perceived in transmission lines. This work has yielded a family of structures that are both pleasing to the eye and may be mass-produced at reasonable cost (Nieminen 1996). In Korea, 300-foot 765 -kV structures were developed to span over trees to completely eliminate ROW clearing and maintenance.

Because of the recent power outages to our transmission systems in California and the Northeast blackout in 2003, Americans are beginning to understand that new transmission lines are essential and necessary. Electricity is fundamental to our quality of life (Tierney 2008). Few citizens, however, are tolerant of high-voltage transmission lines, let alone the superhighway proposed for an extra high-voltage system. This deep protective instinct in their valued viewsheds makes aesthetic mitigation a formidable challenge. Nevertheless, through collaboration – case studies, modern designs, new approaches, and on-going research – we will expand and strengthen the nation's electrical grid, access renewable energy resources, and invent modern solutions to these aesthetic challenges.

## REFERENCES

Center for Smart Energy (2005). *The Emerging Smart Grid: Investment and Entrepreneurial Potential in the Electric Power Grid of the Future*. (October 2005), p. 9.

Edison Electric Institute (2009). "Supply and Demand: Supplies are Shrinking, Systems are Straining." Website, accessed 5 February 2009, from <http://www.getenergyactive.org/supply/problem.htm>.

Federal Power Commission (1970). "Guidelines for the Protection of Natural, Historic, Scenic, and Recreational Values in the Design and Location of Rights-of-Way and Transmission Facilities." Adopted by the Federal Power Commission in Order No. 414 issued November 27, 1970, and now applied by Federal Energy Regulatory Commission. Copies may be obtained from the Office of Public Information, Federal Energy Regulatory Commission, Washington, D.C. 20426.

IEA & LI (Institute of Environmental Assessment and the Landscape Institute) (1995). *Guidelines for Landscape and Visual Impact Assessment*. London: E&FN Spon.

Morris, M. G. (2008). "AEP To Pursue Development Of Transmission Superhighway To Transport Renewable Energy Across The Upper Midwest." Website, news release, accesses 5 February 2009, from <http://www.aep.com/newsroom/newsreleases/?id=1515> (Dec. 2, 2008).

Nieminen, K. (1996). "Poles & Structures Transmission Structures as Landscape Art Artistic and structural design are blended to create a visually appealing transmission line." *Transmission and Distribution World*. Website, accessed 8 January 2009, from <http://www.tdworld.com> (May 1, 1996).

Nowak, C. A., Ballard, B.D., Greninger, L. K., and Venner, M. C. (2008). "Performance Standards for Assessing Vegetation Management on Rights-of-Way: Case Study of New York DOT's Roadside Rights-of-Way Vegetation Management Program," in Goodrich-Mahoney, J. W., Abrahamson, L., Ballard, J. and Takalsky S. (eds.), *8th International Symposium on Environmental Concern in Rights-of-Way Management*, September 12-16, 2004, pp. 113-126. Elsevier Science.

Schmid, W. (2001). The emerging role of visual resource assessment and visualization in landscape planning in Switzerland. *Landscape and Urban Planning*, 54, pp. 213-221.

Tierney, S. F. (2008). "Vision for a 21<sup>st</sup> Century Interstate Electric Highway System," White paper commissioned by AEP from Analysis Group, Boston, MA.

USDA (U.S. Department of Agriculture) (1974). *National Landscape Management, Volume 2 (Visual Management System)*. U.S. Government Printing Office, Washington, D.C.

USDA (U.S. Department of Agriculture) (1995). *Landscape Aesthetics: a handbook for scenery management*. Agriculture Handbook No. 462. U.S. Government Printing Office, Washington, D.C.

USEPA (U.S. Environmental Protection Agency). 2009. Internet website: [www.epa.gov/ems/info/index.htm](http://www.epa.gov/ems/info/index.htm), accessed on 5/29/2009.

USFS (U.S. Forest Service) (2002). *AEP 765kV Transmission Line (Jacksons Ferry, Virginia to Oceana, West Virginia)*. Supplemental Draft Environmental Impact Statement, Volume II, pp. 2-20.

*The authoring team would like to thank Robert Brandner of American Electric Power for his efforts reviewing and editing this paper.*

## Alabama Power Increases Line Capacity Using 3M ACCR Conductor (On Existing Towers)

Howard A. Samms<sup>1</sup>

<sup>1</sup>Southern Company Transmission / Alabama Power Company, 600 North 18<sup>th</sup> Street, Birmingham, AL 35203; PH (205) 257-1959; FAX (205) 257-4364; Email: [hsamms@southernco.com](mailto:hsamms@southernco.com)

### ABSTRACT

Alabama Power has successfully installed the new 3M Aluminum Conductor Composite Reinforced (ACCR) high temperature, low sag conductor on a 2.5 km (1.5 miles) section of a 230 kV transmission line, utilizing the existing lattice steel structures located in a congested corridor with 230 kV and 500 kV line crossings. The upgrade was necessary to provide additional capacity to meet future (short term) load demand and line loading under contingency conditions. This paper provides a case study of the evaluation, selection and installation of the 3M conductor and highlights the challenges during the design and construction stages of the project.

### INTRODUCTION

The Gorgas to Miller 230 kV transmission line was originally designed and constructed in 1956 as the Gorgas to Boyles 110 kV transmission line (North leg). The line consisted of multi-pole wood structures with 795 kcmil 26/7 ACSR conductor. In 1972, with additional insulation and structure modification where necessary, the line was up-rated to operate at the 230 kV voltage level.

With the construction of the Miller Steam Plant in 1975, the Gorgas to Boyles line was sectionalized and looped through the newly constructed Miller SP Substation creating the new line segments; Gorgas - Miller 230 kV transmission line (GMTL) and Miller – Boyles 230 kV transmission line. The two new line sections from the new Miller substation to the existing transmission line were constructed on lattice steel towers with 1351 ACSR conductor.

In 2006, Alabama Power Company (APCo) laid out a multimillion dollar plan to install Flue Gas Desulfurization (Scrubber) facilities at its fossil fuel plants as part of its environmental commitment to reduce sulfur and mercury based emissions. The Miller Steam Plant (SP) was one of the four locations where the Scrubbers would be installed and had a deliverable date of 2010 – 2011. Load flow and system reliability studies by APCo's Transmission Planning identified the existing GMTL as the line to best serve the loading from the new substation required for the Scrubber facilities. The objective was to have a line capacity to satisfy a loading of 1500 Amps (peak and

contingency loadings) by the end of 2010 and a maximum 1900 Amps for future load increase.

The solution, as proposed in the report from Transmission Planning, was to replace the existing conductor on the GMTL with new conductor and have a loop in loop out configuration to the new Miller Scrubber substation as shown in Figure 1. The transmission line segment between the Miller SP substation and the new Miller Scrubber substation would therefore consist of a 0.97 km (0.6 miles) line section of steel lattice towers and a 1.45 km (0.9 miles) line section of single and multi-pole concrete structures including a 0.48 km (0.3 miles) relocated new line section. The steel tower line section is located in a highly congested area due to the presence of nine other transmission lines emanating out of the Miller SP substation (Figure 2). The primary line design objective therefore, was to use the five existing towers to support the new conductor with minimum or no structure modification.

## CONDUCTOR SELECTION

The line parameters for the tower line section are;

Line voltage – 230 kV;

Line Section Length – 0.97 km (0.6 miles);

Ruling Spans – 77 m, 204 m, 363 m, 263 m (254 ft, 670 ft, 1190 ft, 864 ft);

Existing Conductor – 1351 kcmil 54/19 strands ACSR;

Allowable Maximum Conductor Tension (tower design) – 77,872 N (17,500 lbs);

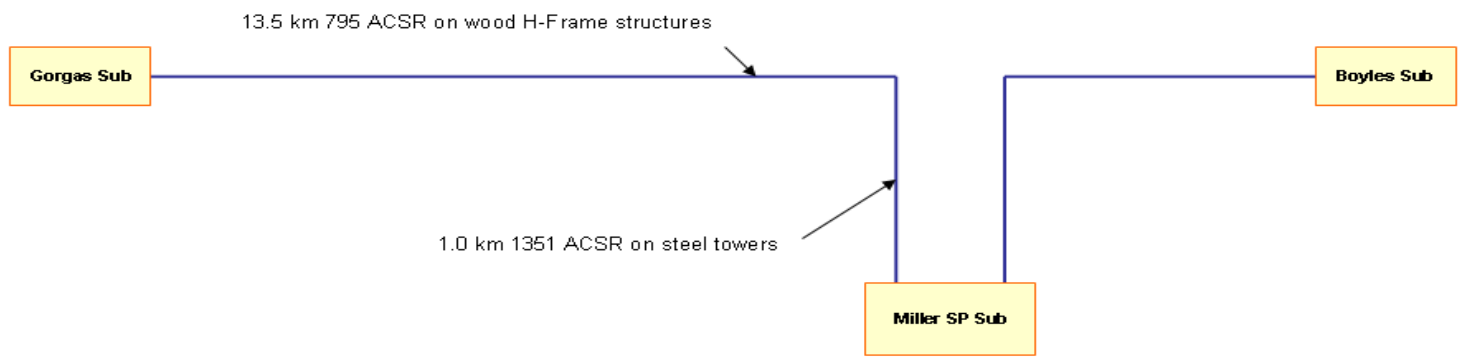
Design Maximum Line Loading – 1900 A

Utilizing aerial survey data, the line sections were modeled in PLS-CADD. Method 4 models were developed for the concrete pole structures using PLS-POLE and method 1 models were used for the lattice steel towers. The initial recommendation from Transmission Planning was to use 1351 54/19 ACSS for the conductor replacement. However, initial line design analysis identified conflict in clearances to ground and obstacle crossings including a railroad and a 230 kV transmission line. Consequently, an alternative solution was explored with the new 1033 54/19 ACCR conductor.

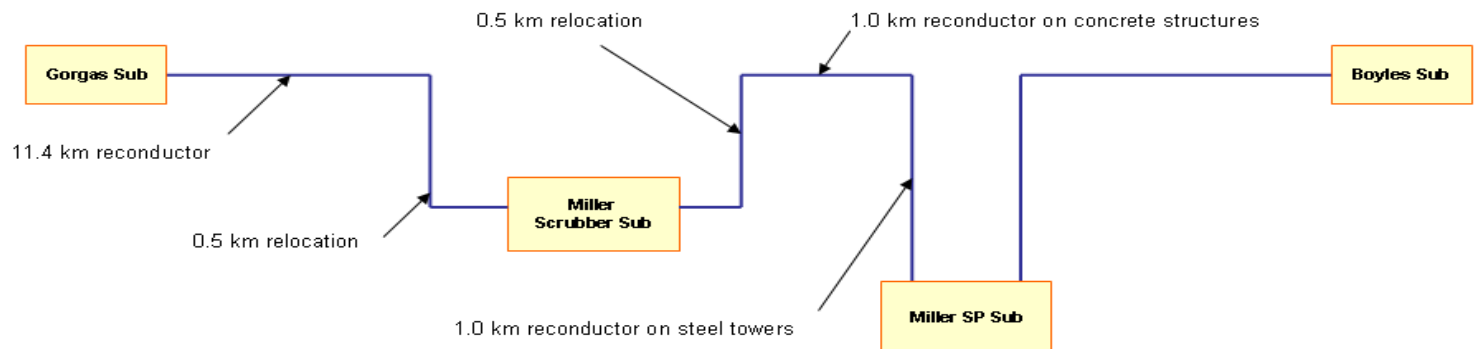
The 1033 ACCR is from a relatively new family of high temperature, low sag conductor manufactured by the 3M Company. The stranded core of metal matrix aluminum composite wires are surrounded by aluminum-zirconium alloy strands resulting in a composite conductor with superior mechanical and thermal properties compared to the more traditional ACSR conductor.

The following details the result of the evaluation of both the 1033 ACCR and 1351 ACSS conductor as a replacement to the existing 1351 ACSR conductor.

**Conductor Ampacity.** Both proposed conductors have the capacity to satisfy the design maximum line loading of 1900 A. At 40 °C ambient temperature, the 1033 ACCR conductor operating at 200 °C has ampacity of 1925 A and the 1351 ACSS conductor operating at 160 °C has ampacity of 1989 A.



*Transmission subsystem before addition of the Miller Scrubber substation*



*Transmission subsystem after addition of the Miller Scrubber substation*

**Figure 1: Schematic of GMTL before and after the Miller Scrubber Substation**

Telegram Channel: @Seismicisolation

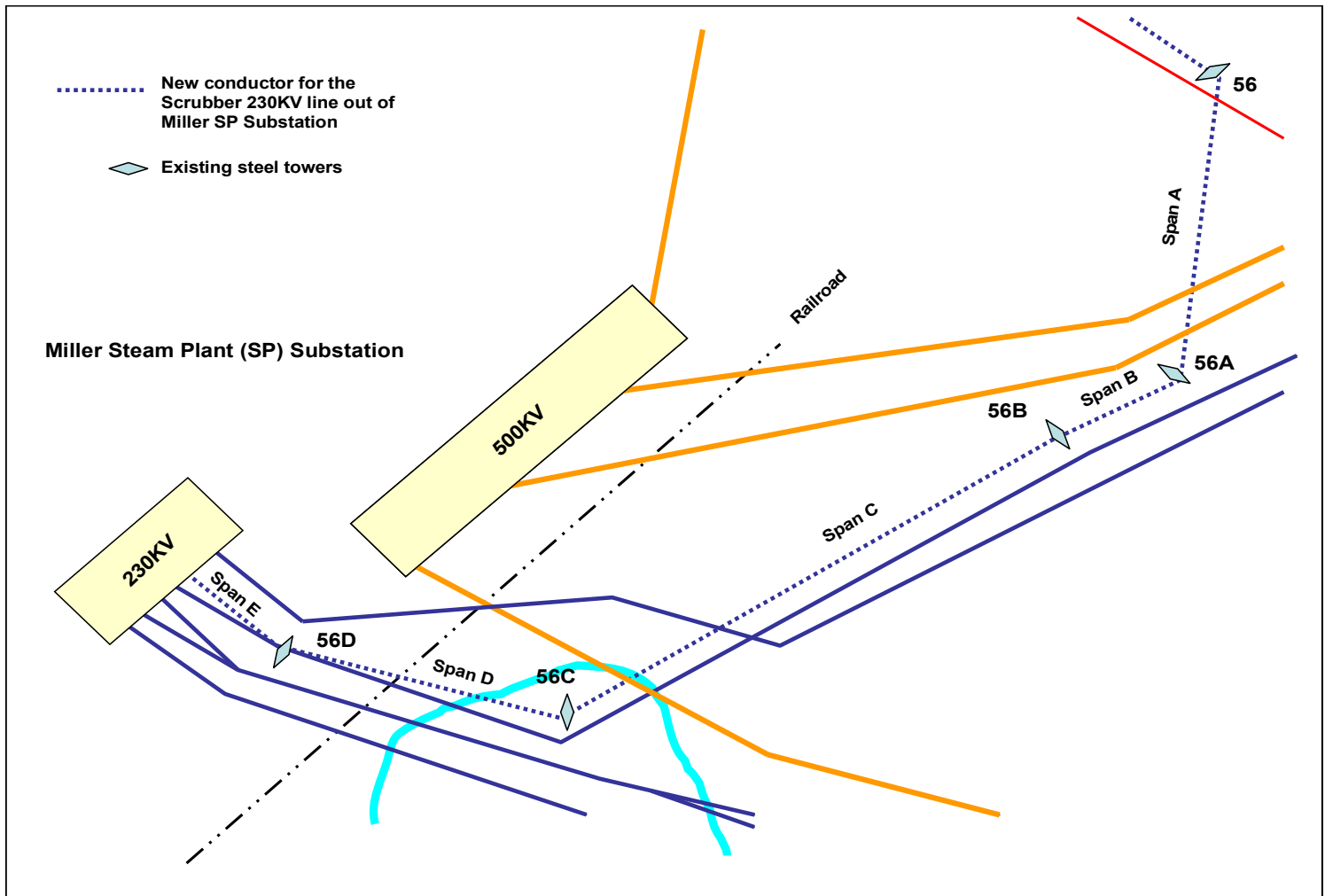


*Figure 2: Transmission Lines out of the Miller SP Substation*

Telegram Channel: @Seismicisolation

**Structure Loading.** The conductor loading criteria was the NESC Medium loading. With the conductors auto sagged in PLS-CADD, the 25% bare final was the limiting condition for both the 1033 ACSR and the 1351 ACSS conductor tension. The maximum tension for the conductors as shown in Table 1, were both below the allowable 77,872 N (17,500 lbs). Table 1 also shows the diameter and unit weight of the 1033 ACSR and 1351 ACSS conductors compared to the existing 1351 ACSR. With the lower tensions and equal or lower unit weight and diameter of the new conductors, the steel towers would not experience an increase in loading compared to the 1351 ACSR conductor; hence the ability to utilize the five existing towers in the main line without any structural capacity improvement.

**Table 1: Comparison of 1351 ACSR with 1033 ACSR and 1351 ACSS**

Description	Conductor Type		
	1351 ACSR	1033 ACCR	1351 ACSS
Stranding	54/19	54/19	54/19
Cable Diameter (mm)	36.1	31.6	36.1
Weight (N/m)	25.3	16.5	25.3
Ultimate Strength (N)	206,000	157,833	161,080
Maximum Tension (N)	75,645	61,410	55,623
Coeff. of Expansion of Core (/ °C)	$6.4 \times 10^{-6}$	$3.5 \times 10^{-6}$	$6.4 \times 10^{-6}$
Ampacity (Amps) & Conductor Temperature -(@ 40 °C Ambient)	1456 100 °C	1925 200 °C	1989 160 °C

**Conductor Sag.** With the conductors displayed at maximum operating temperature of 160 °C (320 °F) for the 1351 ACSS and 200 °C (392 °F) for the ACSR, the final sags were compared with the 1351 ACSR conductor at 100 °C (212 °F). The length and final sags for each span are shown in Table 2.

**Table 2: Comparison of Final Sags**

Span ID.	Span Length (m)	Ruling Span (m)	1351 ACSR Final Sag @ 100 °C (m)	1033 ACSR Final Sag @ 200 °C (m)	1351 ACSS Final Sag @ 160 °C (m)
A	263	263	8.0	8.0	10.2
B	91	363	0.8	0.8	1.0
C	405	363	15.9	15.7	20.7
D	204	204	5.7	5.7	7.4
E	77	77	2.3	2.4	2.8

The 1351 ACSS conductor had higher final sags compared to the existing 1351 ACSR. Span E conductors terminating on the substation structure were sagged in at reduced tension for the conductor models, thus accounting for the smaller variance in final sags.

For the 1351 ACSS conductor, the PLS-CADD report identified clearance violations in 3 of the 5 spans in the tower line section. Ground clearance was not achieved in Span A and obstacle clearances were violated in Spans C and D (the shield wire of a 230 kV line and a rail road crossing respectively). Table 3 shows the extent to which the clearances were exceeded in each span.

**Table 3: 1351 ACSS Clearance Violation in Affected Spans**

Spans ID.	Span Length (m)	Extent of Clearance Violation (m)	Object Under Line
A	263	1.2	Ground / Road
B	91	-	-
C	405	2.4	Shield wire (230 kV TL)
D	204	0.6	Railroad
E	77	-	-

The higher sags of the ACSS conductor reduced clearances to ground and other obstacles crossing under the transmission line. Consequently, the challenge was to achieve the required clearances over ground and the other crossings.

Improving vertical clearances by installing two taller towers at structures 56 (+4.6 m) and 56C (+5.5 m) in the GMTL created new conflicts with the 500 kV transmission lines crossing above in spans A and C (See Figures 3 & 4). Consequently, three new 500 kV towers would be required as intermediate or replacement structures for the crossing transmission lines. The installation of five new towers would present significant challenges with transmission line availability, system exposure during line outages, location of new 230 kV towers and structure installation in a congested and possibly an energized environment.

The lower sags of the 1033 ACCR conductor provided an ideal solution given the various constraints. The lower unit weight and lower coefficient of thermal expansion resulted in final sags of the 1033 ACCR conductor at 200 °C that were comparable (within a 0.5 m variance) to the final sags of the 1351 ACSR at 100 °C; hence the clearances to ground and crossing obstacles were not violated.

**Construction Cost and Time.** The construction cost of the 1033 ACCR option was estimated at **\$2.32 M** which is 12% less compared to the cost for the 1351 ACSS option at **\$2.64 M**, representing a savings of over \$300,000. Unaccounted cost that could also be associated with the 1351 ACSS option includes (a) loss of revenue during outages (minimum 6 days total) on the three 500 kV lines during tower installation; and / or (b) incremental increase in cost for alternative but more expensive power generation or load transfer during line interruptions.

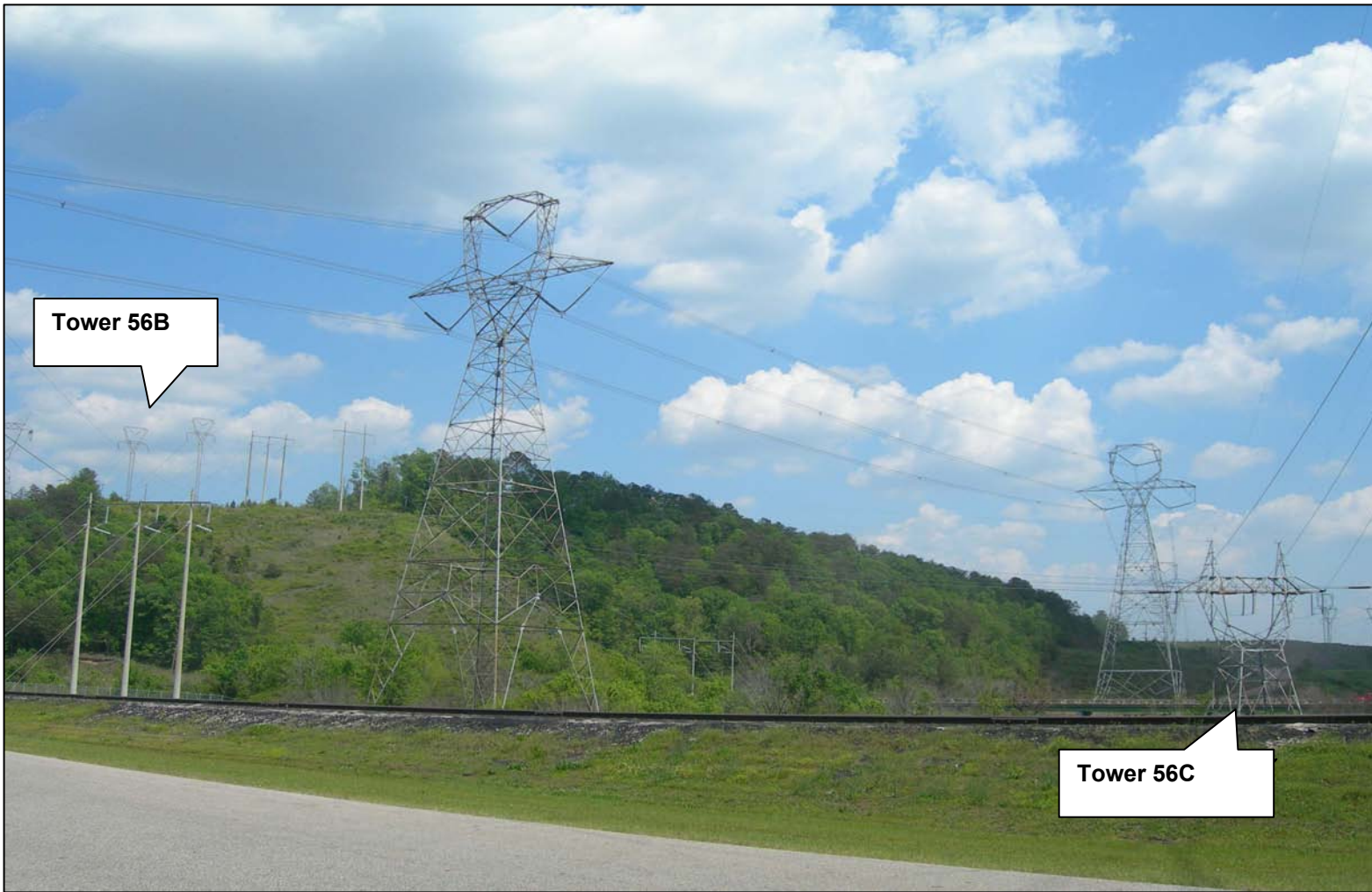


**Figure 3: Conductor in Span C crossing 230 kV and 500 kV transmission lines**

Telegram Channel: @Seismicisolation



**Figure 4: Conductor in Span A crossing (2) 500 kV transmission lines and a roadway**

Telegram Channel: @Seismicisolation

Another significant benefit of selecting the 1033 ACCR option was the time savings that resulted from eliminating the design, manufacture and installation of new towers. The 1351 ACSS option with the five new towers was expected to take a longer time for the design, tower supply and construction; and would also require a higher number of interruptions necessary for installation, including outages on the three 500 kV lines.

The selection of the 1033 ACCR conductor for the Gorgas to Miller Scrubber transmission line job was therefore based on; (a) the adequacy of the conductor in meeting the technical requirement of the project; (b) the overall lower installed cost and shorter construction time; (c) the ability to utilize the existing towers; and (d) that no interruption or modification to the 500 kV transmission lines would be required.

### INSTALLATION OF THE 1033 ACCR

The construction contract for the job was awarded through the normal bidding process. Presentations were made by APCo's construction supervisors and the 3M's installation representative to familiarize the prospective bidders with the particular requirements of the new ACCR conductor. After the bid selection and contract award processes were completed, follow up meetings were held between the successful bidder, 3M and APCo in working out the construction schedule and implementation strategies in more details. 3M's installation representative would be on the job site for the entire construction period.

In consultation with the Alabama Control Center (ACC), the GMTL had to be available for the summer period from June 1 to August 31, 2008. Therefore, the implementation plan was to install the new ACCR conductor on the existing structures up to the point where the relocation started, as the first phase of construction. This phase of the job was done during the period January to May 2008. The line would be returned to service June 1 to August 31 and then the relocation section was done September 1 to December 31, 2008 as the second phase of construction.

The installation of the 1033 ACCR required a few specialized tools and equipment including a 100 ton press, a 10,000 psi pump and high temperature compound for the compression dead end clamps. In order to minimize the bending radius of the conductor, a bull wheel tensioner of 180 cm (72") diameter or larger was recommended. Roller array blocks were used at vertical and or horizontal angles exceeding 30°, as well as break-over angles. Distribution Grips were exclusively used to grip the ACCR conductor and could be re-used for pulling up to 3 times before discarding.

The construction crew experienced no major problems with the installation of the ACCR conductor. With the appropriate on site training and proper coordination at all levels, the job was safely executed and both phases were completed ahead of the planned schedule.

## CONCLUSION

Given the challenges of working in a highly congested area involving some critical 230 kV and 500 kV transmission lines, the 1033 ACCR solution provided an ideal application of the new 3M high temperature, low sag conductor on existing towers in a cost effective manner.

The successful installation of the ACCR conductor was primarily due to the professional and team work approach of the 3M representatives, the contractor, APCo's inspector, construction supervisors and transmission line designers and the ACC.

Our ability to meet the system requirement of increasing the line capacity and satisfying the load demand of the Miller Scrubber facility will serve to ensure the future reduction of emissions and their impact on the environment.

## REFERENCES

- PLS-CADD, (1992), *Power Line Systems – Computer Aided Design and Drafting*,  
Power Line Systems, Inc., Madison, Wisconsin.
- PLS-POLE, (2000), *Analysis and Design of Structures with Wood, Laminated Wood,  
Steel, Concrete and FRP Poles or Modular Aluminum Masts*, Power Line  
Systems, Inc., Madison, Wisconsin.

## Golden Pass LNG 230kV Double Circuit

### FOUNDATIONS

Ernest C. Williamson, Jr.<sup>1</sup>, Ronald L. Rowland<sup>2</sup>

#### Abstract

This paper describes the foundation challenges involved in building a new 12-mile 230kV double circuit line. The project consists of 228 pole structures on base plated steel caissons. Portions of this line are located in a coastal salt marsh, adjacent to a state wildlife sanctuary. Other portions wind their way along an environmental superfund site, and through multiple refinery, petrochemical, and heavy industrial facilities that have been under continuous use since the early 1900's. Current environmental and wildlife restrictions as well as requirements for hurricane loadings ruled out many conventional forms of design and construction, as did restrictions imposed by industrial facilities along the route that severely limited access. Because of this, a decision was made to use helicopter construction over much of the project. Structures and caissons were designed and constructed in sections to allow the use of a helicopter to lift to its maximum capacity. The helicopter then transported and installed each section at its intended location. In some instances where the steel caisson foundations were too heavy for the helicopter to lift, they were manufactured in two pieces and field welded. The various foundations features involved in meeting an aggressive in-service date under difficult conditions are described in the paper.

#### Introduction

Entergy Gulf States Texas initiated this project in the fall of 2004 to provide service to a Liquefied Natural Gas (LNG) facility to be operated by Golden Pass LNG Terminal, LLC located near Sabine Pass, Texas. New Keith Lake Substation serves the facility and is fed from Entergy's Port Acres Bulk Substation located in Port Arthur, via a 230 kV transmission line approximately 12 miles in length.

The bulk of route selection, environmental assessment, preliminary soil testing, and scope document preparation was performed in 2005 and 2006. The Public Utility Commission of Texas requires an application for a Certificate of Convenience and

---

<sup>1</sup> Staff Engineer, Entergy Services, Inc., 120 W. Mayes St., Jackson, MS, 39213, 601-368-2011,  
ewilli2@entergy.com

<sup>2</sup> Manager, Transmission Line Design, 2121 38<sup>th</sup> St., Kenner, LA, 70065, 504-463-2974,  
rrowlan@entergy.com

Necessity, which includes a routing study and Environmental Impact Statement. The northern third of the proposed route passed through a number of industrial properties located southeast of Port Arthur, and continued south along Texas State Highway 87 for the remainder of the distance. A portion of the route had to be reassessed with the proposed addition of a second LNG facility to be operated by Sempra Energy. The second LNG will require construction of future Round Lake Substation located between Port Arthur and Sabine Lake. The location of the new substation required that the line be moved approximately seven tenths of a mile westward into the marsh. Highway 87 is expected to follow the same route around the proposed facility, but relocation of the highway has not yet occurred. A map of the route and surrounding area is presented as Figure 1.

Initially there was considerable resistance to the proposed route from a number of sources. As part of the permitting process, a number of design constraints were introduced to the project, including limiting the height of the proposed line and installing devices on the wires that would make them more visible to the birds in flight. With the assistance of Thomas & Betts, numerous line and structure configurations were evaluated to address feasibility considering the project constraints. PUCT approval of the selected pole and line configurations came in August of 2006.

Additionally the owners of industrial facilities on the north end of the route voiced numerous concerns regarding pole placement, structure type, soil sampling, means of access, etc. These concerns resulted in negotiations that were not satisfactorily resolved until mid

2007. Soil data along industrialized portions of the route became available in September, allowing for final designs and procurement of poles and steel caisson foundations by December. Thomas & Betts received the order to supply the galvanized steel poles and caissons. Project construction was completed between April and July of 2008.

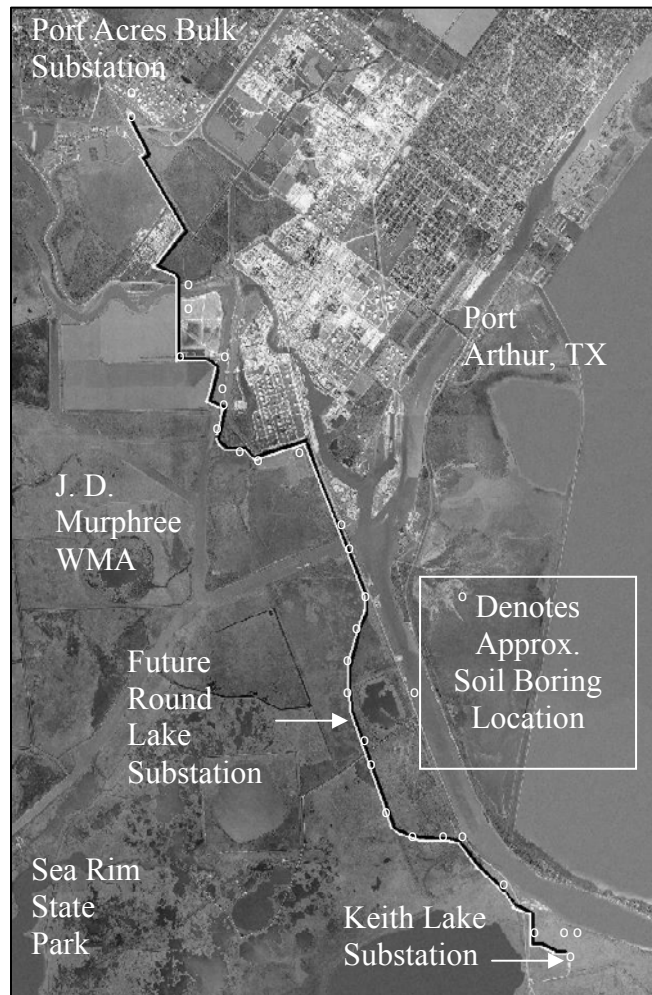


**Figure 1 – Project Map**

## Soil Testing

A total of 30 soil borings were performed in two phases to support this project. While numerous natural variations in stratification and soil properties were observed, soil borings generally conformed to one of four simplified soil profiles as shown in Figures 2.

Initial borings were performed in June of 2005 during preparation of project estimates, and consisted of nine borings along the southern two-thirds of the proposed route. Several existing borings at the Port Acres Bulk Substation on the north end of the project were also available. At the time the initial project estimates were prepared it was assumed that the line would be located just off the highway right-of-way, although the Port Arthur LNG (Sempra) was known to be in the planning stage.

The second phase of collecting data occurred concurrently with final design. At this point the route was altered to follow the future path of Highway 87, and serve a second (future) substation added for Sempra's proposed LNG facility. Agreements had also been reached with the owners of most of the industrial properties allowing soil borings and soil testing along most of the northern third of the route. Six additional borings were planned, but never executed due to a lack of a signed agreement with the property owner. The approximate locations of soil boring locations are also shown in Figure 1.

Near-surface soils showed the most variability. On the north end of the project and on the extreme southern end

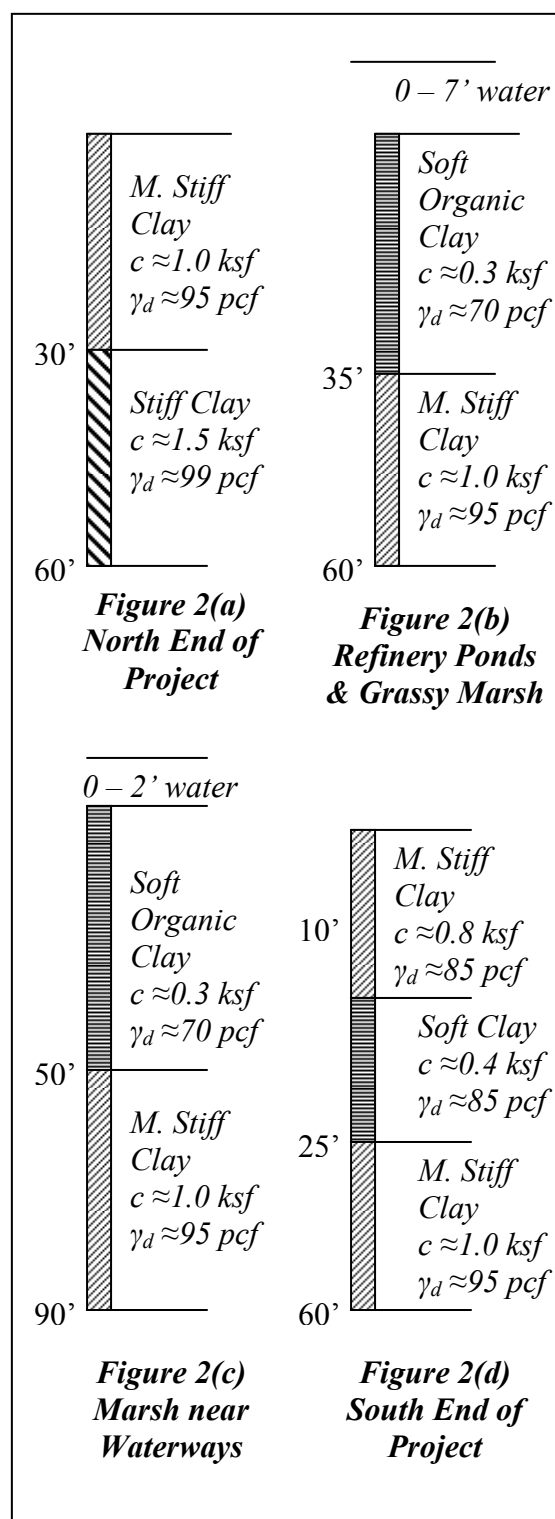


Figure 2 – Typical Soil Profiles

of the project, the near surface soils tended to be medium stiff consolidated clay. In between they tended to be soft unconsolidated clay with considerable organic content. The water table was generally within a few feet of the surface, and in many instances the ground surface is submerged for much of the year. Structures crossing the refinery freshwater storage ponds were typically in three to seven feet of water.

Except at the north end of the project, unconsolidated clays with a low cohesive strength and a high organic content underlay the near-surface soils.

Properties of unconsolidated clay were reasonably uniform with the exception that the thickness of the layer varied considerably in depth. A layer of consolidated medium stiff, to stiff clay was encountered at the bottom of most of the borings.

Shells and thin seams of loose sand were encountered at varying depths in a few locations. Blow counts were generally low, and in only one location did they approach values that might indicate some difficulty in driving a caisson foundation through the layer.

### **Limitations on Design and Construction**

Except for a few locations on the north and south end of the project, initial soil data demonstrated that deep foundations would be required for almost all structures, including the tangent structures. Wetlands permitting did not allow excavation or fill. Similarly, negotiated access through industrial properties on the northern section of the route did not allow for excavation or removal of soil (apart from soil testing samples where this was eventually approved). Additionally, the agreements with the industrial concerns required foundation footprints to be small thereby preventing guying, large reinforced concrete pile caps, etc. Consequently, driven large diameter steel caisson foundations were identified as the most viable solution.

Additionally, access for much of the route was severely restricted, and would have required extensive use of matting, construction of temporary roads, and other means of access. Given the difficulty in moving concrete and other materials along the right-of-way, it was determined that helicopter construction would be cost effect along many portions of the route. Consequently, base-plated steel caisson foundations were selected to facilitate installation by helicopter. Erickson Air Crane (EAC) was consulted, and based on expected availability of their S-64E aircraft; a target lift weight of 16,000 lbs was established. The S-64E has a maximum hook weight of 20,000 lbs, but 4000 lbs was reserved for fuel, rigging and additional forces exerted from the rotor-wash acting downward on the component being lifted. With the assistance of Thomas and Betts (T&B), numerous transmission structure and foundation configurations were evaluated against the target lift weight.

The ability to erect the foundations and structures using helicopters required use of some special details to assist in alignment, and placed some restriction on the structural details being considered. These aspects of the design required a great deal

of input from EAC and T&B. One of the more typical alignment guide details is shown as Figures 3.

One of the concerns initially expressed by operators of the Valero refinery was the potential for excessive disturbance of sediment in the freshwater intake ponds used to supply process water to their plant. That and the relatively shallow pond depths eliminated the potential to work that section of the line from heavy barges. Access to that area with heavy equipment was limited due to numerous underground pipelines and other utilities that would have to be crossed, and by concerns for the stability of the pond levees.



**Figure 3 – Typical Slip Alignment Guide**

Finally, apart from the navigable waterway crossing structures, the Texas Parks and Wildlife Department limited structure height to 85 feet, for protection of birds, on the portion of the line adjacent to the Sea Rim State Park, and the adjacent J. D. Murphree Wildlife Management Area. Although this did not directly affect the foundation design, it was recognized early on that foundations would have to be driven to their full depth regardless of the resistance encountered. Consequently every effort was made to obtain adequate geotechnical data so as to minimize the potential for difficulty in driving caisson foundations.

### **Foundation Design**

This line and its structures and foundations were designed considering a 140 mph wind speed. This design wind speed is determined by the load requirements in the National Electrical Safety Code. Two and three pole structures were used where possible to divide the foundation loads and allow foundations to be as small as possible.

The foundations were designed using MFAD. Steel caisson foundations were modeled as piers, with stiffness of the caisson foundations determined and entered manually. Where feasible foundations were designed: to maintain a maximum ground line deflection of 3"; a maximum foundation rotation of 1.5 degrees; a non-recoverable ground line deflection of 1"; and a non-recoverable foundation rotation of 1.0 degrees. In marshy areas with surface soils contributing little to the foundation strength, the targeted limits were 6", 3 degrees, 2" and 2 degrees, respectively. To accomplish these limits, and maximize foundation stiffness, diameters were selected that were generally 6-7 inches larger than the anchor bolt circle. The typical pole to foundation connection is illustrated in Figure 4.

While the NESC requires only a strength factor of one, dead-end structures were also checked to verify a minimum safety factor of 1.6 against the 140 mph load case. This was done based on past operating experience in the soft soils found in coastal marshes. Past experience suggest that the higher safety factor is needed to improve the overall reliability of the line, minimize foundation deflections resulting from weather events with a higher frequency of occurrence than the 140 mph event, and mitigate potential adverse effects on sag due to excessive foundation rotations.



**Figure 4 – Typical Baseplate Connection**

Many of the foundations on the northern end of the project, including five large angle dead-end structures, had to be designed using data extrapolated from available geotechnical data. Six additional borings were planned between Port Acres Bulk Substation and the northernmost crossing of Taylor's Bayou, but the borings could not be obtained. Foundations were designed considering the weak soils encountered at Taylor's Bayou rather than the comparatively strong soils encountered at Port Acres Bulk. This was done to with the intent of producing the most conservative design possible, but ultimately did complicate installation of the foundations.

Naturally, caisson lengths varied due to changes in soils and loading, but total lengths for tangent structures generally ranged between 30 and 45 feet. Total caisson lengths for dead-end structures typically ranged between 50 and 60 feet, but approached 70 feet in some cases.

The target weight of steel caisson foundations was not possible to achieve in all cases. Many of the foundations for dead-end and navigable waterway structures had to be installed conventionally. Fortunately, access was generally available in these areas. Several other caissons had final weights in excess of 17,000 lbs. There was a helicopter staging area relatively close to the structure locations, so these caissons were able to be flown to their intended location and installed by helicopter. But the additional weight came at the expense of fuel weight and affected flying time and overall installation efficiency.

After initial pole and steel caisson foundation designs were complete, it was determined that two of the 2-pole dead end-end structures would in all likelihood need to be installed by helicopter due to access limitations imposed by the industrial facility crossings involved. With no way of reducing the pole or caisson sizes at this point, it was decided to fabricate these caissons in two pieces and weld them on site.

Again T&B and EAC provided assistance with development of a means to accomplish this. Driving ears were provided on the bottom section of the caisson. Bolt-on guides were also provided to help align the upper caisson section and safely support it while welds were made. These guides and the two-piece steel caisson foundation before welding are shown in Figure 5.

Due to the environment, corrosion protection was provided for all caissons. In addition to galvanizing, Corrocote II was applied to the upper 10 feet of the caissons, and three or more 60 lb sacrificial anodes were attached to each caisson.

### Foundation Construction

The complexity of permitting, Right Of Way acquisition and design, and a rigid in-service date, resulted in a very aggressive construction schedule. Conventional construction and helicopter construction were conducted in parallel to the extent possible to make best use of time. In general, construction by helicopter was done through the marsh and through the refinery ponds. Conventional construction was planned on the north and south ends of the project, and included construction of the navigable waterway crossings from barges. As stated previously, not all foundations could be designed to meet the lift limits of the helicopters. Consequently, these structures had to be added to the scope of the conventional construction crews.

The primary material staging was located on the North end of the project, but smaller staging areas were strategically located along the route to minimize helicopter flight times and maximize the overall efficiency. Notably a temporary mat access road was built and a large area was matted at the future Round Lake Substation.

Helicopter construction consisted of a number of lifts using the S-64E helicopter. Initial lifts were performed to establish working platforms (Figure 6). Aircrews worked in conjunction with small ground crews that included Erickson flight



**Figure 5 – 2-Piece Pile Support**



**Figure 6a – Matting**



**Figure 6b – Modular Barges**

**Figure 6 – Work Platforms**

controllers. Ground crews were typically transported via marsh buggy to the pole location prior to the flight. In marshy areas, the initial lifts at each location consisted of timber matting used to support the hydraulic unit and hammer (figure 6a). At the refinery ponds crews were allowed to bring in small modular shallow draft barges that were secured together and served as work platforms and support the hammer and hydraulic unit (figure 6b). Following this, the hammer and hydraulic units were flown to the site. The hydraulic unit consisted of two sections (figure 7a), a base section containing the hydraulic components and an upper “clam shell” section used to plumb and secure the caisson foundation during driving. The two sections had to be flown to pole locations separately due to weight limitations. The hammer was also selected considering the helicopter’s capabilities, and was an American Piledriving Equipment (APE) model 150.

With the hydraulic unit in place, the caisson was flown to the site and secured using the upper section of the hydraulic unit (figure 7b). The driving hammer was then lifted in place and the caisson driven (figure 7c). Generally speaking, caissons supporting tangent structures were driven without difficulty due to their comparatively small diameters and depths. However, in a few tangent locations and in most angle and dead-end locations, driving resistance was considerably greater than expected, primarily due to a lack of familiarity with the light hammer being used. While most caissons were eventually driven with the model 150, in some cases driving times were considerable. In several of the more accessible locations, a crane and a model 200 hammer had to be brought to the site to complete caisson driving operations. Fortunately, dry weather preceded construction allowing better access that might otherwise have been possible.

As was expected, the most problematic of the foundations during construction were the two-

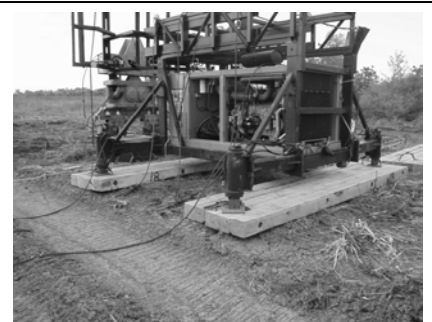


**Figure 7a – Hydraulic Unit**



**Figure 7b – Positioning Pile**



**Figure 7c – Setting Hammer**

**Figure 7 – Foundation Construction**

piece steel caisson foundations. Not only could they not be driven with the lighter hammer, but the alignment of the sections also proved difficult.

Both structures were located in a canal on VALERO property. Helicopter installation for these locations was desirable due to the weight limitations on the access roads leading to the sites, and also due to difficulties in working from the levees on the sides of the canal. The bottom sections of the caissons were driven with difficulty using the helicopter and smaller hammer. But the small hammer was ineffective in driving the caisson much further. Consequently, mats had to be extended into the canal to provide a work surface. Cranes had to be brought to the site in sections to stay within the weight limitations. Caissons were driven to full depth with a Model 300 hammer.

The temporary supports for the two-piece steel caisson foundations worked well for the gross fit-up using the helicopter, but it proved difficult to align the sections sufficiently to achieve the proper weld gaps. Caissons were supplied with backing bars and bevel preparations requiring a tight alignment. Fit-up was complicated by the caisson sections that were slightly oval preventing the backing bar from sliding inside the other section. Jacking nuts had to be welded to the caisson sections to assist in making the alignment. While structural welds were eventually completed in a satisfactory manner, and caisson sections were joined and installed per specification, the process was much more difficult than originally anticipated.

### **Post Foundation Construction**

Following caisson installation, guides were installed (figure 8a) to facilitate seating the pole with the helicopter. Fully framed poles



**Figure 8a – Pole Guides**



**Figure 8b – Pole in Transit**



**Figure 8c – Line Work**

**Figure 8 – Post Foundation Construction**

(including stringing dollies) were flown to the site in one lift where possible (figure 8b).

Slip joints of two part poles were secured together using steel lift straps. Where poles were too heavy to fly in one lift, alignment guides like those shown in figure three were used to align the sections.

Light helicopters flown by Air2, LLC assisted with installing the pull cables through the dollies; and were also used to assist in clamping in the conductors (figure 8c). Following installation of conductors, Air2 also installed bird diverters to shield wires in locations where they were required to meet Texas Parks and Wildlife Department requirements.

### Acknowledgements

Assistance provided by the following companies was instrumental in the successful completion of this project: Air2 (aerial conductor installation); Erickson Air Crane (aerial foundation and pole installation); Fitz & Shipman (surveying); New Park (matting); North Houston Pole Line (conventional pole and caisson installation); S. Bomack (barges and cranes); Stork Southwestern Laboratories (geotechnical testing); T&D (conventional pole and caisson installation) Thomas & Betts (pole and steel caisson foundation design and manufacturing); Turner Industries (on-site welding); and QC Laboratories (geotechnical testing).

The cooperation received from the VALERO refinery was particularly crucial to this project, and the assistance provided by Randy Lowe and Steve Clegg is greatly appreciated.

### Conclusions

1. Emphasis on caisson driving during foundation design is important, but it is extremely important for caissons driven using helicopters. Prior to this project, Entergy had very little experience using the comparatively smaller APE Model 150 driving hammer. Consequently, much of the difficulty encountered in driving was unanticipated.
2. For helicopter installation greater standardization of vibe-hammer driving ears is warranted. Bolt circle variations resulted in variation in driving ear spacing. Frequent adjustments had to be made, and often the hammer had to be flown back to a staging area for adjustment. This affected Helicopter fly-time, and overall efficiency. Additional material costs associated with holding the driving ear spacing constant would have been money well spent.
3. The two-piece steel caisson foundation was an acceptable solution, and necessary in this instance. But the solution came with numerous challenges and will only be repeated as a last resort. The large caissons could not be driven with the helicopter, and it was very fortunate that conventional

equipment could be brought in to finish the job. The temporary supports worked well, but it proved difficult to fit-up the sections to achieve weld gap tolerances. Weld preparation, coating, and cathodic protection issues also exist.

4. The new wind maps introduced in NESC 2002 improve survivability of transmission lines and overall reliability. As a result of Hurricane Betsy, Entergy started designing for wind speeds in excess of NESC requirements long before changes in NESC 2002. Hurricane Ike came ashore with sustained wind speeds in the area approaching 110 mph and with a storm surge in excess of 18 feet. The transmission line discussed in this paper was unaffected due to the 140 mph design wind speed. The new Keith Lake Substation was submerged but structurally intact.
5. Increases in permitting requirements and wetlands rehabilitation costs make similar construction more likely in the future.
6. While effective coordination and communications is important on every project, it is doubly so for projects where a flight crew availability may be limited. Decisions made during design of structures and foundations need be based on careful consideration of flight crew requirements and helicopter limitations. Input from the pole vendor and the representatives of the flight crew should be solicited early and often.

## Deepwater Transmission Line Foundations Meet Trophy Bass Lake Environment

R. Norman, P.E.<sup>1</sup> A. M. DiGioia, Jr., PhD, PE<sup>2</sup> and E. J. Goodwin<sup>3</sup>

<sup>1</sup> Wood County Electric Cooperative, PO Box 1827, 501 S. Main St., Quitman, 75783; PH (903) 763-2203, email: rnorman@wcec.org

<sup>2</sup>DiGioia, Gray & Associates, LLC, 570 Beatty Road, Monroeville, PA 15146: PH (412) 372-4500, email: tony@digioiagray.com

<sup>3</sup>PBS&J, 18383 Preston Rd, Suite 110, Dallas, TX 75252; PH (972) 588-3158, email: ejgoodwin@pbsj.com

### **ABSTRACT**

Wood County Electric Cooperative is serving a new pumping station for the Dallas Water Utilities on Lake Fork in eastern Texas. The optimum route required a lake crossing of over 1,738m (5,700 ft) for a double circuit 138 kV line. Lake Fork is an internationally recognized bass fishing environment, holding the Texas record for the largest bass, weighing over 8kg (18 lbs). The placement of the foundations for the crossing structures presented several unique challenges including limiting the number of structures set in the lake, providing clear channels for boating traffic, minimizing environmental impacts and working in lake depths over 15m (50 ft). This paper discusses the types of foundations considered and the design and installation of the most effective design.

### **Project Description**

Surface reservoirs for water have been built in east Texas for the past 30 years as preparation for future potable water needs in the expanding Dallas, Texas metroplex. In 1975 the Sabine River Authority dammed a branch of the Sabine River and created a water storage area known as Lake Fork. Until recently the lake has served as a recreational area, probably best known internationally as a prime tournament class bass fishing habitat. The top 6 bass and 35 of Texas' top 50 bass caught have been taken from Lake Fork. The lake is poised to enter its primary function as a source of potable water for Dallas via construction of a 2.75m (108 inch) diameter pipe-viaduct transferring water to Lake Tawakoni and eventually to the Dallas municipal water system. The 63,360 kL/D (240 MGD) pump station will be powered by a substation connected to a dedicated 138 kV line. Part of the transmission line supporting the substation will cross the lake, a distance of over 0.6 km (1 mile) in length, see Figure 1. Three transmission structures were installed in the lake, supported by foundations placed at depths of 15-21m (50-70 ft) of water.

The transmission assets are owned and operated by Wood County Electric Cooperative (WCEC). The proposed line also provides an integral part of a loop connection between two substations that were radially fed. The construction of the lake crossing provided the final segment of the loop to afford greater reliability to the WCEC service area and the pumping station. The land-based transmission line section was constructed with double circuit 138 kV structures on concrete poles. The

design of the lake crossing posed several unique geotechnical and construction challenges.

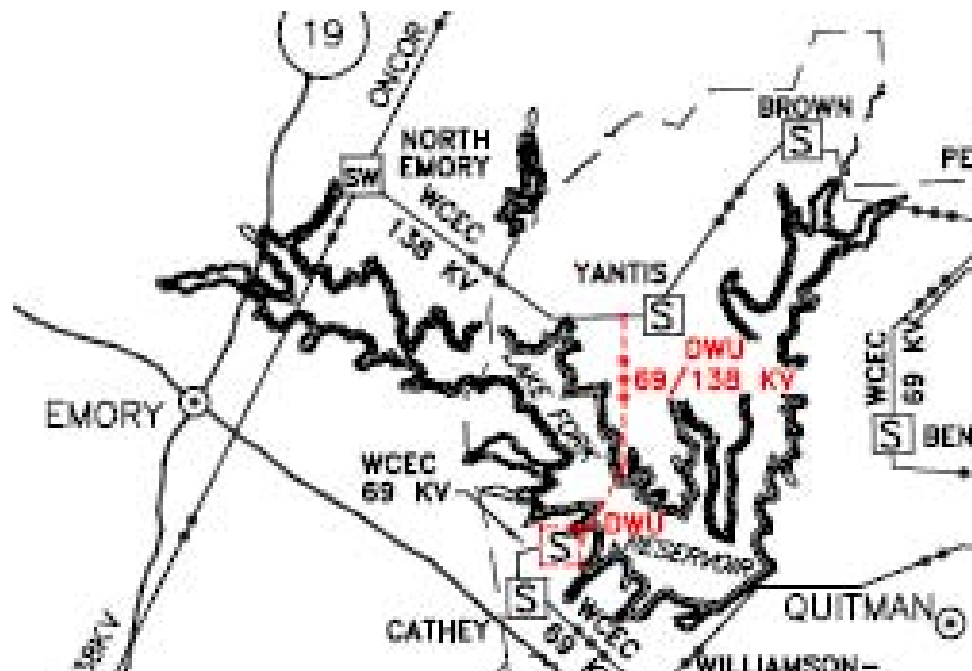


Figure 1 - Project Area Map Showing Lake Fork and Transmission Lines

### Lake Fork's Notoriety Represents Constraints to Construction

Foremost, the fishing habitat and the recreational business based on the international notoriety of Lake Fork necessitated minimal invasion and impact on the lake and water habitat. The Sabine River Authority owner/manager of the lake required that a prime boating channel not be interfered with by the installation of the structures. The first task of the project development was to optimize the type of foundation to be applied and to determine the number of structures to be placed in the lake.

When Lake Fork was developed in the mid 70's, only the main channel was cleared of timber. The rest of the impoundment area was left unchanged. That decision was a boon for the fishing industry and created perfect bass habitat. However, the standing timber continues to be a boating challenge, and in the project's case, an obstruction to construction barges. For safety, the main boating channel required adequate width and a safety buffer to any installed structures. The location of that channel established the required number of structures in the lake. Adding a fourth structure and spacing the structures on near equivalent span lengths interfered with the boating channel. Adding a fifth structure to provide main channel horizontal buffer clearances increased the costs with minimal benefits. Dividing the crossing into four spans – three structures provided the best spacing to preserve the required clearance for the main channel.

## Design Considerations

After the selection of three structures was established, a construction process/foundation design practicality study was initiated. The type of foundation, its size and costs would be driven by the structure loading requirements and the subsurface conditions at the structure sites. The line route was mapped using a hydrograph to determine the lake bottom's contours. The lake elevation was established by maximum pool elevation and a desired ten foot reveal to the base of the poles. See Figure 2 which shows the hydrograph data as a profile for design.

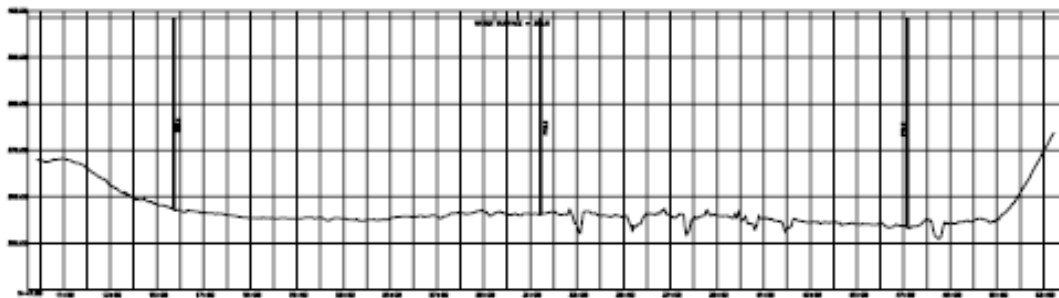


Figure 2 - Hydrograph Profile of Lake Fork Crossing

For a preliminary design of the foundations, several sources of existing boring data were found that provided beneficial insight into the geology of the area. The Sabine River Authority (SRA) shared with the project team the borings they had used in designing the earth retention dam that formed the lake. SRA also had monitoring wells installed along the toe of the dam to detect water leaching and undermining of the structure. In exchange for their sharing of the dam boring data, the project shared its lake bottom hydrograph cross-section with the SRA. They had several cross sections but the crossing area offered them an additional data point for approximating the true retention volume of the lake. This was valuable information to their river management responsibilities.

Additional boring information was obtained from the Texas Department of Transportation (TXDOT). Less than a kilometer upstream of the transmission line crossing location, TXDOT had recently upgraded a bridge across the lake and they shared their boring information with the design team.

Following several preliminary designs of the foundation size, the diameter and embedment depth were designed to support the conductor and structure loads at the base of the steel pole and the "pedestal" length of the structures' length from pole base to lake bottom. The most practical installation was a tubular steel caisson that would be driven into the lake bottom a sufficient length and then extends to 3m (10 ft) above the maximum pool elevation. The actual pole structure would be designed to be socketed into the top "caisson" section, aligned and grouted in place. Installing the caissons into the lake bottom could have been accomplished with one of three techniques. The boring logs showed that the lake bottom consisted of a dense sand and clay mixture for a depth of over in most locations. There was no bedrock or

boulders that would interfere with the placement. The potential placement techniques are addressed below with their perceived pros and cons for the Lake Fork project:

Vibrated Caisson – the caisson would be lowered into position on the lake bottom and then vibrated with a vibratory hammer to the desired depth. The lack of rock made this an attractive alternative. The amount of clay and density of the sands were concerns relative to the ability to vibrate the caisson to the desired depth. The skin friction that would detract from this methodology could be mitigated by using an auger to remove some of the spoils inside the caisson and relieve the friction forces. Advantages of the vibrated caisson were the simplicity of the operation (relative in comparison to the others; not in reference to working in 15-21m (50-70 ft) of water and the minimal disturbance to the lake bottom.

Jetting – using water pressure and jets at the bottom of the caisson, water injection disturbs the soils sufficiently to allow the caisson to be advanced to its embedment depth. This option presented a major effect that was an immediate detractor – the water injection would create a sizable plume of lake bottom material being disbursed into lake water. This was deemed a major environmental concern and a significant potential impact on the fishing habitat. We mentioned the notoriety of Lake Fork's bass fishing, did we mention that the construction window was overlapping or in close proximity to an international invitation bass classic tournament. Both WCEC and the SRA were ever mindful of the fishing habitat impacts.

As you can guess, the vibratory installation method seemed most practical and environmentally acceptable.

### Lake Features Shaped Project

Two additional lake factors played into the project execution: lake elevation and winds. North and East Texas had been experiencing several years of drought and lake elevations were low when the project was being designed. The lower lake elevation increased the issues concerning the still standing timber in the lake; would the barges and working boats be able to maneuver to the structure locations and launch areas. During the season that the line crossing was actually built, rainfall had raised lake elevations above normal and near full pool elevations. This condition increased the water depth that the crews had to work in placing the foundation caissons.

Paradoxically, the water elevation could be a problem if it was high or low as noted above plus the need to reach the exposed caisson top above the lake elevation. If the lake was high, the barge work was in greater depth. If the lake elevation was down, the water depths were better for working but access to the caisson top and the impact of insitu trees were both more of a concern.

In Figure 2, the lake bottom profile shows the west shore on the left. Note that the lake's deep channel is on the east and that the west shore is shallower. The barge ramp and access was from the west shoreline near the crossing location. The issue of the standing timber in the lake was a concern in the shallower area where the top of the trees that were 7-11m (25-30 ft) tall when growing, would now be close to the surface.

The open exposure and length of the lake's open water created windy conditions that again made barge working difficult during the hydrograph, soil boring and construction period. Several barges were tried until one sufficiently large and stable enough provided a platform for the soil boring efforts. The construction crews were familiar with working on lakes, setting transmission poles and they had the proper equipment for executing the foundation installation.

### Crossing Design

Each end of the transmission line crossing was anchored with a self supporting two-pole deadend structure. The east shore structure was an angle structure. The west shore structure had one circuit continue on the tangent line towards another WCEC substation. The pump house feed circuit deadended on the west structure and dropped into a dedicated substation. Figure 3 is a photograph of the west shore termination with the two-pole structure and the pump house under construction adjacent to the line.



Figure 3 - West Shore Pumping Station and Line Structures

The three structures located in the lake required a minimum of 24m (80 ft) long tubular steel caissons that were embedded into the lake bottom a depth of 9m (30 ft) as determined by the foundation design program MFAD. A 50m (165 ft) tall double circuit steel pole structure was socketed into each caisson. The caissons were galvanized, and then coated with corrosion preventive coating along the length of the caisson that could be exposed to air as the elevation of the lake changed seasonally.

### Construction Summary

The construction process was uneventful. The caisson vibration process went smoothly. None of the caissons required internal auguring; the caissons were vibrated to their prescribed depth. The caisson locations had been marked prior to construction

with buoys. When the barge with the caissons were brought to the buoy and jacked into position, see Figure 4. The specific pole location was spotted from the shoreline by survey. Then the steel caisson was stood vertically and lowered to the lake bottom and held in position by a template frame on the edge of the barge, Figure 5. The vibratory hammer was attached to the top of the caisson and was driven to depth, see Figure 5.

Once the caissons were driven to depth, they were filled with low strength concrete to the elevation of the socket plate that was dropped into each caisson to serve as a base to support the pole base section while it was grouted in place, (Figure 6). The original construction specification called for filling the caissons with crushed aggregate to the plate elevation. During construction, however, the concrete backfill was found to be more efficient and less costly than dealing with aggregate handling from the shore onto the barge and then from the barge into the standing caisson. The barge then brought the pole to the location and the base was socketed inside the pile with grout. The three pole base sections were socketed in place before the crew came back and set the top pole sections with attached arms and insulator strings attached. Helicopters were used to pull in a lead line and the conductor was installed. To minimize phase spacing and avoid galloping conditions, the conductor was damped. The dampers are visible in Figure 7, where the line is displayed looking west to east.



Figure 4 - Barge and Hammer in Position to Drive Caisson



Figure 5 - Pile Caisson in Stabilizer Being Driven by Hammer



Figure 6 - Installed Caisson Ready to Accept Single Pole Structure



**Figure 7 - Lake Fork Crossing Structures**

### **Conclusions**

The development of the Lake Fork crossing was built through a delicate coordinated effort between the project owner, Wood County Electric Cooperative, the Sabine River Authority and engineering staffs at PBS&J and DiGioia, Gray & Associates, LLC to provide a lake crossing that met all code and engineering requirements plus minimized the project's impact on the environment, which in this case was a world-class bass fishing habitat. Through the cooperative effort, the preliminary optimization of the design strategy was accomplished by sharing geotechnical information, environmental and recreational constraints presented by the lake and construction experience of several transmission line contractors who frequently erect lake crossings. The collaborative information quickly identified that vibrated tubular steel caissons would be the optimum foundation option to support the three lake crossing structures. Pole site geotechnical information obtained from borings provided the detailed information along with pole loadings to design the caisson foundations. Finally, construction of the crossing proceeded without events, as the preparation in design and collaborative efforts with the Sabine River Authority provided optimum lake access and efficient installation.

230KV Lattice Tower Replacement  
An example of design loadings not addressed in the NESC

Norman P. Hodges, P.E.

Senior Civil Engineer; Seattle City Light, 700 5<sup>th</sup> Ave., Suite 3300, P.O. Box 34023, Seattle, Washington 98124-4023; PH (206) 684-3503; email: norman.hodges@seattle.gov

## ABSTRACT

Seattle City Light (SCL) owns and operates 3 dams in the North Cascades of Washington State which provide about 30% of the utility's needs. Four 230kv circuits carry electricity from these dams to the Seattle area on two parallel alignments of double circuit lattice towers. The alignments cross the Skagit River near the town of Marblemount. At this crossing a major flood event in October of 2003 eroded 50 feet of high river bank in the direction of two lattice towers leaving about 75 feet from the tower bases to the edge of the river bank. In the 1930's the distance from the river bank to the towers was about 200 feet and in the 1950's was about 150 feet. Because of the possibility of further erosion by subsequent flood events Seattle City Light began a study to determine how best to mitigate the risk.

The final design choice was to locate two 175 ft. steel monopoles on drilled pier foundations further from the river. The foundations would remain in place as essentially "bridge piers" in the event that future floods might erode the bank and leave the structures in the river. The future design condition would expose the top 40 feet of a 90 foot pier above the bottom of river scour. Several unique design conditions had to be addressed including a 100 year flood event (103,000 cu. ft/sec) and a seismic design event. The design also had to address how these loading conditions would be combined with the National Electric Safety Code (NESC) weather conditions. In addition the Corp of Engineers river crossing clearance requirements had to be maintained and there were other construction contract elements that had to be met such as sensitive area requirements, impacts to fish, and access.

## INTRODUCTION

In October 2003 heavy rains over a period of several days caused widespread flooding throughout the Pacific Northwest. High river flows can cause riverbanks to erode and even change the course of a river. An alert crew member reported that about 50 ft of high river bank eroded moving the Skagit River to within 75 feet of two lattice towers carrying four 230kv circuits. The potential to undermine the towers from similar flood events in the future initiated an investigation to mitigate the risk.

As designers we refer to widely accepted published industry documents for guidance. The core of this paper is to present a situation where the requirements of the NESC or for that matter American Society of Civil Engineers (ASCE) Manual 74 does not provide sufficient guidance for loading determination to use for design. This paper presents problems in determining design loads and load combinations not typically addressed in transmission line design.

A consultant, Shannon and Wilson, was retained to quantify the risk of future bank erosion. Their report states that “of the top 20 average daily events, two occurred in October 2003.” This was for a recorded time frame since 1943. The largest of these flows was 43,900 cfs. Based on estimates developed by the U.S. Army Corp of Engineers this is a typical 5 year event and equal to about one-half of a 50 year event and considerably less than a 100 year event at an estimated flow of 103,000 cfs.

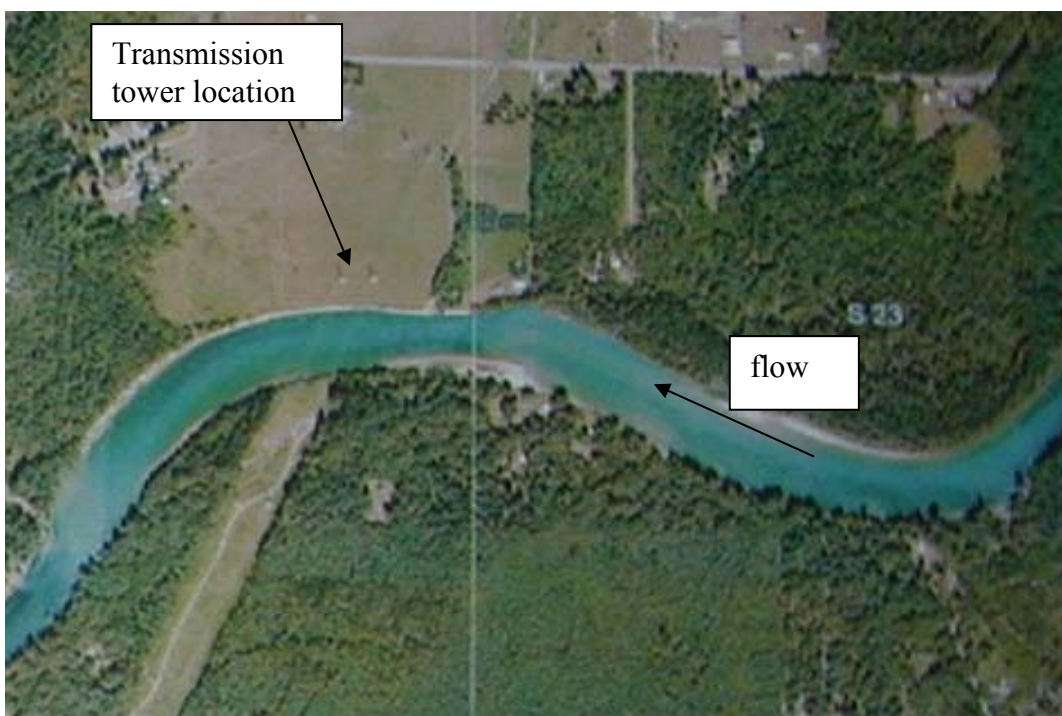


Figure 1. Skagit River and transmission right of way. Note transmission right of way crossing the left bend in the river and the proximity of two towers to the river.  
Seattle City Light aerial photograph

The Shannon and Wilson study, after reviewing prior measurements and historical aerial photographs, found that the rate of erosion had increased more rapidly in the recent past. From 1997 to 2001 the average rate of erosion was 2.6 ft per year and from 2001 to 2004 increased to 13.3 ft per year. The Shannon and Wilson report concluded that “tower stability could be reduced in about five years....and could conceivably occur within one to two years” Reducing risk to the transmission structures was elevated to a high priority in the utility.

The four transmission lines supported by the two towers supply about one-third of the power to Seattle. Loss of these lines would have serious lifeline consequences and cause widespread outages critical to public safety, government response and law enforcement, hospitals, sewer and water operation and last for an undetermined period of time. The loss of these lines would also cause regional constraints on the power system beyond the Seattle City Light service territory. The probability of loss of these towers due to erosion was greater than the occurrence of a design seismic event typically assumed in building codes.

The original lattice towers were 152 feet tall. The first alignment was constructed in the 1930's and the second in the 1950's. The 1930 foundation is a cast in place battered column on a 5ft x 5ft pad buried about 10 feet. The 1950's foundation was a steel grillage foundation buried approximately 8 ½ feet.



Figure 2. Proximity of 230kv towers to river bank. Photograph by unknown Seattle City Light staff.

## DESIGN ALTERNATIVES

Several alternatives were reviewed for mitigating the risk to the transmission lines. The Shannon and Wilson study was also tasked with presenting design alternatives. Some would leave the lattice towers in their present location and others would require relocation further from the current river bank. One suggestion was to prevent bank erosion by lining the bank with rip-rap. This was rejected because of environmental permitting issues for fish such as salmon, eagles and visual impacts in a designated

Wild and Scenic River watershed. Also the length of the rip-rap would extend well beyond the 200 foot width of the transmission right of way onto private property and would also require periodic inspection and maintenance. A sheetpile wall around the lattice towers was also considered. This would create an island supporting the lattice towers if the riverbank were to erode significantly in the future. The sheetpiling would have to be driven well below the bottom of a future channel. Driving the sheet through dense gravel and cobbles could potentially make installation difficult. And the cost of the sheetpiling was estimated to be similar or greater than a drilled pier solution, another option. Moving the towers further from the river bank dictates that the towers be taller, following the rising shape of the catenary curve. The maximum working tension already was 14,500 lbs so increasing the tension to offset increased structure height was not considered. Moving the lattice towers further from the river and raising them or putting the legs on pedestals was considered too. But even so it would be difficult to guarantee what would be a "safe" distance from the river. The selected solution was to use steel monopoles on drilled pier foundations located nominally further from the river to minimize the increased height. The new spans would increase by 60 feet to 1478 feet. The drilled pier foundations would act as "bridge piers" in the future condition that the river were to erode the bank and surround the piers. This would leave the concrete pier approximately 40 ft above the bottom of the river and require a very deep foundation.

## DESIGN LOADING

The National Electrical Safety Code (NESC) weather conditions are generally used as the design criteria at Seattle City Light and they have performed well over the years, but as is clearly stated in the first part of Section 1 they address a limited set of load conditions.

"The purpose of these rules is the practical safeguarding of persons during the installation, operation, or maintenance of electric supply and communication lines and associated equipment.

These rules contain the basic provisions that are considered necessary for the safety of employees and the public under the specified conditions. This Code is not intended as a design specification or as an instruction manual."

As loading of the structures was considered it became clear that this was a unique situation and not all loading was covered in the NESC or ASCE Manual 74. NESC Heavy, NESC Ice and Wind, NESC Extreme wind, and broken conductor criteria are typical SCL transmission design loadings. Other loadings considered were a 100 year flood event, earth pressure on one side of the foundation and a seismic event.

### Flood

A 100 year flood event was selected as the design flood event because of the critical nature of the transmission line and the effort to establish a durable solution to the erosion problem. The 100 year flood event estimated by The Corp of Engineers is 103,000 cfs. To estimate the average velocity of the Skagit River at the transmission

crossing a survey of the channel bottom profile was conducted and the flood stage elevation was determined. Both the American Association of State Highway and Transportation Officials (AASHTO) *Standard Specifications for Highway Bridges* and ASCE 7-02 were consulted for guidance for flood design loading. AASHTO guidance for converting velocity to a vertical pressure distribution against a bridge pier was followed.

$$P_{avg} = K(V_{avg})^2$$

$P_{avg}$  = average stream pressure

$K = 0.7$  for circular piers

$V_{avg}$  = average velocity of water  
in ft/sec.

$V_{avg} = \frac{Q_{100}}{A_{100}}$ , calculated for the  
100 year event.

$Q_{100}$  = cfs flow for 100 year event

$A_{100}$  = cross sectional area based  
on survey

AASHTO directs that the pressure against the pier shall be taken as a triangular distribution with the pressure at the top of water equal to twice the average pressure.

$$P_{max} = 2P_{avg}$$

AASHTO also requires that the “effects of drift buildup shall be considered”. Two scenarios for drift buildup were considered. The potential exists for a debris pile or log jam to develop against the foundation pier and if the river were to erode a relatively small distance beyond the pier a debris pile or log jam potentially could form in this space. The flood loading used for design was a 100 year flood event against such a debris pile pushing on the foundation.

The design also considered a large log carried in a flood event striking the pier. ASCE 7-02 contains a section in the appendix that discusses the impact loading from water borne debris and suggests for the Pacific Northwest that a 4 kip log can be considered typical. The following expression for impact force is presented.

$$F = \frac{\pi W V_b C_I C_O C_D C_B R_{max}}{2g\Delta t}$$

$W$  = the debris weight

$V_b$  = velocity of the object

$C_I$  = importance coefficient

$C_O$  = orientation coefficient, = 0.8

$C_D$  = depth coefficient

$C_B$  = blockage coefficient  
 $R_{max}$  = maximum response ratio for impulsive load  
 $g$  = acceleration due to gravity = 32.2 ft/s<sup>2</sup>  
 $\Delta t$  = the impact duration

Loads were calculated for a log of this size striking the pier in the 100 year flood event.

#### Scour

The geo-technical investigation was asked to provide an estimate of scour depth around the pier. Scour depth determination was based on the empirical formulas of the Colorado State University equations for piers found in the *Integrated Streambank Protection Guidelines 2003*. This additional depth was considered when calculating the foundation design forces

#### Soil pressure

Another design case considered was the situation where the erosion might progress only to the point of removing soil on one side of the foundation leaving the foundation pier subject to earth pressure.

#### Seismic

Transmission structures are generally not designed for earthquake forces. For most steel monopoles on drilled pier foundations the top of the foundation is at or near ground level and seismic forces do not control the design of the pole or foundation.

ASCE Manual 74 (Appendix F) states that:

“Typically, transmission structures are not designed for ground induced vibrations caused by earthquake motion. The standard transmission structure loadings caused by wind/ice combinations and broken wire generally exceed design earthquake loads.”

ASCE Manual 96 states that:

“Transmission lines have been very resistant to earthquake damage: their main vulnerabilities are foundation failure of transmission towers or the loss of a tower due to landslides. Both occurrences are relatively rare. It would appear that the low natural frequencies of lines decouple their mass from the high energy content of earthquakes, and the design for extreme wind, ice, and longitudinal load combinations is adequate for earthquakes.”

There is minimal guidance in the design literature for seismic design of transmission line structures and foundations. The Appendix to Chapter 14 of the National Earthquake Hazard Reduction Program (NEHRP) 2000 Edition of the *Recommended Provisions for Seismic Regulations of New Buildings and Other Structures* includes transmission structures as non building structures and provides the most explicit

direction for seismic design of electrical transmission structures. ASCE 7-02 in Section 9.1.2.1 specifically excludes transmission towers but does include a section for telecommunication poles. NEHRP 2003 excludes “overhead power line support structures” from its scope. ASCE 7-02 and 7-05 explicitly state that transmission towers are beyond the scope of the provisions yet present a R value for telecommunication towers. Presumably the difference between telecommunication towers and transmission towers is that transmission structures interact with the conductors while communication structures are independent structures and the interaction of a tower with conductors is not well codified. Typically if transmission structures are analyzed for seismic forces it is done without the conductor stiffness interaction. The 2003 edition of the International Building Code (IBC) defers to ASCE 7 and the 2006 IBC defers to “other regulations” for seismic design of electrical transmission towers.

Given the future design condition of a tall pole on a large concrete pier, exposed by erosion, projecting almost forty feet above the bottom of river scour and located in an area of potentially significant earthquake activity a seismic analysis was included in the design process. Potential earthquakes affecting the structure could be a magnitude 9 subduction zone earthquake off the coast of Washington State or a rupture of a nearby fault.

Seattle Public Utilities Material Laboratory was retained to conduct a design level geotechnical investigation. Seismic design parameters were provided in accordance with the 2003 International Building Code (2003 IBC) which are based on the 2000 NEHRP provisions. The following parameters were provided.

Site Class:	E
Mapped Spectral Response Acceleration at 0.2 sec. Period, S <sub>S</sub> :	0.670 g
Mapped Spectral Response Acceleration at 1.0 sec. Period, S <sub>I</sub> :	0.223 g
Site coefficient, F <sub>a</sub> :	1.36
Site coefficient, F <sub>v</sub> :	3.12

In the Appendix to Chapter 14 of the 2000 NEHRP/FEMA 368 provisions the familiar equivalent static force expression is recommended for the determination of minimum seismic lateral load for transmission structures. Response modification factors, R, are presented in Table 14A.2.1 for a variety of transmission structure types and lists 1.5 for steel transmission poles. Seattle City Light classifies transmission structures as essential structures and uses 1.5 for the importance factor

$$V = \frac{C_s}{\left(\frac{R}{I}\right)} W$$

V = seismic base shear

R = response modification factor

I = importance factor

C<sub>s</sub> = seismic response coefficient

W = total dead load

The equivalent static force approach was followed assuming two concentrated lumped masses representing the steel pole and the concrete pier above the river bed. In addition a modal analysis was done using the RISA3D software. In the Commentary to Chapter 14 of the 2000 NEHRP/FEMA 369 provisions a damping value of 2% is recommended. The results were scaled up to 85% of the equivalent static force per the 2000 NEHRP provisions and distributed to the steel pole and to the exposed foundation.

Summary of loading:

- 60 degree F, no wind
- NESC Heavy
- NESC Extreme wind
- NESC Extreme Wind and Ice
- 2 broken conductors
- Normal river flow
- 100 year flood event
- 100 year flood event with debris pile/log jam
- Earth pressure on one side
- Seismic event

## LOAD COMBINATIONS

There are a number of codes and design guides to turn to for load combinations but none address the range of loadings that include wind and wire tensions, a significant flood event and seismic activity. Building codes and highway codes in a reciprocal fashion don't address transmission wire tension and wind design loads. Transmission line design guides typically don't include provisions for seismic and flood loads. To proceed to design however reasonable load combinations had to be determined and will be briefly discussed here. Wind direction was assumed to align with the hydrostatic pressure of river flow. Flood events in the Pacific Northwest usually occur with relatively warm wet weather often in conjunction with melting snow. For this reason flood events were not combined with the NESC ice conditions. A high wind event occurring simultaneously with a flood event or seismic event is not likely. The probability of a design seismic event and a flood event occurring simultaneously is small. All river flows, typical and extreme were assumed to act against a debris pile recognizing that if a debris pile were to form it could remain in place for some time. If erosion were to occur on only one side of the foundation pier earth pressure against the pier could be sustained for an extended period and coexist with the NESC weather conditions. Following is a list of load combinations that were considered for design.

Load combinations used for design:

- 60 degree F wire tension, no wind and normal river flow
- NESC Heavy and normal river flow
- NESC Extreme wind and normal river flow

NESC Extreme Wind and Ice normal river flow  
60 degree F wire tension, seismic and normal river flow  
60 degree F wire tension, 100 year flood event  
60 degree F wire tension, Earth pressure and debris pile with 100 year flood event.  
Broken conductor and normal river flow

The use of Load and Resistance Factor Design (LRFD) format for load combinations is widely adopted. The reference documents for the building design community that address concrete, steel, wood and masonry materials either use LRFD exclusively or are migrating to it. The International Building Code (IBC) and the American Society of Civil Engineers publication Minimum Design Loads for Buildings and Other Structures both use a strength based LRFD format but still retain a service load format. The AASHTO Specification for Highway Bridges has adopted a LRFD format. Most load factors come from a statistically based probability analysis of the occurrence of natural phenomena but the NESCC assigns load factors based on historically satisfactory performance rather than a statistically derived method. American Society of Civil Engineers (ASCE) publication *Guidelines for Electrical Transmission Line Structural Loading, Manual 74* presents a reliability based design approach but recognizes that it is not all inclusive and does not address “flooding” and “many other possible load producing events.” This manual has been under review for a number of years and the release of the updated version is widely anticipated. Load factors are not the same across different industry publications for similar design events. The designer must apply engineering judgment in a reasonably conservative manner to decide on load factors for design.

## POLE AND FOUNDATION DESIGN

The seismic load combination was the governing combination for foundation design. The foundation and pole designs were considered without the interaction of the conductor stiffness because of the lack of readily available information and the additional sophistication required of such an analysis.

Soil borings were taken in January of 2006. Alluvium, or soil deposited by rivers, was encountered over the full 98 foot investigation depth. The upper 25 ft consisted of very soft to medium stiff silt. Gravel, gravel with silt and sand, and sand with silt and gravel were encountered to 38 feet. Sand and sand with silt was encountered to the bottom of the borings. Ground water was encountered at 20 feet. Scour depth was estimated at 8 foot for a 10 foot diameter pier. Liquefaction analysis was conducted for a 475 return period earthquake. The risk was found low so no mitigation was recommended for liquefaction. Foundation design software, L-Pile, parameters were provided for foundation design. The size of the pier foundation is 90 feet deep from existing ground elevation and 10 feet in diameter.

Site class E soils identified in the geotechnical report require that the pier design meet the detailing requirements required in higher seismic regions. Originally the confinement reinforcing was called out as continuous spiral reinforcing but the timing

of the construction contract and availability of the spiral reinforcing necessitated a change to hoop reinforcement. The detailing requirements stipulate overlap of the hoop tails and that the ends are turned into the core of the column. See Figure 3. In higher seismic regions the transverse steel, spirals or hoops confine the longitudinal bars and prevent them from buckling under compression.



Figure 3: End of hoops turned into the core.

## CONCLUSIONS

This design presents a situation with unusual loads not covered in the transmission design literature. Codes and design guides are focused on the most common situations and cannot address all possible and less frequently encountered load events or load combinations. Different design references for different industries may need to be consulted for guidance on loads that are more common to a particular industry. The goal of any designer is to address the reality of the design situation, to the extent possible, provide a rational design given the uncertainties with a reasonable factor of safety. Readily available guidelines that address a wider scope of loadings, perhaps including the entire range of loading in ASCE 7, load combinations, and load factors unified across different industry design standards would be helpful to the practicing engineer. Unusual load combinations that include the typical transmission loads of wire tension, wind and ice warrant further study and design recommendations or guidance.

## REFERENCES

- AASHTO (2002). American Association of State Highway and Transportation Officials, *Standard Specification for Highway Bridges*
- ASCE (1990). American Society of Civil Engineers, *Design of Steel Transmission Pole Structures Manual 72*, American society of Civil engineers, New York, N.Y.
- ASCE (1991). American Society of Civil Engineers, *Guidelines for Electrical Transmission Line Structural Loading Manual 74*, American society of Civil engineers, New York, N.Y.
- ASCE (2003). American Society of Civil Engineers, ASCE/SEI Standard 7-02, *Minimum Design Loads for Building and Other Structures*

- ASCE (2006). American Society of Civil Engineers, ASCE/SEI Standard 7-05, *Minimum Design Loads for Building and Other Structures*
- ASCE (1999), Guide to Improved Earthquake Performance of Electric Power Systems, ASCE Manuals and Reports on Engineering Practice No. 96
- IBC (2003). *International Building Code*
- IBC (2006). *International Building Code*
- Integrated Streambank Protection Guidelines 2003, Washington State Aquatic Habitat Guidelines Program, Washington State Department of Fish and Wildlife, Washington State Department of Transportation and Washington State Department of Ecology, 2002.
- LPILE (1999) LPILE Plus 3.0 for Windows, Ensoft, Inc.
- NEHERP (2000), National Earthquake Hazard Reduction Program, *NEHRP Recommended Provisions for Seismic Regulations of New Buildings and Other Structures*, FEMA 368 and 369
- NEHERP (2003), National Earthquake Hazard Reduction Program, *NEHRP Recommended Provisions for Seismic Regulations of New Buildings and Other Structures*, FEMA 450 and 541
- NESC (2002) American National Standard C2, *National Electric Safety Code*
- RISA3D, *Rapid Interactive Structural Analysis – 3 Dimensional*, Risa Technologies, Foothill Ranch, California
- Seattle Public Utilities Material Laboratory (2006). *Geotechnical Report Corkindale Towers Relocation Skagit County, Washington*, NS40123, Seattle, Washington
- Shannon and Wilson (2005), *Final Report, Skagit River Bank Erosion, Seattle City Light Skagit Project, Transmission towers B64/36N and D64/37N, Corkindale, Washington*, Seattle Washington
- U.S. Army Corp of Engineers, *Skagit River Peak Flood Flows, Corkendale Creek*, Seattle City Light drawing files D-37158

## **Design and Construction Challenges of Overhead Transmission Line Foundations**

(NU's Middletown Norwalk Project)

### *Authors*

*Christopher L. McCall*

*James M. Hogan, P.E.*

*David Retz, P.E.*

Over the past 7 years Burns & McDonnell has been given the opportunity to provide program management and detailed design for Northeast Utilities (NU) subsidiary Connecticut Light and Power (CL&P) on their Middletown Norwalk 345-kV Transmission Project. The project includes 69 right-of-way miles of 345-kV and 115-kV overhead and underground transmission line. This \$1.2 Billion project was completed in December, 2009. In order to provide support to the project locally, Burns & McDonnell established an office near the project site that has been staffed with over 70 professionals. Under the final design approximately 45 right-of-way miles of this line were constructed as overhead transmission lines with over 120 actual miles of overhead line. This will require just over 770 new, single, and multiple pole structures to be installed. To accommodate these structures just under 900 foundations will be required. Given the large scale and conditions of this project, there have been many challenges to overcome regarding these foundations. Initially one of the largest challenges was determining the type of foundation to use given the rocky terrain. Creating a design process for the different possibilities was necessary. Geotechnical and environmental questions as well as issues encountered during the actual construction have also provided significant challenges. Additionally, the unusually long project timetable created challenges and required a massive coordination effort. This paper will discuss these different challenges and how they were overcome.

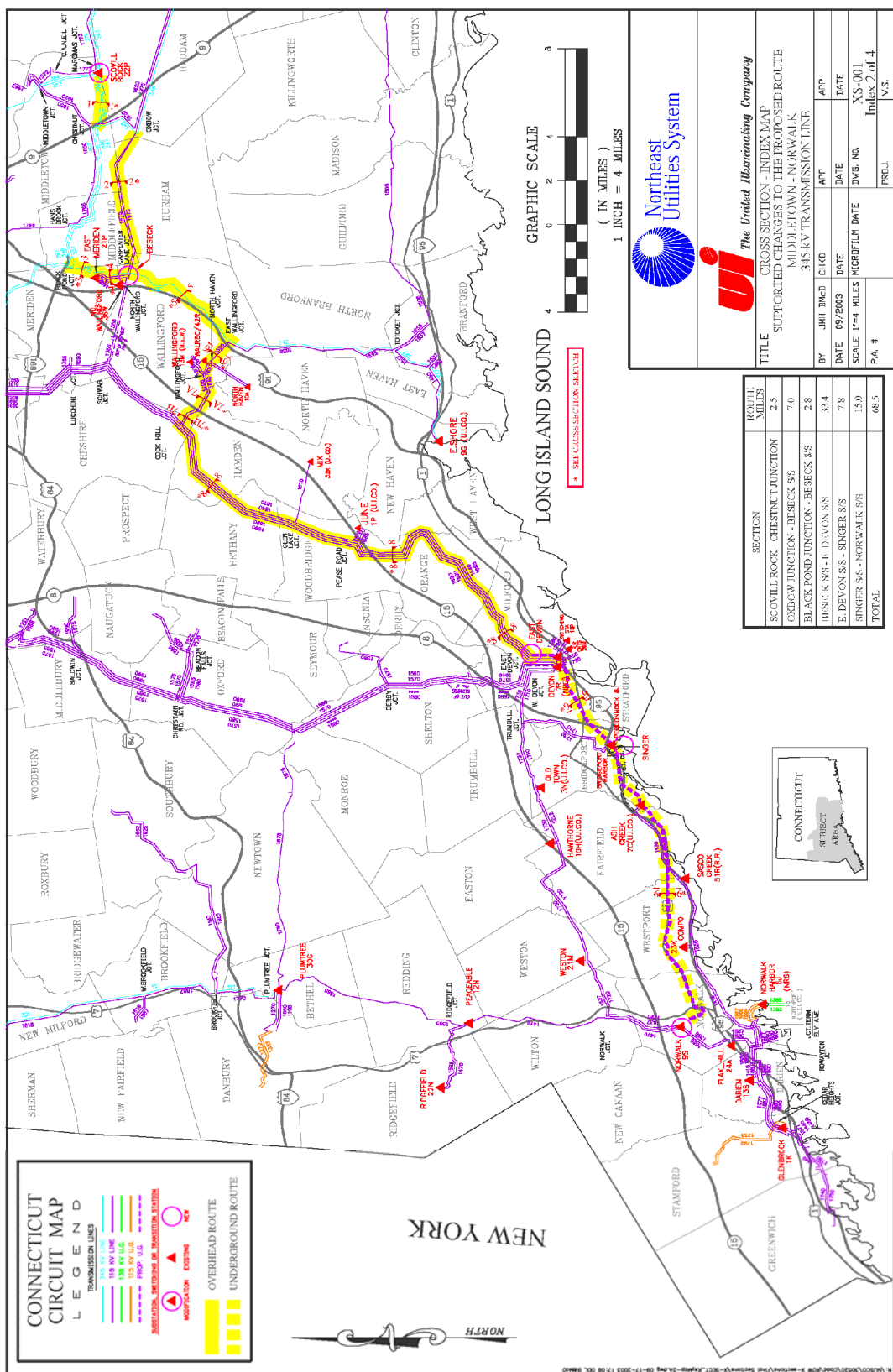


Figure 1 (Middletown Norwalk's Route through Connecticut)

Telegram Channel: @Seismicisolation

### **Route Description**

The Middletown Norwalk 345-kV Transmission Project traverses the state of Connecticut from near the center (Middletown area) to the Southwest corner (Norwalk area). Between Middletown and Norwalk, the project passes through 18 separate municipalities, with the overhead portion of the transmission line extending from Middletown to the town of Milford. The entire line winds its way through rural, suburban, and urban areas. With the exception of small portions of the line, the new route follows existing corridors of 115-kV and 345-kV lines. By making use of several different pole configurations and by replacing and upgrading large portions of the existing lines, the final route minimized the amount of disturbance and additional right-of-way required. In some instances small bypasses were constructed to accommodate residential developments that have been constructed along the corridors. With the expanding development in the area, right-of-way access and expansion became a large coordinated effort. Typical of transmission line projects, construction access also became an issue.

### **Terrain and Soil Conditions**

The first item to consider in foundation design is the condition of the soil in which the foundation is to be placed. With a project of this size traversing 45 miles of ROW, there are numerous variations in the soil conditions. The second issue is the size of the foundations that would be needed. Burns and McDonnell subcontracted Haley and Aldrich, a geotechnical engineering firm with offices in CT to perform soil borings at each proposed structure location. These locations were based on the initial line designs. As we will discuss, changes to these initial locations provided some of our greatest challenges. Various all-terrain drilling rigs were used to perform the necessary borings and collect soil and rock samples. Where required, small track-mounted rigs were used to gain access to areas of steep terrain and heavy vegetation. Laboratory tests including, grain size analysis, moisture content, unconfined compressive strength of soil and rock, split tensile strength of rock, and soil chemistry analysis were performed to provide pertinent design information. Using the information gathered from these soil borings, Burns & McDonnell was then able to begin conceptualizing the types of foundation designs that might be feasible. There was now significant evidence that most of the foundations used would have to be placed in rock. However, given the rolling and sometimes mountainous terrain the depth of the different types of soil and rock sometimes changed between adjacent soil borings let alone the change that occurred between miles of line.

As a generalization, testing results showed bedrock at slightly higher subsurface elevations in Segment 1 of the project. Segment 1 consisted of everything North and East of the Beseck Substation (seen in Figure 1). Bedrock in this area consisted mainly of schist, gneiss, and amphibolite. Topsoil in this area was typically less than 1 ft thick, with thin layers of Subsoil and Colluvium beneath it at maximum thicknesses of 3.5 ft and 3 ft respectfully. Soil in this area consisted of sandy silt to silty sand with increasing amounts of gravel in the Subsoil and beneath. Glacial till consisting of much denser silty sand and gravel containing large cobbles and boulders was found below this. Bedrock in

the remainder of the project was slightly less shallow, and was composed of Sedimentary and Volcanic rock. In these areas various amounts of fill material was encountered at a maximum depth of 23 ft. Topsoil in the area was generally less than 5 ft in thickness with Subsoil up to 5 ft in thickness as well. In some areas, wind blown deposits of loose to medium dense silty sand and sandy silt up to 2 ft thick was found beneath the Subsoil. Beneath the Subsoil and wind deposits more of the same Glacial till was encountered.

### **Foundation Options**

There are numerous structure configurations supporting single and double circuit conductors on structures of moderate to extremely tall heights. Additionally, various required conductor tensions produced structures with a variety of loading conditions. The loads that resulted from some of these structures necessitated extremely large foundations. Drilled shafts are a commonly used foundation for tubular steel transmission structures. Due to their design, drilled shafts tend to have the most capacity for resisting large overturning moments from transmission line structures. In many designs the drilled shafts make use of rock sockets near the base of the foundation to provide the required capacity. In the case of Middletown Norwalk there was initially significant concern expressed with the extremely hard and very shallow rock that existed in some areas. With compressive strengths of over 30,000 psi, there was a concern that the rock could not be drilled with conventional drill rigs. The designers and the construction contractors both believed there could be problems drilling to the required depths for drilled shaft foundations through considerable solid rock. Blasting was considered but was ruled out due to the proximity to businesses and residences in some areas as well as the potential for damage to the remaining rock that was needed to support the foundation. In an attempt to decrease the depth of foundations, two additional foundations types were considered. The idea being that in instances where extremely hard rock was deep or nonexistent, conventional drilled shafts would be used; however, when extremely hard rock was relatively shallow one of the other two designs would be considered, depending on the specific depth of rock. Where more moderate strength rock was encountered, even at shallow depth, conventional rock socketed drilled shafts were still considered most economical.

The first of the alternate foundations was an anchored mat design. This foundation is similar to a spread footing or mat. Instead of installing full length anchor bolts into a thick mat or pedestal, a steel plate placed in the mat is used to transfer the loads from the pole to grouted rock anchors attached to the foundations. These anchors extend from the bottom of the mat and anchor the foundation to solid rock below. This keeps the size of the mat to a minimum while resisting the overturning moments. These types of foundations were intended to be used when very hard rock was extremely shallow, or within a few feet of the ground surface. See Anchored Mat Foundation figure 2.

The second of the alternate foundations was an anchored drilled shaft design. In instances where hard rock was found to be shallow enough to require a rock socket, but not shallow enough to necessitate an anchored mat foundation, an anchored shaft could be used. The concept of these foundations was that a standard drilled shaft foundation

could be designed to the depth of rock. In order to prevent excessive drilling into rock, the foundation would be anchored to the rock with grouted rock anchors that protruded from the base of the foundation. The rock anchors would span the height of the drilled shaft portion of the foundation before extending through the bottom and into the rock. The anchors were assumed to be prestressed to limit shaft deflection and rotation. See Anchored Shaft Foundation figure 2.

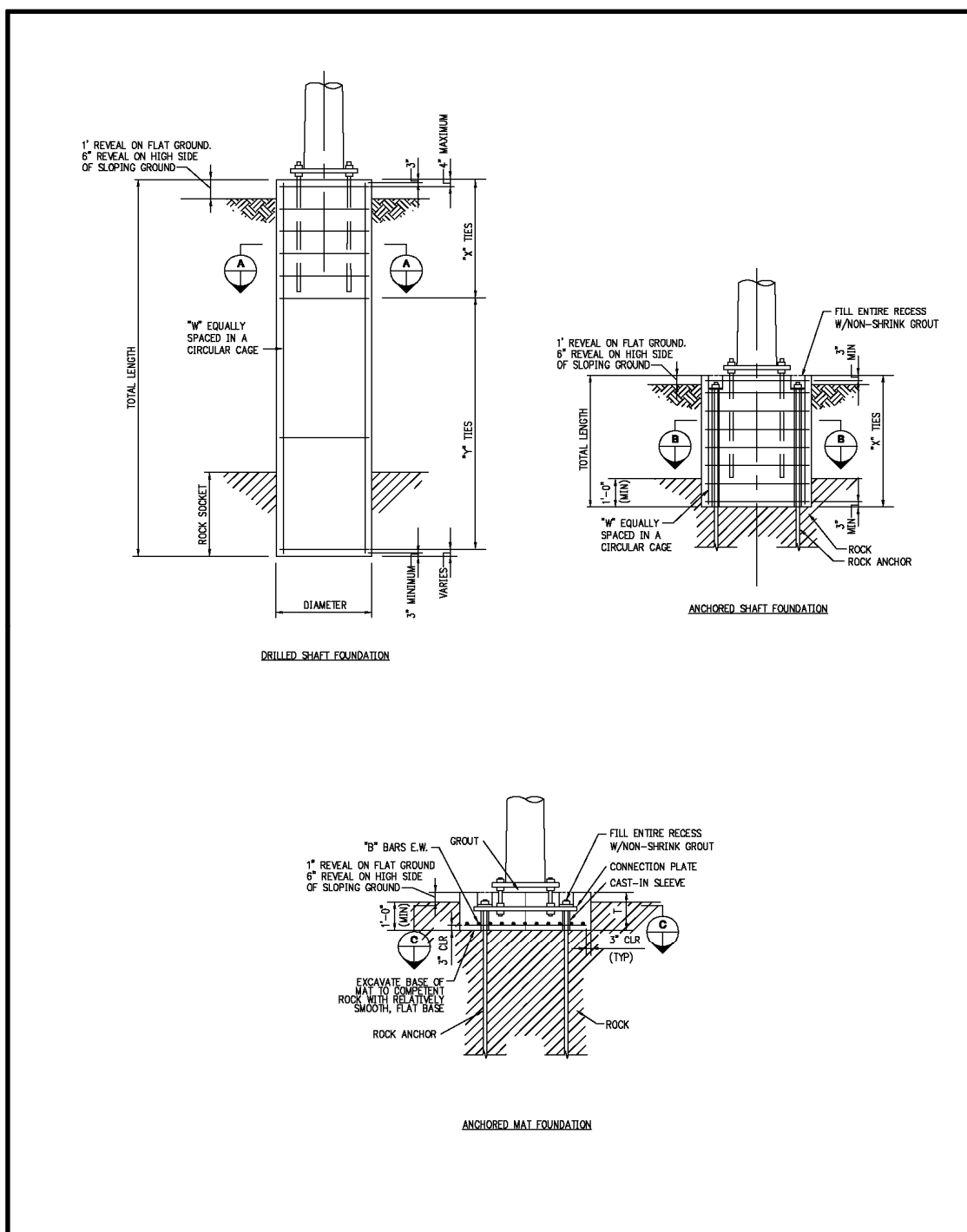


Figure 2 (Various Foundation Designs)

### **Final Decisions**

At this point a framework had been established regarding design concepts. With this framework in place, preliminary design was performed to establish bid quantities. As usual a large majority of the foundation designs incorporated the standard drilled shaft approach. This left around 20% of the foundations, which fell within the parameters initially lending themselves to one of the two alternate designs. Areas where rock was present within a few feet of the groundline utilized mat foundation designs. The remaining areas of concern used the anchored shaft design.

Even though the alternate foundations would ideally save time and money required for the drilling of large quantities of very hard rock, there were several problems with using these foundations discovered through the bid process. The first of which was testing. It became obvious that large scale testing of the rock anchors would be required at each structure site. The problem with on site testing is that the consequences of a test failing would typically render the foundation useless. If one of the rock anchors did not hold its required capacity and pulled out of the rock below, that foundation would no longer be sitting in a viable location. In turn, this would require moving the structure's location and creating another foundation. Another issue dealt with materials. The materials needed to construct the alternative foundations tend to have long lead times. This was especially true of the large metal plates needed for the mat anchor foundations. Each plate was several inches thick to resist the bending moments with unique hole locations placed in each mat. Because final designs were being completed as the installations of previously designed foundations were in progress, this caused serious concerns for procurement. Discussions with the bidders also revealed that the alternate foundations required considerably more labor due the significantly more complex construction. The plates were very heavy and would be difficult to handle in the field and the grouted rock anchors turned out to be a more expensive option than initially considered.

Once construction began, it became apparent that the contractor was not having as much trouble drilling through the hard rock as had initially been expected. With this in mind, the decision was made to redesign all of the alternate foundations so that, if at all possible, drilled shafts could be used. If the rock were to pose serious problems, the original alternate foundation design could still be recalled and put into place. Even though it sometimes required an extended timeframe to drill the newly designed rock sockets in hard rock, it proved to be a more efficient method of foundation placement. Ultimately, there were no structures that have required alternative foundations.

### **Geotechnical Considerations**

Burns & McDonnell's structural department was faced with determining the reactions at each of the roughly 900 different foundation locations for drilled shaft design. Through discussion with NU, parameters for foundation deflection and rotation were determined to be 3 inches and 1.5 degrees respectfully for the entire project. These parameters were used as the basis for the foundation designs. The inconsistent rock depths and varying soil conditions made this a complicated task.

While the presence of shallow rock resulted in shallower drilled shafts for some structures, the internal shear stresses built up in the rock sockets required very tight shear ring spacing for the more heavily loaded drilled shafts.

There were a small number of structures that were placed in areas with very loose soils with shallow groundwater and no rock to provide stability. Providing the required foundation capacities and maintaining the required deflection and rotation criteria in these locations required quite deep foundations. The resulting foundation designs required some of the largest volumes of concrete in the entire project.

Due to the quantity of structures, organizing the different boring logs and keeping them coordinated with the different foundation designs became extremely important. Troubles along the way included changes in the structure numbering during design that caused the boring log numbers to be mismatched with the structure numbering scheme. This was overcome by a coordinated effort in organization. As indicated some individual structure locations changed following the completion of the soil borings. These changes made it necessary to make engineering judgments regarding the actual soil profiles and depth to rock in these new locations.

### **Environmental Considerations / Permitting**

As with any project, particularly one of this magnitude, environmental considerations always need to be kept in mind. Burns & McDonnell employs environmental scientists to do exactly that. As usual it was necessary to establish relations with the different permitting agencies. For Middletown Norwalk the span of the project included a span of different permitting agencies. When it came to foundations there was an increasing concern for the amount of earth that would be displaced during construction. However, the most important environmental issue was the affect the construction would have on the wetlands. In order to decrease wetland disturbances, a great amount of effort was put forth to keep as many of the new structures out of existing wetlands as possible. Once the structures' final locations were known, the overall changes and specific structure locations were compiled so that the overall displacement could be provided to the various permitting agencies as needed. As the project progressed the final displacement information was continuously updated to keep all interested parties up to date.

Overall more than 250 documents were submitted to different permitting agencies, municipalities, and the siting council for review and approval. Permits ranged from items such as road and railroad crossing for the Connecticut DOT to Tidal Wetlands Permits for the Office of Long Island Sound Program. The U.S. Army Corps of Engineers was involved with wetland protection, while the U.S. Fish and Wildlife Service, National Marine Fisheries Service, and the Connecticut DEP were all involved to oversee various other environmental and wildlife concerns. As stated, the Middletown Norwalk Project passes through 18 separate municipalities. Each of these municipalities had various concerned parties ranging from Tree Wardens to Planning and Zoning Commissions. Additionally, approval from the Federal Energy Regulatory Commission and the New England Regional ISO was essential for the technical and monetary authorization of the

project. Lastly, a large majority of the required submittals consisted of Development and Management Plans requested by the Connecticut Siting Council. Any design changes, extended work hour requests, and contractor location information were submitted through these D&M plans.

### **Construction**

Once the Middletown Norwalk Project moved into the construction phase a whole new set of challenges presented themselves. Hard to reach locations caused mobilization issues, the quantity of foundations caused headaches in procurement, and the variable depth to rock over short distances forced many redesigns for structures that were moved even slightly during construction. Actual site conditions caused significant field changes. Timing and coordination between the owner, contractors, designers, and the field representatives became critical. Time required to drill rock sockets determined the pace of foundation placement. Other field changes had to be coordinated with drilling schedules so that the affect on overall time line could be minimized.

As stated, rocky soil conditions were found to pose less of a problem to drilling than they did to engineering. The upper limits of this decision have been tested, and have proved to hold true. Some of our largest rock sockets extended up to 15 feet in depth. Using large, crane mounted drilling equipment the contractor has been able to drill though the largest rock sockets in less than a week. For most rock sockets rock augers and core barrels were used to drill a series of smaller diameter holes to the full length of the rock socket. By drilling a series of smaller holes, the full diameter of the foundation could be reached by breaking up and removing the remaining rock to the appropriate diameter. The exact amount of time it takes to drill these sockets of course depends on the size of the drill rig in use and the actual strength and depth of the rock in question. In the worst cases, it was not a large enough loss of time to make the material lead time and additional construction cost required for the alternate foundation designs worth while.

One issue that caused some scheduling problems was the difference between what could be considered competent rock for design purposes and what was considered rock for payment to the contractor for drilling. The competent rock that is assumed to provide the needed rock socket for support of the foundation designs often laid beneath layers of weathered or less competent rock. Unfortunately, the drilling contractors assumed that any material not specifically called out as rock would be much easier to drill though. In reality the less competent rock still required significant effort to excavate. The contractor's drilling rates for rock were uniform. Any soil that drilled like rock was charged as rock. Once this was realized, the required drilling could be estimated more effectively. This allowed for a much more accurate construction schedule.

In several locations, loose, sandy soils below the water table were encountered during drilling that required installation of temporary casing. In a few instances, the casing was not properly sealed and the sands were found to flow into the shaft during excavation, resulting in relatively large areas of subsidence surrounding the foundations. In areas of subsidence, the soils were assumed to have become very loose. Pressure grouting was

needed to stabilize the soils surrounding foundations and re-establish the anticipated soil strength required to support the foundation. Detailed grouting plans and specifications were prepared to accomplish this work.

Like all projects, field changes had to be dealt with as construction progressed. For foundations, the most significant changes occurred due to the actual depth of competent rock. Initially soil borings were taken for every structure in the initial design of the project. However, issues arose for foundations where borings were taken for a structure that was later relocated, or where borings were used for structures that were in close proximity but not at the exact location. As the foundation installation took place it was monitored by the contractor as well as onsite representatives for the geotechnical consultant and Burns & McDonnell to ensure that the conditions were as anticipated. In the event that the conditions failed to conform to what was expected, a new foundation design could be generated to account for the existing conditions. As noted, the most common cause for a foundation redesign was a significant difference in the depth of competent rock.

When a foundation redesign was required, Burns & McDonnell's on site construction superintendents relayed the information back to the design engineers located in Kansas City, Missouri, where they had a very short amount of time to return a new foundation design that would support the revised subsurface conditions. This type of communication need brings up the most important challenge faced in the Middletown Norwalk Project. Without good communication and timing between all parties involved, there could have been a significant amount of added delay and cost to the project. Burns & McDonnell's on site construction superintendents proved to be the vital link between the field and the design engineers. They have coordinated the transfer of all pertinent information from the on site geotechnical engineers, who provide the required expert opinion of the existing soil conditions. They also coordinated the needs of the construction contractors so that they were able to efficiently use their time and equipment. In addition to coordinating with the field, the design engineers also had to maintain coordination with the pole supplier, Thomas and Betts. In the case of foundation design, all parameters were based on the loads and dimensions that each specific pole originally required. Through cooperation with pole manufactures, delivery of pole designs was coordinated to meet the timing needs of the field for foundation construction. Last, but not least, coordination with NU was critical. Not only so that they could stay informed of progress, but so that their engineers could have a chance to review and make comments regarding the multiple aspects the project.

### **Conclusion**

Overall, NU's Middletown Norwalk 345-kV Transmission Project has been a great success. The overhead line design was completed six months ahead of schedule and under budget. It has shown again the benefits of teamwork within Burns & McDonnell and also within the industry. The foundations in transmission and distribution projects are sometimes overlooked due to the more impressive nature of the project's other aspects, but as engineers we know that these foundations offer the hidden support the

project requires. Overall, the most important lesson learned from Middletown Norwalk has been that an engineer can never be too organized. No matter whether the project in question will require a hundred miles of line or just a few. Being able to offer answers during construction, instead of asking additional questions, has proven to be worth while. It provides a perfect example of the need to prepare for all foreseeable situations in design, so that construction can proceed as scheduled.

## Transmission Line Construction in Sub-Arctic Alaska

### Case Study: "Golden Valley Electric Association's 230kV Northern Intertie"

Gregory E. Wyman, P.E., P.L.S., M.ASCE<sup>1</sup>

<sup>1</sup>Golden Valley Electric Association, Inc., P.O. Box 71249, Fairbanks, AK 99707-1249; PH (907) 451-5629; FAX (907) 458-6371; email: gwyman@gvea.com

#### **ABSTRACT**

Construction projects throughout the world have become more complicated and logically challenging as environmental stipulations become more demanding and the effects climate change become more pronounced. No where is this more evident than in the sub-arctic, in this case interior Alaska, where Golden Valley Electric Association, Inc. (GVEA) is the Owner of the recently constructed 230 kV Northern Intertie transmission line project. This transmission line project is underlain by "warm" discontinuous permafrost prevalent throughout interior Alaska. The potential for change in the marginal permafrost over the life of this project had to be addressed at the design phase to provide the most economical project. This case study discusses the challenge engineers and contractors alike faced in scheduling, accessing and constructing a project across four distinct geographic areas, with an emphasis on permafrost zones. Contractors faced extreme weather conditions where summer sun shown for as much as 21 hours, to winter conditions with as little as 3 hours of daylight. Temperatures during construction varied between 32°C (90° F) and -45° C (-50° F). Without a clear understanding of design parameters between the Engineer and Contractor, projects can easily become problematic.

#### **INTRODUCTION**

Golden Valley Electric Association (GVEA) is a Generation, Transmission and Distribution Co-op serving the interior of Alaska and is headquartered in Fairbanks, Alaska. GVEA is the owner of a 230 kV transmission line that originates at Healy Substation in Healy, Alaska where GVEA owns a mine-mouth coal power plant and has a connection to a single 345 kV transmission line which connects to additional generation in south-central Alaska 483-km (300-miles) to the south. This paper highlights some of the unique challenges for transmission line construction in a Sub-Arctic environment (Interior Alaska). The 154-km (96-miles) of 230 kV transmission line was constructed with four separate construction contracts corresponding to the four distinct geographical and geological zones and extensive areas of discontinuous permafrost.

The first 10-km (6-miles) of the transmission line had to be located between the bank of the Nenana River, a coal mine haul road and 300 foot gravel bluffs (Usibelli Section). The next 38-km (24-miles) crossed mountainous terrain along the northern slopes of the Alaska Range with very limited access (Foothills Section). Dropping out of the mountains, the line crossed 96-km (60-miles) of the Tanana River Valley, a very flat area consisting of swamps and floating bogs (Tanana Flats Section). The final 10-km (6-miles) included a 730-m (2400 ft.) crossing of the Tanana River, then through a lightly populated industrial area into the terminus at Wilson Substation in Fairbanks, Alaska (Fairbanks / Tanana River Crossing Section). (Figure 1.)

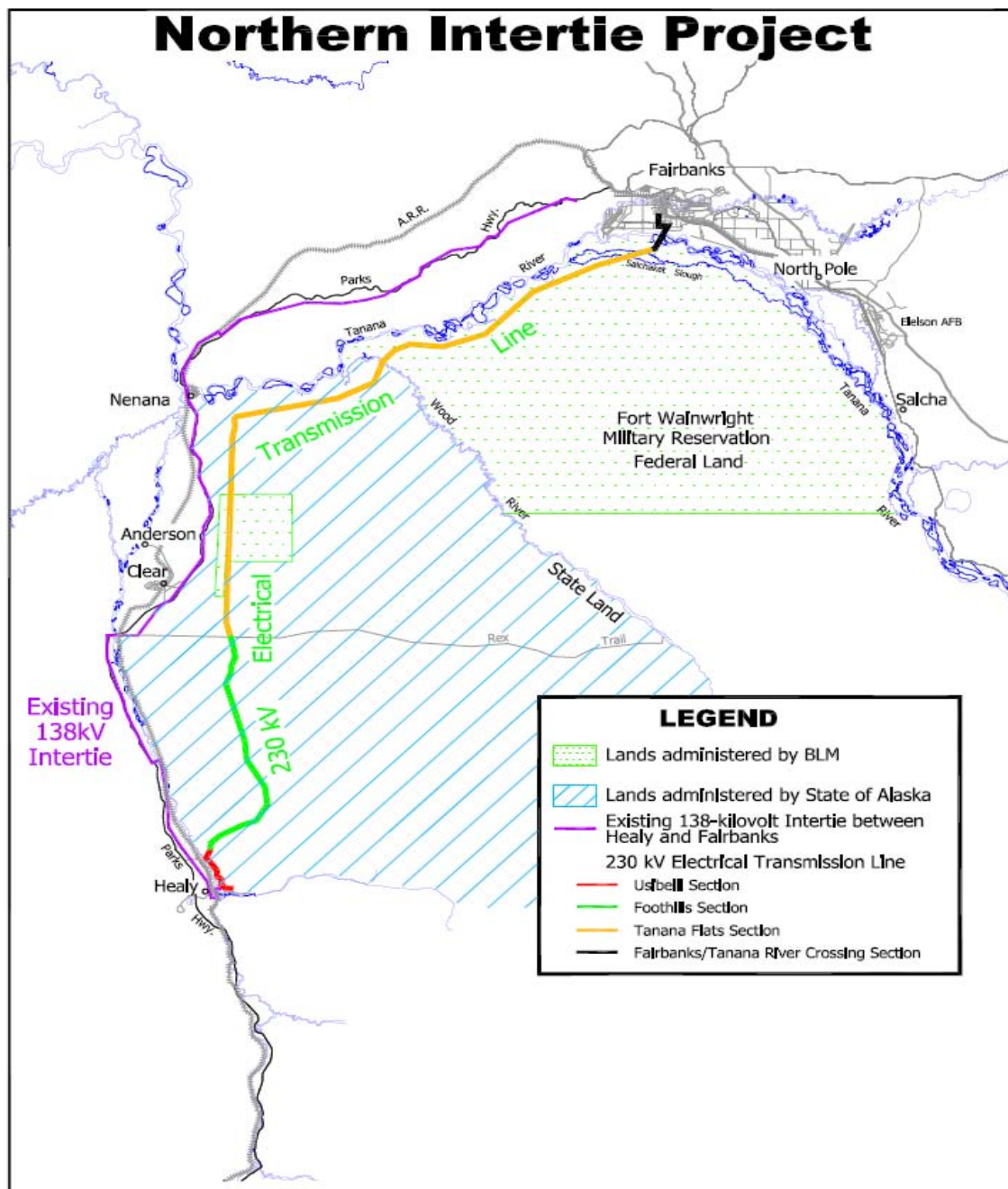


Fig. 1 Northern Intertie Route

Several different types of tubular steel towers were used along the route. Single shaft un-guyed “Y-towers” were used in accessible areas where a small footprint was needed. Fore and aft guyed “X-towers” were most commonly used as the standard tangent and light angle structure. Self supporting “Swing-Set towers” were used for large angles and deadends. All of the towers are supported by driven steel pipe piles varying in size from 12-inch to 66-inch diameters and depths from 24 feet to 80 feet. Typical fore and aft guying was anchored by drilled and grouted rock anchors in the mountains or 10-inch driven piles in the flats.

Telegram Channel: @Seismicisolation

## FOUNDATION DESIGN CONSIDERATIONS

This project overlies vast areas of marginal permafrost that is found at the edges of the world's cold regions. During the life of a project, these areas, by definition, have the potential to change from frozen to thawed states, resulting in the soils ability to carry a load. Ground temperatures in areas of marginal permafrost are typically greater than -1° C (30°F) and often isothermal for some depth. (Musial, 2007)

The foundation design had to recognize that engineering characteristics of the underlying permafrost would change over the life of the project. Not only the load carrying capacity of the soils, but the continuing maintenance costs of subsurface changes had to be addressed. Changes in surface conditions will alter or degrade the permafrost below. (Linell, 1973)

Foundations for the structures in the "Usibelli Section" supported un-guyed single shaft Y-tower adjacent to the Nenana River and were subject to erosion and rock slides; permafrost was not an issue. The subsurface material consisted of glacial outwash and alluvial deposits, ranging in size from sands to large boulders. Since loss of lateral support from river erosion was a large concern deep pipe piles were selected that would allow loss of up to 5-m (16-ft.) of the upper soil layers. A small footprint was needed to fit the structures between the active coal mine haul road and the raveling gravel bluffs. The "Y-Towers" can be seen in Figures 2a. and 2b.



*Fig. 2a (above left) Example of "Y-Towers" with foundation attachment.*

*Fig. 2b (above right) Example of "Y-Tower" with rock deflectors.*

At the 10-km point the line left the active coal mine area and proceeded into the mountains north of Healy where guyed “X-Towers” with a wider footprint were used. (Foothills Section) Subsurface conditions in this section consisted of uplifted lake beds and were found to be densely packed alluvial gravels. With the gravels being non-frost susceptible, a shallow drilled pipe pile grouted in place was used. Existing mining and exploration roads provided vehicle access to about half of the next 38-km; however, the remaining 19-km (11-miles) was restricted to helicopter access only. No disturbance of the root mat was allowed in these areas which made for creative solutions to provide level work pads. (Figures 3a and 3b)

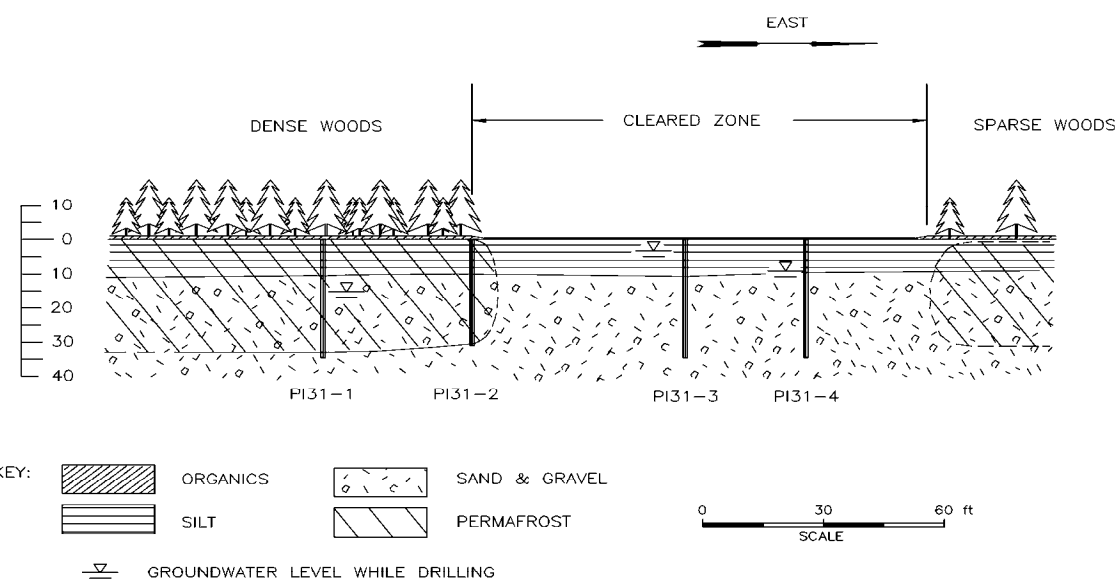


Fig. 3a (top) Work Pad Cribbing on sideslope.  
Fig. 3b (bottom) Foundation pile grouting setup on cribbing.

The transmission line exits the mountains at kilometer 48, extending 96-km (60-miles) across the low-relief terrain of the Tanana River Valley (Tanana Flats Section). The guyed “X-Tower” was used exclusively for all tangent and light angles across the flats, with the un-guyed “Swingset Tower” at deadends and large angles. The tower foundations and anchors consisted of single steel pipe piles. Short term loading from lateral and uplift forces caused by wind and ice controlled the design as sustained loads were relatively small for the X-towers, but much higher for the swing-set towers.

The design of the foundations and anchors had to consider both the frozen and unfrozen state of the soils across the Tanana Flats. Geotechnical investigations for this portion of the project examined an existing GVEA 138 kV right-of-way approximately 5-km (3-miles) west of the Northern Intertie route. When constructed in 1966 the underlying soils consisted of an approximate 9-m (30-ft.) layer of frozen silts and gravels. The original 33-m (100-ft.) wide right-of-way clearing removed all trees and shrubs, leaving the root mat intact. In the 31 years between 1966 and 1997 the permafrost degraded completely in the cleared area as can be seen in Figure 4. This phenomenon has been well established and a well known study by the U.S. Army Corps of Engineers between 1946 and 1972 showed the clear link between the vegetation removal and the resulting degradation of permafrost. (Linell, 1973)

The data collected during November 1997 showed that the permafrost was very marginal and isothermal with ground temperatures warmer than  $-0.3^{\circ}\text{C}$  ( $31.5^{\circ}\text{F}$ ). Isothermal ground temperature is a characteristic indicator of permafrost susceptible to changes in surface conditions. (Musial, 2007)



*Fig. 4 Loss of permafrost due to clearing for construction (Musial, 2007)*

The original foundations on the 138 kV line consisted of 9-m (30-ft.) wooden piling and upon degradation of the permafrost the frost heave jacked the foundations out of the ground 1- to 2-m (3- to 6-ft.). Resulting maintenance costs for this type of foundation failure can be substantial and was a major concern when designing the Northern Intertie.

With the marginal permafrost across much of the area, it was not “if” it thawed, but “when” it thawed that was of concern during the design. When frozen, the soils will provide a sustainable adfreeze resistance of between 488 and 976 kg/m (1000 and 2000 psf) (Golder Associates, May 2 and July 18, 2000). When thaw occurs, that resistance is reduced to an average of about 244 kg/m (500 psf). These conditions regularly create high frost-heave forces.

Frost heave forces will lift a pile out of the ground each season in what is known as frost jacking. This phenomenon was found to control the length of piles used along the route. Significant heave forces were expected because the soils were frost susceptible, meaning that the soils would wick the groundwater up to the freezing front. Frost heave occurs when the pore water in the active layer expands and ice lens’ form at the freezing front in freezing weather.

The active layer in the Tanana Flats, or that layer subject to annual freeze-thaw cycles, varied between 0.6 and 2.4 m (2 and 8 ft.). The active layer thickness and the adfreeze strength was the most significant factor in determining the relatively high frost heave forces that were expected across this area.

Adfreeze skin friction developed by the frozen soil in the active layer will cause the soil around the pile to heave, resulting in an upward load applied to the pile. Figure 5 shows a conceptual frost heave model for a single pile.

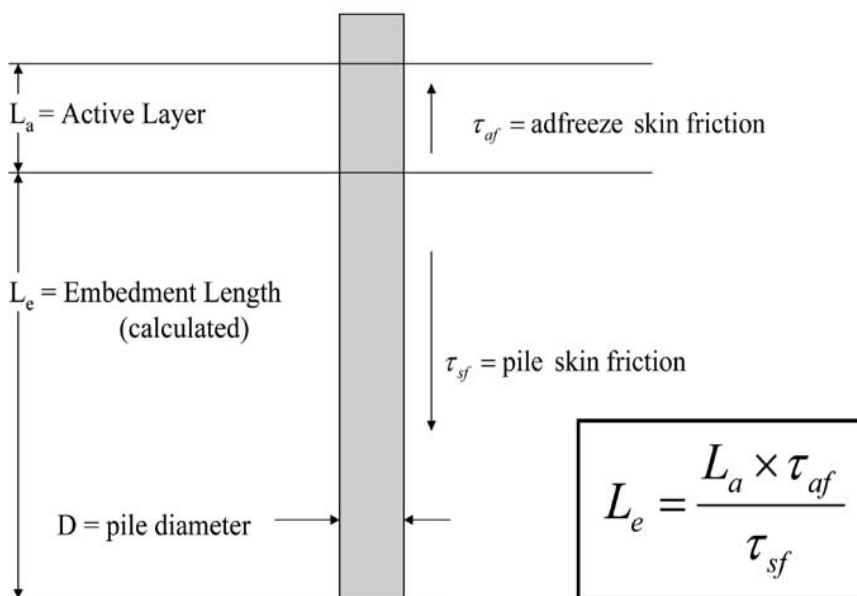


*Fig. 5 Conceptual frost heave model for single pile*

During the initial design we used a 1.2 to 1.5 m (4 to 5 ft.) active layer depth and 2.8 kg/m (40 psf) adfreeze within the active layer. The estimated embedment depths that were developed to resist frost heave ranged from 6 to 24 m (20 to 80 ft.) depending on loads and soil conditions.

The 96 km (60 mile) section across the Tanana Flats consisted of the most unstable soil and would require the deepest embedment depths. GVEA worked with the transmission line designer, Dryden & LaRue, Inc. and the geotechnical consultant, Golder & Associates, Inc. to use probability and statistics in the design process. To develop a business risk model, we estimated the variability in frost heave potential along the alignment. The X-tower has long been used in Alaska due in part to its ability to withstand relatively high differential movement between leg foundations. As the owner, GVEA had to evaluate the question of whether it was important to have no foundation movement through the installation of deep piles, or would on-going maintenance mitigate the significant frost heave (more than 20 cm [8 in.]) if shallower piling were used. Although a probabilistic model was developed, it was ultimately thinking in terms of the risk of change over the life of the project that provided the design guideline. Whether it be in business operations or engineering design:

*"It is better to be roughly right than to be precisely wrong." (John Maynard Keynes)*

The decision was made to install piles to a minimum depth of 11 m (36 ft.) in the flats. For those structures with higher loads, such as large angle swingset towers the depth was 25 m (83 ft.). Some areas in the flats encounter very loose soils and piles were driven to depths in excess of 27 m (90 ft.).



To accommodate the differential movements of the foundation and provide adjustable connections, pile clamps were developed for ease of lowering or raising the tower leg as part of the on-going maintenance. Pin connections to the tower leg also allowed the tower to be assembled flat on the ground and tipped upright into place. (See Figure 6 at left.)

*Fig. 6 (left) Pile clamp*

The X-towers were guyed fore and aft for longitudinal support and the anchors were also driven piles. Guy strand shear release mechanisms were developed to protect the structures from large compressive forces that develop when the towers experience foundation jacking and move differentially to the anchor piling. On GVEA's existing 138kV transmission line in the same area a shear release device was included in the guying system with poor results. Several structures suffered compressive failures when the release mechanisms failed to operate. It appeared that the strength of the shear bolts used in that system were inconsistent and failure occurred in the structure prior to failure of the shear bolt.

The new shear release mechanism uses the same shear pins used in the AB Chance screw anchor torque limiter (Chance catalog #C303-045). The new shear release mechanism was manufactured with positions for seven shear pins in double shear and one in single shear. A shear pin retainer plate keeps the pins in place and allows for replacement if necessary. By varying the number of pins used, release loads between 3,740 Kg (8,250 lbs.) and 7,485 Kg (16,500 lbs.) were developed for the project. Components of the shear device are shown in Figure 7 below.



Fig. 7 Guy strand shear release mechanism

These mechanisms were attached to the guys by creating a loop in the guy wire and inserting the device using pre-formed guy grips. Figure 8 shows a typical X-tower with the shear release mechanism installed.



*Fig. 8a (left) X-tower with shear release mechanism*

*Fig. 8b (above) Shear mechanism after release*

The final 10-km (6-mile) segment of the line into the Fairbanks area (Fairbanks / Tanana River crossing section) consisted of two 56 m (185 ft.) crossing towers and single leg Y-towers and side post structures into the substation in Fairbanks. Soils in the area were either within the thaw bulb around the Tanana River or in areas where the permafrost had degraded due to past development.

## CONSTRUCTION ISSUES

It was natural to divide the project into four separate contracts as they were made distinct by such issues as terrain, logistics and seasonal restrictions. The two largest contracts were the “Foothills Section” and the “Tanana Flats Section” which were also subject to the most restrictions on construction. The contracts for the two 10-km (6-mile) sections at each end of the transmission line were easily accessible and subject to few restrictions.

Communication on any project is key to a project's success, whether it be through the contract documents, pre-construction meetings or during construction itself. Whether through the Owner's inability to communicate the importance of subsurface conditions or the contractor's inability to listen, the issue that created the most challenges was the contractor's lack of understanding of these subsurface conditions.

As part of the bid process, geotechnical information collected during the design phase was made available to contractors at both the Owner's offices and the Engineer's offices; but were not

included as part of the bid package. Unfortunately, several of the contractors did not examine the geotechnical data during the bid process. Add to this the absence of meaningful site visits (some contractors did fly-bys) led to claims of change-in-conditions, etc.

It became apparent early on that pile driving contractors were accustomed to projects where “refusal” was the standard for piling installation. Because of frost heave forces and uplift that were expected and in some cases the erosion possibilities, all of the foundations were specified to a minimum installation depth. The contract recommended pre-drilling to 80% of the diameter and the use of hardened pile tips, but did not require them.

In the “Usibelli Section” the subsurface soils consisted of material ranging from sands to boulders and no permafrost. Within this section the pile driving contractor did not request the geotechnical data or visit the site during the bidding process. Without a clear understanding of the reasons behind a minimum depth burial, the contractor refused to pre-drill or use pile tips, thinking that “refusal” provided an adequate foundation. Figure 9 shows the results when held to the design depths without pre-drilling.



Fig. 9 One of several pile damaged during installation

Unfortunately, it took intervention of the Owner’s Engineer to stop work and require pre-drilling before the contractor was able to successfully install the foundation piles.

In the mountainous area of the “Foothills Section” the soils consisted of dense gravel deposits with sporadic permafrost. The foundation piles were installed to a depth of 7.5 m (25 ft.) by drilling and grouting in place (See Figure 3b). Logistics was made difficult due to the prohibition of constructing trails or work pads. All materials and equipment had to be flown in and construction activities accomplished with minimal disturbance to the natural vegetative mat. Figure 10 illustrates some of the construction techniques used in this section.



*Fig 10a (above left) Wire pulling setup*

*Fig. 10b (above right) Helicopter tower set. (Used with Permission)*

Construction activities within the “Tanana Flats Section” was the most challenging due to the presence of permafrost along the entire 96-km (60-miles) of right-of-way that crossed wetlands and floating bogs. The area is home to a large population of migratory birds during the summer and fall, and virtually impassable. Environmental concerns dictated that all construction activity be done during winter months, which in interior Alaska can be quite inhospitable.

Access to the right-of-way was not permitted until the ground was frozen to a depth of 30.5 cm (12 in.) and there was 30.5 cm (12 in.) of snow cover on the ground. The snow cover had to be compacted and watered to create an “ice road” capable of withstanding continuous construction traffic. Interior Alaska only receives an average of 33.5 cm (13.2 in.) of annual rainfall a year and snowfall amounts can vary greatly. It was unfortunate that construction was done during two seasons of very light snowfall as the contractor was forced to make his own snow along the road prior to moving construction equipment along the right-of-way. (See Figure 11a)

Short daylight hours and frigid temperatures had to be factored into the production and equipment used. The pipe piles in this section were installed using a combination of hydraulic, diesel and vibratory hammers, depending on the pile size and location. The contractor tried numerous foundation installations without the pre-drilling, resulting in either broken piles or meeting refusal well short of the required depth. By drilling pilot holes up to 80% of the pile diameter and using pile tips, the foundations were ultimately installed to the design depths.



© Patrick J. Endres #IMG\_9105



© Patrick J. Endres #B13A3275

*Fig. 11a (above left) Truck with water tanks and snow guns (Used with Permission)*

*Fig. 11b (above right) Hydraulic vibratory driver on 30 in. pile (Used with Permission)*

In developing the construction contracts it became apparent that with several uncontrollable factors such as snowfall and temperature extremes it was necessary to be flexible in the completion time for the contracts. This was done by giving a completion date of two years, but removing liquidation damage and any penalty clauses from the contract. The contractor would therefore be able to use a third winter season if needed. Even with the marginal snowfall the contractor was able to complete the project on time.

It is imperative that contractors are qualified to construct projects in an Arctic environment. The effect of permafrost on subsurface construction, decisions in the equipment used and the logistics of working in extreme cold with little daylight are critical in a projects success.

## REFERENCES

- Musial, M. and Wyman, G.E., 2007, "Marginal Permafrost a Foundation Material in Transition," *Permafrost Foundations: State of the Practice*, Technical Council on Cold Regions Engineering Monograph, pp 30-49, 2007.
- Crowther, G. Scott, 1990, "Analysis of Laterally Loaded Piles Embedded in Layered Frozen Soil," *Journal of Geotechnical Engineering*, Vol. 116, No. 7, July 1990.
- Linell, K.A., 1973, "Long Term Effects of Vegetative Cover on Permafrost Stability in an Area of Discontinuous Permafrost," *Proceedings of the Second International Conference on Permafrost*, Yakutsk, USSR, pp 688-693, 1973.
- Morgenstern, N.R., Roggensack, W.D. and Weaver, J.S., 1980, "The Behavior of Friction Piles in Ice and Ice-rich Soils," *Canadian Geotechnical Journal*, No. 17, pages 405-415, 1980.
- Reese, L.C. and Wang, S.T., 1997, "Documentation of Computer Program LPILE, Plus Version 3.0 for Windows," Ensoft, Inc., Austin, Texas, 1997.
- Weaver, J.S. and Morgenstern, N.R., 1981, "Pile Design in Permafrost," *Canadian Geotechnical Journal*, Volume 18, pp 357-370, 1981.

# The 2008 Iowa Floods: Structural Challenges and Solutions



Electrical Transmission and Substation Structures Conference  
8 – 12 November, 2009  
Fort Worth, Texas USA

James W. Graham  
Pike Energy Solutions

Tim Van Weelden  
Alliant Energy

Marlon Vogt  
Ulteig Engineers

Telegram Channel: [@Seismicisolation](https://t.me/Seismicisolation)

## The 2008 Iowa Floods: Structural Challenges and Solutions

### **Abstract**

Cedar Rapids, IA experienced an unprecedented flood of the Cedar River in June, 2008. The previous record flood was exceeded by over 11 feet, surpassing the 500-year flood zone in much of the city. Over 9.5 square miles of the city was directly affected. Two major generating plants, the central business district underground electric vaults, and over twenty substations were damaged and/or destroyed.

Recovery and rebuilding the system required innovative solutions to emergency restoration of electrical power. This paper will describe the severity of the damage and detail the innovative solutions used to rebuild a key substation required to restore electric service to the city's downtown distribution network.

### **Background**

Cedar Substation is located along the Cedar River in Cedar Rapids, IA. This substation included two 50 MVA transformers fed by three 34.5 kV lines and a metal clad switchgear comprised of two transformer mains, a bus tie, and nine 13.8 kV feeder circuits. The load served by Cedar Substation is primarily commercial and industrial. One feeder serves a heavy industrial customer with a load of approximately 15 MW, three feeders serve an underground network which supplies power to high density office and retail space in downtown Cedar Rapids. The remaining feeders serve industrial, commercial, and some residential loads adjacent to the downtown area.

On June 13<sup>th</sup>, 2008, the Cedar River crested 11 feet above the previous record flood level. Alliant Energy/IPL suffered the total loss of the 6<sup>th</sup> Street and Prairie Creek Stations, representing 380 MW of generating capacity, as well as the associated transmission and subtransmission substations at each plant. The flood waters also caused moderate to severe damage to 23 distribution substations and the complete destruction of Cedar Substation.

Cedar Substation was inundated with water after a heroic effort to sandbag the site. Water levels rose to the roof eaves of the 15 kV switchgear enclosure and inundated the control cabinets of both power transformers. It was clear that the substation would not be returned to service in its original form. The simultaneous loss of both generating stations, the 34.5 kV transmission system, and Cedar Substation resulted in the complete loss of power to downtown Cedar Rapids and a large area along both sides of the Cedar River. City hall, the police station, the county court house, the county jail, county administrative building, the county sheriff's office, 800 businesses and many hundreds of homes were blacked out. Both city hospitals were on emergency back-up generators. It was imperative to get power to this area to support the coming clean up and recovery efforts.

### **Substation Scope Development and Equipment Procurement**

The planning group quickly realized the quickest way to restore power to the city center would be to build a temporary substation and connect it to the downtown underground network. They determined the new substation must have 50 MVA capacity with no fewer than eight distribution circuits. Planning also was working with the transmission service provider to find a way to re-energize at least one of the three 34.5 kV source lines to Cedar Substation to provide power to this substation.

On Sunday June 15<sup>th</sup> a substation team consisting of planners, substation engineers, and a construction manager was formed and given the task of siting, designing and building the Cedar Temporary Substation. Planning determined the temporary substation required a total of 50 MVA capacity and a minimum of eight 13.8 kV distribution feeders. Power would be delivered to the substation by an existing 34.5 kV subtransmission line. Armed with planning's requirements, the substation team put together a conceptual one-line (see figure 1a) and set up a scavenger team to hunt for suitable equipment which could be used to build the substation.

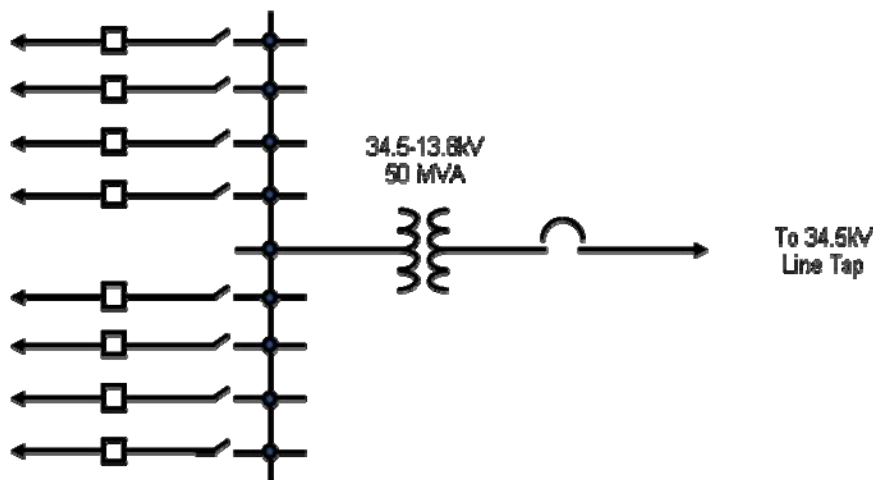


**Figure 1a - Cedar Temporary Substation Conceptual One-Line**

A spare 34.5-13.8 kV 50 MVA transformer purchased in 2004 as a back up to the original Cedar Substation transformers was stored in the regional operation center's material yard. This transformer was standing in four to five feet of mucky water at the crest, which partially flooded the control cabinet. The radiators were stored on the ground, completely inundated. All the bushings were missing, so an emergency purchase order was issued to buy replacements. Another order was placed to procure top and bottom connectors for the bushings.

Waukesha Electric Services was hired to clean the radiators, assemble and test the transformer, and check the control circuits. Fortunately, the transformer passed all tests, and the control circuits functioned normally after some cleaning.

The transformer was too large to fuse, so a circuit switcher was needed. We had taken delivery of a 69 kV circuit switcher for a new substation being built in north

Cedar Rapids. Unfortunately, this circuit switcher was submerged in flood waters and not serviceable. An emergency purchase order was issued, and a new circuit switcher arrived six days later.

This same substation was scheduled to receive a metal clad switchgear in mid-June. The switchgear comprised a 1200A main breaker, a 1200A bus tie breaker, 1200A bus, four 1200A distribution circuits, and associated relay panels. The switchgear alone met neither the 8 circuit nor the 50 MVA requirements.

A small rural substation was also being built in rural north central Iowa. Reviewing the material available from this project yielded a low tension dead end structure, a 69 kV gang operated switch, and a steel box structure comprising a transformer bay and three distribution bays. The bus conductor could support 50 MVA of load but the main disconnect switch was rated 2000A, slightly below the transformer's required full load current of 2091A at 13.8 kV. We debated whether the switch we had would be adequate, but this became a moot point when we salvaged two sets of 15 kV 3000A disconnect switches from yet another project.

On Tuesday, June 17<sup>th</sup>, two days after the water receded, the design team developed the one-line shown in Figure 1, along with an equipment plan and section views for the substation based on the available equipment. The design used the 69 kV switch and a 34.5 kV circuit switcher for primary side transformer protection. We could not locate a 15 kV 3000A circuit breaker in inventory, and lead times for new 15 kV breakers were unacceptably long. This forced us to connect the transformer secondary directly to the box structure bus through the 3000A disconnect switches installed on the transformer main bay. We installed reclosers on the three distribution circuits. Because all four bays of the box were used, we ran a flying tap conductor connecting the cross bus on top of the box structure to the roof bushings of the metal clad switchgear enclosure.

With three circuits coming off the box structure bus and four circuits coming off the switchgear bus, we were still one circuit short. A quick review of the switchgear drawings and a call to the manufacturer confirmed the bus tie position could be converted to a distribution circuit position in the field. This gave us the required eighth distribution circuit.

After consulting their load flow studies, planning was able to assign sufficient loads to the three recloser circuits to keep the remaining load current below the switchgear main breaker's 1200A continuous current rating. This arrangement allowed us to load the transformer to its 50 MVA top rating. Figure 1b shows the final equipment one-line defining the scope of the substation project.

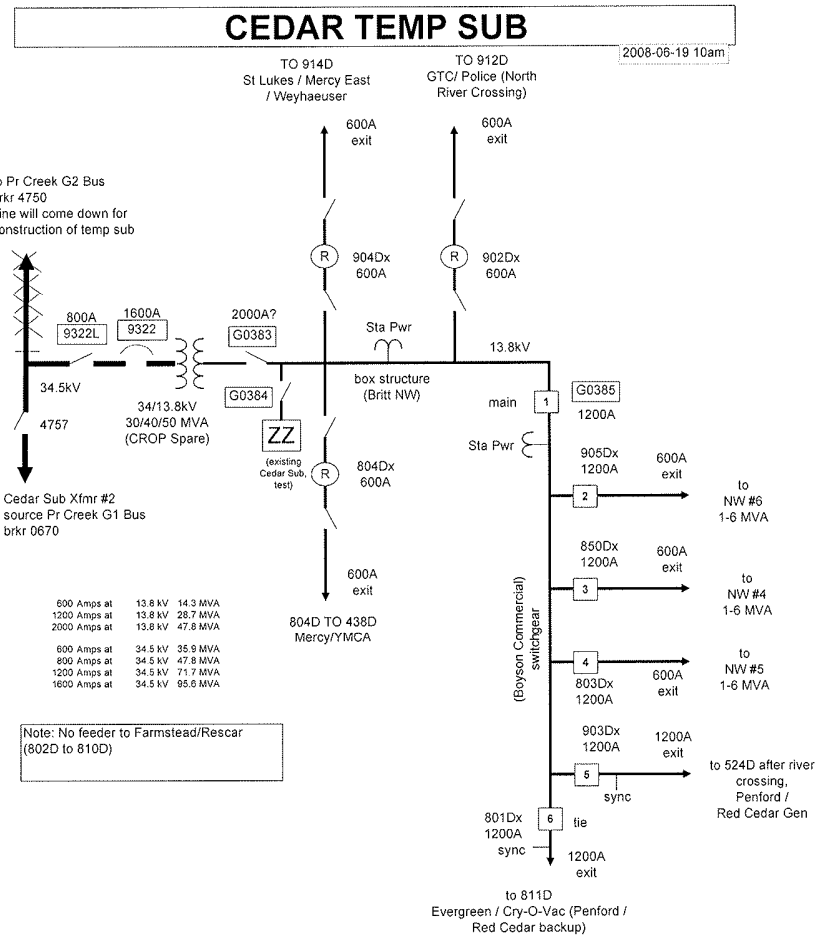


**Figure 1b - Cedar Temporary Substation One-Line**

### **Substation Siting and Contractor Mobilization**

Also on June 17<sup>th</sup>, team members made their first site visit to find a location for the Cedar Temporary Substation. The area around the Cedar Substation is a municipal parking lot, consisting of a concrete surface broken up by landscaped islands that restricted the size of unobstructed areas. We chose an area in the parking lot adjacent to the flooded substation. This location was close to the existing feeder riser poles as well as the existing 34.5 kV lines tied to the flooded substation's subtransmission bus. Cedar Rapids officials were contacted and permission was given to build the substation on the chosen site.

Tim Terrell and Co., a local contractor, was hired to perform initial removal of flood debris from the site and to wash the area down to remove accumulated mud and sand deposited by the flood waters. Hooper Corporation, a utility construction company, was hired to supply labor and equipment for the construction of the substation. The Hooper substation crew demobilized from the construction project they were working on and mobilized to the site.

### **Foundation Layout and Details**

**Telegram Channel: @Seismicisolation**

The foundation designs, by necessity, were low-tech. We did not have time to remove the concrete parking surface, pour concrete pads, or drill and construct pier type foundations so we needed other options. Both our general office and our area maintenance facility were inaccessible due to the flood, which meant the tools available to lay out the equipment foundations were a 100 ft. cloth tape, a can of spray paint and our ingenuity.

We aligned the main bus with the transmission pole which would bring the source 34.5 kV line into the substation by eye and painted the bus center line on the concrete surface. Working from the equipment plan, we measured the center lines for the major structures and equipment, and painted the intersecting centers.

### **Transformer Foundation**

At first glance, a parking lot surface looked level, but in fact the pavement sloped to drain surface water to the storm sewer inlets. Our first structural challenge was to devise a stable, level surface to set the power transformer on. We did not have the time to remove the existing concrete and pour a traditional concrete pad.

We considered setting the transformer on the concrete and shimming the base, but the amount of shims required resulted in an unacceptable stability risk. The contractor suggested building a gravel pad for the power transformer (see Figure 2). The pad was sized to extend about four ft. past the transformer base on all sides to provide a working surface after the transformer was set in place. A line of 8" high railroad ties was set next to the lower edge of the gravel pad. The ties served two purposes. First, to establish the pad thickness, and second, to prevent the road stone from washing away during heavy rains.

An 8 inch layer of gravel (crushed rock with fines typically used to build secondary roads in rural areas) was then laid directly on the concrete surface and compacted, starting at the ties and gradually tapering off up slope. This gave us the required level surface for the transformer. Gravel was chosen because it compacts well, thus giving us the desired stable surface.

Next, copperweld ground mats were laid on top of the base and bonded together to provide a ground plane. The ground mat array was then bonded to the substation ground grid. Finally, a 2" layer of top soil mixed with road stone was placed over the ground mats. This layer provided a measure of self-leveling as the weight of the transformer pressed down onto the pad.

The result of this design was more than satisfactory. After the transformer was set in place, we put a level on the transformer base and found all four sides were almost perfectly level.



Figure 2 - Road Stone Foundation for the Power Transformer

### **Switchgear Foundation**

Our next structural challenge was to come up with a level surface to set the switchgear. Typically our standards call for an array of concrete piers to support a switchgear building, but we did not have time to bring in a drilling rig or pour and cure concrete for the necessary piers before the switchgear arrived on site.

We knew from the equipment plan that the back edge of the switchgear would overlap a curb delineating a landscaped island by about 12 inches. We could not compress the layout to avoid the overlap. This meant we not only had to deal with the slope of the concrete surface, but also had to compensate for the curb height when laying out the support system.

We used the typical footing arrangements from the drawings, and then eyeballed the approximate centerline of the temporary sub layout. We painted an extended substation centerline on the parking lot, then approximated an appropriate offset for the switchgear building centerline. Using this painted “spot” on the parking lot, we laid out the foundation pattern, painting the appropriate ‘dots’ on the concrete.

Wooden railroad ties were cut in half lengthwise, and each piece of wood tie was placed appropriately on each footing spot. Allowances were made for power and control cable exits. After the ties were in place, we checked the height differential between the ties and the top of the curb. We found the top of the curb was actually lower, and the height difference could be made up by simply placing more ties on top of the curb.

When the 68,000 lb switchgear was delivered and set into place (see Figure 3), workers were stationed at each tie to ensure solid contact at each footing location. As the building was slowly lowered onto the ties, the alignment was verified and the building came to rest evenly (miraculously) on all the ties. Only some minor shims

under one corner of the structure were required to level the building. Out of curiosity, a worker put a level on the building's footing rail, and it was only a partial bubble off true level.



Figure 3 - Setting the 15kV Switchgear on Railroad Ties

### **Dead-End Tower Structure**

Our third structural challenge was supporting a 30 ft. tall switch tower and associated 69kV disconnect switch. The incoming 34.5 kV line was a slack span which terminated on this structure. Even so, the structure was still subject to significant overturning moments due to its height.

The dead end tower was a two-leg design, with a bottom plate. No one knew how thick or strong the parking lot concrete was, so it was decided to design a steel base to widen the bearing surface for the structure. The base consisted of two parallel I-beams and a square plate. The plate was welded to the top flanges of the I-beams to form an H pattern. Mounting holes were punched in the plate to match the anchor bolt pattern of the tower leg bases. The lower flanges of the I-beams were punched to accommodate epoxy type anchor bolts set in the parking lot concrete surface. We contacted a local steel fabricator to properly size the steel members and manufacture the bases. Figures 4a to 4d show the completed steel base and details of the bolted connections.



Figure – 4a Dead-End Tower Base

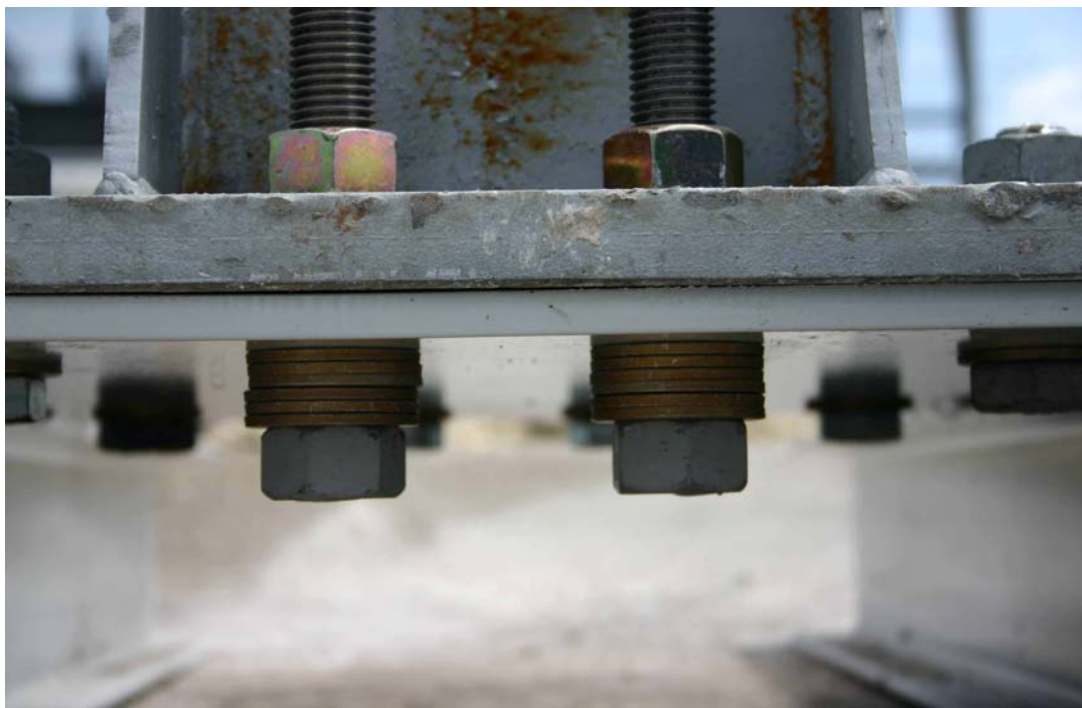


Figure 4b Dead-End Tower Bolted to Steel Base

Telegram Channel: @Seismicisolation



Figure – 4c Steel Base Secured With Epoxy Anchors

### **Circuit Switcher Structure**

The circuit switcher stand was a single leg design and required a similar steel base as used for the dead-end tower for stability. In addition, the steel support stand was too short for our application and needed to be raised a little over seven feet to maintain phase to ground and safety clearances for the conductor leads. With a little more help from our steel fabricator, we designed a seven foot high box beam extension with mounting plates top and bottom. The extension was bolted to the base, then the circuit switcher was mounted on top of the extension. The base was secured to the parking lot surface with epoxy type anchors.

### **Steel Box Structure**

Assembly of the steel box structure commenced on Friday, June 20<sup>th</sup>. The structure could not be assembled in its final location due to space constraint of the site. The switchgear building was not due to arrive until the following day. The size and weight of the switchgear forced the crane to set up in the final location of the steel box structure. Therefore, to keep on schedule the box structure was assembled in an area directly adjacent to its final installation location. The plan was to set the switchgear, relocate the crane, pick up the assembled steel structure, and set it in place.

Assembly of the box structure was completed late Saturday afternoon and set in place early Saturday evening. The structure was secured to the concrete with epoxy type anchors.

### **Substation Completion**

Substation physical construction was essentially completed on Friday, June 27<sup>th</sup>. Fence installation was completed and the site secured the following day. On Wednesday July 2<sup>nd</sup>, the power transformer was energized as system check out continued. Commissioning checkout of the equipment and control panels continued through July 2<sup>nd</sup>.

With the total destruction of Cedar Substation and the limited availability of other distribution substations to phase to, very careful attention was paid to existing phasing. All 13.8 kV distribution feeders left the substation underground, and all paper documents on phasing were destroyed in the flood, so no clear indications of pre-flood phasing existed. Phasing was traced from the 34.5 kV line through the damaged substation to the riser poles, where the phases were taped and color-coded. Starting from the same point, we repeated the process through the temporary substation to the feeder exists. Phases for each distribution line were taped and color-coded to match the riser pole coding. On 3 July, 2008, the temporary substation was in service and ready to serve the available loads.

Typical construction time for a substation similar to Cedar Temporary Substation is six weeks. We were able to go from conception to design to construction completion (see Figure 5) in 18 days.



Figure 5 - Cedar Temporary Substation nearing completion

While the Cedar Temporary Substation was being built, the 13.8 kV underground network circuits serving the downtown loads and fed from this substation were repaired and tested by the underground construction team.

In parallel with these efforts, the transmission provider built a 161-34.5 kV temporary substation and a 161 kV line tap to provide a source of power to the 34.5 kV subtransmission system. Some reconfiguring of existing 34.5 kV lines was required to route power to the substation.

Thanks to a combination of planning, innovation, and good fortune, the transmission, substation, and underground distribution projects were all completed on the same day.

### **Epilogue**

The 161kV transmission and 34.5 kV subtransmission systems were returned to near normal conditions by early fall 2008. At that time the temporary 161-34.5kV substation and the associated line tap were dismantled, but much work remains to restore the previous reliability levels to the transmission and subtransmission systems.

The 13.8 kV distribution network is fully restored. Cedar Temporary Substation is the primary source for the network and is expected to remain in service for a minimum of two years from its in service date. Efforts are continuing to acquire a suitable site and develop plans for a permanent substation to carry the downtown distribution network.

## **TRANSMISSION LINE AT ST. ANDREW BAY**

Rengaswamy Shanmugasundaram, P.E., Program Manager-Civil/Structural  
Mesa Associates, Inc., 832 Georgia Ave., Ste. 300, Chattanooga, TN 37402  
Ph (423) 424-7344, FAX (423) 424-7303, Email: [rshan@mesainc.com](mailto:rshan@mesainc.com)

### **ABSTRACT**

This project resulted in an unusual challenge to augment two existing 46kV underwater circuits with an overhead double circuit line designed for future 115kV operations. The probable reasons to go underwater for the original 46kV circuit lines and the reasons for the new 115kV circuit lines to go overhead are discussed in detail under “Project Background and Requirements”. The new line had to cross approximately 3,600 ft. of the Gulf Intracoastal Waterway at St. Andrew Bay. In addition to constructing facilities in an active waterway, the design of the overhead line had to consider and accommodate water depths of 60 ft. and provide sufficient span and clearance to allow for barge traffic.

The 115kV overhead crossing of the St. Andrew Bay required the installation of four structures within the waterway consisting of tubular steel poles supported by concrete caisson foundations. Foundation and structure installation was performed off of two barges. The concrete caisson foundations were constructed by installing 6 ft. diameter pipe piles with a vibratory hammer and then filling the pipe piles with reinforced concrete. Environmental issues and shoreline stabilization were a part of the consideration for this project.

This paper describes the various design and construction challenges encountered in this project.

## PROJECT LOCATION

The project is located near Panama City, Florida, U.S.A. The transmission line connects Tyndall Air Force Base and the Town of Parker, in St. Andrew Bay, as shown in the map below (see Figure 1).

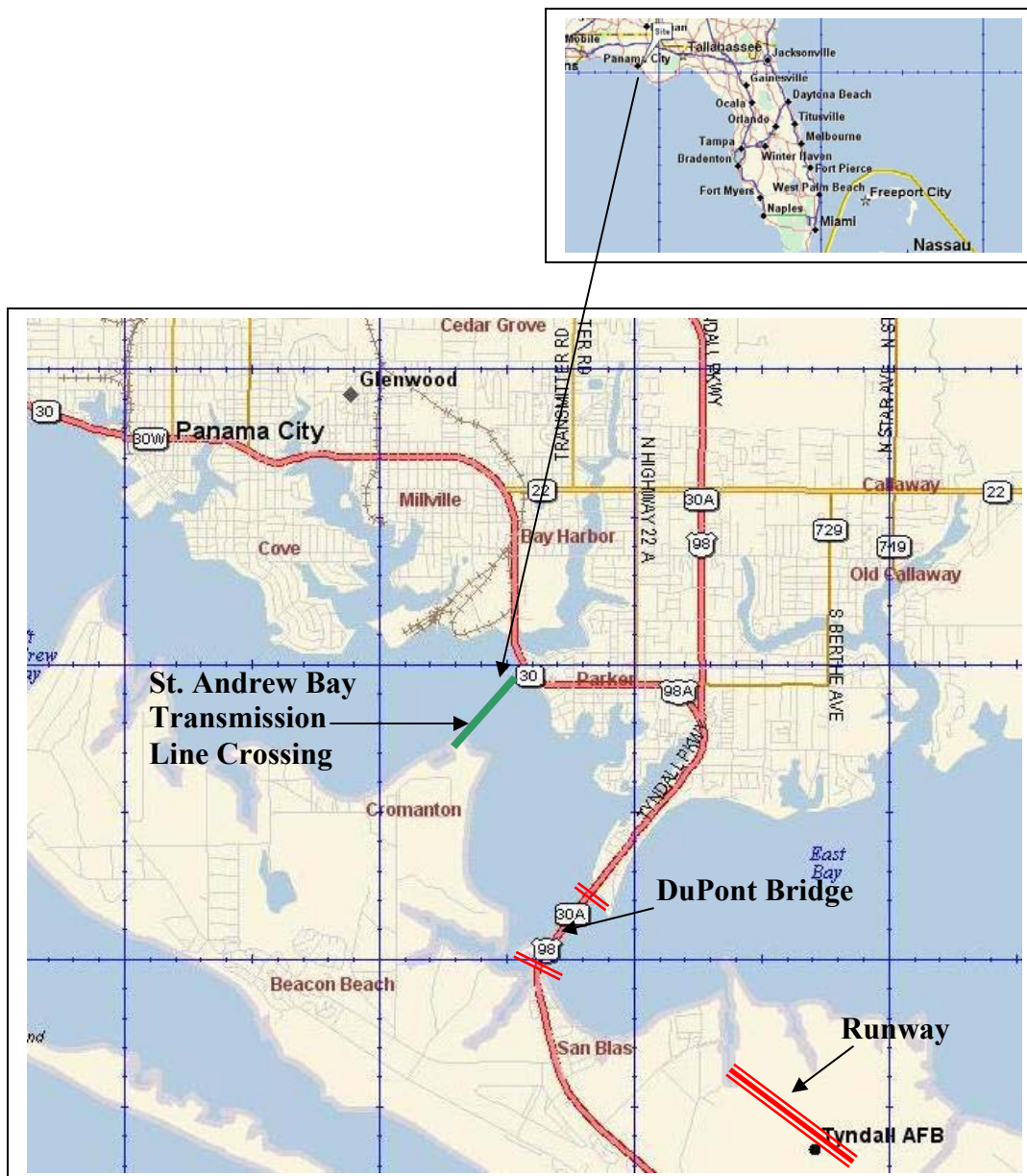


Figure 1.  
Map of Area

## PROJECT BACKGROUND AND REQUIREMENTS

St. Andrew Bay is part of the Gulf Intracoastal Waterway. The length of the bay to cross by transmission line is approximately 3,600 ft. The maximum water depth in the channel in the middle of the bay is approximately 60 ft.

The few available records of the original 46kV underwater cable design and installation for the St. Andrew Bay crossing indicate that the design was done in late 1959 and early 1960 with the installation being completed shortly afterward. The underwater 46kV cables were buried approximately 6 ft. below the bay mud level. The personnel involved in the planning and design have long since retired and research efforts to determine the decision making process at the time has been unsuccessful. The best information that can be obtained is not definitive as to why things were done as they were, but it is reasonable to assume that the design alternatives that were available in 1959, including materials, construction methods and engineering experiences, led to a conclusion that the underwater circuits were less costly. The environmental restrictions were not as broad at the time as they are today. Tyndall AFB was established in 1941, and the proximity of the AFB to the crossing area was not considered an issue. At the time the installation was planned, transmission lines were generally constructed using wood poles or four legged laced steel towers to support the conductors. A design using wood poles of sufficient height and strength to support the design would not have been feasible. A design using the steel towers would have required foundations, structure designs, and construction methods which would have likely been somewhat more costly than the underwater installation decided upon.

The underwater 46kV circuits had to stay in service to provide service to Tyndall Air Force Base while the overhead circuits were being installed. The existing underwater circuits were 40+ years old and were seen as beginning to be unreliable. The old cable had deteriorated some and the importance of the service to Tyndall AFB was a significant factor in making the decision to provide another source of service. The entire new line from the starting point substation to the Tyndall AFB side of the bay substation was to be installed for future 115kV operation. The old underwater circuits and risers on each side of the bay were designed for 46kV operation. If new underwater cable for 115kv operation had been installed, there would have been a requirement for new 115kV risers on each side of the bay as well. The costs associated with installation of new 115kV cable underwater along with the new 115kV risers exceeded the cost of providing the overhead circuits. Access to, and maintenance of an overhead circuit, were additional factors in favor of the overhead circuit as opposed to an underwater circuit. The two underwater 46kV circuits were ultimately tied together on each side of the bay to serve as a secondary source or backup source to serve Tyndall AFB. A switching scheme was designed to be able to use any of the circuits, underwater or overhead, and to also keep some current on the underwater circuits at all times to help preclude further deterioration when the underwater circuit was not the primary source of service.

The overhead route was selected for purposes of more reliability, more readily available maintenance, less environmental impact, and less cost. Alternate routes were evaluated and with each route the new circuits would still have to cross the bay and would have to traverse through residential neighborhoods where there was considerable opposition from property owners. The direct route across the bay was the least obtrusive and the shortest. The second most favorable route would have added several miles to the project and would have been attached to the DuPont Bridge with opposition from the FDOT. Other crossings would have been closer to the runways at Tyndall AFB and would have been longer.

It was necessary to provide sufficient span at the middle of the bay for intracoastal barge traffic. Environmental considerations to protect shoreline transmission and substation structures and extension of stormwater concrete pipe had to also be taken into account.

## TRANSMISSION SOLUTION

This project consisted of two new circuits designed for 115kV operations, but operating at 46kV, starting at Wewa Road Substation, crossing St. Andrew Bay and going to Tyndall Field Substation on the Tyndall AFB property, the total combined length of the two circuits is approximately 8 miles.

The middle span in the bay was made as wide as possible for barge traffic and the centerline of the middle span coincides approximately with the centerline of the Intracoastal Waterway, all in order to provide a low probability of a barge hitting the structures.

The spans were also made longer than the span between piers of the DuPont Bridge, which is located approximately 1-1/2 miles southeast of the bay crossing and where barge traffic goes into the Tyndall AFB property.

Federal Aviation Regulation Part 77 describes the standards for determining obstructions in navigable air space. A study was made to ensure that the new overhead line and structures did not constitute an obstruction. The height of the structures is well below the maximum height restrictions described by the FAA regulations. A report of the new construction was provided to the FAA to provide information to be added to navigation charts. The FAA did not require marker balls, lights, or painting of the structures in the bay area for this design. Two very tall poles, one on each side of the bay, would have caused an obstruction, would have required lighting, and would have been extremely impractical to merge the design back into the existing circuits on each side of the bay. The structures were provided with provisions for climbing for maintenance purposes. Anti-climbing devices were attached to the lower portion of the poles to discourage anyone in a boat from trying to climb a pole. The vertical clearance above the waterway was dictated by the Corps

of Engineers Federal Register rules and regulations for clearances of aerial electric power lines crossing navigable waters of the United States.

The following are the conductor and overhead groundwire used in the line:

Conductor	Hawk, Aluminum Conductor, Aluminum Clad Steel Supported (ACSS/AW) 477,000 Cmil. 26/7 stranding
Overhead Groundwire	Alumoweld 7 No. 8, 7 stranding
Design Tension in the Bay Area for Conductor	8370 lbs.
Design Tension in the Bay Area for Overhead Groundwire	5175 lbs.
Ruling Span in Bay Area	750 ft.

## STRUCTURAL SOLUTION

The crossing of St. Andrew Bay required four structures to be located in the water. The following three types of steel structures were considered in the design:

1. Single steel pole with davit arms with one circuit on each side with steel caisson foundations.
2. Steel H-Frame with bracings and davit arms with one circuit on each side with steel caisson foundations.
3. Lattice tower with cross arms with one circuit on each side with caisson foundations.

The single steel pole with davit arms with one circuit on each side with steel caisson foundations was selected based on being aesthetically pleasing due to the small foot print and due to the overall cost.

The following loads were considered in the design:

1. 2002 National Electrical Safety Code
  - a. Combined ice and wind loading: Light loading 0" radial thickness of ice + 9 lbs. per sq. ft. of horizontal wind pressure load at 30° F.
  - b. Extreme wind loading of 130 mph of horizontal wind pressure at 60°F.

2. American Society of Civil Engineers "Guidelines for Electrical Transmission Line Structural Loading"
  - a. Extreme ice with concurrent wind loading: 0.4" radial thickness of ice + 52 mph wind pressure load at 15° F.
3. Gulf Power Company design loads:
  - a. 135 mph heavy hurricane loading
  - b. Broken shieldwire with 135 mph heavy hurricane loading
  - c. Broken conductor with 135 mph heavy hurricane loading
  - d. Conductor stringing with no wind
  - e. Shieldwire stringing with no wind

Gulf Power Company design loads are critical in comparison with NESC and ASCE loads. Therefore, the structures are designed for Gulf Power loads. Tornado loading was not considered at this location.

The four required structures are numbered 1 through 4 as shown in Figure 2. The engineered poles were designed using flange joints in three sections. The utility company wanted to have spare sections in order to replace any of the poles in water that failed due to heavy hurricane/tornado loading higher than the design loadings. The top sections for all four water structures were designed identically such that the spare top pole sections could be used in any of the four locations. Sufficient spare sections were fabricated to facilitate the assembly of one complete replacement pole for any one of the water structures No. 1 through No. 4.

A comprehensive geotechnical investigation was performed with borings taken at all four water structure locations using a barge mounted drill rig. A soil boring log for one of the middle structures is shown in Figure 3. The soil generally consists of soft to hard clayey sand. The standard penetration blow count number varies from 0 (N-value) at the bottom of the bay (at mud line) to 60 (N-value) at 54 ft. deep into the soil.

The caisson foundations were designed using the engineering software "LPILE Plus", developed by Ensoft, Inc. The foundation caissons were designed to use a permanent pipe pile casing that replaced the interior excavated soil with cast-in-place reinforced concrete. The 6ft. diameter  $\frac{1}{2}$ " thick steel casing was to be the caisson form during construction and then act as a protective covering for the concrete caisson over the life of the project. Due to the salt water in the bay, the steel casings were shop painted, after fabrication, with 20 mil dry film thickness of CorroCote® II Classic on the exterior surfaces for corrosive protection. The reinforced concrete placed within the casings was the structural component of the foundation while the  $\frac{1}{2}$ " thick steel casing was considered as form work and long-term protection.

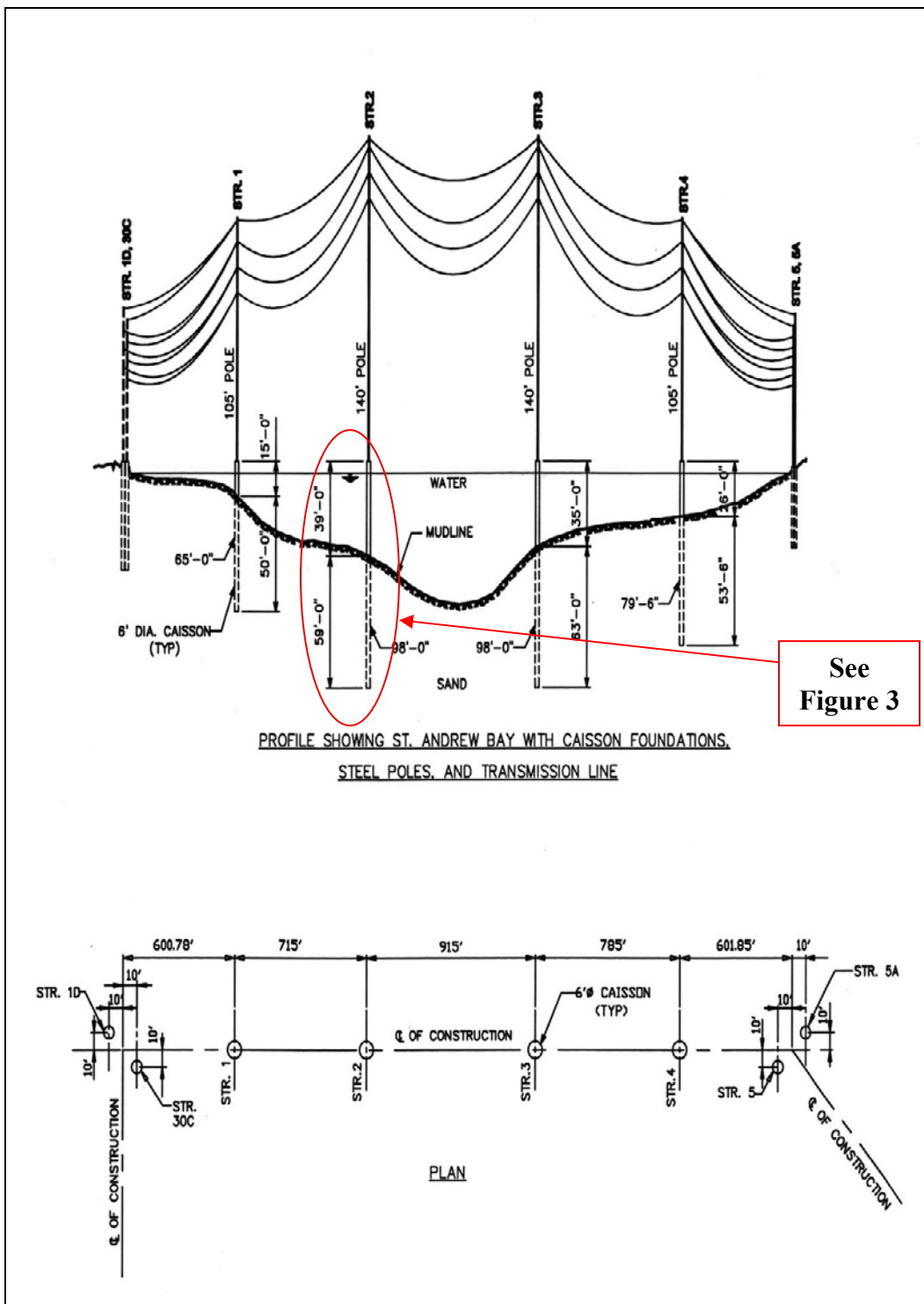


Figure 2.  
Drawing Showing Transmission Line, Steel Poles, and Caisson Foundations

Telegram Channel: @Seismicisolation

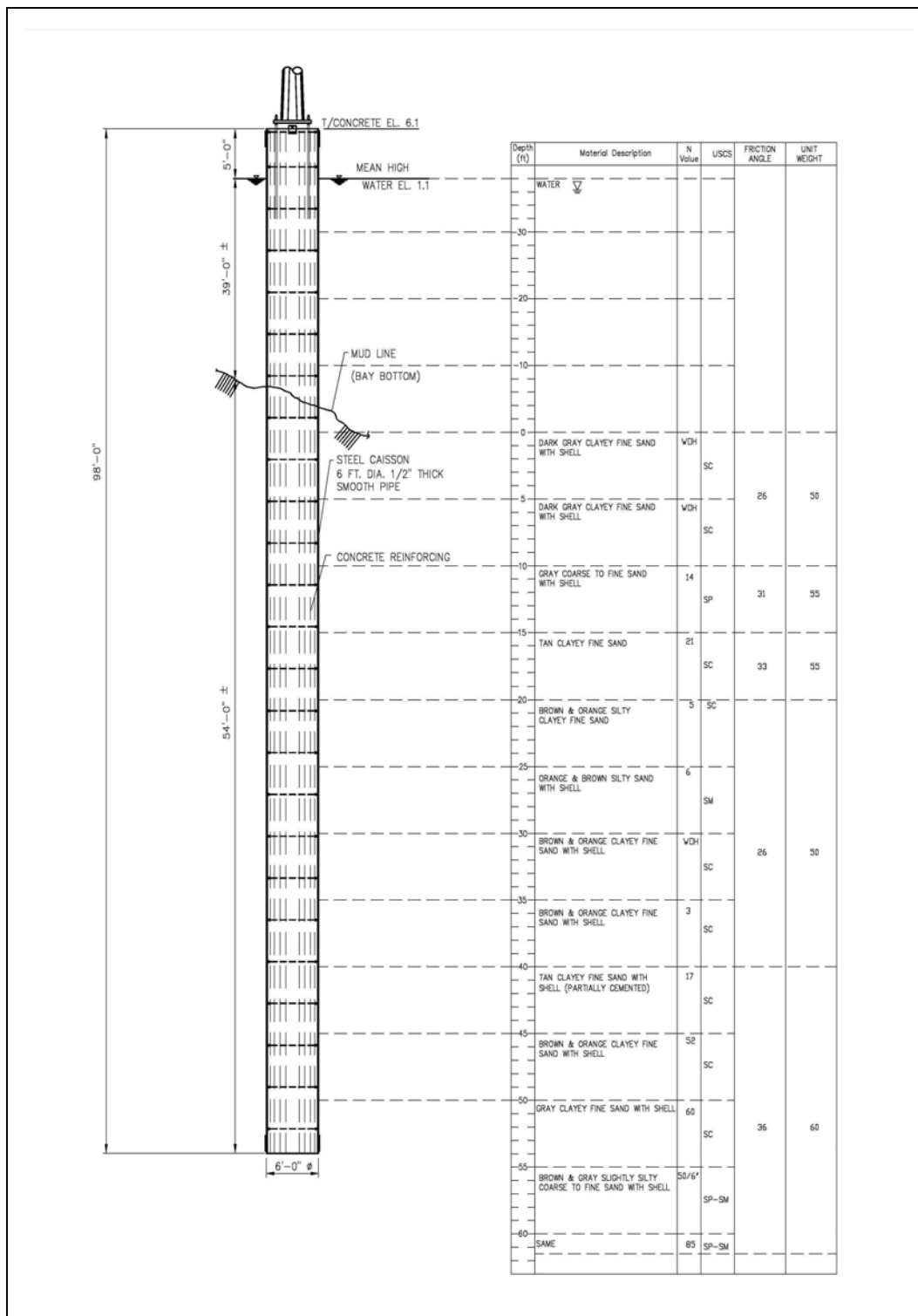


Figure 3.  
Caisson and Soil Boring Detail

Construction was performed from two barges. For the steel casings, 6 ft. diameter  $\frac{1}{2}$ " thick smooth pipes were selected instead of 12-sided pole-type geometry. Steel caissons were installed using the vibratory hammer method. After installation, the material inside each caisson was removed completely down to the bottom level of the caisson. The smooth steel pipe caisson interior helped in effective cleaning, better than a 12-sided geometry pipe. 5500 psi concrete, with approximately 9" of slump maintained by use of a plasticizer, was brought in from an adjacent paper mill loading dock which was approximately one mile from the construction site. From the truck, concrete was transferred by gravity to three 3-cubic yard buckets at the end of the barge. It took approximately 20 minutes for the barge to take the concrete to the site of each foundation. Concrete was placed using the tremie process (underwater placement). With the proper mix design, concrete was plastic throughout the placement time. See Figures 4 and 5.

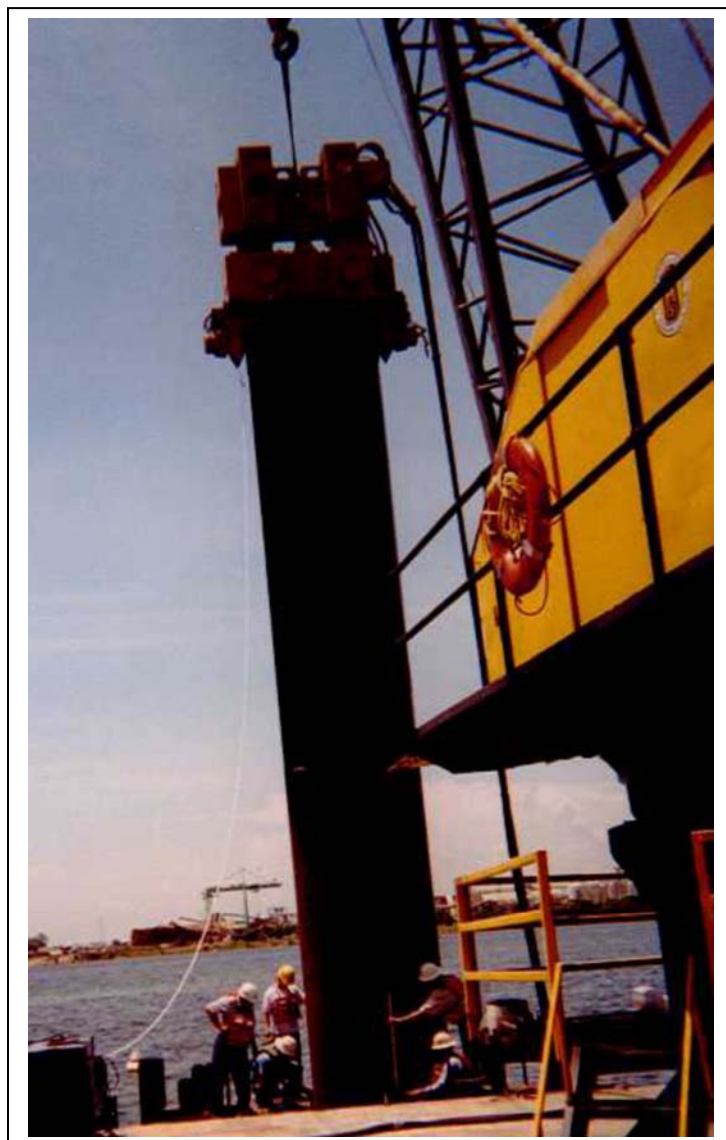


Figure 4.  
Smooth Pipe Caisson  
Installed Using  
Vibratory Hammer



Figure 5.  
Reinforcement Bar Cage Placed Inside Caisson

Telegram Channel: @Seismicisolation

## ENVIRONMENTAL SOLUTION

Environmental issues and regulations for any activity in the bay had changed considerably since the time the original 46kV underwater circuits had been installed 40+ years ago. Current environmental issues that had to be considered and actions taken during the design and construction of the new 115kV overhead circuit lines in the St. Andrew Bay crossing are discussed below.

Coordination was required with the Florida Department of Environmental Protection, Corps of Engineers, and the Federal Aviation Administration for the St. Andrew Bay crossing.

Sea grasses, oyster beds, and sea life, such as the manatee and small and large turtles, required protection from construction. The manatee, a docile creature, is sometimes called a sea cow since they eat sea grasses. In order to protect sea life and grasses, water structures were located away from shore lines at a minimum distance of 60 ft. from sea grass areas. If a manatee was to come within 50 ft. of the work area, the work activity was to be shut down to avoid any harm to the animals. Motorized watercraft had to avoid any sea grass areas where the water level was less than 1 ft. from the sea grasses.

Turbidity curtains were required in the work area. These are floating barriers with curtains designed to control the dispersion of silt and sediment in a body of water. Turbidity curtains surrounded the work area around each structure. Construction forces were to leave nothing in the water, such as drilling mud, dirty water sediment or sludge, and storage tanks were provided on the work barges to contain the waste. A water quality monitoring system was required. The Florida DEP along with Gulf Power Environmental personnel monitored the water conditions for turbidity.

In general, the osprey nesting season begins in January and ends in August in this area. The construction activities were scheduled in such a way that there was no potential for interference with the osprey nesting.

Erosion protection was required on both shores to minimize the environmental impact to the shoreline due to new construction and to protect the new structures on land nearest to the shore from erosion concerns. Erosion protection consisted of embankments on both shores with filter fabric, unopened Quickrete® concrete mix bags, and 6"-10" riprap as shown in Figure 6. Unopened Quickrete® bags, after wetting in place, formed a good foundation for the embankments. An existing drainage pipe on the Panama City side of the bay was modified and protected with riprap.

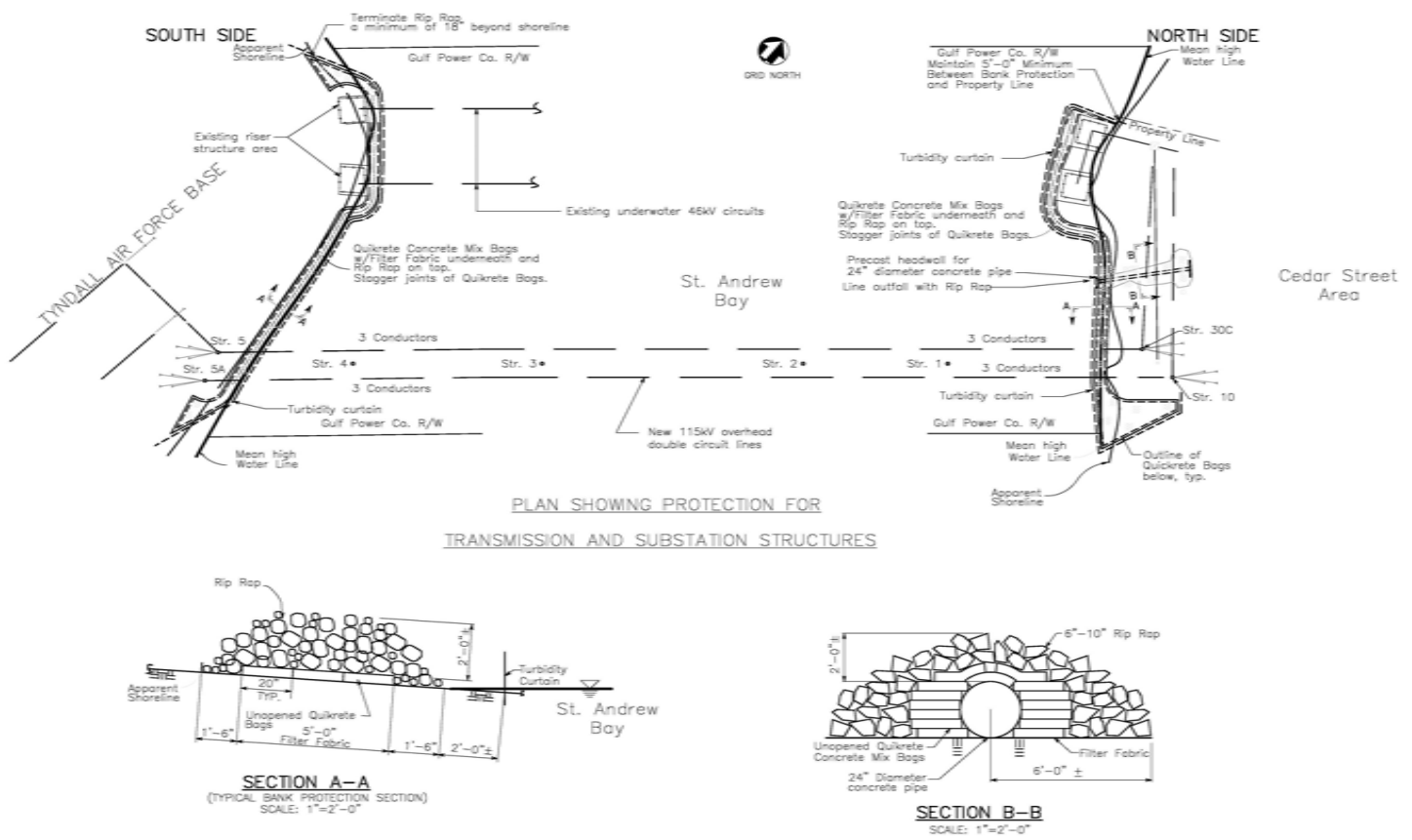


Figure 6.  
Embankment Drawing

Telegram Channel: @Seismicisolation

## CONCLUSION

The project was successfully completed in 2004 due to the excellent pre-planning, dedication, and cooperation from various personnel from the following organizations:

1. Gulf Power Company – Owner of the Project
2. Mesa Associates, Inc. – Consulting Engineers for the Project
3. Newmark Poles – Designer and Fabricator of Steel Poles
4. Asplundh – General Contractor
5. Reliable Constructors, Inc. – Steel Caisson and Concrete Contractor



Figure 7.  
Completed Caissons and Poles with Wires in Place

# Construction Challenges of Extra High Voltage Transmission Lines: Building in the Most Difficult Terrain in the World

Dr. Deepak Lakhapati, PhD

Vice President – Engineering Services, KEC International Ltd., Transasia House,  
3<sup>rd</sup> Floor, Chandidali, Mumbai-400072, INDIA  
Email: [lakhapatidm@kecrpg.com](mailto:lakhapatidm@kecrpg.com)

## Abstract:

This Paper describes the challenges faced during the construction of EHV transmission lines which travel hundred of miles in difficult terrain, under varying and extreme environmental conditions using variety of construction equipment. The engineering challenges become much more difficult with higher voltages as structures become very tall and heavy. Every country has individual challenges which are unique to that country or region. Engineering solutions need to be suitable to overcome working challenges which are described throughout the paper.

## Introduction:

Over the last 60 years, electrical systems worldwide have experienced huge growth in terms of power generation and expansion of EHV transmission systems to transport bulk power from generation to the user end. In India, for example, voltage levels have risen from 132 kV during the 1950s to 765 kV in 2008. Northeast India has a hydropower capacity to generate 50,000 MW of power which has to be transported through a narrow “chicken neck” corridor for which a 1200 kV transmission system is under development. Similar growth has taken place worldwide.

Construction methods vary depending on tower configuration, terrain, right of way and environmental factors which necessitates development of innovative engineering solutions. Interesting examples are presented in the paper along with respective site photographs.

## Afghanistan:

Naibabad – Pul – E – Khumri 220 kV D/C line in Afghanistan had to cross the huge, steep and difficult mountains to reach the substation. After detailed study of the terrain and potential routes, the only feasible solution to reach the substation was to construct the line through a narrow gorge having a width about 35 m (115 ft) and a length of 1.5 km (1 mile). Complicating matters, this gorge also had an existing road and a water canal. (See Exhibit No.1 - 2)



Exhibit No.1: Narrow gorge



Exhibit No.2: Road, water canal and foundation location.

The above terrain needed a unique engineering solution to design narrow base towers for the 220 kV double circuit transmission line.

A detailed survey of the entire gorge was conducted with the help of GPS and all the survey data was electronically transferred and processed by PLS-CADD to spot the towers in such a way that there is sufficient electrical clearance available between the conductors and the sides of the gorge. (See exhibit No.: 3)

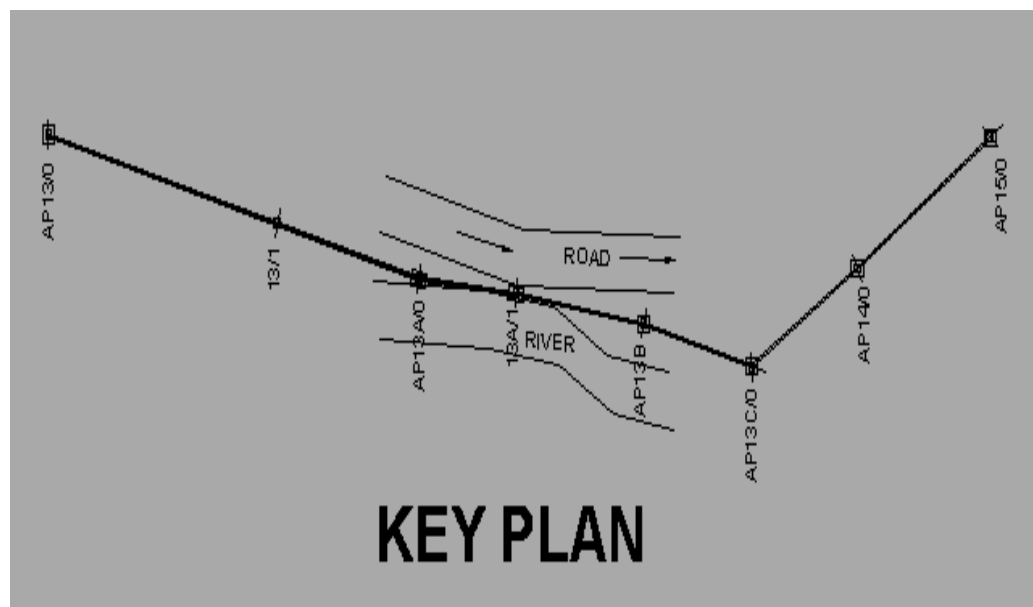


Exhibit No.3: Key plan of the route

Conductor clearances along the length of the line was checked in 3-dimension in the swinging condition and finalized the tower locations. Towers are designed to carry one OPGW and six twin conductors (ASCR-SQUAB).

Space available for design and installation of the tower base was limited to 2.5 Sq. m (27 Sq. ft). There was no space to provide conventional cross arms due to electrical clearance requirements hence the vertical configuration tower was designed where conductors were attached to body directly. Crossarms were provided to accommodate jumpers.

Block foundations of 4 Sq. m (43 Sq. ft) were designed within the space available near the water canal. Due to high water table 9 m (30 ft) deep fully reinforced block foundation were designed to take care of uplift.

Since the transmission line had to follow the road route, all angle towers were provided. (See exhibit Nos.: 4-9)



Exhibit No.4: Foundation excavation



Exhibit No.6: Fixing the reinforcement bars



Exhibit No.5: Placing the reinforcement bars



Exhibit No.7: Arrangement of template



Exhibit No.8: Foundation in progress



Exhibit No.9: Block foundation with stubs

Stringing had to be completed section by section, since every tower was angle tower and finally transmission line was charged and in operation since 2007. (See exhibit Nos.: 10-11)



Exhibit No.10: Fully erected tower

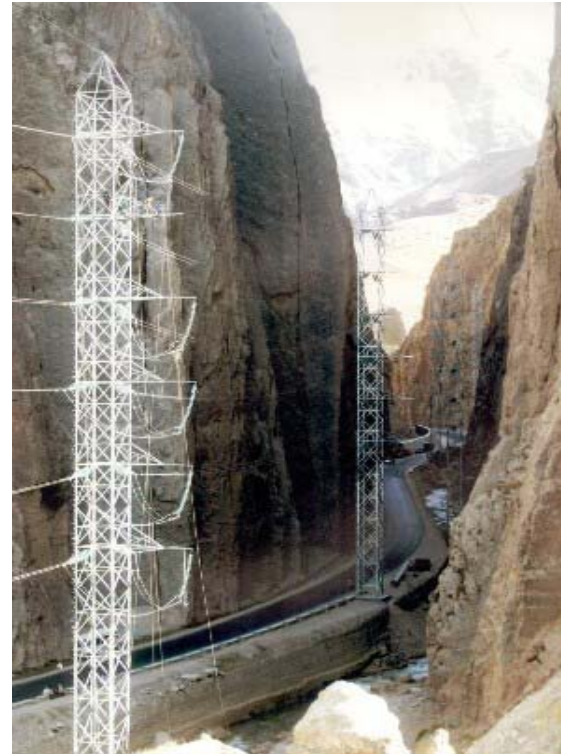


Exhibit No.11: 220 kV D/C Transmission line passing through gorge

#### **Abu Dhabi:**

Per capita energy consumption in Gulf region is very high due resulting in nearly continuous construction of 400 kV delta configuration transmission lines using quad conductors and OPGW. Towers are very heavy and due to sandy soils, heavy piling rigs are required.

**Telegram Channel: @Seismicisolation**

Survey is carried out using high end GPS system and the route is finalized. Access roads are created for movement of heavy duty piling rigs and erections cranes. Sand dunes and extreme hot (+50°C) temperatures made working conditions difficult. (See exhibit Nos.: 12-13)



Exhibit No.12: Sand dunes



Exhibit No.13: Preparation of Access Road.

Vertical as well as battered piles were designed with pile diameters varying from 3.5 ft to 8 ft. For heavier uplift and compressive loads multiple piles and tie beams were required. (See exhibit No.: 14)

Towers were erected in two stages. A 150 ton crane was used for erection up to the waist level and then a 250 ton crane is used for second lift. Civil aviation paint was applied to all towers. (See Exhibit No.: 15)



Exhibit No.14: Driving battered pile



Exhibit No. 15: Erection by crane

Due to congestion of lines, 400 kV multi circuit transmission lines are designed to carry 4 circuits of quad conductors making the construction much more challenging. (See exhibit No.:16)

The weight of the towers ranged from 101 MT to 242 MT since it has an uplift loads range from 300 tons to 900 tons which lead to design a leg with a built up of 4 legs of section 250X250X35 mm (largest angle available in the world).



Exhibit No. 16: 400 kV quad multi circuit undergoing prototype testing

Due to non-availability of right of way through the city, line had to pass through Arabian Sea to reach the substation. Barge were used for construction. (See exhibit Nos.: 17-18)



Exhibit No.17: Erection of tower in Arabian Sea



Exhibit No. 18: Double-deck gantry near GIS substation

Hybrid tower was designed and installed to turn the line. Huge cantilevered auxiliary crossarms' lifting was quite difficult due to weight of structures. (See exhibit No.: 19)



Exhibit No.19: Hybrid Tower

Interconnection of all Emirates is under construction which will exchange power within Emirates. (See exhibit Nos.: 20-21)



Exhibit No. 20: Two 400 kV lines installed with common access road



Exhibit No. 21: 400 kV Constructed on restricted right of way

Telegram Channel: [@Seismicisolation](https://t.me/Seismicisolation)

### Kazakhstan:

Other extreme condition was faced during construction of 600 miles of 500 kV single circuit where the temperature is extremely cold (-40°C) and the site is fully covered by snow and inaccessible for four months each year.

The transmission line had to pass through seven earthquake and wind zones. Towers were configured as guyed towers supported by 4 guys per tower. Guying allowed the towers to become much lighter in weight and the resulting foundations were smaller as well.

With the engineering solution of using precast foundations and prefabricated towers, all towers structures in eight parts were kept ready in the non-working season in the factory. Similarly foundations were casted in the factory. An electric heating system was used for curing of concrete. (See exhibit Nos.: 22-23)



Exhibit No.22: Electric heating system for foundation chimney.



Exhibit No.23: Casting of foundations in factory

Dully assembled towers and precast foundations together were transported to sites. Cranes were used for installation of foundations and erection of towers. (See exhibit Nos.: 24-27)



Exhibit No.24: Assembled tower being transported to site



Exhibit No.25: Precast foundation being lowered into excavated pit

**Telegram Channel: [@Seismicisolation](https://t.me/Seismicisolation)**



Exhibit No.26: Erection by crane



Exhibit No.27: 500 kV S/C complete and energized

Special self supporting angle towers were designed to support one phase per structure, thereby reducing the foundation sizes which allowed for smaller and easier to transport precast foundations. (See exhibit No.: 28)



Exhibit No.28: Angle Tower consisting of one structure per phase

## SOUTH AFRICA

765 kV single circuit transmission line passes through generally flat terrain where V-Guyed suspension towers are more suitable due to light weight supported by four guys.

Due to higher ground clearance requirement and six bundle conductor configuration, the resulting structures are quite tall and erection was a challenge requiring special equipment. (See exhibit No.: 29)

All structures are horizontally assembled, tightened and the lifted one-by-one and guys are tightened by turn-buckle. Balancing the structures during vertical lifting become quite critical. (See exhibit No.: 30)

**Telegram Channel: @Seismicisolation**



Exhibit No.29: Stringing machine for pulling six conductor bundle.



Exhibit No.30: Tower erection by crane.

#### **Libya:**

A 250 mile 400 kV single circuit line has been constructed in the Sahara Desert. Horizontal configuration towers were designed for a triple conductor bundle. Since the line had few obstructions or angles, long spans were used with tall towers by providing body extensions ranging from 90 ft to 240 ft. (See exhibit No.: 31)



Exhibit No.31: 400 kV S/C transmission line in Sahara Desert

A common problem with transmission line construction in remote locations is that lack of locally produced concrete. As such, mobile concrete batch plants were installed and concrete mixers used to transport concrete to each location. Due to hot conditions ice slabs were added into the concrete mix to maintain the temperature.

#### **Algeria:**

We have built 400 kV single circuit and double circuit lines. These lines had passed through hills with snow. Foundations were at high risk due to washing away of soil and creating unequal settlements to the energized line. (See exhibit No.: 22)

**Telegram Channel: @Seismicisolation**



Exhibit No. 32: 400 kV line on hills

Some of the hills and forests were highly inaccessible and dangerous due to land mines and militant activities. We had to take military protection for safety of workers during the construction activities.

#### India:

Line constructed in Himalayan ranges was extremely difficult to access. All the materials had to be head loaded. Erection was manually done with the help of derrick. Towers were designed to carry four bundle conductors on horizontal configuration. (See exhibit Nos.: 33-34)



Exhibit No.33: First 765 kV line in operation

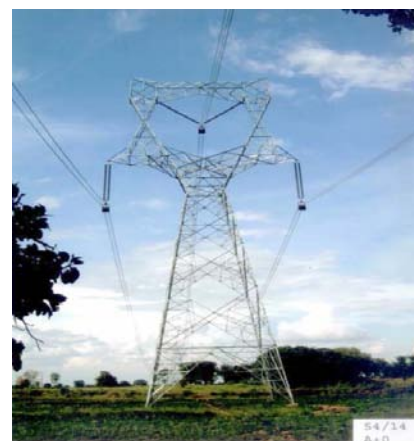


Exhibit No. 34: Latest 765 kV compact design

India has large number of rivers and constructing lines through the river Ganges and Brahmaputra has been a great construction challenge. (See Exhibit No.: 35)



Exhibit No. 35: Brahmaputra River crossing tower

To take care of future energy needs and for transmitting bulk power from North - East India, 1200 kV transmission network is under development. Test line is expected to be ready by end 2009.

#### **Conclusion:**

With the growing power needs worldwide, design engineers have always faced challenges to develop, innovative engineering solutions to produce construction friendly towers. New construction equipments like use of heavy cranes, helicopters are helping to overcome construction challenges in developed countries. However in developing and under-developed countries, it remains as a challenge due to non – availability of equipments and the continuing need to use manual labor methods.

Vegetation Management through LiDAR Derived CADD models:Compliance with NERC Reliability Standard FAC-003-1

N.Ferguson<sup>1</sup>, S.Ryder<sup>2</sup>, S.Verth<sup>1</sup>, P.Richardson<sup>1</sup> and R.Ray<sup>1</sup>

<sup>1</sup> Network Mapping, Unit B1G, Fairoaks Airport, Chobham, UK, GU24 8HU; PH +441276 857800; email: nicholas.ferguson@network-mapping.com

<sup>2</sup> Network Mapping, 24 Lakewood Park Road, Westminster, MA, USA, 01473.

**KEY WORDS** Airborne laser scanning, LiDAR, PLS-CADD™, vegetation clearance, right-of-way, arborist.

## ABSTRACT

Encroaching vegetation poses a continuing threat to transmission line reliability. Vegetation-caused outages can result in heavy fines levied on the service provider. A rapid, accurate and cost efficient system for identifying encroaching and proximate vegetation with the potential to threaten transmission line reliability is described in this paper. The system is based on airborne Light Detection And Ranging (LiDAR) data, downward looking imagery and Global Positioning System (GPS) technology. Following the data collection stage, the geospatial information is processed and then modeled in Power Line Systems® Computer Aided Design and Drafting package (PLS-CADD™). Output data from this software is subject to filtering algorithms and used to create detailed plan sheets, providing a record of encroaching vegetation. This information can form the foundation of an actionable and auditable Transmission Vegetation Management Program (TVMP), as set out by NERC reliability standard FAC-003-01. The system detects and accurately locates trees and other objects that could cause flashovers under multiple line operating conditions, as well as trees that could infringe upon statutory clearance requirements were they to fall into the transmission line right of way (ROW). Predictive growth factors can also be incorporated into the models. The use of LiDAR as an effective vegetation management support tool is then evaluated with a case study in the UK.

## INTRODUCTION

Effective vegetation management along transmission line ROWs is a cornerstone of reliable power delivery. The need to improve vegetation management systems was demonstrated on August 14th, 2003, when parts of eastern Canada and the northeastern United States were plunged into darkness, leaving in excess of 50 million people without electricity. The affected load totaled 61,800 megawatts (FERC, 2004). An investigative committee determined the primary cause was physical contact with conductors sagging into tall vegetation below (NERC, 2004). This was a direct consequence of ineffective vegetation management of transmission ROWs (FERC, 2004). In the UK it has been suggested that tree encroachment is responsible for up to 20% of power outages (McGarrie, 2008).

This paper will first outline the problems facing ROW vegetation management personnel and the traditional techniques employed to identify vegetation threats. The basic concepts of airborne LiDAR, also known as Aerial Laser Survey (ALS), will then be discussed with a methodology proposed for its practical application to ROW vegetation management. The technique is evaluated with a case study on implementation with the National Grid UK vegetation management program.

## TRANSMISSION RIGHTS-OF-WAY AND HAZARDOUS VEGETATION

A transmission line ROW is a cleared strip of land occupied by a transmission line or lines that is maintained by the owning utility. In the USA, ROWs are normally held in easement or fee. Typical easement language often includes the right to "...trim, cut, remove or control by any other means at any and all times such trees, limbs and underbrush within or adjacent to said right of way as may interfere with or endanger said structures, wires or appurtenances, or their operations." (NERC, 2004)

Vegetation control is generally carried out in accordance with regionally or nationally accepted clearance requirements, such as IEEE Standard 516-2003 and the requirements of the National Electrical Safety Code (NESC). They are used to develop vertical and horizontal clearance margins to ensure that no vegetation can encroach close enough to conductors to cause a flashover or physical damage, even at maximum rated operating temperature. However, even with adequately maintained vertical clearance margins, a second risk is posed by falling trees that may contact the line or infringe clearance [Fig.1.].

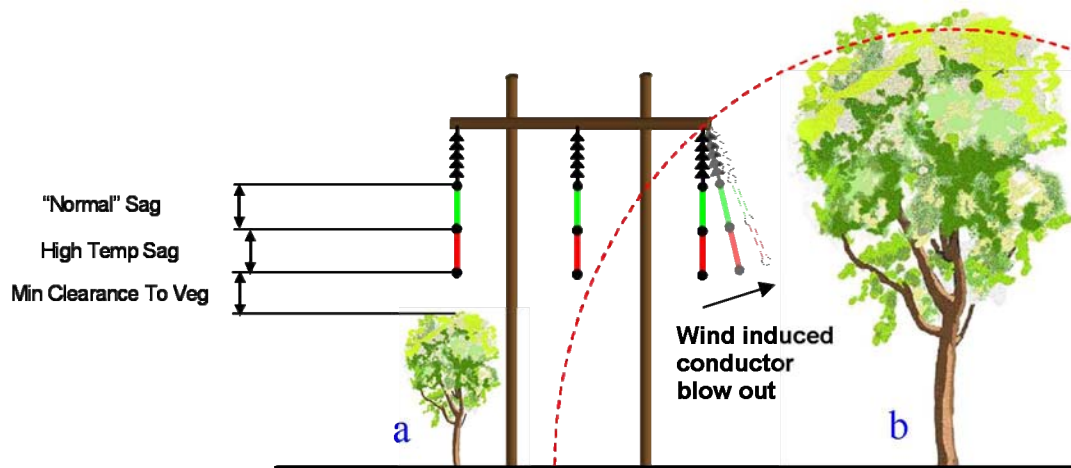


**Figure.1:** A schematic of the two principle hazards posed by vegetation. (a) A tree that has grown in close proximity to the transmission line, and may cause a flashover. This hazard would need to be removed or pruned by arborists on a short return period to prevent infringement of statutory clearance margins. (b) A tree that does not currently infringe statutory clearance, but may infringe clearance or impact the line if it fell.

An effective TVMP is required that mitigates risk to a transmission line through the management of both these hazards, as required by NERC Standard FAC-003-01. Conventional management techniques based on visual estimates can be over-zealous in their maintenance of grow-in infringements, and reactionary to falling tree events. The trim schedules for these conventional management programs are often based on time, and not on need, which can result in inefficiencies and increased risk (PSERC, 2007). To reduce the risk of these hazards, average return periods of 5 years (NERC, 2004) for time based trim schedules should therefore be reduced, or an entirely new methodology is required with factual clearance information at its core.

## SYSTEM AND ENVIRONMENTAL VARIABLES

In order to create a management system based on need, it is essential to acknowledge the system and environmental variables that increase risk. The increased risk stems from either those factors that reduce conductor clearance to vegetation, or the increased likelihood of a hazardous event occurring.

Conductors sag in a catenary curve between attachment points on adjacent strain or suspension structures. As demand levels increase, the higher load levels generate greater demands on both active power (MW) and reactive power (MVar). Resistance within a conductor creates heat, and hence increased flows along the transmission line will cause the conductor metal to expand, and consequently further sag. It is therefore imperative to ensure that clearance to vegetation is determined at the maximum operating temperature for a line, when the conductor sag is at its lowest point. This is required under NERC FAC-003-01.

The weather is a critical component that must be considered when examining clearances to vegetation. Wind can cause the conductor to swing perpendicularly, and clearance should be maintained even at this extended position. Again, this consideration is required when determining clearance requirements for vegetation under NERC FAC-003-01. Ice loading also has a dramatic impact on conductor position, through increased sag. Differential ice accretion in adjacent spans will result in differential sag.

The risk posed to transmission lines varies subtly with vegetation type and climatic zone across the globe, but generally this hazard exists for all lines. However, some vegetation on or adjacent to ROWs should be earmarked for more intensive inspection, due to a higher risk induced by natural hazards. Despite the limitations within the source dataset (cf. PSERC, 2007), **Figure 2** shows the possible level of correlation between vegetation outages and storm conditions for a geographical locality.

In geographical areas prone to earthquakes, high winds, permafrost activity, icing and heavy wet snow, utilities must acknowledge the threat posed by vegetation to transmission lines. They should take measures to mitigate this risk in order to ensure the reliability of the power supply. Lines traversing woodland that becomes desiccated in the summer months should also be checked frequently, as flashovers to encroaching vegetation could start forest fires.

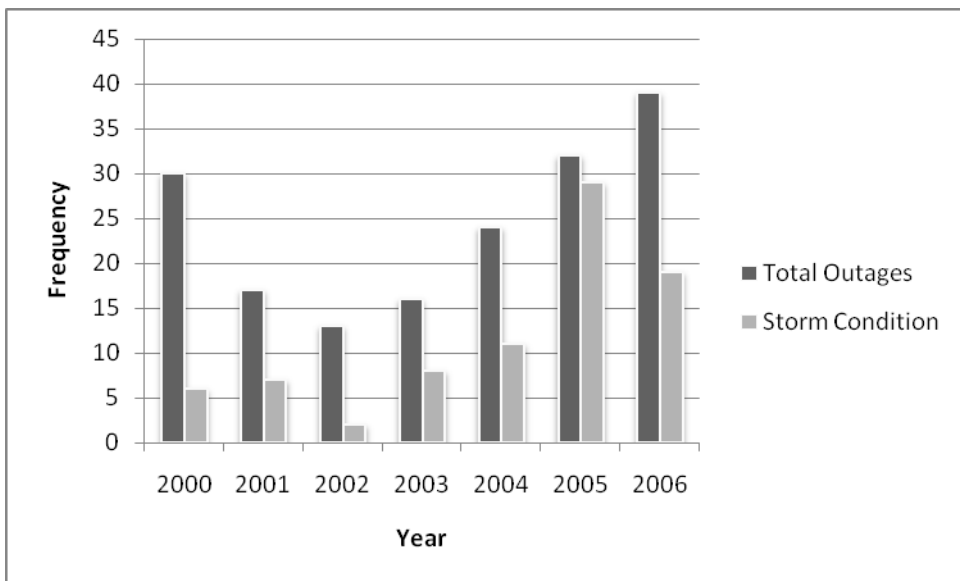


**Figure.2:** A graph showing the vegetation related outage summary for a 32 feeder substation, of which 8 feeders were monitored. Adapted from PSERC, 2007. Despite the limitations of the data (cf. PSERC, 2007), the graph provides an insight into the significantly high percentage of vegetation outages that may be storm induced in some areas.

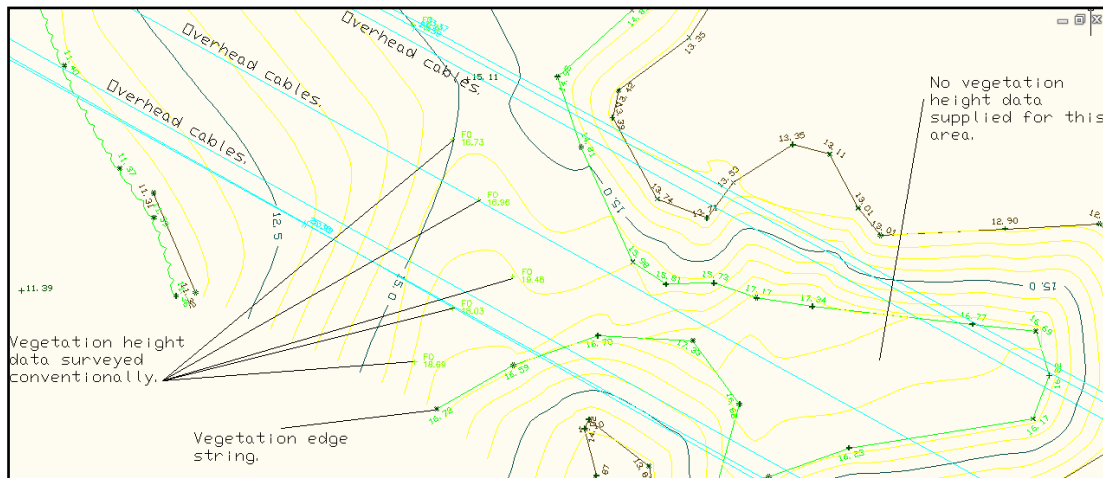
## TRADITIONAL VEGETATION MANAGEMENT TECHNIQUES

Traditionally, and to a certain extent currently, vegetation management needs along transmission line ROWs were identified with terrestrial visual assessment techniques. Experienced foresters would conduct visual inspections along ROWs to identify vegetation that appeared to be encroaching pre-determined minimum clearances based on line voltage. These minimum clearances would typically include a “high operating temperature sag factor” to account for high electrical loading periods. This approach often results in generally more vegetation removal than may be required, “to be on the safe side”. This approach also underestimated conductor sag in long spans, and led to inadequate pruning.

In specific instances where accurate vegetation height with respect to conductors was required (orchards for example), land surveyors would take measurements to the top of any vegetation under or adjacent to the transmission lines using traditional survey equipment. Five points on the conductors and the conductor attachment points would also be surveyed to allow the conductors to be accurately modeled. All clearances from conductor to vegetation could then be calculated. This information was then used to clear any vegetation infringing on the minimum clearance. An example of an output diagram created through this method is provided below [Fig.3.].

This ground survey technique is time and labor intensive, and is consequently impractical for application on more than a handful of spans. Application of this technique on an entire transmission system would be time consuming, costly and unnecessary given the availability of alternative techniques.

A description is now given of Airborne Laser Survey and associated output data [e.g. Fig.4.], and how this addresses the inherent problems of traditional vegetation management techniques, whilst ensuring the system and environmental variables are adequately considered in order to comply fully with NERC FAC-003-01. Laser scanning technology presents a shift from management techniques based on time and judgment, to one based on quantitative data.



## AIRBORNE LASER SURVEY

Airborne Laser Survey is an active form of remote sensing whereby a scanning laser mounted on an aircraft is repeatedly fired at the ground. The laser beams strike an object, causing backscatter [Fig.5.], which is recorded by the sensor. A processing unit on the aircraft uses the timing of the returning light to calculate an accurate distance. The latest generation of airborne laser scanners have a frequency of up to 200 kHz, creating vast 3D point clouds [e.g. Fig.4.] that models the exact lie of the land and above ground objects. The points are referenced to their real world location during data capture by an onboard kinematic Global Positioning System (GPS). This is tied in to ground based differential GPS total stations using processing software, which further increases positional accuracy. Although wide area mapping projects are conducted by installing the laser in a fixed wing aircraft, LiDAR derived engineering products require the most accurate and dense data capture possible. Transmission line surveys should therefore be conducted from a helicopter platform [Fig.6.]. Helicopter platforms benefit from the ability to intimately follow the sometimes angular alignment of transmission lines, and do not require large deviations to reposition themselves between line tangents. The resultant flight path is therefore shorter than the same works conducted using a fixed wing aircraft, and presents a more efficient means of operation.

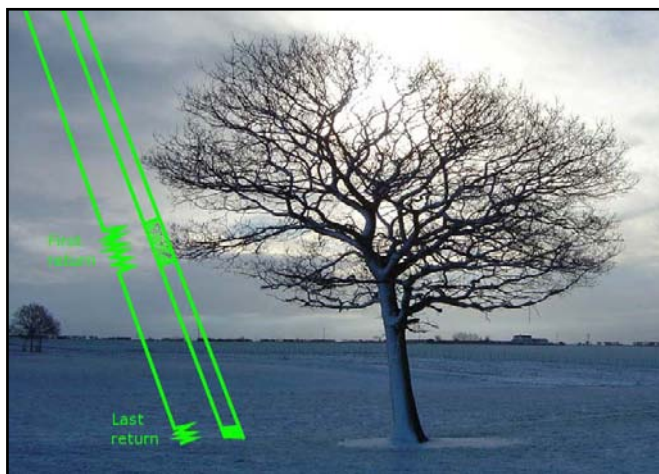


**Figure.5:** A depiction of laser interaction with the ground and an above ground feature. The helicopter mounted laser scanning system fires a pulse of infrared energy. The first contact this makes is with part of the tree structure, which produces backscatter. This is recorded by the sensor head as the 'first return'. The laser then continues and contacts the ground. As the ground is non-permeable, this causes the last backscatter from the original pulse, and is recorded by the scanner as the 'last return'. LiDAR technology can therefore be used to create ground models even when vegetation coverage is present.

Airborne laser scanning systems are usually equipped with a high resolution downward looking metric camera [Fig.6.], providing photographs for a complete coverage of the survey swath. These images are later orthorectified, to ensure the distance between two objects is representative of the actual real world distance.

Aircraft can be equipped with forward looking cameras, and additional downward looking sensor types such as multispectral and thermal cameras.

Following the survey, the collected data is processed to produce a 3D point cloud and photography that is spatially referenced. In order for the data to be meaningful to utilities, it must be populated with attribute data. Feature types within the 3D point cloud are classified by assigning a code to each feature. For example, roads, vegetation and buildings, may be feature codes 108, 109 and 130 respectively. Once imported into PLS-CADD™, the computer can discriminate between these feature types. Statutory clearance values are entered for each feature type according to a country's electrical code. For vegetation clearances in the USA, transmission companies normally base this on published standards, such as ANSI Z133.1 and IEEE Standard 516-2003, which specify minimum clearances for vegetation from various voltage lines. The structures and conductors are modeled within PLS-CADD™ to produce an accurate model of the transmission line at the time of data capture. This model incorporates electrical load information provided by the line operator and meteorological data from locally deployed weather stations and in-flight measurements. PLS-CADD™ allows users to define the size and type of conductor, shield wire or optical ground wire along with associated engineering properties, such as yield strength. Simple frames of structures can be created from circuit diagrams of a route, or full engineering structure models can be modeled or imported. PLS-CADD™ models can be used for a range of applications across all areas of overhead line management, including new line routing and design, thermal rating assessments, re-conductoring projects, and the structural analysis of towers and poles.



**Figure.6:** Optech Incorporated's ALTM 2050 airborne laser scanner. The laser is attached to the front of a Squirrel helicopter with a purpose built mount. The metric camera is installed just behind the scanner, and both of these sensors feed data to the recorder contained within the aircraft.

Field inspection teams previously estimated the conductor position at maximum rated temperature, with inherent subjectivity. PLS-CADD™ allows the user to sag the wire to this position, and then find the vegetation violations for various combinations of conductor temperature, wind and clearance requirements. LiDAR/

PLS derived infringement locations therefore represent not only a great improvement in survey speed, but a quantitative step change for analysis.

The raw datasets used to create the PLS-CADD™ models can also be used to produce models in other power line software packages.

## VEGETATION MANAGEMENT USING ALS

The seasonal nature of vegetation necessitates the rapid turnaround of data from in-flight acquisition to the final delivery of vegetation intelligence that will be used for ROW management. Rapid vegetation check deliverables can be offered within 30 days of data capture, and these depict all vegetation within a pre-defined radius from a conductor, for example, 25 ft. This enables compliance with section R1.5. of NERC FAC-003-1 which states action must be taken on vegetation conditions that present an imminent threat of a transmission line outage. Network Mapping uses the TerraSolid plug-in for Microstation to produce this deliverable, with the simple vectorization of wires and the classification of above ground features as trees. An in-built function then determines any vegetation within the pre-defined distance from these wires to give an idea of the extent of vegetation violations. Violations are highlighted in a plan sheet, and displayed against stock imagery [Fig.7.].

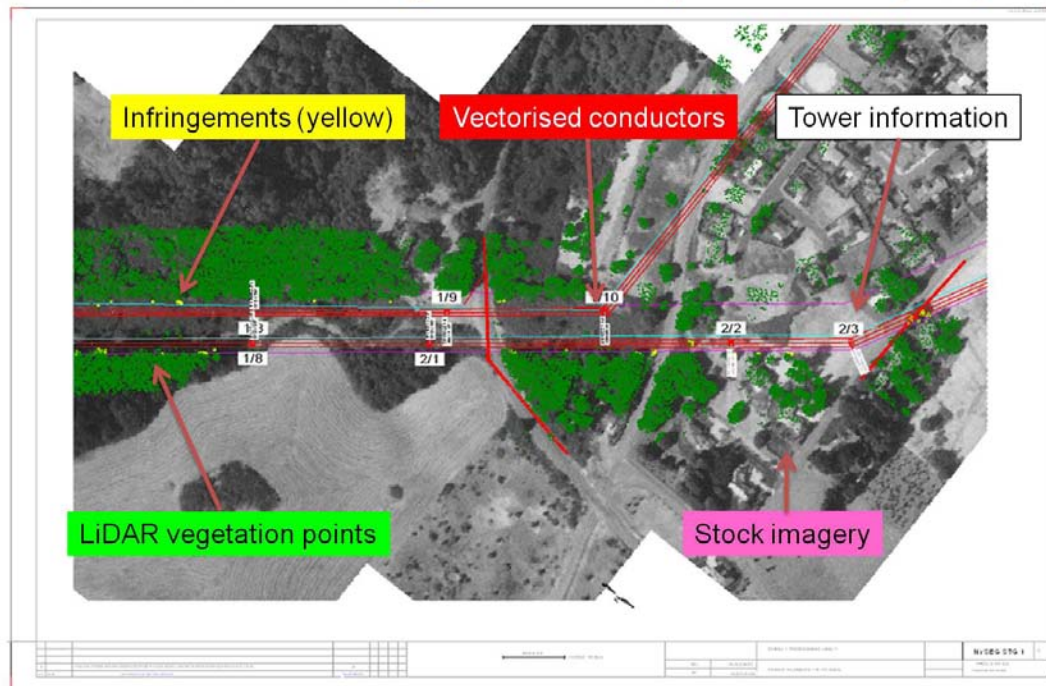


**Figure.7:** Initial vegetation check plan sheet for compliance with NERC FAC-003-1 R1.5. The conductors are vectorized and vegetation points classified. An algorithm highlights all hazardous vegetation within a predefined radius which is displayed against stock imagery.

Pinpoint vegetation checks can be provided 30 – 40 days following data capture. To produce the deliverable, classified Aerial Laser Survey data is imported into PLS-

CADD™, and the conductors are graphically sagged. The ‘Danger Tree Locator’ tool is then used to determine any grow-in or falling tree violations that occur under given parameters, for example maximum sag or blow-out conditions. Plan sheets are produced from this report, and display visually the type and context of each violation within a span [Fig.8.]. Anticipated growth buffers can be incorporated in the analysis. A buffer of 20% may be added to a line that traverses through forests of fast growing trees, where as only 2% may be added to lines traversing forests of predominantly slow growing trees. The report provides intelligence on the three outage categories detailed in FAC-003-1. These are grow-ins inside the ROW, fall-ins inside the ROW and fall-ins outside the ROW.

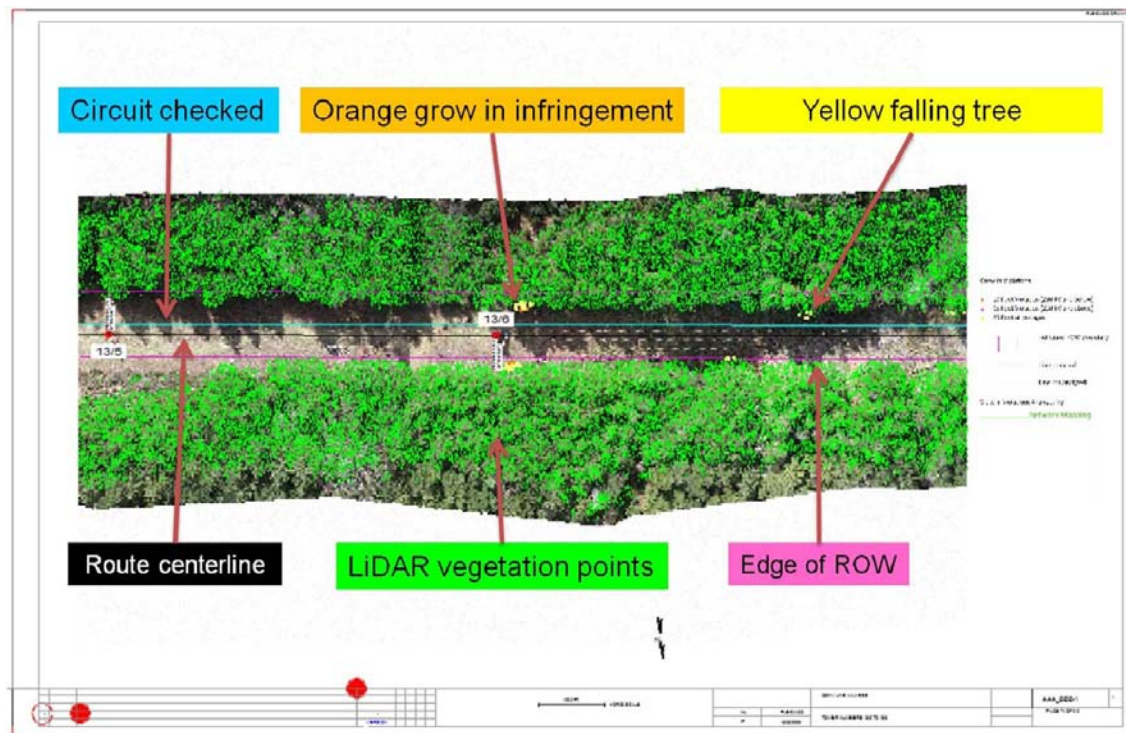


**Figure.8:** Pinpoint vegetation analysis plan sheet. This displays the nature of the infringement, either grow-in or falling tree, against high resolution orthorectified photography. The algorithm used to produce this example plan sheet considered conductor position at maximum sag and a 10% growth buffer.

#### TRENDS IN THE MARKET PLACE TOWARDS ALS

In recent years, the deployment of Airborne Laser Survey for high-voltage transmission line engineering applications has grown exponentially, with most US transmission companies now using ALS derived products as the input for PLS-CADD™ models. The use of this technology as a platform for LiDAR-based vegetation maintenance strategies is also increasing, given the evolving regulation set out in documents like FAC-003-1. There is a growing progressive trend in Europe

with distribution companies harnessing a LiDAR/PLS approach for multiple applications. This has been facilitated, in part, by EU legislation that now requires all distribution companies to map their assets.

### CASE STUDY – IMPROVEMENT OF NATIONAL GRID UK'S ROW VEGETATION MANAGEMENT

Fountain Forestry, a subcontractor to National Grid for ROW vegetation management, has witnessed extensive improvement in their maintenance methodology through the provision of ALS data acquired and processed by Network Mapping.

Fountain Forestry's methodology for vegetation management previously involved walking down a transmission ROW and identifying by eye any trees thought to be an infringement. The distance to the conductors from these infringing trees was then measured, and an additional vertical clearance safety factor for increased sag was applied. This was;

- +1.5 m at the mid point
- +1m at 50 m from the mid point
- +0.5m 100 m from the mid point

The vegetation was then cut to the calculated length.

The problem with this technique is that conductors were measured on the day of survey with no idea of loading or atmospheric temperatures. Increased sag due to temperature can be in excess of 4 m at mid span depending on system and environmental variables. This means that after a tree was cut it could still be infringing by 2.5 m. The devices used to measure such violations were only basic hand-held laser range finders, requiring a line of sight for measurements.

Network Mapping now provides National Grid with full PLS-CADD™ models. These are then used to supply a CAD file of the conductors at rated and ambient temperature to Fountain Forestry. As the tree cutting usually takes place in the summer and during the day, the conductors are unlikely to be at maximum rated temperature and therefore the difference between the two can be used as an accurate safety factor. GPS enabled handheld GIS systems are operated by the field teams, allowing them to record work electronically with accurate positioning. However, maintenance personnel still need to walk the line and take vegetation measurements manually.

Network Mapping will now supply vegetation infringement data for ROWs surveyed using ALS directly to National Grid. This will preclude the requirement for Fountain

Forestry to take measurements manually, and will thus reduce operational expenditure for ROW maintenance. However, for this vegetation infringement data to be of use, it must be current. Network Mapping has therefore realigned internal work flows with a team of technicians now processing data in the field to ensure a quick turnaround of infringement data. National Grid anticipate that this new methodology will allow them to utilize vegetation height data captured during ALS, vastly reducing the time and resources associated with manually walking down the line.

Existing policies concerning the refresh of ALS coverage are normally based on the use of LiDAR derived products for the specific identification of vegetation clearances, and as an audit tool for the effectiveness of existing vegetation management programs. As the capture of LiDAR data becomes more efficient and computer processing power improves; it is increasingly effective to fly larger sections of the power system and produce vegetation management products for immediate use. This is especially true where the electronic records of structures and wires are current, and the worst conductor position already modeled.

Further integration of ALS products with National Grid's vegetation maintenance strategy is expected in the near future. This will most likely entail the provision of vegetation intelligence plan sheets.

## CONCLUSION

Airborne Laser Survey clearly has a huge potential for ROW vegetation management where actionable deliverables are produced within a short time frame. A quick turnaround is essential for this application given the seasonal nature of vegetation and the resultant limited useful lifetime of the data. Commissioning an aerial survey will create quantitative and auditable intelligence on the location of vegetation violations across a transmission network that is compliant with NERC FAC-003-1. The case study demonstrates that ALS is already adding value to transmission companies' maintenance strategies. The demand for transmission line ALS is increasing, given the importance of FERC FAC-003-1 compliance, and the cost savings associated with the technique. It is anticipated that due to regulatory requirements ALS will become the standard approach for US transmission line vegetation management.

## REFERENCES

- Addison, B., Jacobs, K., Richardson, P., Ray, G., Rivkin, L., Merrett, S., (2003). "Wide-scale Application of Lidar Data for Power Line Asset Management in National Grid Transco plc." *International Council on Large Electrical Systems (CIGRE)* Committee SC22 Conference Proceedings.

Addison, B., Ryder, S., Redhead, S., Richardson, P., Ray, G., Jacobs, K., Rivkin, L., Browne, M. and Sullivan, T. (2003) "The Application & Business Benefits of Aerial Laser Survey Techniques used in the Management of Vegetation Encroachment within Transmission Rights of Way" *International Council on Large Electrical Systems (CIGRE)*.

Char, C., and Noda, R. (2006). "Transmission Line Management Using LiDAR and PLS-CADD". *Electrical Transmission Line and Substation Structures Conference*, 286-297.

Federal Energy Regulatory Commission [FERC] (2004) "Utility Vegetation Management And Bulk Electric Reliability Report From The Federal Energy Regulatory Commission". *Vegetation Management Report*.

McGarrie, D. (2008) "Vegetation Management and the Challenge of ESQCR." [http://www.sigmaseven.co.uk/files/Vegetation\\_Mgt\\_Industry\\_Opinion.pdf](http://www.sigmaseven.co.uk/files/Vegetation_Mgt_Industry_Opinion.pdf)>(Jan.05, 2008) Sigma Seven.

North American Electric Reliability Corporation [NERC] (2004) "Final Report on the August 14, 2003 Blackout in the United States and Canada: Causes and Recommendations". *U.S.-Canada Power System Outage Task Force*.

North American Electric Reliability Corporation [NERC] (2006) "Standard FAC-003-1 – Transmission Vegetation Management Program." <http://www.nerc.com/files/FAC-003-1.pdf>>(Oct.04,2008).

North American Electric Reliability Corporation [NERC] (2008) "Vegetation-Related Transmission Outage Report: Third Quarter 2008."

Power Systems Engineering Research Centre [PSERC] (2007) "Reliability Based Vegetation Management Through Intelligent System Monitoring."

Shen, B., Koval, D. and Shen, S. (1999) "Modelling extreme-weather-related transmission line outages". *IEEE Canadian Conference on Electrical and Computer Engineering*, 3, 1271-1276.

## Sequential Mechanical Testing of Conductor Designs

Bruce Freimark<sup>1</sup> Bruce Vaughn<sup>2</sup> Jean-Marie Asselin<sup>3</sup> Craig Pon<sup>4</sup> Zsolt Peter<sup>5</sup>  
P.E., F.ASCE M.IEEE P. Eng., M.IEEE P.Eng., M.IEEE Ph.D., M.IEEE

<sup>1</sup> Principal Engineer, American Electric Power (AEP), 700 Morrison Road, Gahanna, OH 43230, Phone: (614) 552-1944, email: bfreimark@aep.com

<sup>2</sup> Senior Engineer-Utility Products, Alcan Cable, Suite 1600, Three Ravinia Drive, Atlanta, GA 30346, Phone: (770) 677-2613, email: bruce.vaughn@alcan.com

<sup>3</sup> Senior Engineer, Utility Markets – Canada, Alcan Cable, Suite 602 East Tower, 2700 Matheson Blvd. East, Mississauga, Ontario L4W 5H7, Canada, Phone: (905) 206-6874, email: jean-marie.asselin@alcan.com

<sup>4</sup> Manager, T&D Mechanical Laboratory, Kinectrics, Inc., 800 Kipling Avenue, Toronto, Ontario M8Z-6C4, Canada, Phone: (416) 207-6741, email: craig.pon@kinectrics.com

<sup>5</sup> Senior Engineer, Kinectrics, Inc., 800 Kipling Avenue, Toronto, Ontario M8Z-6C4, Canada, Phone: (416) 207-6000 Ext'n 5501, email: zsolt.peter@kinectrics.com

### Abstract

Like many utilities, American Electric Power (AEP) has concerns regarding the longevity of new high temperature low sag conductors using non-traditional materials. For example, conductor designs such as ACCC (Aluminum Conductor Composite Core) and ACCR (Aluminum Conductor Composite Reinforced) that have entered the market in recent years as well as other new conductor designs that may be coming in the future. While vendors of the new conductors generally run their product through individual tests such as sheave, galloping, aeolian vibration, etc., they typically do not run a single sample through a sequence of tests to represent the mechanical loadings that generally occur during installation and operation of an actual line. For example, conductor installation (sheave testing), exposure to galloping conditions, aeolian vibrations and tension cycles due to varying weather loads.

AEP has developed a testing protocol with the goal of evaluating new conductor designs in a few months (approx. 90 days) rather than having to wait years. In order to verify that the testing protocol is not excessively burdensome, AEP has partnered with Alcan Cable and Kinectrics to run samples of commonly used Drake ACSR (Aluminum Conductor Steel Reinforced) and Drake ACSS (Aluminum Conductor Steel Supported) through the same protocol. The only difference between ACSR and ACSS is that ACSR is stranded using hard-drawn aluminum wires, while in ACSS the aluminum wires have been annealed to remove any hardness and strength due to the wire drawing process. This paper discusses the findings of the test program. See Table 1 for the conductor properties.

**Table 1 – Properties of Tested Conductors**

Product Designation	Drake ACSR	Drake ACSS
Cross Section		
Size and Stranding	795 kcmil 26 x 7 ACSR	795 kcmil 26 x 7 ACSS
Outer Diameter	1.108 in.	1.108 in.
Rated Strength	31,500	25,900
Mass	1.093 lb./ft.	1.093 lb./ft.

## Background

Utilities have had extensive experience using ACSR (Aluminum Conductor Steel Reinforced) for about 100 years and ACSS (Aluminum Conductor Steel Supported, which is similar to ACSR but with the aluminum strands fully annealed) for over 30 years. When installed with appropriate consideration for weather loadings, vibration concerns, etc., lines built using these conductors have operated successfully for many decades.

In recent years, new types of bare overhead conductor have entered the market, primarily designed for reconductoring existing overhead facilities. Two products currently on the market are:

- ACCC – Aluminum Conductor Composite Core, manufactured by Composite Technology Corporation (CTC)
- ACCR – Aluminum Conductor Composite Reinforced, manufactured by Minnesota Mining and Manufacturing (3M)

These new conductor types make attractive claims of improving the electrical capacity of the transmission grid when compared to standard ACSR. For example [1]:

- Doubles the current carrying capacity over conventional ACSR - reconductor existing pathways without structural modifications
  - Up to 28% more aluminum to be utilized (based primarily on using TW [Trapezoidal Aluminum Wire] strands instead of round strands to eliminate most voids)
  - Can be operated at higher temperatures - up to 200°C vs. 100°C for conventional cable
- Mitigates clearance issues related to high-temperature sag.
- Reduces construction costs by using fewer support structures (on new lines)
  - Higher strength to weight ratios allows longer spans between support structures reducing project structure requirements by 16% or more
- Resists environmental degradation – will not rust or degrade

An obvious question for the utility considering installing a new type of conductor is:  
Will the new conductor type last 50 years? 10 years? 5 Years?

### Typical Testing by Manufacturers

Conductor manufacturers have typically run their new products through various individual, stand alone, tests such as sheave, aeolian vibration and galloping. Often these conductor tests are based on IEEE Std 1138 [2], which contains various tests for optical overhead ground wires (OPGW). However, once the conductor sample has “passed” any of these tests, the test specimen is typically discarded and a new sample is prepared for the next test. But do these individual tests represent the real world?

### Sequential Test Protocol

When a conductor is installed, it is first pulled over a series of sheaves to place the conductor in position on the structures. After the conductor has been sagged and clipped in, over the next few years it will be exposed to aeolian vibrations and it may also be in an area subject to conductor galloping. Additionally, over the years and seasons the conductor tensions will increase and decrease through numerous cycles. Thus, AEP came up with the following Sequential Test Protocol in an attempt to gain more knowledge regarding the long term performance of new conductors.

Except for the sheave test, all tests are to be run on samples of conductor, using suitable compression-type fittings or other termination intended for deadending the conductors on an actual utility project. If excessive elongation of the aluminum strands due to compressing the fittings in short test span is a concern, then poured epoxy terminations may be used.

### Sheave Test

A suitable length of new conductor (the longer the better) is subjected to multiple back-and-forth passes over a sheave of a diameter and other dimensions as recommended by the conductor manufacturer, for an installation tension of 20% of the conductor’s rated strength for the “Total Conductor Angle Over Sheave” values listed in Table 1, below. In the absence of a manufacturer’s recommendation, a lined sheave with a minimum diameter to the bottom of the groove of  $[20 \times D_C - 4]$  inches, where  $D_C$  is the diameter of the conductor would be used.

The conductor should be at the maximum stringing tension(s) recommended by the conductor manufacturer for each of the “Total Conductor Angle Over Sheave” values listed in Table 2.

**Table 2 – Sheave Test Angles and No. of Passes**

Total Conductor Angle Over Sheave	Minimum Number of Passes
10 Degrees	20
20 Degrees	7
30 Degrees	3



Figure 1 – Photo of Sheave Test

### Aeolian Vibration Test

(Note: The sequencing of the Conductor Galloping and Aeolian Vibration Tests may be reversed.)

After the sheave test, the sample is then subjected to an aeolian vibration test as follows:

- A minimum of 30 m (100 ft) of conductor is installed with a minimum active (driven) span equal to a minimum of 60% of the total span lengths.
- A suitable suspension assembly, as recommended by the conductor manufacturer, is used to support the conductor with a minimum total conductor deflection angle of 5 degrees.

Note: The suspension assembly is centered in one of the sections exposed to the sheave test.

- The conductor is tensioned to a minimum of 20% of its rated tension strength.
- The shaker is set to vibrate the conductor at a frequency equivalent to a 4.5 m/s (10 mph) wind.

Note: Frequency (Hz) =  $830 \div \text{Conductor Diameter, } D_C \text{ (mm)}$

Frequency (Hz) =  $32.7 \div \text{Conductor Diameter, } D_C \text{ (inches)}$

- The conductor shall have a vibration loop antinode displacement (peak-to-peak) of one-half ( $\frac{1}{2}$ ) of the conductor diameter,  $D_c$ .
- The minimum test duration is 100 million cycles.



Figure 2 – Aeolian Vibration Testing

### Conductor Galloping Test

The same sample from the Aeolian Vibration Test is subjected to a galloping test as follows:

- A minimum of 30 m (100 ft) of conductor is installed with a minimum active (driven) span of 20 m (65 ft).
- A suitable suspension assembly as recommended by the conductor manufacturer is used to support the conductor, at a height such that the static total conductor angle through the clamp does not exceed approximately 2 degrees.

Note: The suspension assembly is centered in one of the sections exposed to the sheave testing.

- The suspension assembly is connected to the support structure in such a manner that feed-through galloping will be established in the back span. This can be accomplished by using hardware that provides freedom of movement for the suspension assembly.
- The conductor is tensioned to a minimum of 2% of its rated tensile strength.
- The single galloping loop amplitude is measured.



Figure 3 – Setup for Galloping Conductor Test

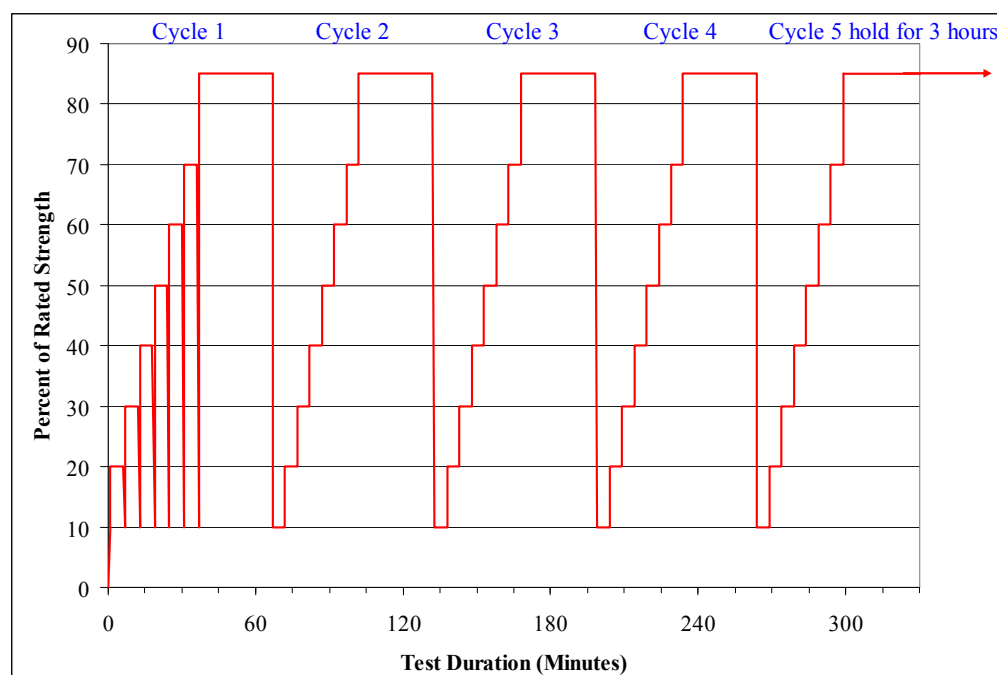
- A suitable shaker is used to excite the cable in the vertical plane with its armature securely fastened to the cable in the vertical plane.
- The test frequency corresponds to the single resonant frequency loop as determined experimentally.
- The peak-to-peak vertical amplitude/loop length ratio is maintained at approximately 1/25 of the active span length. The amplitude (peak-to-peak) in the back span shall be no less than 50% of the amplitude of the active span. Appropriate restraining devices or fixtures are used to maintain the horizontal component of the galloping motion to 300 mm (11.8 inches), peak-to-peak, or less.
- The cable is subjected to a minimum of 100,000 galloping cycles.

### Tension Cycle Testing

Note: If it is necessary to shorten the test sample to fit in the tensile testing machine, the selected test length shall include the section of cable where the suspension assembly was installed, including the length of any associated armor rods, etc.

### Tension Cycle Test Part A

- The sample is placed in a tensile machine and the load is cycled between 10% of the rated strength and 85% of the rated strength, with 5-minute holds at 20, 30, 40, 50, 60, and 70% of the rated strength and a minimum of a 30-minute hold at 85%. After each hold period, during this initial load cycle only, the tension is reduced to 10% of the rated strength and the sample is visually examined for evidence of loosening of the aluminum strands. After examining the conductor, the tension is increased to the next increment.
- The above loading sequence is repeated without the tension reductions and visual examinations for four additional cycles with a 3-hour hold at the 85% loading on the last (fifth) cycle. The sample is removed and the test proceeds to Part B.



Graph 1 – Representation of Tension Cycle Test – Part A

### Tension Cycle Test Part B – Detailed Examination of Components

Note: For the verification testing of the protocol using standard Drake ACSR and Drake ACSS conductors, the detailed examination of the conductor and deadends was dispensed with.

A length of conductor from the tensioned sample from Part A is selected for examination as follows:

- Starting at the deadend installed closest to the suspension assembly , a length is cut off beginning at the deadend and extending to just past the center of the suspension clamp but not including the full length of any armor rods.

The conductor sample is carefully disassembled (including the deadend fitting) and all layers and components of the conductor are examined for cracks, etc., that could lead to moisture coming into contact with critical materials. Carefully examine the outer surface of the core for any defects:

- Cut cross sections from the core, and
- Examine the cross sections using a microscope, etc.
- Perform dye penetration tests using Zyglo or other appropriate media.

### Tension Cycle Test Part C – Test to Failure

A new termination is installed on a suitable length of the remaining tortured specimen and tested to failure, which should meet or exceed 95% of the rated strength of the conductor.

### Test Results for ACSR and ACSS

In order to verify that the testing protocol is not excessively burdensome, AEP, Alcan Cable and Kinectrics partnered to prove the validity of the sequential testing protocol. Samples of Drake ACSR and Drake ACSS (both 795 KCM 26/7) were tested at Kinectrics using the criteria described above.

### Sheave Test

Due to the setup in the lab (see Figure 1) the actual sheave portion of the testing was somewhat more conservative than specified, as shown in Table 3.

**Table 3 – Actual Sheave Test Angles and No. of Passes**

Specified Conductor Angle Over Sheave	Specified Minimum Number of Passes	Actual Number of Passes
10 Degrees	20	--
20 Degrees	7	27
30 Degrees	3	3

### Aeolian Vibration and Galloping Tests

The ACSR conductor was supported in suspension by a standard suspension clamp installed directly on the conductor strands for the galloping and aeolian vibration tests.

For the galloping and aeolian vibration tests, the ACSS conductor was (initially) supported by a standard suspension clamp installed over a set of armor rods. This arrangement met the minimum recommendations of Alcan Cable and also was AEP's standard practice for this product. When the armor rods were removed in preparation

for the tension tests, it was found that a number of the annealed aluminum strands had failed in fatigue in the vicinity of the suspension clamp (see Figure 4).

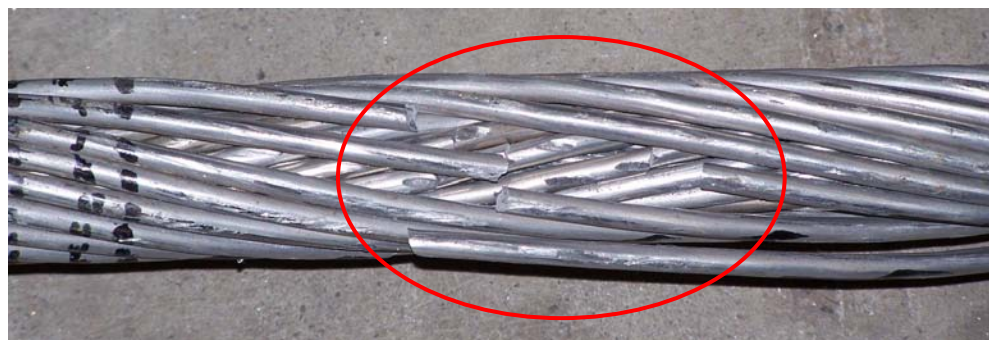


Figure 4 – Fatigue Failures of ACSS Conductor Supported by a Standard Suspension Clamp installed over a set of armor rods

Upon seeing the fatigue damage, a manufacturer of conductor support hardware was contacted and advised us that this failure was likely due to the rigors of the test protocol. The use of a cushioned suspension assembly was recommended, as pictured in Figure 5.



Figure 5 – Cushioned suspension assembly

We obtained a cushioned suspension assembly and repeated all of the tests on a new sample of ACSS conductor. After the aeolian vibration and galloping tests, the second sample of ACSS was examined and we found that the formed wire rods on the cushioned assembly had fatigue failures as shown in Figure 6.



Figure 6 – Fatigue failure of formed rods on suspension assembly

After removal of the suspension assembly, we saw no damage to the outer aluminum strands on the ACSS. We carefully tried to examine the inner strands (without damaging the soft aluminum) and did not see any damage.

We then proceeded to the tension tests using poured epoxy terminations.

### Tension Tests

The ACSR was then subjected to the tension cycling tests using poured epoxy terminations (see Figure 7) without any undue occurrence. The tension in the ACSR sample was then increased to failure, which occurred at 103.6% of the rated breaking strength.

The second ACSS sample was also subjected to the tension cycling tests using poured epoxy terminations without any undue occurrence. The tension in the ACSS sample was then increased to failure, which occurred at 109% of the rated breaking strength.

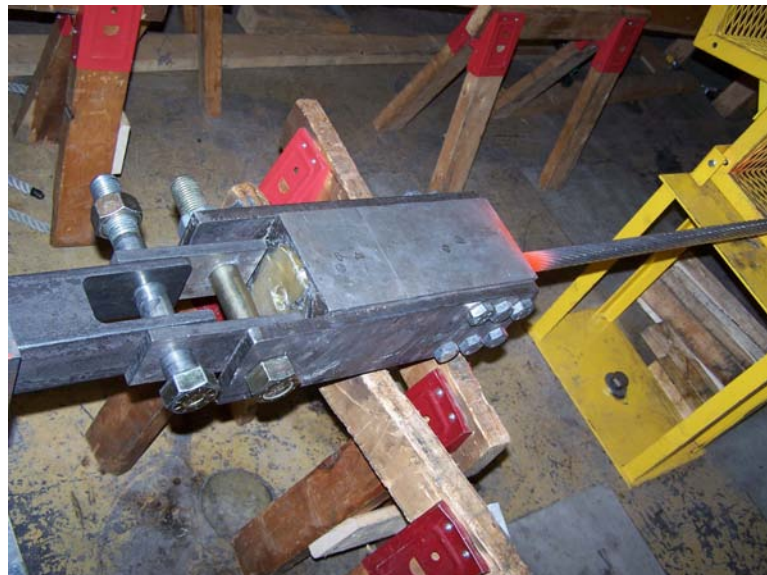


Figure 7 – Poured Epoxy Deadend

After the completion of the tension tests, the conductors were carefully examined. On the ACSR, most of the strands had the classic “cup and cone” indicators of tensile failure. However, 4 of the 10 strands in the inner aluminum layer had the shear-plane appearance of a fatigue failure; see Figure 8.

During the tension tests the movement of the hydraulic cylinder was monitored and recorded. There were no obvious indications that any strands were failing prior to reaching 103.6% of the rated strength. It could be that these wires were already broken prior to the tension testing, or that they failed at the same time as the others.

(in tension) but had partially cracked during the aeolian vibration and/or galloping test and would have eventually severed at some point in the future. At this point this is not known. Additionally, later examination of this ACSR sample at Alcan's Technical Center revealed extensive fatigue damage to the sample, with fatigue breaks in the inner layer under the suspension assembly.

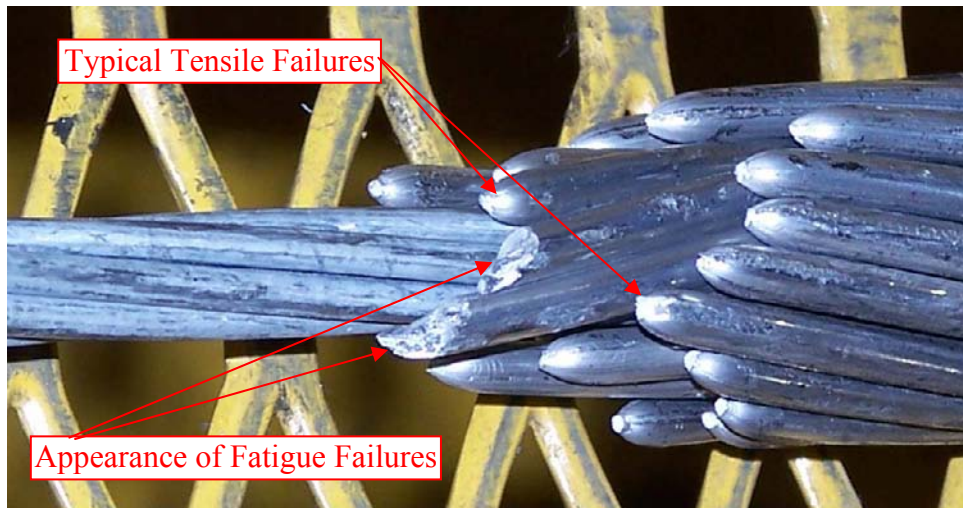


Figure 8 – Detail photo of ACSS after tension test.

Similarly, on the ACSS, most of the strands had the classic “cup and cone” indicators of tensile failure. However, 7 of the 10 strands in the inner aluminum layer had the shear-plane appearance of a fatigue failure. Figure 9 shows the fatigue failure patterns from the different tests.

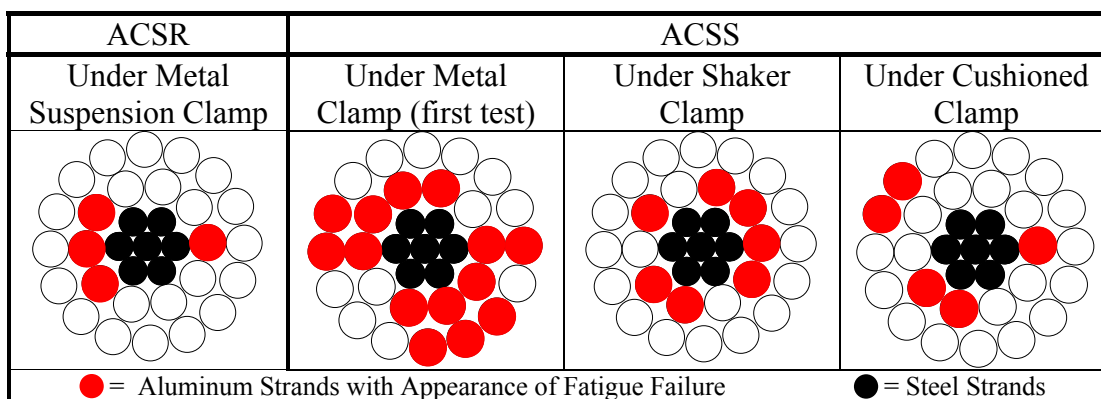


Figure 9 – Fatigue Failures of Various Samples

### Observations and Conclusions

As mentioned above, in testing the ACSS conductor:

- On the first ACSS sample that was supported by a standard suspension clamp installed over standard armor rods, we found fatigue failures of the annealed aluminum strands after the aeolian vibration and galloping tests

- The second ACSS sample was supported by a cushioned suspension assembly. During the examination following the tension testing, extensive fatigue damage was observed on the sample. Fatigue breaks were observed in the inner layer under the suspension assembly and the shaker clamp. Also, as stated above, we did see fatigue failures in the formed wire rods of the cushioned assembly.
- The ACSR sample was tested supported by a standard suspension clamp. Four fatigue failures were found in the aluminum strands after the tension test.

We feel that these results prove the rigor of the testing protocol. Although it will not provide any direct measure of the potential longevity of a new conductor type, the use of the Sequential Mechanical Testing of Conductor protocols described above may be a valid method of collecting information and may assist in identifying potential weaknesses in conductor types. At the moment there are few data points in this collection and conclusions cannot be drawn more precisely.

At AEP's request, Composite Technology Corp. (CTC) ran a sample of their ACCC conductor through the above test protocol. As a result of this, they are considering including new design criteria and recommendations to users regarding design limitations for their conductor as presently specified in their data sheets.

---

### References:

- [1] From CTC and 3M websites:  
(<http://www.compositetechcorp.com/cabadv.htm>);([http://solutions.3m.com/wps/porta1/3M/en\\_US/EMD\\_ACCR/ACCR\\_Home/Proven\\_Benefits/More\\_Amps/](http://solutions.3m.com/wps/porta1/3M/en_US/EMD_ACCR/ACCR_Home/Proven_Benefits/More_Amps/))
- [2] IEEE Std 1138-1994 (R2002) – IEEE Standard Construction of Composite Fiber Optic Overhead Ground Wire (OPGW) for Use on Electric Utility Power Lines, Copyright © by the Institute of Electrical and Electronics Engineers, Inc.

## H<sub>2</sub>S ENTRAPMENT AND CORROSION ON DIRECT EMBEDDED GALVANIZED STEEL TRANSMISSION POLES

Ajay Mallik <sup>1</sup>, PE, A.M.ASCE and Andy Cooper <sup>2</sup>

<sup>1</sup> President, SANPEC, Inc, 11819 Skydale Drive, Tomball, TX 77375; PH: (832) 392-4230, FAX: (832) 550-2634; email: [ajmallik@sanpec.com](mailto:ajmallik@sanpec.com)

<sup>2</sup> Safety Manager, LCRA Transmission Services Corporation, 3505 Montopolis Drive, Austin, Texas, 78744; PH: (512) 356- 6442, FAX: (512) 356-6054, email: [andy.cooper@lcra.org](mailto:andy.cooper@lcra.org)

### ABSTRACT

Hydrogen sulfide (H<sub>2</sub>S) is a colorless, toxic, and flammable gas with a characteristic odor of rotten eggs. It occurs naturally in crude petroleum, natural gas, volcanic gases, and hot springs. It can also result from bacterial breakdown of sulfates in organic matter, such as in swamps and sewers. H<sub>2</sub>S gas forms sulfuric acid when concentrations exceed approximately 2.0 ppm and causes corrosion on many underground construction materials and is particularly devastating to concrete and steel. Temperature can accelerate chemical corrosion due to creation of sulfuric acid. Warmer climates -southern US cities, for example - have more corrosion problems. It can also lead to sulfide stress cracking.

This paper addresses the corrosion issues due to H<sub>2</sub>S gas on some galvanized steel transmission poles and the precautions taken related to the removal and replacement of the direct embedded steel poles with base plated steel poles on a traditional concrete pier foundation. This was a dangerous situation, but also an interesting exercise in developing a solution to the abatement of the toxic and corrosive gas, as well as evaluation and removal of the pole itself. Special techniques that were necessary in dealing with the toxic gas that may prove beneficial to others who may come across similar situations.

### I. INTRODUCTION

In 2004, during routine maintenance inspections for LCRA Transmission Services Corporation, American Electric Power (AEP) reported that visible and severe exterior corrosion had developed on one or more direct embedded steel transmission poles near Corpus Christi, Texas. After investigation, it was determined that the cause of the severe corrosion was a very high concentration of H<sub>2</sub>S gas at and around the top of the steel poles. For public safety, LCRA decided to remove the embedded steel poles, which had the toxic and potentially explosive H<sub>2</sub>S gas trapped inside.

### A. Background

Transmission lines T436 (now T522) and T437 were constructed in 2002 by utilizing direct embedded steel poles. These lines are located in Corpus Christi area. AEP first noticed a rust spot on pole # 106 (T522) in 2004. The assumption was made that the pole had been struck by lightning. The rusty area was painted with cold galvanize paint. Four years later, Jan 2008, AEP reported a visible exterior corrosion on another pole # 71 (T437). Structures #106 and #71 are adjacent to each other and are separated by approximately 60 feet.

LCRA Transmission Lines:



**Visible Corrosion on Two Steel Poles**

When the AEP crew went up to investigate the corrosion issue, they noticed an unusual smell. Subsequently, AEP performed atmospheric sampling on Pole # 71. They discovered very high concentrations of H<sub>2</sub>S gas at the top of the pole. There were no traces of the gas at the ground level.

## II. LCRA SAMPLING

On June 2008, LCRA sampled suspected toxic atmospheres within six (6) transmission poles on both lines (T437 and T522 - Pole # 70, 71, and 72 on T437 and Pole # 105, 106, and 107 on T522). The sampling target compound was H<sub>2</sub>S gas.

The sampling team confirmed the presence of H<sub>2</sub>S gas within two (2) poles. Pole # 106 contained harmful concentrations of H<sub>2</sub>S gas and elevated levels of flammable gas. Pole # 71 contained deadly concentrations of H<sub>2</sub>S gas and explosive

concentrations of flammable gas. Both the poles had severe external corrosion on the top of the poles.

### SAMPLE RESULTS:

The following results represent data gathered on site on June 2<sup>nd</sup> and 3<sup>rd</sup>, 2008 with two (2) calibrated Industrial Scientific M40 4-gas monitors, and four (4) calibrated ToxiRAE 3 H<sub>2</sub>S personal monitors.

Structure #	~ Height (ft.)	H2S (ppm)	% Lower Explosive Limit	Oxygen	Personal H2S Monitoring	Notes
106	*0	0.0	0	21.0	0.0	
106	**25	0.0	0	21.0	† 0.0	
106	**50	0.0	0	21.0	† 0.0	
106	**60	0.0	0	20.9	† 0.0	
106	**70	0.0	0	20.9	† 0.0	
106	***75	47	8	< 19.5	† 0.0	5 minute sample peak
71	*0	0.04	0	21.0	0.0	
71	**25	0.0	0	21.0	† 0.0	
71	**30	0.0	0	21.0	† 0.0	Seam at upper/ lower structure connection
71	**50	0.0	0	21.0	† 0.0	
71	**60	0.0	0	20.9	† 0.0	
71	**70	0.0	0	20.9	† 0.0	
71	***80	> 500	> 10	< 19.5	† 0.0	2 second sample

\* Ground level sample

\*\* Elevated sample (sample at height from bucket truck basket) exterior of structure

\*\*\* Elevated sample (sample at height from bucket truck basket) interior of structure

† Personal sample (exterior of structure) within bucket truck basket

Note 1: samples were taken up wind of suspected source

Note 2: The limit of detection for H<sub>2</sub>S was 0.01-500 ppm

Note 3: Samples were also taken from structures 105, 72, 107 and 70. Sample results indicated no hydrogen sulfide contamination, or any other known contamination.

### III. EXTERIOR CORROSION ON STEEL POLES

Pole # 71

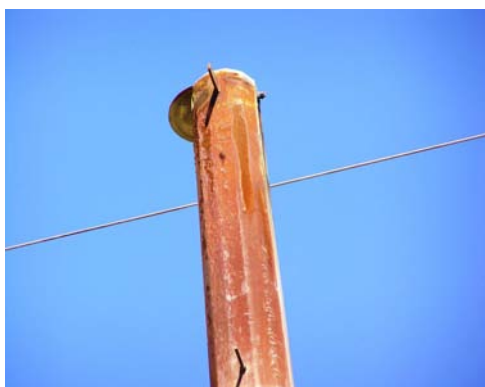


Pole # 71



#### Severe Exterior Corrosion

Pole # 71



Pole # 106

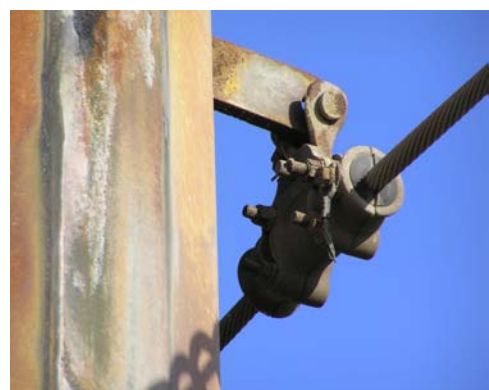


#### Severe Exterior Corrosion

Pole # 71



Pole # 106



#### Severe Exterior Corrosion

Telegram Channel: [@Seismicisolation](https://t.me/Seismicisolation)



### No Visible Inside Corrosion

#### A. Source of H<sub>2</sub>S Gas:

Based on interviews with AEP, Texas Rail Road Commission (TRRC) and a Certified Petroleum Geologist, it is believed that the source of the H<sub>2</sub>S is from naturally occurring subsurface gases that are diffusing through the surface and soils and are occupying the void, or open space, that exists inside the transmission structures. It is believed that the gas is present but under only normal atmospheric pressures that vary based on ambient temperature, as well as venturi effects from wind blowing past small openings in the top of the poles. It has been verified by LCRA staff and TRCC that there are no measureable ground level concentrations of H<sub>2</sub>S present at or near the poles

#### B. H<sub>2</sub>S Hazards

Hydrogen sulfide is explosive, toxic and corrosive by nature. It is considered to be an extremely toxic gas, which targets the respiratory system and central nervous system. In low concentrations, the gas resembles the smell of rotten eggs. Lower concentration exposures can cause eye irritation, cough, headache, and fatigue. H<sub>2</sub>S can also cause olfactory fatigue. This toxic effect is caused by the gas overwhelming the sinuses and the ability to smell. This is of particular as one could smell low concentrations of gas, but suddenly lose the sense and think that the gas has diminished, but in fact has increased in concentration and could be causing significant harm.

H<sub>2</sub>S single breath knock-down level is approximately 300 ppm for the average person. Lower level concentrations may cause difficulty in breathing. Brief exposure to concentrations of 500 ppm can cause loss of consciousness or death. Such exposures, where individuals regain consciousness, can result in long term effects such as headaches, poor attention span, poor memory, and poor motor function.

Hydrogen sulfide is a flammable gas. It is often found with other hazardous gases, such as methane. Such gases can present explosive atmospheres.

**C. H<sub>2</sub>S Physical and Chemical Properties:** Two atoms of Hydrogen and one atom of sulfur

Description: Colorless Gas	Molecular weight : 34.08 g/mol
Gas density: 1.4 g/L @ 25 °C	Specific gravity : 1.192 @15 °C (59 °F) (20% heavier than air)
Boiling point : -60.7 °C	Melting point : -85.5 °C
Vapor pressure : 15,600 torr @ 25 °C	Solubility : Soluble in water
Order threshold : 8.1 ppb (11µg/ m <sup>3</sup> )	Flash Point : -85 °C
Lower Exposure Limit : 4%	Solubility Soluble in water

**H<sub>2</sub>S Exposure Limits:**

Ceiling Level : 50 ppm (10-minutes)                    STEL: 20 ppm  
IDLH : 100 ppm

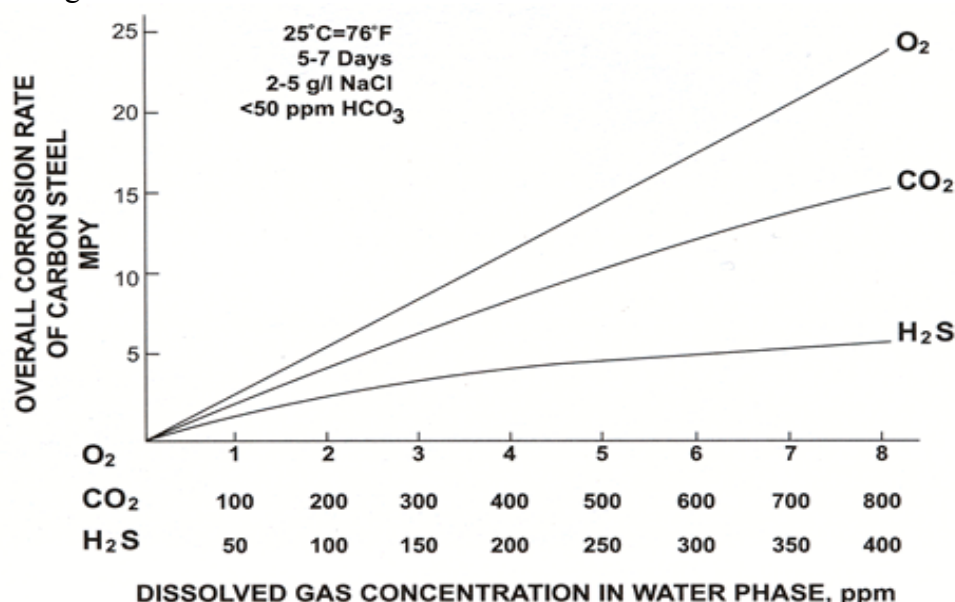
Ceiling Level: Worker exposure concentration not to exceed at any time  
STEL (short Term Exposure Limit) : Worker exposure concentration limit for one 15-minutes period  
IDLH (Immediately Dangerous to Life and Health): Worker exposure limit that could result in death

**D. Corrosive Gases and Microbes**

Common Corrosive gases:

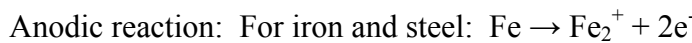
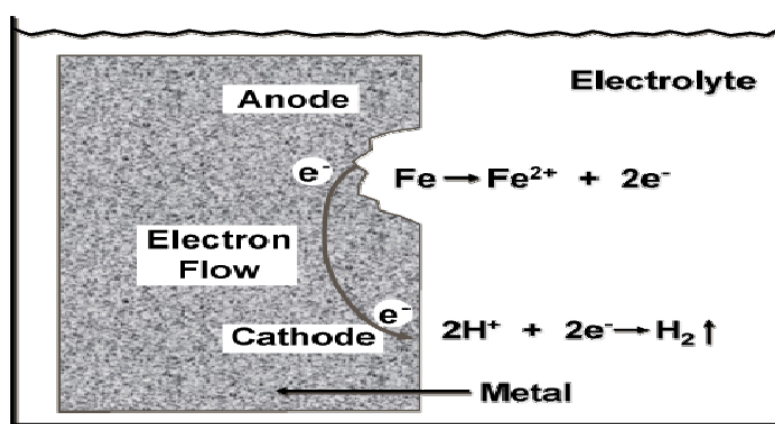
Oxygen (O<sub>2</sub>) - It is a strong oxidizer and one of the most corrosive gases when present  
Carbon dioxide (CO<sub>2</sub>) – Form weak acid in water  
Hydrogen sulfide (H<sub>2</sub>S) – Form weak acid in water  
Microbial Activity- It may cause corrosion alone and create more corrosive gases

Corrosion rates of steel versus oxygen, carbon dioxide, and hydrogen sulfide. Note the different gas concentrations on the x axis



### E. Corrosion Theory

Corrosion is defined as the destruction of a metal by a chemical or electrochemical reaction. It occurs when a metal in contact with water forms a corrosion cell. The corrosion cell has four components, the aqueous phase (water) which acts as an electrolyte (through which ions migrate), an anode on the metal surface (where the metal is oxidized and goes into solution as metal ions), a cathode (where excess electrons are consumed) and a metallic path connecting the cathode to the anode.

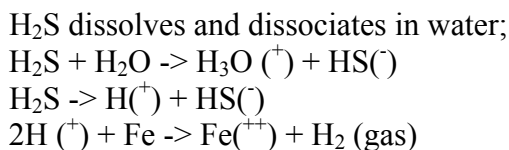


Cathodic reactions:

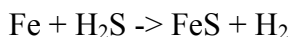
- $\text{O}_2 + 4 \text{H}^+ + 4\text{e}^- \rightarrow 2 \text{H}_2\text{O}$   
(Oxygen reduction in acidic solution)
- $1/2 \text{O}_2 + \text{H}_2\text{O} + 2\text{e}^- \rightarrow 2 \text{OH}^-$   
(Oxygen reduction in neutral or basic solution)
- $2 \text{H}^+ + 2\text{e}^- \rightarrow \text{H}_2$   
(Hydrogen evolution from acidic solution)
- $2 \text{H}_2\text{O} + 2\text{e}^- \rightarrow \text{H}_2 + 2 \text{OH}^-$   
(Hydrogen evolution from neutral water)

Corrosion is an electrochemical reaction composed of two half cell reactions, an anodic reaction and a cathodic reaction. The anodic reaction releases electrons, while the cathodic reaction consumes electrons. If the overall cell potential is positive, the reaction will proceed spontaneously.

### F. Mechanism H<sub>2</sub>S Corrosion:



Bisulfide ion may react with the dissolved metal ions and precipitate as metal sulfides. Hydrogen sulfide is a weak acid when dissolved in water, and can act as a catalyst in the absorption of atomic hydrogen in steel, promoting sulfide stress cracking (SSC) in high strength steels



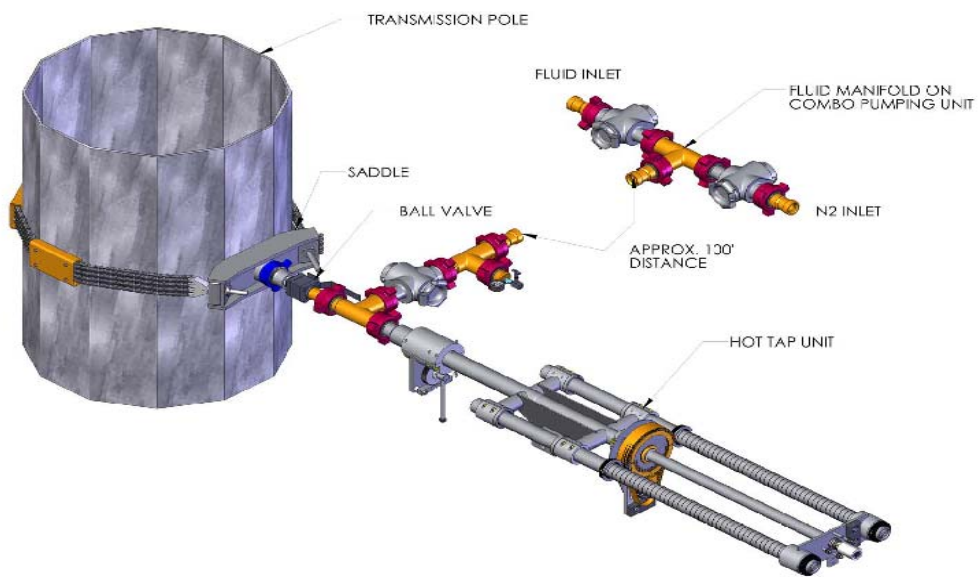
Hydrogen is evolved as a corrosion by-product. Main corrosion by-product that indicates H<sub>2</sub>S corrosion is Pyrite (FeS<sub>2</sub>), Pyrrhotite (Fe<sub>7</sub>S<sub>8</sub>), and troilite (FeS), which are iron sulfides. In environments with hydrogen sulfide (H<sub>2</sub>S) corrosion, the most common types include uniform corrosion, pitting corrosion, corrosion fatigue, sulfide stress cracking, hydrogen blistering, hydrogen embrittlement, and stepwise cracking

#### IV. CONCLUSION

For public safety, LCRA decided to remove the embedded steel poles, which had the toxic and potentially explosive H<sub>2</sub>S gas entrapped inside. Two replacement base-plated steel poles were ordered. Traditional concrete pier foundations were used with Type V cement (high sulfate resistance) and Class F fly ash (beneficial to sulfate resistance). The conductors and shield wires were transferred from existing poles to new poles

##### A. New base plated galvanized steel poles Installation:



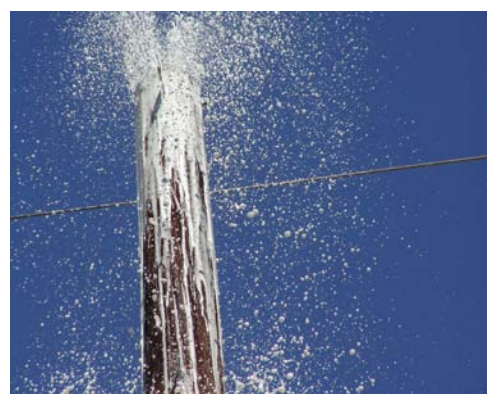
**B. Unique design and method to remove H<sub>2</sub>S gas and embedded steel poles:****LCRA TRANSMISSION POLE DECOMMISSIONING****C. Existing Pole Removal Steps**

Remediation:

- Rig up custom designed saddle, valves, 4-way spool, and hammer union.
- Rig up hot tap unit. Use mats and jack stands to support saddle and hot tap unit

Telegram Channel: @Seismicisolation

- Rig up fluid pump, pump lines and tanks
- Set up N<sub>2</sub> pump, 100 bbl open top tank, 25 bbl mixing plant, transfer diaphragm pump
- Run N<sub>2</sub> flow line, 2 in. pump hose to each pole
- Rig up nitrogen equipment and lay pump line up to flow tee
- Shut valve
- Negative pressure test seal element to 500 psi over calculated pressure drop across hole when pumping
- Tap 1 in. hole
- Back out hot tap and swap valves to pump fluid volume into pole volume below surface.
- Pump approximately 50 bbl at 1 bpm until fluid displaces internal volume up to tapped hole level. Fluid should be double concentration of H<sub>2</sub>S scavengers in fresh water.
- Bleed off system making sure fluid level is at or near tap height.
- Swap valves to pump nitrogen
- Pump nitrogen at 700 scfm from hole level to top to displace gases. Estimated 350 scf (50 bbl equivalent) for 1 volume.
- Pump at least 15 volumes or until gases are evacuated. Verify using monitors.
- Follow with 80 quality flame retardant foam. Pump 0.25 bpm fluid, 300 scfm N<sub>2</sub>, and 3% foamer
- Pump enough until visual confirmation out the top of the pole.
- Shut down and bleed off any pressures.
- Rig up exothermic cutting rods (est. 5 rods per circumferential cut) and gas oxygen bottle rack.
- Cut poles near tapped hole level
- Pump fluid out of embedded pole section and fill embedded section of pole with concrete approximately five feet up from the bottom
- Cut off pole approximately three feet below grade and fill with soil
- Level site and Repeat on next pole.





## V. REFERENCES:

Currah, Mitch, and Cooper, Andy (2008), Transmission & Substation Design & Operation Symposium (TSDOS) -138kV Transmission Pole H<sub>2</sub>S Corrosion Remediation

Gundiler, Dr. Ibrahim (2005), New Mexico Water and Infrastructure Data System  
<http://octane.nmt.edu/waterquality/corrosion/H2S.htm>

CUDD Energy Services (2009), Power Transmission Pole Purge

REA BULLETIN 1751F-670 (1993), Outside Plant Corrosion Considerations

## Line Rating: It's all about the Temperature!

Ryan Bliss, P.E., S.E., M.ASCE

Transmission Engineering, Electrical Consultants, Inc., 660 W. 700 South, Woods Cross, Utah 84087; PH (801) 292-9954; FAX (801) 292-9177; email: Ryan.Bliss@ecislc.com

### Introduction

Line rating and uprating techniques have become very popular methods for evaluating and increasing the capacity of existing transmission lines. Highly accurate aerial LiDar surveys have enabled transmission engineers to precisely model wire attachment points and corresponding conductor sag. The utility industry has then used several methods of calculating, predicting and or measuring the conductor temperature and then calibrated it to the highly accurate survey data. The models of each transmission line are then used to evaluate the respective electrical capacity of each line and the results are used as a tool in determining the extent of uprating required. The line rating studies have resulted in many transmission uprating projects where significant capital has been invested to increase the electrical capacity in each line. The line rating and uprating processes have leveraged technology to maximize capital investments; however, how accurate are the results? Are the results conservative? Are they too conservative? What is the margin of error?

Is there a disconnect between the Operation's system models and Engineering's models used for Line Rating Analysis? Planning and Operations department typically use the Institute of Electrical and Electronic Engineers' (IEEE) Standard 738 calculation methods to predict operating temperatures on transmission lines per some set of operating criteria for a given season. This standard states in the introduction that "*because there is great diversity of weather conditions and operating circumstances for which conductor temperatures and/or thermal ratings must be calculated, the standard does not undertake to list actual temperature-current relationships for specific conductors or weather conditions.*" Is this standard applicable or helpful to Line Rating analysis?

This paper will explore many of the methods used in line rating analysis, focusing on the methods of determining the calibrating conductor temperature. A comparison of each method will include a brief methodology and an error analysis of maximum possible error and probably error, positive and negative.

The results of this comparative analysis will answer the questions of the importance of calibrating conductor temperature accuracy and the significance in line rating and uprating results. The inaccuracy of conductor temperature calibration can cause potential violations to be missed or can cause significant increase in project cost to achieve the same rating.

## Observations of Current Industry Practices

### *Ambient Temperature Method*

The simplest approach to calibrating the conductor temperature is using an ambient temperature that was measured and collected during the survey. At first glance, this appears to be a conservative method, because this should be the coldest theoretical temperature that the wire could be. There are a few questions that should be realized with this approach.

- I. Is calibrating with the coldest temperature always the most conservative?
- II. Where was this ambient temperature measured? (conductor elevation, under line, on some control point 5 ft off the ground shielded by trees)
- III. How conservative is this approach?

There are situations with multiple circuits on a single transmission line that the controlling condition of thermal ratings is the clearance to the other circuits on the transmission line. In this case and in the case of analyzing ratings to crossing circuits, using the coldest temperature is not being conservative and could be masking potential clearance deficiencies. Often the ambient temperature measurements that are recorded during a survey are five feet above the ground and surrounded by vegetation, near some control point used by the survey company that happens to be a significant distance from the transmission line. The ambient temperature is typically much cooler at the elevation of the conductors; also the wind can be dramatically different at the conductor as compared to the wind measured near the ground.

These errors can cause both non-conservative and over-conservative conductor temperature calibrations and therefore inaccurate thermal ratings, resulting in the possibility and probability of clearance violations not discovered or much more capital than is really needed to restore the transmission line's capacity rating. The errors of this approach get dramatically worse if the line is heavily loaded electrically during the survey. This data is good to tabulate and evaluate but this method is not recommended for conductor temperature calibration.

### *Predictive methods*

The need to calibrate conductor temperature with highly accurate aerial LiDar survey data has caused several predictive methods to be used in the attempt to be more accurate.

#### *I. IEEE*

The most common approach currently used to predict and calibrate the conductor temperature to the LiDar survey data is the use of IEEE Standard 738, calculations of steady state conductor temperature. There are many variables that make up these calculations, some of which are easy to collect and be very accurate, while others simply must be estimated with very little accuracy and can introduce significant error in calibration. One of the goals of

this study was to find the limits of potential error, which required in over 37 billion calculations to reach the following observations. The variations identified are the extreme limit of fluctuation, the actual amount of error in each case is expected to be less. The variables include:

- a. **Date & Time** – The date and time variables are easy input variables to be very accurate. The 2006 update to the IEEE Standard 738 added sensitivity to the equations to account for small incremental adjustments to the sun's angle to the wire and the resulting impact on the conductor. There is a period of time required to survey a transmission line, this time would introduce some error as many of the input variables could vary. The amount of this error is very difficult to predict and for the purposes of this paper will be assumed as minimal.
- b. **Atmosphere** – The atmosphere variable where there are only two options, either clear or industrial. The atmosphere variable does not consider all the variations of sky conditions between clear and cloudy that would typically exist during a survey. The variation of results from this input variable can be as much as 15 degrees F. and highest variation occurs on low electrical loads. Some error from this input variable is likely to be included in the results from the IEEE calculations.
- c. **Latitude & Elevation** – The latitude and elevation input variables are also easy to be very accurate as they relate to geospatial location of the transmission line under evaluation. Each transmission line is different and that would cause some variation in the input variables, but if either latitude or elevation caused significant variation in the results of the IEEE calculations, each section of line could use the average latitude and elevation of the corresponding section. The amount of this error is assumed minimal for the purposes of this paper.
- d. **Line Azimuth** – The azimuth of a transmission line is also an input variable that can be determined per section of line, although any type of running angles present in a section of line makes it difficult to determine since the azimuth varies. Once again minimal error is expected by small variations in an azimuth angle of a line; although, if the angle varies significantly, 15 to 20 degrees F. of variation occurs and it would be expected that some error would be included in the IEEE results for heavy and light loaded transmission lines.

**Wind Pressure** – The wind input variable is also a difficult variable to collect. Weather data is usually collected during the survey, but it is typically near a survey control point which could be some distance from the transmission line and the weather station is typically at an elevation near the ground and possibly shielded by surrounding vegetation. The transmission conductor on the other hand is typically 25 – 50 feet above the ground, where the expected wind would be

greater. The variation results between a 0 foot per second wind and an 8 foot per second wind vary from 50 degrees F. on lightly loaded lines to 380 degrees F. on heavily loaded lines, it is expected that significant error would be included in the IEEE results. The amount of error expected would also increase as the load on the transmission line increases.

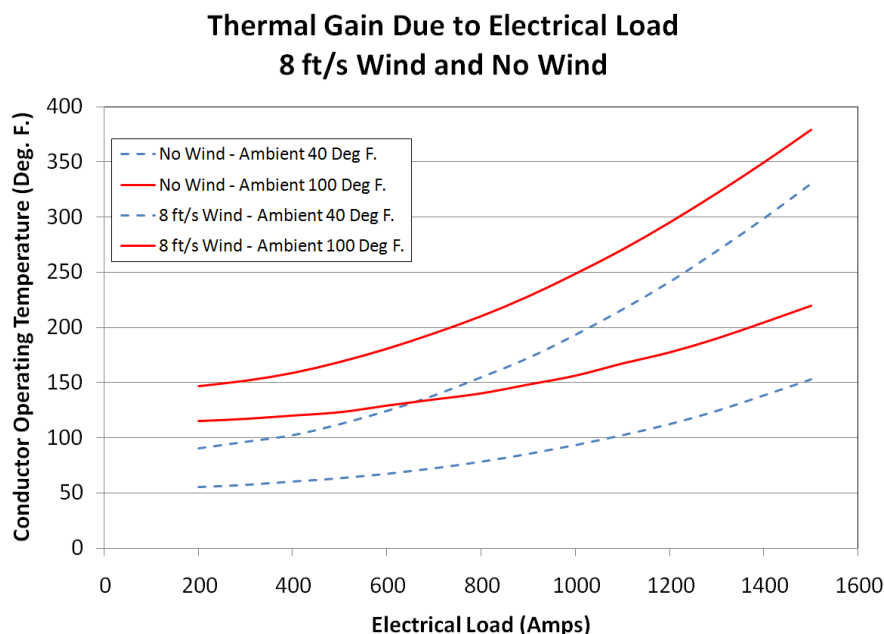


**Figure 1 - This graph shows the thermal gain comparison between a "No Wind" condition and an "8 ft/s Wind" condition.**

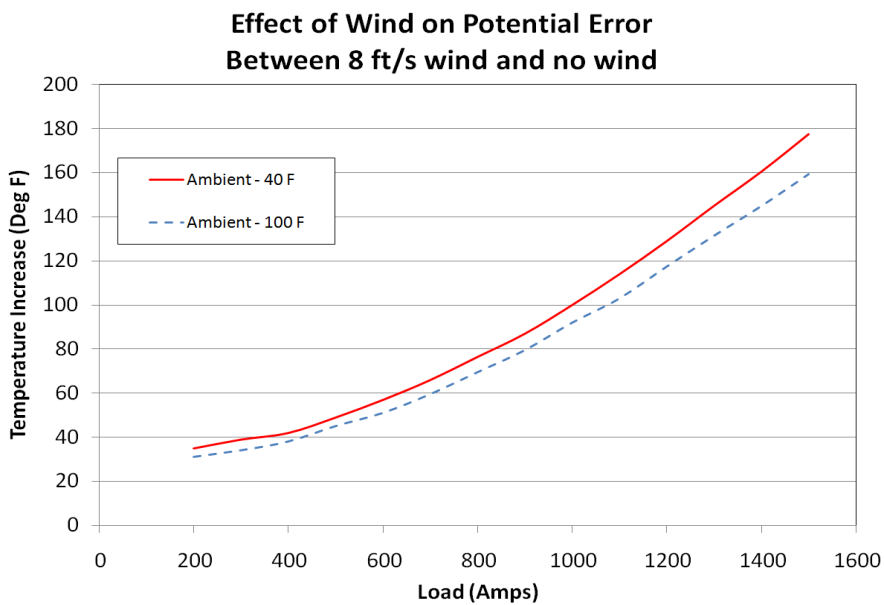


**Figure 2 - The difference between the curves in Figure 1 is represented this graph to show the potential error that could exist between the two wind pressure values of "No Wind" and "8 ft/s".**

- e. **Wind Conductor Angle** – The wind conductor angle is a very difficult input variable to determine, since wind direction is continually changing and the azimuth of each transmission line often changes frequently. The variation of results from the wind angle can vary from 20 degrees F at lightly loaded lines to 180 degrees F on heavily loaded lines, it is expected that significant error would be included in the IEEE results. It should also be mentioned that the IEEE equations can also completely break down under very light loaded conditions.

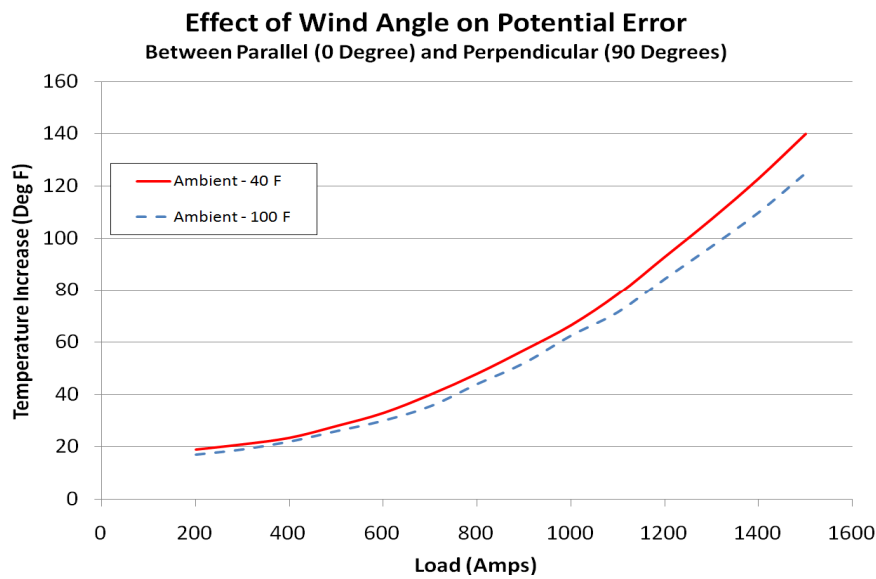


Figure 3 - Similar to the effect of Wind Pressure is the Wind Angle, this graph shows difference in thermal gain between a parallel wind and a perpendicular wind on the wire.

- f. **Electrical Load** – The electrical load is an input variable that is also very easy to be very accurate to collect and document from the system operators. The input variable of electrical load is the main cause of heat in transmission lines and the error of all other variables are impacted by the amount of electrical load. In operation logs it will be observed that the electrical load is not constant, therefore the greater the variation in the load the greater the potential error in IEEE calculations. IEEE calculations assume constant electrical flow.
- g. **Emissivity & Solar Absorption** - The emissivity and solar absorption input variables are also very difficult to determine and theoretically would vary on almost every conductor. Most utilities use set values used by their operations group in the line rating capacity criteria. The variation of results for emissivity varied from 15 degrees F. on a lightly loaded line to 400 degrees F. on a heavily loaded line. The amount of error is expected to be between 10 degrees F. for a lightly loaded line and 80 degrees F. for a heavily loaded line.

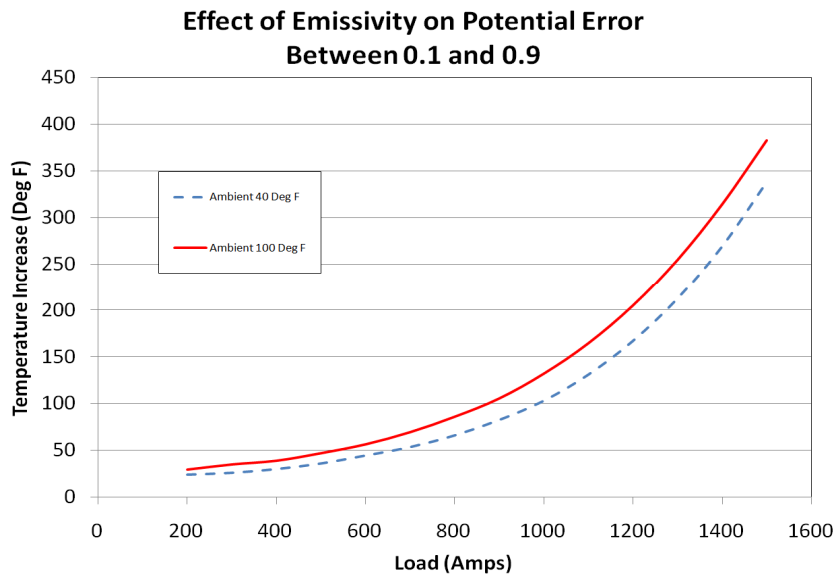


Figure 4 - This graph shows difference in thermal gain between the extreme values of Emissivity.

The variation results for solar absorption was much less and varied from 25 degrees F. on a lightly loaded line to 20 degrees F. on a heavily loaded line. The amount of error expected would be between 5 – 10 degrees F.

- h. **Conductor Thermal Coefficients** – The input variables associated with the thermal properties for each conductor type was assumed to be accurate for the purposes of this paper.

The IEEE calculations are also only mathematical models that have limited accuracy even with accurate input variables. After a review of all the input variables it is concluded that the IEEE calculations for conductor temperature will include significant error.

## II. Infrared

Infrared temperature sensors have over the last few years become effective at measuring relative surface temperatures and with calibrating the solar absorption and emissivity coefficients, absolute surface temperatures can be measured very accurately. The application of this technology is limited to relatively close distances so that there are several pixels of the sensor on the surface being measured; and when the background temperature is not drastically different than the desired surface. Although, this technology has

great application for finding hot spots in substations, transmission lines are typically too high to measure and the sky washes out the sensors ability to measure. The other difficulties would be to calibrate the solar absorption and emissivity coefficients which as discussed earlier can dramatically impact the predicted temperature.

### ***Direct Measurement method***

There are a few instruments that have been produced that can be mounted on a hotstick and safely measure the surface temperature of the conductor while energized or the resistance of the conductor, which then can produce the conductor temperature.

#### **I. Temperature Probe**

These instruments have proven to be accurate to less than one degree for the surface temperature of a conductor. There are three drawbacks for this method; first, instrument availability; second, utility operations practices for hotline clearances and third, there is an increase in cost to collect these measurements. The availability of these instruments has diminished due to lack of demand from the utility sector and therefore that are currently no known manufacture of a hotline temperature probe. Many utilities have adopted safety policies which prohibit any contact with a transmission line while circuit reclosures are in place therefore making it more difficult to get hotline clearances, especially on heavier loaded lines. Some utilities have reviewed the procedure of collecting a temperature reading and were able to get an exception to that type of policy and still collect temperature readings. The last concern of cost for the additional personnel, which is typically a very small percent of LiDar line rating project and easily offset by the value of the information collected, where the cost will be offset by the savings of being more accurate.

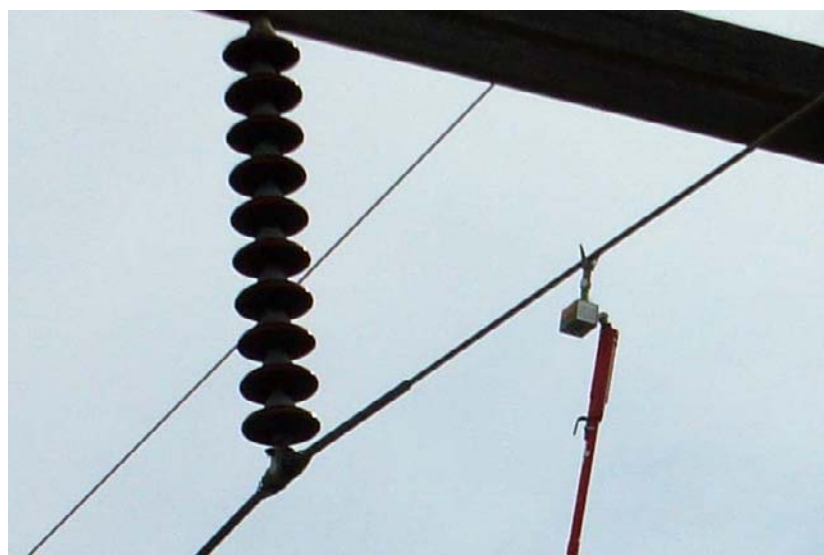


**Figure 5 - AB Chance Temperature Probe making direct energized conductor surface temperature measurement.**

## ***II. Resistance Measurements***

Temperature and resistance are directly related. If the temperature of the conductor increases, the resistance will also increase at the same rate. It does not matter if the line is heated by the sun or cooled by wind. The correlation between temperature and resistance is relatively linear for the temperature range for this application.

The temperature of ACSR can be different between the surface and the core of the conductor. The key temperature that determines sag is the cross-sectional temperature of the conductor. The resistance temperature correlation is this cross sectional temperature.

In 1996 SensorLink Corporation invented a process to measure current and micro-ohm resistance on high voltage lines. (Up to 500 kV) They integrated this process into a live-line meter called the Ohmstik. The primary application for this meter is evaluating the reliability of in-service connectors. By adding a longer probe to their present Ohmstik, reliable resistance readings can be collected for the purpose of determining the cross-sectional temperature of conductors.

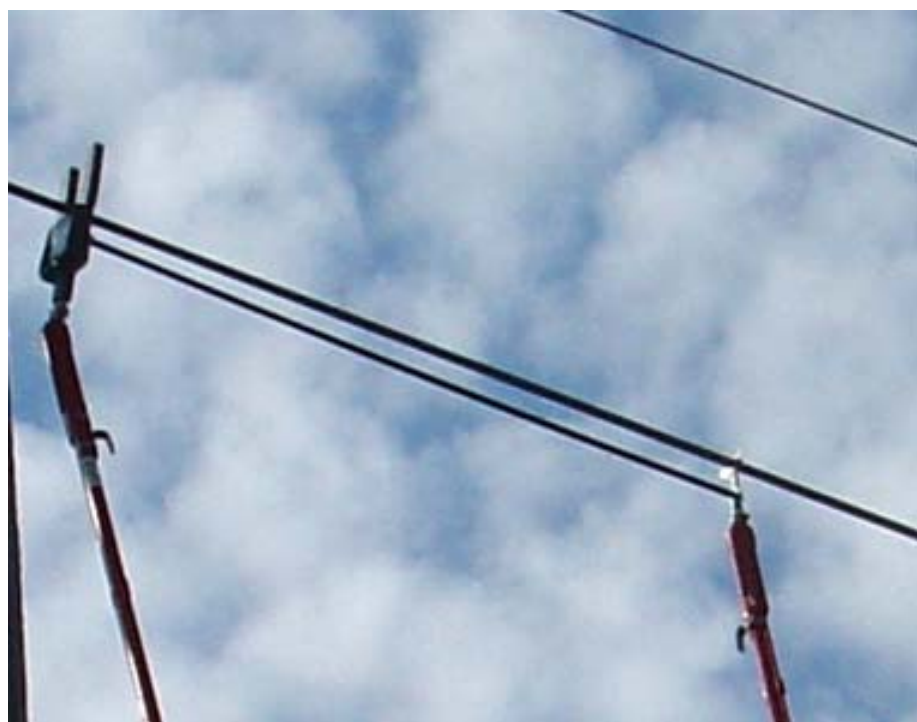


**Figure 6 - Sensorlink's Ohmstik modified to make resistance readings over five feet instead of one foot to increase the accuracy of the instrument.**

### Conclusions – Accuracy and Precision

Typically, very small increments of temperature can make significant variations of the uprating work recommended from a line rating analysis. It is clear that there is no single solution for determining conductor temperature; the direct methods achieve the accuracy of collecting real world values but have limited availability of instruments and difficulty in collecting measurements in each section of a line; while the predictive methods of determining conductor calibrating temperature have significant variations from input variables that cannot be determined accurately and will contain significant error. The resistance method shows great promise and currently could be used to get very accurate and precise calibrating temperatures. The ideal meter still needs to be developed, one that can be hung on the conductor prior to survey and log temperature, resistance, electrical load and weather data for a period of time when a survey could be completed.

The recommended line rating philosophy is to collect as much information as possible of both predictive and direct measurement techniques. Adding an error analysis to the IEEE calculation procedures would allow for the possible error limits to be identified for specific lines and compared to direct measurements, thus somewhat calibrating the IEEE calculations to real world direct measurements.

The issue of conductor temperature calibration is not an issue of being conservative, it is an issue of being accurate and precise. A more appropriate place to be conservative would be in the clearance criteria requirements used for line rating evaluation and in uprating design engineering. The IEEE calculations are valuable information to consider but should not be used blindly or by themselves. The input variables for the IEEE calculations are also not repeatable, therefore there is no precision. It is important to assemble as much information as possible for each section being rated; preferably some direct temperature readings to correlate and validate IEEE calculation conditions for some sections of data to determine accuracy and gain confidence in the calibrated conductor survey temperature. A philosophy of accuracy and precision ultimately will be the most cost effective on uprating projects and clearance compliant approach to line rating and uprating engineering.

### References:

IEEE Standard for Calculating the Current-Temperature of Bare Overhead Conductors (738-2006), IEEE Power Engineering Society, Transmission and Distribution Committee.

## Dynamic Wind Analyses of Transmission Line Structures

Ferawati Gani<sup>1</sup>, Frederic Legeron<sup>1</sup> and Mathieu Ashby<sup>1</sup>

<sup>1</sup>Industrial Research Chair of NSERC/Hydro-Québec TransÉnergie on Overhead Transmission Lines Structures, Department of Civil Engineering, Université de Sherbrooke, Quebec, Canada, J1K 2R1; email: ferawati.gani@usherbrooke.ca, frederic.legeron@usherbrooke.ca, mathieu.ashby@usherbrooke.ca

### ABSTRACT

Transmission line (TL) structures are generally designed with a simplified static-equivalent approach described in the industry documents (IEC 60826, CENELEC, ASCE 74). These static equivalent methods are based on extensive in-situ testing and have been shown to be appropriate for typical TL structures. However, wind loading is a dynamic loading, and for certain cases it is difficult to capture dynamic response of the structure by a static equivalent method. As well, static equivalent method has limitations and the industry documents do not give any directions to design structures out of their scope.

In this article, a set of numerical tools were used in order to assess wind-structure interaction for TL structures. At the present, the dynamic/turbulent wind loading data were numerically generated. The TL structures were modelled using finite element (FE) method that takes into account the inherent nonlinearities.

Two wind loading studies are presented here: (i) a guyed tower; and (ii) a river crossing. The guyed tower was studied to show that its dynamic behaviour can have significant impact on wind effect on the structure which cannot be captured by static equivalent method provided in the industry documents. The river crossing was studied to understand better the implications of applying wind loads extrapolated from the ones used for normal TL structures, as compared to dynamic wind loading. For each case, comparisons with results obtained with static equivalent method are presented and discussed.

### INTRODUCTION

Wind loading is one of the important types of loadings that need to be considered for transmission line (TL) structures design. Several industry documents exist and they have relatively similar approaches for wind loading analysis. These documents apply static-equivalent approach. For typical TL the wind loading described in IEC 60826 (2003) have shown to be satisfactory (Houle et al 1991). Other documents are used such as guide ASCE 74 and CENELEC standard which used similar method to calculate wind loading.

The main interest in the present study is the assessment of dynamic wind loading on TL structures that have a dynamic behaviour that can be different from the one evaluated in in-situ tests or for structures outside the scope of the industry documents. The focus of this study is to compare directly between the code static-

equivalent wind loading and direct dynamic analysis of TL structures under dynamic wind loading for two TL structures.

The first study concerns a guyed tower, which is more flexible than typical self-supporting towers and have a dynamic behaviour that cannot be captured easily by a static approach. The dynamic interaction between the cables (conductors, ground-wire and guyed cables) and the tower mast could greatly contribute to possible dynamic amplification under dynamic wind loading.

The second study deals with a river crossing, which have towers and cable spans with much greater dimensions than typical TL structures. Spatial variability under turbulent wind loading has more influence on the overall magnitude of wind loading applied to the structure.

## ANALYSIS PRINCIPALS

For the dynamic wind analysis of these TL, it is necessary to: (i) generate a whole wind field with the right spatial and temporal correlation to be applied on the TL; and (ii) model adequately the tower and conductors so the structural behaviour is accurately represented. The methods used for the wind generation and structural modelling are presented in this section.

**Transmission line finite elements model.** The FE models of the TL structures include geometrically non-linear static and transient-dynamic (TD) analyses. The cables (conductors, ground-wires and guy-cables) are modelled using tension only cable element with large displacement-small strain kinematics. For the damping consideration, aerodynamic damping is modelled in accordance with current practice (Gani & Légeron, 2008). The structural damping is assumed as 0.5%. When truss/lattice tower is modelled, in order to reduce the computational burden, the lattice tower mast was modelled as equivalent beam-column elements using equivalent plate-thickness theory (Meshmesh et al., 2006).

**Wind loading.** The wind forces were applied on a set of chosen points along the span and the tower. The complete application of these wind points on the FE model will be shown in the next sections. The static-equivalent wind loading is calculated in accordance with the current industry documents (e.g. IEC-60826, 2003; CENELEC EN-50341-1, 2000; ASCE Manual No.74 – Draft, 2005).

In a real structure, under a real wind, at a given time, the dynamic wind force on the conductor is varying along the span. The spatial correlation is important as it has considerable influence on the propagation of the conductor force along the conductor span. The dynamic wind forces are also varying along the tower height at a given time. Wind force on structures depends on the total wind speed  $U(z, t)$ , which is random in nature. The wind speed  $U(z, t)$  is divided into two parts, the mean wind part  $U(z)$  and the turbulent wind part  $u(z, t)$ .

For TD analysis, the turbulent wind part  $u(z, t)$  was generated numerically using the in-house program WindGen (Hang et al. 2005), based on spectral representation method as detailed in Deodatis (1996). Using this numerical approach,

the spatial and temporal correlations of the wind loading are taken into account. Verifications of the generated wind speed and the target spectra showed good agreement. An example of the auto-spectra verification is given in Figure 1. The generated wind speed was then incorporated into the FE model as a time-varying loading. Further details on the dynamic wind loading analysis were given in Gani & Légeron (2008). It is to be noted that if real measured wind data are available for the structure to be analysed, this real time wind record could also be incorporated to the FE model accordingly. However, due to the size of a real structure it is unpractical to record real wind data for the analysis.

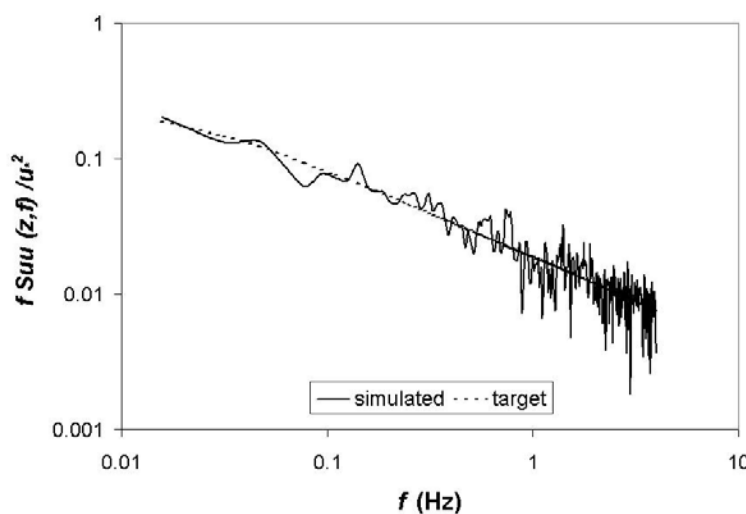


**Figure 1 Auto-spectrum of wind applied at mid-height of tower mast ( $U(10) = 35\text{m/s}$ )**

## GUYED TOWER WIND STUDY

Guyed tower is a competitive option to support high-voltage (HV) transmission line (TL) structure. They are about 50% lighter than conventional lattice self-supporting towers, easy to install, allow pre-assembly, and the foundation is simple to design and construct.

Since guyed towers are more flexible and have a different structural system than typical self-supporting towers, their dynamic behaviour can be different from self supporting towers. In IEC-60826 (2003) code, the wind loading coefficients were developed for self-supporting towers. It is therefore questionable whether these coefficients could be applied directly for guyed towers and other flexible types of supports.

Previous numerical studies on guyed tower for TL structures were focused on the galloping phenomenon (Tsui, 1978; Mathur et al., 1987). More recent works on the dynamic wind-loading for TL structures, such as the study by Yasui et al. (1999) and Battista et al. (2003) did not involve flexible type towers such as guyed tower. Studies on dynamic wind loading on guyed towers were mostly aimed for the communication tower type (Sparling & Davenport, 1998).

**Description of the structure and wind loading.** A single mast guyed lattice tower (suspension type) with four guy cables and a pinned base connection was chosen (Figure 2 &Figure 3). The guy cable configuration is as such that torsion effect is minimized and possibility of large moment due to unbalanced longitudinal load is reduced. The tower geometry is adapted from the guyed tower for 450kV DC used in study by Oakes (1971). To reduce the computation burden, the truss tower masts were simplified to equivalent beam-column pole model. Details of the tower modelling used in this study are given in Gani & Légeron (2008). Figure 2 shows the calibration between the full truss model and the simplified model.

To evaluate different dynamic guyed tower response, two guyed towers were analysed (see Figure 3): a two-phase tower that would be used for a direct-current (DC) line with both conductor arms located above the guy-cable attachment point; and a three-phase tower that would be used for an alternating current (AC) line with two conductor arms located below and one conductor arm located above the guy-cable attachment point. The tower height is 52.18 m, the height of guy cable attachment point on the tower mast is 38.04 m and the conductor and ground wire span length is 480 m.

A total of four loading cases, with and without ice, were studied. For brevity, only two cases will be detailed here. The two phase guyed tower with mean wind  $U(10) = 35 \text{ m/s}$  normal to the line (*Case 2P90w*) and the three phase guyed tower with the same wind condition (*Case 3P90w*) will be discussed here. Wind points applications were as shown in Figure 4. The terrain type is B in which the roughness characteristics are categorized as open country with very few obstacles (IEC-60826 2003) with roughness length  $z_0 = 0.05 \text{ m}$ . For comparison with static-equivalent of IEC-60826 (2003), the TD analysis used 10 wind record samples of ten minutes each. The TD results detailed herein are the mean of maximum of the available samples.

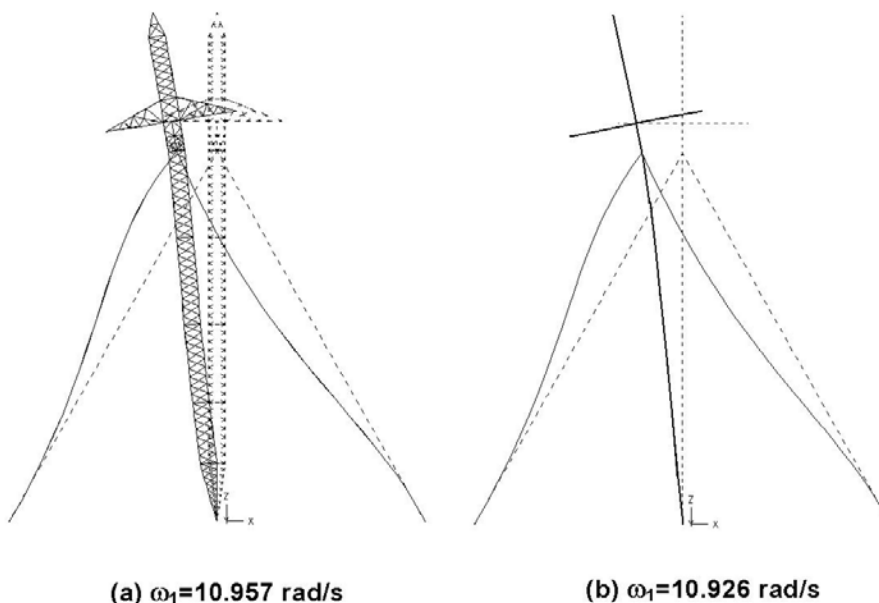


**Figure 2. Equivalent model verification of first transversal mode: (a) truss model; (b) beam-column model**

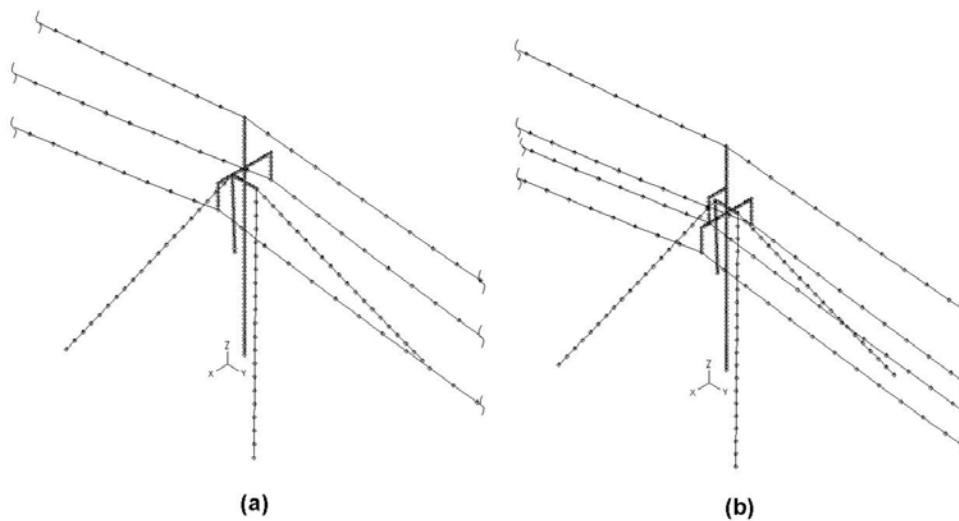


**Figure 3. FE model outline: (a) two-phase guyed tower; (b) three-phase guyed tower**

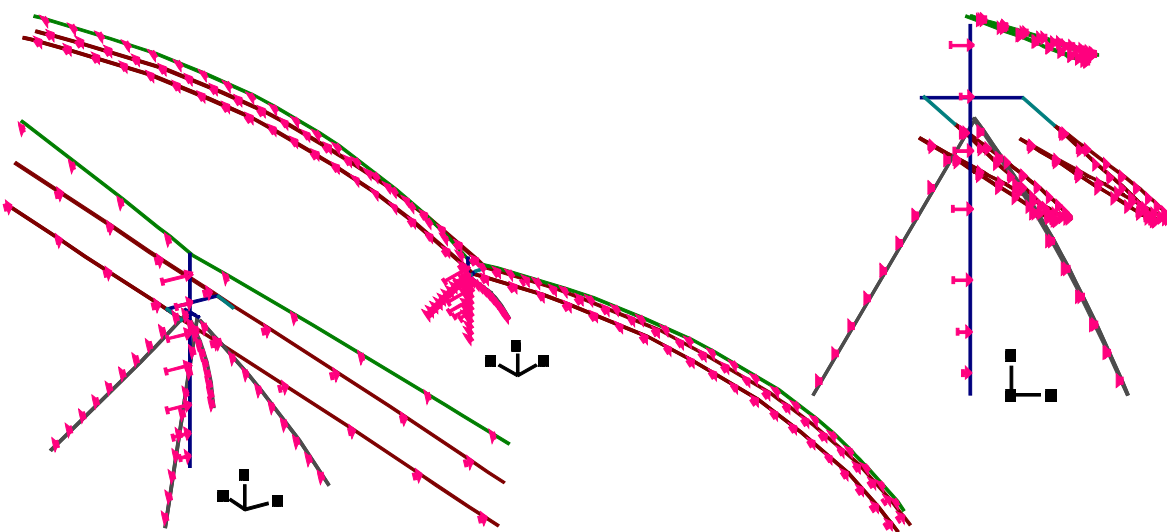


**Figure 4. Two-span FE model with the applied wind loading points**

**Difference between static-equivalent and nonlinear dynamic analyses.** Table 1 summarized some of the results for this study. For the cable response, in terms of cable tension, the differences between the two methods are relatively small. This highlights the fact that the overall wind loading magnitude along the cable spans for the static and dynamic analyses are relatively comparable. However, looking at the structural responses of the tower mast, it could be observed that the static method

tend to result in lower response than the dynamic method on locations that could be considered critical for the structural design on the tower mast.

Therefore, it can be concluded that dynamic effects due to wind loading for guyed tower type supports is not fully taken into account in the static-equivalent method provided in IEC-60826 (2003). Considering the complexity of the transient dynamic analyses performed in this study, it would be of interest to find a simpler way that bridges the gap between the two methods and includes the dynamic effects of guyed towers.

**Table 1. Summary of results for guyed tower wind study: Static-equivalent vs. TD analyses**

<b>Parameters</b>	<b>Case 2P90w</b>		<b>Case 3P90w</b>	
	<b>IEC-60826</b>	<b>TD</b>	<b>IEC-60826</b>	<b>TD</b>
Tower transversal reaction (kN)	3.96	11.75	14.49	18.29
Average conductor tension (kN)	48.92	45.95	34.39	33.59

**Contribution of TL components to overall tower mast response.** Turbulent wind loading, depending on the location of the transferred loading along the mast, could cause positive bending moment (in the central part of the mast) and negative bending moment (in the top part of the tower). If a simple summation such as the static-equivalent method is utilized, the influence of this opposite sign bending moment will cancel one another. However, in reality, the possible maximum loading on each different TL component will less likely occur at the same time, as the frequency of conductor and tower are very different. Hence, it is possible that the turbulent wind will cause all positive moment or vice-versa or at least it could add partially.

**Comparison of the three methods evaluated.** For final comparison, all the results of the transversal bending moment of the tower mast, shown in Figure 5 (a) and (b) were evaluated. In the present study, a simplified dynamic method, based on SRSS principle, was proposed (see Gani & Légeron (2008) for more details), in which the basic wind loading coefficients are taken from IEC-60826 (2003) code. In general, good match and practically similar results could be observed for mean of maximum of TD and SRSS method in *Case 2P90w, 3P90w*. Both TD and SRSS methods resulted in higher value if compared to static-IEC for the lower part of the tower mast: below  $z \approx 30$  m for both cases. At points where the moments sign change, the static-IEC and SRSS are always within the limit of mean of maximum  $\pm$  standard deviation from TD samples.

Based on the comparison of the three methods for the loading cases, it can be concluded that depending on the guyed tower configuration, the possible dynamic loading caused by the turbulent wind part could be important to the overall transversal bending moment of the tower mast. The simplified dynamic approach by

SRSS could predict relatively well the TD response, except for the area near the guyable attachment point in *Case 2P90w*, *Case 3P90w* where the static-equivalent approach provides good results.

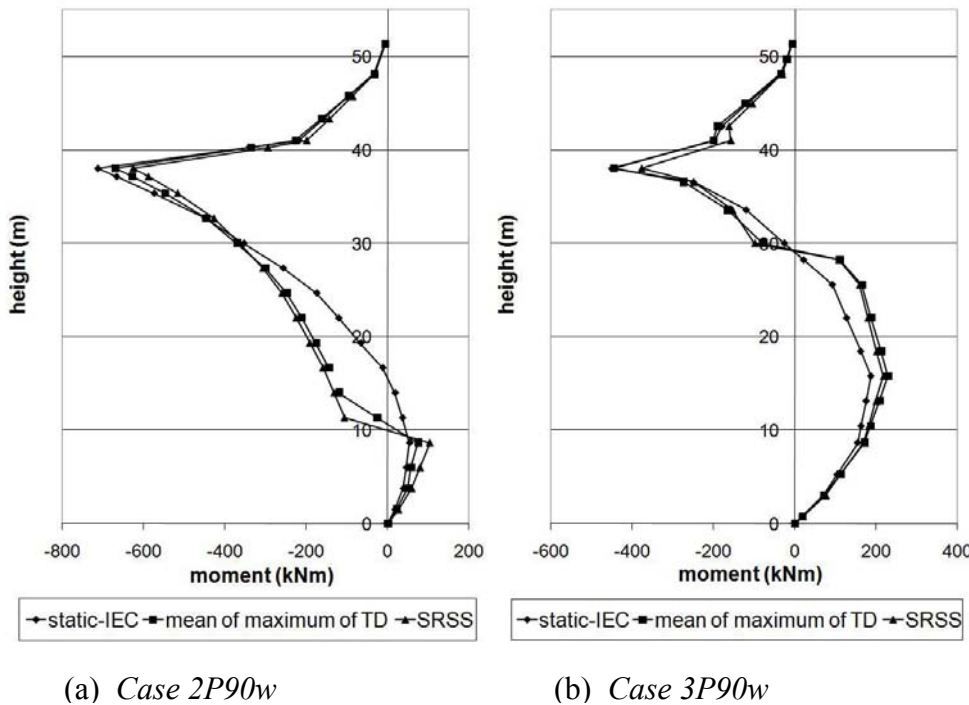


**Figure 5. Transversal bending moment: (a) Case 2P90w; (b) Case 3P90w**

## RIVER CROSSING WIND STUDY

River crossings generally consist of long-span conductors that are usually outside the range of span and height considered in transmission line industry documents. As defined in CIGRÉ SCB2.08 (2009), river crossings or large overhead line crossings, are TL structures with spans larger than 1000 m and/or with tower heights larger than 100 m. In IEC 60826, the limitation for normal span range is between 200 and 800 m and height of tower is up to 60 m. In this standard, for span over 800 m and height above 60 m, the criteria given there, could still be used, but the validity of the approach could be questioned. This is due to the fact that the spatial correlation for very long-span conductor (limitation of gust widths) is generally not taken completely into account in the current industry documents.

Comparison between the wind loading defined in the industry documents and the one actually encountered in the field has been a continuous effort for transmission line designers (Houle et al., 1991). Their study were based on normal range of conductor span (max span tested was 457 m), with wind speed up to 30 m/s in terms of gust velocity at the conductor level, for terrain with very few obstacles, typical for normal transmission lines. Over the years, with the continuous improvement, it has

been well accepted that the requirements given in the industry documents are providing relatively good agreement for wind loading of conductor within the normal span range. For overhead line crossing, recent study by Paluch et al. (2007), which was based on field observations, did not include comparison with the requirements from the code utilized in that study.

**Description of the river crossing.** This study was focused on a typical overhead transmission line crossing. The maximum span of this river crossing is 1100 m and the maximum height of the tower is 145 m (Ghannoum et al., 1990). It is composed of 3 suspension towers and 2 dead-end towers. The two-phase transmission line is spaced out by 26 m and it carries two conductors and one ground wire per phase. The conductors are attached to the towers by 4 insulator chains. For an overview of the overhead-line crossing, see Figure 6. For this study, only the insulator strings and the main spans of the conductors were modelled.

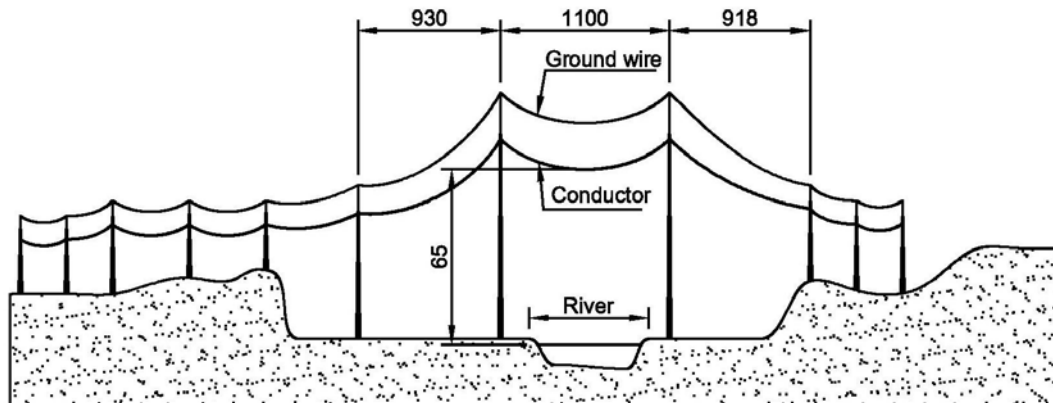


Figure 6. Schema of the overhead line crossing studied

**Comparison with the current industry documents.** Before pursuing the wind loading analysis on the river crossing, a benchmark study was done using normal three-span conductors (380 m - 450 m - 380 m). While for the river crossing, the three-span conductors consists of 930 m - 1100 m - 917.6 m, respectively. The summary of results is given in Table 2. From the results obtained, it could be seen that for the benchmark, the transmission line industry documents IEC-60826 and CENELEC EN-50341 are comparable to dynamic analysis, with less than 8% difference. The code ASCE Manual 74 underestimated the wind loading by as much as 20% if compared to the other documents and the dynamic analysis result. For the river crossing three-span conductors, it could be observed that this time the difference for transversal force between the dynamic results and the ones from the documents is more pronounced, by up to 18% if compared to CENELEC. Hence, it has been highlighted that for the river crossing, the percentage of difference between the industry documents and the dynamic analysis is relatively higher than for the normal span range from the benchmark study. To illustrate that the industry documents

provide relatively higher wind loading, Figure 7 shows a sample of 10 minutes time history of the transversal forces obtained from dynamic analysis versus the values obtained from these documents.

**Table 2. Forces transmitted to the tower**

Model	Force (kN)	IEC	ASCE	CENELEC	NL Dynamic
Benchmark	Transversal	43.47	34.41	44.77	41.35
River-crossing	Transversal	228.9	223.00	249.00	210.71

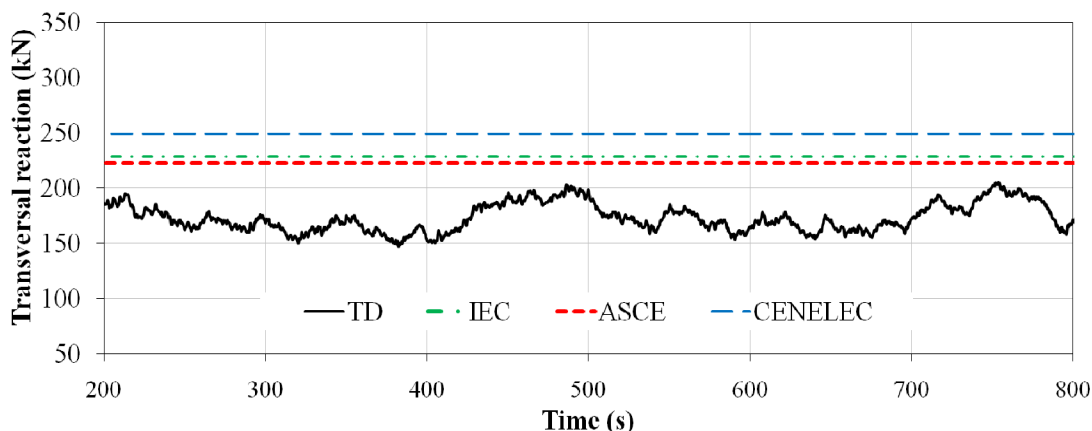


**Figure 7. Time-history of transversal force for one sample of 10 minutes**

**Along the wind correlation.** In real wind, correlation between along-wind turbulent component exists. This correlation, defined by the decay coefficient in the along-wind direction,  $C_x$ , is more important for wind over water than on land. For normal transmission lines, constructed on land, where the decay coefficient,  $C_x = 6$ , it could be justified that the parallel-phased conductors would mostly act in a synchronized manner. Nonetheless, for river crossing, built over water, where the decay coefficient is lower,  $C_x = 3$  (Simiu & Scanlan, 1996), the interaction between parallel phases under wind loading could be more important than expected. In order to accommodate the conductor wind and ice/wind motions as a result of the larger sags, the overhead line crossing towers usually have longer conductor arms, if compared to ordinary transmission line towers. However, the current industry documents do not explicitly include this type of correlation for the wind loading calculation. In addition to this, the consideration of along the wind correlation would also mean a lower wind loading than if it is not considered. Therefore, it would be of interest to evaluate the importance of this correlation for typical river crossing.

To understand better the influence of along the wind correlation for parallel-phased conductors, the middle main span (1100 m) of the river crossing was modelled, three different conductor spacing were studied: i) 10 m spacing that represents ordinary transmission line spacing; ii) 25 m spacing, representing the spacing for the evaluated overhead line crossing; and iii) 50 m spacing, which could represent parallel spacing from a portal type tower.

The results that will be highlighted here, as summarized in Table 3, is the maximum value of transversal force transmitted to the tower, force differences between the conductor cross arm and the possible torsion of the tower mast due to the difference in longitudinal forces (occurred due to difference of the time varying wind loading along the span). From this table, it could be concluded that larger spacing resulted in slightly lower total transversal force due to the wind. Nonetheless, for the possible overall torsion, larger spacing is more likely to induce larger torque in the tower.

**Table 3. Maximum values of forces & possible torsion**

Conductor spacing (m)	Total transversal (kN)	Force difference (kN)			Torsion (kNm)
		Transversal	Longitudinal	Vertical	
10	204.67	5.01	16.52	2.80	82.60
25	196.61	6.86	23.26	4.19	290.75
50	192.00	9.73	35.16	5.74	879.00

## CONCLUSION

The present study has shown the versatilities of dynamic analyses for TL structures. Each structure presented here pointed out different aspects of the necessity for more complete dynamic analyses.

For the guyed tower study, depending on the tower configuration and the type of climatic loading, the dynamic effect could have a large influence in the overall response of the tower mast under wind loading. Therefore, the application of static-equivalent method, which is an algebraic summation of mean wind effect and turbulent wind effect, does not always provide a conservative estimate of the possible dynamic response.

While in the study of the river crossing, a more complete consideration of the spatial correlation resulted in lower wind loading than the ones obtained from the industry documents. Also, the necessity to reconsider the current practice for large parallel spacing for the tower cross-arms was highlighted.

Overall, the present study is a first step towards a more reliable and economical design for overhead line crossings where the conductor spans are longer than what are covered in the current transmission line industry documents. Further study that involves comprehensive field measurement of the wind loading on site specific terrain or river crossing would be interesting in order to validate the numerical approach proposed here.

## ACKNOWLEDGEMENT

This study was carried out as part of the research projects of the Natural Sciences and Engineering Research Council of Canada (NSERC)/Hydro-Québec Trans-Énergie (HQTÉ) Industrial Research Chair on Overhead Transmission Line Structures at Université de Sherbrooke, Quebec. The financial support provided by NSERC and HQTÉ is well appreciated.

## REFERENCES

- ADINA R&D Inc. (2004). *Automatic Dynamic Incremental Nonlinear Analysis (ADINA)*. ADINA R&D Inc.
- ASCE Manual No.74 – Draft (2005). *Guidelines for electrical transmission line structural loading*, American Society of Civil Engineers, USA.
- Battista, R.C., Rodrigues, R.S. and Pfeil, M.S. 2003. "Dynamic behavior and stability of transmission line towers under wind forces". *Journal of Wind Engineering and Industrial Aerodynamics*, 91, 1051-1067.
- CAN-CSA-S37.01 2001. *Antennas, towers and antenna supporting structures*. Canadian Standard Association.
- CENELEC EN-50341-1 (2000). *Overhead electrical lines exceeding AC 45 kV*, European Committee for Electrotechnical Standardization.
- CIGRÉ SCB2.08, (2009). Large overhead line crossings. CIGRE. Technical brochure to be published by CIGRÉ.
- Deodatis, G. (1996). "Simulation of ergodic multivariate stochastic processes", *Journal of Engineering Mechanics*, 122(8), 778-787.
- Gani, F. and Légeron, F. (2008), "Dynamic wind loading analysis of transmission lines with guyed towers", submitted to *Canadian Journal of Civil Engineering*.
- Ghannoum, E., Bell, N., Binette, L., Ouellet, P. , Manoukian, B. (1990). "Use of reliability techniques in the design of Hydro-Quebec's 1100 km Radisson-Nicolet-des-Cantons ±450kV HVDC line", *Proceedings of the 1994 35th International Conference on Large High Voltage Electric Systems: Part 1*, Paris, France, no. 22-201 (7p).
- Hang, S., Gani, F. and Légeron, F. (2005). *Générateur de vent appliqué au génie civil: WindGen*, Manuel du logiciel, Université de Sherbrooke.
- Houle, S., Hardy, C. and Ghannoum, E. (1991),"Static and dynamic testing of transmission lines subjected to real wind conditions", *CIGRE Symposium: Compacting Overhead Transmission Lines*, Leningrad, USSR, Paris, France, no. 200-02 (6p).
- IEC-60826 (2003). *International Standard: Design criteria of overhead transmission lines*, International Electrotechnical Commission.
- Mathur, R.K., Shah, A.H., Trainor, P.G.S. and Popplewell, N. (1987). "Dynamics of a guyed transmission tower system". *IEEE Transactions on Power Delivery*, 2(3), 908-916.
- Meshmesh, H., Sennah, K. and Kennedy, J.B. (2006). "Simple method for static and dynamic analyses of guyed towers". *Structural Engineering and Mechanics*, 23(6), 635-649.
- Oakes, D.L.T. (1971). "Nelson River HVDC transmission line towers". In *Proceedings of the Manitoba Power Conference EHV-DC*, Winnipeg, Manitoba, Canada, 7-10 June 1971, 441-458.
- Paluch, M.J., Cappellari, T.T.O. and Riera, J.D. (2007). "Experimental and numerical assessment of EPS wind action on long span transmission line conductors", *Journal of Wind Engineering and Industrial Aerodynamics*, 95, 473-492.

- Simiu, E. and Scanlan, R. (1996) *Wind Effects on Structures*, 3<sup>rd</sup> Edition. John Wiley & Sons Inc.
- Sparling, B.F. and Davenport, A.G. (1998). "Three dimensional dynamic response of guyed towers to wind turbulence". *Canadian Journal of Civil Engineering*, 25, 512-525.
- Tsui, Y.T. (1978). "Dynamic behavior of a pylône à chaînette line: Part I Theoretical studies". *Electric Power Systems Research*, 1, 305-314.
- Yasui, H., Marukawa, H., Momomura, Y. and Ohkuma, T. (1999). "Analytical study on wind-induced vibration of power transmission towers". *Journal of Wind Engineering and Industrial Aerodynamics*, 83, 431-441.

## Temporary Support of Lattice Steel Transmission Towers

Scott Monroe P.E.<sup>1</sup>, Rodger Calvert P.E.<sup>2</sup> and John D. Kile<sup>3</sup>

<sup>1</sup>Osmose Utilities Services, Department of Transmission and Underground, 215 Greencastle Rd. Tyrone, GA 30290-2944; PH (662) 694-9251; FAX (678)-364-0844; email: jkile @osmose.com

<sup>2</sup>Mesa and Associates, Inc., Engineering, 9238 Madison Blvd # 116 Madison, AL 35758; PH (256) 258-2100; email: rcalvert@mesainc.com

<sup>3</sup>Osmose Utilities Services, Manager- Department of Transmission and Underground, 215 Greencastle Rd. Tyrone, GA 30290-2944; PH (770) 632-6715; FAX (678)-364-0844; email: jkile @osmose.com

### ABSTRACT

Lattice steel transmission towers have been used to support transmission lines over the past 120 years. Many events have been known to damage these towers to an extent to which they must be repaired structurally. These events include but are not limited to vehicle impacts, agricultural equipment damage, corrosion damage, vandalism, and initial fabrication / construction errors. It has been the standard practice of transmission utilities in the past to produce the steel detail drawings in house, and either have their own line maintenance crews make the steel changeout or to have an electrical contractor perform the work. Most often, the responsible engineer at the utility will specify a load that must be supported during the work.

There is an old wives tale prevalent among electrical contractors that the towers are “designed” to stand on three legs. This no doubt comes from the fact that many of the foreman and supervisors in the industry have personally seen the towers stand with one leg removed. In fact, many tangent and light angle towers will stand with one leg disconnected with no temporary support. However, with the many combinations of tangent, light angle, heavy angle, and dead end configurations, wire tensions, and construction / design practices, it is imperative to communicate that a general “blanket” statement that the towers will stand on three legs not true. In fact, allowing this blanket statement to be used in the industry is incorrect.

It is the purpose of this paper to discuss the correct procedure(s) for temporary support of towers and outline the correct safety factors that are given by OSHA, ASME, and the governing utility. The focus will be on cranes supporting towers and the applicable safety factors. Additionally, alternative temporary support options shall be discussed.

### Temporary Loading and Applicable Safety Factors

Repairing or replacing of tower members, including the repair of below ground steel grillage members, will not take place during extreme weather events such as icing or high wind. Therefore, guidelines needed to be established to instruct construction personnel when these repairs can be made. The chances of no wind being present during construction is very low so a maximum wind speed needed to be determined as a limit when these repairs should be made. This maximum wind speed will be used to determine reactions in the tower that will be provided to construction personnel as a load that must be safely supported during repair work.

This maximum wind speed limit was discussed with utilities as well as construction personnel and determined that 20 mph of wind (equal to approximately 1 psf of pressure) would be sufficient to accomplish the required work and also give reactions that could be safely supported by a crane. Because many utilities use a safety factor of 2 during construction work, this safety factor would be used. A drawing issued for repair work indicates no work will be performed should the wind increase over 20 mph.

An example of this drawing is shown below:

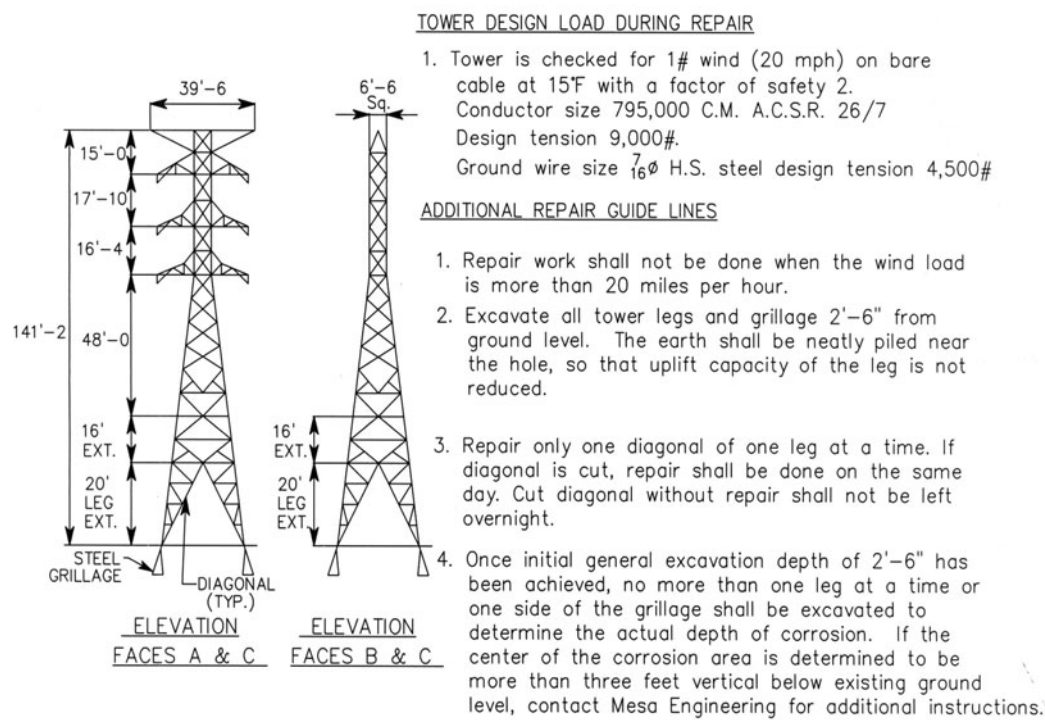


Figure 1 Typical Tower Design Loads and Repair Guidelines

**Temporary loads should be calculated for the following condition:**

- 20 mph wind (1 psf) on wire and tower with a safety factor of 2

The following loads should be combined to determine the post leg reactions:

1. Wind on wire
2. Wind on tower
3. The line angle load based on wire tension at 1psf wind
4. Weight of tower
5. Weight of wire

All loads listed above will have a safety factor of 2 applied.

Because similar repairs are often made on many towers of the same type, the maximum wind span, weight span, and line angle are often used for these load calculations.

Angle towers and dead end towers will most likely produce higher loads than tangent towers. Because dead end towers often have unbalanced tensions producing longitudinal loads, these towers should be evaluated on an individual basis.

### **Methods of Measuring Wind Speeds**

As stated above, the repair work should not be started if the wind speed is above 20 mph. Construction personnel must check this wind speed before beginning work. There are several ways of determining wind speed at the tower site. One way is simply by observing the wind, calm days and days having high wind are easily determined. The Beaufort wind scale can be used when simple observations are accurate enough. On days when the wind speed is in question, local weather reports from the weather channel website or a pocket anemometer can be used. This device is inexpensive, simple to use, and will measure maximum wind speed as well as average wind speed.

### **Calculation of Reaction Loads**

#### **PLS TOWER With Overload Factors**

Once all wire loads are calculated with the appropriate overload factors, the next step is to model the tower in PLS-TOWER. This model is very useful when completed. The model will give reactions in all members as well as the reactions at the base of the tower. These reactions at the base of the tower are provided to construction personnel to size the crane. Members can be easily removed to determine the structural stability of the tower without these members. Vertical load from tower weight is automatically calculated in PLS-TOWER based on a safety factor of 2 input by the user.

#### **Effect of Disconnecting Single Members and Multiple Members**

Tower members are designed to carry tension and compression loads only. The detailing of tower member joints takes special care to avoid inducing bending in these members. The removal of any tower member may create bending stress in the adjacent remaining members. Often times the remaining members can safely carry the additional forces caused by removing a member. The PLS-TOWER model is very useful for removing members and checking the structural stability of the tower. Removal of multiple members should be avoided if possible. This type of removal may induce bending stress in the adjacent members, which the members are not designed to carry. When multiple members are to be replaced, the best practice is to replace one at a time. Replacement of tension members such as the diagonal at the bottom of the tower can be achieved with the addition of a come-a-long where the member is located before it is removed. Member removal for this type of repair work requires checking by a qualified individual experienced with this type of repair. Remember, tower members are under stress and construction personnel will need to use extreme caution while making repairs.

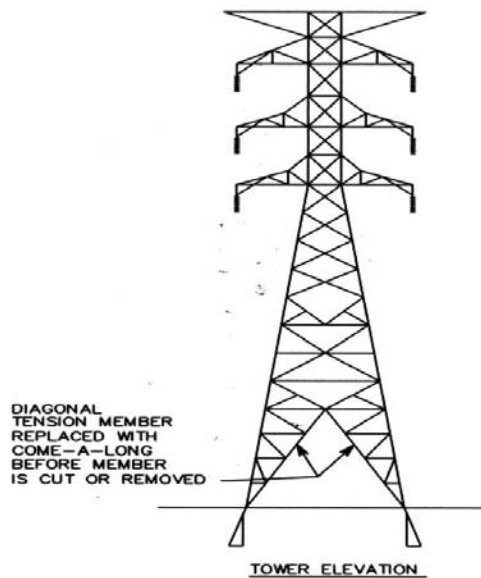


**Figure 2 Members to Be Temporarily Disconnected**

### **Types of Temporary Support**

#### Crane Support

Crane Support of transmission towers is the most commonly used and accepted practice today. The work is usually done under caution order with the line hot. This is because it is not possible or convenient to schedule outages for this type of work. The work then

becomes inefficient. It is important to note that sometimes clearances may dictate the radius of the crane, as minimum clearances to high voltage lines must be maintained. ASME 30.5 shows minimum required clearances to energized lines of various normal voltages for cranes.

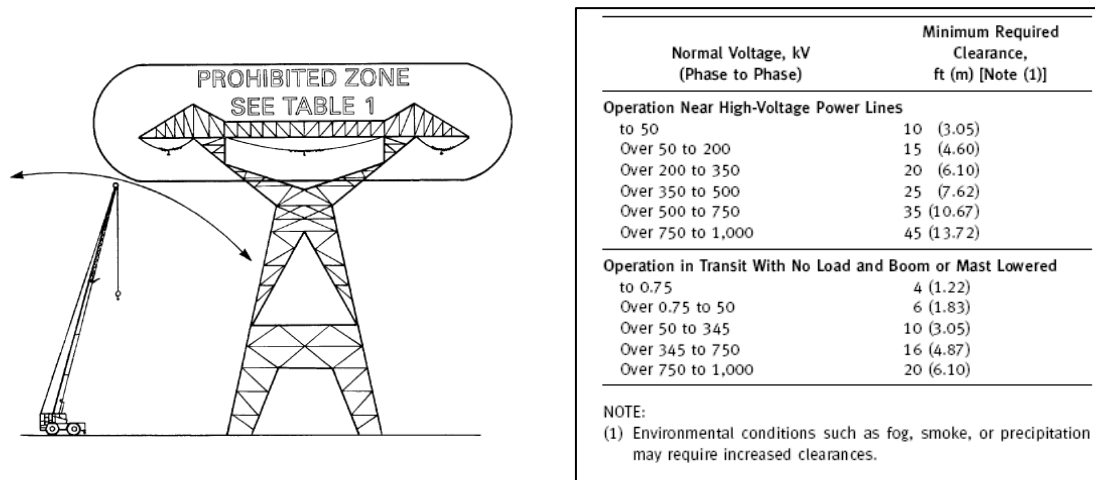
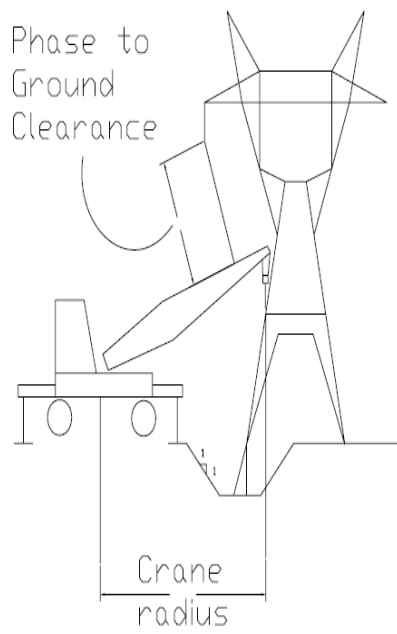


**Figure 3 Required Clearance Illustration   Table 1 Required Clearance Distances**

OSHA also gives required clearance values for high voltage lines in section 1926.550(a)(15)(i). These values calculate to be the same as in Table 1.



The first step in crane support of a transmission tower after determining the reaction load is the crane radius required for construction. This is necessary to calculate very early in the process due to the fact, that the crane must be sized for a particular load and radius. This is a source of error for many construction crews that assume that an 80 ton crane, for instance, is good for 80 tons. This is certainly not the case at a 40 ft. radius which is typical with this work. OSHA excavations must be considered, as this will dictate the radius that the crane will have to be placed away from the tower leg. Note that the radius is measured from the center pin of the crane to the attachment point on the diaphragm joint. The measurement is often taken to the post leg which is incorrect.

**Figure 4 Crane Radius**

The next step after determining the correct crane radius is to determine the crane size. This is not as simple as it may seem. Let us investigate what OSHA regulations say about sizing the crane.

### **1926.550(a)(1)**

The employer shall comply with the manufacturer's specifications and limitations applicable to the operation of any and all cranes and derricks. Where manufacturer's specifications are not available, the limitations assigned to the equipment shall be based on the determinations of a qualified engineer competent in this field and such determinations will be appropriately documented and recorded. Attachments used with cranes shall not exceed the capacity, rating, or scope recommended by the manufacturer.

Also referring to ASME 30.5:

Type of Crane Mounting	Maximum Load Ratings %
Crawler or Wheel Mounted – outriggers set	85
Crawler or Wheel Mounted – w/o outriggers set	75

This specification only allows 85 % (for outriggers fully extended and set) of the ultimate capacity of the crane to be published in the manufacturers' load charts. The specification requires a 25 % reduction for cranes without outriggers fully extended and set. This reduction is already taken into account in crane manufacturers load tables.

Assuming outriggers to be fully extended and set for most utility cranes, this translates into a safety factor

$$\text{F.S.} = 1/.85 = 1.18$$

However, the reaction load calculated on the tower is a dynamic load (due to variable wind loading). A minimum factor of safety of 2.0 is recommended. Ultimate capacity = F.S. x S.W.L.

This is in line with most utilities safety standards. Therefore, a factor must be applied to the safe working loads of the tower reaction to have a factor of safety of 2.0 on the crane capacity.

Correction Factor =  $1 / (1.18 / 2.0) = 1.7$  (use instead of 2.0 for sizing the crane because a 15% strength reduction is already used in the crane chart). It is the purpose of this factor to translate a static load factor into a dynamic load factor. This factor can be used by field personnel to multiply the working loads in order to use the manufacturers' load tables directly.

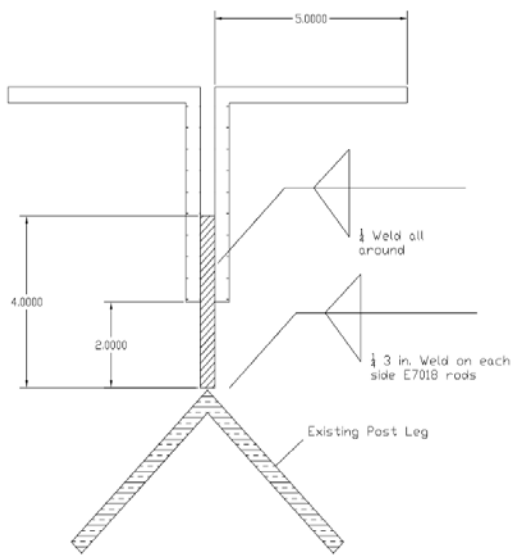
Note that this results in a crane that has 44 % more capacity than if the minimum OSHA / ASME factors are used.

ASME 5-1.11 States that for cranes used for non-lifting purposes the load ratings shall be established by a qualified person. This qualified person, either from the utility or contractor, must understand the load factors or apply them correctly. Many times, there are only a limited number of crane sizes available. A crane can always be chosen that far exceeds the capacities specified here. In many cases, availability will dictate if this is the case.

Many times, a factored load with an overload factor already applied is given by the responsible engineer or utility. It is important to know what overload factor was used so as not to apply more than one load factor to the safe working load (SWL).

### Welded Support

It has been found to repair localized damage to towers, a temporary support can be welded to the tower member spanning the damaged area, the damaged area removed and butt spliced, and then removed.



Several drawbacks to this construction method make it less desirable. These include but are not limited to: wariness of field welds by utilities, many variations in support member configurations / sizes, and the need for certified welders in the field. The temporary welds that attach the temporary member to the tower are usually ground flush and recoated to avoid future corrosion. The temporary support member should be engineered and sized for load and the welds or bolted connections should be specified.

**Figure 5 Example of Welded Temporary Support Member**

This is quite difficult, as field personnel tend to use what is readily available for this member.

### Integral Temporary Support / Repair



It has been found that an integral bolted temporary support and bolted repair splice can be prefabricated and installed in one process. This eliminates the need for cranes or other temporary support mechanisms. The negative aspect of this design is that it requires design for the specific tower prior to field work.

This repair works well for corrosion damage but not very well for vehicular impacts or agricultural damage.

**Figure 6 Integral Temporary Support Member**

### **References**

American Society of Mechanical Engineers , “Below the Hook Lifting Devices” Safety Standard for Cableways, Cranes, Derricks, Hoists, Hooks, Jacks, and Slings.  
ASME B30.20-2003 Revision of ASME B30.20-1999.

Newberry, W.G. (Bill), “Handbook For Riggers”, 1989 Revised Edition. Copyright W.G. Newberry, 1967.

Huler, Scott, “Defining the Wind: The Beaufort Scale, and How a 19<sup>th</sup>-Century Admiral Turned Science into Poetry”.

IEEE, 2007 National Electric Safety Code.

PLS-TOWER, By Powerline Systems Inc., Madison, Wisconsin.

## Power Restoration Solution after Major Cyclone: “Gonu” Hit Oman in June 2007

Deepak Lakhapati, Ph.D.

Vice President – Engineering Services, KEC International Ltd., Transasia House,  
3<sup>rd</sup> Floor, Chandidali, Mumbai-400072, INDIA

Email: [lakhapatidm@kecrpg.com](mailto:lakhapatidm@kecrpg.com)

### Abstract:

Paper describes the major storm event which happened when a cyclone ‘GONU’ lashed OMAN on 5<sup>th</sup> June 2007. OMAN electricity and Transmission Company asked for quickest restoration solution. Damaged sites were not reachable due to floods. Various solutions were considered and finally quickest solution was adopted to erect 50 wooden poles. Restoration of one circuit of 132 kV Transmission line was done in 8 days after mobilizing men and material. Power was restored on 20<sup>th</sup> June 2007. Paper describes entire event, engineering solutions along with actual site photographs.

### Major Storm Event:

MUSCAT, 03<sup>rd</sup> June 2007 – The Country declared Red alert warning for the CYCLONE GONU, the strongest tropical storm hit the region with winds of 105 miles an hour. Weather officials said the Cyclone was strongest to hit the peninsula since 1977.

Cyclone Gonu reached Oman’s Eastern coast producing strong winds and waves. The Cyclone, which had been churning North West through the Indian Ocean could endanger Oil installations near Southern Iran. (June 5, 2007). (See exhibit Nos. 1-3)



Exhibit No. 1: 20 feet waves during cyclone.

The streets of Muscat were almost deserted, thousands of residents were evacuated from Eastern Coastal areas. The Army, Police and Civil defense troops were mobilized and about 18,000 people were evacuated across the Country.



Exhibit No. 2: Evacuation of people

Flights were suspended at Oman's Muscat Airport but the Cyclone had not affected shipping through the Strait of Hormuz, where atleast a quarter of world oil supplies passes.

Oil prices had risen on Monday 4<sup>th</sup> June 2007 on news of the Cyclone but subsided on Tuesday. Oil expert said on Wednesday that any impact from disruption to shipping would be only temporary, provided oil facilities in the region remained intact.



Exhibit No. 3: Heavy winds

The Country issued several alert notifications to all ministries including Power stations and Distribution companies to take precautionary measures and to activate their respective internal emergency procedures, as well as to keep available the necessary facilities.

The neighboring Countries UAE, IRAN, SAUDI ARABIA and YEMEN were also put on alert for the effects of Cyclone GONU.

The Cyclone caused widespread damage to many installations including Power Transmission System. Oman Electricity and Transmission Company's 132 kV transmission system got damaged and Six Towers totally collapsed and washed away with the floods and eight towers were affected. For instance, the tower which links Madinat Sultan Qaboos with Jahloot Circuits 1 & 2. This caused electrical shutdown on Jahloot Grid station, which feeds the entire Welayat Al Amerat and Welayat Qurayat region, which has more than 40 villages and 5 major towns. (See exhibit Nos. 4-7)



Exhibit No. 4: Conductors are grounded



Exhibit No. 5: Damaged Tower



Exhibit No. 6: Damaged tower



Exhibit No. 7: Damaged tower

Several roads and bridges were also washed away creating a massive damage of infrastructure. (See exhibit Nos. 8-10)



Exhibit No. 8: Damaged Highway



Exhibit No. 9: Damaged Bridge



Exhibit No. 10: Damaged Road

#### **Emergency Solution for Restoration of Power:**

The client immediately called KEC to report to the incident site with the help of Army Vehicles since there was no approach road to access the site. We proposed our restoration procedures and methodology to restore the line.

Various solutions were considered. Towers availability, time for work and access issues were the main problems.

We looked for readymade material in the stores like conductor, insulators, lattice towers, wooden poles etc.

As wooden poles and insulators and conductors were available in stores and there were no spare lattice tower or steel/concrete poles. So the obvious choice was the wood poles. (See exhibit Nos. 11-14)



Exhibit No. 11: Unique solution for immediate Restoration of power by using wooden frame



Exhibit No. 12: Erection of the wooden frame.

Then we mobilized man power and it was decided to evacuate power on one circuit. Computer aided solution was worked out overnight. Three wood poles and connecting beam was good enough to carry conductors over 300 ft span.



Exhibit No. 13: A wooden frame with insulators



Exhibit No. 14: Stringing the conductors

Block foundations were designed as a quick solution. (See exhibit Nos. 15 - 16)



Exhibit No. 15: Excavating the soil



Exhibit No. 16: Block foundation

KEC, organized materials, men and machines at site on 12<sup>th</sup> June 2007 and completed the entire proposed work with in 8 days and commissioned one circuit on 20<sup>th</sup> June 2007.



Exhibit No. 17: Emergency line Restoration in 8 days

**Original Line Restoration:**

After the power was restored KEC signed contract to re-build a new transmission line in the damaged section, and connection to the original line. (See exhibit No.18 - 23)



Exhibit No. 18: Construction of the newly designed transmission towers



Exhibit No. 19: Erection of the new transmission towers



Exhibit No. 20: Stringing of the Conductors



Exhibit No. 21: New Transmission line diverted on the hill



Exhibit No. 22: Original line restored

Telegram Channel: [@Seismicisolation](https://t.me/Seismicisolation)



Exhibit No. 23: Original line restored

**Conclusion:**

This event has given us a good opportunity to learn techniques that can be used for power restoration in shortest possible time and earned the goodwill from the customer.

**ACKNOWLEDGEMENT**

I gratefully acknowledge the contribution of the entire design & engineering team for successfully developing the emergency solution and project team to install the line. We were also acknowledged by the customer. I also acknowledge the encouragement given by the Top Management of KEC International Limited to prepare the paper.

## **ANALYSIS CHALLENGES IN THE EVALUATION OF EXISTING ALUMINUM TOWERS**

Rengaswamy Shanmugasundaram, P.E., Program Manager-Civil/Structural  
Jason W. Kilgore, P.E., S.E., Project Engineer-Civil/Structural  
Rodger Calvert, P.E., Project Engineer-Civil/Structural  
Mesa Associates, Inc., 832 Georgia Ave., Ste. 300, Chattanooga, TN 37402  
Ph (423) 424-7344, Fax (423) 424-7303, Email: [rshan@mesainc.com](mailto:rshan@mesainc.com)

### **ABSTRACT**

Existing structures were aluminum double-circuit lattice towers with a single circuit installed and had to be evaluated for the proposed addition of a second circuit. Original design data drawings were not available for these towers. Therefore, field measurements of towers with an energized single circuit were performed to determine overall tower geometry, individual member sizes and connection configuration. Field hardness testing and sample coupons were taken for laboratory analysis to determine material properties.

Loadings for the towers were determined in accordance with the 2007 edition of the National Electrical Safety Code. Analysis and qualification of the towers were performed using the software program "Tower" by Power Line Systems (PLS Tower), and the "Guide for the Design of Aluminum Transmission Towers" as published in the December 1972 *Journal of the Structural Division, Proceedings of the American Society of Civil Engineers*. The existing foundations were checked against the support reactions from the PLS Tower Analysis.

This paper describes the various analysis challenges encountered in this project.

## PROJECT REQUIREMENTS

Four existing structures were aluminum double circuit lattice towers with a single circuit installed and had to be evaluated for the proposed addition of a second circuit. Three towers are dead-end towers and one tower is a tangent tower supported by a portal frame as shown in Figure 1.

## FIELD INSPECTION FOR TOWER DIMENSIONS

Original design data drawings were not available for these towers and, therefore, tower dimensions and member sizes were not known.

Mesa personnel along with linemen from Shaw Energy Group field measured the four existing double-circuit aluminum transmission towers to determine overall tower geometry, individual member sizes, and connection configuration. Dimensions of legs and web members were carefully taken by maintaining electrical clearance from the energized conductors. Cross arm dimensions were taken from the un-energized side of the towers.

Field measured dimensions of one of the towers are shown in Figure 2. Cross section area and moment of inertia of the unusual shape of the members with bulb or stem at the end were calculated using AutoCAD program.



Figure 1.  
Tangent Tower Supported By A Portal Frame  
(Linemen taking dimensions, individual member sizes, and connection configuration on this energized tower)

Telegram Channel: @Seismicisolation

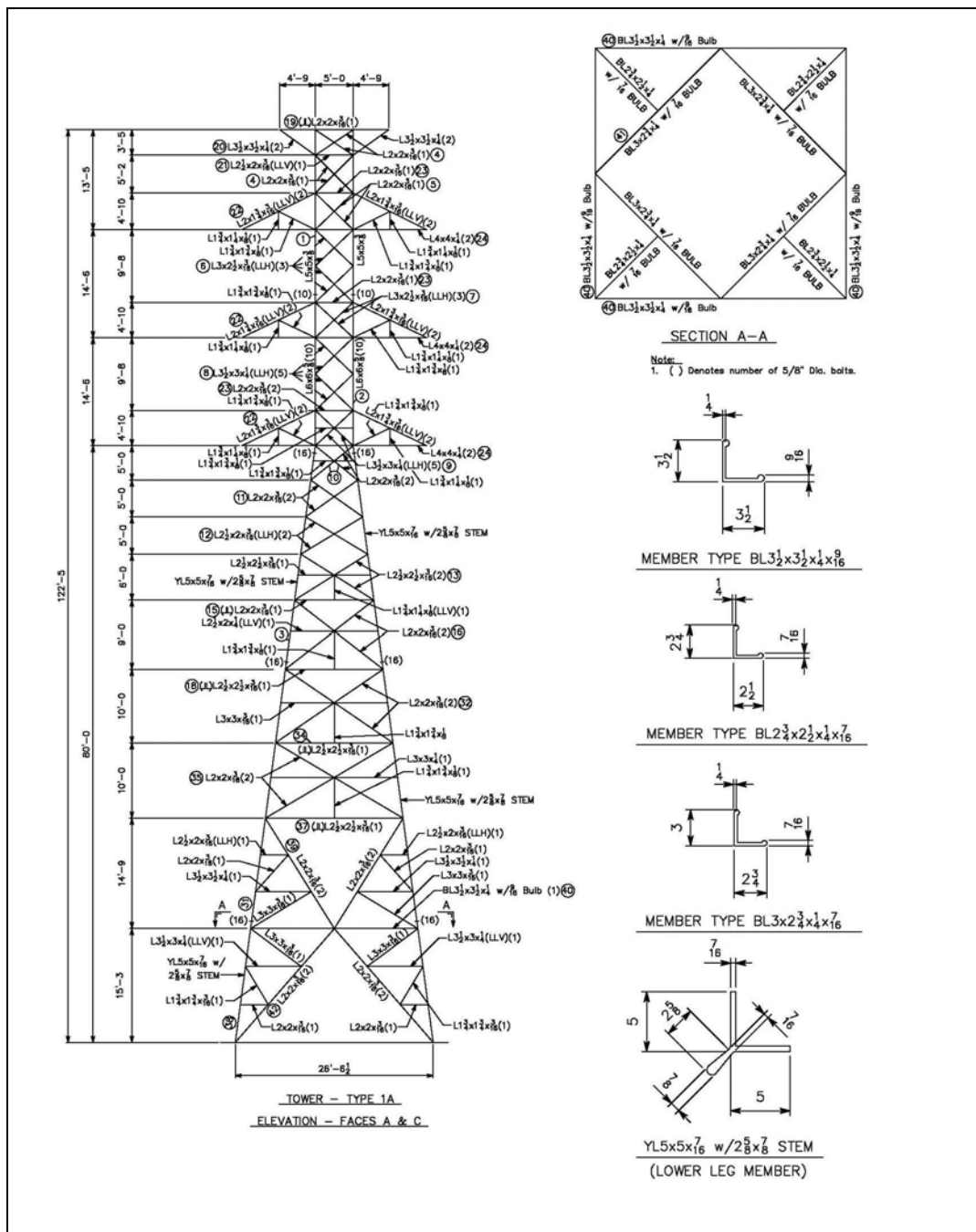


Figure 2.  
Field Measured Dimensions of One of The Towers

Telegram Channel: @Seismicisolation

## FIELD INSPECTION FOR TOWER MEMBER PROPERTIES

Since tower member properties were not known, field testing was performed as detailed below:

A representative from Materials Technology, Inc. performed field hardness testing and took sample coupons for laboratory analysis. Field hardness tests were performed in accordance with ASTM E18 at sixteen locations around the base of the tower encompassing a representative sample of angle members, connection plates, and bolts. Two sample coupons were collected for laboratory chemical analysis (ASTM E415), one each from a main leg and a web member. Coupons were taken from the outstanding corner at the end of the members to avoid compromising the members strength.

The results of the chemical analysis indicated that the "Y" shaped main leg members were aluminum alloy 6070 and the web members were aluminum alloy 6061. "L" shaped leg members above the waist were assumed to be alloy 6061. Hardness results indicated a temper level of T6.

Based on the above, yield strength is estimated as shown below:

Lower Leg Members = 45,000 psi  
 Web Brace Members = 35,000 psi

The above information matched the values given in an aluminum design manual published by the Aluminum Association as detailed below:

<b>Member</b>	<b>Alloy</b>	<b>Fy</b>	<b>Fu</b>	<b>Modulus of Elasticity</b>
Lower Legs	6070-T6	45 ksi	48 ksi	10,000 ksi
Web Braces	6061-T6	35 ksi	38 ksi	10,000 ksi

5/8" diameter tower bolts are assumed as aluminum alloy 2024-T4 with the following properties: Fs = 37,000 psi, Fu = 62,000 psi

Test results for the above materials are attached at the end of this paper, see Figures 3 and 4.

## DESIGN LOADS

Line loads were determined in accordance with the 2007 edition of the National Electric Safety Code.

NESC Section	Description	Values
250B	Medium wind and ice	40 mph wind on $\frac{1}{4}$ " radial ice at $15^\circ$
250C	Extreme wind	90 mph wind, no ice at $60^\circ$
250D	Light wind on extreme ice	30 mph wind on $\frac{3}{4}$ " radial ice at $15^\circ$

## ANALYSIS

Using the field measurements, the towers were modeled in the software program "Tower" by Power Line Systems (PLS Tower). The members were checked against two independent design criteria: ASCE 10-97, "Design of Latticed Steel Transmission Structures", and the article "Guide for the Design of Aluminum Transmission Towers" as published in the *Journal of the Structural Division, Proceedings of the American Society of Civil Engineers*, December 1972. In general, the ultimate stresses allowed by the ASCE "Guide" are more conservative than those allowed by ASCE 10-97.

The maximum stress level in each tower from the PLS Tower program is given below:

Tower No.	Member	Load Case – NESC Section		
		250B	250C	250D
1A	Diagonals	73.8%	97.5%	67.3%
	Legs Above Waist	46.4%	46.1%	35.8%
	Legs Below Waist	51.7%	54.6%	38.2%
2A	Diagonals	58.0%	91.7%	69.6%
	Legs Above Waist	56.4%	81.8%	38.6%
	Legs Below Waist	31.5%	53.2%	15.8%
3A	Diagonals	95.7%	94.8%	85.5%
	Legs Above Waist	57.7%	49.4%	44.8%
	Legs Below Waist	64.6%	57.5%	49.0%
4A	Diagonals	87.2%	98.0%	57.1%
	Legs Above Waist	22.9%	25.3%	18.5%
	Legs Below Waist	25.7%	29.7%	20.7%

The steel portal frame supporting one of the four towers and spanning over an access road was analyzed in STAAD Pro using the tower support reactions from PLS Tower.

All existing foundation footings consist of four steel piles each with a concrete pile cap and concrete pedestal.

The existing foundations, including steel piles, were checked against the support loads from the analysis in assumed soft clay and found to meet the appropriate factor of safety requirements.

## CONCLUSION

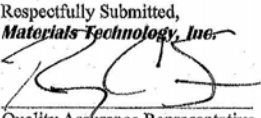
All four steel towers, the steel portal frame, and the foundations are capable of safely supporting the addition of a second circuit with no structural modifications.

The project was successfully completed in the year 2007 due to excellent pre-planning, dedication, and cooperation from various personnel from the following organizations:

1. Aluminum Company of America – owner of the project
2. Mesa Associates, Inc. – consulting engineers for the project
3. Shaw Energy Group – field support to measure dimensions of four towers
4. Materials Technology, Inc. – field and laboratory testing of tower members

TEST RESULTS OF TOWER MEMBERS					
 <b>MTI</b> MATERIALS TECHNOLOGY INCORPORATED			www.TestMetal.com 213 Lyon Lane Birmingham, AL 35211 205.940.9480 866.RUN.TEST		
<b>REPORT OF ANALYSIS</b>					
Mesa Associates, Inc. Attention: Rodger Calvert 9238 Madison Boulevard, Suite 116 Madison, AL 35758			Test Date: 01/29/2007 Report Date: 02/07/2007 Lab Number: 70354 P. O. Number:		
Sample Identification: (2) Aluminum Tower Hardness Inspection					
<b>SPECIMEN IDENTIFICATION</b>					
<b>Properties</b>	<b>Unit</b>	<b>Brace</b>	<b>Leg</b>		
<b>Chemical Composition</b>					
Silicon	%	0.68	1.22		
Manganese	%	0.02	0.62		
Chromium	%	0.05	0.06		
Copper	%	0.25	0.27		
Magnesium	%	0.92	0.80		
Titanium	%	0.03	0.08		
Iron	%	0.26	0.35		
Zinc	%	0.02	0.02		
<b>Alloy Classification</b>					
		6061	6070		
<b>Tensile Properties</b>					
Estimated Yield Strength	psi	35,000	45,000		
Test Method(s): ASTM E415					
Remarks: Alloy classification is indicated above and is based on the chemical analysis. Field hardness readings on page 2 and indicate both are T-6 tempers – this was the basis of the estimated yield strength.					
Respectfully Submitted, <b>Materials Technology, Inc.</b>  Quality Assurance Representative					
<i>Tests and analysis performed in accordance with procedures derived from methods described and approved by the ASTM and other accepted industry practices. This report shall not be reproduced, except in full, without the prior written approval of Materials Technology, Inc.</i>					
<i>Testing efforts were in accordance with MTI QA Program, Rev. 2 –February 15, 2002</i>					
<i>Page 1 of 2</i>					

Figure 3.  
 Test Results, Page 1

TEST RESULTS OF TOWER MEMBERS						
 <b>WEATHERING TECHNOLOGY INCORPORATED</b>			www.TestMetal.com 213 Lyon Lane Birmingham, AL 35211 205.940.9480 866.RUN.TEST			
<b>REPORT OF ANALYSIS</b>						
<b>Mesa Associates, Inc.</b> Attention: Rodger Calvert 9238 Madison Boulevard, Suite 116 Madison, AL 35758			Test Date: 01/29/2007 Report Date: 02/07/2007 Lab Number: 70354 P. O. Number:			
<b>Sample Identification:</b> (4) Aluminum Tower Hardness Inspection						
<b>SPECIMEN IDENTIFICATION</b>						
Properties	Unit	Tower #1	Tower #2	Tower #3	Tower #4	
<b>Hardness Testing</b>						
Tower Leg						
#1	HRB	64	64	60	67	
#2	HRB	62	-	64	66	
#3	HRB	63	-	61	69	
#4	HRB	65	61	62	69	
Cross Brace						
Angle	HRB	50	55	53	49	
Connector	HRB	61	-	59	62	
Angle	HRB	52	-	52	50	
Connector	HRB	63	59	59	65	
Fasteners						
Leg #1	HRB	75	74	74	72	
Leg #2	HRB	77	-	78	74	
Leg #3	HRB	75	-	76	71	
Leg #4	HRB	74	75	74	75	
Base Joint						
Joint #1	HRB	56	58	55	50	
Joint #2	HRB	54	-	50	51	
Joint #3	HRB	55	-	50	52	
Joint #4	HRB	53	56	52	55	
<b>Test Method(s):</b> ASTM E18						
<i>Respectfully Submitted, Materials Technology, Inc.</i>  Quality Assurance Representative						
<i>Tests and analysis performed in accordance with procedures derived from methods described and approved by the ASTM and other accepted industry practices. This report shall not be reproduced, except in full, without the prior written approval of Materials Technology, Inc.</i>						
<i>Testing efforts were in accordance with MTI QA Program, Rev. 2 –February 15, 2002</i>						
<i>Page 2 of 2</i>						

**Figure 4.**  
**Test Results, Page 2**

**Electrical and Mechanical Considerations  
in 765kV (Insulator) Hardware Assembly Design**

John Kuffel<sup>1</sup>                    Ziqin Li<sup>2</sup>                    Bruce Freimark<sup>3</sup>    Teja Rao<sup>4</sup>  
Ph.D, P.Eng., F.IEEE      PhD P.Eng., SM.IEEE      P.E., F.ASCE      AVNG

<sup>1</sup> Chief Engineer, Kinectrics, Inc., 800 Kipling Avenue, Toronto, Ontario M8Z-6C4, Canada, Phone: (416) 207-6047, email: john.kuffel@kinectrics.com

<sup>2</sup> Principal Engineer, Kinectrics, Inc., 800 Kipling Avenue, Toronto, Ontario M8Z-6C4, Canada, Phone: (416) 207-6000 Extension 6489, email: ziqin.li@kinectrics.com

<sup>3</sup> Principal Engineer, American Electric Power (AEP), 700 Morrison Road, Gahanna, OH 43230, Phone: (614) 552-1944, email: bfreimark@aep.com

<sup>4</sup> Engineer, American Electric Power (AEP), 700 Morrison Road, Gahanna, OH 43230, Phone: (614) 552-1865, email: trao@aep.com

## Abstract

Starting in 1969, American Electric Power (AEP) built a 765kV transmission network that amounted to over 2,000 circuit miles by 1984. The system utilized four-conductor bundles of Rail and Dipper conductors. Operational experience with the network revealed issues around audible noise due to corona from the lines.

In 1990, when the need arose to expand the network, it was decided that audible noise issues would be addressed by utilizing a new bundle design that consisted of a 6-conductor bundle using Tern conductors. The intent of the design change was to eliminate corona and thus resolve the audible noise issues associated with previous designs. The new design would also allow the use of non-ceramic insulators, which are susceptible to damage from long term exposure to corona. The move to the 6 x Tern phase bundle posed significant mechanical and electrical challenges to the engineers involved in hardware development.

This paper describes the extensive electrical testing programs carried out to prove the performance of the new 6-conductor bundle design.

## The “Traditional” Method of Corona Testing

Traditionally corona testing has been performed in laboratories by mounting a single-phase full size mock-up of the conductor-hardware-insulator assembly at a height above the ground representing the minimum design clearance of the line and applying 110% of the rated line-to-ground operating voltage. If the test setup is

shown to be free of corona by this test, then it is considered that the assembly will be free of corona under operating conditions. This method does not appear in any standards, but is used as a generally accepted test method. In spite of its general acceptance, this test method can give erroneous results. This is due to the fact that the inception of corona occurs at a given electric field gradient rather than a given absolute voltage. Under actual operating conditions, the electric field gradient at the conductor-hardware-insulator assembly is a function of phase spacing, the local geometry, the applied 3-phase voltage, and the line's elevation (air density). In order to correctly perform such a test in a laboratory, it is essential that the maximum gradients occurring on the conductors in the field be reproduced in the laboratory test.

### **Introduction to the Improved Method**

To reflect the true operating environment, corona testing of equipment should be carried out at a specified gradient related to the actual system-operating gradient. To establish this gradient in the test setup, three alternatives are possible. These are:

1. Build an accurate mock up of the three-phase system utilizing representative energized conductors, phase spacing and ground planes (including the structure), etc.
2. Test the hardware on a conductor of the same size upon which will be used in service and set the test gradient to that representative of the maximum 3-phase gradient present at the location where the test object will be installed. The test gradient can be obtained by calibrating the test setup through the use of corona calibrating spheres.
3. Test the hardware as above in 2, but calculate the applied voltage necessary to achieve the required gradient for the test setup used.

The first of these alternatives requires the use of a 3 phase supply, and an extremely large laboratory in which real setups can be constructed. In most High Voltage labs this is not possible. Therefore, the latter two alternatives are of most interest. These methods are based on the use of calculated or calibrated field gradients which are used during the testing.

The third alternative is based upon the calculation of the electric field surrounding the insulator assembly or hardware under test. Currently, there are a number of electric field plotting software packages available. Some of these are commercially available, while others have been developed in-house by research and development institutes engaged in testing, which requires characterization of the electric fields surrounding high voltage equipment. While such software has undergone marked improvement over the past decade, there is still significant concern on the effects of modeling details on calculated results. The second method is based on the use of gradient calibrating spheres. While this method is slightly more time consuming to implement, it has the advantage of actually measuring the electric field in areas of

interest in the test setup while avoiding the need to create an accurate mathematical model.

A calibrating sphere is a small sphere, which is mounted on a circular clip and can be attached to a conductor [1, 2]. Figure 1 shows the design details of the calibrating sphere, and how it is attached to the conductor under test.

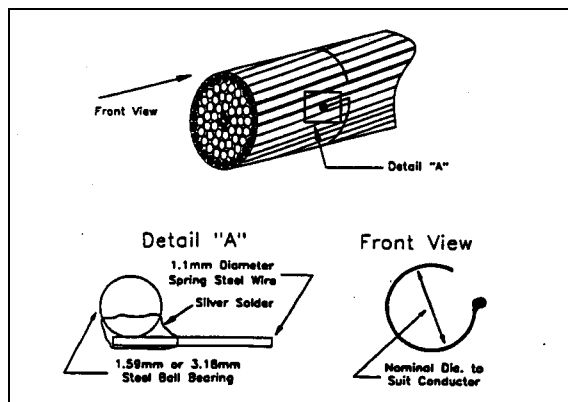


Figure 1 – Conductor surface gradient calibration sphere

The spheres are themselves calibrated on various sizes of conductor to establish the relation between the electric field gradient at which the particular unit will go into positive corona for the conductor diameter being studied.

When performing the laboratory corona test, the previously calibrated sphere is mounted at the center of a length of conductor in the phase bundle and is used as a calibration device to relate applied voltage and ground planes in the lab to the conductor gradient. After the applied voltage – conductor surface gradient calibration factor is established, the sphere is removed and the hardware under test installed. Since the applied voltage is directly proportional to the measured surface gradient, the applied voltage is then raised to the level required to produce the maximum conductor surface gradient as calculated under the specified operating conditions.

In the third approach, the required test voltage is calculated through the use of electric field modeling computer programs. These modeling techniques are then used to establish the single phase test voltage which, when applied to a test assembly in the laboratory, will produce gradients on the equipment that are equal to those the equipment sees when installed on the transmission line.

This paper describes a series of tests utilizing the second of these methods. This test method is described in detail in Canadian standard CAN/CSA-C411.4-98 [1] and in IEC Publication 61284, 1987 [2]. The tests were performed on a variety of suspension and dead-end assemblies utilizing polymer and porcelain suspension insulators intended for use on AEP's new 765-kV line design using the 6 x Tern phase bundle, which was adopted for the 90 mile (145 km) line in Virginia and West Virginia that was placed in service in June, 2006. The goal of implementing the 6-conductor bundle design was to provide a reduction in audible and electrical noise generated by corona discharges. Gaining assurance that the line would operate

corona-free was particularly important in this case since polymer insulators were used extensively on the line. The tests were intended to demonstrate that the new design would be corona free under normal operation, eliminating the possibility of in-service corona discharges and the potential life reduction of the polymer insulators and also improving the audible noise performance. Kinectrics, in Toronto, Canada worked with AEP in the design and performance of the corona and RIV test program.

## Test Program

The first step in the test program development was the calculation of the values of the maximum midspan operating gradients characterizing the line design. Based on these, the voltage gradient at which the testing was to be performed was established, which included factors to account for aging of the hardware and for the lower air density at the elevations that the lines would be built. Following the establishment of the target voltage gradient, full scale suspension and dead-end assemblies were erected in the high voltage laboratory and subjected to visual corona testing.

### Calculation of the mid-span conductor surface gradients

The mid-span conductor surface gradients were calculated for the line design provided by AEP. The maximum operating voltage of the AEP 765-kV system is 805 kV. Based on this value, the maximum mid span sub-conductor surface voltage gradient on the operating line with a ground clearance of 13.7 m (45 ft) was calculated as being 18.27 kV/cm. In order to account for the reduced air density in the highest area of the AEP service territory in which this design could be utilized, and for the surface aging that occurs on line hardware exposed to nature, the value of the subconductor surface voltage gradient set for acceptance was set at 1.3 times the maximum operating gradient. Therefore, the assemblies were tested at a subconductor surface gradient of 23.7 kV/cm.

### Calibration of the single phase test setup

The first step in the calibration of the full single phase test setup comprised the calibration of the corona calibrating sphere which would be utilized in establishing the relationship between the voltage applied to the full single phase test setup and the electric field at the outside surface of the individual subconductors [3].

The diameter of the calibrating sphere chosen for use was 3mm. Calibration of the calibrating sphere on a conductor of the same diameter as that of the bundle subconductors was performed so that the sphere could be used to set the test voltage to the value which would produce the required electric field at the bundle subconductor surface.

The calibration procedure is based on the use of a geometry characterized by a known and easily calculable electric field distribution. Typically the geometries used are either a single conductor positioned above a ground plane or a coaxial geometry with the conductor placed in the central axis of a metal cylinder. Both of these geometries

allow for accurate and simple calculation of the electric field at the conductor surface. The calibrating sphere is mounted on a conductor at its midpoint. The length of the conductor used is sufficient to ensure that the electric field at the center of the conductor is not subject to end effects. In this case the calibration of the corona calibrating sphere was done utilizing a single conductor positioned a given distance above the laboratory ground plane (i.e. the floor).

The calibration was performed by raising the voltage applied to the conductor and determining the applied voltage at which the corona calibration sphere went into positive corona. This was repeated 5 times for two different heights of conductor above ground. The positive corona inception voltage was established as the average of the 5 measurements taken at each of the two heights above ground. This value was then used to establish the electric field occurring on the conductor surface at the inception of positive corona on the calibrating sphere. For the single conductor above ground geometry utilized, the relation between the applied voltage and the electric field at the conductor surface is given by:

$$E = \frac{V}{r \ln \frac{2h}{r}}$$

where: E = the Voltage Gradient  
 V = is the applied voltage  
 r = the radius of the conductor  
 h = the height of the conductor above ground.

This value of electric field was then assigned to the particular corona calibration sphere as the electric field at which the calibrating sphere goes into positive corona when mounted on this particular diameter of conductor.

Figures 2 and 3 show the setup used for calibration of the corona calibrating sphere and the details of how the calibrating sphere is attached to the conductor. The results of the calibration are shown in Table 1.



Figure 2 – Setup for calibration of the corona calibrating spheres



Figure 3: Details showing installation of the corona calibrating spheres

Table 1 – Calibration data for 3mm sphere on 26.8 mm bus

Height Above Ground	Corona Inception Voltage (kV)						Surface Gradient (kV/cm)
	1	2	3	4	5	Average	
0.63 m (2 ft)	92.7	91.6	91.6	91.2	91.7	91.6	15.49
0.91 m (3 ft)	101.5	100.5	100.0	100.0	100.0	100.5	15.48

Upon completion of the calibration process for the corona calibrating sphere, the sphere was used to obtain a calibration between the applied voltage and the electric field present at the surface of the test setup's single phase conductor bundle. The single phase test setup consisted of a length of 6-conductor bundle utilizing smooth metal tubes as subconductors and was erected in the center of the high voltage laboratory. One end of the conductor bundle was shielded using corona rings and the other was shielded by inserting the bundle into the corona ring of the voltage divider. The use of smooth metal tubing in place of stranded conductor represents a practical simplification to assist in the test setup, negating the need to apply tension to control the position of individual wire strands. The "conductor" used was a rigid aluminum tube having a diameter equal to the Tern conductor. The error introduced through this substitution of smooth aluminum tubes for stranded conductors is accepted as being negligible and allowed in the standards [1, 2].

The length of the bundle was 50 feet. The center of the bundle was 15 feet 10 inches above the laboratory floor. The bundle was located 22 feet 8 inches from the south wall of the laboratory and 24 feet from the north wall of the laboratory. A structural beam with its full length covered with an 8-ft wide screen (used to represent the tower cross arm) was hung 20 feet 5 inches above the midpoint of the bundle. The beam was oriented perpendicular to the bundle. The diameter of the sub-conductors making up the bundle was 27 mm and the bundle diameter was 762 mm (30 inches). A photograph of the setup used for calibration of the applied voltage vs. bundle subconductor surface gradient is shown as Figure 4.

The calibration of the setup was performed by attaching the 3 mm diameter calibrating sphere to the bundle sub-conductors at a position mid-way along the bundle length. Calibration of the sphere had shown that, when mounted on a 27mm

diameter conductor, it would have a positive corona inception gradient of 15.49 kV/cm. Utilizing this calibration data for the sphere, the relation between applied voltage and subconductor surface gradient was established by mounting the calibrating sphere on each of the sub-conductors in turn and following the procedure outlined below.

Voltage was applied to the conductor bundle, and the test voltage at which positive corona inception occurred on the calibrating sphere was established. This was done by first raising the voltage to above the corona inception level to condition the calibrating sphere and to allow the observer to locate the sphere. The voltage was then lowered to below the corona extinction level, and then respectively raised and lowered to the positive corona inception voltage and 30% below the positive corona extinction voltage of the calibrating sphere. The voltage was raised and lowered five times. During the voltage excursions, the voltage at which positive corona inception occurred on the calibrating sphere was recorded. Following this, the positive corona inception voltage was calculated as the average of the inception readings obtained during the 5 voltage excursions. This procedure was repeated for each of the 6 subconductors in the bundle.

Based on the determined positive corona inception voltage, the required test voltage for the assembly, was calculated using the relation shown below.

$$V_r = \frac{E_s}{E_c} V_c$$

where:

$V_r$  = The required applied test voltage

$E_s$  = The voltage gradient at which the test assembly must be free of positive corona

$E_c$  = The positive corona inception voltage gradient for the sub-conductor mounted calibrating sphere (in this case 15.49 kV/cm)

$V_c$  = The applied voltage corresponding determined as the positive corona inception voltage obtained during the bundle calibration.

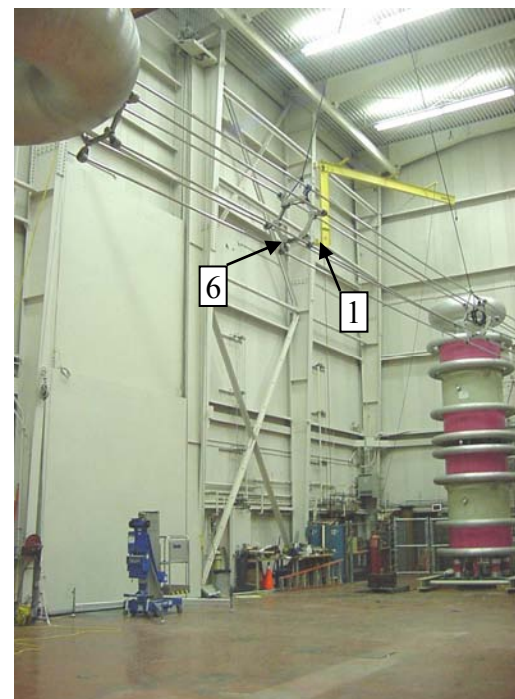


Figure 4 – The six-conductor bundle set up for calibration

Table 2 shows the results. Based on these data, it was agreed that 530 kV was to be used as the pass/fail voltage criterion of the transmission suspension assemblies.

Table 2: Suspension Bundle Calibration Results

Sub-conductor	Average Test Voltage for 15.49 kV/cm (kV)	Voltage for 23.7 kV/cm (kV)
1	348.0	532
2	337.0	516
3	347.5	531
4	353.2	540
5	340.0	520
6	333.0	510

### Testing of the Assemblies and Results

Full scale replicas of the following 7 single phase test assemblies were erected in the laboratory:

1. 2 Designs of Single “V” Suspension Assemblies  
Polymer and Porcelain
2. 2 Designs of Double “V” Suspension Assemblies  
Polymer and Porcelain
3. 1 Design of a Quadruple Polymer Insulator Deadend Assembly.
4. 1 Design of Jumper Loop Support Assembly using Polymer Insulators

The suspension and jumper assemblies under test were installed in the same location as the bundle conductor assembly used for calibration had been mounted. Due to physical constraints, the deadend assembly used actual Tern conductor and was mounted slightly closer to the ground; a separate calibration study was performed on this bundle.

As required by the standard test procedure [1, 2], the effects of the grounded structures in the vicinity of the suspension and tension assemblies (i.e., the towers) were simulated through the use of large grounded metallic screens. The location of these screens was adjusted to approximate the location of the tower present in the in-service installation.

The visual corona testing of the various assemblies was performed in a darkened laboratory with the aid of an image intensifier, as well as in a fully lit laboratory with the aid of a Coronascope and a Daycor corona camera.

The test procedure comprised raising the applied voltage to above the level at which positive corona appeared on the assemblies under test, and then lowering the voltage until corona extinction was observed. In each case, the corona extinction and inception voltages were based on the average values as determined from a series of 5 voltage excursions. If the voltage at corona extinction was above the required 530-kV test voltage, then the assembly was considered to have passed the test.

If corona extinction did not occur until the test voltage was reduced to below 530-kV, then the assembly was considered to have failed the test.

Sample photographs of the double V, single V, and the quadruple tension assemblies showing the setup, and the corona extinction and inception details are shown in Figures 5 to 7.

In many cases the assemblies passed the test successfully, while in others they failed. On assemblies which initially failed to pass the test, modifications were made during the testing. In some cases, the assemblies could be made to pass the test through simple modifications such as moving, adjusting, or re-orientating the corona rings. In these cases, the new positioning and orientation of the rings was included as a part of an immediate design revision. In other instances, more extensive modifications were required. Here, solutions such as changing the shape or increasing the diameter or the size of tubing used in the ring construction were identified and proven to work in mock-up form. Following the identification of the potential solutions, the design was revised, new rings were manufactured, and the assemblies were later re-tested to ensure that the revised designs met the test requirements.

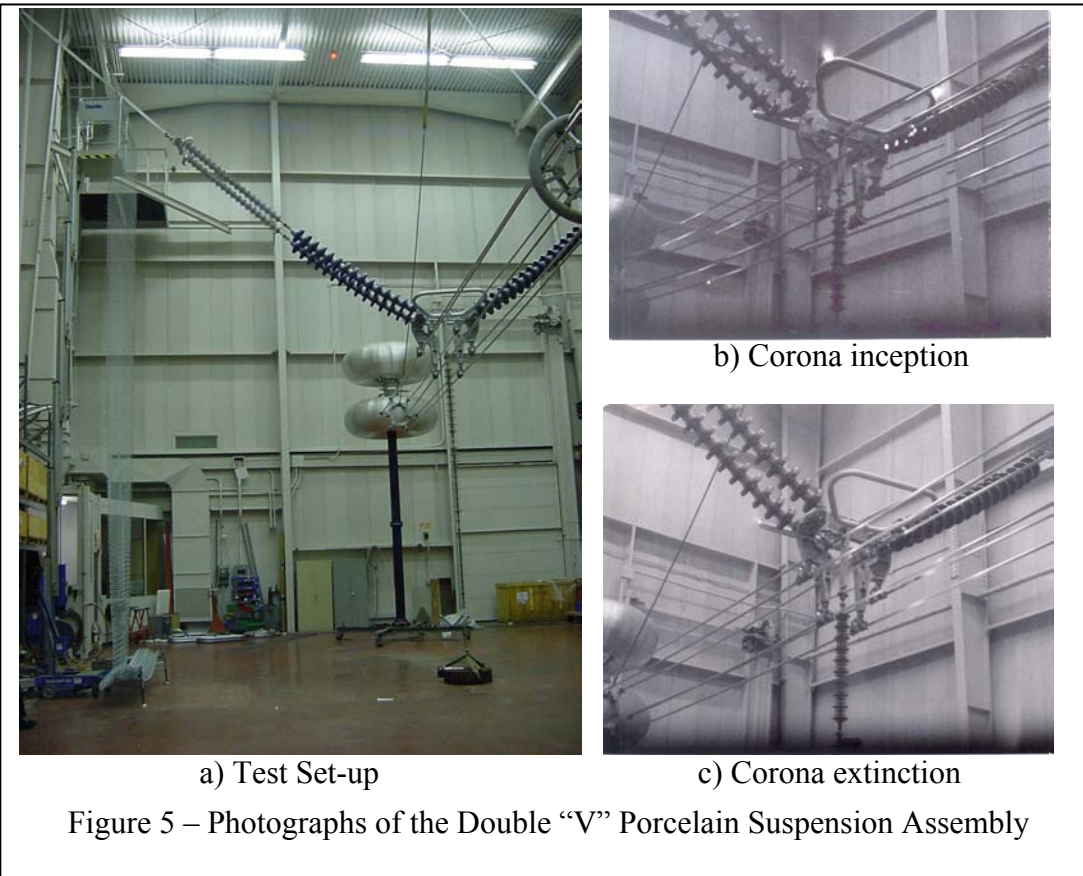


Figure 5 – Photographs of the Double “V” Porcelain Suspension Assembly

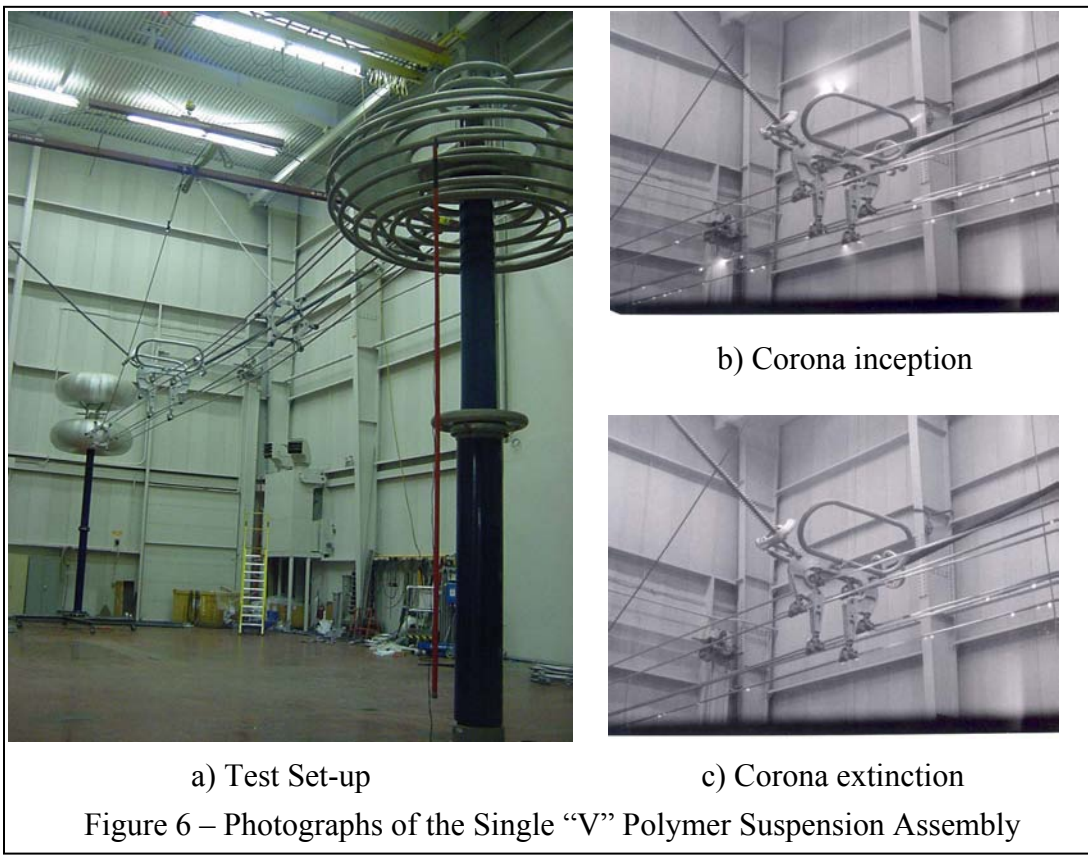


Figure 6 – Photographs of the Single “V” Polymer Suspension Assembly

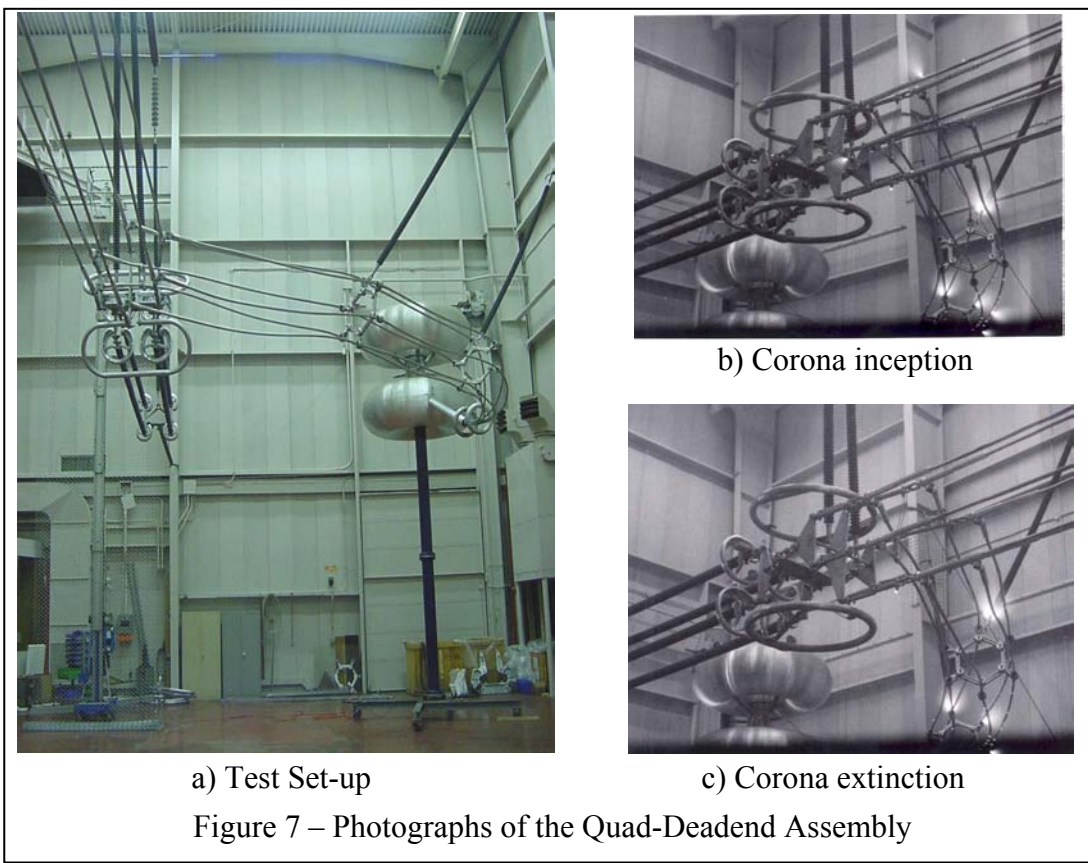


Figure 7 – Photographs of the Quad-Deadend Assembly

Telegram Channel: @Seismicisolation

## Conclusions

Voltage gradient based visual corona tests [1,2] were carried out in accordance with accepted standards and guidelines for visual corona and RIV testing for transmission line insulator assemblies and line hardware. The tests were performed on several assemblies for use in AEP's new 765-kV transmission construction. The tests confirmed that several of the assemblies would operate free of positive corona in fair weather conditions. In some instances, the initial designs did not meet the test requirements and in these cases, improvements to the design were formulated and their effectiveness was checked during the testing. Assemblies requiring significant modification were re-tested after the identified modifications had been made.

During the tests, several instruments were used to detect and observe visual corona on the insulator assemblies and hardware. These included a standard image intensifier, a Daycor camera and a Coronoscope. It was also determined that a tripod mounted (non-commercial) camcorder with low-light capabilities was quite effective in recording the tests. All of the instruments proved capable of detecting the presence of positive corona, and resulted in the same assessment of corona inception and extinction levels.

---

## References:

- [1] CAN/CSA-C411.4-98, "Composite Suspension Insulators for Transmission Applications"
- [2] IEC Publication 61284, 1997, "Overhead lines – Requirements and tests for fittings"
- [3] O. Nigol, "Development and Testing of Corona-Free High Voltage Line and Station Hardware", 3rd International Symposium on High Voltage Engineering, Milan, Italy, 1979.

## STRENGTH OF STEEL ANGLES SUBJECT TO SHORT DURATION AXIAL LOADS

Jared J. Perez<sup>1</sup>  
Wendelin H. Mueller III<sup>2</sup>  
Leon Kempner Jr<sup>3</sup>.

<sup>1</sup>Bonneville Power Administration (BPA), P.O. Box 61409 (TELS-TPP3), Vancouver, Washington, 98666-1409; email: [jjperez@bpa.gov](mailto:jjperez@bpa.gov),

<sup>2</sup>infra-Structure Testing and Applied Research (iSTAR) Laboratory, Civil and Environmental Engineering, P.O. Box 751, Portland, Oregon, 97207, website: [www.istar.cee.pdx.edu](http://www.istar.cee.pdx.edu); email: [wendell@cecs.pdx.edu](mailto:wendell@cecs.pdx.edu)

<sup>3</sup>Bonneville Power Administration (BPA), P.O. Box 61409 (TEL-TPP3), Vancouver, Washington, 98666-1409; email: [lkempnerjr@bpa.gov](mailto:lkempnerjr@bpa.gov),

### SUMMARY

This research presents the results of a test program to determine the compression strength of single angle members subjected to short duration axial load. Lattice steel transmission towers are largely constructed of single angle members. When a conductor breaks, the load on the tower is of large magnitude but short duration. This research attempts to answer two questions: 1) do angles in transmission towers have a higher compressive strength under short duration axial loads than they have for static loads; and 2) if they have a higher short duration axial capacity, how can this be used by transmission tower engineers. The parameters of the short duration axial load to simulate a broken conductor applied to the angles, as a function of the time, were determined using CIGRE B2-308 (2004). This reference discusses a full-scale test of a broken conductor and insulator on a transmission line. Time history plots of transmission line component loads are presented and used to develop the short duration load function for this study.

The angles used in this study include two sizes: 76 X 76 X 6.4 mm (3 X 3 X 1/4 in.) and 89 X 89 X 9.5 mm (3-1/2 X 3-1/2 X 3/8 in.), and four slenderness ratios, (L/r): 70, 100, 140, and 180. The member end supports studied include 1) Ball Joints at each end, 2) Single Leg Bolted at both ends, and 3) One end with Single Leg Bolted and the other with Partial End Restraint.

This research was preformed at the infra-Structure Testing and Applied Research (iSTAR) Laboratory, Portland State University. The study was funded by the Bonneville Power Administration (BPA), and the CEATI International, Inc. (CEATI), Overhead Line Design Issues & Wind and Ice Storm Mitigation Interest Group (WISMIG). The Interest Group consists of Utilities from the USA, Canada, France, and Japan. The complete research report referenced in this paper is CEATI REPORT No. T063700-3336. Mike J. Riley of the BPA was a contributing author.

## APPLICATION

Broken conductors are one of the extreme event loads used to design high voltage transmission lines. This load case can be a controlling load for the design of a tower or components, such as cross-arms. The broken conductor load is a short duration load compared to the traditional static loads used to design for wind and ice. It has been demonstrated in other structural engineering applications that members have higher compression capacities when subjected to short duration loads.

Traditional high voltage transmission line towers are designed using industry codes that base member capacity on nominal strength values. Tension members and compression members with low slenderness ratios are designed using the nominal yield strength, whereas compression members with high slenderness ratios are designed using Euler buckling, which is independent of yield strength.

New transmission line tower designs currently use the nominal member capacities to resist all design loads. In special cases where an existing high voltage transmission line is being assessed for upgrading and reliability, capacities higher than the nominal value may be used in structural assessment of the transmission line. Investigation of transmission line failures involving short duration loads may benefit by considering the increase in compression capacity of individual members.

Tension members are designed to the nominal yield strength. A tension member can have an increase in capacity on the order of 10–20 percent, when the actual yield strength is considered. This would also be true for low slenderness ratios compression members. The compression capacity of members with high slenderness ratios are not controlled by yield strength. In this case the increased as a result of RL compression capacity could be beneficial.

## TESTS

Both static and RL Tests were performed as part of this research. Angles tested were of two (2) different cross sectional areas and four (4) different slenderness ratios. The angle sizes were 76 X 76 X 6.4 mm (3 X 3 X 1/4 in.) and 89 X 89 X 9.5 mm (3-1/2 X 3-1/2 X 3/8 in.), and the slenderness ratios, L/r's were 70, 100, 140 and 180. The angles were cut from 12.2 m (40 ft.) sections and piece marked accordingly in order to account for material property variations. To determine the yield strength, a coupon was cut from each 12.2 m (40 ft.) section and tested in accordance with ASTM E8 (2001).

Members were first tested under normal static loading conditions to determine the static capacity of the member. These tests are referred to as the Pre-Static Tests. The capacity of the member is defined as the point where the member could no longer support additional applied load. Three (3) Pre-Static Tests were performed for each angle size and L/r. The RL Tests began once the Pre-Static Tests were complete. At least five (5) RL Tests were performed for each angle group. A group consists of angles of the same slenderness ratio, cross sectional area and end support.

The RL Test was performed in a series of load steps that were each a percentage of the ultimate load estimated using the Pre-Static Test capacity and calculated values. The percentage varied slightly from test to test. A typical RL Test started at 50% of

ultimate static load and continued in 20% steps until failure. Failure is defined as the load at which a permanent set in lateral deflection occurred or when the load resistance of the member did not increase. Each RL step started and ended at a load equal to zero. Whenever possible, a static load test to failure was conducted for each member after it failed in the RL Test.

## TEST SETUP

Three types of end supports were tested with the two angle sizes and all four L/r's. They included: 1) Ball Joints at each end, 2) Single Leg Bolted at both ends and 3) One end with Single Leg Bolted and the other with Partial End Restraint.

End Support Type 1, ball joint at each end, is shown in Figure 1. The angle was bolted to a channel that was welded to a base plate on each leg at both ends. The angle had slotted bolt holes so that when loaded, the angle would slip into place and bear directly onto the end plate. This was to ensure that the load applied was transferred through the plate and into the angle, as opposed to being transferred through the bolt. The load was applied through the Center of Gravity (CG) of the angle.

End Support Type 2, single leg bolted at both ends is shown in Figure 2. The angle was bolted on one leg at both ends of the member. This end support was also hinged on both ends. This is different from End Support Type 1 not only because of the hinge, but also because the angle did not bear against the plate. The load was instead transferred through the base plate and then through the angle via the bolts. The end support consisted of a staggered five bolt-hole pattern. The hinge allowed rotation about an axis along the outside surface of the bolted leg. The load was not centered on the centroid of the angle, but at the outside of the bolted leg at the centroid of the bolt pattern representing normal frame eccentricity.

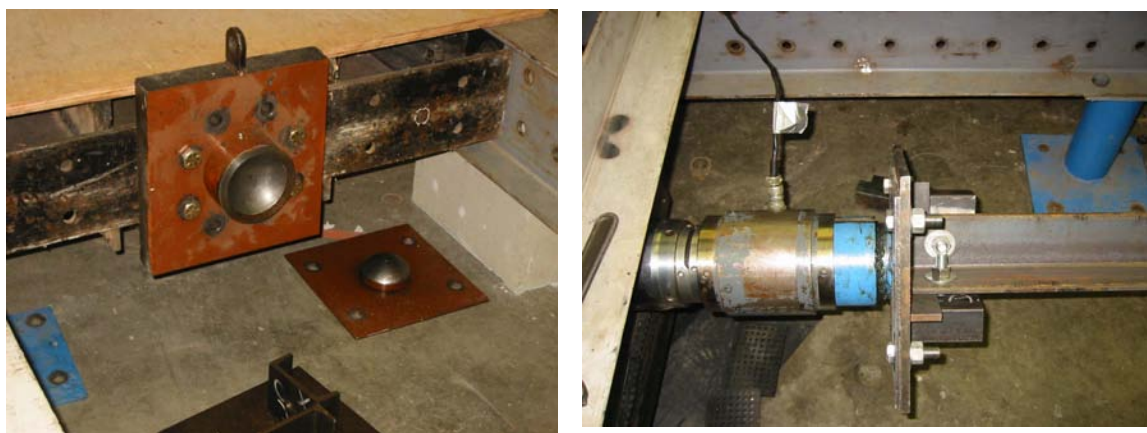


Figure 1, Ball Joint on Both Ends, Type 1



**Figure 2, Single Leg Bolted at Both Ends, Type 2**

End Support Type 3 had a single leg bolted on one end of the member and a partial end restraint on the other end. The load transfer mechanism is similar to that of End Support Type 2 except no rotation was allowed by the partial end restraint, as was the case with the hinge and the ball joint. An example of this type of support is shown in Figure 3.



**Figure 3, Single-Leg Bolted on one end and Partial End Restraint on the other end, Type 3**

## SUMMARY OF RESULTS

### Short Members – L/r of 70 and 100

The Average RL Factors (Avg. RL Factor) for both size angles with L/r of 70 and 100 are very close to 1.0, indicating that there is no increase in the load resistance of the members as the rate of loading increases. A RL Factor close to 1.0 for Short Members is consistent with information provided by others (Ari-Gur, J., Weller, T., and Singer J., 1982, Galambos, T. V., 1998, and Hoff, N. J., 1951).

### Long Members – L/r of 140 and 180

The Average RL Factors (Avg. RL Factor) for both size angles with L/r of 140 and 180 are larger than 1.0, indicating that there is an increase in the load resistance of the members as the rate of loading increases. The values range from 1.25 to 2.8. RL Factors greater than 1.0 for Long Members is consistent with information provided by others, per the listed literature search references in Appendix A (Ari-Gur, J., Weller, T., and Singer J., 1982, Galambos, T. V., 1998, and Hoff, N. J., 1951).

For members with L/r of 140 and 180 the Avg. RL Factors consistently trend lower as the member cross section increases. The mass of the member increases as the member size increases. It is the authors' opinion that the trend to smaller RL Factors as the member size increases is caused by the increase in inertia of the larger cross section angle. The increase in lateral deflection as a result of lateral inertial effects could cause yielding at a lower test load.

## CONCLUSION

The results of this research show that an increase in compression load capacity can be expected for "long" members (L/r of 140 and 180) when subjected to rapid loads. Based on the test results of this study a Rapid Load Factor of 1.5 may be a reasonable value to represent this type of behaviour. This increased compression capacity was not seen in "short" members (L/r of 70 and 100). This is encouraging because long members fail by compression buckling while short members fail by yielding. A buckling failure load of long members is not dependent on the yield strength of the member, thus yield strength higher than that specified is of no benefit. In short member's, the capacity is dependent on the material's yield strength, which is normally higher than that specified by the material specification (nominal yield strength). In addition, strain hardening of the steel occurs before a "yielding" failure. Short members have the potential for additional compression capacity due to the actual yield strength exceeding the nominal yield strength.

These results of this study are consistent with published papers (Ari-Gur, J., Weller, T., and Singer J., 1982, Galambos, T. V., 1998, and Hoff, N. J., 1951) which address rapid loading of structural members for applications other than transmission line towers. Additional research should be performed on individual members with other slenderness ratios. Also substructure and full-scale tests should be performed to determine if the individual members of these assemblies attain the increased compression capacity reported here, when subjected to a more complex structural load path.

## REFERENCES

- Ari-Gur, J., Weller, T., and Singer J., (1982) "Experimental and Theoretical Studies of Columns under Axial Impact," International Journal of Solids and Structures, Vol. 18, No. 7.
- CIGRE B2-308 (2004) "Testing and Numerical Simulation of Overhead Transmission Line Dynamics under Component Failure Conditions", Vincent, P., Huet C., Charbonneau M., Guibalt P., Lapointe M., and Banville D., et. al., Paris, France.
- Galambos, T. V., (1998) "Selected Topics in Dynamic Stability," Guide to Stability Design Criteria for Metal Structures, Fifth Edition, John Wiley & Sons, Inc.
- Hoff, N. J., (1951) "The Dynamics of the Buckling of Elastic Columns," Journal of Applied Mechanics, American Society of Mechanical Engineers.

## CEATI INTERNATIONAL, INC. CONTACT INFORMATION

CEAT International, Inc. (CEATI), 1010 Sherbrooke Street West, Suite 2500, Montreal, Quebec, Canada H3A 2R7, Website: [www.ceati.com](http://www.ceati.com)

## Residual Capacity in Compression of Corroded Steel Angle Members

L.-V. Beaulieu<sup>1</sup>, F. Légeron<sup>1</sup>, S. Langlois<sup>1</sup> and S. Prud'homme<sup>1</sup>

<sup>1</sup>Industrial Research Group NSERC/Hydro-Québec TransÉnergie on Overhead Transmission Lines Structures, Department of Civil Engineering, Université de Sherbrooke, Sherbrooke, Quebec, Canada, J1K 2R1

Email: [frederic.legeron@usherbrooke.ca](mailto:frederic.legeron@usherbrooke.ca)

### ABSTRACT

Over time, steel structures are affected by corrosion and their capacity is therefore affected. To estimate the capacity of structures with corrosion, it is necessary to estimate the residual capacity of corroded members. The objective of this article is to evaluate the structural behaviour of corroded steel angle members under compressive load in order to provide practical data to engineers. An accelerated corrosion procedure was used on 16 angle members. The angle members were then tested in compression. The influence of corrosion on compressive capacity was measured and compared to analytical methods accounting for weight loss. Recommendations are drawn from this research to provide guidance to engineers on how to evaluate compressive capacity of corroded members. Needs for future work are also highlighted.

### INTRODUCTION

Steel structures exposed to environmental condition are subject to corrosion. Even galvanized steel can experience corrosion after some time. Corrosion can be particularly important in the foundation, for example, where steel is in direct contact with the soil. For companies managing large structure networks, such as transmission line utilities, it is extremely difficult to assess the residual capacity of an existing structure and determine when it is no longer safe. One method based on qualitative parameters was developed by Hathout (2004) to evaluate the reliability of transmission lines. To examine the problem in more details, it would be useful to develop a model predicting the residual capacity of corroded members.

The phenomenon of corrosion is well-studied. However, very little research has been done on how the capacity of steel members is affected once corrosion has developed. The objective of this study is to provide data on compressive capacity of corroded angle steel members that could be used by practicing engineers. A model to predict residual capacity of members is evaluated.

## EXPERIMENTAL PROGRAM

In order to evaluate the residual capacity of angle members, an experimental program was performed. The main parameters of this study are: (i) the overall slenderness ratio ( $KL/r$ ), (ii) the width-to-thickness ratio (w/t), and (iii) the corrosion level.

The slenderness ratio ( $KL/r$ ) is one of the main factors affecting the capacity of steel members under compression load. This is the ratio of the unsupported length (effective length  $KL$ ) to the radius of gyration. The length of the test specimens were selected such that two levels of this variable are investigated: (i) slenderness ratio of approximately 25, and (ii) slenderness ratio of approximately 70. Originally,  $K$  is assumed to be equal to 1.

The width-to-thickness ratio ( $w/t$ ) is defined as the ratio of the leg flat width to the leg thickness. This ratio affects the value of  $F_{cr}$  of the member based on the definitions of the ASCE 10-97 standard (1997), and therefore the calculated compression capacity of the member. The two levels of width-to-thickness ratio studied are 5.72 and 12.4. The corrosion level is measured as a mass loss percentage. Three levels of this variable were investigated: 0% (not corroded), 25% (moderate corrosion), and 40% (severe corrosion).

Table 1 shows all specimens and their level for each variable mentioned above, as well as the section, length, and gross area.

**Accelerated corrosion procedure.** The steel members were corroded by the galvanic corrosion process. The members were immersed in a conductive solution saturated with copper sulphate, and connected to the positive node of an electric circuit. The galvanized steel piece then plays the role of the anode. A copper plate cathode was also immersed in the solution and connected to the negative node of the circuit. Current was applied with a constant intensity generator to oxidize the steel member (from the anode to the cathode). The steel members were submitted to the process for durations between 253 and 1819 hours. Measurements of the leg width ( $b$ ) and leg thickness ( $t$ ) were taken during and after the corrosion process at four locations along the member. Current intensity and voltage were monitored. Standard assemblies for the corrosion process are shown in Figure 1.

**Experimental set-up.** The experimental set-up developed by Morissette (2008) to study the compression capacity of single diagonal bracing members was used here to assess the strength in compression of the corroded members. A sketch of the test set-up is shown in Figure 2.

**Table 1 Test specimens**

Specimen	Section	L (mm)	% of corrosion	w/t	KL/r	A (mm <sup>2</sup> )
48S-00-1	L64X64X4.8	500	0	12.4	39.7	582
48S-00-2	L64X64X4.8	500	0	12.4	39.7	582
48L-00-1	L64X64X4.8	1358	0	12.4	108	582
48L-00-2	L64X64X4.8	1358	0	12.4	108	582
95S-00-1	L64X64X9.5	500	0	5.72	40.3	1120
95S-00-2	L64X64X9.5	500	0	5.72	40.3	1120
95L-00-1	L64X64X9.5	1358	0	5.72	110	1120
95L-00-2	L64X64X9.5	1358	0	5.72	110	1120
48S-25-1	L64X64X4.8	500	25	12.4	39.7	582
48S-25-2	L64X64X4.8	500	25	12.4	39.7	582
95S-25-1	L64X64X9.5	500	25	5.72	40.3	1120
95S-25-2	L64X64X9.5	500	25	5.72	40.3	1120
48L-25-1	L64X64X4.8	1358	25	12.4	108	582
48L-25-2	L64X64X4.8	1358	25	12.4	108	582
48S-40-1	L64X64X4.8	500	40	12.4	39.7	582
48S-40-2	L64X64X4.8	500	40	12.4	39.7	582
95S-40-1	L64X64X9.5	500	40	5.72	40.3	1120
95S-40-2	L64X64X9.5	500	40	5.72	40.3	1120
95L-25-1	L64X64X9.5	1358	25	5.72	110	1120
95L-25-2	L64X64X9.5	1358	25	5.72	110	1120
95L-40-1	L64X64X9.5	1358	40	5.72	110	1120
95L-40-2	L64X64X9.5	1358	40	5.72	110	1120
48L-40-1	L64X64X4.8	1358	40	12.4	108	582
48L-40-2	L64X64X4.8	1358	40	12.4	108	582

Compressive tests were performed under displacement control using a 500 kN hydraulic actuator. The angle members were connected to the frame with bolted connections on one leg only (three bolts per connection). Holes in the angle members were drilled after the corrosion process.

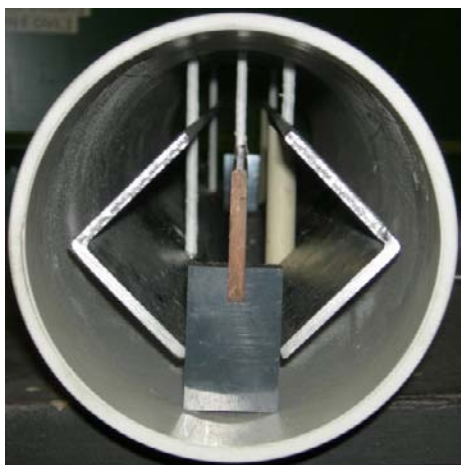


**Figure 1 Standard assembly.**

LVDT at the center of the member and adjusted relative to the connections measured by a LVDT.

As shown in Figure 3, the displacement in the axial (z-axis), in-plane buckling (x-axis) and out-of-plane buckling (y-axis) directions were measured during the tests to observe the non-linear behaviour of the steel members. The axial displacement was measured using a potentiometer fixed at the center bolt of both connections. The displacement in the y-axis at the center of the angle member was measured by a linear variable differential transformer (LVDT) and adjusted relative to the displacement at the connections, which were measured with potentiometers aligned with the center bolt of each connection. Similarly, the displacement in the x-axis was measured by a

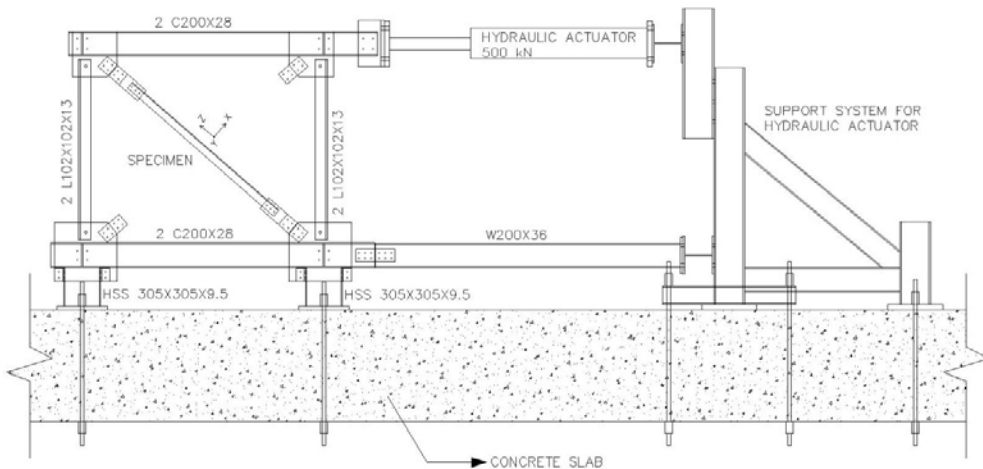


**Figure 2 Sketch of the compression test assembly, profile view.**

## CALCULATION OF THEORETICAL STRENGTH.

The ASCE 10-97 was used to calculate the theoretical capacity in compression of the corroded steel members based on the dimensions measured in the laboratory. The modulus of elasticity  $E$  used in the calculations is 200,000 MPa. The measured yield stress  $F_y$  is 365 MPa for L64X64X4.8 members, and 345 MPa for L64X64X9.5 members as measured on coupons cut from the members before the corrosion process. The yield stress was measured as per the ASTM E8-61T (1961) standard.

The length of the member taken in the calculation is the theoretical value from centroid of connection to centroid of connection. In accordance with ASCE 10-97, the radius of gyration of the member is the radius about the principal minor axis. Experimental evidence has however shown that the effective length may be different from theoretical length and that buckling may not occur around the minor axis. This phenomenon is due to the effect of the connections and is currently studied at the University of Sherbrooke. Nevertheless, because the gusset plates in the tests had flexibility very close to the flexibility of gusset plates used in practice, it was considered that the code should take this effect into account, at least in a limited way. Indeed, ASCE 10-97 allows modifying  $KL/r$  for members with normal framing eccentricities at both ends of the unsupported panel and for members partially restrained against rotation at both ends of the unsupported panel (ASCE 10-97, 1997).

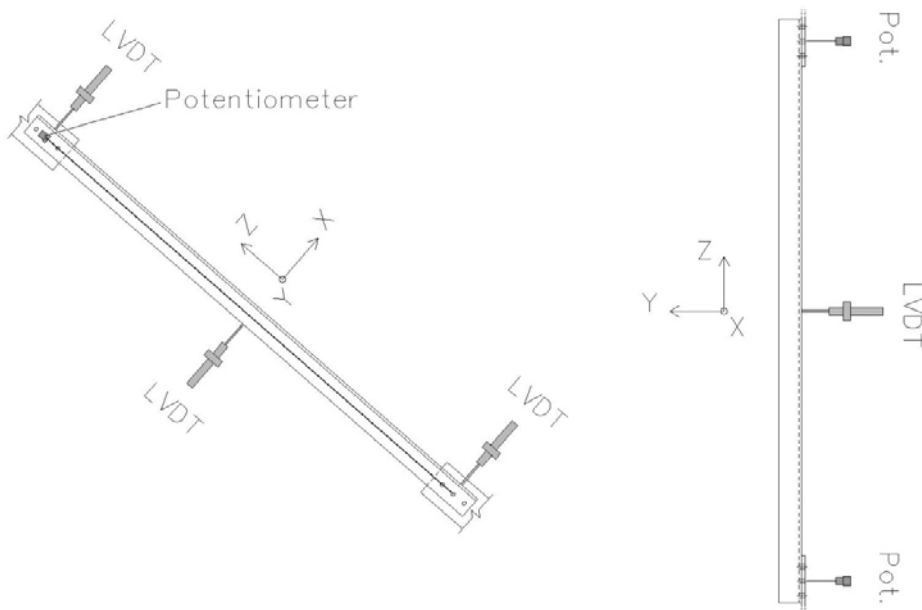


**Figure 3 Position of the instruments**

## EXPERIMENTAL RESULTS

**Accelerated corrosion procedure.** The steel members reached corrosion levels between 20% and 50% when submitted to the accelerated corrosion process. The main properties after corrosion are shown in Table 2. The leg width ( $b$ ) for corroded members was approximately constant at 63 mm.

To provide more information on the uniformity of the corrosion, the thickness of some members was measured at each point of the grid shown in Figure 4. A sample of the results is shown in Figure 5. These measurements show that the uniformity of the corrosion seems to decrease with the level of corrosion increasing. It is also

observed that the corrosion is more uniform for the 9.5 mm thick members than for the 4.8 mm thick members, suggesting that corrosion uniformity is less for smaller thicknesses.

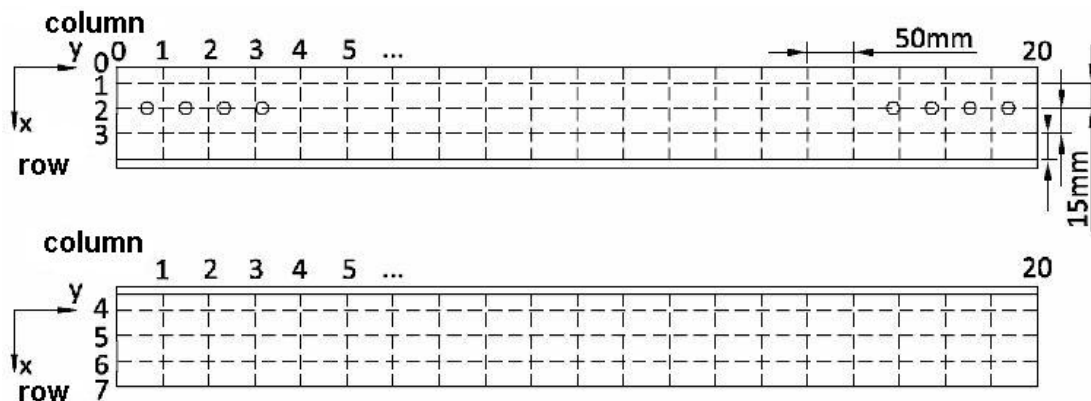


Figure 4 Sketch of thickness measurements.

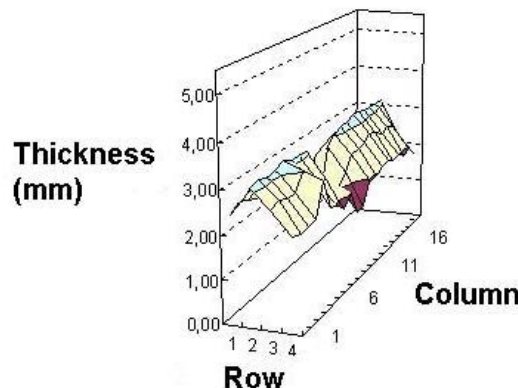


Figure 5 Thickness of members with original thickness and level of corrosion of a 4.8 mm and 40%

**Compression tests.** Figure 6 shows the results of the tests in terms of ratio between residual strength and uncorroded strength. The value of the uncorroded strength is taken as the average of the experimental strength of the two members of the same series that are not corroded. Table 2 also shows the capacity obtained in laboratory and the observed failure modes. It should be noted that the type of failure was either local or global and the buckling occurred at various locations along the members. In two cases, complete perforation of the member was observed. The type of failure is an important parameter and should be considered in the analysis of the results. It should be noted that the classification of failure modes is not straightforward and therefore these observations should be analysed with care.

**Table 2 Results of the corrosion process and compression tests.**

Specimen	% of corrosion	<i>t</i> (mm)	w/t (mm)	<i>KL</i>	<i>KL/r</i> (ASCE)	<i>A</i> (mm <sup>2</sup> )	Exp. capacity (kN)	Failure mode*
48S-00-1	0.00	4.76	12.4	39.7	79.9	582	n/a	3
48S-00-2	0.00	4.76	12.4	39.7	79.9	582	114	2
48L-00-1	0.00	4.76	12.4	108	114	582	91	1
48L-00-2	0.00	4.76	12.4	108	114	582	88	4
95S-00-1	0.00	9.53	5.72	40.3	80.2	1120	323	1
95S-00-2	0.00	9.53	5.72	40.3	80.2	1120	335	1
95L-00-1	0.00	9.53	5.72	110	115	1120	168	1
95L-00-2	0.00	9.53	5.72	110	115	1120	167	4
48S-25-1	26.4	4.32	13.8	40.0	80.0	526	57	3
48S-25-2	26.6	4.18	14.3	40.0	80.0	509	n/a	2
95S-25-1	26.9	7.28	7.79	40.5	80.3	864	253	1
95S-25-2	25.3	7.18	7.91	40.5	80.2	853	251	1
48L-25-1	27.4	3.86	15.6	108	114	471	80	1
48L-25-2	27.3	3.84	15.7	108	114	469	79	1
48S-40-1	37.2	3.51	17.2	39.8	79.9	430	66	2
48S-40-2	37.3	3.37	18.0	39.8	79.9	413	63	2
95S-40-1	37.1	6.43	8.95	40.4	80.2	769	216	1
95S-40-2	36.1	6.25	9.24	40.4	80.2	748	202	2
95L-25-1	22.4	7.80	7.21	110	115	922	151	1
95L-25-2	21.5	7.98	7.02	110	115	942	150	1
95L-40-1	30.7	6.79	8.43	110	115	809	99	3
95L-40-2	27.2	7.08	8.04	110	115	842	99	1†
48L-40-1	40.7	3.28	18.5	108	114	403	65	1
48L-40-2	47.1	2.63	23.3	108	114	324	25	1†

\* Legend for failure modes: 1- global buckling, 2- local buckling near connections, 3- local buckling near center, 4- mode not clearly identified in the test.

† Perforated members.

Specimen 48S-00-1 and 48S-25-2 did not produce any compressive capacity results due to difficulties in the experimental procedure.

It was observed that the effective length remained constant throughout the corrosion process. The radius of gyration varied moderately due to the moderate change of the leg width which affects the moment of inertia of the member. The slenderness ratio is

directly dependent on the variation of the radius of gyration and therefore was subject to minor modifications only. However, the section area of the members varied significantly, causing major changes to the compressive capacity of the angle steel members.

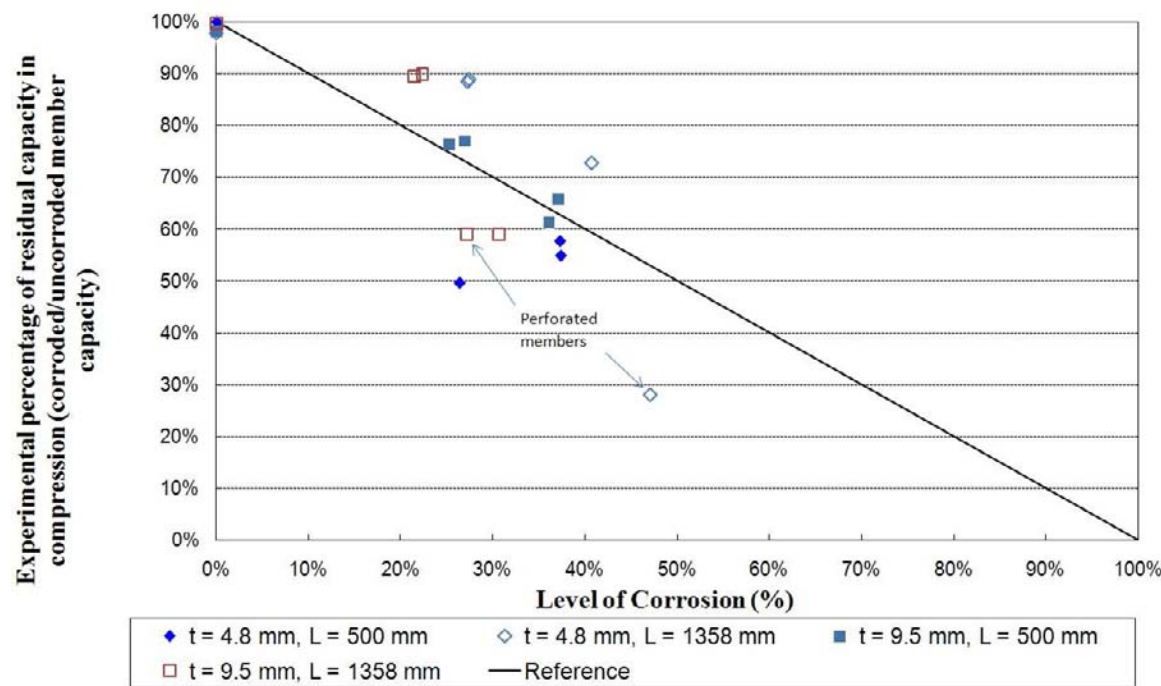


Figure 6 Experimental percentage of residual capacity in compression versus level of corrosion.

## ANALYSIS OF RESULTS

**Comparison of experimental and theoretical results.** The experimental results for the capacity in compression of the angle members are compared in Table 3 to the theoretical results from the ASCE standard. The calculation of the theoretical strength was based on an average thickness measured in laboratory, assuming that the thickness of corroded members is constant. It is however obvious from the failure modes observed in Table 2 that the corrosion was not uniformly distributed. The compression capacity is largely dependent on the extent and the location of the corrosion. This non-uniformity of the phenomenon explains in large part the difference between the experimental and theoretical results. In fact, complete perforation was found on two members (see Figure 7). In particular, the capacity of member 48L-40-2 was greatly reduced due to perforation because most of one leg was lost near the center. Another example is member 48S-25-1 which is particularly weaker than its predicted capacity. The failure mode of this member was very localized on one leg near the center. The failure in this case was due to the large w/t

and is not influenced by its  $KL/r$  value. The thickness near its failure point is approximately 3.3 mm, nearly 1 mm smaller than its average measured thickness. The experimental capacity of 57 kN would be obtained theoretically for a thickness of approximately 3.1 mm with the ASCE 10-97. As seen in these two examples, the compression capacity is largely dependent on the extent and the location of the corrosion. Concentration of corrosion reduces in an acute way the capacity of the member, specifically when such concentration occurs near the middle of the member. Corrosion is critical at the middle of the member because this is where the moment due to the eccentricities of the connections is a maximum. This non-uniformity of the phenomenon explains in large part the differences between the experimental and theoretical results.

Figure 8 shows the ratios of the experimental to the theoretical compression capacities versus the level of corrosion. This figure clearly shows the weakened capacity of the 48S-25-1 member.

To further analyse the results obtained and to focus on capacity reduction due to corrosion rather than the theoretical prediction of compression strength, the experimental and theoretical results are presented in Figure 9. The vertical axis is the ratio between the experimental and predicted percentage of residual capacity as compared to the uncorroded strength. This value compares the predicted loss of capacity and the loss of capacity measured during the test. From this figure, it is seen that there is a wide scatter in the results. Up to about 25% of corrosion, predictions are in line with experimental results. For corrosion level above 25%, experimental results and predictions do not match. However, there is not enough data between 0 and 25% to conclude that the analytical approach is satisfactory in this range of corrosion level.

It is interesting to note that predictions of the capacity of members with 9.5mm legs are better than the predictions on 4.8mm leg members. The average of the predictions is actually close to experimental results for 9.5mm leg members and variability is acceptable when we consider the rough method of estimating the capacity as compared to the complex development of corrosion. The predictions for members with 4.8mm leg thickness present more variability. The scatter in the ratio experimental/prediction observed on 4.8-mm leg thickness members might be attributed to the irregularity of the corrosion process when corrosion level increases.

**Table 3 Experimental and theoretical results for the compression capacity.**

Specimen	% of corrosion	Exp. capacity (kN)	Prediction ASCE (kN)	Exp. / ASCE
48S-00-1	0.00	n/a	142	n/a
48S-00-2	0.00	114	142	0.80
48L-00-1	0.00	91	88.6	1.03
48L-00-2	0.00	88	88.6	0.99
95S-00-1	0.00	323	278	1.16
95S-00-2	0.00	335	278	1.21
95L-00-1	0.00	168	168	1.00
95L-00-2	0.00	167	168	0.99
48S-25-1	26.4	57	121	0.47
48S-25-2	26.6	n/a	114	n/a
95S-25-1	26.9	253	214	1.18
95S-25-2	25.3	251	212	1.19
48L-25-1	27.4	80	70.4	1.13
48L-25-2	27.3	79	69.9	1.13
48S-40-1	37.2	66	80.6	0.82
48S-40-2	37.3	63	73.0	0.86
95S-40-1	37.1	216	191	1.13
95S-40-2	36.1	202	186	1.09
95L-25-1	22.4	151	137	1.10
95L-25-2	21.5	150	140	1.07
95L-40-1	30.7	99	121	0.82
95L-40-2	27.2	99	126	0.79
48L-40-1	40.7	65	54.3	1.20
48L-40-2	47.1	25	32.1	0.78



Figure 7 Perforated members 95L-40-2 and 48L-40-2.

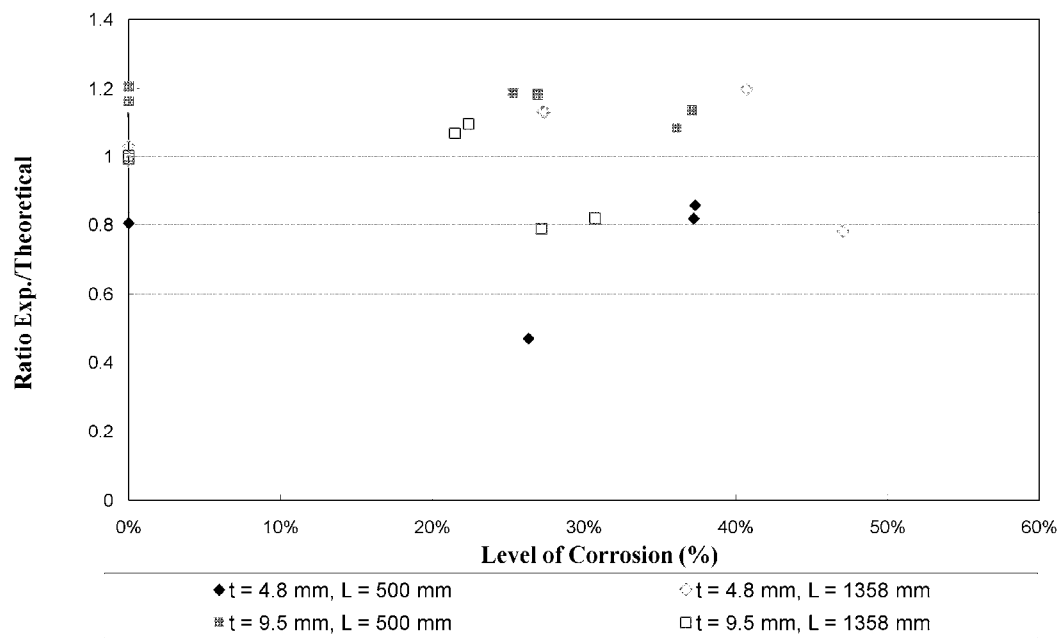
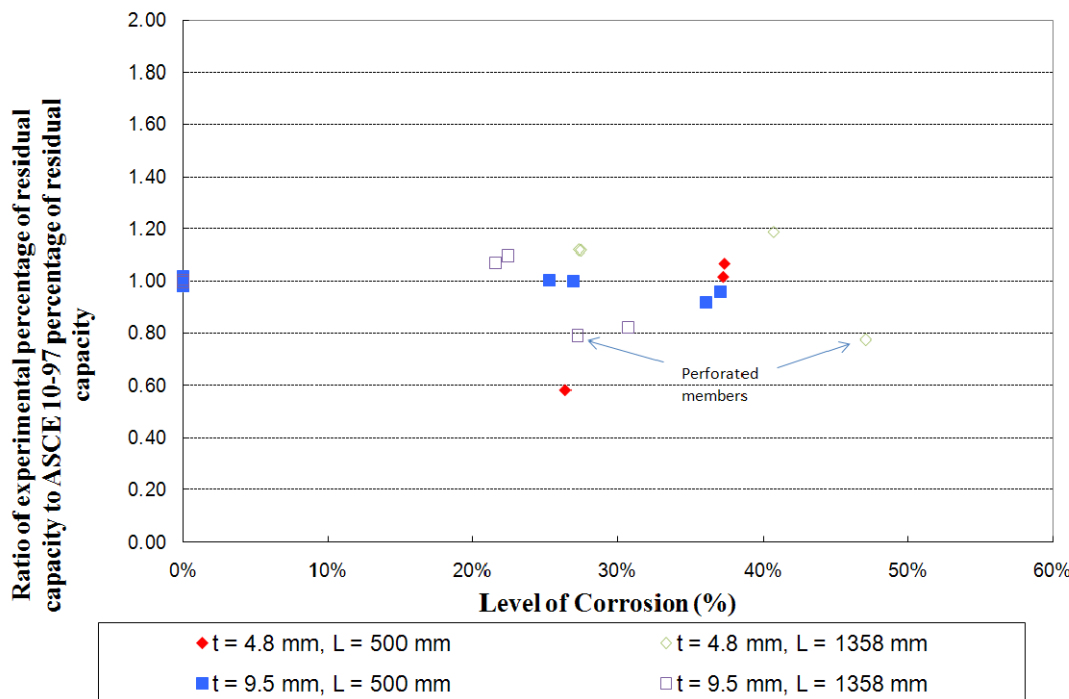


Figure 8 Ratio of the experimental to the theoretical compression capacity (ASCE 10-97) versus the level of corrosion.



**Figure 9 Ratio of experimental percentage of residual capacity to predicted ASCE 10-97 percentage of residual capacity.**

## CONCLUSIONS AND RECOMMENDATIONS

The capacities of many members were not predicted accurately using the ASCE 10-97 standard. The variation in the results can be explained by the non-uniformity of corrosion. ASCE 10-97 predicts the strength of members reasonably because it offers a way to predict local buckling due to large width-to-thickness ratio, and because it allows accounting for the influence of the connections through the modification of the slenderness ratio.

This experimental program showed that it may be possible to estimate the capacity of a corroded angle steel member using a prediction method based on average residual thickness of member. For members with initial thickness of 9.5mm, estimates of the capacity show an acceptable variability considering the uncertainty of the variables in practice. For members with 4.8 mm, the predictions are within 40% of experimental values with a large scatter.

The method needs improvement to be able to predict accurately residual strength. For example, it is required to take into account the unevenness of corrosion and concentration of corrosion as well as location of those concentrations.

To develop empirical charts that can be used in practice to evaluate directly the residual strength, it is believed that additional experimental data would be required, in

particular for members with level of corrosion between 0 and 20%. Additional data for other leg thickness and  $KL/r$  would also be interesting. For utilities, residual strength curves as a function of time are also necessary to plan asset repairs and replacements. For this purpose, additional research is required to transform corrosion level into time, depending on environment aggressiveness. Finally, it is also necessary to verify that the actual corrosion pattern found on steel structures is similar to the corrosion pattern obtained in this experiment through an accelerated corrosion method.

## REFERENCES

ASCE 10-97. (1997). *Design of Latticed Steel Transmission Structures*. American Society of Civil Engineers, USA.

ASTM E 8-61T. (1961). *Tentative Methods of Tension Testing of Metallic Materials*. American Society for Testing and Materials, USA.

Hathout, I. (2004). *Damage assessment and soft reliability evaluation of existing transmission lines*. In Proceedings of the International Conference on Probabilistic Methods Applied to Power Systems, Piscataway, NJ, 12-16 Sept. 2004, IEEE, pp. 980-986.

Morissette, E. (2008). *Évaluation des normes de calcul et du comportement des cornières simples en compression utilisées comme contreventements dans les pylônes à treillis en acier*. Thèse de maîtrise, Département de génie civil, Université de Sherbrooke, Sherbrooke, QC.

## Steel Structure Surface Preparation for Below Grade Coatings

Edward M. Jacobs

Director of Quality and R&D, Thomas & Betts Corporation, 8155 T&B Boulevard,  
2D-15, Memphis, TN 38125; Ph (901)-252-5349; Fax (901)-252-1312, email:  
[ed\\_jacobs@tnb.com](mailto:ed_jacobs@tnb.com)

### **Abstract**

This paper covers the importance of achieving good adhesion strength when applying Below Grade Coatings to steel structures. In particular, galvanized structures.

Through research, development and testing in accordance with ASTM D4541 we have concluded that there is a very meaningful correlation between a high pull-off adhesion value and the durability of an applied coating on a steel structure. The higher the pull-off adhesion strength, the better the bond to the substrate material. Having a superior bond will better enable the coating to withstand harsh weather and physical conditions.

It is imperative that when using a blast technology to prepare a surface for a Below Grade Coating that a high level of attention be placed on not only the profile of the galvanized steel surface after blasting but also the surface roughness achieved.

Having an insufficient surface roughness can lead to an undesirable adhesion strength of the Below Grade Coating and may compromise the intended performance for which it was engineered/developed.

The importance of establishing a reliable and consistent surface preparation method is critical for providing a foundation that will enable a superior pull-off adhesion value, which will provide a more robust coating solution.

## Introduction

Below Grade Coatings is a means of protecting steel structures at the ground line & below grade. Figure 1 is an example of galvanized steel structures with a below grade coating applied.

Protective coatings provide a barrier coating that protects the steel from corrosion and should be applied whenever there is a possibility of corrosive soil conditions. The dielectric properties of urethane coatings insulate poles from stray currents that may be present in the immediate area. Figure 2 illustrates a typical spray application process for a Below Grade Coating

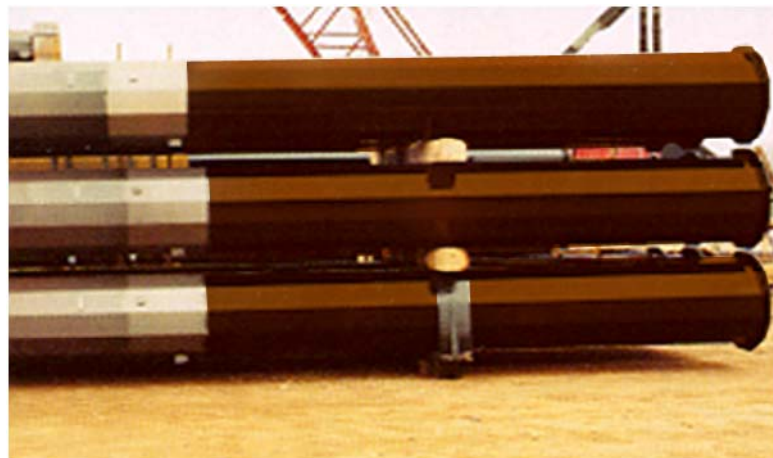


Figure 1: Below Grade Coating on a Steel Structure

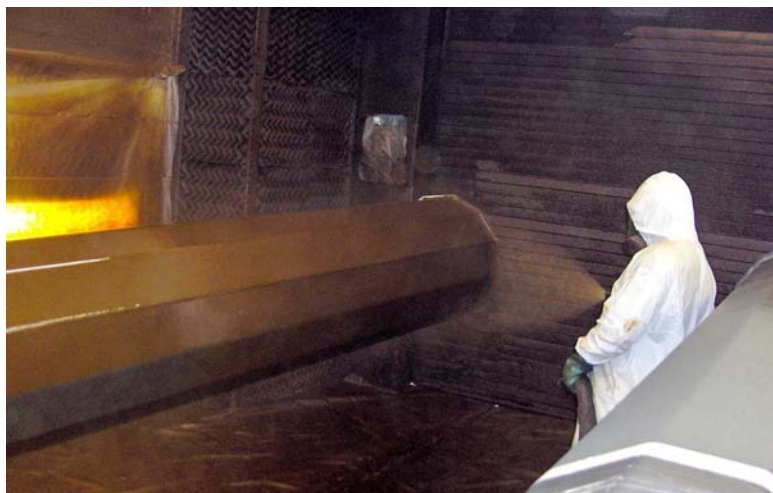


Figure 2: Application Process

## **Background**

Over the past several years Thomas & Betts has performed numerous and extensive tests through the efforts of our Research & Development Department on below grade coating products in order to identify the best method for surface preparation and subsequent coating applications.

We considered a range of coatings formulas, as well as surface preparation methods. Some of the tests were successful and some did not perform as originally hypothesized. The testing program played a significant role by helping us increase our knowledge base and improve our processes and product performance.

Since we are only aware of a minimal number of field performance problems when coating weathering steel, we used A871 panels to benchmark our results. History indicates that most performance challenges were associated with coating over galvanized structures made of A572 steel.

## **Testing**

We identified and tested multiple combinations of blasting media, surface profiles, coatings formulations and adhesion promoters.

Test panels of each combination were prepared. Substrate temperature, dew point, temperature, humidity, time and any special comments were recorded immediately prior to coating. Galvanize thickness and coating thickness measurements were taken in three places for each panel and surface profiles were recorded.

After the panel preparation was complete, we selected samples that best represented each individual test group. A fully accredited ISO registered third party test facility performed all testing.

Testing consisted of:

X-Cut Adhesion per ASTM D6677

Pull-Off Adhesion per ASTM D4541

Cathodic Disbondment per ASTM G95 modified to 60 days

QUV Accelerated Weathering testing per ASTM G154-06 at 1000 hour intervals.

All adhesion tests were performed 5 days after application. Additional adhesion tests were conducted after 1000 hours of QUV for a degradation check/comparison. No significant changes in performance were observed when compared to the initial tests.

After reviewing the results of the various tests that were performed, we concluded that the most meaningful information was obtained by conducting the Pull-Off Adhesion test per ASTM D4541.

### Testing (continued)

There was a direct correlation between the adhesion strength values obtained and the surface preparation method and media used. The higher performing test plates had both a higher profile and a higher “surface roughness,” which was achieved by following the rigorous process parameters that were set and controlled along with the blast media that was specified.

For the purpose of this report we are only going to focus on the correlation between an improved Pull-Off Adhesion test value and the benefits of a superior surface preparation practice. Figure 3 shows one of the Pull-Off Adhesion test panels after testing. The face of the test stub is shown on the left and the coated steel surface being tested for adhesion strength is shown on the right. Note that the percent of coating and/or glue remaining on the steel plate provides indication of the failure mode as shown in Table 1.



Figure 3. Typical Pull-Off Adhesion test panel

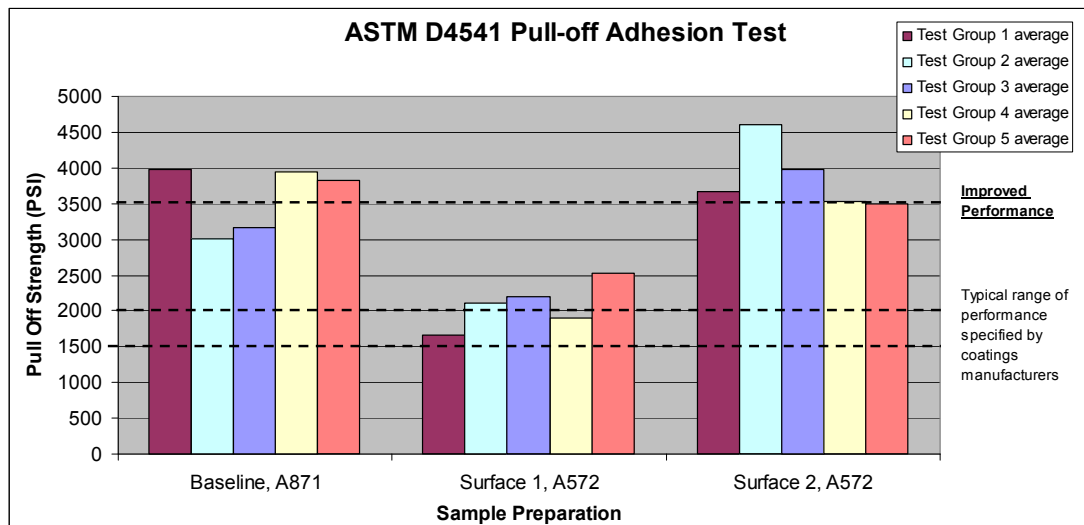


Figure 4: Pull-Off Adhesion test results.

Figure 4 summarizes the Pull Of adhesion test results. A871 material was utilized as a baseline for the test. Surface 1 represents a previously acceptable profile on galvanized steel which is typical for the industry. Surface 2 represents improved surface roughness characteristics on galvanized steel which was obtained by altering the blast process and media. Surface 2 provided adhesion test results that were much higher than the typical range of performance specified by coatings manufacturers for galvanized surfaces.

Testing (continued)

## ASTM D4541, Pull-off Adhesion Test

Test Group	Surface	#	Point 1 Thickness (Mils)	Point 2 Thickness (Mils)	Point 3 Thickness (Mils)	Average Mils	Failure Mode				Pull Off Strength (Actual PSI)	Mean PSI
							% Glue	% Coating Cohesion	% Substrate Adhesion	% Substrate Cohesion		
1	Baseline, A871	5	14.4	10.6	10.6	12	95	3	2	0	4149	3986
		7	22.5	12.3	15.3	17	100	0	0	0	3823	
	Surface 1	3	19.4	17.8	18.1	18	0	5	90	5	2112	1664
		6	27.6	27.1	27.3	27	0	5	95	0	1216	
	Surface 2	6	21.1	16.0	17.7	18	80	5	15	0	4068	3661
		7	20.9	16.7	15.7	18	85	5	10	0	3253	
2	Baseline, A871	7	17.7	16.9	18.4	18	35	5	60	0	3579	3579
		8	39.7	35.2	35.2	37	3	12	0	85	1623	
	Surface 1	5	24.3	25.5	25.6	25	2	8	90	0	2031	2113
		7	22.2	19.6	21.2	21	0	5	35	60	2194	
	Surface 2	2	28.3	26.3	26.3	27	100	0	0	0	4557	4598
		3	23.4	25.6	25.0	25	98	2	0	0	4638	
3	Sample	#	Point 1 Thickness (Mils)	Point 2 Thickness (Mils)	Point 3 Thickness (Mils)	Average Mils	% Glue	% Coating Cohesion	% Substrate Adhesion	% Substrate Cohesion	Pull Off Strength (Actual PSI)	Mean PSI
	Baseline, A871	5	17.4	17.1	18.2	18	100	0	0	0	2601	3172
		8	16.2	16.7	17.9	17	100	0	0	0	3742	
	Surface 1	3	23.4	25.9	24.5	25	20	5	65	10	1623	2194
		7	22.9	21.6	21.9	22	90	5	5	0	2764	
	Surface 2	6	26.7	26.6	25.9	26	100	0	0	0	3171	3986
		7	26.5	28.0	25.8	27	93	5	2	0	4801	
4	Surface	#	Point 1 Thickness (Mils)	Point 2 Thickness (Mils)	Point 3 Thickness (Mils)	Average Mils	% Glue	% Coating Cohesion	% Substrate Adhesion	% Substrate Cohesion	Pull Off Strength (Actual PSI)	Mean PSI
	Baseline, A871	6	17.1	20.3	17.9	18	99	1	0	0	4231	3946
		8	18.2	25.4	23.8	22	93	7	0	0	3660	
	Surface 1	1	26.7	20.3	17.4	21	2	3	95	0	2031	1909
		2	21.8	26.5	26.5	25	0	5	95	0	1786	
	Surface 2	3	18.9	20.7	21.3	20	45	5	50	0	2927	3538
		5	23.8	22.6	22.4	23	100	0	0	0	4149	
5	Surface	#	Point 1 Thickness (Mils)	Point 2 Thickness (Mils)	Point 3 Thickness (Mils)	Average Mils	% Glue	% Coating Cohesion	% Substrate Adhesion	% Substrate Cohesion	Pull Off Strength (Actual PSI)	Mean PSI
	Baseline, A871	2	14.4	15.0	14.0	14	10	5	85	0	4394	3824
		3	10.3	12.1	9.9	11	2	3	95	0	3253	
	Surface 1	4	17.3	17.1	17.8	17	0	5	95	0	2275	2520
		7	24.3	22.4	23.5	23	0	5	95	0	2764	
	Surface 2	4	14.9	15.9	17.8	16	0	5	95	0	3742	3498
		6	18.7	19.9	16.1	18	0	5	95	0	3253	

Table 1: Pull-Off Adhesion test results data

As shown in Table 1 the low performers exhibited a high percentage of failure between the substrate and coating. An insufficient surface roughness was attributable to these results. Most samples that exhibited a high (over 3000 psi) pull-off adhesion value failed in the glue area which is an indication that the coating was still adhered to the substrate material.

## **Surface Preparation**

A common practice for determining a surface profile which is accepted throughout many industries entails measuring the height of the highest profile peak within a sample area.

While the use of this method serves its intended purpose for surface measurements involving many applications, we found that there are other variables, which when defined and controlled will provide a more robust surface enabling better adhesion for Below Grade Coatings.

Roughness is a texture measurement of a surface. It is quantified by the frequency and short wavelength of surface deviations from its ideal form. If these deviations are large, the surface is rough; if they are small the surface is smooth.

We found that identification and controlling of the optimum vertical deviation or amplitude along with the slope and spacing of peaks and valleys (peak density) is critical to obtaining a good anchor profile.

Having an optimum profile will increase the total surface area and provide superior adhesion performance. The optimum profile must be determined for the specific application being considered.

It is imperative that very strict process parameters are in place as well as the blast media used.

## **Manufacturing Practices**

Controlling the blasting media and process along with selection of a robust coating product provide the best adhesion performance available.

### **These Items are Critical to Performance:**

- Leading-Edge Coating Formulations
- Qualified Blast Media
- Qualified and Certified Application Practices
- Trained, Experienced and Certified Applicators
- Monitoring of Process Control Parameters
- Well Maintained Equipment PM Schedule
- Performance Verification by Third Party Testing

## Conclusion

Superior adhesion is the key for overall performance of a Below Grade Coating.

Aromatic coatings typically provide superior adhesion when applied using best manufacturing practices and best surface preparation methods. Coatings of this type have less gloss retention over an extended period of time, but out perform aliphatic coatings when used for below grade applications. Performance vs. aesthetics must be considered when choosing a Below Grade Coating.

It is critical that blast practices and media used be optimized in order to achieve the best surface roughness possible in order to provide superior adhesion.

Robust Surface Roughness = Superior Adhesion = Superior Performance

Thomas & Betts has performed over five years of Research and Development which involved four manufacturing plants, consultants, independent test laboratories and a significant financial investment in order to provide our customers with the best below ground coating protection available.

We have invested in new technology and equipment, developed process control guidelines for surface preparation at our own plants and at galvanizing subcontractors, and partnered with our coatings supplier to define the ultimate coatings solution.

This study enabled us to surpass what was originally thought to be good adhesion by a significant amount. Feedback from the field allowed us to confirm a marked improvement in performance since we implemented these changes and refined our processes.

Thomas & Betts is confident that what we are currently doing is the best combination of surface preparation and coatings in our industry and we are committed to continuing research to maintain that position.

## IMPACT OF ALTERNATIVE GALLOPING CRITERIA ON TRANSMISSION LINE DESIGN

D. Boddy<sup>1</sup> and J. Rice<sup>2</sup>

### **ABSTRACT**

With the ever increasing demand on high voltage transmission systems minimizing outages has become an even higher priority. For transmission lines located in regions of the country that experience conductor galloping, this phenomenon can significantly contribute to the flashover rate if not properly accounted for in the design of the line.

Recent experience in some areas has shown that traditional methods of calculating the magnitude of galloping ellipses do not provide adequate phase separation. An alternative method being evaluated is the design approach proposed by CIGRE. The CIGRE methodology is derived from actual galloping observations and incorporates conservative empirical approximations. While this conservatism minimizes the probability of flashover or conductor impact during galloping, it also leads to larger vertical and horizontal phase spacing which directly affects structure configuration and cost. The impact can be even more significant for rebuild or reconductor projects where the original design criteria did not consider the larger CIGRE galloping ellipses.

This paper provides a comparison of galloping ellipses calculated by CIGRE with traditional methods and includes several examples of the impact on structure configuration, structure weight, and foundation size.

### **INTRODUCTION**

The electric transmission line industry has been witnessing an increasing demand for reliability in high voltage transmission lines. This has been the effect of growing demand creating network strain, increasing cost of new transmission lines, and new FERC regulations regarding service outages. Galloping is a factor in the design of transmission lines throughout much of the United States. This phenomenon is difficult to predict and can contribute to increased flashovers if it is not properly accounted for during design.

Recently, a new methodology has emerged and is gaining favor for design calculations. The CIGRE method of estimating the galloping ellipses is based on empirical calculations from observed galloping conditions for different wire diameters, tensions, and spans. This differs from the traditional galloping estimation using A.E. Davidson and L.W. Toye methodology which is based on theoretical assumptions.

---

<sup>1</sup> Sargent and Lundy LLC, Power Delivery Services, 55 E. Monroe, Chicago, IL 60603; PH (312) 269-2000; email: [david.m.boddy@sargentlundy.com](mailto:david.m.boddy@sargentlundy.com)

<sup>2</sup> Sargent and Lundy LLC, Power Delivery Services, 55 E. Monroe, Chicago, IL 60603; PH (312) 269-2000; email: [jonathan.a.rice@sargentlundy.com](mailto:jonathan.a.rice@sargentlundy.com)

## GALLOPING METHODOLOGY OVERVIEW

### A.E. Davidson Methodology Overview

The first of two modern-day systematic procedures for estimating galloping ellipses was proposed by A.E. Davidson in 1939. Davidson's method prescribes that wire during galloping moves in an ellipse (Figure 1) defined by the following equations<sup>3</sup>:

$$A_1 = D_L \text{ (loaded sag)}$$

$$A_2 = (A_1)/4$$

$$A_3 = 0.3 \text{ m (1 foot)}$$

$$A_4 = 1.25 * D_L + 1 \text{ (foot)}$$

$$A_5 = 0.4 * (A_4)$$

$$Q = F / 2$$

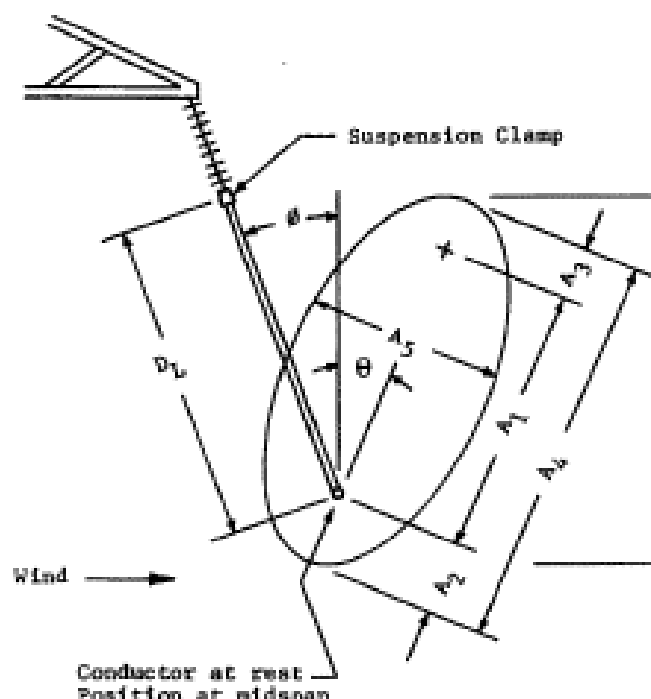


Figure 1. Galloping ellipse notation<sup>4</sup>.

Davidson Methodology is widely practiced throughout North America with utilities including minor modifications of the equations to better represent their own experiences.

<sup>3</sup> Electric Power Research Institute, Transmission Line Reference Book: Wind-Induced Conductor Motion, Palo Alto, California, 1979.

<sup>4</sup> Electric Power Research Institute, Transmission Line Reference Book: Wind-Induced Conductor Motion, Palo Alto, California, 1979.

### L.W. Toyes Methodology Overview

The other common procedure for estimating galloping ellipses is that introduced by L.W. Toye in 1951. Toye, employed then by the Public Service Electric and Gas Co. of New Jersey, considered galloping to occur with two ellipses along the span length. Consequently, Toye proposed ellipses defined by the following dimensions<sup>5</sup>:

$$A_4 = D_L / 2 * \text{sqrt}(2)$$

$$A_5 = 2 * \text{sqrt}(A_4)$$

In comparison, the Toye methodology produces ellipses of less magnitude than that of Davidson. It is this comparison that prompts debate concerning the point where galloping transitions from a single ellipse to two ellipses. This transition zone between ‘single loop’ and ‘double loop’ galloping often varies between design criteria documents as utilities again strive to incorporate past experience with the phenomenon.

### CIGRE Methodology Overview

The CIGRE State-of-the-Art Conductor Galloping Task Force B2.11.06<sup>6</sup> used measurements from actual galloping events as a basis to formulate empirical equations. The empirical equations derived were based on a conservative data fit approach. One of the key observations observed was that for longer spans the generally accepted assumption of double loop galloping was not valid. Due to this observation, the CIGRE formulations consider round conductor to always be in single loop galloping regardless of span length. Typical design standards currently employ a combination of Davidson for shorter spans and Toyes for larger spans which creates a sharp discontinuity when graphed. The CIGRE method does not have discontinuities since it is an empirical method based on field observations. It should also be noted that the conductor ellipse shall be taken as vertical which is in contrast to the Davidson and Toye methodologies which have a tilted ellipse. The following equations are used to determine the galloping ellipse for the CIGRE methodology.

$$A_4 = 80 * d * \ln\left[\frac{8f}{50d}\right]$$

$$A_1 = 0.7 A_4$$

$$A_2 = \frac{A_4}{4}$$

$$A_5 = 0.4 * A_4$$

Where,

d = Wire diameter (meters)

f = Sag of wire at 32F; ½ in. ice; no wind (meters)

---

<sup>5</sup> Electric Power Research Institute, Transmission Line Reference Book: Wind-Induced Conductor Motion, Palo Alto, California, 1979.

<sup>6</sup> International Council on Large Electric Systems (CIGRE), State of the Art conductor Galloping, Task Force B2.11.06, 2006

$A_4$  = Major axis of amplitude (meters)

$A_1$  = Vertical distance from wire sag point to top of ellipse (meters)

$A_2$  = Vertical distance from bottom of ellipse to wire sag point (meters)

$A_5$  = Minor axis of ellipse (meters)

## CONDUCTOR GALLOPING COMPARISONS

To select wires for a sample set, several items and design parameters were considered. Since galloping is a concern for longer span lengths, which are typical for higher voltages, conductors for 115kV to 345kV were considered. A shield wire was also selected since depending on the structure configuration, shield wire-conductor galloping interference can be a design consideration. Only round wire was selected for this paper since galloping design conditions are most prevalent when round wire is used. For the purpose of this paper, “round wire” is defined as non wind-induced, motion-resistant (T2) wire.

With these parameters and considerations, the following three conductors and one shield wire were selected as typical industry examples for regions that exhibit galloping.

795kcmil Drake ACSR

954kcmil Cardinal ACSR

2156kcmil Bluebird ACSR

7/16in. x 7 strand steel EHS

To compute the sag of the wires, the governing tension condition was selected as 20% rated tensile strength (RTS) at 0 deg F final condition and 16% RTS at 0 deg F final condition for conductors and shield wire respectively.

To display the conductor galloping ellipse information, ruling spans from 500 to 1200ft were chosen. This range was selected so that both the ends of the galloping design spectrum were accounted for. For simplicity of this paper, the ruling span was used to determine galloping ellipse magnitude.

### CIGRE Galloping Amplitudes

To gain a high level overview of the CIGRE method impacts, Figure 2 was created to display the galloping ellipse amplitudes. Figure 1 displays the sample wire set for various ruling spans.

For the ruling span length of 900ft, the conductor amplitudes range from 27.2ft to 38.9ft. These are substantial amplitudes when compared to the Toye method which, in S&L’s experience, is the most common method for such span lengths. This difference is due to the assumption in the Toye method that the wire will undergo double loop galloping and thus reduces the ellipse amplitude significantly.

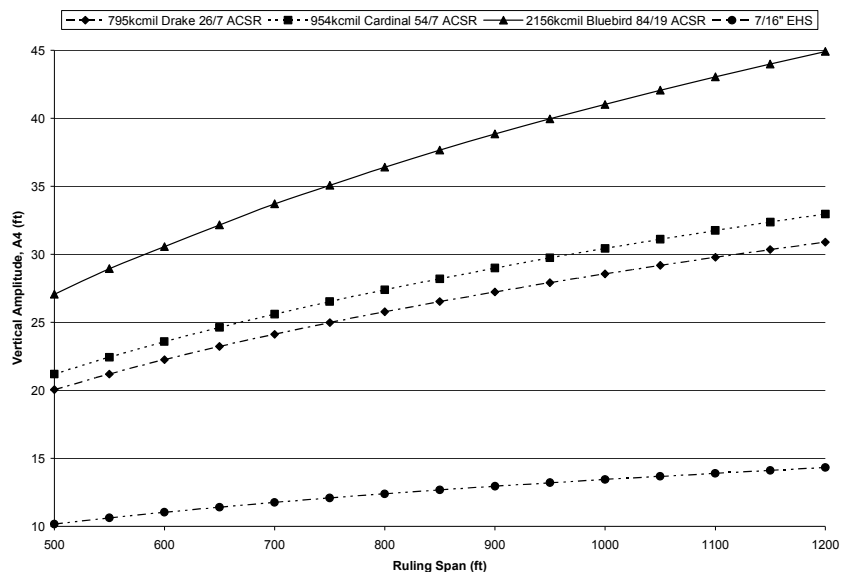


**Figure 2.** Vertical ellipse amplitude,  $A_4$ , for sample wire set using CIGRE method.

#### Galloping Methods Comparison

To examine the effects of implementing the CIGRE method versus the traditional Davidson and Toye methods, Figures 3-6 were created for the sample set of wires for a direct comparison. These figures display the galloping ellipse amplitude for the Davidson, Toyes, and CIGRE methodologies for the same tension and ruling span conditions.

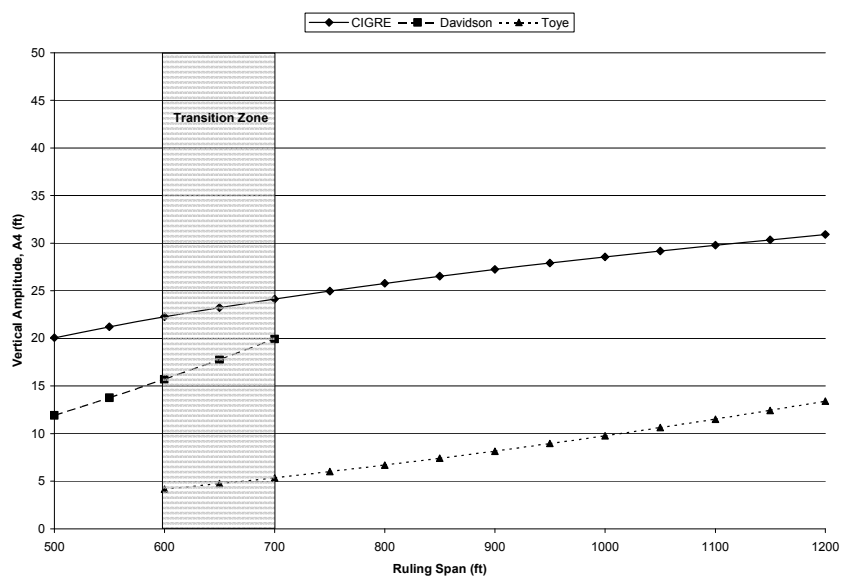


**Figure 3.** Galloping method comparison for 795kcmil Drake ACSR.

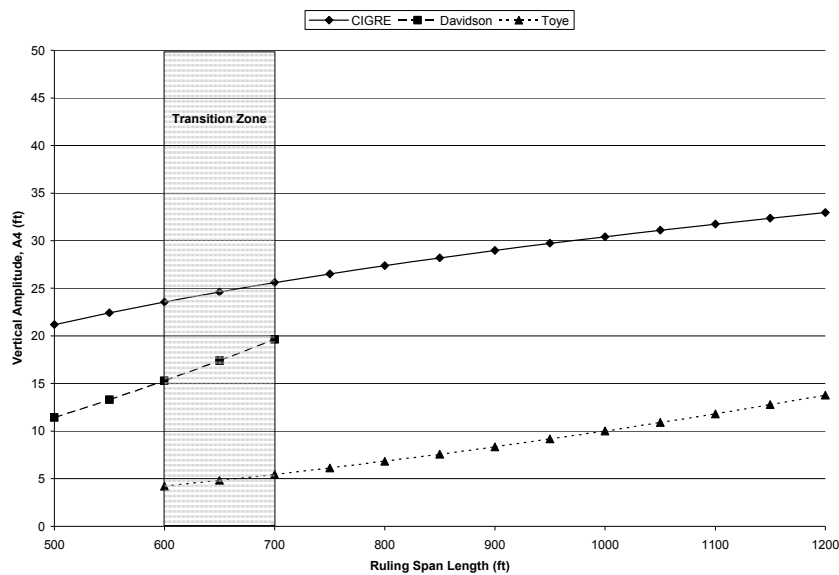


Figure 4. Galloping method comparison for 954kcmil Cardinal ACSR.

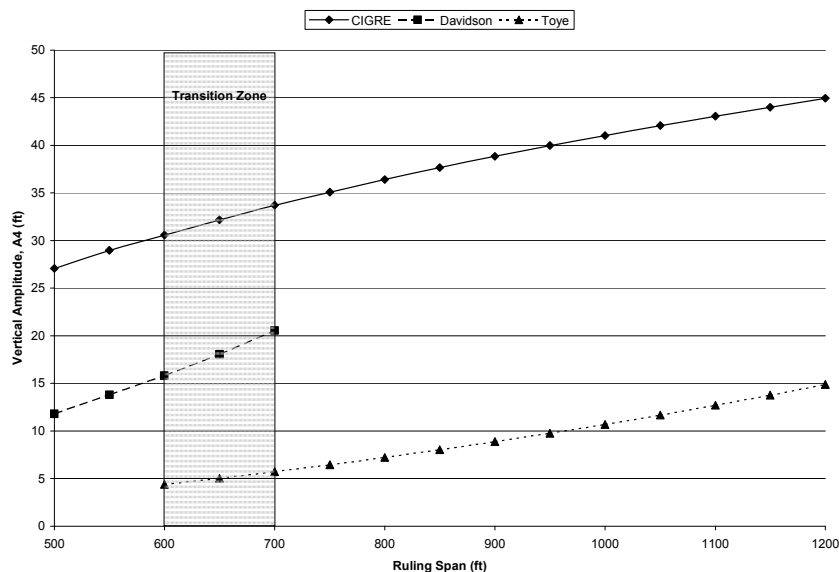
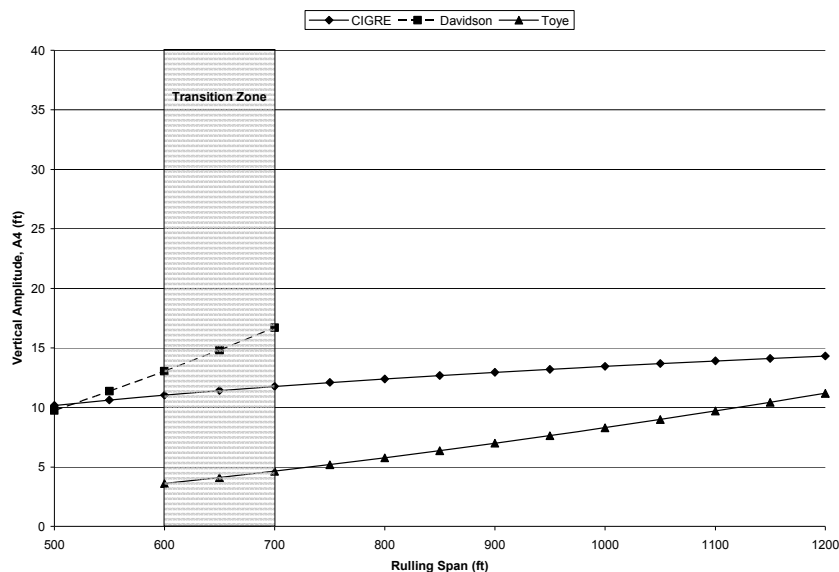


Figure 5. Galloping method comparison for 2156kcmil Bluebird ACSR.



**Figure 6. Galloping method comparison for 7/16in. x 7 Strand Steel EHS.**

With the examination of figures 3 to 6, three key observations are noted. For all the sample conductors chosen, the CIGRE method has larger amplitudes when compared to the Davidson method for shorter spans (500ft to 700ft). The maximum difference observed is between 8.8 to 15.3ft in vertical amplitude which corresponds to percent increases of 78.8% to 129%.

The CIGRE method amplitudes are always substantially larger than the Toy's method by 300-400% for the sample conductors. This is due to the method's fundamental assumptions regarding double loop galloping. A change of this magnitude for longer spans could greatly affect the configuration of the structure.

The 7/16x7 EHS displays the CIGRE method as the moderate method by having a smaller amplitude than the Davidson method but a larger amplitude than the Toy's method. This is a stark difference compared to the sample conductors.

## STRUCTURE CONFIGURATION IMPACT

To further highlight the differences between the different methods, three typical structure configurations were selected to display the galloping ellipses. These examples were chosen in an effort to best highlight structure configurations used in the utility industry.

### 138kV H-Frame

One of the most common structures used in the utility industry is the H-frame. For this example a 138kV H-frame with 15.5ft horizontal phase spacing is shown in figure 7. From the sample set of conductors, the 795kcmil Drake ACSR was selected with a 600ft ruling span. Both shield wires were selected as 7/16x7 EHS steel strands.

Due to the moderate span length of 600ft, coupled with design practices observed by S&L, only the CIGRE and Davidson galloping methods were applied. The CIGRE method in figure 7 is displayed using a solid line while the Davidson method is displayed using a hidden (dashed) line.

Even though the CIGRE method has substantially larger ellipses, it is evident in figure 7 that none of the galloping ellipses overlap. This is to be expected since over the many years and numerous applications, H-frame structures have had minimal flashover occurrences due to galloping events.

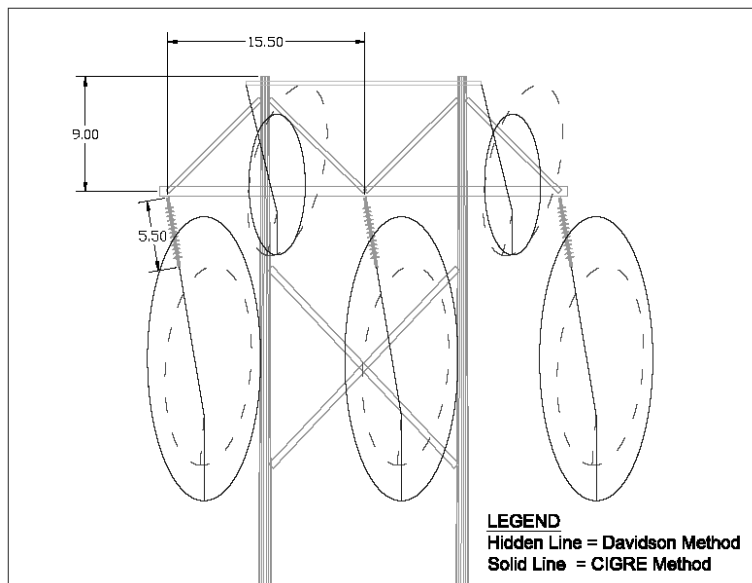


**Figure 7. Typical 138kV H-frame with 795kcmil Drake ACSR, 7/16x7 EHS steel strand shield wires and a ruling span of 600ft.**

#### 138kV Double Circuit Steel Pole

One of the structure types most susceptible to galloping flashover is the vertical double circuit steel pole configuration. For this structure configuration, the conductor was chosen to be 954kcmil Cardinal ACSR with 7/16x7 EHS steel as the shield wires. To emphasize the effects of the CIGRE method the ruling span length was selected as 900ft.

Due to this span length, the Toye method (double loop galloping) was employed since this is typical design practice observed by S&L. Figure 8 displays the example with the CIGRE method as a solid line and the Toye method as a hidden (dashed) line.

From figure 9, one can conclude that the CIGRE method would require substantial arm and/or phase spacing adjustments. This is in contrast to the Toye method which would require no configuration alterations.

The structure alterations required to ensure that no CIGRE ellipse overlap occurs include extending the middle arm to at least 18.25ft which is an increase of 25%. This increase in arm length is just the minimal amount required to ensure that the ellipses do not overlap. (If a

requirement is used that ellipses shall maintain an additional 1.5ft<sup>7</sup> as the EPRI “Orange Book” recommends to avoid phase-phase flashover, then the arm would need to be a minimum of 19.75ft which is an increase of 36%).

Not only does the increase in arm length change the phase spacing but it would also have an adverse effect on structure cost due to the increased arm length and weight, increase pole shaft size for extra capacity, and larger foundation to account for the larger overturning moment. While some of these changes may seem relatively minor, for large projects this can add substantial cost due to total quantities.

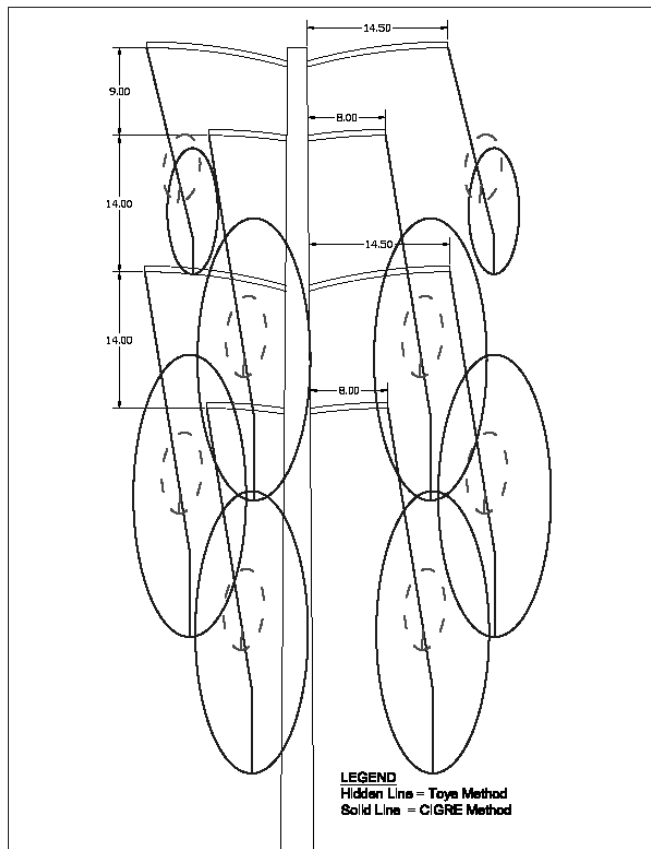


**Figure 8. Typical 138kV double circuit steel pole with 954kcmil Cardinal ACSR, 7/16x7 EHS steel strand shield wires and a ruling span of 900ft.**

#### 345kV Double Circuit Steel Pole

To further illustrate the vertical configuration example, a typical 345kV double circuit steel pole example was selected (figure 9). For structures of this configuration, the span lengths are typically longer so a ruling span length of 900ft was used with the 2156kcmil Bluebird ACSR conductor.

<sup>7</sup> Electric Power Research Institute, Transmission Line Reference Book: Wind-Induced Conductor Motion, Palo Alto, California, 1979.

As was the case in the 138kV double circuit example above (figure 8), the 345kV double circuit configuration has extensive galloping ellipse overlap for the CIGRE method and no overlap for the Toye double loop method. If the current vertical spacing was held constant, the middle phase arm would require an increase in length by 8ft (40%) to ensure no overlapping of the CIGRE galloping ellipses. The shield wire arm would also require a 2ft extension (10% increase).

The extension of the middle phase arm 8ft would increase the required pole shaft and foundation capacity but could also cause right-of-way (ROW) issues.

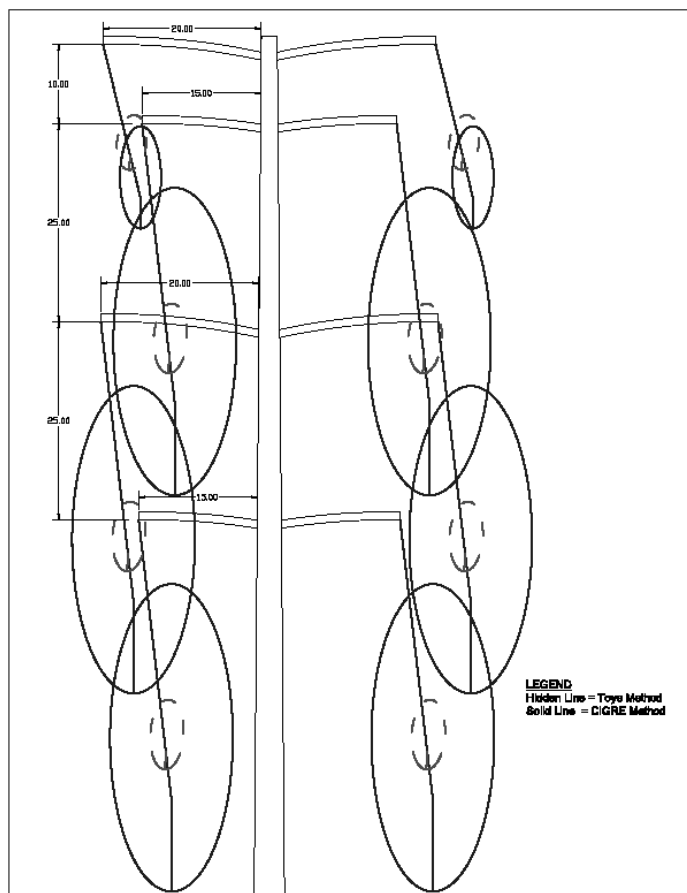


**Figure 9. Typical 345kV double circuit steel pole with 2156kcmil Bluebird ACSR, 7/16x7 EHS steel strand shield wires and a ruling span of 900ft.**

## DESIGN CRITERIA CONSIDERATIONS

### Current Design Criteria Considerations

A typical reference for transmission line design, the RUS Design manual for High Voltage Transmission Lines states “Single-loop galloping rarely occurs in spans over 600 to 700 feet”<sup>8</sup>. This statement has led many past and current design criteria to implement a combination of Davidson/Toye methods based on a determined span length.

By using the Davidson method for shorter spans and Toye method for longer spans, design criterias have an inherent discontinuity at a span length determined by the criteria. The span length determined by the criteria can result in two different configurations with span lengths that differ by as little as 100 feet. This discontinuity can be just as difficult to predict as the galloping occurrence.

### Design Criteria Considerations for CIGRE Implementation

Design criterias employing the CIGRE method also include key assumptions that have a conservatism constructed into the empirical equations. Figure 10 displays the empirical curve fit based on the observations used for the CIGRE method. As can be seen there are few outliers above the CIGRE method curve.

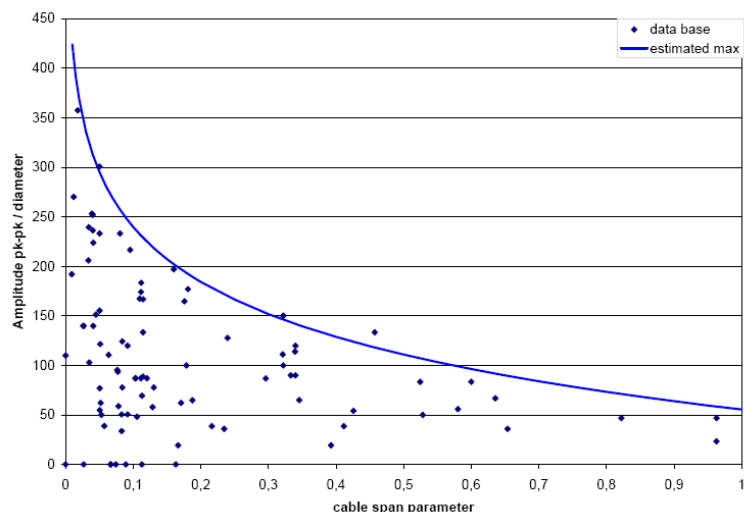


**Figure 10. CIGRE variation of observed galloping amplitude versus span parameters<sup>9</sup>.**

With the implementation of the CIGRE method, a new set of questions arise. Since the amplitude has a degree of conservatism built in the empirical equations additional ellipse spacing for flashover may be overly conservative.

<sup>8</sup> RUS Bulletin 1724E-200, DESIGN MANUAL FOR HIGH VOLTAGE TRANSMISSION LINES, Section 6.5.1, May 2005

<sup>9</sup> International Council on Large Electric Systems (CIGRE), State of the Art conductor Galloping, Task Force B2.11.06, 2006, Figure 8.44

One potential issue with the CIGRE method is maximum amplitude of the ellipses. The CIGRE method does not have a maximum ellipse amplitude so for longer spans the amplitude keeps increasing. This can be viewed as having an excessive design conservatism which may not be economically justified. Similar to the Davidson & Toye method utilities could set a maximum amplitude.

## CONCLUSION

While the design criteria considerations mentioned above influence the galloping analysis, the real impact of the galloping method chosen is most evident in the structure configuration. One of the main differences when first examining the CIGRE calculations is the amplitude of the galloping ellipses for longer spans. The CIGRE methodology when compared to A.E. Davidson methodology has much larger amplitudes that can significantly affect structure configuration, size, and cost. The effects on the structure configuration were shown above for a select set of wires and structure types. The increase in structure size and therefore weight also affect the foundation design and potential ROW width. If the ROW width is fixed which is typical for a rebuild project, the options are limited to increasing phase spacing and thus structure height, decreasing span length with additional structures, or changing conductor.

Design for galloping occurrences can be a challenging problem with many influencing factors. The solutions to address the galloping concerns may prove to be economically inefficient depending on the project. With these economic factors, a balancing act occurs between project cost and project design when addressing galloping concerns.

## REFERENCES

Electric Power Research Institute, Transmission Line Reference Book: Wind-Induced Conductor Motion, Palo Alto, California, 1979.

International Council on Large Electric Systems (CIGRE), State of the Art conductor Galloping, Task Force B2.11.06, 2006

United States Department of Agriculture Rural Utilities Service, Design Manual for High Voltage Transmission Lines, Bulletin 1724E-200, 2004

# Author Index

## A

**Amundsen, T. A.**

Analytical Techniques to Reduce Magnetic Force from High Fault Current on Rigid Bus

**Andrews, Trevor**

Estimation of Containment Loads on a 230kV Steel Transmission Line Using Finite Element Model

**Ashby, Mathieu**

Dynamic Wind Analyses of Transmission Line Structures

**Asselin, Jean-Marie**

Sequential Mechanical Testing of Conductor Designs

## B

**Baker, Brent**

Are Wood Poles Getting Weaker?

**Bazán-Zurita, E.**

Seismic Design of Substation Structures

**Beaulieu, L. -V.**

Residual Capacity in Compression of Corroded Steel Angle Members

**Beehler, Michael E.**

Lessons Learned on Mega Projects

**Bégel, C.**

3D Automated Design of Substations

**Behncke, Roberto H.**

Review of Span and Gust Factors for Transmission Line Design

**Benavides, C.**

Telegram Channel: @Seismicisolation

3D Automated Design of Substations

**Bielak, J.**

Seismic Design of Substation Structures

**Bingel, Nelson G. III**

Assessment and Repair of Steel Tower and Steel Pole Foundations

**Bliss, Ryan**

Line Rating: It's All about the Temperature!

**Boddy, D.**

Impact of Alternative Galloping Criteria on Transmission Line Design

**Brown, Michael D.**

Are Wood Poles Getting Weaker?

## C

**Calvert, Rodger**

Temporary Support of Lattice Steel Transmission Towers

Analysis Challenges in the Evaluation of Existing Aluminum Towers

**Carrington, Ron**

The Effects of Ice Shedding on a 500 kV Line

**Catchpole, P. G.**

Large Catenary Structures for High Voltage Transmission Lines

**Chau, Max**

Aesthetic Mitigation—The Challenge Confronting Future Expansion of Transmission Lines

**Cooper, Andy**

H<sub>2</sub>S Entrapment and Corrosion on Direct Embedded Galvanized Steel Transmission Poles

**Crissey, Dana R.**

345 kV High Ampacity OH/UG Project

## D

Telegram Channel: @Seismicisolation

**DiGioia, A. M. Jr.**

Seismic Design of Substation Structures

Deepwater Transmission Line Foundations Meet Trophy Bass Lake Environment

**Drolet, Y.**

3D Automated Design of Substations

**F****Fan, Quan He**

Lessons Learned from Design and Test of Latticed Steel Transmission Towers

**Ferguson, N.**

Vegetation Management Through LiDAR Derived CADD Models: Compliance with NERC Reliability Standard FAC-003-1

**Foster, Michael**

Integration of Optimum, High Voltage Transmission Line Foundations

**Freimark, Bruce**

Laboratory and Field Testing of Steel Davit Arm Fatigue Failures on Concrete Poles

Sequential Mechanical Testing of Conductor Designs

Electrical and Mechanical Considerations in 765kV (Insulator) Hardware Assembly Design

**G****Gajan, Sivapalan**

Transmission Pole Foundations: Alternate Design Methods for Direct-Embedded Round, Wood Transmission Poles

**Gani, Ferawati**

Dynamic Wind Analyses of Transmission Line Structures

**Goodwin, E. J.**

Deepwater Transmission Line Foundations Meet Trophy Bass Lake Environment

**Graham, James W.**

The 2008 Iowa Floods: Structural Challenges and Solutions

Telegram Channel: @Seismicisolation

## H

**Haldar, Asim**

Estimation of Containment Loads on a 230kV Steel Transmission Line Using Finite Element Model

**Hastings, Aaron**

Integration of Optimum, High Voltage Transmission Line Foundations

**Ho, T. C. Eric**

Review of Span and Gust Factors for Transmission Line Design

**Hodges, Norman P.**

230kV Lattice Tower Replacement: An Example of Design Loading Not Addressed in the NESC

**Hogan, James M.**

Design and Construction Challenges of Overhead Transmission Line Foundations (NU's Middletown Norwalk Project)

## J

**Jacobs, Edward M.**

Steel Structure Surface Preparation for Below Grade Coatings

**Jarenprasert, S.**

Seismic Design of Substation Structures

**Johnson, Kristofer**

Geotechnical Investigations for a Transmission Line are More Than Drilled Borings

## K

**Kempner, Leon Jr.**

Wind Load Methodologies for Transmission Line Towers and Conductors

Strength of Steel Angles Subjected to Short Duration Axial Loads

**Kennedy, Scott**

Aesthetic Mitigation—The Challenge Confronting Future Expansion of Transmission

Telegram Channel: @Seismicisolation

Lines

**Khattak, Anwar**

Integration of Optimum, High Voltage Transmission Line Foundations

**Kile, John D.**

Temporary Support of Lattice Steel Transmission Towers

**Kilgore, Jason W.**

Analysis Challenges in the Evaluation of Existing Aluminum Towers

**Kuffel, John**

Electrical and Mechanical Considerations in 765kV (Insulator) Hardware Assembly Design

**L**

**Lacroix, C.**

3D Automated Design of Substations

**Lakhapati, Deepak**

Construction Challenges of Extra High Voltage Transmission Lines: Building in the Most Difficult Terrain in the World

Power Restoration Solution after Major Cyclone: "Gonu" Hit Oman in June 2007

**Langlois, S.**

Residual Capacity in Compression of Corroded Steel Angle Members

**Légeron, F.**

Residual Capacity in Compression of Corroded Steel Angle Members

**Legeron, Frederic**

Dynamic Wind Analyses of Transmission Line Structures

**Lemelin, D. R.**

3D Automated Design of Substations

**Li, Ziqin**

Electrical and Mechanical Considerations in 765kV (Insulator) Hardware Assembly Design

**Lynch, Otto J.**

Common Sag and Tension Errors: It's Time for Template Technology to be Put in the Drawer Forever

Telegram Channel: @Seismicisolation

## M

**Mallik, Ajay**

H<sub>2</sub>S Entrapment and Corrosion on Direct Embedded Galvanized Steel Transmission Poles

**Malmedal, Keith**

Substation Bus Design: Current Methods Compared with Field Results

**Malten, K. C.**

Analytical Techniques to Reduce Magnetic Force from High Fault Current on Rigid Bus

**McCall, Christopher L.**

Design and Construction Challenges of Overhead Transmission Line Foundations (NU's Middletown Norwalk Project)

**McNames, Cassie**

Transmission Pole Foundations: Alternate Design Methods for Direct-Embedded Round, Wood Transmission Poles

**Monroe, Scott**

Temporary Support of Lattice Steel Transmission Towers

**Mueller, Wendelin H. III**

Strength of Steel Angles Subjected to Short Duration Axial Loads

## N

**Niles, Kevin D.**

Assessment and Repair of Steel Tower and Steel Pole Foundations

**Norman, R.**

Deepwater Transmission Line Foundations Meet Trophy Bass Lake Environment

## O

**Oliphant, Wesley J.**

The Chaotic Confusion Surrounding "Wood Equivalent" Non-Wood Poles

Telegram Channel: @Seismicisolation

**Oster, J. L.**

Analytical Techniques to Reduce Magnetic Force from High Fault Current on Rigid Bus

**P****Peabody, Alan B.**

The Effects of Ice Shedding on a 500 kV Line

**Perez, Jared J.**

Strength of Steel Angles Subjected to Short Duration Axial Loads

**Peter, Zsolt**

Sequential Mechanical Testing of Conductor Designs

**Peyrot, Alain H.**

Wind Loading: Uncertainties and Honesty Suggest Simplification

**Pon, Craig**

Sequential Mechanical Testing of Conductor Designs

**Prud'homme, S.**

Residual Capacity in Compression of Corroded Steel Angle Members

**Pugh, Archie**

Aesthetic Mitigation—The Challenge Confronting Future Expansion of Transmission Lines

**R****Rao, Teja**

Electrical and Mechanical Considerations in 765kV (Insulator) Hardware Assembly Design

**Ray, R.**

Vegetation Management Through LiDAR Derived CADD Models: Compliance with NERC Reliability Standard FAC-003-1

**Retz, David**

Design and Construction Challenges of Overhead Transmission Line Foundations (NU's Middletown Norwalk Project)

Telegram Channel: @Seismicisolation

**Rice, J.**

Impact of Alternative Galloping Criteria on Transmission Line Design

**Richardson, P.**

Vegetation Management Through LiDAR Derived CADD Models: Compliance with NERC Reliability Standard FAC-003-1

**Rowland, Ronald L.**

Golden Pass LNG 230kV Double Circuit: Foundations

**Ruggeri, E. A.**

Large Catenary Structures for High Voltage Transmission Lines

**Ryder, S.**

Vegetation Management Through LiDAR Derived CADD Models: Compliance with NERC Reliability Standard FAC-003-1

**S****Salisbury, Nick**

Integration of Optimum, High Voltage Transmission Line Foundations

**Samms, Howard A.**

Alabama Power Increases Line Capacity Using 3M ACCR Conductor (On Existing Towers)

**Shanmugasundaram, Rengaswamy**

Transmission Line at St. Andrew Bay

Analysis Challenges in the Evaluation of Existing Aluminum Towers

**T****Thompson, Freeman**

Integration of Optimum, High Voltage Transmission Line Foundations

**V****Vaughn, Bruce**

Sequential Mechanical Testing of Conductor Designs

Telegram Channel: @Seismicisolation

**Veitch, Maria**

Estimation of Containment Loads on a 230kV Steel Transmission Line Using Finite Element Model

**Verth, S.**

Vegetation Management Through LiDAR Derived CADD Models: Compliance with NERC Reliability Standard FAC-003-1

**Vogt, Marlon**

The 2008 Iowa Floods: Structural Challenges and Solutions

**W****Weelden, Tim Van**

The 2008 Iowa Floods: Structural Challenges and Solutions

**Wendelburg, John**

Substation Bus Design: Current Methods Compared with Field Results

**Whapham, Robert**

Laboratory and Field Testing of Steel Davit Arm Fatigue Failures on Concrete Poles

**Williamson, Ernest C. Jr.**

Golden Pass LNG 230kV Double Circuit: Foundations

**Wong, C. Jerry**

Fact or Fiction—Weathering Steel Can Provide Effective Corrosion Protection to Steel Structures

**Wyman, Gregory E.**

Transmission Line Construction in Sub-Arctic Alaska Case Study: "Golden Valley Electric Association's 230kV Northern Intertie"

**Z****Zhu, Meihuan (Nancy)**

Laboratory and Field Testing of Steel Davit Arm Fatigue Failures on Concrete Poles

Telegram Channel: @Seismicisolation